



MONASH University

Studies on obesity-associated Advanced Glycation Endproducts and female fertility

Jennifer Claire Hutchison

Bachelor of Science (Honours)

A thesis submitted for the degree of Doctor of Philosophy at
Monash University in 2021

Department of Molecular and Translational Science,
Faculty of Medicine, Nursing, and Health Sciences

&

Centre for Reproductive Health,
Hudson Institute of Medical Research

Under the supervision of:

Professor Lois A. Salamonsen, Professor David K. Gardner,
Professor Guiying Nie (2019-2021), & Dr Jemma Evans (2017-2019)

Copyright notice

© Jennifer Hutchison (2021)

I certify that I have made all reasonable efforts to secure copyright permissions for third-party content included in this thesis and have not knowingly added copyright content to my work without the owner's permission.

Abstract

Globally, 39% of the adult population is overweight or obese, with prevalence of obesity following an upward trajectory over the recent decades. Up to 30% of women of reproductive age in Western countries are obese before conception, and obese women experience higher rates of infertility and pregnancy complications than lean women; however, the mechanisms underpinning obesity-related infertility are poorly understood. Advanced Glycation Endproducts (AGEs) are a proinflammatory modification of proteins exposed to sugars, formed through the Maillard reaction. Prior to my candidature, my laboratory identified AGEs as elevated four-fold in the uterine fluid of obese, infertile women, compared to lean. AGEs equimolar to the obese uterine fluid microenvironment negatively impacted the functions of endometrial epithelial and stromal cells, and adhesion and invasion of trophoblast cells. The work in this thesis further investigated obesity associated AGEs and their functional impact on female fertility.

The earliest stages of embryo development are finely balanced, and altered local environments can set offspring up for a lifetime of health or disease (DoHAD); thus, uterine AGEs may contribute to the prevalence of non-communicable disease in children of obese parents. AGEs representative of the obese uterine microenvironment impacted the formation and function of the preimplantation embryo: hatching rates were reduced; trophoctoderm comprised fewer cells; and blastocyst outgrowth on fibronectin was reduced. Trials of therapeutic interventions revealed modest benefit of RAGE antagonism on trophoctoderm cell number, but no effect of metformin or antioxidants. Thus, obesity-associated AGEs link obesity and reduced fertility through poor placentation potential of embryos.

Therapeutic intervention was then trialled to normalise the implantation environment in obese women and support establishment of healthy pregnancy. Antioxidants successfully normalised the rate of proliferation of endometrial epithelial cell lines exposed to obese levels of AGEs. Subsequently, human endometrial epithelial organoid culture was utilised as a more physiologically relevant experimental paradigm. Obesity-associated AGEs altered the function of these epithelial cells, particularly increasing the secretion of proinflammatory CXCL16. As the inflammatory milieu is altered in idiopathic infertile women, AGEs may promote an infertile endometrial inflammatory environment.

Further experimentation characterised protein biomarkers of endometrial receptivity, potential molecular targets for AGEs induced endometrial non-receptivity. The human endometrial epithelial “receptome” and embryo-epithelial “adhesome” were previously determined by proteomic interrogation of trophoctoderm spheroids adherent to primary human endometrial epithelial cells, a

model which reflects the fertility of donors. Here, immunoreactive Positive Cofactor 4 (PC4), highly upregulated in receptive endometrial epithelial cells versus non-receptive, was detected at significantly higher levels in fertile early- and mid-secretory endometrium. Stem-Loop-Interacting RNA binding Protein (SLIRP) was reduced in the epithelium following adhesion of trophectoderm spheroids, and its reduction in endometrial epithelial cell lines relaxed tight junctions, required for the embryo to traverse the epithelial barrier.

In conclusion, AGEs link obesity and reduced fertility, and are detrimental to preimplantation embryo development and endometrial function when present at concentrations equal to those in the obese uterine fluid. This research provides evidence supporting AGEs as a factor contributing to obesity-related infertility, and as an emerging frontier for reproductive health.

| | |
|---|--------------|
| COPYRIGHT NOTICE | II |
| ABSTRACT | III |
| DECLARATION | XI |
| THESIS INCLUDING PUBLISHED WORKS DECLARATION | XII |
| ACKNOWLEDGEMENTS | XV |
| LIST OF ABBREVIATIONS | XVIII |
| CHAPTER 1: INTRODUCTION | 2 |
| 1.1 THE CLINICAL PROBLEM OF OBESITY-RELATED INFERTILITY | 2 |
| 1.2 THE FEMALE REPRODUCTIVE TRACT | 2 |
| 1.2.1 THE OVARIES | 3 |
| 1.2.2 THE UTERUS | 4 |
| 1.2.2.1 THE ENDOMETRIUM | 4 |
| 1.2.2.1.1 Stromal fibroblasts | 4 |
| 1.2.2.1.2 Endometrial Glands and Secretions | 5 |
| 1.2.2.1.3 Epithelium | 5 |
| 1.3 THE MENSTRUAL CYCLE OF THE ENDOMETRIUM | 6 |
| 1.3.1 MENSES | 7 |
| 1.3.2 THE PROLIFERATIVE PHASE | 8 |
| 1.3.3 THE SECRETORY PHASE | 8 |
| 1.4 ENDOMETRIAL RECEPTIVITY | 9 |
| 1.4.1 THE ROLE OF THE LUMINAL EPITHELIUM | 9 |
| 1.4.2 WHAT AFFECTS ENDOMETRIAL RECEPTIVITY? | 10 |
| 1.4.3 THE HUMAN ENDOMETRIAL EPITHELIAL RECEPTOME | 10 |
| 1.5 PREIMPLANTATION EMBRYO DEVELOPMENT | 11 |
| 1.5.1 DEVELOPMENTAL TIMELINE | 13 |
| 1.6 MATERNAL-FETAL INTERACTION: EMBRYO-ENDOMETRIUM CROSSTALK | 14 |
| 1.6.1 ADHESION AND IMPLANTATION | 15 |
| 1.6.2 MODELS TO STUDY EMBRYO-EPITHELIAL INTERACTIONS | 16 |
| 1.6.3 THE ADHESOME | 17 |
| 1.7 OBESITY | 17 |
| 1.7.1 EFFECTS OF OBESITY ON REPRODUCTION | 18 |
| 1.7.1.1 Female reproduction | 18 |
| 1.7.1.1.1 The endometrium | 20 |
| 1.7.1.1.2 Ovarian effects | 21 |
| 1.7.1.1.3 Gestational Disorders | 22 |
| 1.7.1.2 Male reproduction | 22 |
| 1.7.1.3 Combined parental obesity | 23 |
| 1.7.1.4 Obesity and ART | 23 |
| 1.7.1.4.1 Effects on the embryo | 24 |

| | |
|--|-----------|
| 1.8 ADVANCED GLYCATION END PRODUCTS | 25 |
| 1.8.1 STRUCTURE AND FORMATION | 25 |
| 1.8.2 ACCUMULATION OF AGES IN THE BODY | 26 |
| 1.8.3 SIGNALLING PATHWAYS OF AGES | 26 |
| 1.8.4 PHYSIOLOGICAL FUNCTION | 27 |
| 1.8.5 AGES AND FEMALE REPRODUCTION | 27 |
| 1.8.5.1 AGEs in the ovary: implications for oocyte development, maturation, and competency | 28 |
| 1.8.5.2 AGEs and the early embryo | 29 |
| 1.8.5.3 RAGE and AGEs in the uterus: implications for embryo development and implantation | 30 |
| 1.8.5.4 The placenta: AGEs may affect establishment and continuation of pregnancy | 30 |
| 1.8.5.4.1 Evidence of AGEs in miscarriage and recurrent pregnancy loss | 31 |
| 1.8.5.4.2 Evidence of AGEs in preeclampsia | 31 |
| 1.8.5.5 AGEs influence the outcome of ART | 32 |
| 1.8.5.6 Maternal AGEs and offspring outcome | 33 |
| 1.8.6 CURRENT INTERVENTIONS TO REMEDIATE AGES INDUCED DAMAGE | 34 |
| 1.8.6.1 Prevention of formation and accumulation | 34 |
| 1.8.6.2 Inhibition of AGEs signalling | 35 |
| 1.8.6.3 Remediation of downstream effects | 35 |
| 1.9 SUMMARY AND CONCLUSIONS | 36 |
| 1.10 THESIS AIMS AND HYPOTHESES | 36 |
| 1.10.1 OVERALL AIM | 36 |
| 1.10.2 SPECIFIC AIMS | 37 |
| 1.10.2.1 Aim 1: Examining the effect of the obese uterine environment on pre-implantation embryonic development. | 37 |
| 1.10.2.2 Aim 2: Investigating pharmaceutical intervention to remediate the effects of AGEs on the human endometrial environment | 37 |
| 1.10.2.3 Aim 3: Optimisation of human endometrial epithelial organoid culture to validate the effects of AGEs on human endometrial epithelium | 37 |
| 1.10.2.4 Aim 4: Characterization of the proteins of the human adhesome and endometrial epithelial receptome and investigation of the effects of AGEs | 38 |
| 1.11 TRANSLATIONAL IMPACT OF THIS RESEARCH | 38 |
| 1.12 NECESSITY AND SIGNIFICANCE OF THIS STUDY | 38 |
| | |
| CHAPTER 2: OPTIMISATION OF MATERIALS AND METHODS | 41 |
| | |
| ETHICAL APPROVALS | 41 |
| 2.1 DATA REPRESENTATION AND STATISTICAL ANALYSIS | 41 |
| 2.2 IN VITRO GENERATION OF AGES | 41 |
| 2.3 OBESITY ASSOCIATED AGES AND THE PREIMPLANTATION EMBRYO | 42 |
| 2.3.1 STANDARD PROTOCOLS | 43 |
| 2.3.1.1 Embryo generation | 43 |
| 2.3.1.2 Cell lineage allocation | 43 |
| 2.3.1.3 Immunolocalisation of RAGE and TLR4 | 44 |
| 2.3.2 OPTIMISATION OF PROTOCOLS | 45 |
| 2.3.2.1 Dose response of AGEs | 45 |
| 2.3.2.2 Embryo developmental morphokinetics | 46 |
| 2.3.2.3 Blastocyst outgrowth | 49 |

| | | |
|------------|--|-----------|
| 2.3.2.4 | Optimisation of therapeutic intervention | 50 |
| 2.3.2.4.1 | FPS-ZM1: RAGE antagonist | 50 |
| 2.3.2.4.2 | Metformin | 51 |
| 2.3.2.4.3 | Antioxidants | 52 |
| 2.4 | AGES AND THE UTERINE ENVIRONMENT | 53 |
| 2.4.1 | STANDARD PROTOCOLS | 53 |
| 2.4.1.1 | Generic cell culture | 53 |
| 2.4.1.1.1 | Cell lines | 53 |
| 2.4.1.1.2 | Trophectoderm cell culture | 54 |
| 2.4.1.1.3 | Cryopreservation | 54 |
| 2.4.1.2 | Isolation and culture of primary human endometrial epithelial and stromal cells | 54 |
| 2.4.1.3 | Decidualisation of primary human endometrial stromal cells | 54 |
| 2.4.1.4 | Real Time Cell Analysis (xCelligence) | 55 |
| 2.4.1.4.1 | Adhesion and proliferation | 55 |
| 2.4.1.4.2 | Invasion | 55 |
| 2.4.1.5 | Western Immunoblotting | 56 |
| 2.4.2 | OPTIMISATION OF PROTOCOLS | 57 |
| 2.4.2.1 | Measurement of reactive oxygen species | 57 |
| 2.4.2.2 | Optimisation of therapeutic intervention for endometrial cells | 59 |
| 2.4.2.2.1 | Viability of cells in the presence of therapeutics | 60 |
| 2.4.2.2.2 | Optimising the dose of selected therapeutics | 61 |
| 2.5 | HUMAN ENDOMETRIAL EPITHELIAL ORGANIDS AS A PRIMARY MODEL OF THE HUMAN ENDOMETRIUM | 64 |
| 2.5.1 | STANDARD PROTOCOLS | 64 |
| 2.5.1.1 | Immunohistochemistry | 64 |
| 2.5.1.2 | Multiplex analysis of chemokine and cytokine secretion | 64 |
| 2.5.2 | ESTABLISHMENT OF ORGANOID CULTURE | 65 |
| 2.5.2.1 | Histological examination of human endometrial epithelial organoids | 66 |
| 2.5.2.2 | Characterisation of secretions | 67 |
| 2.5.2.3 | Immunohistochemical staining | 69 |
| 2.5.2.3.1 | A note on the immunolocalisation of cytokeratin | 69 |
| 2.6 | THE HUMAN ADHESOME AND RECEPTOME | 71 |
| 2.6.1 | STANDARD METHODOLOGIES | 71 |
| 2.6.1.1 | Spheroid adhesion assay | 71 |
| 2.6.1.2 | siRNA knockdown | 71 |
| 2.6.1.3 | Transepithelial resistance | 72 |
| 2.6.1.4 | Validation of siRNA by quantitative PCR | 72 |
| 2.6.1.4.1 | RNA extraction | 72 |
| 2.6.1.4.2 | cDNA synthesis | 72 |
| 2.6.1.4.3 | PCR | 73 |
| 2.6.2 | OPTIMISATION OF PROTOCOLS | 73 |
| 2.6.2.1 | Generation of spheroid-epithelium interfaces | 73 |
| 2.6.2.2 | Immunolocalisation of receptome and adhesome proteins | 75 |

CHAPTER 3: THE EFFECT OF OBESITY ASSOCIATED ADVANCED GLYCATION ENDPRODUCTS ON PREIMPLANTATION EMBRYO DEVELOPMENT **80**

3.1 CHAPTER SUMMARY **80**

| | |
|------------------------|-----------|
| 3.2. MANUSCRIPT | 81 |
|------------------------|-----------|

CHAPTER 4: NORMALISING THE FUNCTIONS OF ENDOMETRIAL CELLS EXPOSED TO OBESITY ASSOCIATED AGES **93**

| | |
|---|------------|
| 4.1 INTRODUCTION | 93 |
| 4.2 METHODOLOGY | 94 |
| 4.2.1 DONOR DEMOGRAPHICS FOR HUMAN ENDOMETRIAL STROMAL CELL EXPERIMENTATION | 94 |
| 4.2.2 THERAPEUTIC INTERVENTION | 95 |
| 4.2.3 WESTERN IMMUNOBLOTTING | 95 |
| 4.3 RESULTS | 96 |
| 4.3.1 AGE RECEPTORS ARE AFFECTED BY OBESITY ASSOCIATED AGES | 96 |
| 4.3.2 THE EFFECTS OF AGES ON ENDOMETRIAL EPITHELIAL CELL PROLIFERATION ARE PARTIALLY NORMALISED BY ANTIOXIDANTS | 97 |
| 4.3.3 ASSESSMENT OF ENDOPLASMIC RETICULUM STRESS | 102 |
| 4.3.4 ENDOMETRIAL STROMAL CELL DECIDUALISATION | 103 |
| 4.3.5 IMPLANTATION COMPETENCE: INVASION OF TROPHOBLAST CELLS | 105 |
| 4.4 DISCUSSION AND CONCLUSIONS | 107 |
| 4.4.1 RAGE ANTAGONISM WAS INSUFFICIENT TO IMPROVE ENDOMETRIAL CELL OUTCOMES | 107 |
| 4.4.2 ANTIOXIDANTS IMPROVED ECC-1 CELL FUNCTION IN THE PRESENCE OF OBESE AGES | 108 |
| 4.4.3 MECHANISMS UNDERPINNING THE EPITHELIAL RESPONSE TO AGES | 108 |
| 4.4.4 THE ORGANOID PHENOMENON: RESTRUCTURE OF MY EXPERIMENTAL PARADIGM | 109 |
| 4.5 “TAKE HOME” MESSAGE | 109 |

CHAPTER 5: USE OF HUMAN ENDOMETRIAL EPITHELIAL ORGANOID CULTURE TO INVESTIGATE THE EFFECTS OF AGES ON THE HUMAN ENDOMETRIAL EPITHELIUM **111**

| | |
|--|------------|
| 5.1 INTRODUCTION | 111 |
| 5.2 METHODS | 113 |
| 5.2.1 DONOR DEMOGRAPHICS | 113 |
| 5.2.2 IMMUNOHISTOCHEMISTRY | 113 |
| 5.2.3 WESTERN IMMUNOBLOTTING | 113 |
| 5.2.4 REAL TIME CELL ANALYSIS (XCELLIGENCE) | 113 |
| 5.2.5 MULTIPLEX ANALYSIS OF ORGANOID SECRETIONS (LUMINEX) | 114 |
| 5.3 RESULTS | 114 |
| 5.3.1 HĒEO MAINTAIN MORPHOLOGY AND SECRETORY CHARACTERISTICS OF DONOR ENDOMETRIUM | 114 |
| 5.3.2 HĒEO MAINTAIN ENDOMETRIAL EPITHELIAL CELL CHARACTERISTICS | 115 |
| 5.3.2.1 hĒEO express hormone receptors characteristic of the human endometrium | 116 |
| 5.3.3 HĒEO MAINTAIN APPROPRIATE MECHANISMS BY WHICH TO RESPOND TO AGES AND HAVE LIMITED PRIOR EXPOSURE TO ENDOMETRIAL AGES | 118 |
| 5.3.4 EPITHELIAL CELLS DERIVED FROM HĒEO HAVE A DISTINCT KINETIC PROFILE COMPARED TO COMMONLY USED CANCER CELL LINES | 120 |
| 5.3.5 OBESITY ASSOCIATED AGES DO NOT AFFECT RECEPTOR EXPRESSION | 122 |
| 5.3.6 OBESITY ASSOCIATED AGES IMPACT ORGANOID FUNCTIONS | 122 |
| 5.3.6.1 Gross organoid morphology is not impacted by AGES | 122 |
| 5.3.6.2 AGES equimolar with the obese uterine fluid impact the proliferation of organoid derived epithelial cells | 123 |

| | |
|--|------------|
| 5.3.6.3 Obesity associated AGEs affect hEEO secretion of chemokines and cytokines | 126 |
| 5.4 DISCUSSION AND CONCLUSIONS | 129 |
| 5.4.1 ORGANOID CULTURE: THE FUTURE OF CELL LINE RESEARCH? | 129 |
| 5.4.2 AGEs INFLUENCE FUNCTION BUT NOT MORPHOLOGY | 130 |
| 5.4.3 POTENTIAL MEDIATORS OF THE DIFFERENTIAL RESPONSE TO AGEs IN PRIMARY ENDOMETRIAL EPITHELIAL CELLS | 131 |
| 5.4.4 OBESITY ASSOCIATED AGEs MAY LEAD TO A PRO-INFLAMMATORY ENVIRONMENT ADVERSE TO ESTABLISHMENT OF A HEALTHY PREGNANCY | 133 |
| 5.4.4.1 Potential fertility limiting effects of AGEs induced inflammation | 135 |
| 5.4.5 THERAPEUTIC POTENTIAL AND FUTURE DIRECTIONS | 136 |
| 5.5 “TAKE HOME” MESSAGE | 137 |

CHAPTER 6: VALIDATION AND INTERROGATION OF NOVEL PROTEIN BIOMARKERS OF ENDOMETRIAL RECEPTIVITY **139**

| | |
|---|------------|
| 6.1 INTRODUCTION | 139 |
| 6.2 MATERIALS AND METHODS | 141 |
| 6.2.1 DONOR DEMOGRAPHICS | 141 |
| 6.2.2 DIGITAL QUANTIFICATION OF IMMUNOHISTOCHEMISTRY | 142 |
| 6.2.3 qPCR ASSESSMENT OF siRNA KNOCKDOWN AND HORMONAL REGULATION OF RECEPTOME AND ADHESOME GENES IN ECC-1 | 142 |
| 6.2.4 TRANSEPITHELIAL RESISTANCE | 143 |
| 6.2.5 DATA MINING | 143 |
| 6.3 RESULTS | 143 |
| 6.3.1 INDEPENDENT INTERROGATION OF RECEPTOME-SPECIFIC PROTEINS | 143 |
| 6.3.1.1 Positive Co-factor 4 | 143 |
| 6.3.1.2 Stathmin1 | 146 |
| 6.3.1.3 Cytidine deaminase | 148 |
| 6.3.2 INDEPENDENT INTERROGATION PROTEINS COMMON TO THE RECEPTOME AND ADHESOME | 149 |
| 6.3.2.1 Kynureninase | 149 |
| 6.3.2.2 Legumain | 152 |
| 6.3.2.3 Stem-Loop-Interacting RNA-binding protein | 155 |
| 6.3.3. INDEPENDENT INTERROGATION OF ADHESOME-SPECIFIC PROTEINS | 158 |
| 6.3.4 HORMONAL REGULATION OF RECEPTOME AND ADHESOME PROTEINS IN ECC-1 CELLS | 162 |
| 6.3.5 RECEPTOME AND ADHESOME PROTEINS IN HUMAN ENDOMETRIAL EPITHELIAL ORGANOIDs | 163 |
| 6.4 DISCUSSION AND CONCLUSIONS | 167 |
| 6.4.1 HOW PHYSIOLOGICAL IS THE SPHEROID ADHESION MODEL? | 173 |
| 6.4.2 TRANSLATIONAL IMPACT AND FUTURE DIRECTIONS | 175 |
| 6.5 “TAKE HOME” MESSAGE | 176 |

CHAPTER 7: GENERAL DISCUSSION **178**

| | |
|---|------------|
| 7.1 MAJOR FINDINGS OF THIS THESIS | 178 |
| 7.2 CLINICAL IMPLICATIONS OF THIS RESEARCH | 181 |
| 7.2.2 TO WHOM DOES THIS RESEARCH APPLY? | 181 |
| 7.2.1 WHAT ARE THE CLINICAL IMPLICATIONS OF THIS WORK? | 181 |
| 7.2.3 APPLICATION OF TARGETED AGEs REDUCTION STRATEGIES | 182 |

| | |
|--|------------|
| 7.3 IDENTIFYING THE PRIORITY FOR TARGETED AGE_s REDUCTION: THE EMBRYO OR THE ENDOMETRIUM? | 183 |
| 7.4 STRENGTHS AND LIMITATIONS OF THIS RESEARCH | 184 |
| 7.4.1 PHYSIOLOGICAL RELEVANCE OF THE MODELS USED | 185 |
| 7.5 FUTURE DIRECTIONS | 186 |
| 7.5.1 PERSONALISED MEDICINE: MODIFICATION OF ENDOMETRIAL RECEPTIVITY | 186 |
| 7.5.2 CONTINUED DEVELOPMENT OF MODELS | 186 |
| 7.5.3 EXAMINATION OF DOWNSTREAM CONSEQUENCES OF ELEVATED AGE _s IN THE MICROENVIRONMENT OF IMPLANTATION AND PLACENTATION | 186 |
| 7.5.4 AGE _s AND MALE FERTILITY | 186 |
| 7.6 CONCLUDING REMARKS | 187 |
| | |
| REFERENCES | 189 |
| <hr/> | |
| APPENDIX 1: WIDELY USED SOLUTIONS | 225 |
| | |
| A1.1: TRIS BUFFERED SALINE (10X) | 225 |
| A1.2: PHOSPHATE BUFFERED SALINE (10X) | 225 |
| A1.3: SODIUM CITRATE ANTIGEN RETRIEVAL SOLUTION (10X) | 225 |
| A1.4 SDS BUFFER FOR GEL ELECTROPHORESIS (4X) | 225 |
| | |
| APPENDIX 2: ENDOMETRIAL 3D CO-GEL | 227 |
| <hr/> | |
| APPENDIX 3: THE HUMAN ADHESOME AND RECEPTOME | 228 |
| | |
| A3.1 STRING ANALYSIS OF PROTEIN INTERACTIONS | 228 |
| A3.1.1 STRING ANALYSIS: TOTAL UPREGULATED PROTEINS OF THE RECEPTOME | 228 |
| A3.1.2 STRING ANALYSIS: TOTAL DOWNREGULATED PROTEINS OF THE RECEPTOME | 230 |
| A3.1.3 STRING ANALYSIS: TOTAL PROTEINS UPREGULATED IN THE ADHESOME | 231 |
| A3.1.4 STRING ANALYSIS: TOTAL PROTEINS DOWNREGULATED IN THE ADHESOME | 233 |
| A3.2 UNIQUE PROTEINS OF THE RECEPTOME | 234 |
| A3.2.1 PROTEINS UNIQUELY UPREGULATED IN THE EPITHELIAL RECEPTOME | 234 |
| A3.2.2 PROTEINS UNIQUELY DOWNREGULATED IN THE RECEPTOME | 236 |
| A3.3 UNIQUE PROTEINS OF THE ADHESOME | 237 |
| A3.3.1 UPREGULATED PROTEINS OF THE ADHESOME | 237 |
| A3.3.2 PROTEINS DOWNREGULATED IN THE ADHESOME | 239 |
| A3.4 PROTEINS COMMON TO THE RECEPTOME AND ADHESOME | 241 |
| A3.5 PROTEINS DIFFERENTIALLY REGULATED IN THE RECEPTOME AND ADHESOME | 243 |
| | |
| APPENDIX 4: PUBLICATION OF THE HUMAN RECEPTOME AND ADHESOME | 246 |
| <hr/> | |

Declaration

This thesis is an original work of my research and contains no material which has been accepted for the award of any other degree or diploma at any university or equivalent institution and that, to the best of my knowledge and belief, this thesis contains no material previously published or written by another person, except where due reference is made in the text of the thesis.

Signature: J. Hutchison

Print Name: Jennifer Claire Hutchison

Date: 18th March 2021

Thesis including published works declaration

I hereby declare that this thesis contains no material which has been accepted for the award of any other degree or diploma at any university or equivalent institution and that, to the best of my knowledge and belief, this thesis contains no material previously published or written by another person, except where due reference is made in the text of the thesis.

This thesis includes **2** original papers published in peer reviewed journals, and **0** submitted publications. The core theme of the thesis explores the impact of Advanced Glycation Endproducts on female fertility. The ideas, development and writing up of all the papers in the thesis were the principal responsibility of myself, the student, working within the Centre for Reproductive Health, Hudson Institute of Medical Research, and the department of Molecular and Translational Science, Faculty of Medicine, Nursing and Health Sciences, under the supervision of Professor Lois Salamonsen, Professor Guiying Nie, Professor David Gardner, and Dr Jemma Evans.

The inclusion of co-authors reflects the fact that the work came from active collaboration between researchers and acknowledges input into team-based research.

In the case of chapter 3, and appendix 4 my contribution to the work involved the following:

| Chapter # | Publication Title | Status (<i>published, in press, accepted or returned for revision</i>) | Nature and % of student contribution | Co-author name(s) Nature and % of Co-author's contribution* | Co-author(s), Monash student Y/N* |
|-----------|--|---|---|--|---|
| 3 | Preimplantation embryo development is compromised by concentrations of Advanced Glycation Endproducts found within the obese uterine environment | Published | 70%: Performed experiments, data collection and analysis, preparation and editing of manuscript, manuscript revisions | 1: Thi Thanhmai Truong (17.5%) performed embryo culture, assisted with experimental methodologies and input into manuscript 2: David Gardner (5%) assisted with experimental design and input into manuscript 3: Lois Salamonsen (2.5%) input into manuscript | No |

| | | | | | |
|-------------------|--|-----------|--|--|----|
| | | | | 4: Jemma Evans (5%) involved in project conception, experimental design, input into manuscript | |
| Appendix 4 | Proteomic insights into endometrial receptivity and embryo-endometrial epithelium interaction for implantation reveal critical determinants of fertility | Published | 15%: performed validation experiments (Figure 6), assisted with gene ontology data analyses | 1: Jemma Evans (40%): conception of project and experimental design, performed experiments, data analysis, preparation of manuscript. 2: Lois Salamonsen (5%) input into manuscript 3: David Greening (40%) performed proteomic experiments, data analysis, input into manuscript | No |

**If no co-authors, leave fields blank*

I have not renumbered sections of submitted or published papers in order to generate a consistent presentation within the thesis.

Student signature: J. Hutchison **Date:** 18th March 2021

The undersigned hereby certify that the above declaration correctly reflects the nature and extent of the student's and co-authors' contributions to this work. In instances where I am not the responsible author, I have consulted with the responsible author to agree on the respective contributions of the authors.

Main Supervisor signature: L. Salamonsen **Date:** 18th March 2021

Other research outputs:

Azlan, A., Salamonsen, L A., **Hutchison, J. C.**, and Evans, J (2020). Endometrial inflammasome activation accompanies menstruation and has implications for systemic inflammatory events of the menstrual cycle. *Human Reproduction*, 35 (6), 1363-1376.

I contributed immunofluorescent localisation of inflammasome proteins in the human endometrium (Figures 2F and 3F), technical assistance with primary cell culture techniques and protocols, and assistance with Western immunoblotting. I also contributed to editing the manuscript.

Salamonsen, L. A., **Hutchison J C.**, Gargett, C. (Submitted). Cyclical endometrial repair and regeneration in women: mechanisms, insights, and opportunities. *Development*.

Professor Salamonsen was invited to write this review for the journal *Development*. I contributed to the section on endometrial organoids and provided an original figure from work done during the course of this thesis. Some of my intellectual contributions during discussions with Professor Salamonsen are also included as insights and opportunities.

Acknowledgements

This research was supported by an Australian Government Research Training Program (RTP) Scholarship.

This thesis is only possible due to the support, encouragement, and help of a large number of people.

To my network of supervisors: you have provided me with incredible opportunities, insight, and advice over the last few years. To say I am extremely thankful for this would be an understatement. I hope that I have done justice to the opportunity you have given me. Jemma, I would not have been able to do this project without you: you took a chance on me and opened my eyes to the world of research within the endometrium and your crazy ideas inspire me to be more creative with the way I view and approach research.

Lois. There are no words to describe the gratitude I feel when I think about the support and mentoring you have given me. You truly stepped up to the mark when I went through difficult times and your patience and guidance made this monumental task possible.

David Gardner, Mr IVF. What a wonderful mentor you have been. You and your lab were so welcoming and accommodating when I started my work with you.

Guiying. Thank you for your kindness, support, and willingness to talk ideas through with me, and also the support from your entire team.

Mai and Shanti, I honestly don't know where I would be without your support and technical help. You are both so patient and so generous with your time and knowledge. Working with you was an absolute pleasure.

To the other members of the Endometrial Remodelling lab past and present, and the wider Centre for Reproductive Health, it has been a privilege working with you. To the students who came through, Anika, Manizha, Jasmine, Emily, and Aida, thank you for letting me part of your experience. Harriet and Nick, I owe you a large thanks for showing me the ropes and giving me a kick start in the lab.

I have said on multiple occasions that my acknowledgements would be a love letter to histology and the people therein. To all the wonderful staff at the Monash Histology Platform, I cannot thank you enough for the encouragement and advice you have given me. I truly loved spending time at histology: you gave me a safe space to be myself, explore ideas, and let me develop my technical skills. Some of my fondest memories from my PhD will definitely be from the time spent in the histology department.

There are friends who I have made along the way, and friends I knew before who have all played a significant role in making my PhD experience what it was. I apologise if I have missed naming you in person, but I appreciate everything you have done for me. Sarah, Rama, and Sam: you are friends that I have made for life. You have made such an impact on me professionally and personally, and you brought such joy to my time at the Hudson Institute. Elly, Rheannon, Sigrid and Ruby: the aggressive support and motivation squad. May I one day be able to repay the favour! Mary, from desk-mate to friend, you have provided support and advice that I truly appreciate. Kathryn, thank you for being second set of eyes, an independent advisor, and patient friend. I really enjoyed working with you, and thank you for encouraging me to take days off when I needed them. Mike and Kirsty, you provided me with so much love and conversations from across the other side of the world, and supported me when I needed it most, for which I am truly grateful.

Two foundations of any research are samples and finance. This work would not have been possible without the generous donation of endometrial tissue, and the collection of mouse embryos. It has been an honour to work with these samples. I would like to thank Sr Judi Hocking, for consenting the patients and collecting the samples—it has been a pleasure to work with you. I also acknowledge the financial support of the Research Training Program stipend that I was fortunate enough to be awarded, the Hudson Institute Centre for Reproductive Health travel award, and Ferring Pharmaceuticals sponsorship of the FSA-ESHRE exchange award. This support made many opportunities possible.

At this point, three acknowledgements remain, these being the three strongest pillars of support outside of my academic group anyone could hope for.

Xander. Having known you for several years, you have always been a strong member of my support network, listening when I needed to vent, providing advice when I needed help, challenging my opinions, and making me smile on a regular basis. To you and David, I promise to help out more with the housework now this thesis is over!

My family who are in New Zealand have been incredibly supportive and encouraging throughout my life. When we were not able to physically see each other due to the health pandemic of COVID19, you made sure that I was not without support or conversation and did not feel isolated. I cannot thank you enough for the laughs, the tears, and the socially distanced wine.

Finally, to my fiancé, David. I cannot imagine having done this without you being by my side. The love and support you have given over all these years are truly indescribable. You are the kindest,

most selfless, and loving person I know. In addition to helping me generate figures to express my ideas in a better form than my scribble on the back of napkins, this PhD was made possible by the foundation of support you provided. I cannot thank you enough.

Much love to each and every one of you,

Jen xx

P.S.: It's been amazing.

List of Abbreviations

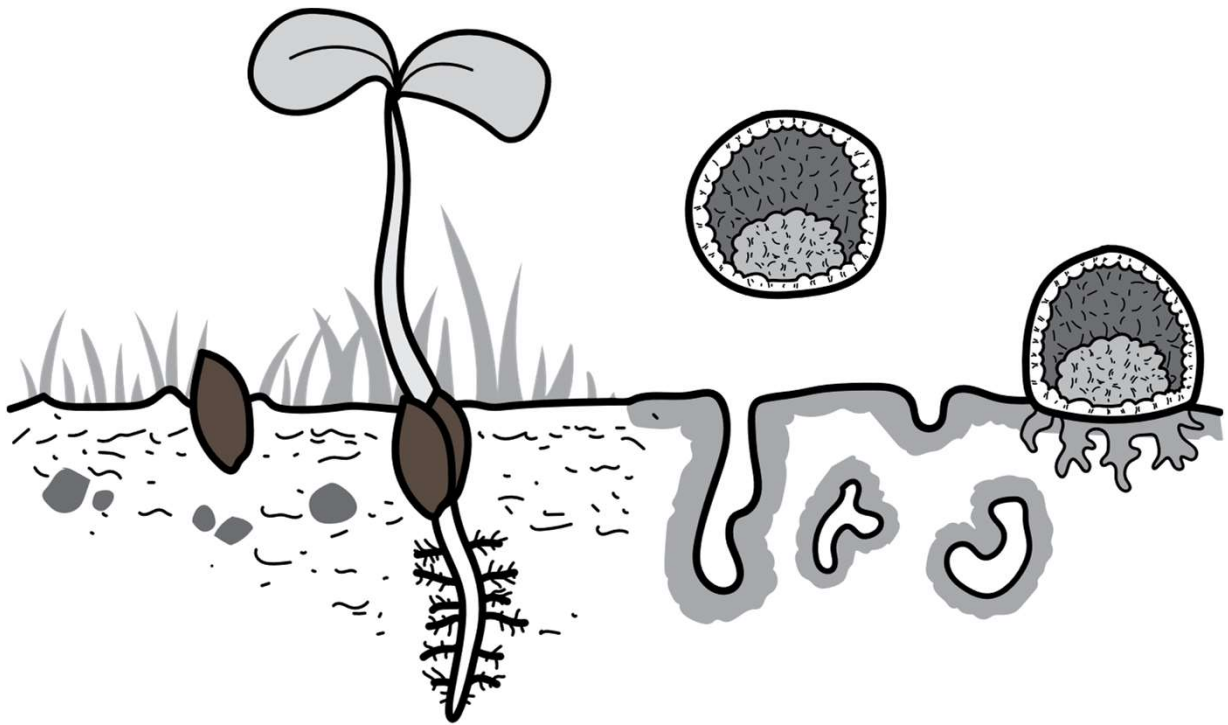
| | |
|------------------|--|
| °C | Degrees Celsius |
| AB | Alcian Blue |
| Ab/Am | Antibiotic-Antimycotic |
| aDMEM | advanced DMEM |
| AGEs | Advanced Glycation End Products |
| ART | Assisted Reproductive Technologies |
| BMI | Body Mass Index |
| CDA | Cytidine Deaminase |
| cDNA | Complimentary deoxyribonucleic acid |
| CHOP | C/EBP Homologous Protein |
| CML | N-ε-Carboxymethyl lysine |
| csFCS | Charcoal stripped fetal calf serum |
| CXCL-6/16 | CXC motif chemokine ligand 6/16 |
| DCF-DA | 2'-7'-Dichlorofluorescin diacetate |
| DMEM | Dulbecco's Modified Eagle Medium |
| DNA | Deoxyribonucleic acid |
| E | 17β-Estradiol |
| EDTA | Ethylenediamine Tetraacetic Acid |
| ELISA | Enzyme Linked ImmunoSorbent Assay |
| ERA | Endometrial Receptivity Assay |
| ERα | Estrrogen receptor alpha |
| ExM | Expansion Media |
| FCS | Fetal Calf Serum |
| FPKM | Fragments per kilobase transcript per million mapped reads |
| FSH | Follicle Stimulating Hormone |
| GCFS | Granulocyte colony stimulating factor |
| GE | Glandular Epithelium |
| h | hours |
| H&E | Haematoxylin and Eosin |
| HEECs | Human Endometrial Epithelial Cells |
| hEEO | Human Endometrial Epithelial Organoid |
| HRP | Horse Radish Peroxide |
| ICM | Inner Cell Mass |
| ICSI | Intra-Cytoplasmic Sperm Injection |
| IL-x | Interleukin x |
| IU | International units |
| IVF | <i>In Vitro</i> Fertilisation |
| KRT7 | Cytokeratin 7 |
| KYNU | Kynureninase |
| L | Litre |
| LE | Luminal Epithelium |
| LFQ | Label Free Quantitation |
| LGMN | Legumain |

| | |
|------------------|--|
| LH | Leuteinising Hormone |
| LH | Luteinising Hormone |
| LoD | Limit of detection |
| M | Molar |
| MAGT1 | Magnesium Transporter 1 |
| min | minutes |
| mL | millilitre |
| mM | millimolar |
| mol | moles |
| MPA | Medroxyprogesterone acetate |
| NAC | N-Acetyl-L-Cysteine |
| NBF | Neutral Buffered Formalin |
| NFκB | Nuclear Factor Kappa-light-chain-enhancer of activated B cells |
| ng | nanogram |
| nM | nanomolar |
| nm | nanometer |
| PAS/AB | Periodic Acid Schiff / Alcian Blue |
| PBS | Phosphate Buffered Saline |
| PC4 | Positive Cofactor 4 |
| PCNA | Proliferating Cell Nuclear Antigen |
| PFA | Paraformaldehyde |
| pM | picomolar |
| PR | Progesterone Receptor |
| PRL | Prolactin |
| PTGS2 | Prostaglandin G/H Synthase 2 |
| RAGE | Receptor for Advanced Glycation End Products |
| RCF | Relative centrifugal force |
| RIPA | Radioimmunoprecipitation assay |
| RNA | Ribonucleic acid |
| ROS | Reactive Oxygen Species |
| RPL | Recurrent Pregnancy Loss |
| scRNA-seq | Single cell RNA sequencing |
| SEM | standard error of the mean |
| SERPINE1 | Serpin family E member 1 (also known as Plasminogen activator inhibitor 1) |
| siRNA | Small interfering ribonucleic acid |
| SLIRP | Stem-Loop Interacting RNA binding Protein |
| STMN1 | Stathmin 1 |
| TBS | Tris Buffered Saline |
| TBS-T | Tris Buffered Saline - Tween 20 |
| TE | Trophectoderm |
| TER | Transepithelial resistance |
| TLR4 | Toll Like Receptor 4 |
| TNFα | Tumour necrosis factor alpha |
| uNK | Uterine Natural Killer cell |
| VIPER | Viral Inhibitory Peptide for TLR4 |

| | |
|------------|-----------------------------|
| WHO | World Health Organisation |
| α- | Anti (relating to antibody) |
| μg | microgram |
| μL | microlitre |
| μm | micrometer |
| μM | micromolar |

Chapter 1:

Literature review
&
Aims and hypotheses



Chapter 1: Introduction

1.1 The clinical problem of obesity-related infertility

Infertility can be defined as the inability of a couple to conceive within twelve months of unprotected intercourse and affects one in six couples worldwide, disproportionately obese women. With the average age of first-time mothers increasing (Mills et al., 2011), and a general decline in fertility (Lutz, 2006), much research has been done to optimise ovulation procedures and to produce high quality, viable embryos. Even with advances in assisted reproductive technologies (ART), many embryos still fail to implant and the live birth success rate of ART has remained at approximately 25% (Centres for Disease Control and Prevention et al., 2017). In each normal monthly cycle for a couple with no known fertility issues, the success of conception is between 15% and 20%, with most couples able to conceive within 2 years (Taylor, 2003). Chambers *et al.*, (2009) reviewed the cost and success rate across multiple countries and estimated the cost per live birth following ART in Australia to be approximately \$34,000 (in 2006). With the considerable financial, physical, and psychological implications of repeated ART attempts, it is important to maximise the success rate of such technologies (Boivin and Takefman, 1996; Domar et al., 1993; Rajkhowa et al., 2006), or possibly to improve the chance for natural conception. Establishment of pregnancy requires an appropriately prepared endometrium (the lining of the uterus) into which a hatched and appropriately developed embryo must implant before the placenta is formed. The endometrium plays an essential role in establishing pregnancy, as it must be receptive to an implanting embryo for adhesion and implantation to occur. Considerably less research has focussed on the receptivity of the endometrium than on the embryo, an equal partner in ART, and it is in this direction we turn to further understand adhesion and implantation of embryos, and to find ways to improve the success rate of ART, particularly in light of rising levels of obesity, which are detrimental to fertility.

1.2 The female reproductive tract

The female reproductive tract consists of the vagina, the uterus, Fallopian tubes, and ovaries. Within the ovaries, oocytes mature and ovulate (usually one per cycle in women) in concert with the menstrual cycle, and pass into the Fallopian tubes via the fimbriae. The vagina is the entry point for sperm, which travel upwards through the mucus-secreting cervix into the uterus and then to the Fallopian tubes where fertilisation of the ovulated oocyte occurs. The dynamic lining of the uterus, the endometrium, undergoes cyclical remodelling throughout the menstrual cycle, and is the site of embryo implantation following successful fertilisation.

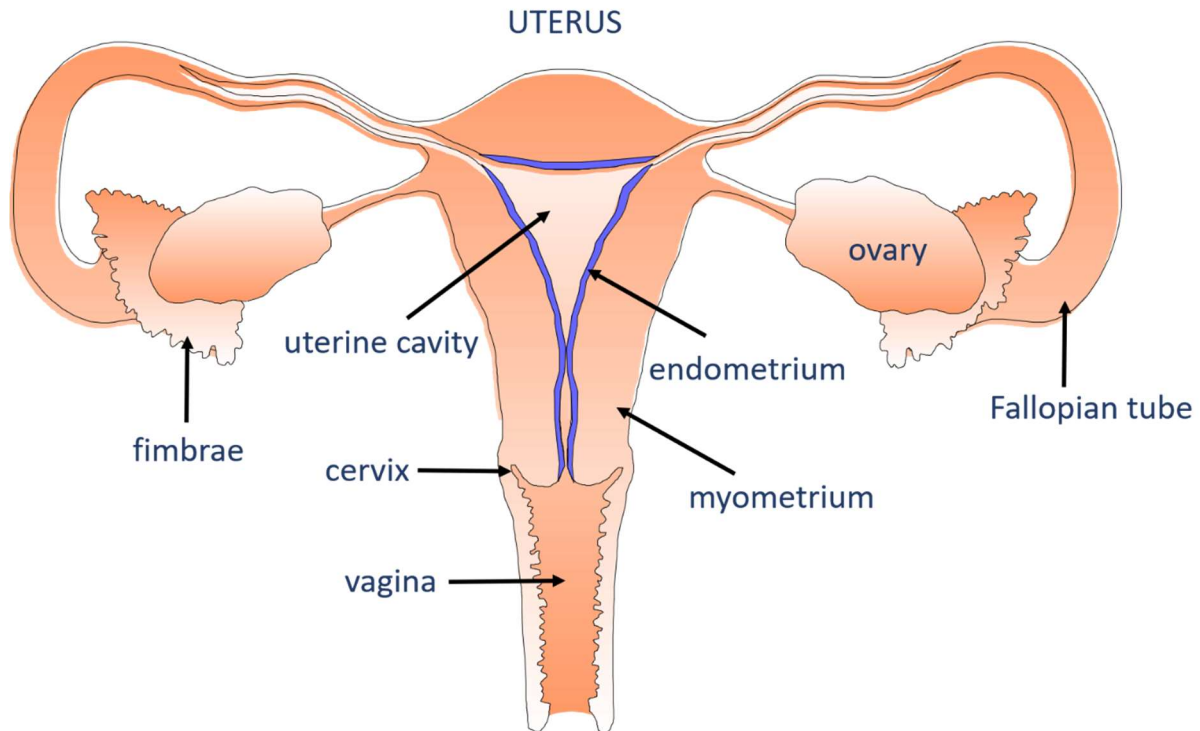


Figure 1.1: Anatomy of the female reproductive tract. The female reproductive tract consists of the ovaries, Fallopian tubes, uterus, cervix, and vagina. The endometrium (purple) is the innermost layer of the uterus and is the site of implantation. ©Lois Salamonsen, used with permission.

1.2.1 The ovaries

The ovaries contain the maturing oocytes, housed in individual follicles. Follicles mature at different times and so at any given time the ovary consists of follicles at a variety of developmental stages (Peters et al., 1975). Follicles mature in waves, with each cohort selected by a small rise in basal levels of follicle stimulating hormone (FSH). They then progress from the primordial state (an oocyte surrounded by a single layer of granulosa cells) through primary and secondary phases, marked by granulosa cell proliferation and subsequent formation of a fluid-filled antrum (Emori and Sugiura, 2014; McGee and Hsueh, 2000). The dominant follicle, which will eventually release its oocyte, secretes 17β -estradiol which suppresses further development of other follicles and causes atresia of the rest of the developing cohort (Fortune, 1994; McGee and Hsueh, 2000). Ovulation from the dominant follicle occurs in response to the surge of luteinising hormone (LH) at the end of the proliferative phase of the menstrual cycle. The follicle from which the oocyte was expelled becomes the corpus luteum, secreting progesterone and suppressing FSH. It regresses by a process known as luteolysis in the absence of pregnancy, and the cycle begins again. If a pregnancy is established, then an anti-luteolytic signal from the implanting embryo (human chorionic gonadotrophin in women) maintains the corpus luteum until the placenta forms sufficiently to maintain the pregnancy.

1.2.2 The uterus

The uterus is a major female reproductive organ, being the site of both implantation and gestation. The development of the uterus starts from the embryonic progenitor tissue, the paramesonephric or Mullerian ducts. For a review of uterine development, see Gray et al. (2001). These ducts develop into the Fallopian tubes, the uterus, and part of the vagina. The uterus is a hollow organ, consisting of three distinct tissue layers: the outer perimetrium or serosa, the muscular myometrium, and the endometrium. The architecture relating to the uterus can be divided into 3 major components: the uterine or Fallopian tubes, the body or corpus of the uterus, and the cervix which links the uterus to the vagina (Figure 1.1).

1.2.2.1 The endometrium

The endometrium is the innermost layer of the uterus and is cyclically remodelled in preparation for pregnancy in the menstrual cycle (Section 1.3). There are two major layers of the endometrium: the basalis and the functionalis. Across the menstrual cycle, these cell types undergo extensive phenotypic and transcriptomic alterations, identified by single cell RNA-sequencing (Giudice, 2020; Wang et al., 2020). During menses the functionalis is completely shed, and regenerates largely from the basalis layer in the next menstrual cycle, undergoing cyclical shedding, repair and regeneration. Cells of the functionalis proliferate and secrete factors into the uterine cavity throughout the menstrual cycle. The functionalis consists of the stroma, comprising fibroblastic cells which late in each cycle undergo a differentiation process known as decidualisation, a variable range and number of immune cells along with cells of the vascular system, and is protected and covered by an outer layer of luminal epithelial cells which are the first point of contact for an approaching embryo. The endometrium and its cycle have recently been comprehensively reviewed (Evans et al., 2016).

1.2.2.1.1 Stromal fibroblasts

Stromal cells (fibroblasts) of the endometrium form the bulk of the functionalis. Some of the stromal cells undergo differentiation known as decidualisation, late in the menstrual cycle in women and subsequently form the maternal component of the placenta. They are highly responsive to hormones and in response to a reduction in progesterone, secrete inflammatory mediators into the endometrial tissue (Evans and Salamonsen, 2014). Decidualisation in non-menstruating species can be induced as a response to damage sustained by the endometrial lining or contact with an embryo. In contrast, menstruating species exhibit spontaneous decidualisation as a response to ovarian progesterone during the secretory phase of the cycle, and this is not dependent on an embryo (for a review of menstrual evolution and significance, Jarrell (2018)). Implantation of the embryo requires it to traverse initially between the endometrial epithelial cells and then through the developing decidua, in which extensive remodelling of the maternal vasculature subsequently occurs.

1.2.2.1.2 Endometrial Glands and Secretions

Uterine glands are formed by invagination of the luminal epithelium and proliferation through the stroma. In humans this begins soon after birth and is completed by puberty (Gray et al., 2001). The bottom two thirds of the uterine glands are located within the basalis (Padykula et al., 1989) and are a key source of epithelial progenitor cells for re-epithelialisation of the endometrium after menses (Kaitu'u-Lino et al., 2010; Nguyen et al., 2017). Gland knock-out mouse and sheep models have shown that uterine glands are essential for blastocyst survival and implantation (Filant and Spencer, 2013; Gray et al., 2002, 2000) and decidualisation of the surrounding stroma (Filant and Spencer, 2013) as well as endometrial receptivity and regulation of the uterine fluid (Kelleher et al., 2016).

The glandular epithelium provides the bulk of the numerous soluble factors and extracellular vesicles in the uterine cavity which are essential for embryo survival, implantation, and early placentation (Gray et al., 2001; Greening et al., 2016b, 2016a). Mucin secretion is highlighted in Figure 1.2. The embryo completes its final stages of development within the gland-conditioned uterine fluid, which provides a medium for cross-talk between the embryo and endometrium, to orchestrate adhesion and implantation (Section 1.6). Thus, aberrations in this fluid microenvironment may alter both embryo competency and endometrial receptivity.

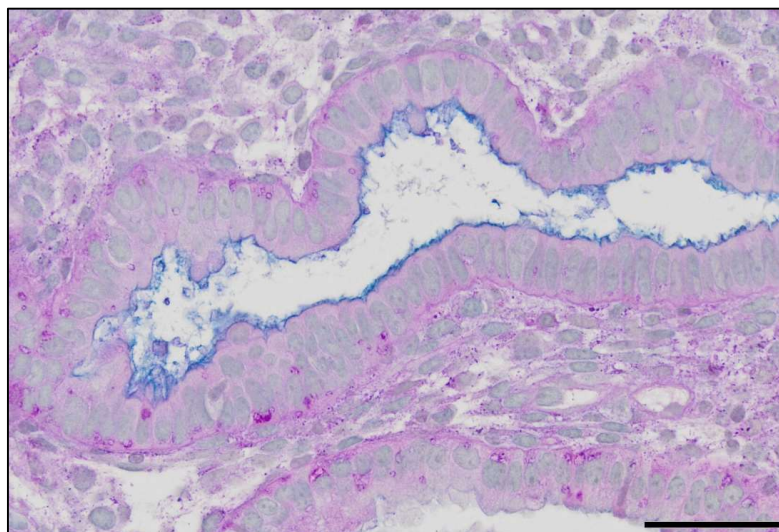


Figure 1.2: Mucin secretion of the mid secretory endometrium. Periodic acid Schiff (pink) and alcian blue (blue) staining identify secretion of acidic and neutral mucins into the lumen of the endometrial glands, which will contribute to the composition of the uterine fluid. Scale bar represents 50 μm .

1.2.2.1.3 Epithelium

The luminal epithelium is formed during reepithelialisation of the endometrium, outgrowing from residual glands after menstruation (Kaitu'u-Lino et al., 2010; Ludwig and Spornitz, 1991). Luminal epithelial cells provide an impermeable layer which covers the stroma and provides a barrier between the stromal cells and the uterine cavity; from this layer, glands provide invaginations into the tissue.

Luminal epithelial cells undergo significant changes throughout the menstrual cycle, particularly changing the composition of their glycocalyx and their polarity to enable penetration by trophoblastic cells at implantation (Aplin and Ruane, 2017; Whitby et al., 2018). They also contribute to the hormonally regulated secreted proteins and vesicles present in the fluid microenvironment of the uterus (Greening et al., 2016b). Since the luminal epithelium faces the uterine cavity, it is the first point of contact for an approaching embryo.

1.3 The menstrual cycle of the endometrium

The uterine environment undergoes significant physical changes in preparation for pregnancy, and is “reset” during menstruation: the shedding of the functionalis layer of the endometrium at the end of a menstrual cycle in which no pregnancy occurs. As reviewed by Emera et al., (2012), spontaneous menstruation is known to occur only in humans, Old World Monkeys, the Elephant Shrew, four species of bat, and has recently been shown to be present in the Spiny Mouse, *Acomys cahirinus* (Bellofiore et al., 2017). Spontaneous menstruation is the result of irreversible decidualisation; other species require the presence of an embryo to induce decidualisation, preparing the endometrium for implantation only once successful fertilisation has occurred.

Endometrial remodelling is orchestrated by the ovarian steroid hormones, 17β -estradiol (estrogen) which rises and falls with follicular development and ovulation (Section 1.2.1), and progesterone released from the corpus luteum following ovulation (Figure 1.3). The physiology of the endometrium throughout the menstrual cycle has been extensively studied and reviewed, classically by Noyes (1950). More recently, single-cell transcriptomics have profiled the cells present within the endometrium across the menstrual cycle and have provided significant detail on temporally regulated gene expression (Giudice, 2020; Wang et al., 2020).

The menstrual cycle is of approximately 28 days duration and can be broken into three discrete phases: menses, the proliferative phase, and the secretory phase. If no pregnancy occurs, the endometrial functionalis is shed at menses and the cycle begins anew.

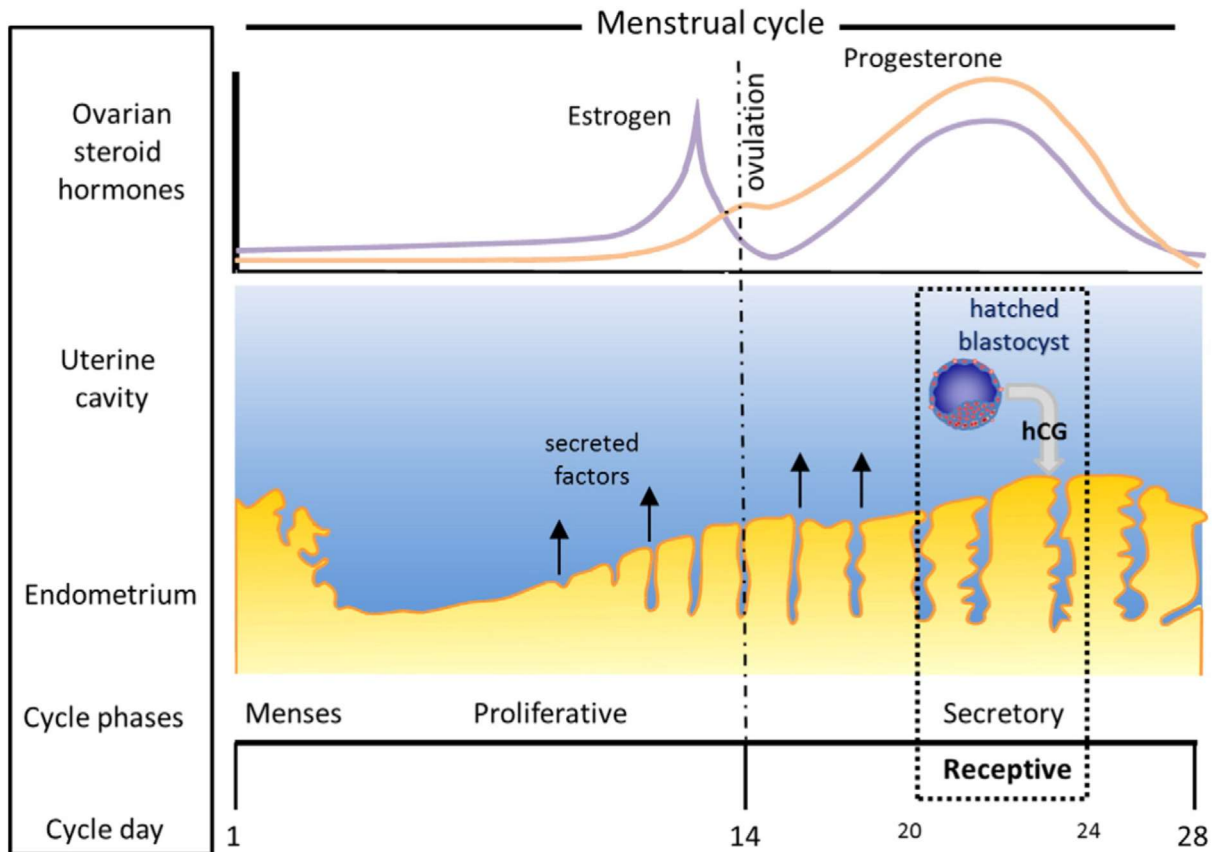


Figure 1.3: Schematic representation of the menstrual cycle. Diagrammatic representation of endometrial remodelling and relative hormone concentrations across the phases of the menstrual cycle normalised to 28 days. Regression of the endometrial functionalis occurs in response to withdrawal of progesterone in a non-conception cycle, the secretion of hCG from an approaching blastocyst maintains the endometrium for implantation. Adapted with permission (Greening et al., 2016b).

1.3.1 Menses

Menses is the process of the shedding of the functionalis at the end of a menstrual cycle in which no embryo successfully implanted into the endometrium. As the corpus luteum begins to degrade, there is a concurrent fall in progesterone levels (Chabbert-Buffet and Bouchard, 2002; Reed and Carr, 2015). This reduced progesterone concentration starts a cascade of events resulting in the piece-meal degradation of the endometrial functionalis (Reed and Carr, 2015).

Re-epithelialisation starts directly after the onset of menstruation, thus in the endometrium tissue breakdown and repair occur simultaneously for the first six days of the cycle (Ludwig and Metzger, 1976; Ludwig and Spornitz, 1991). After the tissue surrounding an endometrial gland has been degraded, the glandular cells proliferate and new luminal epithelial cells grow outwards from the exposed surface of the gland to cover the surrounding tissue (Ludwig and Metzger, 1976; Ludwig and Spornitz, 1991). The basal region of the glandular epithelium is a source of epithelial progenitor cells which reform the glands (Kaitu'u-Lino et al., 2010; Nguyen et al., 2017). Complete re-epithelialisation

must occur before the proliferation of the epithelial and stromal cells can occur in the proliferative phase (Ludwig and Spornitz, 1991).

1.3.2 The proliferative phase

The proliferative phase proceeds under the influence of estrogen, and is approximately 14 days long, the end signalled by ovulation and the corresponding surge in luteinising hormone. Following re-epithelialisation (throughout and following menses), the stromal and glandular cells proliferate (Johannisson et al., 1987; Padykula et al., 1989) to regenerate an endometrial thickness of approximately 6-9 mm required for successful embryo implantation (Hoad et al., 2005; Tomic et al., 2020). During this time, the uterine glands are relatively straight (Figure 1.4), and spiral arterioles begin formation by the elongation of existing vessels (Maas et al., 2001). The post-ovulation rise in progesterone, signals the transition from the proliferative phase to the secretory.

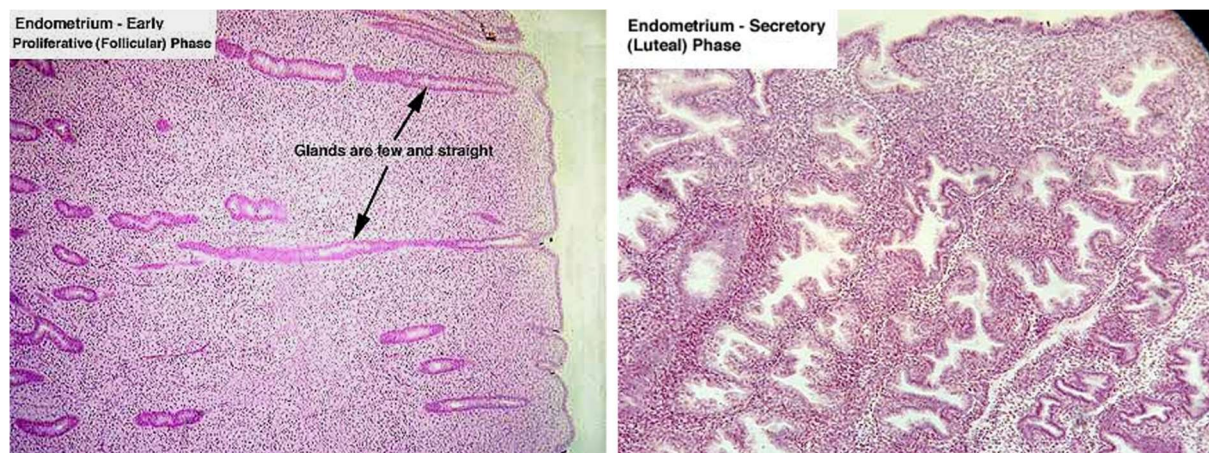


Figure 1.4: The proliferative and secretory phase human endometrium. Left: Proliferative phase endometrium. Glands are few and relatively straight. Stroma maintain a fibroblastic morphology. Right: Secretory phase endometrium. Glands are tortuous and many. Stroma become rounded as they undergo decidualisation. ©Lois Salamonsen, used with permission.

1.3.3 The secretory phase

The secretory phase occurs after ovulation between days 14 and 28 of the menstrual cycle. Under the influence of progesterone, the secretory phase prepares the endometrium for implantation and encompasses the period of endometrial receptivity. Proliferation of the stromal cells is reduced in the early secretory phase, and proliferation of the glandular epithelial cells reduces from just prior to the LH surge to the mid-secretory phase (Johannisson et al., 1987; Padykula et al., 1989), with all of the cell types undergoing differentiative changes. Coiling of the endometrial glands occurs (Figure 1.4) and may be associated with the slight compaction of the endometrium soon after ovulation, as the endometrium thins out by approximately 1 mm (Hoad et al., 2005). Although the glandular epithelial cells are no longer proliferating, the diameter of the glands significantly increases throughout the

secretory phase of the menstrual cycle (Johannisson et al., 1987). The epithelium becomes highly secretory with upregulation of proteins involved in cell adhesion, metabolism, and transcriptional regulation, and downregulation of several members of the integrin family (Greening et al., 2016b). During the early secretory phase, the endometrium is also highly angiogenic as the spiral arterioles elongate and coil (Maas et al., 2001).

1.4 Endometrial receptivity

Endometrial receptivity can be defined as the ability of the endometrium to accept an embryo of the correct developmental stage for adhesion and implantation. During the menstrual cycle, the endometrium becomes receptive to an approaching embryo only for a brief period in the mid-secretory phase (between 6 and 10 days after ovulation). For successful implantation to occur, both the endometrium and the blastocyst must be in synchrony and at an appropriate stage of development and receptivity (Wilcox et al., 1999). This time period is also known as the “window of implantation” (Evans et al., 2016; Lessey, 2011; Salamonsen et al., 2009). At this time in the mid-secretory phase, the endometrium undergoes significant alterations in protein and gene expression and regulation to achieve a state of receptivity (Evans et al., 2016; Greening et al., 2016b; Kukushkina et al., 2017).

The gene expression profile of the “receptive” endometrium has been defined, and developed into an assay known as the endometrial receptivity array (ERA) to investigate the window of implantation in individual women (Díaz-Gimeno et al., 2011). A displaced or disrupted window of implantation, identified by the ERA, identifies some causes of recurrent implantation failure (Sebastian-León et al., 2018), and a need to personalise the timing of blastocyst transfer (Ruiz-Alonso et al., 2013). Current research is identifying the efficacy of clinical use of the ERA to improve implantation success and live birth rates following IVF (Cozzolino et al., 2020; Simón et al., 2020). The proteins involved in endometrial epithelial receptivity and embryo adhesion (Sections 1.4.3 and 1.6.3) are the subject of Chapter 6 of this thesis.

1.4.1 The role of the luminal epithelium

Both the trophoderm of an approaching embryo and the luminal epithelium, the first point of contact for an approaching embryo, have a polarized phenotype. During the proliferative phase, the luminal epithelium maintains high expression of polarity markers, which act to deter the implantation of an embryo at an inappropriate stage of the menstrual cycle. During the secretory phase, the luminal epithelium transiently becomes less polarised and thus more receptive to an approaching embryo (Whitby et al., 2018). Significant structural alterations are observed in the receptive endometrium, with alterations seen in the ciliation, cytoskeleton, and glycocalyx of the endometrial epithelium, as part of the plasma membrane transformation (Murphy, 2004).

1.4.2 What affects endometrial receptivity?

Endometrial receptivity is orchestrated by a fine balance of numerous factors, aberrations to which may detrimentally affect endometrial receptivity. Assisted reproductive technologies (ART) use the application of exogenous hormones, namely FSH agonists or antagonists, to stimulate the ovaries to superovulate. Whilst increasing the oocytes available for ART, the hormones also elicit effects on other tissues in the reproductive tract. Histological comparisons between the endometrium of a natural cycle and a stimulated cycle show considerable alterations in the endometrial architecture and markers of endometrial differentiation, with these differences being most pronounced in women who then did not achieve pregnancy (Evans et al., 2012). This indicates that hormonal stimulation may affect endometrial receptivity, which is decreased by up to 20% in a stimulated cycle (Evans et al., 2012; Gardner et al., 2000b).

Lifestyle factors including body weight also influence endometrial receptivity, with obese women tending to have a non-receptive endometrium as determined by an endometrial receptivity assay (Lathi et al., 2014). The effects of obesity on reproduction are discussed in Section 1.7.

It is critical that the approaching embryo and the endometrium are concurrently receptive for implantation to occur. Recurrent implantation failure has been linked to altered endometrial receptivity: it is possible for the window of implantation to be disrupted at the molecular level, be out of synchrony with the menstrual cycle, or a combination of both, leading to a possible explanation for recurrent implantation failure (Sebastian-León et al., 2018).

1.4.3 The human endometrial epithelial receptome

During the window of receptivity, the luminal epithelium of the endometrium undergoes significant alterations in terms of the proteins expressed and secreted (Evans et al., 2016; Whitby et al., 2018), and gene expression and regulation (Kukushkina et al., 2017). Our group recently determined a cohort of proteins altered in a model of endometrial epithelial receptivity (Evans et al., 2020b), by state-of-the-art proteomic evaluation (Evans et al., 2020a). The proteins altered during the state of receptivity are collectively known as the “receptome” and can provide insights into potential biomarkers for receptivity, or targets for therapeutics or contraceptives.

Utilising a novel assay in which a spheroid of human trophectoderm cells approximating the size and shape of a human embryo is placed onto a monolayer of endometrial epithelial cells, mimicking the initial adhesive phase of embryo implantation (Evans et al., 2020b), Dr Evans demonstrated that these trophectoderm spheroids appear to differentiate between endometrial epithelial cells derived from infertile and fertile women: they do not adhere to cells isolated from endometrial tissue of infertile women. Endometrial epithelial cells which allowed trophectoderm spheroid adhesion were

designated 'adhesive co-cultures', with the corresponding cell monolayer designated 'adhesive' monolayer. Protein differences between adhesive monolayers and non-adhesive monolayers were detected using proteomics to identify the human epithelial "receptome." This work underpins the data in Chapter 6 of this thesis.

1.5 Preimplantation embryo development

The development of a preimplantation embryo is a highly regulated and precisely timed cascade of events (review: Niakan et al., 2012; Wale and Gardner, 2016). Upon fertilisation within the Fallopian tube, the second polar body (resulting from meiosis as the oocyte completes metaphase II) is extruded. The two nuclei from the gametes are pulled together by microtubules and fuse to form the embryonic genome. For the early mitotic divisions, cell processes are governed by maternal mRNA and factors present within the oocyte. The embryonic genome becomes activated at the 4-8 cells stage and embryonic genes are transcribed to progress development (reviews: Hogg and Western, 2015; Tadros and Lipshitz, 2009).

Mitotic division continues until the embryo is a small ball of cells called a morula. At this point in time, compaction begins to occur and the first cell fates are determined: the outer cells differentiate to become a layer of epithelial cells termed the trophectoderm, and inner cells form a compact ball of pluripotent cells termed the inner cell mass (ICM). The trophectoderm, in the absence of Hippo signalling, expresses the marker *Cdx2*, whereas Hippo signalling drives the expression of *Oct4* and *Nanog* in the inner cell mass (review: Leung and Zernicka-Goetz, 2015). The embryo then undergoes cavitation, as the fluid-filled blastocoel begins to form between the trophectoderm and the inner cell mass (Figure 1.5 A, B). These cell types can be identified by staining methods to examine their formation in experimental settings (Figure 1.5 C). Fluid accumulation is facilitated by aquaporins and ion transport into the blastocoel which generates an osmotic gradient: sodium enters the trophectodermal cells through ion exchangers and is extruded into the blastocoel by sodium-potassium ATPases (Barcroft et al., 2003; Houghton et al., 2003; Manejwala et al., 1989). In addition, fluid transport can be stimulated by maternal derived growth factors including EGF (Dardik and Schultz, 1991). Expansion of the blastocyst occurs as fluid accumulates in the blastocoel, a process in the human embryo which takes approximately 20 h (Huang et al., 2016). The mechanical stimulus of expansion, increasing internal pressure of the blastocyst, provides positive feedback on the differentiation of the trophectoderm and inner cell mass (Wang et al., 2018).

The inner cell mass will continue to differentiate to form the primitive endoderm and the epiblast during the second cell fate specification. These cells contribute the fetal tissues and extra-embryonic membranes during fetal development and gestation. The trophectodermal cells contribute the

embryonic components of the placenta, differentiating into a variety of trophoblastic cells as they invade and remodel the maternal endometrium.

With the development of the blastocoel and differentiation of trophectoderm and inner cell mass, the embryo is now considered a blastocyst, and at this stage it enters the uterine cavity where it hatches from the surrounding glycoprotein zona pellucida, a process governed by embryonic and maternal proteases coupled with increasing internal pressure (Leonavicius et al., 2018; Seshagiri et al., 2009). The final stages of preimplantation development occur in the uterine cavity where the embryo is exposed to a milieu of factors secreted by the endometrium into the fluid microenvironment.

The early preimplantation embryo metabolises pyruvate as its primary energy source; however, following embryonic genome activation the blastocyst predominantly utilises glucose to meet increasing energy demands (reviews: Gardner et al., 2002; Gardner and Harvey, 2015). The glycolytic blastocyst releases lactic acid into the surrounding fluid, generating a highly localised microenvironment characterized by a low pH: this acidic microenvironment is proposed to facilitate maternal-fetal interactions (Gardner, 2015). Glucose metabolism is strongly correlated to quality, healthy embryos: a high rate of glucose consumption is correlated to higher quality scores using the Gardner grading system and developmental morphokinetics, and indicators of post-transfer success such as the KIDscore (Ferrick et al., 2020).

It is clear that the preimplantation embryo is a complex entity which is highly attuned to the surrounding environment. For example, independent of the factors present within the uterine fluid, development *in vitro* is highly sensitive to fluctuations in temperature (Choi et al., 2015; Walters et al., 2020) and oxygen concentration (Gardner, 2016; Wale and Gardner, 2010). Appropriate development of this blastocyst is essential for the establishment of a healthy pregnancy and offspring, as abnormalities in the early stages of development can establish susceptibility to a lifetime of disease (Barker, 1995). The effect of an altered maternal environment, related to obesity, on critical aspects of preimplantation embryo development and function is the focus of Chapter 3 of this thesis.

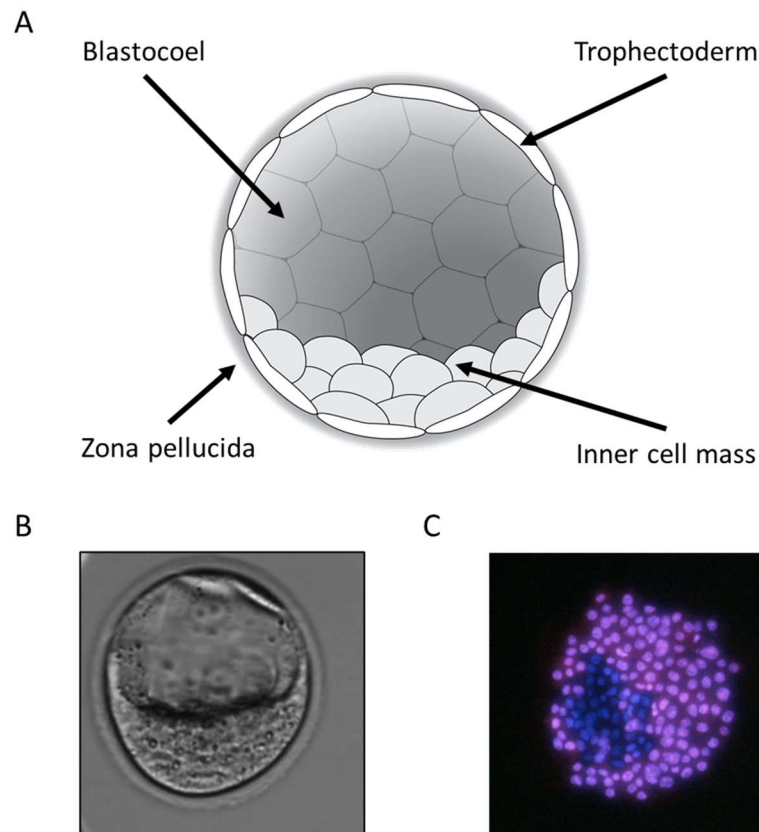


Figure 1.5: The preimplantation blastocyst. **A)** The preimplantation blastocyst is a spherical structure encased in a protective glycoprotein barrier, the zona pellucida, from which it must hatch before implantation. The blastocyst comprises two distinct cell lineages, the inner cell mass and the trophectoderm, and contains a fluid filled cavity known as the blastocoel. The trophectodermal cells are involved in implantation and placentation of the embryo, and the inner cell mass consists of pluripotent cells which give rise to the embryonic tissues. The blastocoel provides a medium for communication between these cell types. The structures of the blastocyst can be seen under brightfield microscopy (**B**) and the two cell types identified with a differential nuclear stain (**C**), showing the trophectoderm in pink and the inner cell mass in blue. Figure A generated by David Young, used with permission.

1.5.1 Developmental timeline

Fertilisation of the oocyte by a spermatozoon occurs in the upper region of the Fallopian tube. After fertilisation, the resultant zygote travels through the Fallopian tube towards the uterus as it continues to develop (Figure 1.6). The first cleavage and progression to a four-cell embryo occurs within the first 48 hours. As the cells continue to divide, the embryo forms a morula and reaches the uterine cavity approximately 3 days after fertilisation. In the uterine cavity, compaction occurs and the embryo develops into a blastocyst by approximately day 5, with hatching from the zona pellucida and

implantation occurring between days 6 and 7. These last few stages of development occur in the uterine cavity where the embryo is bathed in uterine fluid and is able to communicate with the maternal endometrium.

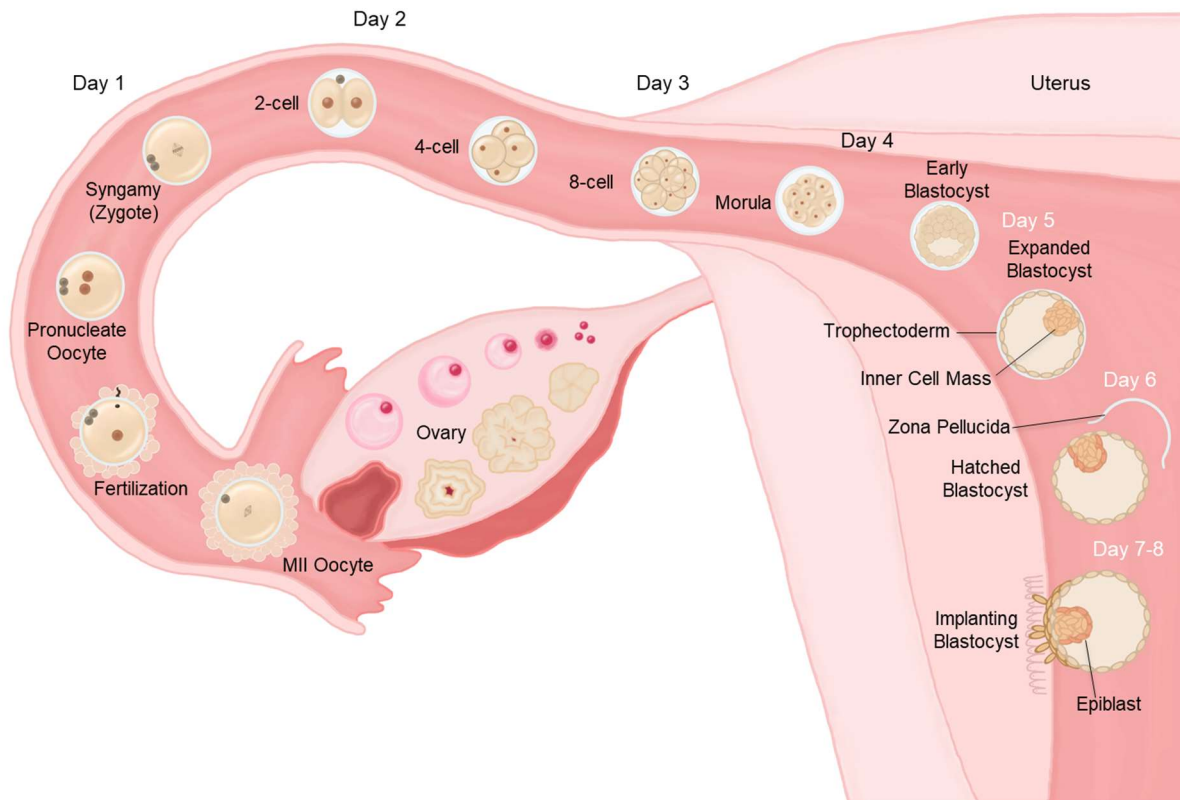


Figure 1.6: Timeline of human embryonic development. Schematic showing location and timing of significant developmental events. From: Gardner, D. K. (2018). Human Embryo Development and Assessment of Viability. In M.K. Skinner (Ed.), Encyclopaedia of Reproduction. Vol. 5, pp. 176–185. Used with permission.

1.6 Maternal-fetal interaction: embryo-endometrium crosstalk

Final development of the blastocyst occurs within the uterine cavity where embryo-endometrial interactions take place. These are mediated via the microenvironment of uterine fluid which contains secretions from both embryo and endometrium and prepare both the trophoctodermal and endometrial epithelial surfaces for adhesion and implantation (Salamonsen et al., 2016). Since trophoctodermal cells are also epithelial, and epithelial cells are mutually repulsive, both must be modified to enable adhesion (Owusu-Akyaw et al., 2019; Whitby et al., 2018).

Significant factors within the uterine fluid which may mediate maternal-fetal communications either through autocrine or paracrine mechanisms include proteins (Greening et al., 2016b; Heng et al., 2011), growth factors (Gurner et al., 2020), miRNA (Cuman et al., 2015), and exosomes (Greening et al., 2016a). For reviews on the factors related to receptivity and implantation, see Dimitriadis *et al.* (2005, 2010). Extracellular vesicles are secreted by both the maternal endometrium (Greening et al.,

2016a; Homer et al., 2016) and the embryo (Giacomini et al., 2017), with the cargo of endometrial exosomes modulated by the hormonal milieu of the menstrual cycle (Greening et al., 2016a). Exosomes retrieved from the human endometrial epithelium modulate the functions and implantation potential of the embryo, increasing blastocyst cell number, hatching rate, and embryo outgrowth (Gurung et al., 2020). This highlights the important contributions from the maternal uterine environment to supporting embryonic and fetal growth.

Dysregulation of the factors within the uterine fluid across the menstrual cycle has the potential to impact or disrupt maternal-fetal interactions. Indeed, an altered cytokine profile within the uterine fluid has been identified in women who experience idiopathic infertility, which may impact endometrial function and receptivity in later phases of the menstrual cycle (Fitzgerald et al., 2016). Research is beginning to identify altered uterine environments in women who suffer from conditions such as PCOS and obesity, and as is the focus of this thesis, how they impact maternal-fetal interactions which may underpin the poor fertility outcomes of these women.

1.6.1 Adhesion and Implantation

The blastocyst must approach the receptive endometrium and adhere to the luminal epithelium via cell-cell interactions before invasive implantation can occur (Figure 1.7). The embryo forms a reversible attachment during apposition, proposed to activate the trophoblast cells into an invasive phenotype (Ruane et al., 2017). Following apposition, the embryo adheres to the epithelium, forming a more stable maternal-fetal complex. The trophoblast extends in a bipolar manner on the epithelium and penetrates between the epithelial cells and then through the decidualizing stromal compartment (Bentin-Ley et al., 2000). In a model of early implantation, it has been suggested that the trophoblast senses the orientation of the underlying stroma and aligns itself during invasion, giving rise to the axis for embryonic development (Carver et al., 2003).

The details of initial phase of implantation, embryo adhesion, are widely debated. Evidence exists both for direct cell-cell interaction of the trophoblast and luminal epithelium, but it is also possible that the embryo invades between epithelial cells without direct contact (Bentin-Ley et al., 2000; Lopata, 1996). In the mouse, direct contact of these two cell types occur, before embryo-mediated entosis of epithelial cells allows for invasive implantation (Li et al., 2016). There are significant differences in the mode of adhesion and implantation between species (review: Lee and DeMayo, 2004), resulting in the need for *in vitro* methods to improve our understanding of human embryo adhesion and implantation.

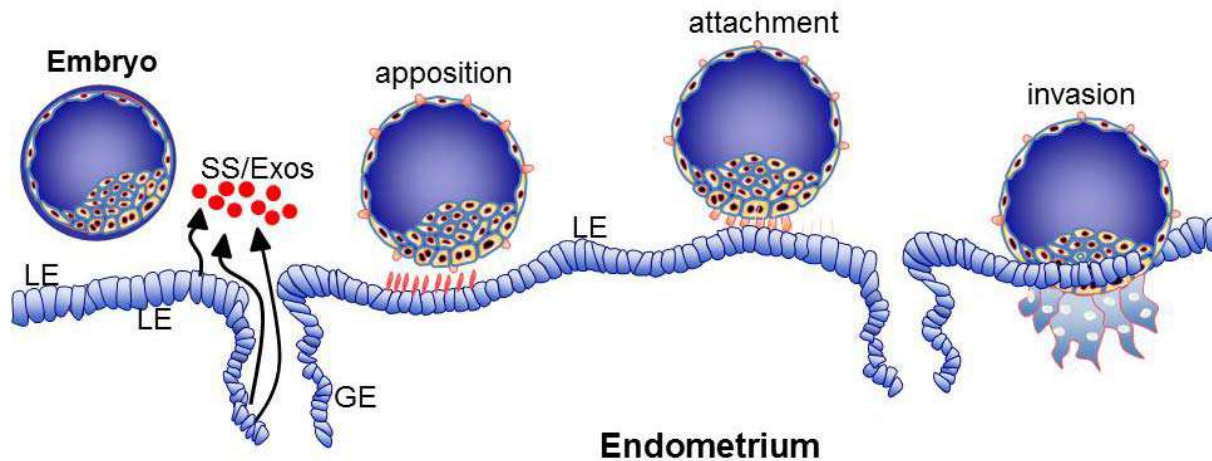


Figure 1.7: Embryo adhesion and implantation. The embryo approaches the luminal epithelium (LE) where it is exposed to soluble secreted factors (SS) and exosomes (Exos) secreted from the uterine glands (glandular epithelium, GE), undergoes apposition then adhesion to the LE, and finally invasion between the epithelial cells into the stromal layer. ©Lois Salamonsen, used with permission.

1.6.2 Models to study embryo-epithelial interactions

The complex maternal-fetal interactions during implantation are difficult to study, and many must be extrapolated or inferred from animal models. However emerging technologies such as endometrial and trophoblast organoids may provide experimental means by which to study these earliest stages of human pregnancy *in vitro* (Abbas et al., 2020; Haider et al., 2018; Turco et al., 2017). Interactions between spheroids of trophoblast or trophoblast cells and monolayers of human endometrial epithelium provide means by which to examine adhesive interactions (John et al., 1993; Thie and Denker, 2002), similar to *in vitro* investigation of cancer metastasis, however cell line investigations have inherent limitations in their physiological representation (review: Weimar et al., 2013). Some models, including those used in this thesis, use a monolayer of epithelial cells, whereas other models provide a more comprehensive overview though modelling of the endometrial and stromal compartment in culture (Wang et al., 2012). The spheroids formed in such models often utilise trophoblastic cells such as BeWo, or HTR8/SVneo that are more representative of differentiated and invasive cells (Szklańska et al., 2017). Work in the Salamonsen laboratory has extended these spheroid adhesion assays to utilise trophoblastic stem cells to be as representative as possible when investigating ‘embryo-epithelium’ interactions (Evans et al., 2020b; Kinnear et al., 2019).

Recent developments in organoid culture of cells from the human endometrium and trophoblast have greatly improved upon the physiological relevance of current models of maternal-fetal interactions (Abbas et al., 2020; Fitzgerald et al., 2021; Haider et al., 2018; Turco et al., 2018). Human endometrial epithelial organoids retain characteristics of donor tissue; application of hormones related to the menstrual cycle and pregnancy drive alterations to cell function, morphology,

ciliation, and secretory capacity (Boretto et al., 2017; Fitzgerald et al., 2019; Haider et al., 2019; Turco et al., 2017). Organoids of the human endometrial epithelium may be utilised to examine functions of primary endometrial epithelial cells and both validate and build upon results from cancer cell lines: they enable investigation of mechanisms underpinning endometrial pathology and responses to sexually transmitted infections such as chlamydia (Bishop et al., 2020; Boretto et al., 2019). In addition, endometrial glandular organoids can be derived from the decidua of term placenta, allowing experimentation on tissue with a known pregnancy outcome (Marinić et al., 2020). Organoids of the human endometrial epithelium have been used in this thesis as a primary cell model, detailed in Chapter 5.

1.6.3 The Adhesome

Adhesion of an embryo to the endometrium is an essential yet under-studied process. Investigation of the proteins involved and their functions may provide critical insights into *in vivo* adhesion, while study of their functions and alterations in pathologies may provide targets for both therapeutics and non-hormonal contraceptives.

The “adhesome” is a term newly coined by Dr Evans in the Salamonsen laboratory at the Hudson Institute of Medical Research (Evans et al., 2020a). It describes the protein cohort involved in the adhesion of an embryo to the endometrium, which is essential for reproduction as the embryo may not implant without first having successfully adhered to the endometrium. Adhesion occurs between an apposed blastocyst and the receptive luminal epithelium. As such the adhesome reflects the total cohort of proteins altered when the receptive endometrial epithelium is exposed to an adhering embryo, modelled using the adhesion of trophectoderm spheroids to primary endometrial epithelial cells (Evans et al., 2020a).

1.7 Obesity

Obesity, defined by the World Health Organisation (WHO), as the accumulation of excess fat which can affect an individual’s health, is diagnosed by having a body mass index (BMI) equal to or greater than 30 kg/m². The percentage of obese adults is highest in developed, Western countries, including Australia. In 2016 the WHO found 29% of Australian adults to be obese, including 28.4% of female adults (Global Health Observatory data; Figure 1.8). The WHO have shown obesity to follow an increasing upwards trend over the last 30 years, termed ‘Globesity’ and have urged for health interventions to prevent or reduce the physical, mental, and financial burdens that come with obesity.

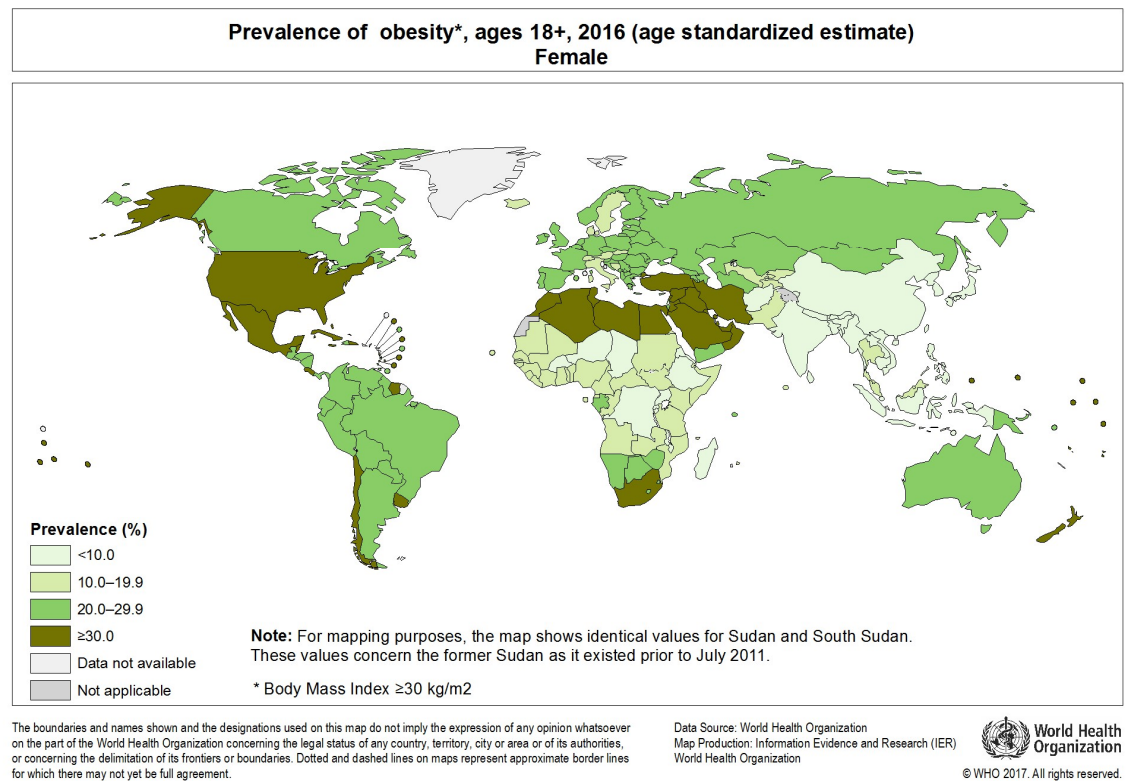


Figure 1.8: Global levels of obesity in female adults. Percentage of the female adult population that are obese (BMI ≥ 30 kg/m²). Map obtained from WHO Global Health Observatory map gallery.

1.7.1 Effects of obesity on reproduction

In Australia, almost half of the women who give birth are overweight or obese (Australian Institute of Health and Welfare, 2017). Obesity has been shown to affect fertility and menstruation (Rogers and Mitchess, 1952), to increase maternal and fetal risk during gestation, and to predispose offspring to non-communicable diseases (Heerwagen et al., 2010; Jungheim et al., 2010). For both men and women, an increasing BMI is correlated with increased subfecundity, a prolonged period before conception (Ramla-Hansen et al., 2007). With an increasing prevalence of obesity amongst both men and women of reproductive age, it is important to understand the impact of obesity on reproductive health and offspring.

1.7.1.1 Female reproduction

Obesity has numerous effects on the female reproductive system, culminating in reduced overall fertility. Menstrual irregularities have long been associated with obesity. Among women experiencing menstrual disturbances including amenorrhea, infertility, and recurrent pregnancy loss, there is a significantly higher prevalence of obesity compared to women experiencing normal menstrual cycles (Rogers and Mitchess, 1952). Obesity is further correlated to irregular menstrual cycle length,

amenorrhea and oligomenorrhea (Castillo-Martínez et al., 2003; Zhang et al., 2012), and increased serum FSH concentrations in infertile women (Seth et al., 2013).

A normal body mass index (BMI) is considered to be within the range 18.5 to 24.9. For every 1 unit increase of BMI over 29, the probability of a spontaneous pregnancy in ovulatory women decreases by 4% (Van Der Steeg et al., 2008). Likewise, increasing BMI and associated fat distribution reduced the probability of conception in a natural cycle, as a 0.1 increase of waist to hip ratio was associated with a 30% reduction in conception rate (Zaadstra et al., 1993). In contrast, one study has shown that obese women have an increased propensity to achieve pregnancy in a shorter period of time, termed 'superfertility' (Bhandari et al., 2015), but have an increased prevalence of recurrent pregnancy loss (Bhandari et al., 2015; Sugiura-ogasawara, 2015). Obesity has likewise been shown to be highly related to miscarriage as it significantly increased the odds of experiencing a miscarriage compared to non-obese women (Lashen *et al.*, 2004; Sugiura-ogasawara, 2015; Veleva *et al.*, 2008; Wittemer *et al.*, 2000). In particular, obesity is associated with an increased frequency of euploid miscarriage in natural cycles (Boots et al., 2014).

The effects of obesity on pregnancy outcomes are not consistent within the literature, as several studies have shown no correlation between BMI and reproductive outcomes following ART cycles (Insogna et al., 2017; Jungheim et al., 2013; Martinuzzi et al., 2008; Schliep et al., 2015; Wattanakumtornkul et al., 2003). However, a consensus appears to be building on the detrimental effects of obesity on a variety of reproductive measures (Sermondade et al., 2019).

Weight alteration between pregnancies has been investigated, with overweight or obese women who lost weight between pregnancies showing a significantly reduced time to pregnancy compared to women who maintained their weight. Conversely, underweight women who gained weight between pregnancies showed an increase in time to pregnancy (Ramlau-Hansen et al., 2007). If an obese woman does become pregnant, she is more likely to suffer from early and recurrent miscarriage (Bhandari et al., 2015; Lashen et al., 2004; Sugiura-Ogasawara, 2015; Wittemer et al., 2000). It should be stressed that weight loss is not a cure-all solution, particularly for infertile women approaching reproductive senescence. For example, even following an average weight loss of almost 10 kg, while some benefit was evident for spontaneous conception, live births following IVF were not significantly improved for obese women (Legro et al., 2015). The underlying mechanisms of obesity-related infertility should be addressed, as a mechanism has not yet been identified for how obese women suffer from a disproportionate number of adverse outcomes.

1.7.1.1.1 The endometrium

The effect of obesity on the endometrium has been highlighted in oocyte donation models, which control for gametic effects. Increasing BMI in recipient women has been significantly correlated with reduced implantation, and an increased risk of pregnancy loss (Bellver et al., 2007; DeUgarte et al., 2010; Provost et al., 2016). As oocytes were donated from women of normal weight, these results highlight an effect of obesity on the endometrium, and suggest an unfavourable intrauterine environment for establishing pregnancy (Bellver et al., 2007; Bellver et al., 2013). Obese women have an increased loss of transferred cryopreserved genetically euploid embryos, further highlighting the role of the endometrium (Tremellen et al., 2017).

The regeneration of the endometrial functionalis in the menstrual cycle is reliant largely on the stem cell population of the basalis. Proliferation of the stromal layer is also required during invasive implantation and placentation to remodel the endometrium towards sustaining pregnancy. During the window of implantation, 6-10 days after ovulation, the obese endometrium has been found to have a reduced population of endometrial mesenchymal stem cells which may negatively impact the subsequent ability of the endometrium to undergo the remodelling required for invasive implantation and healthy placentation, resulting in an increased risk of pregnancy loss and complications (Murakami et al., 2013).

Uterine natural killer cells (uNK) which regulate the remodelling of the endometrial vasculature during the cycle and implantation, have also been shown to be affected by obesity (Parker et al., 2013; Perdu et al., 2016). In a mouse model, obesity reduces leukocyte expression of interferon- γ (important for arterial remodelling), along with a reduced population of uNK, and altered T-cell profiles (Parker et al., 2013). Perdu et al., (2016) examined the effects of obesity on uNK which are important in vascular remodelling and trophoblast invasion during placentation: a reduction in both the total number of uterine natural killer cells and their different gene expression patterns was seen in cells isolated from endometrium from obese compared with lean women. Although uterine natural killer cells were able to proliferate, the obese uterine environment appears to be detrimental to their survival. Interestingly, the uterine natural killer cells of the obese endometrium overexpressed decorin which blocks placental trophoblast outgrowth, and increases extracellular matrix signalling molecules and growth factor receptors. The signalling in this environment was more representative of a fibrotic and inflammatory pregnancy compared to control and may partially explain the increased miscarriage rate. The functionality of the uNK was also changed in terms of angiogenesis, with the obese endometrium showing narrower arteries with thicker smooth muscles. This indicates that obesity affects endometrial vascular remodelling and promotion of an environment which is hostile to placentation.

Endometrial remodelling is further affected by obesity: in a mouse model, diet-induced obesity reduced the decidualisation of stromal cells, while exposure to fatty acids prevalent in the Western diet reduced the decidualisation of human endometrial stromal cells (Rhee et al., 2016). Decidualisation requires proliferation and energy, and it is hypothesized that autophagy—cellular recycling—is important in this process. In mouse and human models, obesity and exposure to the unsaturated fatty acid palmitic acid, reduced markers of autophagy, implying that obesity reduces the ability of the endometrium to recycle cellular components and meet the energy demands of decidualisation (Rhee et al., 2016).

Endometrial receptivity has also been shown to be altered on a genetic level, as during the window of implantation the expression of genes involved in transcriptional regulation, development, and basic metabolic processes are negatively impacted by obesity, especially in combination with polycystic ovary syndrome, a common comorbidity of obesity. This aberrant gene expression also affects pathways involved in implantation (Bellver et al., 2011; Comstock et al., 2015). Recent evidence suggests that obesity, while detrimental on its own, does not necessarily exacerbate all endometrial pathologies: for example, an elevated BMI does not further alter the endometrial gene expression in the endometrium from women with endometriosis (Holdsworth-Carson et al., 2020).

1.7.1.1.2 Ovarian effects

There is significant evidence that obesity impacts the oocyte, with continuing effects on embryonic development (Robker, 2008). Approximately 25% of ovulatory infertility can be attributed to an overweight or obese BMI while an increase in BMI is associated with an increase in relative risk for anovulatory infertility (Rich-Edwards et al., 2002). Follicular fluid contains nutrients required for oocyte development and competence, and the balance of its various components is altered in obese women (Robker et al., 2009; Valckx et al., 2012). In overweight and obese women, increased levels of triglycerides and insulin were demonstrated in the follicular fluid of oocytes after ovarian hyperstimulation, but no direct effect of BMI on oocyte quality was found (Valckx et al., 2012). However, other research has found a significant effect of BMI on different markers of oocyte quality. Metaphase I and II oocytes, which are considered to be good quality oocytes, were reduced in overweight and obese women, who tended to have more oocytes retrieved that were premature, or had fractured zona pellucida (Witteimer et al., 2000). The diameter of oocytes retrieved from overweight and obese women during ART are significantly smaller than those from normoweight women: as smaller oocytes are less likely to cleave and form blastocysts: this is an indicator of poor quality of resultant embryos (Atzmon et al., 2017; Leary et al., 2015). Oocytes from overweight and obese women also have an altered profile of fatty acids, important in cellular function, as the fatty acids within a cell determine cell membrane properties and influence their biological functions.

(Matorras et al., 2020). Matorras *et al.*, (2020) propose that the reduced polyunsaturated fatty acid content in oocytes from obese women may impair the cellular processes of fertilisation, and contribute to the poor reproductive outcomes.

The effects of obesity on the oocyte have more extensively been examined in mouse models. The “blobby” mouse, containing an *Alms1* mutation, overeats and develops obesity. Following the onset of obesity, these mice exhibit fewer ovulated oocytes, analogous to reduced ovulation in obese women (Wu et al., 2015). Oocytes from these obese “blobby” mice exhibit poor mitochondrial function, spindle formation, and expression of extracellular matrix proteins important in fertilisation (Wu et al., 2015). Additionally, in both diet and genetic models of obesity in mice, expression of epigenetic machinery and methylation is significantly impacted, which may impact long term offspring health (Hou et al., 2016).

Of concern, mitochondrial damage observed in obese mothers is transmitted to the offspring, altering growth trajectories and mitochondrial copy number in “blobby” mice (Wu et al., 2015). This highlights the need to alleviate obesity-induced damage to support healthy maternal-fetal interactions and embryo development. The impacts of obesity on oocyte mitochondrial function and lipid accumulation are not necessarily reversible by diet, indicating that short term weight loss, whilst beneficial in normalising whole body measures of metabolism, may not be as beneficial to gamete quality and fertility (Reynolds et al., 2015).

1.7.1.1.3 Gestational Disorders

Obese women are at a higher risk of first trimester and early miscarriage, and are more likely to suffer from recurrent miscarriage and pregnancy loss (Bellver et al., 2003; Lashen et al., 2004; Sugiura-ogasawara, 2015). Once the pregnancy is well established, an obese woman is subject to further risk during gestation, with increased likelihood of pre-eclampsia (Roberts et al., 2011), gestational diabetes (Chu et al., 2007), intrauterine growth restriction (Wu et al., 2004) and pre-term birth (Cnattingius et al., 2013).

1.7.1.2 Male reproduction

Obesity has been correlated with reduced testicular function: obese men with a history of fertility have a significantly lower sperm count than fertile men with a normal BMI or those who are underweight (Stewart et al., 2009). However, the association of BMI with sperm count is not consistent: several studies find no correlation between the two variables (MacDonald et al., 2013). Furthermore, some studies show no effect of overweight or obesity on sperm quality, and when partnered with a normoweight woman, no significant impact on reproductive outcome following ART (Thomsen et al., 2014). BMI has also been shown to have a significant negative effect on the reproductive hormones testosterone and free testosterone, and on sex hormone binding globulin

(MacDonald et al., 2013; Stewart et al., 2009). Further, elevated male BMI in conjunction with age negatively impacts the quality of embryos produced through IVF and subsequent live birth rate (Anifandis et al., 2013).

Although obesity detrimentally affects male reproduction, the paternal effects of obesity will not be discussed in detail here, as this research aims to understand perturbations in maternal-fetal interactions mediated by obesity.

1.7.1.3 Combined parental obesity

As obesity increases in prevalence, there is a greater occurrence of both maternal and paternal obesity. Finger et al., (2015) investigated the effect of combined parental obesity on reproduction, a relatively understudied area. It was known that the obese male phenotype may confer epigenetic programming onto the offspring, so the combination of male and female obesity needed to be examined. In a mouse model of combined parental obesity, there was a reduction in successful mating as evidenced by the lack of a vaginal plug, when compared to individual obesity, along with alterations in embryo developmental morphokinetics, reduction of total cell count and proportion of cells in the trophoctoderm (Finger et al., 2015; McPherson et al., 2015). Embryos resulting from parents both with obesity, also had increased glucose consumption but no increase in lactate, indicating altered embryo viability (Finger et al., 2015). In addition, such offspring had reduced fetal and placental weight (McPherson et al., 2015). In humans, a study of ART cycles examined the effect of individual and combined parental obesity, and noted no significant effect of combined parental obesity on the clinical pregnancy rate following IVF or ICSI treatments (Kupka et al., 2011). The authors of this study noted that previous studies have not agreed on the effects of obesity on implantation rate and ART outcomes, and caution that their dataset may have underestimated the prevalence of obesity. Further studies have shown that couples where both partners are overweight or obese, have an increased risk of experiencing subfecundity than normal weight couples (Anifandis et al., 2013; Ramlau-Hansen et al., 2007).

1.7.1.4 Obesity and ART

It is debated in the literature whether obesity is significantly associated with a reduced rate of implantation and pregnancy in ART cycles. However a recent meta-review found a significant negative correlation between obesity and live birth rate in women who underwent IVF (Sermondade et al., 2019). Kupka (2011) found a significant increase in clinical pregnancy rates when an obese woman underwent ICSI, or if the male partner undergoing ICSI or IVF was obese. Some studies have shown no effect of obesity on implantation rate following fresh or frozen thawed embryo transfer (Insogna et al., 2017; Valckx et al., 2012). However female obesity has also been linked to significant adverse

outcomes including reduced clinical pregnancy rate, live birth rate, and increased rate of miscarriage following embryo transfer (Bu et al., 2020; Fedorcsak et al., 2004; Provost et al., 2016; Rittenberg et al., 2011; Tremellen et al., 2017). Indeed, with live birth rate following embryo transfer was approximately 30%, increasing BMI significantly reduced this by up to 10%: women with a BMI > 50 kg/m² had a live birth rate of 21.2% (Provost et al., 2016).

Gonadotrophin requirement for ovarian stimulation is increased in obese women compared to those of normal weight, with FSH required for longer periods of time and at higher doses (Orvieto et al., 2009). Even so, obese women are at increased risk of insufficient follicle development (Fedorcsak et al., 2004). Obesity also reduces the number of oocytes retrieved following ovarian hyperstimulation, inherently limiting the success of IVF (Valckx et al., 2012; Wittemer et al., 2000), with those retrieved being of lesser quality (Wittemer et al., 2000).

1.7.1.4.1 Effects on the embryo

Parental obesity at the time of conception may impact embryonic development through gametic effects, epigenetic programming, or via alterations in the tubal or uterine microenvironments (review: Lane *et al.*, 2015). Fewer quality embryos form from fertilized oocytes retrieved from obese women than from those of normal BMI (Valckx et al., 2012), suggesting that obesity may somehow affect *in vitro* embryonic development. Conversely, in follicles of > 15 mm diameter, optimal for ART, retrieved oocytes from obese women are able to generate embryos which are appropriately developed by day 3 of culture (Orvieto et al., 2020): however the persistence of these effects to day 5 of culture was not examined in either study.

Preimplantation embryo morphokinetics have been used as a marker of embryo quality and viability (Del Canto et al., 2012; Hlinka et al., 2012). While assessment of early embryo morphokinetics showed no detrimental effect of female obesity on embryo quality in the first three days of development (Bellver et al., 2013a), embryos from obese and overweight women develop to morula and subsequent blastocyst stages significantly faster than embryos from normoweight women (Leary et al., 2015). Leary *et al.*, (2015) also investigated multiple parameters indicative of human embryo quality from overweight and obese women in comparison to normoweight women, showing that the oocytes from overweight and obese women, and the resultant embryos, were significantly smaller, and had a lower total cell count with fewer cells present in the trophectoderm. As the trophectoderm is involved in placentation this could correlate to the increase in pregnancy loss seen in obese women. Furthermore, this study demonstrated that 'overweight and obese' embryos have an increased amino acid turnover, specifically consuming more methionine, serine, and glutamine. Glucose consumption was also reduced in these embryos. Interestingly 'overweight and obese' embryos had a significantly higher level of endogenous triglycerides than 'normoweight' embryos, which are also significantly

increased in embryos which arrested. Thus obesity and overweight negatively affect both the metabolism and development of the preimplantation embryo (Leary et al., 2015).

Though obesity has been strongly implicated in impaired embryonic development, the mechanism by which it does so is still not understood. As the follicular microenvironment mirrors some of the abnormalities seen in the serum of obese women (Valckx et al., 2012), it was hypothesized that metabolic changes may alter meiotic division and result in aneuploid embryos (Goldman et al., 2015). In a mouse model, obesity is associated with an increased occurrence of aneuploidy, this has not been reflected in human studies (Goldman et al., 2015). This implies that an alternative mechanism is responsible for the reproductive outcomes seen in obese women. In a sheep model of obesity, differential expression of genes important in embryogenesis and placental development was observed (McCoski et al., 2018). Additionally, Tremellen et al. (2017) theorise that there may be an epigenetic mechanism affecting the expression of critical genes in obese origin embryos to explain the loss of euploid embryos in obese women undergoing ART.

1.8 Advanced Glycation End Products

Advanced Glycation End Products (AGEs) are a family of non-enzymatic protein modifications which cause down-stream inflammation. They affect multiple tissues and are associated with the complications of a number of diseases including diabetes, cardiovascular disease and stroke. AGEs are elevated in people who suffer from obesity and are associated with the development of metabolic syndrome (Uribarri et al., 2015). Of relevance to this thesis, AGEs are significantly elevated in the uterine fluid of obese women, and impair endometrial function (Antoniotti et al., 2018), thus they may contribute to the poor reproductive outcomes experienced by obese women.

1.8.1 Structure and Formation

AGEs are formed in several different ways, both endogenously and exogenously. Endogenous AGEs can be formed by proteins and glucose undergoing transformation primarily via the Maillard reaction. Glucose is covalently bonded to free amino acids or lipids and undergoes either oxidation or hydrolysis. For a review of AGEs biochemistry and analysis, see Perrone et al. (2020). This spontaneous reaction is used *in vitro* to prepare AGEs solutions for experimentation (Figure 1.9).

AGEs and their precursors can also be absorbed from external sources including cigarette smoke and the consumption of highly heated and processed foods. Browning of food during cooking generates large quantities of AGEs through the Maillard reaction. Factors that enhance AGE formation in foods include high lipid and protein content, and application of dry heat. Fewer AGEs are generated

in gentler cooking methods with higher water content, for example boiling and steaming. For reviews see (Sharma et al., 2015; Zhang et al., 2020).



Figure 1.9: *In vitro* formation of AGEs. Following 3 months of incubation, a golden colour was observed in the HSA solution containing glucose, indicating the formation of AGEs, in comparison to control (A). These solutions were depleted of endotoxin prior to experimental use (B).

1.8.2 Accumulation of AGEs in the body

Exogenous AGEs consumed through the diet contribute to the AGEs burden in the body. Approximately 10% of dietary AGEs are absorbed and either enter the circulation eventually being excreted through the urine (only approximately a third of absorbed dietary AGEs), or accumulate within organs and tissues (Koschinsky et al., 1997). Dietary AGEs and their absorption have recently been comprehensively reviewed (Guilbaud et al., 2016; Zhang et al., 2020). Their absorption is dependent on the molecular structure, as the Maillard reaction leads to a heterogenous array of AGEs: dicarbonyls such as methylglyoxal are broken down during digestion and are unlikely to influence serum methylglyoxal levels; however, structures such as n- ϵ -carboxymethyl lysine (CML) are more readily absorbed in the gastrointestinal tract. Rodent models demonstrate that dietary CML not only enters circulation, but can accumulate throughout the body.

How AGEs accumulate within the reproductive tract, including the uterine fluid, is poorly understood as this unique environment is regularly remodelled with shedding of the endometrium during menses. Diet is known to modulate the composition of human uterine fluid, thus it may also be impacted by exogenous AGEs (Kermack et al., 2015).

1.8.3 Signalling pathways of AGEs

AGEs can bind to a variety of signal receptors to induce multiple responses, (reviews: Ott et al., 2014; Xie et al., 2013). AGEs receptors include the receptor for advanced glycation end products (RAGE), advanced glycation end products receptor complex (AGE-R, also known as OST48), Toll Like Receptor 4 (TLR4) (Noguchi et al., 2010), and macrophage scavenger receptors including LOX-1 (Ott et al., 2014; Xie et al., 2013). RAGE is approximately 35 kDa, and consists of an extracellular ligand binding domain,

two cytosolic domains, a transmembrane helix, and a cytosolic signal transduction domain. Although it does not induce signal transduction by itself, activated RAGE recruits different transducers to mediate the cellular effects. One example is Src, which upon recruitment, phosphorylates the cytosolic signal transduction domain, and produces reactive oxygen species (ROS). Through signal transduction and oxidative stress on the Golgi and mitochondria, NFκB is activated and translocates to the nucleus, where it increases the expression of genes involved in the inflammatory response and receptor upregulation (Ott et al., 2014). AGEs-stimulated RAGE also activates ERK1/2 and JNK kinases to activate the transcription factors NFκB and activator protein-1, in turn upregulating the expression of lysyl oxidase and endothelin-1, which can lead to altered ECM constituents, and vascular dysfunction (Adamopoulos et al., 2016). Soluble (s)RAGE is a soluble ligand for RAGE which may act as a decoy to this receptor, and its elevation in bodily fluids may confer beneficial effects (Ott et al., 2014). However, sRAGE will not be the primary focus of this thesis. AGEs exert additional cellular effects through TLR4 signalling (Noguchi et al., 2010), activating NFκB and promoting inflammation; for a review of TLR4 signal transduction refer to Lu et al. (2008). AGEs and their precursors (such as glycoaldehyde) can also be directly taken up into the cells, leading to endoplasmic reticulum stress, and activation of the unfolded protein response, which ultimately induces apoptosis (Yamabe et al., 2013).

1.8.4 Physiological function

AGEs are involved in the inflammatory response, causing translocation of NFκB to the nucleus and resulting in the expression and release of a milieu of pro-inflammatory factors. Furthermore, signalling through the receptor for AGEs (RAGE) via other ligands can stimulate cellular proliferation and induce apoptosis (Arumugam et al., 2004; Jin et al., 2011; Rani et al., 2014). AGEs have been identified in the pathology of several conditions including diabetes, Alzheimer's disease, and cardiovascular health (review: Singh et al., 2001). In some conditions, AGEs can be synthesized and secreted by macrophages to stimulate inflammation. Their secretion is significantly upregulated during post ischemic reperfusion injury, and exacerbates muscle cell death. Inclusion of sRAGE during therapeutic application of stem cells helps to prevent cell death and improve tissue recovery (Son et al., 2017).

1.8.5 AGEs and Female Reproduction

AGEs accumulate throughout the human and mammalian reproductive tracts, and tend to be elevated in people who are subfertile, including those who suffer from obesity (Antoniotti et al., 2018), diabetes (Mallidis et al., 2008), and polycystic ovary syndrome (Diamanti-Kandarakis et al., 2005). Whilst AGEs and their signalling may play a physiological role in human reproduction, their elevation and dysregulation of RAGE signalling is likely detrimental to fertility.

AGEs and their receptors have been localised and examined throughout the female reproductive tract and associated with various gynaecological pathologies in which altered localisation and expression of AGEs and their receptors are apparent. AGEs within the female reproductive tract have the potential to impact oocyte development and competency, preimplantation embryo development, placental formation and function, and ultimately the final outcome of pregnancy.

1.8.5.1 AGEs in the ovary: implications for oocyte development, maturation, and competency

The location and pathological implications of AGEs within the ovary have been described and previously reviewed (Merhi, 2014). Healthy ovarian function is critical for maintaining gamete quality and fertilisation potential. Within the ovary, follicles exist in a heterogenous array of developmental stages, and selection and ovulation of one or two follicles is directed under the fine control of FSH and LH. As gametes are not generated *de novo* within the ovary through a woman's reproductive life, AGEs have the potential to influence a woman's entire cohort of germ cells. It is therefore necessary to understand the physiological and pathological effects of AGEs on follicular development and gamete health, and whether interventions may normalise any adverse effects to optimise reproductive health for women with elevated AGEs. Contents of the follicular fluid are critical for healthy oocyte development and maturation—indeed Takahashi et al. (2019) demonstrate elevated follicular fluid levels of AGEs to be associated with poor quality embryos developing from the follicles. Levels of AGEs in follicular fluid correlate with impaired follicular growth, fewer recovered oocytes, reduced fertilisation during ART cycles, and a lower probability of ongoing pregnancy following ART (Jinno et al., 2011). Importantly, cumulus cells, which surround the oocyte, derived from women undergoing IVF, are impacted by AGEs in terms of steroidogenic enzyme expression, and estrogen profile; expression of steroidogenic enzymes improved by Vitamin D3. Thus elevated follicular AGEs may impact oocyte and follicular synchrony (Merhi et al., 2018). *In vitro*, anti-mullerian hormone signalling is altered by AGEs, potentially impacting folliculogenesis in women with elevated follicular AGEs (Merhi, 2019). Granulosa cells and monocytes within follicular fluid also accumulate AGEs, and express RAGE in correlation with a patient's age (Stensen et al., 2014).

Ovarian ageing appears to be influenced by AGEs-modified extracellular matrix proteins, possibly contributing to the declining follicular reservoir. Indeed, *in vitro*, AGEs-fibronectin resulted in the cell death and detachment of granulosa lutein cells which normally adhere to fibronectin alone (Stensen et al., 2014). Furthermore, with advancing maternal age, a reduction in plasma sRAGE is observed—as sRAGE may act as a decoy receptor and mitigate AGEs induced signalling, this reduction may exacerbate the effects of ovarian AGEs (Fujii and Nakayama, 2010).

Elevated levels of AGEs have been implicated in pathologies of the ovary, including Polycystic Ovary syndrome (PCOS) (Diamanti-Kandarakis et al., 2005). This syndrome, affecting between 3 and

10% of women, alters hormonal profiles, hyperglycaemia, ovulation, and subsequently fertility (Wolf et al., 2018). Associated insulin resistance and resultant hyperglycaemia would imply accelerated formation of AGEs. Indeed, regardless of insulin resistance, women with PCOS have higher serum concentrations of AGEs (Diamanti-Kandarakis et al., 2005) and there appears to be a synergistic effect of AGEs and insulin resistance on folliculogenesis (Jinno et al., 2011).

1.8.5.2 AGEs and the early embryo

Given the sensitivity of the embryo to environmental cues, exposure to AGEs or conditions promoting their formation may have long term consequences for development. Under *in vitro* oxidative stress, human embryonic stem cells upregulate mRNA and protein expression of RAGE, while somatic cells accumulated CML, embryonic stem cells did not. However, upon differentiation towards cardiac myocyte identity, RAGE expression was reduced, with a concurrent increase in proteasome activity (Barandalla et al., 2017). This indicates that the regulation of RAGE signalling is important in embryonic stem cell differentiation, and has a potential role in early embryo development.

At the time of writing, the process of fertilisation within an AGEs-rich environment has not been examined. With elevation of AGEs in the uterine fluid of obese women, sperm ascending the female reproductive tract are open to assault by AGEs, which may influence their motility and capacitation, though evidence suggests short term exposure to glycating agents has limited effects on human sperm function (Nevin et al., 2018). Levels of AGEs within the Fallopian tube are unknown, but may potentially affect the site of oocyte fertilization and development to morula. *In vitro* studies of fertilization may shed light on the effects of AGEs on this critical interaction and subsequent development. Uterine fluid is a conduit for maternal-fetal interactions, and elevated levels of AGEs within this fluid microenvironment may detrimentally impact blastocyst hatching and development. AGEs-modified BSA and glyoxal increased cellular fragmentation and significantly reduced the proportion of rat embryos forming blastocysts *in vitro* (Hao et al., 2008). These studies utilized naturally-mated embryos, hence conclusions cannot be drawn as to effects of AGEs on fertilization.

Preimplantation embryos *in vivo* also show detrimental development in an AGEs-rich environment. In a rabbit model of maternal diabetes, AGEs were elevated in the blood plasma and endometrium of the rabbits, and critically both AGEs and RAGE accumulated significantly more in the embryonic cells and blastocoel fluid compared to embryos derived from control animals (Haucke et al., 2014). Aberrant AGEs accumulation and RAGE signalling, or exposure to an AGEs rich environment may compromise early embryo development. This provides the first major research aim of this thesis (Chapter 3).

Recent research also demonstrates a lasting effect on offspring after *in utero* exposure to elevated AGEs (Merhi et al., 2020). Following a maternal diet rich in AGEs, mouse offspring were born early, exhibited a low birth weight, and delayed reproductive parameters. Subsequently, adiposity, folliculogenesis, and steroidogenesis were detrimentally impacted, even though the offspring themselves had a low AGE diet (Merhi et al., 2020). This implies that elevated maternal AGEs may result in epigenetic programming which impacts the reproductive system in female offspring.

1.8.5.3 RAGE and AGEs in the uterus: implications for embryo development and implantation

AGEs and additional ligands for RAGE (CML, HMGB1) accumulate within the endometrium and the uterine fluid (Antoniotti et al., 2018; Bhutada et al., 2014). AGEs are located in the stromal and epithelial cells of the human uterus, exacerbated by obesity. AGEs are also present within uterine fluid and in obese infertile women, their levels are four-fold higher than in the uterine fluid of lean, fertile women (Antoniotti et al., 2018). *In vitro*, concentrations of AGEs equimolar with the obese uterine environment reduced endometrial epithelial cell adhesion and proliferation, and reduced the adhesive and invasive capacities of trophoblast and trophoblast cells (Antoniotti et al., 2018), likely reducing implantation competence. Furthermore, HMGB1 can induce proinflammatory responses and cytokine secretion by activation of RAGE and TLR4. Its interaction with RAGE may contribute to the control of timing of implantation, as it is elevated in the non-receptive phase of the menstrual and estrous cycles, and application of exogenous HMGB1 reduces the implantation of rat embryos into the endometrium (Bhutada et al., 2014).

Elevated AGEs appear to increase the extent of decidualisation (reflected in elevated PRL expression) maybe leading to an altered ratio between senescent and decidual cells, which in turn may limit recruitment of uNK and thus poor decidual remodelling (Brighton et al., 2017). Indeed uNK have previously been identified as negatively impacted by obesity (Perdu et al., 2016), perhaps linked through AGEs. Additionally, elevated RAGE has been identified in the follicular and peritoneal fluid from women with endometriosis (Fujii et al., 2008), and in endometrial stromal cells from women with endometriosis (Sharma et al., 2010). RAGE has been identified in both eutopic and ectopic endometrial biopsies, indicating the involvement of the AGE-RAGE signalling axis in proinflammatory endometrial pathologies (Fujii et al., 2008; Shimizu et al., 2017).

1.8.5.4 The placenta: AGEs may affect establishment and continuation of pregnancy

Proper formation and function of the placenta is vital for a healthy pregnancy, coordinating nutrient and waste exchange. Low level AGEs may be tolerated during pregnancy; indeed, RAGE may contribute to the inflammatory cascade of implantation and placentation, but perturbations may be linked to preeclampsia and recurrent pregnancy loss.

The human placenta and gestational tissues are able to respond to AGEs *ex vivo*, and RAGE signalling through a number of pathways, which activate proinflammatory pathways and the secretion of chemokines through NFκB and ERK1/2 signalling (Lappas et al., 2007). In isolated first trimester trophoblasts, AGEs increased the secretion of the chemokines MIP1-α and MIP1-β approximately 3-fold, increased apoptosis, and reduced the secretion of hCG. The elevated chemokine secretion was reversed using antiaminoguanidines and namafostatin which inhibit nitric oxide synthase and NFκB respectively (Konishi *et al.*, 2004). Additionally, in SW61 trophoblast cells, AGEs activated both JNK and ERK signalling pathways, and elevated the secretion of pro-inflammatory cytokines TNFα, and IL-1β (Alexander et al., 2016; Shirasuna et al., 2016).

1.8.5.4.1 Evidence of AGEs in miscarriage and recurrent pregnancy loss

Miscarriage and recurrent pregnancy loss (RPL: loss of three or more pregnancy losses under 20 weeks of gestation) affect a significant number of clinical pregnancies (15% and 1%, respectively (Rai and Regan, 2006; Wu et al., 2017)), but the aetiology of these conditions is poorly understood. Whilst RAGE is downregulated in the sera of RPL patients (Wu et al., 2017), serum levels of sRAGE were 1.5 times the level of control patients (Ota et al., 2014). Further, in the placentas from pregnancies that resulted in still birth, the prevalence of CD163⁺ macrophages expressing RAGE was significantly elevated, whilst overall RAGE protein expression was reduced in the placenta (Kerby et al., 2021). Together these data imply a dysregulation of physiological AGEs-RAGE signalling associated with RPL.

1.8.5.4.2 Evidence of AGEs in preeclampsia

Whilst pregnancy itself does not increase the concentration of AGEs in the serum, preeclampsia is associated with two-fold elevated serum AGEs and AGEs accumulate in the preeclamptic placenta, particularly in the syncytiotrophoblast and the endothelial cells (Chekir et al., 2006). Additionally, RAGE protein and mRNA are elevated in the preeclamptic placenta versus healthy placenta (Alexander et al., 2016).

AGEs demonstrate a dose-dependent relationship with numerous factors associated with preeclampsia. Treatment of HTR8/SVneo extravillous trophoblast cells with AGEs resulted in increased s-Flt1, VEGF, and ROS production, effects mitigated using a neutralizing antibody against RAGE, and apocynin, which inhibits NADPH oxidase (Huang et al., 2013). This implicates the RAGE signalling axis as important in the aetiology of preeclampsia. Likewise, in the human trophoblast cell line, BeWo, elevated AGEs significantly compromised tight junction integrity, partially reversed by an inhibitor of RAGE and NFκB (Y. Shi et al., 2020)

Independent to the trophoblast, AGEs disturb vascular systems in general, contributing to the pathology of preeclampsia (Guedes-Martins et al., 2013): elevated serum AGEs and CML correlate to

increased vascular and arterial stiffness independent of other factors in large vessel hypertension (McNulty et al., 2007; Semba et al., 2009). RAGE is significantly elevated in the myometrial blood vessels of women with preeclampsia, beyond the elevation seen in healthy pregnancy (Cooke et al., 2003). Within the umbilical cord blood, pentosidine (a form of AGEs) was moderately, yet significantly, elevated in women with preeclampsia and positively correlated with birthweight, a significant observation as altered birthweight could set the child up for a lifetime of altered health consequences (Tsukahara et al., 2004).

The soluble receptor for RAGE (sRAGE) acts as a decoy receptor, binding RAGE ligands, thus modulating RAGE signalling. Perturbations of sRAGE expression may lead to exacerbation or suppression of RAGE signalling, resulting in downstream complications. For example, in women with type 1 diabetes, a reduced level of sRAGE is associated with later development of preeclampsia (Yu et al., 2012). Conversely, sRAGE is elevated in severe preeclampsia both in maternal serum and amniotic fluid, and is proposed as overcompensation for elevated RAGE signalling (Oliver et al., 2011). In addition, ligands for RAGE including HMGB1 and S100A12 are elevated in the maternal serum of women with early and late onset preeclampsia (Naruse et al., 2012). Cumulatively, this provides further evidence that the AGEs-RAGE signalling axis plays an important role in the maintenance of healthy pregnancy with alterations of signalling associated with pathological conditions including preeclampsia.

TLR4 expression is evident in the healthy first trimester and term placenta, but is increased in the placenta from women with preeclampsia (Pineda et al., 2011). Physiological activity of TLR4 may be a response to inflammatory stimuli from the maternal environment. Low level activation of TLR4 by LPS in a rodent model resulted in the development of preeclampsia, attenuated by the curcumin inhibition of TLR4 (Fan et al., 2019; Gong et al., 2016), supporting the idea that TLR4 stimulation by elevated AGEs may contribute to the development of this pathology.

1.8.5.5 AGEs influence the outcome of ART

The female contribution of elevated AGEs to outcomes of ART have been examined in a number of studies. Increased AGEs in follicular fluid correlates with reduced number of collected and fertilized oocytes, their fertilisation and production of high quality embryos (Yao et al., 2018) whilst sRAGE in follicular fluid inversely correlates with the amount of gonadotrophins required for ovulation (Merhi et al., 2014). Furthermore, increased intrafollicular sRAGE correlated to poor quality embryos on day 2 and day 3 following ICSI (Bonetti et al., 2013). However, this study would have been more convincing if day 5 morphology and Gardner grading (Gardner et al., 2000a) had been applied. Finally, elevated serum AGEs correlate with reduced live birth outcomes following IVF (Jinno et al., 2011).

1.8.5.6 Maternal AGEs and offspring outcome

The Barker hypothesis, now termed Developmental Origins of Health and Diseases (DOHaD), states that prenatal exposure to toxins may set the offspring up for a lifetime of health or disease (Barker, 1995). It is now understood that prenatal epigenetic modifications mediated by the maternal environment have lifetime consequences for health. Thus, prenatal exposure of the embryo and developing fetus to excessive concentrations of AGEs may lay the foundation for altered development and long-term health.

Following the development of a haemochorial placenta, the fetus is dependent on the maternal bloodstream as a source of nutrition, and may be exposed to maternal AGEs. Indeed, serum AGEs in the mother correlate with serum AGEs in newborns, and elevated AGEs transferred by the mother may predispose offspring to the development of diabetes. Indeed maternal serum CML is related to increased insulin resistance and adiponectin levels in the offspring (Meriq et al., 2010).

The embryo is also exposed to AGEs within the uterine fluid prior to implantation, particularly in obese women (Antoniotti et al., 2018). Whilst preimplantation embryo development in such an AGEs rich environment is not well understood, and is explored in chapter 3 of this thesis, recent research demonstrates a lasting effect on the offspring of *in utero* exposure to elevated AGEs (Merhi et al., 2020). Following a maternal diet rich in AGEs, mouse offspring were born early, exhibited a low birth weight, and delayed reproductive parameters. Offspring adiposity, folliculogenesis, and ovarian steroidogenesis were also detrimentally impacted, even though the offspring themselves followed a low AGEs diet (Merhi et al., 2020). In another rodent model, elevated AGEs in maternal diet during pregnancy and before weaning of the offspring resulted in an increased bodyweight of young adult male offspring and earlier demonstration of key reflexes indicative of neuronal development (Csongová et al., 2018). These effects continued through development, with offspring exposed to high maternal AGEs demonstrating memory and behavioural differences compared to those not exposed to maternal AGEs (Csongová et al., 2019). This implies that maternal AGEs may result in epigenetic programming which impacts offspring development.

In addition to epigenetic programming propagating the effects of AGEs proposed by Merhi *et al.*, (2020), maternal levels of AGEs directly influence offspring AGEs following gestation: AGEs can be transferred from mother to child through lactation (Meriq et al., 2010). Lactation is an important process by which offspring accumulate critical maternal factors which influence their lifetime immunity and growth trajectory, as demonstrated in the Tammar wallaby (Trott et al., 2003). Francisco et al. (2018), using a rodent model in which lactating female rats were exposed to methylglyoxal (significantly altered milk composition in relation to glyucose, insulin, cholesterol, triglycerides, and fructosamine concentrations), demonstrated that offspring had higher final bodyweight, altered fat

storage, and lipid profile. Of significance, offspring had elevated blood glucose, coupled with impaired glucose tolerance and insulin sensitivity, indicative of a diabetic phenotype in the offspring.

1.8.6 Current interventions to remediate AGEs induced damage

Therapeutic interventions targeting AGEs can be placed into three broad categories: prevention of formation or accumulation, inhibition of signalling, and remediation of downstream effects. Therapeutics can act in multiple ways, and it is important to understand the role of AGEs within a particular disease to enable selection of the most appropriate approach. Many inhibitors of these signalling pathways and downstream effects are known: vitamin D (Merhi, 2019), metformin (Tanaka et al., 1999), antioxidants (Thieme et al., 2016), and statins including pravastatin (Ishibashi et al., 2012). For a review of anti-AGEs compounds, see Nenna et al. (2015). Most of these have not yet been tested in the context of early pregnancy.

1.8.6.1 Prevention of formation and accumulation

As exogenous AGEs can be consumed through diet and absorbed into the body (Koschinsky et al., 1997), dietary intervention is a promising first-line defence against AGEs accumulation in the body. Kellow and Savige (2013) performed a systematic review and meta-analysis of a low AGEs diet in healthy and diabetic individuals and found limited evidence that a low AGEs diet would be beneficial in improving inflammatory profiles and oxidative stress. A more recent meta-analysis investigated obese individuals undertaking an AGEs restricted diet; if continued for greater than 8 weeks, weight-loss and an improvement in leptin and adiponectin profiles were reported (Sohouli et al., 2020). Such low AGEs diets are beneficial in improving hormonal profiles in women with PCOS. In addition to low dietary AGEs, caloric restriction and weight-loss significantly impact serum AGEs. For example a low fat and low calorie diet resulted in approximately 10kg weight-loss coupled with 17% reduction in serum CML (Deo et al., 2017). While these data are promising, the effect of dietary AGEs restriction on the reproductive tract has not yet been investigated, and further study is required to understand the efficacy of such intervention on obese women.

To reduce the accumulated AGEs, or prevent accumulation following other therapeutic interventions, a crosslink breaker such as Alagebrium (ALT711) can be applied. The reduction in AGEs-related collagen crosslinking mediated by Alagebrium improved vascular stiffness in a rodent model of diabetes (Wolffenbittel et al., 1998), which may be beneficial for the process of endometrial remodelling as indicated previously. Some AGEs effects on mitochondrial stress including superoxide production, can be relieved by treatment with Alagebrium (Coughlan et al., 2007). Such AGEs-reducing therapies may be of benefit in conjunction with dietary AGEs restriction.

1.8.6.2 Inhibition of AGEs signalling

Once AGEs have accumulated within tissue or are elevated within the bloodstream, the next therapeutic option is to block their signalling. As previously discussed, RAGE and TLR4 present two major signalling pathways of AGEs ligands.

In a pig model of acute respiratory distress, intravenous application of a RAGE antagonist peptide or recombinant soluble RAGE (acts as a decoy receptor) successfully reduced several parameters including tissue histology and inflammation: IL1 β , IL6, IL8, and TNF α were significantly reduced by both treatments (Audard et al., 2019). These authors suggested further investigation using small molecular antagonists such as FPS-ZM1 (used in this thesis), and highlighted that the long-term effects of RAGE antagonism were not investigated.

Deane et al. (2012) identified FPS-ZM1 to be a highly specific RAGE antagonist which was non-toxic to mice, and permeable across the blood-brain-barrier. It has been successful in reducing mouse neuroinflammation and RAGE-mediated influx of amyloid beta peptides associated with Alzheimer's disease into the brain, and reduced proinflammatory activation of NF κ B both *in vitro* and *in vivo* (Deane et al., 2012; Shen et al., 2017). Clinical trials of RAGE antagonism as a treatment for Alzheimer's disease demonstrated drug safety, but mixed therapeutic efficacy (Walker et al., 2015). In the reproductive tract, RAGE and TLR4 antagonism similarly reduced the secretion of proinflammatory cytokines in AGEs-treated trophoblast cells *in vitro* (Shirasuna et al., 2016). Together this data supports RAGE antagonism as a promising avenue for remediating AGEs induced effects. Further studies are required on RAGE antagonist pharmacokinetics and the efficacy of this treatment on reproductive disorders associated with obesity.

1.8.6.3 Remediation of downstream effects

The final but least favourable option in alleviating AGEs effects, is to repair or minimise cellular damage by targeting pathways and mechanisms downstream of AGEs signalling molecules. These include inhibition of ER stress, ROS production, and apoptosis. ER stress appears to be a significant mediator of AGEs-induced damage. Knockout of TLR4 in mice prevented weight gain and upregulation of ER stress and downstream signalling molecules following 18 weeks of a high fat diet (Pierre et al., 2013). Additionally, metformin and specific antioxidants can alleviate AGEs induced cellular stress: in trophoblast cells N-Acetyl-L-Cysteine (NAC) reduced secretion from AGEs treated trophoblast cells (Shirasuna et al., 2016). An added benefit of metformin as a therapeutic is its potential to reduce the *de novo* formation of AGEs (Tanaka et al., 1999). Further information on the therapeutics tested in this thesis (RAGE antagonist FPS-ZM1, metformin, and antioxidants (Truong et al., 2016)) is provided in Sections 2.3.2.4 and 4.4.1.

1.9 Summary and conclusions

It is clear that obesity-associated AGEs within the uterine fluid microenvironment have the potential to negatively impact the endometrium and the blastocyst on a cellular level. The elevated concentrations of inflammatory molecules and AGEs in the 'obese' uterine environment may further affect the receptivity of the endometrium and alter preimplantation blastocyst development, and potentially placentation. These findings clearly require more comprehensive molecular investigation to determine the potential mechanisms of action of elevated AGEs in reducing establishment and continuation of pregnancy in an 'obese' uterine environment.

In obese women there is an increased loss of genetically euploid embryos (Tremellen et al., 2017), and an increased loss of embryos derived from oocytes donated by normoweight women (Bellver et al., 2013b, 2007). Furthermore obese women experience reduced implantation rates, and increased numbers of pregnancy complications such as recurrent pregnancy loss (Bellver et al., 2007; DeUgarte et al., 2010; Provost et al., 2016). Thus, there is a need for further studies examining the mechanism by which AGEs may impact these processes. Indeed AGEs are highly pro-inflammatory moieties which are associated with poor endometrial cell function (Antoniotti et al., 2018), and poor reproductive outcomes following assisted reproduction (Jinno et al., 2011).

Overall, there is significant evidence that elevated maternal AGEs are detrimental to fertility and long-term offspring health. Reproductive AGEs present a novel aspect of preconception health which provide new avenues for clinician-led counselling of obese couples wanting to conceive.

1.10 Thesis aims and hypotheses

The overall hypothesis underpinning this thesis, proposed that the detrimental effects of obesity on establishing pregnancy in women are mediated at least in part by AGEs, providing a potential target for new therapeutics that will mitigate AGEs-induced effects. The specific hypotheses and aims were based on literature available at the commencement of this candidature (June 2017) but were adjusted accordingly as research proceeded. Organoid culture was initially established in this laboratory in late 2019 and further developed here to provide a valuable mechanism of primary cell validation of research.

1.10.1 Overall aim

To examine in the context of physiologically relevant concentrations of AGEs, preimplantation embryo development, embryo adhesive capacity and endometrial receptivity. Further, to identify and examine potential therapeutic interventions to remediate observed and previously published effects of AGEs on embryo development and endometrial cell function.

1.10.2 Specific aims

1.10.2.1 Aim 1: Examining the effect of the obese uterine environment on pre-implantation embryonic development.

Preimplantation development was assessed within the context of AGEs levels equimolar with those within the obese uterine cavity. This work specifically investigated:

1. Embryo development (morphokinetics)
2. Cell specification to trophoctoderm or inner cell mass
3. Apoptosis of embryonic cells
4. Implantation potential: blastocyst outgrowth

After characterizing the effects of AGE on preimplantation embryonic development, potential therapeutic interventions were examined by co-culturing embryos in media containing obese levels of AGEs and treatments targeting the cellular stress caused by AGEs, specifically:

1. Antagonism of AGEs related receptors (RAGE)
2. Metformin
3. Antioxidants (Truong et al., 2016)

1.10.2.2 Aim 2: Investigating pharmaceutical intervention to remediate the effects of AGEs on the human endometrial environment

This aim was to replicate the previous findings within the Salamonsen laboratory that AGEs impacted endometrial cell functions including: epithelial cell adhesion and proliferation, stromal cell decidualisation, and trophoblast adhesion and invasion. Therapeutics outlined in aim 1 were to be utilised to normalise these cell functions.

1.10.2.3 Aim 3: Optimisation of human endometrial epithelial organoid culture to validate the effects of AGEs on human endometrial epithelium

Novel organoid culture systems enable long term culture of primary human endometrial epithelial cells. This thesis aimed to determine the following:

1. Validation of our human endometrial organoid culture compared to published data and confirmation of the retention of characteristics from donor endometrium.
2. Confirmation that epithelial cells can be retrieved from organoid culture and provide sufficient numbers to be used in functional analysis.
3. Assessment of impact of obesity-associated AGEs on organoid-derived cell adhesion and proliferation.

1.10.2.4 Aim 4: Characterization of the proteins of the human adhesome and endometrial epithelial receptome and investigation of the effects of AGEs

This work confirmed and further characterized the relative importance of novel protein biomarkers of endometrial receptivity and embryo adhesion identified in this laboratory (Evans et al., 2020a) to provide groundwork for future investigation in the context of obesity-associated AGEs. While beyond the scope of this thesis, it was hypothesized that AGEs will affect endometrial receptivity and blastocyst adhesion by altering the expression of proteins in the epithelial receptome and endometrial adhesome. This aim was addressed by the following methods:

1. Immunolocalisation of receptome and adhesome proteins in the human endometrium across the menstrual cycle in both fertile and infertile women.
2. Generation of spheroid-monolayer interface sections to immunolocalise adhesome proteins and validate their presence in this model.
3. siRNA knockdown of individual proteins and assessment of spheroid adhesion, and tight junction regulation.

Should circumstances have been normal during the final year of my candidature (2020), the expression of validated receptome and adhesome proteins would have been investigated in the endometrium of obese women compared to lean, and in epithelial cells co-cultured with physiologically lean and obese concentrations of AGEs. Addition of therapeutics would have attempted to mitigate any AGEs induced effects on the expression of receptome proteins in epithelial cells and adhesome proteins at the maternal-fetal interface. Loss of access to fresh clinical material due to the COVID-19 pandemic, made this impossible.

1.11 Translational impact of this research

Collectively these studies will provide critical information of the mechanisms underpinning embryo development, endometrial receptivity and embryo implantation, and particularly how an altered endometrial environment, characterized by high AGE levels, may detrimentally impact each of these and how potential treatments to reduce or block AGEs actions may mitigate these negative effects. The work aimed to generate data which may be translated to the clinic to improve fertility and ultimately both pregnancy and offspring outcomes in women with metabolic disorders.

1.12 Necessity and significance of this study

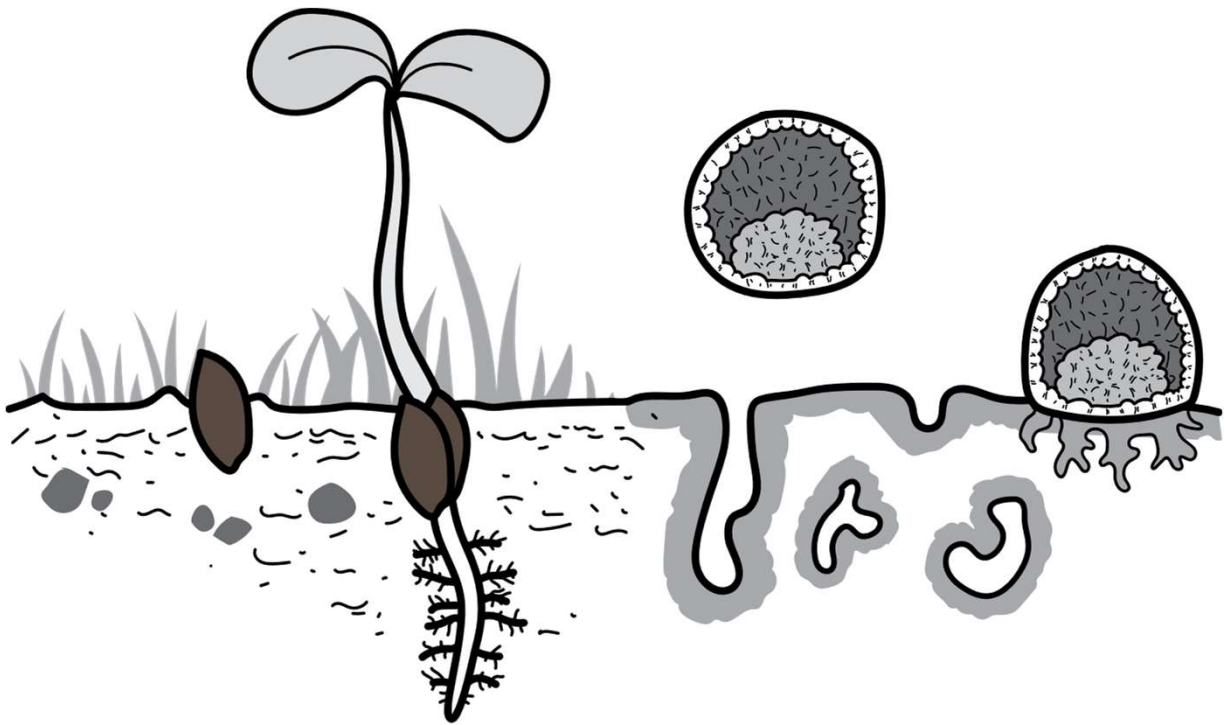
Many papers finding a significant link between obesity and poor reproductive outcome recommend women wishing to become pregnant adopt a “healthy lifestyle” or reduce their weight by “any means necessary” before conception (Bellver et al., 2013b, 2007, 2003; Boots et al., 2014; DeUgarte et al., 2010). Whilst maintenance of a healthy weight should be encouraged, and it is acknowledged that

weight-loss improves the reproductive outcomes of obese women (Best et al., 2017; Broughton and Moley, 2017), weight-loss as an initial and blanket prescription does not take into consideration underlying factors that influence reproduction, and to which obese women are more prone. Dietary action for obesity takes a long time to reduce weight and for some can be extremely difficult. With the increasing age of first-time mothers, it is important to remember that any intervention for fertility is fighting against the ticking of the biological clock, and therefore for an obese woman in her mid-late 30's, therapeutic interventions for obesity-related infertility are needed to maximise the time she has to achieve pregnancy. AGEs have a long half-life, particularly evident in the glycation of extracellular matrix proteins, and so even after weight has been lost, they may still exert their detrimental effects on the endometrium and the embryo, making it is critical to understand their mechanisms of action and potential interventions. Finally, it is essential to remember that underpinning obesity there are many physical, financial, and psychological factors which are private and specific to an individual, and that must be respected at all times. Obesity should be treated as a condition from which a patient suffers, the effects of which can be reduced or remediated using fertility interventions, and scientific research performed without judgement or trivialisation.

As an increasingly large proportion of the global population suffer from obesity and obesity-related infertility, this study has the potential to impact many people worldwide. Understanding the mechanisms underpinning effects of obesity on embryonic development and endometrial receptivity could lead to novel targets for fertility. By normalising altered factors within the obese endometrium, we can improve ART outcomes for these women.

Chapter 2:

Optimisation of materials and methods used in this thesis



Chapter 2: Optimisation of materials and methods

This chapter describes methods widely used in the following chapters, and those for which preliminary experimentation and optimisation was performed.

Ethical approvals

All mouse experimentation (Chapter 3) was approved by the Ethics Committee of the University of Melbourne (#1814430).

Ethical approval for human tissue collection (Chapters 4-6) was obtained from Institutional Ethics Committees at Monash Health (#03066B) and Monash Surgical Private Hospital. Following detailed explanation, written informed consent was obtained from each patient prior to tissue collection by a research nurse.

2.1 Data representation and statistical analysis

Unless otherwise stated, all data representation and analyses were performed using GraphPad Prism (Version 9.0), and data presented as mean \pm SEM. Individual dot points represent independent replicates. $P < 0.05$ was considered to be statistically significant.

All data were subjected to the Shapiro-Wilks normality test before statistical analysis. Data with three or more groups were assessed with a one-way ANOVA (normal distribution), or a Kruskal-Wallis test (data not normally distributed) followed by appropriate post-hoc testing. Data containing only two groups were assessed using a Student's t-test (normal distribution) or Mann-Whitney U-test (data not normally distributed).

Multiplex cytokine and chemokine (Luminex) analyses were conducted using a two-way ANOVA with repeated measures. Samples below the limit of detection were assigned a value of half the lowest detected concentration, and samples above the limit of detection assigned double the highest detected concentration, so that statistical analysis could be performed, a method previously reported (Fitzgerald et al., 2016).

2.2 *In vitro* generation of AGEs

Advanced Glycation Endproducts (AGEs) were prepared as described previously (Antoniotti et al., 2018). In brief, 10 mg/mL human serum albumin (HSA, Sigma) in 0.2 M Na₂HPO₄ (Sigma) buffer pH 7.5 containing 0.5 M D-glucose (Sigma) was sterile-filtered before incubation under aerobic conditions at 37°C for 3 months. Excess glucose was removed by dialysis against pH 7.5 phosphate buffered saline (PBS) at 4°C with regular buffer changes (twice daily for 48 h), using Snakeskin™ dialysis tubing (Thermofisher) with a high molecular weight cut off. AGEs were again sterile filtered, and endotoxins

depleted using Detoxi-Gel™ Endotoxin Removing Resin (Thermofisher). Resultant solutions were stored at -80°C until required.

Table 2.1: Concentration of AGEs as determined by ELISA assay. The concentration of AGEs in the original and new preparations of AGEs-HSA. No AGEs were detected in the HSA control solutions (n.d.: not detected).

| | AGEs-HSA (original) | HSA control (original) | AGEs-HSA (new) | HSA CONTROL (new) |
|----------------------|--------------------------------|-----------------------------------|---------------------------|------------------------------|
| Concentration | 72.98 µg/mL | n.d. | 30.31 µg/mL | n.d. |

The concentration of AGEs was measured using a commercial AGEs ELISA assay (Abcam #238539, range 0.36-100 µg/mL). The concentration of AGEs generated previously (Antoniotti et al., 2018) and for this study were determined as per manufacturer's instructions. All samples were assayed in triplicate, and AGEs were not detected in the co-incubated HSA control (Table 2.1). Both solutions of AGEs were compared using xCelligence to ensure consistency in biological effect. ECC-1 were hormonally primed in the presence of 'lean' and 'obese' concentrations of AGEs and adhesion and proliferation assessed for a period of 48 h (Section 2.4.1.4). Pilot data indicated that newly prepared AGEs, when applied at an equivalent concentration, elicit the same anti-adhesive and anti-proliferative effect (approximately 40% reduction across various time points, data not shown) as the previous batch of AGEs, thus confirming their appropriate biological activity for use. Sufficient quantity of original AGEs-HSA was available for aim 1 (Chapter 3), with the newly prepared batch used for aims 2 and 3 at an equivalent concentration.

The concentrations used by Antoniotti *et al.* (2018) to represent the lean and obese uterine fluid were 2 µmol/mol lysine, and 8 µmol/mol lysine respectively (herein referred to µmol). The equivalent concentrations of the recently prepared batch of AGEs are 0.73 µg/mL and 2.9 µg/mL AGEs respectively, the concentration of lysine was not measured in these samples.

2.3 Obesity associated AGEs and the preimplantation embryo

To examine the effects of obesity-related AGEs on preimplantation embryo development, mouse embryos were cultured for up to five days in the presence of physiologically relevant concentrations of AGEs prior to use in a number of experimental methodologies assessing preimplantation development and function. Presented here is the optimisation of several techniques and the standard protocols required. Additional methods are presented in Chapter 3.

All mouse experimentation and imaging were performed at the University of Melbourne.

2.3.1 Standard protocols

2.3.1.1 Embryo generation

F1C57 X CBA mice (Florey Institute, University of Melbourne) were housed in a 12-hour light/dark cycle and given food and water ad libitum. Follicular maturation in virgin 3- to 4-week-old female mice was stimulated by administration of 5 international units (IU) of pregnant mare serum gonadotrophin (PMSG; Intervet). To induce ovulation 48 h later, female mice were administered 5 IU human chorionic gonadotrophin (hCG; Chorulon Intervet) before mating overnight with male mice less than one year of age. After 21.5 h, female mice were checked for the presence of a vaginal plug as an indicator of mating and euthanised by cervical dislocation.

Isolation of pronucleate oocytes from the oviduct ampullary region was performed under an SMZ 1500 dissection microscope (Nikon, USA) with a heated stage (Tokai Hit, Japan) to maintain approximate physiological temperature. Unless otherwise specified, this temperature was continued for experimental protocols. Tubal ampullae were dissected and placed in pre-warmed G-MOPS™ Plus media (Vitrolife) for embryo collection. In a fresh 500 µL drop of G-MOPS™ Plus, ampullae were opened using fine forceps and embryo-cumulus cell complexes expelled into the media. 500 µL hyaluronidase (final concentration 300 IU/mL; Sigma) was added to the G-MOPS™ Plus droplet to remove the cumulus cells. Denuded embryos were washed in G-MOPS™ Plus three times prior to allocation to culture treatments. Pronucleate embryos were selected on the presence of 2 pronuclei, a tight zona pellucida, co-localised polar bodies, and the absence of degeneration. Embryos from multiple animals were pooled to reduce variability.

Unless otherwise stated, embryos were cultured in 60 mm dishes (Falcon, Corning LifeSciences) in groups of 10 in 20 µL G-1™ Plus droplets containing experimental treatments under an OVOIL (Vitrolife) overlay in a 60 mm dish (Falcon, Corning LifeSciences) and incubated at 37°C under 5% O₂, 6% CO₂, 89% N₂ in a Sanyo incubator. Embryos were cultured in G-1™ Plus medium for 48 h, then transferred into G-2™ Plus media for a further 24 h (experiments requiring day 4 blastocysts) or 48 h (day 5 blastocysts).

2.3.1.2 Cell lineage allocation

To assess allocation of cells to the inner cell mass (ICM) or trophectoderm (TE) in blastocysts, differential nuclear staining was performed following termination of culture on day 4 or 5, per standard protocols (Hardy et al., 1989; Kelley and Gardner, 2016). All steps were performed on a heated stage, and embryos were rinsed in G-MOPS™ Plus between all steps. The zona pellucida was removed by 5-minute incubation in 0.5% Pronase (Sigma) in G-MOPS™ Plus (Vitrolife), before thorough rinsing in G-MOPS™ media. TE cells were labelled with 10%

trinitrobenzenesulfonic acid (TNBS, Sigma), 10% polyvinyl pyrrolidone (PVP, Sigma) in simple G1 media (prepared in house). After thorough rinsing, embryos were incubated in anti-dinitrophenyl antibody (anti-DNP, Sigma) for 10 min. TE membranes underwent complement mediated lysis, and TE nuclei were visualised by incubation in 10 µg/mL propidium iodide (Sigma) in guinea pig serum (Intervet). Complement reaction was observed under a microscope and considered complete once blebbing of the membranes occurred (approximately 30 seconds). All nuclei, including the ICM, were then visualised by immediate transfer into 0.1 mg/mL bisbenzimidazole (Sigma) diluted in 10% ethanol (Sigma) and incubation for 20 min under dark conditions. Embryos were washed in GMOPS PLUS™, mounted in 100% glycerol (Sigma), imaged using a Nikon Eclipse TS100 inverted fluorescence microscope fitted with a digital camera, and cells manually counted using ImageJ software (NIH).

2.3.1.3 Immunolocalisation of RAGE and TLR4

To confirm that mouse embryos express an appropriate mechanism by which to respond to AGEs, the receptors RAGE and TLR4 were immunolocalised on the day 4 blastocyst. Embryos were grown under standard group culture conditions in G1 PLUS™ media (Vitrolife) for 48 h before incubation in G2 PLUS™ media for a further 48 h. Embryos were washed three times in phosphate buffered saline (PBS, Thermofisher) and fixed in 4% paraformaldehyde (PFS; Sigma) for 15 min at room temperature. Embryos were then rinsed 3 times in phosphate buffered saline (PBS) before permeabilisation in PBS containing 0.01% Triton X-100 for 10 min. Following rinsing, embryos were blocked in PBS containing 2.5% fish skin gelatin (Sigma), 10% goat serum, and 2% mouse serum (both Thermofisher), before a final wash in 0.5% mouse serum and 1% Tween-20 (Blocking base; Sigma) and incubation in primary antibody or matched isotype control overnight (1:100 RAGE (5.94 µg/mL) and 1:100 TLR4 (10 µg/mL); both Abcam) at 4°C under humidified conditions. Embryos were rinsed 3 times in blocking base and incubated in biotinylated goat anti-rabbit secondary antibody for 90 min at room temperature before further rinsing and incubation for 45 min in streptavidin conjugated Alexa Fluor™ 488 (Gibco, Life Technologies). Subsequent incubations were performed under foil to protect from light. Embryos were further rinsed and all nuclei visualised by incubation in 0.1 mg/mL bisbenzimidazole for 10 min. Embryos were thoroughly washed, mounted in 100% glycerol and imaged using a Nikon Eclipse TS-100 inverted fluorescence microscope. Both RAGE and TLR4 showed punctate staining in the blastocyst (Figure 2.1 A and B). At the same exposure, isotype controls showed no fluorescence. Regrettably, isotype control images at a higher exposure were incorrectly taken and potential non-specific staining or autofluorescence was recorded (Figure 2.1 C). Owing to an absence of an appropriately imaged negative control, these images are not suitable for publication. Due to the low

availability of mouse embryos, and the pronounced effect of AGEs on cell lineage allocation, further immunofluorescence was not performed.

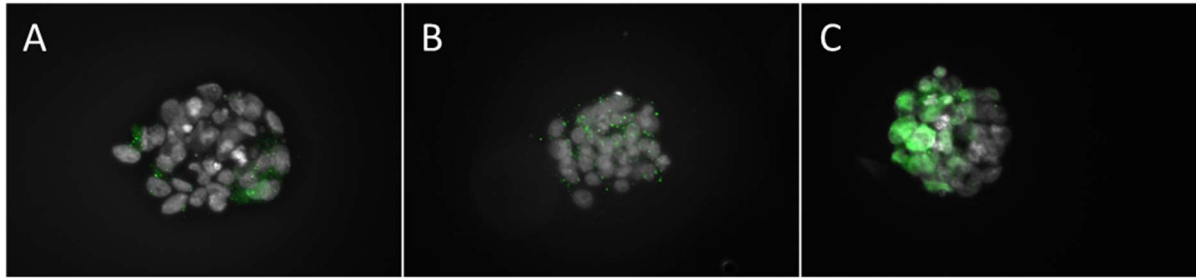


Figure 2.1: Immunolocalisation of RAGE and TLR4 in the mouse blastocyst. Mouse blastocysts express both TLR4 (A, 40 ms exposure) and RAGE (B, 40 ms exposure), demonstrating a potential mechanism by which to respond to AGEs. Isotype control (C, 300 ms exposure) showed evidence of non-specific staining or autofluorescence at a higher exposure. Green represents target fluorescence; grey represents nuclear staining.

2.3.2 Optimisation of protocols

2.3.2.1 Dose response of AGEs

To determine an effective dose of AGEs for a mouse experimental model, a dose response encompassing biologically relevant concentrations of *in vitro* prepared AGEs (as described by Antoniotti et al. (2018)) was performed. Embryo development was assessed by analysis of cell number following 5 days of culture: nuclear visualisation performed by incubation in 0.1 mg/mL bisbenzimidazole in the dark for 20 min. Following 5 days in culture, 8 μ M AGEs mediated an approximate 20% reduction in total cell number compared to culture in 0, 2, and 4 μ M AGEs (Figure 2.2; $P < 0.05$). As the difference in cell number following culture in 1 μ M AGEs compared to 8 μ M was approaching significance ($P = 0.08$), it was decided that in subsequent experiments, all doses would be utilised to elucidate the effects of a range of physiologically relevant concentrations of AGEs.

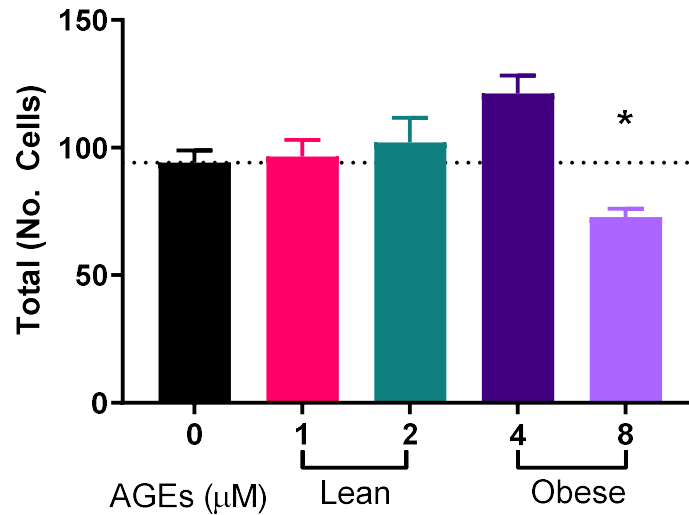


Figure 2.2: Obese concentrations of AGEs reduce total cell number. Mean \pm SEM total cell number. Following 5 days culture in 8 μ M AGEs, mouse blastocysts had significantly fewer cells than lean and control conditions. Mean in each group is the derivative of 4 biological replicates with a minimum of 44 embryos per group. One-way ANOVA: * $P < 0.05$ vs 0, 2, and 4 μ M AGEs.

2.3.2.2 Embryo developmental morphokinetics

EmbryoSlide™ Culture Dishes (Vitrolife, Sweden) were prepared by addition of 25 μ L of treatment specific G-1™ Plus media to each well, and application of a 1.5 mL OVOIL™ overlay to prevent media evaporation. Dishes were pre-equilibrated for a minimum of four hours by incubation at 37°C under 5% O₂, 6% CO₂, 89% N₂. Embryos were transferred into the EmbryoSlide™ and incubated in the Embryoscope™ (Vitrolife, Sweden) time-lapse incubator. Each EmbryoSlide™ held a total of 12 embryos (1 per well). After 48 hours, embryos were transferred to an EmbryoSlide™ containing pre-equilibrated G-2™ PLUS media with experimental conditions continued. The time taken to reach each developmental time point was determined using EmbryoViewer software (Vitrolife, Sweden), and normalised to the time of pronuclear fusion (tPNF). Times t2, t3, t4, t5, t6, t7, t8, t9+, tM, tSB, tB, tEB, tHB represent time to cleavage to 2-cell, 3-cell, 4-cell, 5-cell, 6-cell, 7-cell, 8-cell, 9 or more cells (cell borders blurring), morula (no clear cell outlines, reduced embryo volume), starting blastocyst formation (first appearance of blastocoel), blastocyst blastocoel approximately 50% of embryo volume), expanding blastocyst (blastocoel > 50% of embryo volume), and first evidence of blastocyst hatching, respectively.

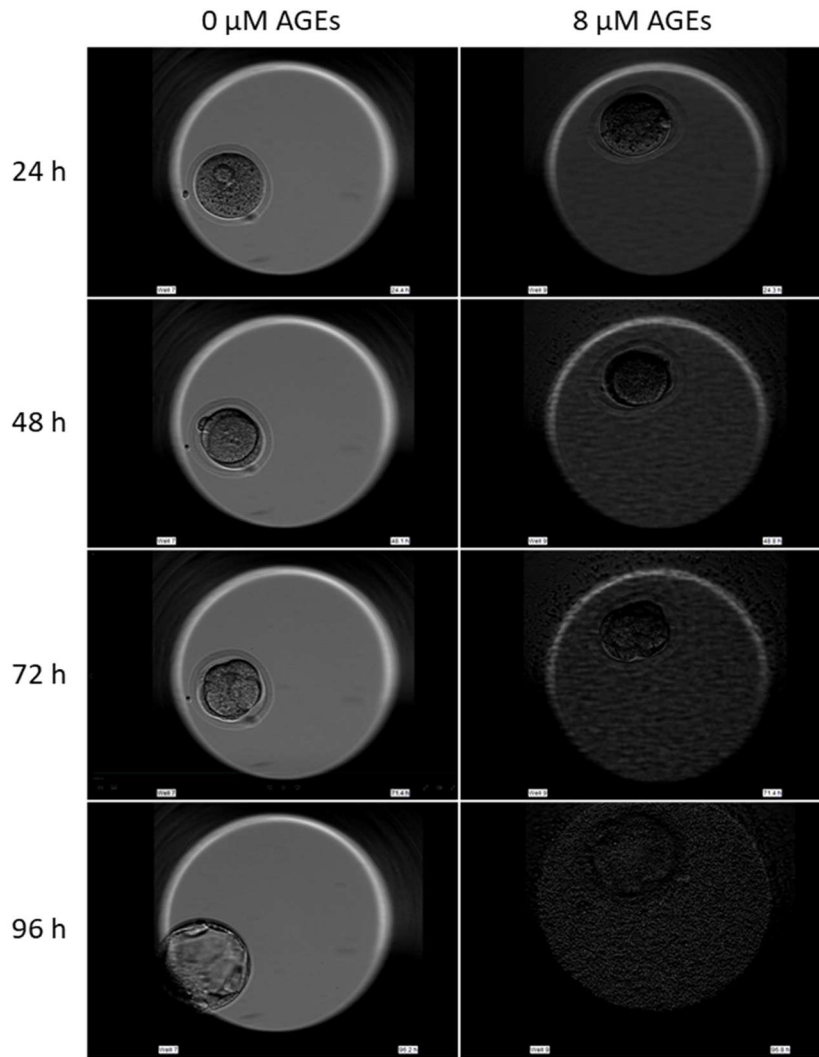


Figure 2.3: AGEs precipitate in the presence of individually cultured blastocysts. 8 μM AGEs showed steady precipitation when in the presence of individually cultured embryos. This was not evident in lower concentrations. Precipitation began after 24 h of culture, and by 72 h, it was difficult to identify precise timings of developmental stages. This was evident in wells across two biologically independent replicate experiments.

Following approximately 24-36 h in culture, a dark precipitate was observed in all wells containing 8 μM AGEs (Figure 2.3), making analysis difficult, particularly of later developmental timepoints. This was not observed in cultures containing lower concentrations of AGEs. However, preliminary data was obtained. Obese (8 μM) AGEs significantly increased the time taken to reach almost all developmental time points compared to embryos cultured in the absence of AGEs (Figure 2.4 A). While developmental timings were delayed, there was no significant impact on the rate of expansion of the blastocyst (tEB-tSB, Figure 2.4 B). Due to the potential bias caused by precipitation, this data was not presented for publication (Chapter 3). In individual culture, preimplantation embryos

may secrete factors which affect the stability of AGEs in media, resulting in this precipitation. Such precipitation was not observed in other cell culture methodologies utilised in this thesis.

Embryos incubated in individual culture for developmental morphokinetics were also subjected to differential nuclear staining to assess cellular allocation in the mouse preimplantation blastocyst using standard protocols (Section 2.3.1.2, Figure 2.4 C). AGEs equimolar to those measured in the uterine fluid of obese women significantly reduced the number of cells allocated to both the TE and the ICM when individually cultured ($P < 0.001$). This effect on the ICM was not observed under group culture after the same period of incubation in 8 μ M AGEs (Chapter 3). In group culture, it is possible that healthier embryos can secrete factors into the culture medium and stimulate growth of the less healthy embryos (Lane and Gardner, 1992). In comparison, individual culture may result in the dispersal of secreted factors with their autocrine effect being reduced (Vutyavanich et al., 2011), making these embryos more sensitive to stimuli. This may explain why this phenomenon is only evident in individually cultured blastocysts. This method of differential nuclear staining was subsequently applied only to group cultured blastocysts following 4 or 5 days in culture in physiologically relevant concentrations of AGEs.

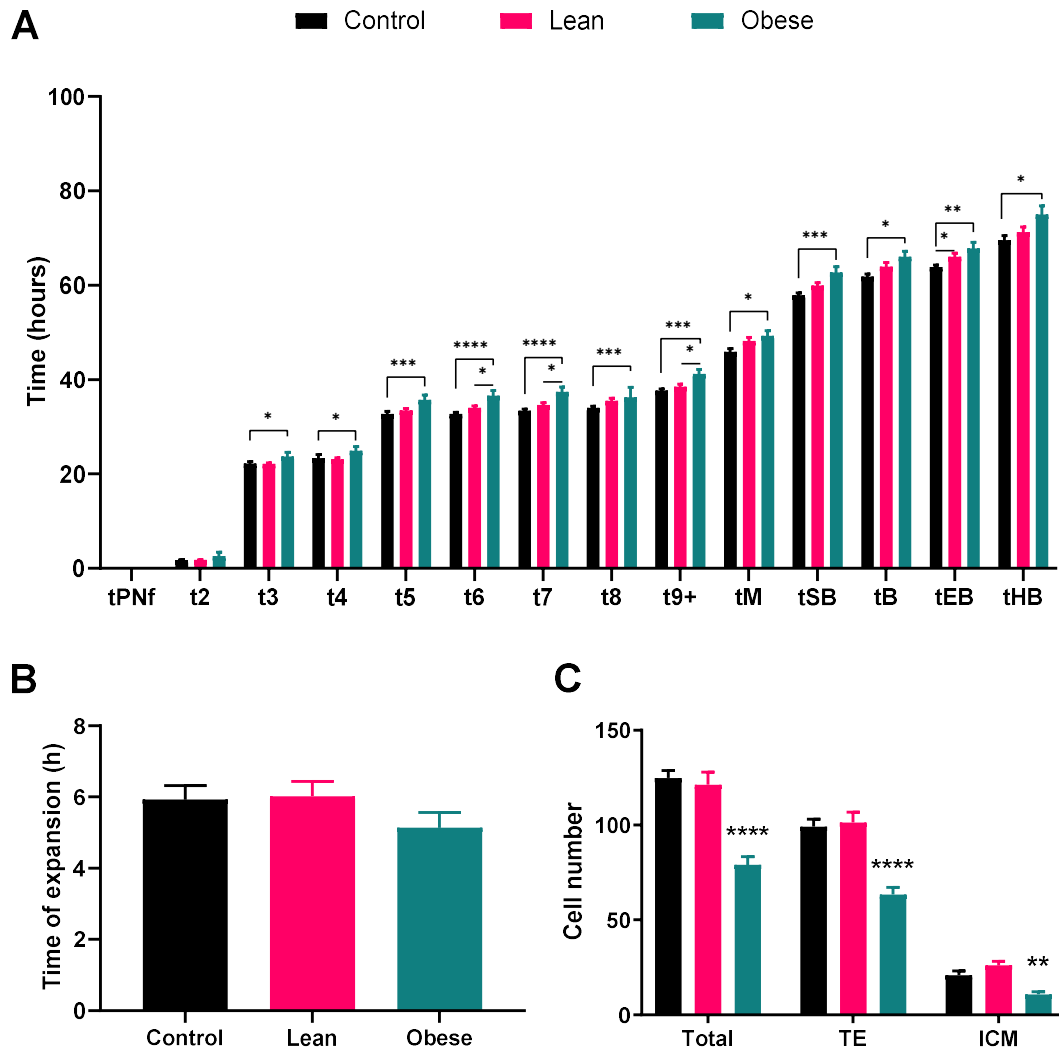


Figure 2.4: Obese concentrations of AGEs affect preimplantation embryo developmental morphokinetics and cell number. Embryos were cultured individually in AGEs equimolar to that in lean (pink, 1-2 μM) and obese (green, 8 μM) uterine fluid. Black represents untreated control conditions. Embryos cultured in obese (8 μM) concentrations of AGEs were significantly delayed in reaching all developmental milestones **(A)**. The time taken for blastocyst expansion was not significantly affected **(B)**. Obese concentrations of AGEs reduced the total number of cells in the blastocyst **(C)**, an effect seen in both the TE and ICM. For each, mean and SEM are derived from 2 biologically independent replicates, with the exception TE and ICM staining which are derived from one replicate with a minimum of 23 embryos per group. One-way ANOVA/Kruskal-Wallis: *, **, ***, **** $P < 0.5, 0.1, 0.01, 0.001$ compared to control, or bracketed group.

2.3.2.3 Blastocyst outgrowth

Following the observation that AGEs appeared to precipitate in solution following individual embryo culture, it was considered this may obscure cell borders and hinder the measurement of embryo outgrowths as these are also cultured individually. To mitigate this, cell borders were fluorescently visualised in a pilot trial (Figure 2.5). Following outgrowth on BSA and fibronectin coated plates for 96

h (Binder et al., 2015), blastocysts were fixed in 4% PFA for 15 min and stored at 4°C under 0.4% PFA overnight in a humidified chamber. Wells were rinsed 3x with PBS and incubated with 50 µL CellMask (1:1000, Thermofisher) for 45 min at room temperature. Following PBS rinsing, nuclei were visualised with bis-benzimide (Thermofisher; 5 µg/mL in PBS) for 2 min at room temperature. Outgrowths were visualised using a Nikon Ti-U Eclipse inverted fluorescence microscope with a heated stage fitted with a digital camera. Images were obtained using NIS Elements BR 3.00, SP7 imaging software (Nikon, Figure 2.5). This process resulted in loss of some blastocysts from wells. Following the first experimental replicate, it was decided that standard outgrowth measurements would be appropriate as precipitation was not noted.

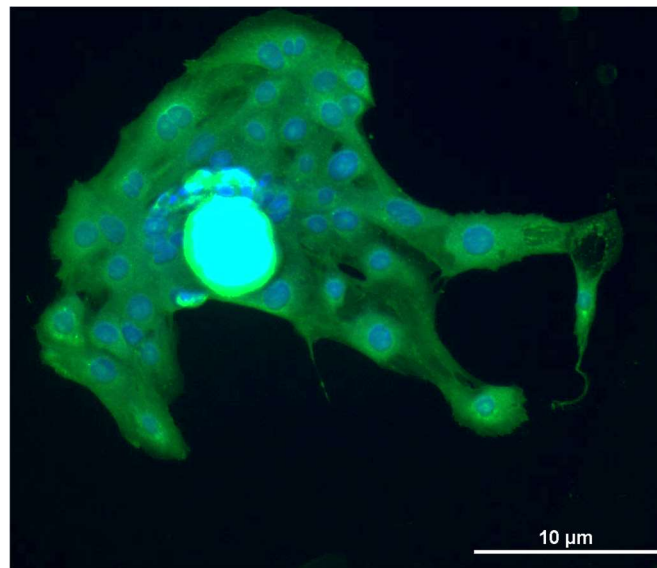


Figure 2.5: Fluorescently labelled blastocyst outgrowth. Cell membranes of outgrowing blastocysts were fluorescently labelled in an attempt to more easily determine the outgrowth area. Scale bar represents 10 µm.

2.3.2.4 Optimisation of therapeutic intervention

Embryos were to be incubated in a variety of potential therapeutics in an effort to remediate the effects of obese concentrations of AGEs. To determine the appropriate therapeutic dose of the RAGE antagonist FPS-ZM1 (Tocris), and Metformin (Sigma), a dose response in the presence of 8 µM AGEs was performed for each therapeutic. The use and optimal dose of antioxidants had previously been optimised for mouse embryo culture (Truong et al., 2016).

2.3.2.4.1 FPS-ZM1: RAGE antagonist

RAGE is a major mediator of AGEs induced damage, promoting an inflammatory response once activated (Ott et al., 2014). FPS-ZM1 is a specific antagonist against RAGE (Deane et al., 2012; Shen et al., 2017), and was selected to prevent signalling of AGEs through this receptor and hence mitigate AGEs detrimental effects. The RAGE antagonist FPS-ZM1 has previously been used in the context of

primary rat microglial cells, applied at a concentration of 25 nM (Shen et al., 2017). Doses trialled here were 12.5, 25, and 50 nM FPS-ZM1.

Following culture in 8 μ M AGEs supplemented with increasing doses of FPS-ZM1, embryos were subjected to differential nuclear staining (Figure 2.6 A). 12.5 nM FPS-ZM1 was selected as the therapeutic dose as this concentration mediated a significant increase in TE cell number compared to embryos cultured in 8 μ M AGEs alone ($P = 0.02$), but no significant effect on the ICM was observed ($P = 0.7$). Total cell number was not significantly increased in embryos treated with 12.5 nM FPS-ZM1 ($P = 0.058$).

The optimal concentration of FPS-ZM1 was redetermined in the context of cell culture in later experiments (Section 2.4.2.2).

2.3.2.4.2 Metformin

The oral anti-diabetic drug metformin has a significant positive impact on reproduction, increasing the ongoing pregnancy rate for women undergoing a repeated course of IVF, and reducing the risk of early pregnancy loss in women with PCOS (Al-Biate, 2015; Jakubowicz et al., 2014; Jinno et al., 2010). Metformin can reverse the negative effects of AGEs on osteoblastic cells, specifically oxidative stress and cell death (Schurman et al., 2008), while in aortic endothelial cells it reduces RAGE expression (Ouslimani et al., 2007). Metformin (1 - 10 μ M) applied to bovine oocytes and preimplantation embryos had no effect on embryo formation from cumulus cell oocyte complexes, but reduced embryo development past the 2 and 8 cell stage (Hong et al., 2009; Pikiou et al., 2013). In contrast, Hong et al. (2009) showed no significant effect of 10 μ M metformin on bovine embryo development to 8 or 16 cells versus control. Mouse embryos from a genetic model of obesity, had improved reproductive outcomes and blastocyst metabolism when treated with the much higher dose of 25 μ g/mL (0.19 mM) metformin (Louden et al., 2014). At 6 mM, metformin increased glucose uptake and expression of glucose transporter proteins of gestational day 8.5 mouse embryos following 12 hours of culture (Smoak, 1999). Together these data suggest metformin may be a promising therapeutic to remediate the negative effects of AGEs on mouse embryo preimplantation development.

In my preliminary testing, the dose range of Pikiou et al., (2013) was modified for mouse embryos, and doses of 0.01 nM, 0.1 nM, 1 nM, 0.1 μ M, and 1 μ M were trialled. 0.1 nM metformin significantly increased all cell parameters investigated when embryos were co-cultured in 8 μ M AGEs, compared to AGEs alone (Figure 2.6 B). This was selected as the therapeutic dose. The therapeutic concentration of metformin was reoptimized for cell culture using a dose range in accord with previous literature (Section 2.4.2.2).

2.3.2.4.3 Antioxidants

Antioxidants are beneficial to preimplantation embryo culture to mitigate oxidative stress (Truong et al., 2016; Truong and Gardner, 2017). The antioxidants contained in this cocktail, namely 10 μM N-acetyl-L-cystine, 10 μM N-acetyl-L-carnitine, and 5 μM α -lipoic acid, exhibit beneficial effects against AGEs with regards to endoplasmic reticulum stress, the production of reactive oxygen species, and apoptosis (Loske et al., 1998; Thieme et al., 2016; Wang et al., 2016), and can reduce the *in vitro* formation of AGEs (Ghelani et al., 2018). Thus antioxidants were adopted for use in these studies at concentrations previously optimised for embryo culture (Truong et al., 2016).

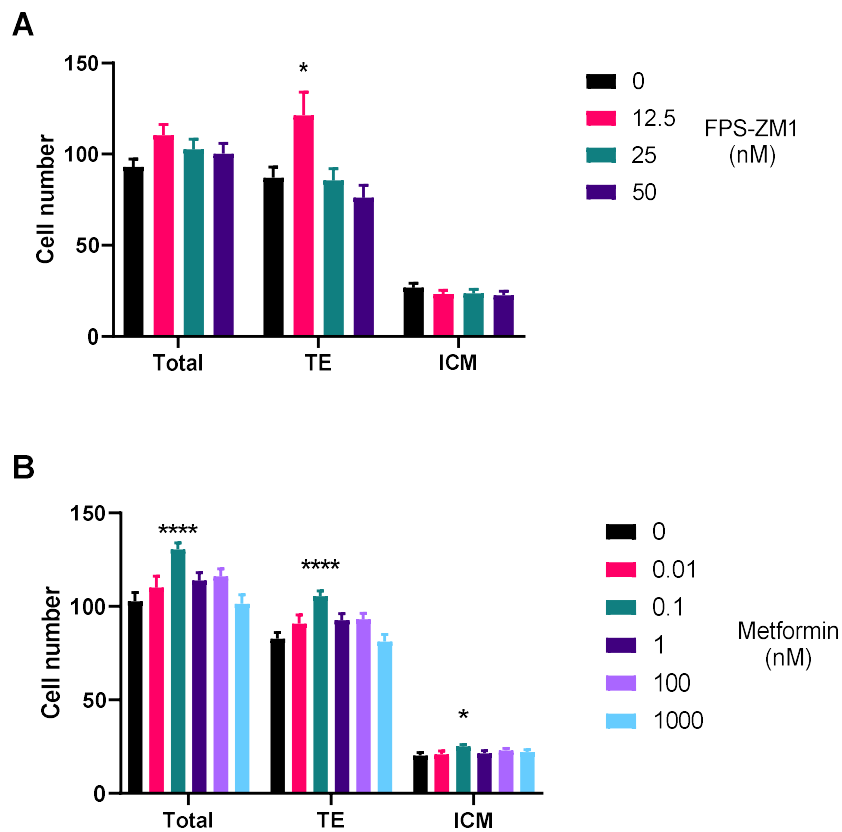


Figure 2.6: Optimisation of therapeutic intervention to remediate the effects of obese concentrations of AGEs on preimplantation embryo cell number. Mean \pm SEM cell number of total blastocyst, trophoctoderm (TE), and inner cell mass (ICM) of embryos cultured in AGEs and therapeutics. To determine the optimum therapeutic dose, embryos were cultured in the presence of AGEs either alone or with FPS-ZM1 (12.5-50 nM) or metformin (0.01-1000 nM). **A)** Embryos cultured in 8 μM AGEs supplemented with 12.5 nM FPS-ZM1 had significantly improved trophoctoderm (TE) cell number compared to 8 μM AGEs alone. Mean (\pm SEM) derived from 39 (total cell number) or 8 embryos per group (TE and ICM). **B)** Embryos cultured in 8 μM AGEs supplemented with 0.1 nM metformin had significantly increased total and TE cell number compared to 8 μM AGEs alone. Mean (\pm SEM) is derived from a minimum of 34 embryos per group for all. 12.5 nM FPS-ZM1 and 0.1 nM metformin were selected as the therapeutic doses. One-way ANOVA: * $P < 0.05$; **** $P < 0.0001$ versus control.

2.4 AGEs and the uterine environment

2.4.1 Standard protocols

2.4.1.1 Generic cell culture

Unless otherwise stated, all cell culture was performed under sterile conditions in a biosafety cabinet, and cells incubated in a humid environment at 37° under 5% CO₂ in air.

2.4.1.1.1 Cell lines

ECC-1 (American Type Culture Collection) and Ishikawa cells (kindly gifted to Professor Nie by Professor Masato Nishida of National Hospital Organization, Kasumigaura Medical Center, Ibaraki-ken, Japan) were used as a model of the human endometrial epithelium. Cells were routinely maintained in 75 cm² Nunc EasyFlasks (Corning), in basal medium containing appropriate supplementation (Table 2.2), with media replenished every 2-3 days. Once cells were approximately 80-90% confluent, they were passaged by twice rinsing with PBS and incubation in 2 mL of TrypLE Express dissociation solution (Gibco, Thermofisher) at 37 °C until cells were lifting from the base of the flask. The enzymatic reaction was quenched with 5 volumes of basal medium with appropriate supplementation, and cells thoroughly resuspended by repetitive pipetting. Cells were then seeded in fresh culture flasks (1:10 dilution for routine maintenance), seeded for experimentation, or cryopreserved (Section 2.4.1.1.3). The first trimester extravillous trophoblast cell line HTR8/SVneo was routinely maintained in the same manner as the epithelial cell lines. Characteristics of these cell lines are detailed in Hannan et al (2010).

Table 2.2: Standard culture media for maintenance of cell types used in this research. Basal medium and general supplementation for each cell type for general culture. Supplementation altered if necessary, according to experimental design. Supplementation with fetal calf serum (FCS), Glutamax, and antibiotic/antimycotic (Ab/Am) was performed as % vol/vol.

| Cell type | Basal medium | Supplementation |
|---|----------------------------|---|
| ECC-1 | DMEM/F-12 Glutamax (Gibco) | 10% FCS (Bovogen), 1% Ab/Am (Gibco, Thermofisher) |
| Ishikawa | MEM (Gibco) | 10% FCS, 1% Glutamax (Gibco), 1% Ab/Am |
| Primary human endometrial epithelial cells | DMEM/F-12 Glutamax | 10% FCS, 1% Ab/Am |
| Primary human endometrial stromal cells | DMEM/F-12 Glutamax | 10% charcoal stripped FCS (Gibco), 1% Ab/Am |
| HTR8/SVneo | DMEM/F-12 Glutamax | 10% FCS, 1% Ab/Am |
| L2-TSC | DMEM/F-12 Glutamax | 10% FCS, 1% Ab/Am, 10 nM SB41352 (Tocris) + 10 ng/mL bFGF (R&D systems) |

2.4.1.1.2 Trophectoderm cell culture

The trophoblast stem cell line (kind gift of Professor Susan Fisher, University of California San Francisco) termed L2-TSC (Zdravkovic et al., 2015), were routinely maintained in 25 cm² Nunc EasyFlasks (Corning), with media changes every 2-3 days. Flasks were coated in sterile 0.5% Type B gelatin in H₂O (Sigma Aldrich) for 30 min prior to use. Once cells were approximately 80% confluent, they were passaged (1:2 dilution for routine maintenance), seeded for experimental use, or cryopreserved (Section 2.4.1.1.3).

2.4.1.1.3 Cryopreservation

For cryopreservation, cells were pelleted by centrifugation at 300 RCF for 5 min, and resuspended in 90% FCS, 10% DMSO at approximately 1 x 10⁶ cells per mL. One mL of cells was transferred to a cryovial (Corning), and brought to -80°C at a rate of -1°C/min (CoolCell, Biocision), before storage in vapour phase liquid nitrogen.

2.4.1.2 Isolation and culture of primary human endometrial epithelial and stromal cells

Human endometrial biopsies were obtained, and isolated cells cultured blind to the fertility history of the subject. Biopsies were fixed in 10% neutral buffered formalin (NBF; Trajan) and preserved in paraffin wax for immunohistochemical investigation (Section 2.5.1.1), or stored in DMEM containing 1% Antibiotic-Antimycotic (Ab/Am, Invitrogen) at 4°C for cell isolation. Within 24 h of collection, tissue was finely scissor minced and digested in the presence of 7.5 IU/mL of Collagenase III (ThermoFisher) and 25 µg/mL DNase I (Roche) at 37°C under agitation for a total of 45 min. The enzymatic reactions were quenched by addition of 5 volumes of warm serum free DMEM, and solution passed through a 45 µm nylon mesh filter (Allied Filter Fabrics). The retained glandular fragments were rinsed off the 45 µm filter and pelleted to give the epithelial fraction. The human endometrial epithelial cells (HEECs) were seeded evenly in a 24 well plate and maintained in DMEM/F-12 GlutaMax + 1% Ab/Am + 10% FCS (Bovogen). The filtrate was passed through an 11 µm nylon mesh filter (Allied filter fabrics) to purify the stromal cell fraction. Stromal cells were pelleted by centrifugation at 300 RCF for 5 min, thoroughly resuspended in DMEM F/12 Glutamax + 10% charcoal stripped FCS (csFCS, Gibco Life technologies) + 1% Ab/Am, seeded into a 25 cm² Nunc EasyFlask and allowed to settle for 30 min. Medium was transferred to a secondary flask, and media replenished in the primary flask. Following 1 h incubation, the medium was exchanged on the secondary flask.

2.4.1.3 Decidualisation of primary human endometrial stromal cells

Isolated primary human endometrial stromal cells were grown to confluence in a 25 cm² Nunc EasyFlask with regular media changes. Preparations were visually assessed for purity (<5% epithelial cell contamination) before use. Stromal cells were lifted from the base of the flask using TrypLE express dissociation reagent, and seeded evenly in 12 well plates (approximately 1.25 x 10⁵ cells per

well). Cells were allowed to grow until 90% confluent before starting decidualisation treatment using routine protocols (Evans and Salamonsen, 2014). Stromal cells were incubated for 12 days in DMEM/F-12 Glutamax + 1% Ab/Am+ 2% csFCS + 10^{-8} M 17β -Estradiol (E, Sigma) + 10^{-7} medroxyprogesterone acetate (MPA, Sigma) to mimic the physiological hormonal milieu. Media were exchanged every 2 days, with conditioned media collected on day 2 and day 12 for Prolactin analysis by Monash Health Pathology. After culture, cells were rinsed twice with PBS and lysed in ice cold RIPA buffer (Abcam) containing protease inhibitor cocktail III (Roche) for subsequent protein analysis.

2.4.1.4 Real Time Cell Analysis (xCelligence)

The xCelligence system for label free, real time cell analysis (ACEA Biosciences) was used to measure adhesion and proliferation of epithelial cells, and invasion of trophoblast cells. All data recording and processing was performed using the RTCA data analysis software (Version 1, ACEA biosciences).

2.4.1.4.1 Adhesion and proliferation

Unless otherwise specified, endometrial epithelial cells were seeded at a density of 5×10^5 cells per well in a 6 well plate and allowed to settle overnight. Cells were twice rinsed in PBS and deprived of serum for 6 h, before incubation in DMEM/F-12 Glutamax containing 1% Ab/Am, 0.5% charcoal stripped FCS (csFCS) + 10^{-8} M E for 24 h containing appropriate experimental treatments, and an additional 24 h in 10^{-8} M E + 10^{-7} M MPA with experimental treatments continued. Each well of a 96 well E-plate (ACEA biosciences) was twice rinsed with sterile PBS and coated with 100 μ L of 20 μ g/mL recombinant human Fibronectin (Sigma), diluted in serum free medium, for a minimum of 45 min before experimental set up. Fibronectin solution was removed, and wells rinsed twice with PBS. Media containing treatments at 2x concentration was added to each well (100 μ L), and plate inserted into xCelligence machine. Electrode connections were confirmed and a background reading taken. Pre-treated epithelial cells were lifted from the culture plate and resuspended in serum free DMEM/F-12 Glutamax + 1% Ab/Am. An aliquot of 100 μ L containing 2×10^4 viable cells was added to each well of the E-plate and measurements of electrical impedance started immediately. Measurements were taken every 15 s for 5 h to measure adhesion, and every 15 min for up to 72 h to measure proliferation.

2.4.1.4.2 Invasion

The trophoblast cell line, HTR8-SVneo, was seeded at a density of 5×10^5 cells per well in a 6 well plate and allowed to settle overnight. Following 6 h serum starvation, cells were treated for 24 h in DMEM/F-12 Glutamax supplemented with 0.5% csFCS + 1% Ab/Am containing AGEs equimolar to the lean or obese uterine fluid either alone or in combination with therapeutics (Table 2.3). The upper chamber of each well in a cell invasion and migration plate (ACEA Bioscience) was coated with 25 μ L of growth factor reduced, phenol red free Matrigel (Corning) diluted 1:10 in cold serum free DMEM/F-12 Glutamax medium. Matrigel was allowed to set for a minimum of 30 min by incubation at 37°C. To

the basal chamber of the plate, 160 μ L of DMEM/F12 Glutamax supplemented with 1% Ab/Am and 10% FCS was added to act as a chemoattractant. Fifty μ L of serum free DMEM/F-12 Glutamax + 1% Ab/Am containing experimental treatments was added to each well of the upper chamber, and the two chambers gently interlocked together. The plate was inserted into the machine, electrode connections confirmed, and background readings recorded.

Pre-treated HTR8/SVneo cells were rinsed gently with serum free DMEM/F-12 +1% Ab/Am before lifting with TrypLE express dissociation reagent. Since PBS caused premature lifting of the cells, serum free media were used to rinse the cells before dissociation. An aliquot of 100 μ L media containing 4×10^4 viable HTR8 cells with experimental treatments continued was added to the upper chamber of the plates, and measurements of electrical impedance started immediately. Measurements were taken every 15 min for up to 72 h to monitor cell invasion.

2.4.1.5 Western Immunoblotting

Cell samples were lysed in ice-cold RIPA buffer containing 0.001% protease inhibitor cocktail III, vortexed thoroughly, and clarified by centrifugation at 14,000 x g for 30 min at 4°C. Protein content was determined using a Pierce BCA Protein Assay kit per manufacturer's instructions (ThermoFisher). Samples were stored at -80°C prior to use. Samples were thawed on ice, and 10 μ g protein denatured in SDS sample buffer containing 0.1 M dithiothreitol (Sigma) for 5 min at 96°C. Proteins were separated on a 4-20% SDS Mini-Protean TGX stain free gel (Bio-Rad), using Kaleidoscope precision plus protein standards (Bio-Rad) as a marker of molecular weight. Proteins were transferred onto a polyvinylidene fluoride (PVDF) membrane using the TransTurbo system (Bio-Rad) according to manufacturer's recommendations. Membranes were rinsed in Tris buffered saline containing 0.2% Tween 20 (TBS-T), and blocked using a 5% skim milk solution in TBS-T for 30 minutes. Membranes were incubated at 4°C overnight with the appropriate primary antibody at an optimised concentration. An appropriate horseradish peroxidase (HRP) conjugated secondary antibody was applied for 1 hour, before the membrane was developed using ECL Clarity substrate (Bio-Rad). Bands were visualised using a Chemidoc and analysed using Image Lab software Version 6.1 (both Bio-Rad). Antibodies were stripped from the membrane by 30-minute incubation in Reblot Plus Strong solution (Millipore, Sigma). After thorough washing and re-blocking in 5% skim milk, a normalisation control was performed by probing the membrane for β -actin (HRP conjugated; Cell Signalling Technology), and relative density calculated for each sample. Densitometry analysis was performed using Image Lab software.

2.4.2 Optimisation of protocols

2.4.2.1 Measurement of reactive oxygen species

Both RAGE and TLR4 signalling stimulate the production of cellular reactive oxygen species (ROS). 2'-7'-dichlorofluorescein diacetate (DCF-DA) is a cell permeable molecule which is cleaved to highly fluorescent DCF in the presence of ROS, and can be used to quantify the production of ROS within cells in a plate-reader based fluorometric assay. To determine an appropriate cell density for this assay, a titration of ECC-1 cells was seeded in technical duplicate (range 5000-60,000 cells per well), in a clear bottomed, black walled, 96-well plate (Corning) and allowed to settle overnight. Cells were twice rinsed in PBS before incubation in DMEM supplemented with 0.5% csFCS and 10 μ M DCF-DA. Cells were rinsed twice with PBS and stimulated with 0.03% H₂O₂ in serum free DMEM as a positive control for 30 min. Cells were washed twice with PBS, and the fluorescence of each well immediately determined using an excitation wavelength of 485 nm and an emission wavelength of 535 nm, using a ClarioStar microplate reader (BMG Labtech). To normalise DCF fluorescence to total number of cells, wells were subsequently fixed in 4% PFA for 15 min at room temperature. Following 2 washes with PBS, all nuclei were visualised with bis-benzimide (Thermofisher; 5 mg/mL in PBS) for 2 min at room temperature. Following three PBS rinses, intensity of bis-benzimide was quantified using the excitation wavelength of 352 nm and emission wavelength of 461 nm. As the fluorescent readout was within the linear range of the titration for both DCF and bisbenzimidide, 2 x 10⁴ cells per well was selected as the most appropriate cell density for this assay (Figure 2.7).

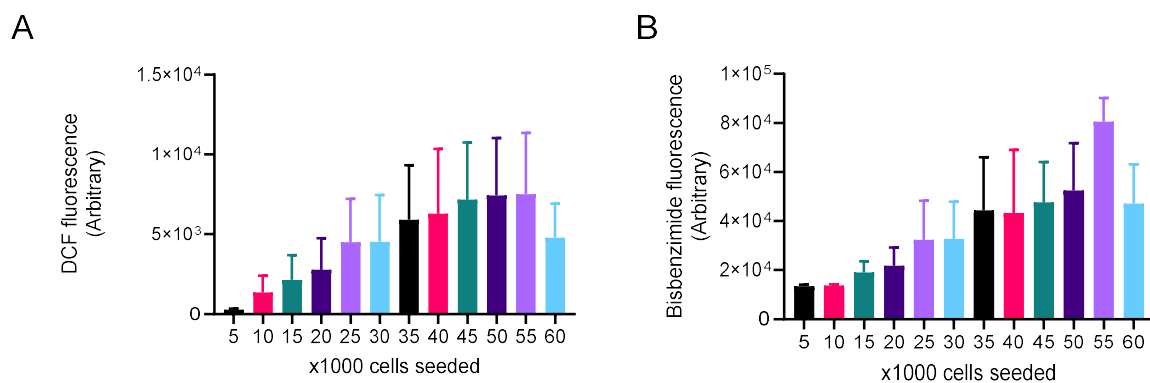


Figure 2.7: DCF fluorescence is proportional to cell number and can be normalised to Hoechst fluorescence intensity. Mean \pm SEM fluorescence. Mean is the derivative of 3 biological replicates. Increasing numbers of ECC-1 show an approximately linear increase in DCF (A) and biz-benzamide fluorescent intensity (B) at less than 50 x 10³ cells per well, allowing for normalisation of ROS production to cell number as approximated by bisbenzimidide intensity.

As a test study to confirm the production of ROS by AGEs in endometrial epithelial cells, ECC-1 were seeded at 2.5 x 10³ cells per well of a 24 well plate (Corning) in basal medium, and allowed to

settle overnight. Cells were deprived of serum for 6 hours, before hormonal priming for 24 h in the presence of 10^{-8} M E and an additional 24 h in 10^{-7} MPA + 10^{-8} E in DMEM/F-12 Glutamax + 1% Ab/Am + 0.5% csFCS. Throughout hormonal priming, cells were cultured in media containing physiologically lean (2 μ M) or obese (8 μ M) concentrations of AGEs. After priming, cells were trypsinised and seeded into a clear bottom, black walled 96 well plate at a density of 2×10^4 cells per well and allowed to settle overnight with treatments continued. ROS production was detected by application of treatment media supplemented with 10 μ M DCF-DA as above, and DCF fluorescence normalised to bis-benzamide. No significant effect was detected ($P = 0.5$), thus obesity-related AGEs do not affect ROS production in ECC-1 cells (Figure 2.8).

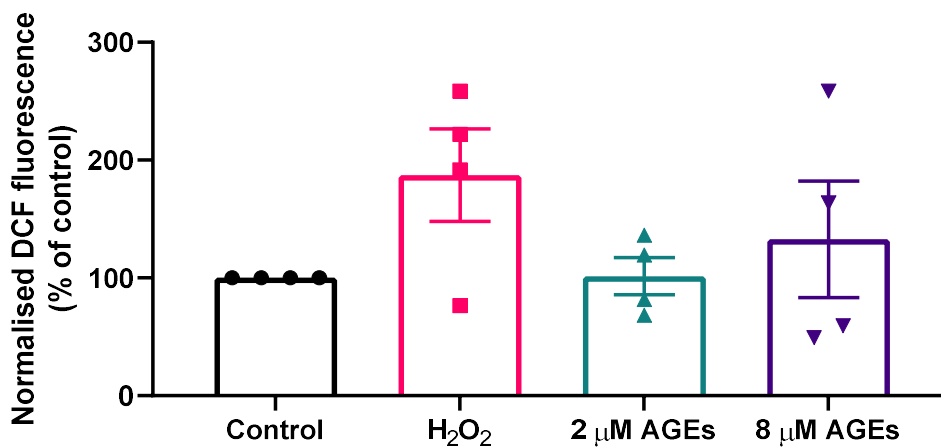


Figure 2.8: AGEs may not induce ROS production in cell lines. Mean \pm SEM of DCF fluorescent intensity normalised to bis-benzimide, expressed as % of control. Individual points represent independent replicates. No significant effect of any treatment was detected (Kruskal-Wallis: $P = 0.5$). 8 μ M AGEs do not affect ROS production in ECC-1 cells.

To visualise ROS production following hormonal priming and treatment, cells were seeded at the same density in a Falcon® CultureSlide (Corning, USA), and allowed to settle overnight. Following DCF-DA treatment as indicated above, nuclei were visualised with bisbenzimidazole, twice rinsed in PBS, and immediately imaged using a fluorescence Olympus microscope (Figure 2.9).

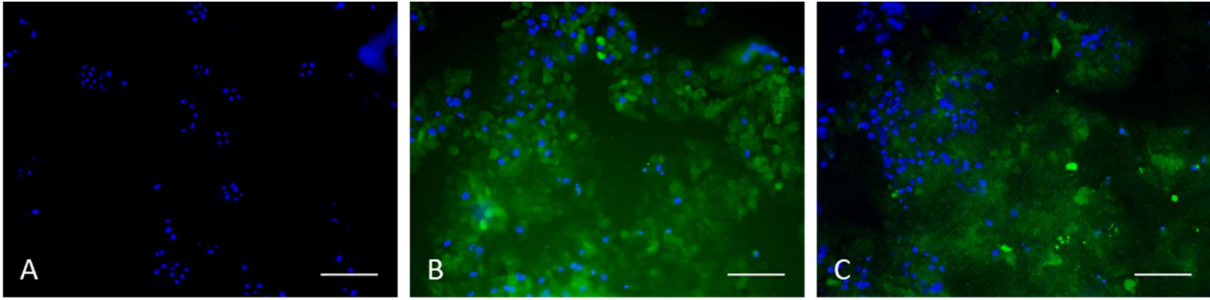


Figure 2.9: ROS visualisation using fluorescence microscopy. ECC-1 cells were hormonally primed and stained for ROS content using DCF-DA. Visualisation showed no significant elevation of DCF fluorescence after stimulation with 0.03% H₂O₂. A) Autofluorescence control, B) DCF-DA loaded, untreated control, C) DCF-DA loaded, treated with H₂O₂. Scale bar represents 100 µm.

Due to high variation in results and no significant effect of AGEs on ROS production, ROS measurement was not used in later work (Chapter 4). The positive control, hydrogen peroxide, did not elicit a consistent response in either assay, as had been anticipated. AGEs increase ROS presence in first trimester trophoblast cells (Shirasuna et al., 2016), however, given the lack of ROS responsiveness of the ECC1 cells to hydrogen peroxide, there can be no confidence in applying the assays in the present context. Tert-butyl hydrogen peroxide could be used as an alternative positive control to determine this. Alternatively, a commercial assay such as CellROX (ThermoFisher) could be used. However, given the cost of commercial assays, and the time it would take to further optimise this protocol, ROS production was deemed not to be a critical endpoint to be examined in this thesis, but may be an interesting avenue for future studies.

2.4.2.2 Optimisation of therapeutic intervention for endometrial cells

Substantial and significant effects of AGEs were previously observed on the adhesion and proliferation of ECC-1 cells (Antonioti et al., 2018). Hence, using standard culture conditions, therapeutics targeting the known AGEs receptors RAGE (FPS-ZM1, Torc1s) and TLR4 (VIPER, Novus biologicals), metformin (Sigma), and a cocktail of antioxidants (Truong et al., 2016) were trialled. Results of testing are shown in Table 2.3. While AGEs did not impact ROS generation, specific antioxidants can remediate effects of AGEs (Wang et al., 2016), and were continued in this study as they may act through a different mechanism in AGEs treated epithelial and stromal cells.

Therapeutics optimised for preimplantation embryo culture (Section 2.3.2.4) were re-optimised for cell culture. In addition to these, an inhibitor of TLR4 was included (Viral Inhibitor peptide of TLR4, VIPER; Novus Biologicals) as AGEs can interact with TLR4 to increase cellular stress (Noguchi et al., 2010; Shirasuna et al., 2016).

Table 2.3: Concentrations of therapeutics optimised for use in reducing the effects of AGEs on the uterine environment. A large range of concentrations of each pharmaceutical were applied to assess their impact on viability of endometrial epithelial cells. A narrower range of concentrations was used to optimise the therapeutic dose. Antioxidants were tested at 1 and 10 times the concentrations previously optimised for mouse preimplantation embryo culture (Truong et al., 2016).

| <i>Compound</i> | <i>Viability range</i> | <i>Optimisation range</i> | <i>Optimised concentration</i> |
|-----------------------|------------------------|---------------------------|--------------------------------|
| <i>FPS-ZM1</i> | 0-50 nM | 12.5-50 nM | 25 nM |
| <i>Metformin -HCL</i> | 0-1 mM | 1-100 μ M | 100 μ M |
| <i>VIPER</i> | 0-40 μ M | Not suitable | Not suitable |
| <i>Antioxidants</i> | N/A | 1X and 10X | 1x |

2.4.2.2.1 Viability of cells in the presence of therapeutics

The xCELLigence RTCA system was used to assess the viability of ECC-1 cells in the presence of selected therapeutics to ensure these compounds were not toxic to the cells before proceeding with complete optimisation. Three to four biologically independent replicates seeded in technical triplicate were performed for this pilot data.

ECC-1 cells were seeded at a density of 2×10^4 viable cells in 100 μ L of DMEM/F-12 + 1% Ab/Am + 1% FCS in an e-plate prepared as per Section 2.4.1.4.1. Proliferation was assessed by measuring cell index every 15 min for up to 24 h post seeding. After 24 h, 100 μ L of 1% FCS containing either vehicle control or therapeutic at 2x concentration was added to each well (FPS-ZM1 range 0-50 nM, vehicle DMSO; Metformin range 0-1 μ M, vehicle water; VIPER range 0-40 μ M, vehicle CP7) and continued proliferation measured for 48 h. Viability was assessed by determining the continued rate of proliferation over 12 h following compound addition (Fig. 2.10).

The viability of ECC-1 cells was not affected by either metformin or the antagonism of RAGE using FPS-ZM1. The application of the small peptide inhibitor VIPER at or above 10 μ M was cytotoxic to ECC-1 cells, with a negative rate of proliferation following compound addition indicative of cellular deadhesion. Thus, TLR4 signalling is likely important in ECC-1 viability and proliferation, and consequently, this therapeutic was deemed unsuitable for use at this time.

As the antioxidants used in this study were not cytotoxic to the preimplantation embryo, they were utilised in this thesis without additional viability studies.

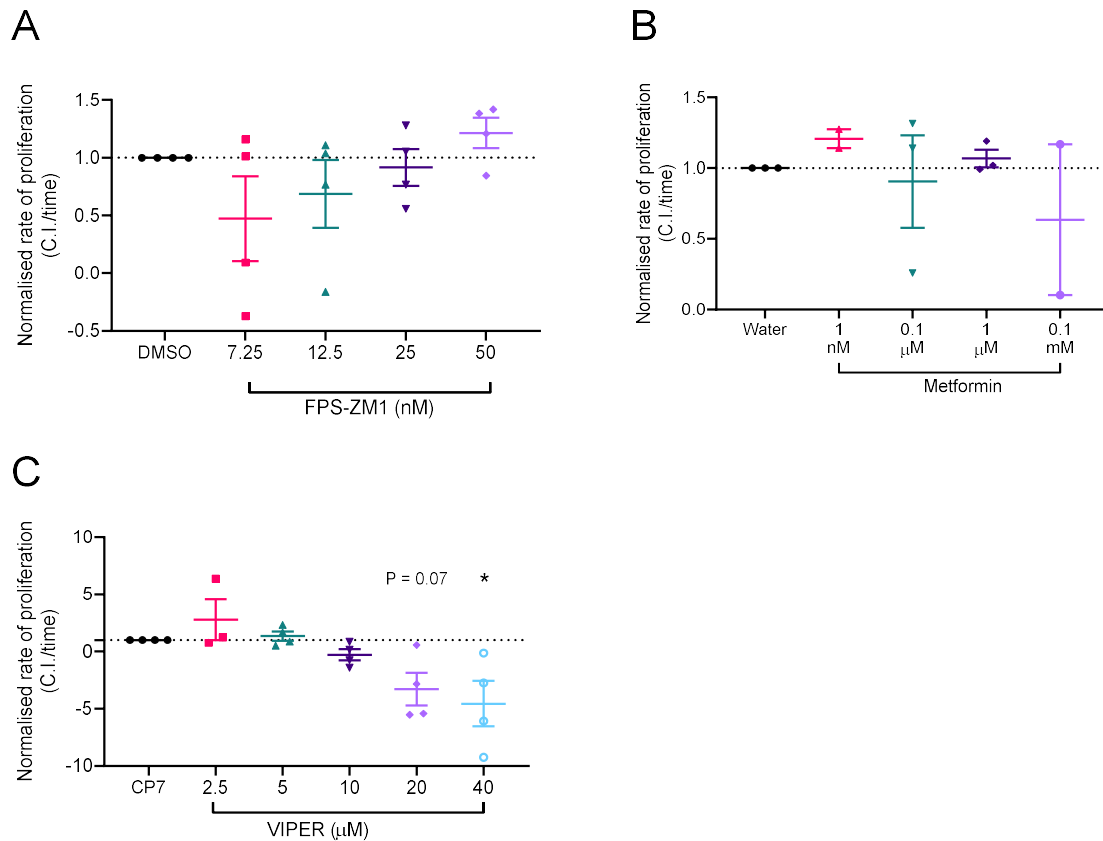


Figure 2.10: Viability of ECC-1 treated with potential therapeutics. Mean \pm SEM rate of proliferation for 12 h following addition of therapeutics ($n \geq 3$ biologically independent replicates for all, represented by individual data points). Neither FPS-ZM1 (**A**) nor metformin (**B**) affected the continued rate of proliferation of ECC-1 cells ($P = 0.24, 0.68$ respectively). Inhibition of TLR4 using an inhibitory peptide (VIPER) is cytotoxic to ECC-1 cells ($P < 0.01$) (**C**). Viability assessed as continued proliferation following therapeutic addition at 24 h. Rate of proliferation normalised to control conditions. Negative rate of adhesion demonstrates a reduced viability. One-way ANOVA/Kruskal-Wallis: * $P < 0.05$ vs control.

2.4.2.2.2 Optimising the dose of selected therapeutics

Therapeutic doses were optimised by assessing the effect of each compound on ECC-1 cells which had been hormonally primed in the presence of lean and obese concentrations of AGEs. ECC-1 cells were serum starved for 8 h, and hormonally primed as previously described in the presence of lean or obese concentrations of AGEs further supplemented with therapeutics. Treated cells were seeded at a density of 2×10^4 cells per well in a fibronectin-coated 96 well E-plate (ACEA biosciences) with treatments continued, and adhesion and proliferation measured for 48 h (Section 2.4.1.4.1). The rate of adhesion (rate of change in cell index 0- 5 h), and rate of proliferation (rate of change in cell index 12-48 h) are shown in Figure 2.11.

FPS-ZM1 (Figure 2.11 A-B) showed no significant beneficial effects on adhesion and proliferation in the presence of obese (8 μ M AGEs). Therefore, the K_i of 25 nM was selected for future use in the assumption that it may be beneficial in modulating other effects of AGEs.

Addition of 100 μ M metformin (Figure 2.11 B) somewhat improved the relative cell index up to 24 h (data not shown) but did not show significant effects on cell adhesion and proliferation. As 100 μ M metformin does not reduce the proliferative capacity of endometrial cancer cells, and does not significantly reduce glyoxalase 1, a protein involved in the detoxification of the AGE methylglyoxal (Dong et al., 2012), 100 μ M metformin was selected to investigate its effects on trophoblast invasion and other endometrial cell functions.

As antioxidants had no effect on embryo trophectoderm cell number when exposed to obese concentrations of AGEs, a higher concentration was also trialled. These antioxidants when applied at 10-fold higher concentrations appeared to synergise with obese concentrations of AGEs and reduced ECC-1 cell adhesion and proliferation, whereas lower concentration antioxidants prevented the reduction in rate of proliferation in the presence of obese AGEs (Figure 2.11 F). The previously published cocktail containing of 10 μ M N-acetyl-L-carnitine, 10 μ M N-acetyl-L-cysteine, and 5 μ M α -Lipoic acid were adopted for use.

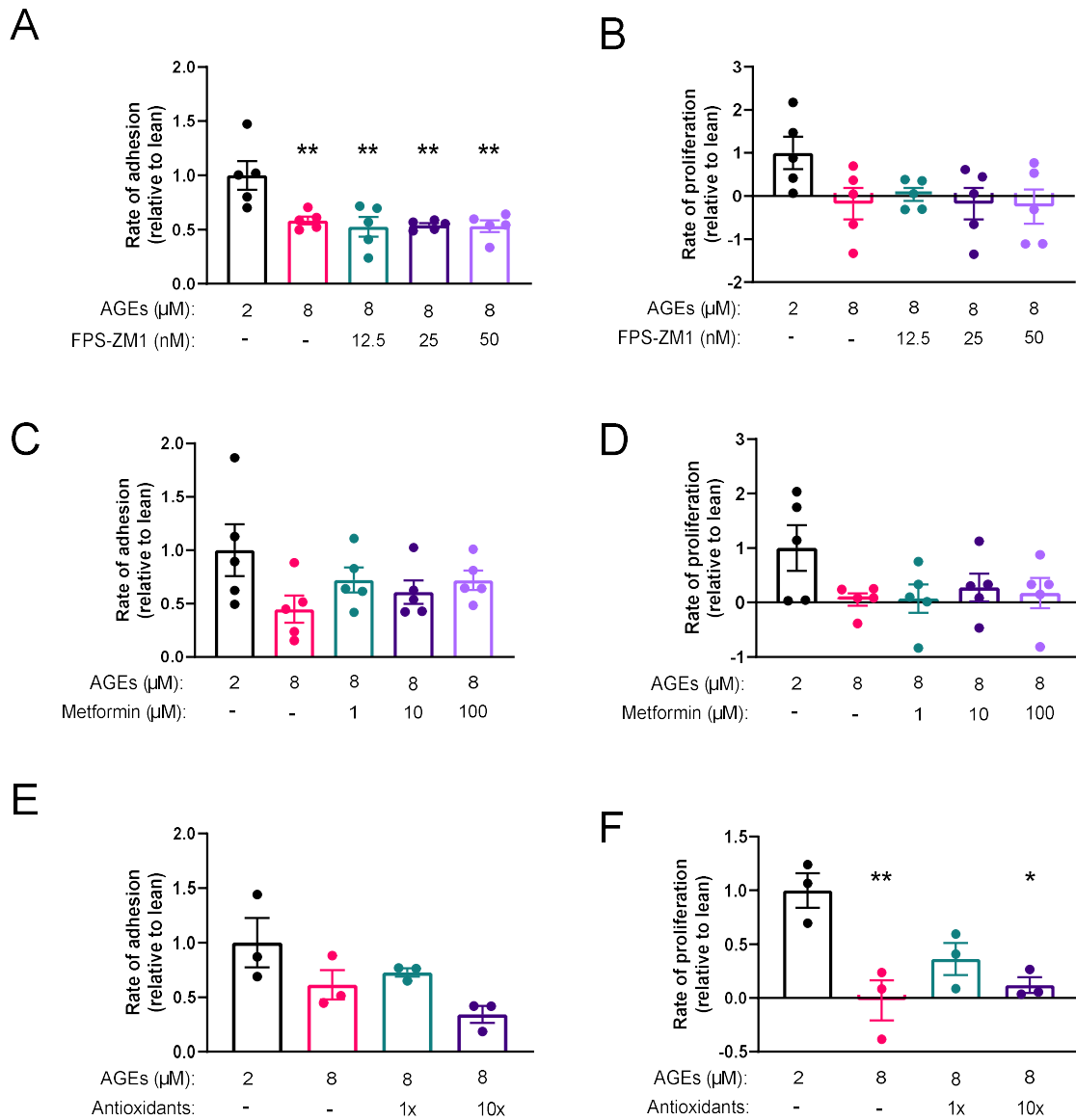


Figure 2.11: Optimisation of pharmaceutical intervention to remediate the effects of AGEs on endometrial epithelial cell proliferation. ECC-1 cells were hormonally primed in media containing either lean (2 μM) or obese (8 μM) AGEs alone or obese AGEs further supplemented with either increasing doses of the RAGE antagonist (FPS-ZM1, **A-B**), metformin (**C-D**), or a combination of antioxidants (**E-F**). Rate of adhesion was determined over the first 5 h of culture, and rate of proliferation determined between 12 and 48 h. Rate of adhesion and proliferation are normalised to lean, and data are expressed as mean \pm SEM. Minimum $n=3$ biologically independent replicates performed, denoted by individual data points. One-Way ANOVA/Kruskal Wallis: *, ** $P < 0.05$, 0.01 vs 2 μM .

2.5 Human Endometrial Epithelial Organoids as a primary model of the human endometrium

Since the work in this thesis was commenced, new developments in human endometrial epithelial organoid (hEEO) culture have provided an exciting possibility for validation of the effects of obesity-related AGEs on primary endometrial epithelial cells. Presented here are the standard methodologies and optimisation of histological techniques, required to validate and investigate the cellular nature of hEEO.

2.5.1 Standard protocols

2.5.1.1 Immunohistochemistry

Formalin fixed, paraffin embedded endometrium was sectioned at 4 μm . Tissue sections were dewaxed in two changes of xylene and rehydrated in decreasing concentrations of ethanol before immersion in distilled water. Sections were washed twice in TBS-T and once in TBS following each subsequent step. Antigen retrieval was performed by boiling slides in 10 mM sodium citrate (Chem Supply) containing 0.5% Tween 20 at pH 6.0, and an endogenous peroxidase block performed using 3% H_2O_2 for a period of 30 min. Non-specific binding was prevented by a non-immune block for a period of 1 hour. Antibodies were applied at an appropriate concentration following optimisation for a minimum of 16 hours at 4°C. An appropriate biotinylated secondary antibody (Vector Labs) was applied for 1 hour at 37°C, after which signal was amplified by application of VECTASTAIN® ABC solution (Vector Labs) for 30 min at 37°C. Immunostaining was visualised using DAB+ liquid chromogen substrate. Slides were dehydrated and mounted in DPX. Slides were either scanned using a VS120 Slidescanner (Olympus) or imaged using an Olympus B52 microscope fitted with a digital camera.

2.5.1.2 Multiplex analysis of chemokine and cytokine secretion

Conditioned medium was collected from hEEO: 48 h after media were replenished, prior to hormonal priming and AGEs treatment (basal); following 24 h in the presence of E and lean or obese AGEs; and following 24 h in the presence of E + MPA + AGEs. PBS was used as a vehicle control for AGEs-HSA. Media were immediately stored at -80°C for later analysis.

Secretion of inflammatory factors was assessed in technical duplicate using a Luminex BioPlex® 200 system (Bio-Rad) and Milliplex® MAP human cytokine/chemokine (Milliplex #HCYTOMAG-60K) and cardiovascular disease (Milliplex #HCVD1MAG-67K) kits as per manufacturer's recommendations.

2.5.2 Establishment of organoid culture

The culture of primary human endometrial epithelial cells as organoids has been extensively optimised and validated in other laboratories (Boretto et al., 2017; Fitzgerald et al., 2019; Turco et al., 2017). As biopsy collection and cell dissociation protocols vary between laboratories, preliminary validation studies were performed to ensure similarities in my hEEO cultures to those described in Turco et al., (2017). Human endometrial epithelial cells (hEEC) were isolated as per Section 2.4.1.2, thoroughly washed and resuspended in advanced DMEM (aDMEM; Themofisher), and pelleted by centrifugation. hEEO were formed in 48 well plates by seeding of a predominantly single cell solution of epithelial cells, formed by mechanical dissociation of glandular fragments, in 20 μ L droplets of growth factor-reduced, phenol red-free Matrigel (Corning) and covered in 250 μ L organoid expansion media (ExM, Table 2.4) as previously detailed (Turco et al., 2017). Proliferation of epithelial cells over approximately one week resulted in the formation of hEEO: hollow spherical structures with highly defined cell boundaries (Fig. 2.12 A). Matrigel droplets contained organoids in a heterogenous array of sizes and polarization (Fig 2.12 B), and hEEO appeared to bud off from each other as they proliferated (Fig 2.12 C). When hEEO approached confluency within the Matrigel droplet, they were passaged by mechanical dissociation from Matrigel, rinsed twice in aDMEM, brought to a predominantly single cell suspension by repetitive pipetting, and reseeded as described previously in additional wells.



Figure 2.12: Culture of primary hEECs as endometrial organoids. **A)** Isolated primary hEECs are seeded as single cells in Matrigel, allowing the formation of organoids (hEEO). White arrow indicates a single cell starting to form an organoid, black arrow an early hEEO, and black and white arrow indicates a growing hEEO (10x magnification). **B)** After a few days of growth, hEEO show significant expansion, and clear cell borders imply polarization of cells (black arrow), however some hEEO demonstrate polarisation to lesser extent (white arrow, 10x magnification). **C)** hEEO split from each other during growth (20x magnification).

Cryopreservation was performed by mechanical dissociation of hEEO from Matrigel, pelleting by centrifugation at 1000 RCF for 5 minutes, and two rinses in aDMEM with gentle resuspension. hEEO were resuspended in freezing medium containing 70% ExM, 20% FCS, and 10% DMSO and taken to -80°C before storage in vapour phase liquid nitrogen. hEEO were thawed by two rinses in warm

aDMEM, and organoid fragments seeded in Matrigel overlaid with ExM. Post-thawing, the ROCK1/2 inhibitor Y-27632 was included in ExM for three media changes to promote cell survival.

Table 2.4: Components of organoid expansion media. ExM was prepared under sterile conditions in Advanced DMEM and sterile filtered before use. Y-27632 was only included in ExM for the first three media changes after thawing of hEEO.

| Reagent | Supplier | Concentration |
|---|------------------------|---------------|
| GlutaMAX | Invitrogen | 2 mM |
| N2 Supplement | Invitrogen | 1X |
| B27 Supplement (without vitamin A) | Invitrogen | 1X |
| Primocin | Invivogen | 100 µg/mL |
| N-Acetyl-L-Cysteine | Sigma | 1.25 mM |
| Recombinant human EGF | Peptotech | 100 ng/mL |
| Recombinant human Noggin | Sinus Biologicals | 100 ng/mL |
| Recombinant human FGF-10 | Sinus Biologicals | 100 ng/mL |
| Recombinant human HGF | Sinus Biologicals | 50 ng/mL |
| A83-01 | Stem cell technologies | 500 nM |
| Nicotinamide | Sigma | 10 mM |
| Recombinant human Rspodin-1 | Sinus Biologicals | 500 ng/mL |
| Y-27632 (post-thaw only) | Stem cell technologies | 10 µM |

2.5.2.1 Histological examination of human endometrial epithelial organoids

Six confluent wells of hEEO were disaggregated from Matrigel, centrifuged at 1000 RCF for 10 min, washed twice in PBS, and transferred to a medium sized cryomould (TissueTek), with 5% agar (% wt/vol; Sigma) overlaid. Once set, the agar plug was fixed in 10% NBF for 24 h and processed through to paraffin wax.

Unpublished work in the Salamonsen laboratory demonstrates that extensive hormonal priming of hEEO within an extracellular matrix results in a highly polarised and ciliated phenotype of the endometrial epithelial cells containing basally located nuclei, with proliferation indicated by the presence of mitoses. Furthermore, expression of the progesterone receptor was noted following

hormonal priming (Figure 2.13). This is in concordance with experiments reported by Turco et al. (2017).

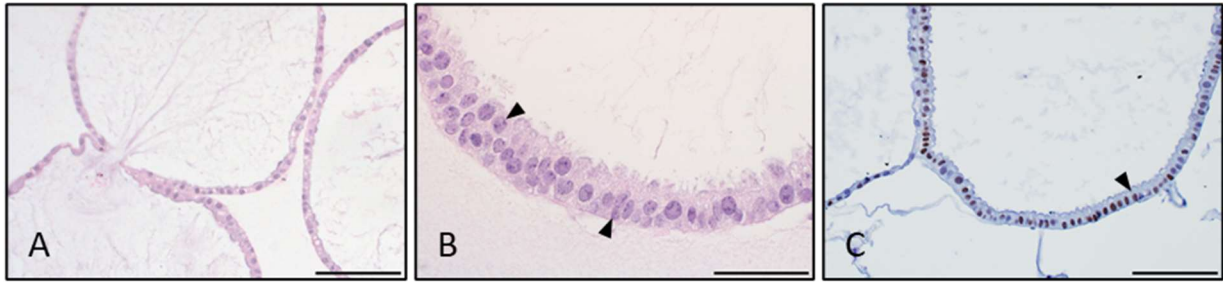


Figure 2.13: hEEO contain proliferating cells and hormonal stimulation promotes progesterone receptor expression. A) Organoids tend to grow close to each other in culture due to their ability to bud off from each other. **B)** Mitoses (black arrow) indicate proliferation of epithelial cells in hEEOs. The cuboidal shape, evidence of apical cilia, and basal location of the nuclei suggests polarisation of epithelial cells. Progesterone receptor was immunolocalised to nuclei following hormonal priming **(C)**. Scale bars represent 100 μm (A, C) and 50 μm (B). Experiments performed by Dr Jemma Evans.

2.5.2.2 Characterisation of secretions

Initial H&E staining indicated that hEEOs maintained their secretory nature, with a pink stain appearing in the organoid lumen, and it was considered these may be mucin secretions. Routine protocols for alcian blue (AB), periodic-acid-schiff (PAS), and a combination of the two (PAS/AB) were trialled to examine the contributions of acid and neutral secretions. Prior literature demonstrates that hEEO secretions increase with hormonal priming (Boretto et al., 2017; Turco et al., 2017); this was not further examined here.

Individually, each stain indicated significant secretions from both the uterine glands in tissue sections and hEEOs (Figure 2.14). The organoids exhibit reduced staining intensity compared to endometrial glands; as the epithelial cells are dissociated and thoroughly rinsed with each passage of hEEO, accumulation of secretions will be less than in intact endometrium.

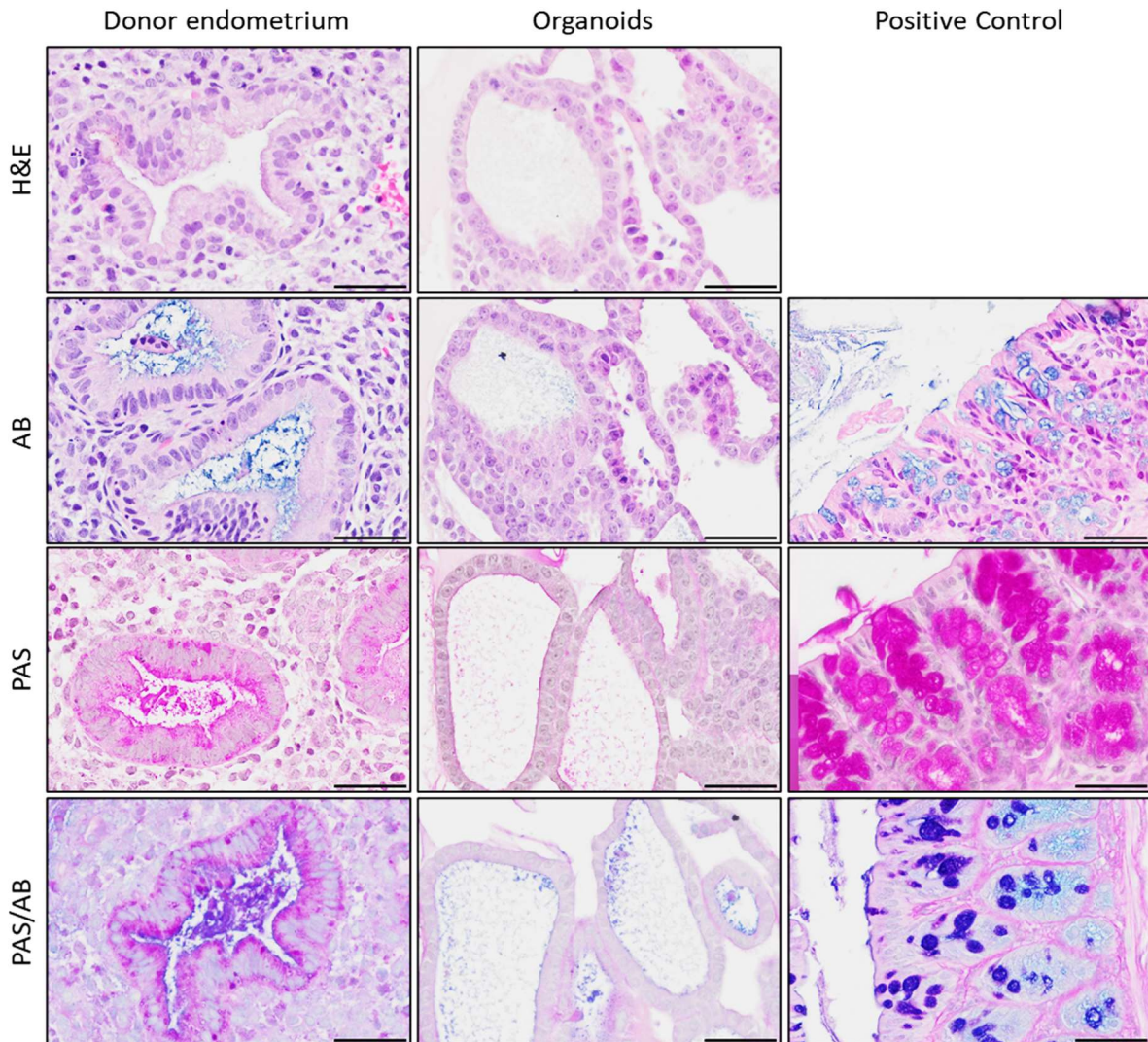


Figure 2.14: Secretion identification in human secretory endometrium and donor-matched organoids. Acidic and neutral mucin secretions are identified by AB and PAS staining respectively in the secretory endometrium and donor-matched organoids. The endometrium shows acidic (AB) and neutral (PAS) mucin secretion into the lumen of the gland, maintained in organoid culture. Highest identification of secretions was identified by PAS/AB. Mouse colon was used as a positive control for each stain. Scale bars represent 50 μ M.

Neutral mucins and polysaccharides were identified by PAS⁺ staining in the extracellular matrix and are localised to the apical and basal regions of luminal and glandular epithelial cells in tissue sections. Some glandular secretions are also PAS⁺ (pink). hEEOs derived from the same tissue also exhibit PAS⁺ staining. Residual Matrigel in the organoid pellet is also positively identified with this stain. AB⁺ staining was evident strongly in glandular and hEEO secretions indicating the presence of acidic mucins. As both secretions were evident, the combination stain of PAS/AB was elected for further use.

2.5.2.3 Immunohistochemical staining

Immunohistochemistry (Section 2.5.1.1) was utilised to validate characteristics of these hEEO as similar to those described in previous literature. The tested conditions for each antibody are detailed in Table 2.5 with optimised antibody dilutions identified in bold. Full immunohistochemical validation and characterisation and investigation is presented in Chapter 5.

2.5.2.3.1 A note on the immunolocalisation of cytokeratin

Clear and specific staining was identified for pan-cytokeratin, KRT7, and KRT13 using the conditions listed in Table 2.5. KRT13 has been previously reported as a marker of endometrial luminal epithelium (Mo et al., 2006), however the antibody trialled here was unable to discriminate between these types of epithelium and the optimisation of an additional antibody was beyond the scope of this thesis. KRT7 was selected for use in this thesis to align with previous validation studies on hEEO (Turco et al., 2017).

Table 2.5: Optimised IHC conditions for hEEO validation. Summary of optimisation and optimised staining conditions for each protein. All immunohistochemistry was performed following citrate antigen retrieval. Optimised antibody dilutions identified in bold. Staining of the glandular and luminal epithelium (GE, LE) and endometrial stroma are denoted as present (+) or strong (++). (-): no significant staining was noted.

| Protein | Primary antibody | Blocking solution | Primary antibody dilution | Staining | Notes |
|-----------------------|--|-----------------------------------|---------------------------|---|---|
| ER α | Rabbit- α -ER α (Santa cruz) 0.2 mg/mL | 10% Goat serum 2% Human serum | 1:100 | Overstaining of the endometrium. Signal detection in the isotype control. | Manufacturer's recommendation. |
| | | | 1:1000 | Nuclear and cytoplasmic staining. GE (+), LE (+), Stroma (++) | 1:1000 dilution selected as optimised condition. |
| Progesterone receptor | Mouse- α -PR (Novocastra) 0.36 mg/mL | 10% Horse serum 2% Human serum | 1:100 | Nuclear staining. GE (-), LE (-), stroma (++) | Dilution previously used in this laboratory. No further optimisation required |

| | | | | | |
|-----------------|---|-----------------------------------|--|---|--|
| PCNA | Mouse- α -PCNA (Santa Cruz) <i>0.2 mg/mL</i> | 10% Horse serum 2% Human serum | 1:500, 1:1000, 1:2000 | Nuclear staining. GE (++) LE (+), Stroma (++) | 1:2000 dilution selected as optimised condition. |
| Pan-cytokeratin | Rabbit- α -pan cytokeratin (Dako) <i>10.7 mg/mL</i> | 10% Goat serum 2% Human serum | 1:50 | Overstaining of the endometrium. Signal detection in the isotype control. | |
| | | | 1:2000 | Cytoplasmic staining. GE (++) LE (++) | 1:2000 dilution selected as optimised condition. |
| Cytokeratin 7 | Mouse- α -KRT7 (Dako) <i>0.5 mg/mL</i> | 10% Horse serum 2% Human serum | 1:500, 1:1000, 1:2000 , 1:4000 | Cytoplasmic staining. GE (++) LE (++) | 1:2000 dilution selected as optimised condition. |
| Cytokeratin 13 | Mouse- α -KRT13 (Santa Cruz) <i>0.2 mg/mL</i> | 10% Horse serum 2% Human serum | 1:50, 1:100, 1:200, 1:400 | Cytoplasmic and some nuclear staining. GE (+), LE (+) | Not specific to luminal epithelium. |
| RAGE | Rabbit- α -RAGE (Abcam) | 10% Goat serum 2% Human serum | 1:100 | No evident staining. | Used in Chapter 3 for embryo IF. |
| | Mouse- α -RAGE (Santa Cruz) <i>0.2 mg/mL</i> | 10% Horse serum 2% Human serum | 1:1000 | GE (+), LE (+), stroma (+) | Reported in Antoniotti et al. (2018, this laboratory). No further optimisation required. |
| TLR4 | Rabbit- α -TLR4 (Abcam) <i>1 mg/mL</i> | 10% Goat serum 2% Human serum | 1:100, 1:250, 1:500, 1:1000 | GE (++) LE (++) stroma (++) | 1:1000 dilution selected as optimised condition. |
| CML | Mouse- α -CML (Santa Cruz) <i>0.25 mg/mL</i> | 10% Horse serum 2% Human serum | 1:1000, 1:10,000 | Cytoplasmic staining. GE (+), LE (+), stroma (++) | 1:10,000 reported in Antoniotti et al. (2018). Confirmed as optimised concentration. |

2.6 The human adhesome and receptome

Work initiated by my supervisor, Dr Jemma Evans, had proteomically defined a number of proteins specific to the human adhesome and receptome (Evans et al., 2020a). One of my major aims had been to validate and further investigate these findings. However, given the success of the other aims of my work related to obesity-associated AGEs, and Dr Evans leaving the Hudson Institute, along with the loss of experimental time due to COVID19, this work was given a lower priority and was not completed. The extensive methodology development is detailed here.

2.6.1 Standard methodologies

2.6.1.1 Spheroid adhesion assay

Trophectoderm cell (Zdravkovic et al., 2015) spheroids were used to investigate adhesion to ECC1 cells as previously reported (Evans et al., 2020b). ECC-1 cells were seeded at a density of 2.5×10^5 cells per well in a 12 well plate and allowed to settle overnight. L2TSC (routinely maintained as per Section 2.4.1.1.2) were seeded at a density of 2.5×10^3 cell per well in an ultralow adhesion, round bottom well 96 well plate (Corning), in a total of 150 μ L of media (Table 2.2). Spheroids were allowed to form over a period of 48 h while ECC-1 cells were simultaneously hormonally primed. Spheroids were inspected visually, and those which had not formed compact spheroids (<5%) excluded from experimental use. Thirty spheroids per treatment group were removed from the 96 well plate using a 1 mL wide bore pipette tip (Axygen) to prevent damage, and centrifuged at 300 RCF for 5 min. Supernatant was removed and spheroids washed twice in PBS. Spheroids were gently resuspended in DMEM + 1% FCS + 1% Ab/Am containing 10^{-7} M E and 10^{-8} M MPA. Hormonally primed ECC-1 cells were twice rinsed in PBS and spheroids placed in the wells. Spheroids were allowed to adhere for a period of 6 hours before gentle washing with PBS. Adherent spheroids were expressed as % adhered.

2.6.1.2 siRNA knockdown

ECC-1 cells were seeded per standard protocols at 2×10^5 cells per well in a 12 well plate for siRNA knockdown, allowed to settle overnight, and rinsed twice in PBS before application of siRNA. For each target, 4 μ L of 10 μ M siRNA (all Santa Cruz, Table 2.6) and 4 μ L lipofectamine RNAiMAX (Thermofisher) were equilibrated at room temperature in 100 μ L OptiMEM (Thermofisher) for 5 min before combination and incubation for a further 30 min. siRNA solutions were made to 1 mL and applied to ECC-1 cells. After 24 hours of incubation at 37°C, medium was replaced with Ab/Am free DMEM/F-12 + 10% FCS for a further 48 hours. Individually, siRNA knockdown was performed for each of PC4, LGMN, KYNU, STMN1, SLIRP, PTGS2, and SERPINE1. Scramble siRNA was used as a control (Table 2.6). Control and knockdown cells were then subject to hormonal priming for transepithelial resistance (Section 2.6.1.3) or spheroid adhesion assay: 6 h in serum free DMEM/F-12 + 1% Ab/Am; 20 h

incubation in 10^{-7} M E; 20 h incubation in 10^{-7} M E + 10^{-8} M MPA both in DMEM/F-12 + 1% Ab/Am + 0.5% csFCS.

Table 2.6: siRNA information. Target and catalogue information for each siRNA used. All sourced from Santa Cruz.

| Target | Catalogue number |
|-----------|------------------|
| PC4 | sc-106359 |
| KYNU | sc-95023 |
| LGMN | sc-60930 |
| STMN1 | sc-36127 |
| SLIRP | sc-92406 |
| SERPINE1 | sc-36179 |
| PTGS2 | sc-29279 |
| Scrambled | sc-37007 |

2.6.1.3 Transepithelial resistance

ECC-1 cells were seeded in 12 well plate 0.4 μ m transwell inserts (Corning) at 1.5×10^5 viable cells per well in basal medium, and underwent siRNA knockdown as above. Cells were hormonally primed, and transepithelial resistance measured using Millicell® electrical resistance system (Merk) after: 6 h in serum free DMEM/ F-12 + 1% Ab/Am; 24 h incubation in 10^{-7} M E; and again after 24 h incubation in 10^{-7} M E + 10^{-8} M MPA both in DMEM/F-12 + 1% Ab/Am + 0.5% csFCS.

2.6.1.4 Validation of siRNA by quantitative PCR

2.6.1.4.1 RNA extraction

Following siRNA knockdown, cells were rinsed twice in PBS and lifted from the base of the plate using TrypLE express. When cells were visually confirmed to be lifting from the base of the plate, the reaction was quenched using 5 volumes of ice-cold PBS. Cells were pelleted by centrifugation at 300 RCF for 5 min. Supernatant was removed and pellet snap frozen on dry ice. Cells were immediately stored at -80°C until RNA extraction using the RNEasy Mini Kit (Qiagen) as per manufacturer's instructions. Contaminant DNA was removed using an on column DNase treatment (Qiagen) during RNA extraction. RNA was solubilised in 30 μ L RNase free water, and concentration determined using a Nanodrop ND-1000 spectrophotometer (Thermofisher). RNA stored at -80°C until further use.

2.6.1.4.2 cDNA synthesis

Complementary DNA (cDNA) was generated using the SuperScript III synthesis system (Thermofisher) as per manufacturer's instructions from 500 ng sample RNA using random hexamer primers. A Veriti

PCR machine (Applied Bioscience, Thermofisher) was used for thermal cycling. cDNA stored at -20°C until further use.

2.6.1.4.3 PCR

Relative mRNA levels of specific adhesome and receptome proteins were determined using PCR. Amplification of 25 ng cDNA was performed using 500 nM each of pre-designed forward and reverse primers (Table 2.7; KiCqStart™, Sigma Aldrich). PowerSYBR Green mastermix (Applied Bioscience, Thermofisher) and primers were added to each well, with cDNA. Nuclease free water was used to adjust reaction volume to 10 µL. Reactions were performed in technical triplicate and analysed using the Quant studio™ Real Time PCR software version 1.7.1 (Applied Biosystems, Thermofisher). Relative expression was calculated using the $2^{-\Delta\Delta CT}$ method using RPL19 as a housekeeper, and data normalised to scramble siRNA control.

Table 2.7: Primer sequences. Sequences of predesigned KiCqStart™ primers used in the validation of siRNA knockdown by qPCR.

| Target | Direction | Primer sequence (5'-3') |
|----------|-----------|-------------------------|
| PC4 | Forward | TTCAGATTGGGAAAATGAGG |
| | Reverse | TGTCAGAAATCTGTTCCCTC |
| KYNU | Forward | AACTCTACTTACATGACTGGG |
| | Reverse | ACTGCAGTTTGTATCCATC |
| LGMN | Forward | ACTATGATGAGAAGAGGTCC |
| | Reverse | GGTGGAGATTGTTTTGTTTC |
| STMN1 | Forward | AGATGTACTTCTGGACTCAC |
| | Reverse | GATCAGACCAGGTAATCAATG |
| SLIRP | Forward | GCGTAGAAGTATCAATCAGC |
| | Reverse | CTTCTGAAGAAAAGTGAACCC |
| SERPINE1 | Forward | ATCCACAGCTGTCATAGTC |
| | Reverse | CACTTGCCCATGAAAAG |
| PTGS2 | Forward | AAGCAAGGCTAATACTGATAGG |
| | Reverse | TGTTGAAAAGTAGTTCTGGG |
| RPL19 | Forward | CAGAAGATACCGTGAATCTAAG |
| | Reverse | TGTTTTTGAACACATTCCCC |

2.6.2 Optimisation of protocols

2.6.2.1 Generation of spheroid-epithelium interfaces

The work in this thesis required preservation of spheroid-epithelium interfaces as previously developed in this laboratory (Evans et al., 2020b, 2020a; Kinnear et al., 2019). However, this process has been difficult to replicate for the immunolocalisation of adhesome proteins. I had previously

attempted culturing endometrial epithelial cells on a Matrigel coated, sectionable coverslip (Thermanox), and separately on a thin layer of collagen type I (Sigma). However, there were inconsistencies in the transfer of the monolayer to the agar plug into which the adhesive co-culture was embedded, and H&E staining revealed no spheroid-epithelium interfaces. Other issues with this model lay in the coverslip itself, occasionally coming loose and falling away during fixation of the agar plug in formalin, or during processing of the agar plug for paraffin embedding. After embedding, it is possible for the coverslip to shift during microtomy, leading to potential disruptions of the spheroid-epithelium interface, and other limitations of this model.

To improve this process, ECC-1 cells were seeded on a gel-like structure encased in a trans-well insert. This allowed removal of the insert membrane and preservation of the gel within an agar plug, ensuring that no shear stress was applied to the monolayer. For the model to be most biologically representative, a 3D co-gel model developed by a previous PhD student (Harriet Fitzgerald) in the Salamonsen laboratory was adapted (Appendix 2). This model uses fibrinogen, thrombin, and collagen type I to mimic the extracellular matrix of the human endometrium.

In short, fibrinogen, thrombin, and collagen are combined in the presence of CaCl_2 and protease inhibitors and allowed to set at 37°C for approximately one hour in a 12 well plate trans-well insert. ECC-1 cells were seeded on the co-gel in media containing protease inhibitors, and allowed to settle overnight. As previously described, a spheroid adhesion assay was performed on the co-culture (Section 2.6.1.1). Simultaneously, an adhesive co-culture was attempted with ECC-1 cells directly seeded onto a trans-well insert. The co-cultures were then preserved in a 5% agar solution, and the base of the trans-well insert was cut away from the plastic insert. The entire structure was removed and fixed in 10% NBF overnight before being processed through to paraffin wax.

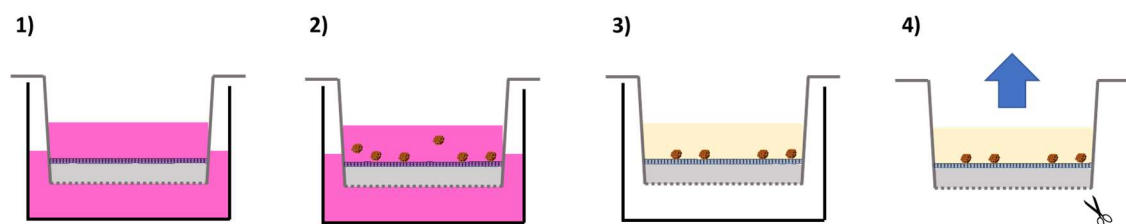


Figure 2.20: Schematic of 3D Co-gel for generation of spheroid-epithelium interface sections. (1) ECC-1 cells are seeded on a co-gel and hormonally primed before spheroids of trophectodermal stem cells are allowed to adhere **(2)**. Structure is embedded in agar **(3)** and removed for embedding in paraffin wax **(4)**.

A monolayer was successfully sectioned from ECC-1 cells seeded directly on a trans-well insert (Figure 2.21). Haematoxylin and eosin staining of sections from ECC-1 cells grown on a co-gel matrix indicate a poor monolayer (data not shown): it was difficult to observe the health of the monolayer

on the co-gel during culture, and it may be that the cells were not viable or did not grow correctly. This could be optimised by confirming the pH of the gel and attempting seeding of cells at varying densities.

Following completion of serial sectioning of the monolayer seeded directly on the trans-well insert, sections potentially containing spheroids have been identified (Figure 2.21). As the spheroid is very small, adjacent slides are being examined to see if the size of the spheroid changes. To confirm that these structures are indeed spheroids of trophectoderm cells, they could be stained for a protein marker known to be expressed in these cells (Zdravkovic et al., 2015). If this spheroid-endometrium interface is able to be replicated using this process, this protocol will be considered to be optimised. Due to the time-consuming nature of this technique, other research aims were prioritised to complete this thesis, however this technique provides an interesting avenue for future research.

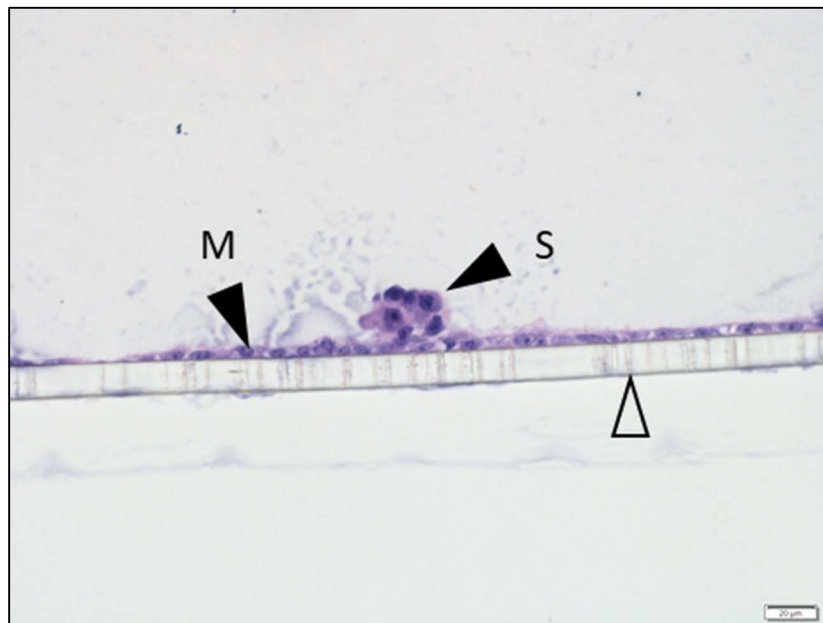


Figure 2.21: Cross section of a spheroid adherent to endometrial epithelial cell monolayer. A cross section of a presumptive spheroid of trophectoderm stem cells (S) adhered to a monolayer of epithelial cells (M), seeded on a trans-well insert (open arrow). Perpendicular lines within the trans-well insert are the pores which allow passage of nutrients. Scale bar represents 20 μm .

2.6.2.2 Immunolocalisation of receptome and adhesome proteins

Immunohistochemistry was performed using standard protocols described in Section 2.5.1.1. Optimisation of immunohistochemical staining for each receptome and adhesome protein investigated in this thesis is detailed in Table 2.8. Additional antibodies optimised but not used further include MAGT1, ACOT1, DENR, and S100A13. Due to an external data processing error independent of the Salamonsen laboratory, DENR and MAGT1 were originally included in the upregulated proteins of the receptome and adhesome but were later removed. ACOT1 was unable to be fully investigated

due to time constraints. Despite extensive efforts, the immunolocalisation of STMN1 was unable to be optimised, with trialled conditions listed in Table 2.9.

Antigen retrieval was generally performed using 10 mM sodium citrate containing 0.5% Tween 20 at pH 6.0, some specific antibodies were trialled with 0.1 M EDTA at pH 9.5. To optimise staining, two thermal conditions were used during antigen retrieval:

1. Standard retrieval: 5 min microwaving on medium-high, left immersed in hot buffer for 20 min.
2. Strong retrieval: 5 min microwaving on high, 3 min microwaving on medium-high, left immersed in hot buffer for 20 min.

The temperature of primary antibody incubation was also subject to optimisation:

1. Incubation 1: 16 h at 4°C
2. Incubation 2: 30 min at 37°C followed by 16 h at 4°C

Table 2.8: Optimisation of immunolocalisation of receptome and adhesome proteins in the human endometrium. Conditions trialled are given for each protein, with optimised antibody dilutions identified in bold. Staining of the glandular and luminal epithelium (GE, LE) and endometrial stroma are denoted as present (+) or strong (++). If not listed, no significant staining was noted.

| Protein | Primary antibody | Antigen retrieval | Blocking solution | Primary antibody dilution + incubation | Staining | Notes |
|----------|--|-------------------|-----------------------------------|--|---|-----------------------------------|
| PC4 | Mouse- α -PC4 (Santa Cruz) <i>0.2 mg/mL</i> | Standard citrate | 10% Horse serum 2% Human serum | 1:250 ; Incubation 1 | Nuclear staining GE (++) stroma (+) | No further optimisation required. |
| SERPINE1 | Mouse- α -SERPINE1 (Santa Cruz) <i>0.2 mg/mL</i> | Standard citrate | 10% Horse serum 2% Human serum | 1:100 ; Incubation 1 | GE (+), LE (++); Stroma (+) | No further optimisation required. |
| PTGS2 | Mouse- α -PTGS2 (Santa Cruz) <i>0.2 mg/mL</i> | Standard citrate | 10% Horse serum 2% Human serum | 1:100; Incubation 1 | GE, LE (+); Stroma (+) | Limited staining. |

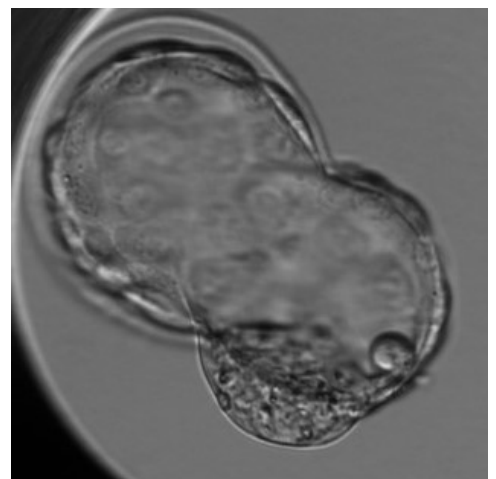
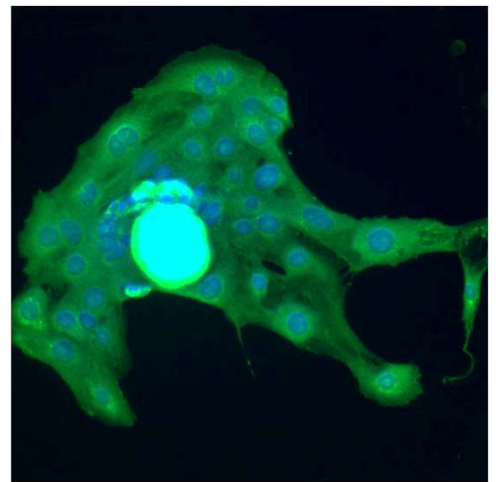
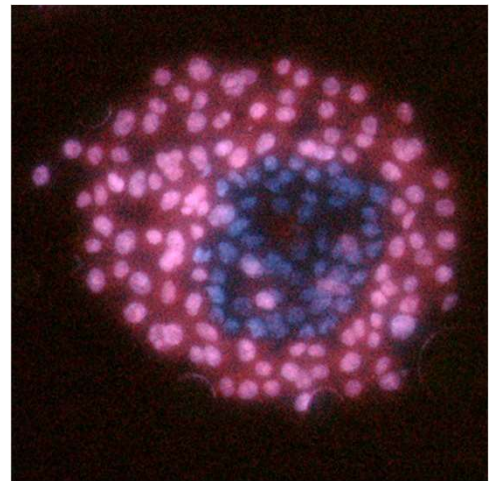
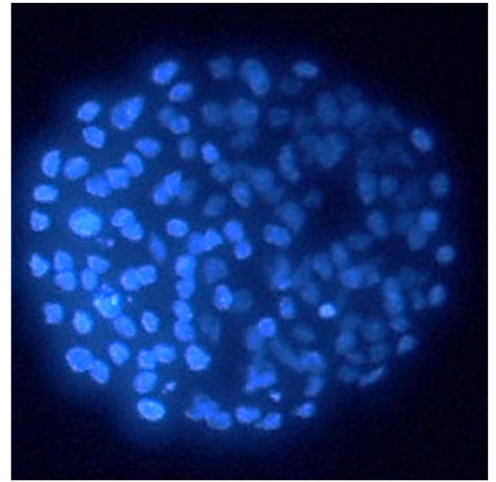
| | | | | | | |
|-------|--|---------------------|--------------------------------------|---|--|---|
| | | | | 1:50, 1:100 , 1:200, 1:400; Incubation 2 | GE (++), LE (+); Stroma (+) | 1:100 dilution selected as optimised condition. |
| KYNU | Mouse- α - KYNU (Santa Cruz) <i>0.2 mg/mL</i> | Standard citrate | 10% Horse serum 2% Human serum | 1:250; Incubation 1 | None | Higher antibody concentration to be trialed |
| | | | | 1:50, 1:100, 1:200; Incubation 1 | None | Limited staining |
| | | Strong citrate | | 1:50 Incubation 2 | GE (+) | 1:50 dilution / strong citrate selected as optimised condition. |
| LGMN | Mouse- α - LGMN (Santa Cruz) <i>0.2 mg/mL</i> | Standard citrate | 10% Horse serum 2% Human serum | 1:250 ; Incubation 1 | GE (++), LE (++) | No further optimisation required. |
| SLIRP | Mouse- α - SLIRP (Santa Cruz) <i>0.2 mg/mL</i> | Standard citrate | 10% Horse serum 2% Human serum | 1:250; Incubation 1 | Signal detection in isotype control | |
| | | Strong citrate | | 1:100 , 1:200; Incubation 2 | GE (+) | 1:100 dilution / strong citrate selected as optimised condition. |
| CDA | Mouse- α - CDA (Santa Cruz) <i>0.2 mg/mL</i> | Standard citrate | 10% Horse serum 2% Human serum | 1:250; Incubation 1 | GE (+), LE (+) | Staining evident in one tissue only. |
| | | | | 1:200 ; Incubation 1 | GE (+), LE (+) | 1:200 dilution selected as optimised condition. |

Table 2.9: Optimisation of STMN1 immunolocalisation in the human endometrium. Conditions trialled in the optimisation of STMN1. Staining of the glandular and luminal epithelium (GE, LE) and endometrial stroma are denoted as present (+) or strong (++) . If not listed, no significant staining was noted. This antibody was unable to be fully optimised. An alternative antibody could be tested.

| Protein | Primary antibody | Antigen retrieval | Blocking solution | Primary antibody dilution + incubation | Staining | Notes |
|---------|--|-------------------|--|--|---|------------------------|
| STMN1 | Goat- α -STMN1 (LS Bio) 0.5 mg/mL | Standard citrate | 10% Horse serum 2% Human serum | 1:250, 1:500; Incubation 1 | GE (+), LE (+); Stroma (+); Signal detection in isotype control | Wash of light staining |
| | | Standard citrate | 10% Horse serum 2% Human serum 10% fish skin gelatin | 1:100, 1:200; Incubation 2 | | No staining detected |
| | | Strong citrate | 5% Horse serum 2% Human serum 10% fish skin gelatin | 1:100, 1:200; Incubation 2 | GE (+) | Very faint staining |
| | | Strong EDTA | 5% Horse serum 2% Human serum 10% fish skin gelatin | 1:100, 1:200; Incubation 2 | GE (+) | Very faint staining |

Chapter 3:

The effect of obesity associated AGEs
on preimplantation embryo
development



Chapter 3: The effect of obesity associated Advanced Glycation Endproducts on preimplantation embryo development

Published manuscript

3.1 Chapter summary

The preimplantation embryo is exposed to the uterine fluid milieu as it undergoes the early and critical stages of development before adhesion and implantation into the maternal endometrium; perturbations of this environment may impact development, and the establishment and continuation of a healthy pregnancy. The work in this chapter aimed to determine if the altered uterine environment in relation to obesity-associated AGEs affected preimplantation embryo development.

Mouse embryos were collected at the 1 cell stage and cultured in concentrations of AGEs equimolar to the lean and obese uterine environment. As a comparison, embryos were also cultured under standard conditions without addition of AGEs or equivalent non-glycated protein to show the effects standard culture had on the same cohort of embryos, allowing comparison of how embryos from the same donor may develop *in utero* when exposed to AGEs, or *ex vivo*, when cultured for example after IVF.

Following exposure to concentrations of AGEs representative of the obese uterine environment, preimplantation embryo development, specifically trophectoderm formation and function, were compromised significantly in comparison to embryos exposed to lean concentrations of AGEs, or no AGEs. Pharmaceutical intervention was applied in the form of metformin, antagonism of the receptor for AGEs (RAGE), and a combination of antioxidants known to benefit preimplantation embryo development. Trophectoderm cell number was used as the experimental endpoint, and was only modestly improved by RAGE antagonism, but not by application of metformin or antioxidants. Future investigation could examine other cellular mechanisms through which AGEs may be exerting their effects including TLR4 activation and endoplasmic reticulum stress.

I have demonstrated that the obese uterine environment, containing elevated levels of AGEs, significantly compromises preimplantation embryo development. This provides a link between an altered maternal environment, and the poor reproductive outcomes experienced by women who are obese. As this early chapter reinforced the necessity for a quality microenvironment for preimplantation development, this thesis then examined the potential of pharmaceutical intervention in an attempt to normalise the functions of endometrial cells in the obese peri-implantation environment (Chapter 4).

The data from this chapter is here presented as a manuscript published in Reproductive Biomedicine Online (Impact factor 2.93, quartile 1 in Reproductive Biomedicine and Obstetrics and

Gynaecology). Author contributions are provided in the thesis including published works declaration at the start of this thesis.

3.2. Manuscript

Hutchison, J. C., Truong, T. T., Salamonsen, L. A., Gardner, D. K., Evans, J. (2020). Advanced Glycation End Products present in the obese uterine environment compromise preimplantation embryo development. *Reproductive Biomedicine Online*, 41 (5), 757-766.

ARTICLE



Advanced glycation end products present in the obese uterine environment compromise preimplantation embryo development



BIOGRAPHY

Jennifer Hutchison is currently completing her PhD under the primary supervision of Professor Lois Salamonsen at the Hudson Institute of Medical Research, Melbourne, Australia. Her major interests are understanding maternal–fetal communications and improving reproductive success for people who experience infertility.

Jennifer C. Hutchison^{1,2}, Thi T. Truong³, Lois A. Salamonsen^{1,2,*}, David K. Gardner³, Jemma Evans¹

KEY MESSAGE

Advanced glycation end products (AGE) link obesity with reduced fertility. Preimplantation embryo development within an AGE-rich environment detrimentally impacts trophoblast cell number and blastocyst outgrowth *in vitro*. Pre-conception reduction of intrauterine AGE may improve fertility outcomes for women with obesity or other metabolic syndromes associated with elevated AGE.

ABSTRACT

Research question: Proinflammatory advanced glycation end products (AGE), highly elevated within the uterine cavity of obese women, compromise endometrial function. Do AGE also impact preimplantation embryo development and function?

Design: Mouse embryos were cultured in AGE equimolar to uterine fluid concentrations in lean (1–2 $\mu\text{mol/l}$) or obese (4–8 $\mu\text{mol/l}$) women. Differential nuclear staining identified cell allocation to inner cell mass (ICM) and trophoblast (TE) (day 4 and 5 of culture). Cell apoptosis was examined by terminal deoxynucleotidyl transferase-mediated dUDP nick-end labelling assay (day 5). Day 4 embryos were placed on bovine serum albumin/fibronectin-coated plates and embryo outgrowth assessed 93 h later as a marker of implantation potential. AGE effects on cell lineage allocation were reassessed following pharmacological interventions: either 12.5 nmol/l AGE receptor (RAGE) antagonist; 0.1 nmol/l metformin; or combination of 10 $\mu\text{mol/l}$ acetyl-L-carnitine, 10 $\mu\text{mol/l}$ N-acetyl-L-cysteine, and 5 $\mu\text{mol/l}$ alpha-lipoic acid.

Results: 8 $\mu\text{mol/l}$ AGE reduced: hatching rates (day 5, $P < 0.01$); total cell number (days 4, 5, $P < 0.01$); TE cell number (day 5, $P < 0.01$), and embryo outgrowth ($P < 0.01$). RAGE antagonism improved day 5 TE cell number.

Conclusions: AGE equimolar with the obese uterine environment detrimentally impact preimplantation embryo development. In natural cycles, prolonged exposure to AGE may developmentally compromise embryos, whereas following assisted reproductive technology cycles, placement of a high-quality embryo into an adverse ‘high AGE’ environment may impede implantation success. The modest impact of short-term RAGE antagonism on improving embryo outcomes indicates preconception AGE reduction via pharmacological or dietary intervention may improve reproductive outcomes for overweight/obese women.

¹ Hudson Institute of Medical Research, 27–31 Wright Street Clayton VIC 3168, Australia

² Department of Molecular and Translational Science, Monash University Clayton VIC 3800, Australia

³ School of BioSciences, University of Melbourne, Parkville VIC 3010, Australia

KEYWORDS

Advanced glycation end products
Implantation
Obesity
Pregnancy
Preimplantation embryo development
Trophoblast

INTRODUCTION

Obesity, defined as a body mass index (BMI) ≥ 30 kg/m², is a rising global crisis, with the World Health Organization (WHO) estimating that globally almost 40% of adults are overweight or obese. In developed countries, around 60% of adults are overweight or obese (*World Health Organization, 2018*). Multiple comorbidities are associated with obesity, including diabetes, cardiovascular disease and cancer (*Khaodhiar et al., 1999*). While still under debate (*Insogna et al., 2017; Schliep et al., 2015*), a growing body of evidence implicates a detrimental impact of obesity on fertility (*Rittenberg et al., 2011*). Obese women take longer to achieve a pregnancy, and are less likely to conceive in a natural cycle (*Gesink Law et al., 2007*). Indeed, every one unit increase in BMI above 29 kg/m² reduces the probability of achieving a natural pregnancy by 4% (*Van Der Steeg et al., 2008*). Studies in assisted reproductive technology (ART) cycles further highlight these detrimentally affected outcomes in obese women. Maternal obesity is associated with reduced implantation and clinical pregnancy in comparison to lean women (*Moragianni et al., 2012*), and 15% reduction in live birth rate (*Sermondade et al., 2019*).

Obesity may impact female reproductive potential in various ways, including ovarian and oocyte function, embryo development and uterine receptivity. In animal models, diet-induced obesity detrimentally impacts follicle and oocyte health, and adversely affects embryo development (*Jungheim et al., 2010; Luzzo et al., 2012*). In humans, obesity reduces the number of oocytes retrieved, oocyte quality and fertilization success, and blastocyst formation following induced ovulation for ART (*Comstock et al., 2015; Kudesia et al., 2018; MacKenna et al., 2017; Shah et al., 2011; Wittemer et al., 2000*).

Independent of the impact of obesity on oocyte function, the obese uterine environment plays an important role in fertility outcomes. Obese women have an increased risk of early pregnancy loss (*Lashen et al., 2004; Metwally et al., 2008*), and their increased incidence of euploid embryo loss (*Landres et al., 2010; Tremellen et al., 2017*) implicates a detrimental impact of obesity on

endometrial function and implantation competency. Indeed, obesity has been suggested to affect the window of implantation in obese women, and alter expression of receptivity genes determined by the endometrial receptivity array (*Comstock et al., 2017*). Studies in which embryos obtained from donor oocytes from lean women, and transferred into obese women, show reduced ongoing clinical pregnancy and live birth rates compared with autologous transfers in lean women (*Bellver et al., 2013*).

The mechanisms that underpin the relationship between obesity and adverse reproductive outcomes are still largely unclear; however, recent data implicates intrauterine advanced glycation end products (AGE) in altered pregnancy outcomes (*Antonioti et al., 2018*). AGE are formed via the Maillard reaction when sugars glycate proteins, which can occur endogenously, or exogenously when foods are browned or heat-treated for preservation; thus AGE can be ingested from the diet (*Kellow and Coughlan, 2015; Poulsen et al., 2013*). AGE are proinflammatory and have been linked to many adverse conditions including cardiovascular disease and diabetes (*Ott et al., 2014; Zhou et al., 2016*). Their role in reproduction is starting to be elucidated: clinical studies show that follicular fluid and serum concentrations of AGE are negatively associated with ovarian response, embryo quality and live birth following ART (*Jinno et al., 2011; Takahashi et al., 2019; Yao et al., 2018*). Of particular relevance for this study, AGE within the intrauterine environment of obese women (BMI ≥ 30 kg/m²), where final preimplantation embryo development occurs (*Salamonsen et al., 2016*), are four-fold elevated compared with lean women (BMI < 25 kg/m²) (*Antonioti et al., 2018*).

This study aimed to elucidate the effect of AGE, equimolar with the obese uterine environment, on mouse preimplantation embryo development, and the impact of pharmacological interventions (RAGE antagonism, metformin, and an antioxidant cocktail shown to benefit preimplantation embryo development in culture (*Truong et al., 2016*)) on improving AGE-mediated effects. The findings demonstrate clearly that obesity-related AGE detrimentally affect preimplantation embryo development

and implantation potential. Importantly, these effects are partially ameliorated with antagonism of RAGE, providing a potential means to improve reproductive outcomes of women with obesity and other conditions associated with elevated AGE.

MATERIALS AND METHODS

In-vitro preparation of AGE

AGE were prepared and quantified previously (*Antonioti et al., 2018*). In brief, 10 mg/ml human serum albumin (HSA, Sigma, Castle Hill, NSW, Australia) in 0.2 mol/l Na₂HPO₄ (Sigma) buffer pH 7.5 containing 0.5 mol/l D-glucose (Sigma) was sterile-filtered before incubation under aerobic conditions at 37°C for 3 months. Excess glucose was removed by dialysis against pH 7.5 phosphate-buffered saline (PBS) at 4°C with regular buffer changes. AGE were again sterile-filtered, and endotoxins depleted using Detoxi-Gel™ Endotoxin Removing Resin (ThermoFisher, Scoresby, VIC, Australia). The concentration of AGE (μ mol/l AGE/mol lysine, reported here as μ mol) was determined using an in-house enzyme-linked immunosorbent assay (*Coughlan et al., 2011a*) and normalized to lysine content, as measured by mass spectrometry (*Degenhardt et al., 2002; Forbes et al., 2001*).

Embryo collection

Mice (C57BL/6xCBA) were housed in a 12 h light–dark cycle with food and water *ad libitum*. F1 virgin female mice (3–4 weeks old) were super-ovulated by intraperitoneal administration of 5 IU pregnant mare's serum gonadotrophin (Folligon; Intervet, UK). Ovulation was induced 48 h later by intraperitoneal administration of 5 IU of human chorionic gonadotrophin (Chorulon; Intervet, UK), followed by mating with F1 male mice (≥ 12 weeks of age). Mice with a vaginal plug, indicative of successful mating, were sacrificed by cervical dislocation 22 h after mating, and pronucleate oocytes collected in 37°C handling medium (G-MOPS PLUS; Vitrolife AB, Sweden) by dissection and tearing of the ampullae, as previously described (*Gardner and Truong, 2019*). Pronucleate oocytes were denuded of the surrounding cumulus cells by incubation in G-MOPS PLUS media containing 300 IU/ml hyaluronidase (bovine testes type IV, Sigma Aldrich, NSW, Australia). Embryos were then washed twice in G-MOPS PLUS, followed by a wash in G1™ PLUS media (Vitrolife) prior to

culture. Within each biological replicate, embryos were collected from multiple mice and pooled prior to allocation to experimental groups to control for inter-animal variation. A minimum of three biologically independent replicates were performed for each experiment, with a minimum total of 20 embryos per treatment group. All mice experimentation was approved by the University of Melbourne's Animal Ethics Committee (1814430, 29 March 2018).

Embryo culture

Unless otherwise stated, embryos were cultured in groups of 10 in 20 μ l drops of treatment-specific media under paraffin oil (Ovoil; Vitrolife) in 6% CO₂, 5% O₂ and 89% N₂ at 37°C in a humidified multi-gas incubator (Sanyo, Japan). Embryos were cultured in G1™ PLUS media (Vitrolife) for 48 h before a further 48 h culture in G2™ PLUS media (Vitrolife); treatments were maintained throughout culture.

AGE dose-response

Embryos were cultured as described above with the addition of 0, 1, 2, 4 or 8 μ mol/l AGE supplemented in both G1 and G2 medium. 1–2 μ mol/l AGE encompass the physiological concentrations of AGE in the lean human uterine environment, while 4–8 μ mol/l AGE represent the obese uterine environment (Antoniotti *et al.*, 2018). G1 and G2 medium with no AGE served to replicate standard in vitro culture conditions.

Therapeutic intervention

Dose-responses determined the optimal dose for RAGE antagonist (FPS-ZM1, Tocris; range 12.5–50 nmol/l) and metformin (Sigma; range 0.01 nmol/l to 1 μ mol/l) in the presence of 8 μ mol/l AGE. The therapeutic doses selected for FPS-ZM1 and metformin were 12.5 nmol/l and 0.1 nmol/l, respectively (dose-response data not shown). Antioxidant treatment has previously been optimized for embryo culture (Truong *et al.*, 2016), using a combination of acetyl-L-carnitine (10 μ mol/l, Sigma), N-acetyl-L-cysteine (10 μ mol/l, Sigma) and alpha-lipoic acid (5 μ mol/l, Sigma). The impact of therapeutic intervention was examined by assessing cell lineage allocation, as described below, following embryo culture in 0, 1 or 8 μ mol/l AGE, or 8 μ mol/l AGE supplemented with the optimal dose of FPS-ZM1, metformin or combined antioxidants.

Cell number and lineage allocation in the blastocyst

To assess allocation of cells to the inner cell mass (ICM) or trophectoderm (TE) in blastocysts, differential nuclear staining was performed following termination of culture on day 4 or 5 per standard protocols (Hardy *et al.*, 1989; Kelley and Gardner, 2016). The zona pellucida was removed using pronase (Sigma), TE labelled with propidium iodide, and all nuclei stained with 0.1 mg/ml bisbenzimidazole (Sigma). Blastocysts were mounted in 100% glycerol and imaged using a Nikon Eclipse TS100 microscope fitted with a digital camera, and cells counted using ImageJ software (National Institutes of Health [NIH], Bethesda, MD, USA).

Apoptosis within the embryo: terminal deoxynucleotidyl transferase (TUNEL) staining

Embryos were assessed for apoptosis using a DeadEnd™ Fluorometric TUNEL system (Promega, USA) according to the manufacturer's instructions. Embryos were fixed in 4% paraformaldehyde (PFA) in PBS for 1 h at room temperature, and washed twice in G-MOPS PLUS. Blastomeres were permeabilized with 0.125% Triton X-100 (Sigma) in 0.1% sodium citrate for 30 min at room temperature and washed three times with G-MOPS PLUS. Apoptotic cells were labelled with terminal deoxynucleotidyl transferase (TdT) by incubation for 60 min at 37°C in a humidified dark chamber. All nuclei were visualized with 0.1 mg/ml bisbenzimidazole. Embryos were imaged under a FITC filter and number of apoptotic nuclei determined and expressed as per cent total cells.

Blastocyst outgrowth

Ninety-six-well culture plates were rinsed with sterile PBS and coated with 10 μ g/ml fibronectin (BD Biosciences, NJ, USA) overnight at 4°C, as previously described (Binder *et al.*, 2015). After rinsing wells with sterile PBS, they were incubated with 4 mg/ml BSA for 2 h at room temperature. Wells were rinsed with PBS followed by G2 medium and filled with 150 μ l treatment-specific G2 medium supplemented with 5% fetal calf serum (Gibco, Life Technologies). Wells were equilibrated at 37°C under paraffin oil (Ovoil, Vitrolife) under 5% oxygen for 4 h before the addition of blastocysts. Embryos cultured in 0, 1 or 8 μ mol/l AGE which had reached or surpassed expanded blastocyst stage were

transferred to individual wells after 4 days of culture in the continued presence of AGE supplemented with 5% fetal calf serum. Blastocysts were imaged 45, 69 and 93 h after plating, and the area of the embryo outgrowth was measured using ImageJ software (NIH).

Statistical analysis and data representation

Analyses and representation performed using GraphPad Prism Version 8.2 (San Diego, CA, USA). Data were assessed for normality using a Shapiro–Wilk test. Normally distributed data were analysed using a one-way analysis of variance, followed by Tukey's post-hoc comparison testing. Those not normally distributed were analysed using a Kruskal–Wallis test, followed by Dunn's multiple comparisons test. Developmental stage and hatching rates were subjected to arcsine transformation before statistical analysis. Data are presented as mean \pm SEM. Biological significance was considered at $P < 0.05$.

RESULTS

Obese AGE compromise embryo development rates

The proportion of embryos developing to the blastocyst stage was determined in the presence of lean (1–2 μ mol/l) and obese (4–8 μ mol/l) AGE. Obese AGE did not significantly reduce the proportion of embryos reaching the blastocyst stage by day 4 (FIGURE 1A, $P = 0.14$), but by day 5, there was a significant reduction in the proportion of embryos forming hatching blastocysts when exposed to 8 μ mol/l AGE, compared with embryos that were exposed to no AGE throughout culture (FIGURE 2A, $P < 0.01$). In cultures maintained for 5 days, at the time of media changeover on day 3, AGE mediated no significant impact on the proportion of embryos containing 8 or fewer cells (TABLE 1, $P = 0.26$). Treatment with 8 μ mol/l AGE significantly impaired embryo development, as manifested by an increase in the proportion of embryos at compaction compared with lean concentrations or no AGE (TABLE 1, $P < 0.01$), and a reduction in the proportion of embryos that had reached or exceeded morula compared with no AGE in the culture medium (TABLE 1, $P = 0.04$).

AGE impact cell lineage allocation

Blastocysts cultured in obese concentrations of AGE (8 μ mol/l) for 4

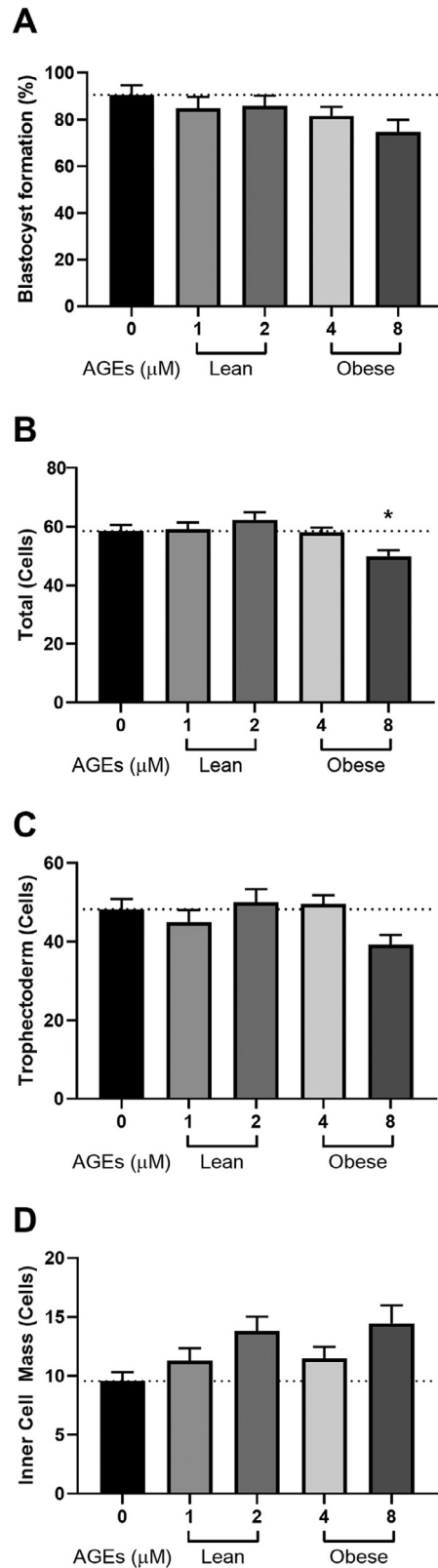


FIGURE 1 Obese concentrations of advanced glycation end products (AGE) affect total cell number, but not inner cell mass (ICM) or trophectoderm (TE) in the day 4 blastocyst. (A) The proportion of embryos in a group culture droplet forming blastocysts was not significantly affected by lean (1–2 $\mu\text{mol/l}$) or obese (4–8 $\mu\text{mol/l}$) concentrations of AGE ($P = 0.14$). (B) Embryos cultured in 8 $\mu\text{mol/l}$ AGE had significantly fewer total cells compared with those cultured in 0 $\mu\text{mol/l}$ ($P = 0.02$), 1 $\mu\text{mol/l}$ ($P = 0.02$), 2 $\mu\text{mol/l}$ ($P < 0.001$), or 4 $\mu\text{mol/l}$ ($P = 0.02$) AGE. Increasing concentrations of AGE did not significantly affect TE (C) ($P = 0.06$). AGE impacted ICM cell number ($P = 0.03$), but no statistical difference was detected between treatments (D). Controls were embryos cultured in media with no AGE (0 $\mu\text{mol/l}$, standard culture conditions). Mean in each case is the derivative of at least five biologically independent replicates with a minimum of 26 embryos per group. * $P < 0.05$ versus all other conditions.

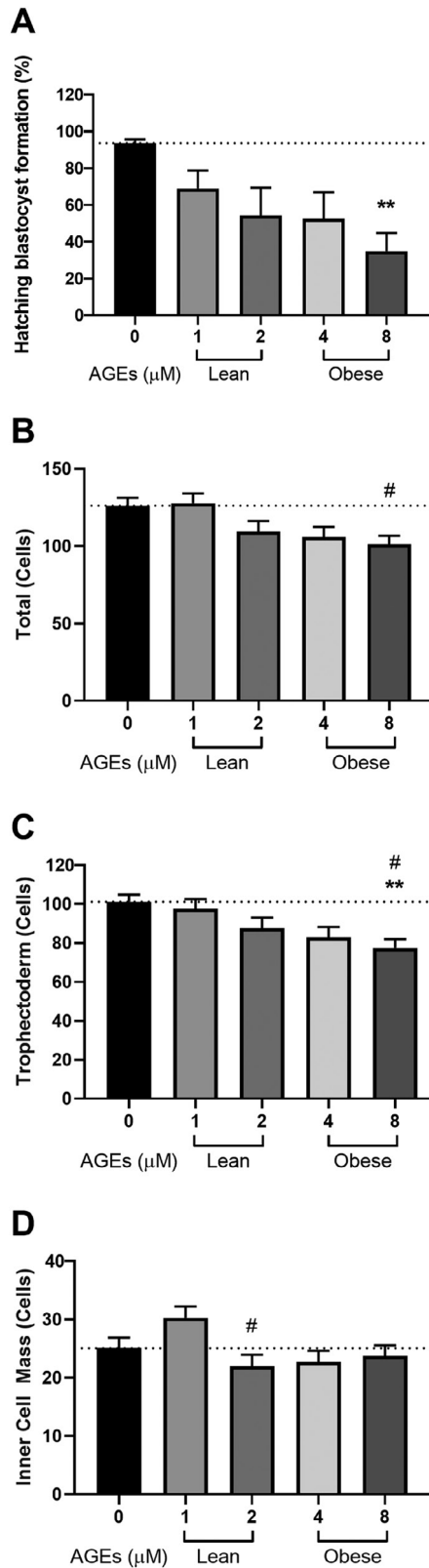


FIGURE 2 Obese concentrations of AGE affect embryo hatching, total, and TE cell number in the day 5 blastocyst. (A) The proportion of embryos forming hatching blastocysts was significantly reduced when embryos were cultured in obese (8 $\mu\text{mol/l}$) concentrations of AGE compared to 0 $\mu\text{mol/l}$ AGE (standard culture conditions ($P < 0.01$)). (B) 8 $\mu\text{mol/l}$ AGE reduced the total number of cells compared with 1 $\mu\text{mol/l}$ ($P = 0.03$), no group was significantly different in comparison to standard culture ($P \geq 0.052$ for all). (C) Embryos cultured in 8 $\mu\text{mol/l}$ AGE had fewer TE cells compared with 0 $\mu\text{mol/l}$ ($P < 0.01$) and 1 $\mu\text{mol/l}$ AGE ($P = 0.04$). (D) Lean 2 $\mu\text{mol/l}$ AGE reduced the number of ICM cells compared with lean 1 $\mu\text{mol/l}$ AGE ($P = 0.02$), no group was significantly different in comparison to standard culture ($P \geq 0.43$ for all). Controls were embryos cultured in media with no AGE (0 $\mu\text{mol/l}$, standard culture conditions). Mean in each case is the derivative of four biological replicates with a minimum of 33 total embryos per group. ****** $P < 0.01$ versus 0 $\mu\text{mol/l}$ AGE. **#** $P < 0.05$ versus 1 $\mu\text{mol/l}$ AGE.

TABLE 1 OBESE CONCENTRATIONS OF AGE AFFECT EMBRYO DEVELOPMENTAL RATES

| Developmental stages of embryos on day 3 of culture (mean % ± SEM) | | | | | |
|--|------------|-------------|-------------|-------------|--------------|
| AGE (μmol/l) | 0 | 1 | 2 | 4 | 8 |
| ≤8 cells | 4.6 ± 4.6 | 9.6 ± 4.8 | 14.8 ± 10.2 | 17.3 ± 9.1 | 28.6 ± 10.1 |
| Compacting | 17.6 ± 5.8 | 19.3 ± 7.3 | 13.1 ± 5.4 | 25.9 ± 5.0 | 46.7 ± 7.2*# |
| ≥Morula | 77.9 ± 8.5 | 71.0 ± 11.4 | 72.2 ± 12.3 | 56.8 ± 13.1 | 24.7 ± 9.9* |

Mean % ± SEM of embryos in a culture drop at each developmental stage at the time of media changeover on day 3 in cultures that were continued for 5 days. Exposure to AGE did not impact the proportion of embryos containing 8 or fewer cells ($P = 0.26$). Treatment with 8 μmol/l AGE was associated with significantly more embryos at compaction compared to lean (1 μmol/l ($P = 0.03$) and 2 μmol/l ($P < 0.01$)) or no AGE ($P = 0.02$). Treatment with 8 μmol/l AGE was associated with fewer embryos that had reached or exceeded morula stage compared to standard culture conditions ($P = 0.04$). * $P < 0.05$ vs 0 μmol/l AGE

$P < 0.05$ vs 1 or 2 μmol/l AGE.

days had a reduced total cell number compared with all other conditions (FIGURE 1B, $P < 0.01$), with a decrease in the number of TE cells approaching significance (FIGURE 1C, $P = 0.058$). A significant effect of AGE on ICM number following 4 days of culture was detected ($P = 0.03$), but multiple comparisons testing did not detect a difference between groups, the increase in number of ICM cells in embryos exposed to 8 μmol/l AGE approaching significance compared with standard culture (FIGURE 1D, $P = 0.056$). After 5 days of culture in 8 μmol/l AGE (obese), embryos exhibited a significant reduction in total cell number (FIGURE 2B) compared with lean 1 μmol/l ($P = 0.03$), but not standard culture ($P = 0.052$). Around 20% fewer cells were identified within the TE compared with standard culture ($P < 0.01$) and lean conditions (1 μmol/l, $P = 0.04$) (FIGURE 2C). The ICM had a higher number of cells when cultured with 1 μmol/l AGE, compared with 2 μmol/l AGE (both lean; FIGURE 2D,

$P = 0.02$). No significant difference was seen between standard culture and any other treatment ($P \geq 0.43$ for all).

AGE do not increase cell apoptosis in the embryo

Apoptosis was investigated as a potential mechanism to explain the reduced cell number in blastocysts cultured with obese AGE. Obese AGE did not alter the percentage of cells undergoing apoptosis as determined by TUNEL assay (4 μmol/l [$1.07 \pm 0.34\%$] or 8 μmol/l [$1.55 \pm 0.32\%$]), compared with standard culture and lean conditions (0 μmol/l [$1.54 \pm 0.54\%$], 1 μmol/l [$0.62 \pm 0.25\%$], 2 μmol/l [$1.50 \pm 0.44\%$] ($P = 0.12$)). Mean is the derivative of three biologically independent replicates with a minimum of 30 embryos per experimental group (immunofluorescence not shown).

AGE impair TE function

Neither lean nor obese concentrations of AGE impacted embryo outgrowth

at 45 h ($P = 0.75$) or 69 h ($P = 0.17$), however obese AGE (8 μmol/l) significantly reduced embryo outgrowth at 93 h compared with 0 μmol/l AGE ($P < 0.01$), but not in comparison to 1 μmol/l AGE (FIGURE 3).

Effects of AGE are partially attenuated by RAGE inhibition

Neither metformin nor a cocktail of antioxidants improved embryo outcomes, as assessed by total cell number and TE/ICM cell number, in the presence of 8 μmol/l AGE (FIGURE 4A-C). However, co-treatment with the RAGE antagonist FPS-ZM1 partially attenuated AGE impacts such that the total cell number (FIGURE 4A), TE (FIGURE 4B) and ICM (FIGURE 4C) cell numbers were not significantly different to culture without AGE (standard culture). Treatment with 8 μmol/l AGE mediated an approximately 20% reduction in TE ($P < 0.01$) and total cell number ($P < 0.01$) in comparison to standard culture, and in the presence of FPS-ZM1, this was approximately a 10% ($P = 0.92$) or 12% ($P = 0.35$) reduction, respectively, compared with standard culture. Culture in 8 μmol/l AGE reduced the ICM in comparison to 1 μmol/l AGE ($P < 0.01$), but not standard culture ($P > 0.99$). With the addition of the RAGE antagonist, ICM was not significantly different to 1 μmol/l AGE (lean) or culture in 8 μmol/l AGE without therapeutics (obese), however both TE and total cell number remained significantly reduced in comparison to 1 μmol/l AGE ($P < 0.01$), and were not significantly increased in comparison to culture in 8 μmol/l AGE without therapeutics.

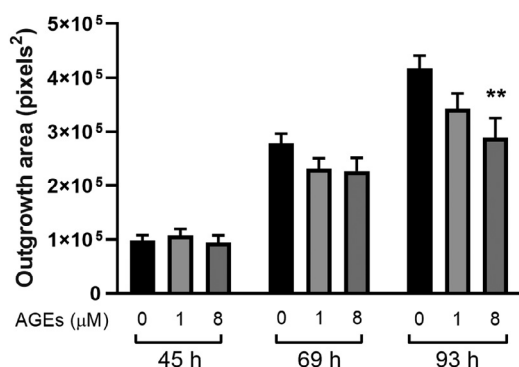


FIGURE 3 AGE impact embryo outgrowth. Blastocyst outgrowth was not significantly affected after 45 h ($P = 0.75$) or 69 h ($P = 0.17$) by either lean (1 μmol/l) or obese (8 μmol/l) concentrations of AGE. Compared with 0 μmol/l AGE, embryos cultured in 8 μmol/l AGE had reduced outgrowth after 93 h ($P < 0.01$). Culture in 1 μmol/l AGE did not significantly affect blastocyst outgrowth compared with 0 μmol/l AGE ($P = 0.08$) or 8 μmol/l AGE ($P = 0.45$). Controls were embryos cultured in media with no AGE (0 μmol/l, standard culture conditions). Mean is the derivative of three biological replicates with a minimum of 20 total embryos per group. ** $P < 0.01$ versus 0 μmol/l AGE.

DISCUSSION

This study provides strong evidence to support clinical reports of an adverse impact of obesity on fertility outcomes.

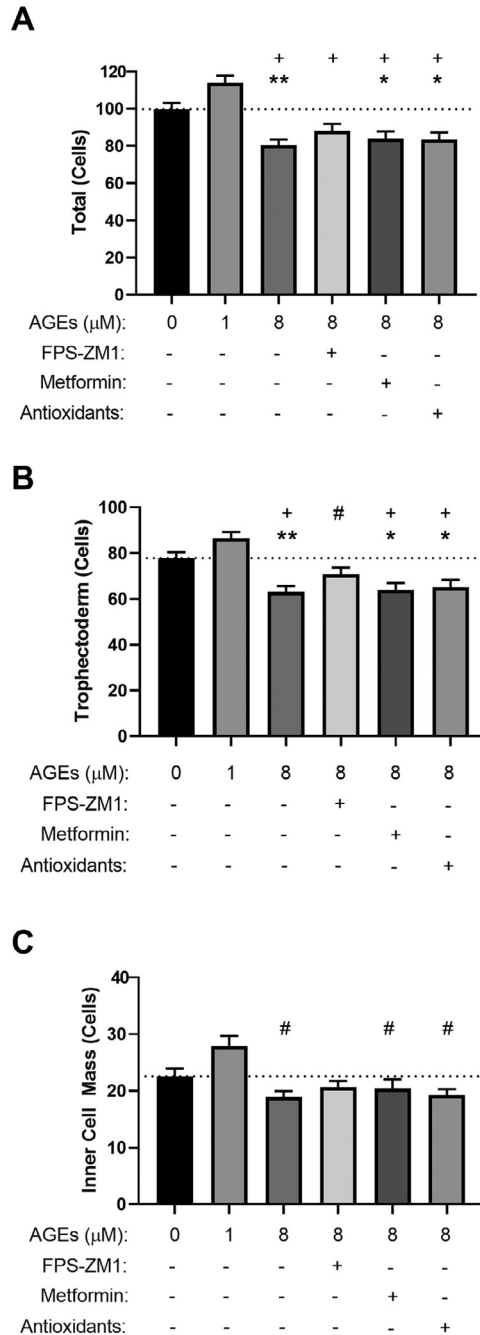


FIGURE 4 RAGE antagonism reduces the effects of AGE on the day 5 blastocyst. Cell number (mean \pm SEM) of (A) total blastocyst, (B) TE and (C) ICM, when treated with lean (1 μ mol/l) and obese (8 μ mol/l) concentrations of AGE and the addition of therapeutics. 8 μ mol/l AGE significantly reduced the number of TE ($P < 0.01$) and total ($P < 0.01$) cells in comparison to 0 μ mol/l and 1 μ mol/l AGE. Embryos cultured in 8 μ mol/l AGE supplemented with 12.5 nmol/l RAGE antagonist (FPS-ZM1) had fewer total and TE cells compared with 1 μ mol/l ($P < 0.01$) but not 0 μ mol/l AGE (standard culture conditions; $P = 0.35$, 0.92 , respectively). The total cell number was significantly lower than 0 and 1 μ mol/l AGE following culture in 8 μ mol/l AGE with the addition of either 0.1 nmol/l metformin ($P = 0.03$, <0.0001 , respectively) or antioxidants ($P < 0.03$, <0.0001 , respectively). The TE cell number was significantly lower than 0 and 1 μ mol/l AGE following culture in 8 μ mol/l AGE with the addition of either 0.1 nmol/l metformin ($P = 0.01$, <0.0001 , respectively) or antioxidants ($P = 0.02$, <0.0001 , respectively). The ICM was significantly reduced in comparison to 1 μ mol/l AGE following culture in 8 μ mol/l AGE either alone ($P < 0.01$) or containing metformin or antioxidants (both $P < 0.01$), but not in comparison to 8 μ mol/l AGE supplemented with FPS-ZM1 ($P = 0.14$). The ICM of embryos under standard culture conditions (0 μ mol/l AGE) was not significantly different to 1 μ mol/l ($P = 0.62$), or 8 μ mol/l either alone or with therapeutics ($P > 0.99$ for all). No condition significantly reduced ICM cell number in comparison to 0 μ mol/l AGE (standard culture conditions). Mean is the derivative of six biological replicates with a minimum of 52 embryos per group. *,** $P < 0.05$, 0.01 versus 0 μ mol/l AGE. # $P < 0.01$ versus 1 μ mol/l AGE, + $P < 0.0001$ versus 1 μ mol/l AGE.

Specifically, it demonstrates that AGE equimolar with those within the obese uterine fluid microenvironment (Antoniotti *et al.*, 2018) compromise preimplantation embryo development and function relating to implantation potential, as demonstrated by reduced blastocyst outgrowth. Given the need for synchronous development of the endometrium and embryo for successful implantation, alterations in developmental timing and embryo function induced by exposure to AGE as shown here, may contribute significantly to the sub-fertility and increased time to pregnancy experienced by obese women (Gesink Law *et al.*, 2007; Van Der Steeg *et al.*, 2008). Indeed, delayed embryo development will create dys-synchrony between embryonic and endometrial development, a significant issue given that late implantation of an embryo is more likely to result in early pregnancy loss (Wilcox *et al.*, 1999). Thus, the data presented here are highly pertinent to the clinical observation that obese women are more likely to undergo spontaneous abortion of euploid embryos (Tremellen *et al.*, 2017).

Hatching from the zona pellucida, facilitated by mechanical force exerted by the expanding blastocyst (Leonavicius *et al.*, 2018) and trypsin-like protease production (Perona and Wassarman, 1986; Vu *et al.*, 1997), is a critical step towards an implantation-competent blastocyst (Balaban *et al.*, 2000). Exposure to obese concentrations of AGE for 5 days significantly reduced the rate of hatching of mouse embryos compared with lean concentrations. Of the potential mechanisms underpinning this, the reduced cell number in day 5 embryos may impact the mechanical contribution of the embryo to hatching (Leonavicius *et al.*, 2018). Although not examined here, there is evidence that AGE can inhibit proteolytic activity (Ott *et al.*, 2014), and this may also be relevant. Future work will examine whether embryonic protease expression and activities are altered by obese AGE.

Appropriate allocation of blastocyst cells to either TE or ICM is critical for a healthy pregnancy. Inappropriate TE formation may 'feed forward' to compromise implantation competency or placental development, while variation in the ICM is associated with altered birthweight (Licciardi *et al.*, 2015), which may set the offspring up for a lifetime of

altered health outcomes (*Leddy et al., 2008*). Here, AGE-mediated differential effects on embryo cell lineage allocation were dependent on time in culture. After 4 days in culture, the total number of cells in the blastocyst was significantly reduced by obese concentrations of AGE, probably due to reduction in TE cell number. Reduced blastocyst cell number in the absence of increased apoptosis, and reduced proportion of embryos having reached or exceeded morula on day 3, implies AGE mediate an anti-proliferative effect as observed in endometrial epithelial cells (*Antonioti et al., 2018*). This observation persisted to day 5, with a significant decrease in TE cells observed in embryos cultured in obese concentrations of AGE, and may indicate that the function of the TE may be adversely impacted by elevated AGE.

The reduced TE cell number in the presence of obese AGE implies fewer functioning cells to adhere to and traverse the endometrial epithelium at implantation. In addition, the reduced in-vitro blastocyst outgrowth seen at 93 h in such culture provides an indication of in-vivo adhesion and implantation potential (*Binder et al., 2015*). AGE-mediated effects on TE formation and function are of clinical significance in light of the increased risk of pre-eclampsia and related disorders experienced by obese women (*Poorolajal and Jenabi, 2016*), because subsequent to implantation, trophoblastic cells then differentiate into the range of invasive and syncytial trophoblast cells that provide the embryonic component of the placenta. Indeed, AGE have previously been associated with poor placental function, and can increase oxidative stress in placental cells (*Konishi et al., 2004; Shirasuna et al., 2016*). In-vitro outgrowth experiment results warrant future validation and investigation by embryo transfer into recipient females.

Clinically, overweight and obese women are at an increased risk of developing gestational complications, including recurrent implantation failure and pre-eclampsia (*Boots et al., 2014; Roberts et al., 2011; Sugiura-Ogasawara, 2015*), all of which are in part attributable to poor implantation and placentation (*Saito and Nakashima, 2014*). The reduction in TE cell number and outgrowth of mouse blastocysts cultured in high concentrations of AGE provides a link between obesity and these pathologies.

By attempting to reduce or neutralize the effects of AGE before conception, it may be possible to significantly improve pregnancy outcomes for these women.

Of the three therapeutics trialed (RAGE antagonist, metformin and a combination of antioxidants), only RAGE antagonism mediated a small improvement in embryo development, implying that in the mouse embryo, RAGE signalling may be one mechanism by which AGE exert their detrimental effects. It is important to note that RAGE is not the only receptor activated by AGE. AGE can also interact with and signal through Toll-like receptor 4 (TLR4) and AGE receptor complex (*Ott et al., 2014; Shirasuna et al., 2016; Xie et al., 2013*). Thus, a signalling blockade including multi-receptor antagonism may be necessary. However, a longer-term, preconception therapy to reduce uterine AGE through either diet or prolonged pharmacological intervention with an AGE targeting drug such as the AGE crosslink breaker Alagebrium (*Coughlan et al., 2011b*) may be more appropriate. While the antioxidants used in this study have been shown to benefit embryo outcomes (*Liang et al., 2017; Truong et al., 2016; Truong and Gardner, 2017*) and exhibit anti-AGE effects (*Hao et al., 2008; Hsuuw et al., 2005*), the concentrations used exceed the concentrations utilized here. The concentrations used in this study were previously optimized for embryo culture with significant benefits to TE cell numbers (*Truong et al., 2016*). However, further studies trialling higher concentrations of these antioxidants on potential AGE-induced oxidative damage and reactive oxygen species production in the preimplantation embryo may be helpful.

Cellular mechanisms underpinning the reduced TE cell number and blastocyst outgrowth mediated by obesity-associated AGE are still to be elucidated. Activation of RAGE can induce cellular endoplasmic reticulum stress, reported in decidualized human endometrial stromal cells exposed to AGE equimolar with the obese uterine environment (*Antonioti et al., 2018*). Endoplasmic reticulum stress detrimentally impacts oocyte mitochondrial function, and subsequent development of mouse embryos (*Wu et al., 2015, 2012*), and may be activated by AGE in the preimplantation embryo.

Further to endoplasmic reticulum stress, metabolism and epigenetic regulation may be impacted by

obesity-associated AGE. Combined parental obesity in a mouse model demonstrating compromised TE shows increased glucose consumption per cell in an embryo but no increase in lactate production (*Finger et al., 2015*), and the metabolic profile of human embryos from obese women is altered compared with lean counterparts (*Bellver et al., 2015; Leary et al., 2015*). Epigenetic regulation is important in the specification of TE and ICM cells, and in obese mice, epigenetic modifications are altered in the oocyte in both diet-induced and genetic models of obesity (*Hou et al., 2016*). Linking elevated AGE to any of the above in the preimplantation embryo would provide a mechanism for AGE-induced effects, and identify novel therapeutic targets.

While highly pertinent, the data presented here using a mouse model may not transfer directly to human biology. In support of their relevance, in women, elevated serum and follicular fluid AGE have been correlated to poor ovarian response, reduced embryo quality and lower ongoing pregnancy rates following ART (*Jinno et al., 2011; Takahashi et al., 2019; Yao et al., 2018*), while obese concentrations of AGE reduce adhesion of spheroids of human TE stem cells to human endometrial epithelial cells (*Antonioti et al., 2018*). Together the evidence to date supports detrimental effects of AGE in the uterine microenvironment of implantation and establishment of a healthy pregnancy, but further studies in human cell lines and clinical trials need to occur before AGE targeting becomes clinical practice.

Two translational conclusions can be drawn from the data presented here. Firstly, it may be possible to improve embryo development within the uterine cavity of obese women by either pharmacological intervention or preconception dietary reduction of AGE. Secondly, an assay of uterine AGE may be applied before obese women undergo fertility treatments including embryo transfer or intrauterine insemination, to assess the AGE concentrations, and to follow any effort to reduce these before treatment. Thus, this research provides critical evidence of the need for preconception interventions to reduce or inhibit the activity of intrauterine AGE and optimize pregnancy outcomes for women with obesity.

ACKNOWLEDGEMENTS

The authors acknowledge Ms Kathryn Gurner for her technical assistance, and Professor Melinda Coughlan for quantification of AGE-HSA.

This work was supported in part by: a bridge grant from the Study for Reproductive Investigation (to JE); the Victorian Government Operational Infrastructure support program to the Hudson Institute; University of Melbourne (to TTT and DKG); Australian Government Research Training Program (RTP) Scholarship (to JH); Fielding Foundation fellowship (to JE).

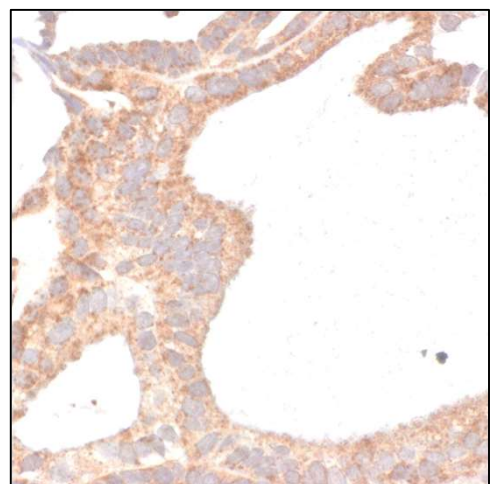
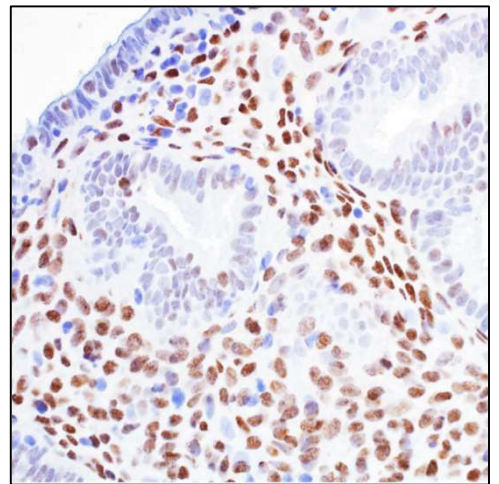
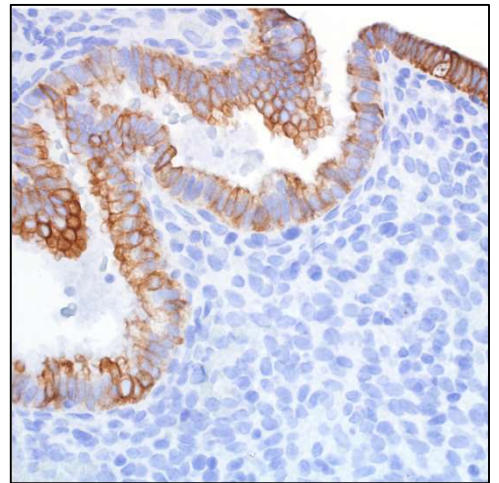
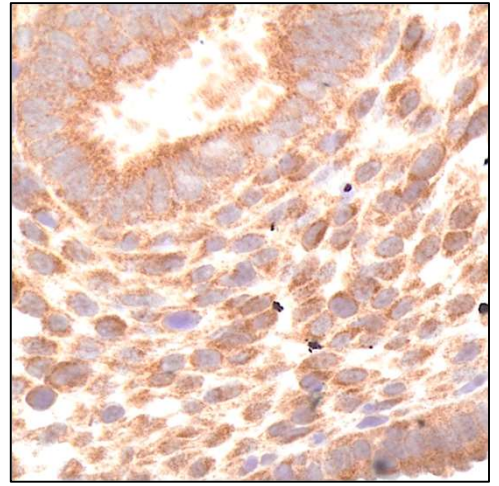
REFERENCES

- Antoniotti, G.S., Coughlan, M., Salamonsen, L.A., Evans, J. **Obesity associated advanced glycation end products in the uterine cavity adversely impact endometrial function and embryo implantation competence.** *Hum. Reprod.* 2018; 33: 654–665. doi:10.1093/humrep/dey029
- Balaban, B., Urman, B., Sertac, A., Alatas, C., Aksoy, S., Mercan, R. **Blastocyst quality affects the success of blastocyst-stage embryo transfer.** *Fertil. Steril.* 2000; 74: 282–287. doi:10.1016/S0015-0282(00)00645-2
- Bellver, J., De Los Santos, M.J., Alamá, P., Castelló, D., Privitera, L., Galliano, D., Labarta, E., Vidal, C., Pellicer, A., Domínguez, F. **Day-3 embryo metabolomics in the spent culture media is altered in obese women undergoing in vitro fertilization.** *Fertil. Steril.* 2015; 103. doi:10.1016/j.fertnstert.2015.03.015
- Bellver, J., Pellicer, A., García-Velasco, J.A., Ballesteros, A., Remohí, J., Meseguer, M. **Obesity reduces uterine receptivity: Clinical experience from 9,587 first cycles of ovum donation with normal weight donors.** *Fertil. Steril.* 2013; 100: 1050–1058. doi:10.1016/j.fertnstert.2013.06.001
- Binder, N.K., Hannan, N.J., Gardner, D.K. **In vitro embryo outgrowth is a bioassay of in vivo embryo implantation and development.** *Asian Pacific J. Reprod.* 2015; 4: 240–241. doi:10.1016/j.apjr.2015.06.009
- Boots, C.E., Bernardi, L.A., Stephenson, M.D. **Frequency of euploid miscarriage is increased in obese women with recurrent early pregnancy loss.** *Fertil. Steril.* 2014; 102: 455–459. doi:10.1016/j.fertnstert.2014.05.005
- Comstock, I.A., Diaz-Gimeno, P., Cabanillas, S., Bellver, J., Sebastian-Leon, P., Shah, M., Schutt, A., Valdes, C.T., Ruiz-Alonso, M., Valbuena, D., Simon, C., Lathi, R.B. **Does an increased body mass index affect endometrial gene expression patterns in infertile patients? A functional genomics analysis.** *Fertil. Steril.* 2017; 107: 740–748. doi:10.1016/j.fertnstert.2016.11.009
- Comstock, I.A., Kim, S., Behr, B., Lathi, R.B. **Increased body mass index negatively impacts blastocyst formation rate in normal responders undergoing in vitro fertilization.** *J. Assist. Reprod. Genet.* 2015; 32: 1299–1304. doi:10.1007/s10815-015-0515-1
- Coughlan, M.T., Patel, S.K., Jerums, G., Penfold, S.A., Nguyen, T.V., Sourris, K.C., Panagiotopoulos, S., Srivastava, P.M., Cooper, M.E., Burrell, L.M., MacIsaac, R.J., Forbes, J.M. **Advanced glycation urinary protein-bound biomarkers and severity of diabetic nephropathy in man.** *Am. J. Nephrol.* 2011; 34: 347–355. doi:10.1159/000331064
- Coughlan, M.T., Yap, F.Y.T., Tong, D.C.K., Andrikopoulos, S., Gasser, A., Thallas-Bonke, V., Webster, D.E., Miyazaki, J., Kay, T.W., Slattey, R.M., Kaye, D.M., Drew, B.G., Kingwell, B.A., Fourlanos, S., Groop, P.-H., Harrison, L.C., Knip, M., Forbes, J.M. **Advanced Glycation End Products are direct modulators of β -cell function.** *Diabetes* 2011; 60: 2523–2532. doi:10.2337/db10-1033
- Deegenhardt, T.P., Alderson, N.L., Arrington, D.D., Beattie, R.J., Basgen, J.M., Steffes, M.W., Thorpe, S.R., Baynes, J.W. **Pyridoxamine inhibits early renal disease and dyslipidemia in the streptozotocin-diabetic rat.** *Kidney Int.* 2002; 61: 939–950. doi:10.1046/j.1523-1755.2002.00207.x
- Finger, B.J., Harvey, A.J., Green, M.P., Gardner, D.K. **Combined parental obesity negatively impacts preimplantation mouse embryo development, kinetics, morphology and metabolism.** *Hum. Reprod.* 2015; 30: 2084–2096. doi:10.1093/humrep/dev142
- Forbes, J.M., Soulis, T., Thallas, V., Panagiotopoulos, S., Long, D.M., Vasan, S., Wagle, D., Jerums, G., Cooper, M.E. **Renoprotective effects of a novel inhibitor of advanced glycation.** *Diabetologia* 2001; 44: 108–114. doi:10.1007/s001250051587
- Gardner, D.K., Truong, T.T. **Culture of the Mouse Preimplantation Embryo.** *Methods Mol. Biol.* 2019; 2006: 13–32
- Gesink Law, D.C., Maclehorse, R.F., Longnecker, M.P. **Obesity and time to pregnancy.** *Hum. Reprod.* 2007; 22: 414–420. doi:10.1093/humrep/del400
- Hao, L., Noguchi, S., Kamada, Y., Sasaki, A., Matsuda, M., Shimizu, K., Hiramatsu, Y., Nakatsuka, M. **Adverse effects of Advanced Glycation End Products on embryonal development.** *Acta Med. Okayama* 2008; 62: 93–99
- Hardy, K., Handyside, A.H., Winston, R.M. **The human blastocyst: cell number, death and allocation during late preimplantation development in vitro.** *Development* 1989; 107: 597–604
- Hou, Y.J., Zhu, C.C., Duan, X., Liu, H.L., Wang, Q., Sun, S.C. **Both diet and gene mutation induced obesity affect oocyte quality in mice.** *Sci. Rep.* 2016; 6: 18858. doi:10.1038/srep18858
- Hsuuw, Y.-D., Chang, C., Chan, W., Yu, J. **Curcumin Prevents Methylglyoxal-Induced Oxidative Stress and Apoptosis in Mouse Embryonic Stem Cells and Blastocysts.** *J. Cell. Physiol.* 2005; 205: 379–386. doi:10.1002/jcp.20408
- Insogna, I.G., Lee, M.S., Reimers, R.M., Toth, T.L. **Neutral effect of body mass index on implantation rate after frozen-thawed blastocyst transfer.** *Fertil. Steril.* 2017; 108: 770–776. doi:10.1016/j.fertnstert.2017.08.024
- Jinno, M., Takeuchi, M., Watanabe, A., Teruya, K., Hirohama, J., Eguchi, N., Miyazaki, A. **Advanced glycation end-products accumulation compromises embryonic development and achievement of pregnancy by assisted reproductive technology.** *Hum. Reprod.* 2011; 26: 604–610. doi:10.1093/humrep/deq388
- Jungheim, E.S., Schoeller, E.L., Marguard, K.L., Loudon, E.D., Schaffer, J.E., Moley, K.H. **Diet-induced obesity model: abnormal oocytes and persistent growth abnormalities in the offspring.** *Endocrinology* 2010; 151: 4039–4046. doi:10.1210/en.2010-0098
- Kelley, R.L., Gardner, D.K. **Combined effects of individual culture and atmospheric oxygen on preimplantation mouse embryos in vitro.** *Reprod. Biomed. Online* 2016; 33: 537–549. doi:10.1016/j.rbmo.2016.08.003
- Kellow, N.J., Coughlan, M.T. **Effect of diet-derived advanced glycation end products on inflammation.** *Nutr. Rev.* 2015; 73: 737–759. doi:10.1093/nutrit/nuv030
- Khaodhiar, L., McCowen, K.C., Blackburn, G.L. **Obesity and its comorbid conditions.** *Clin. Cornerstone* 1999; 2: 17–31. doi:10.1016/S1098-3597(99)90002-9
- Konishi, H., Nakatsuka, M., Chekir, C., Noguchi, S., Kamada, Y., Sasaki, A., Hiramatsu, Y. **Advanced glycation end products induce secretion of chemokines and apoptosis in human first trimester trophoblasts.** *Hum.*

- Reprod. 2004; 19: 2156–2162. doi:10.1093/humrep/deh389
- Kudesia, R., Wu, H., Hunter Cohn, K., Tan, L., Lee, J.A., Copperman, A.B., Yurttas Beim, P. **The effect of female body mass index on *in vitro* fertilization cycle outcomes: a multi-centre analysis.** J. Assist. Reprod. Genet. 2018; 35: 2013–2023. doi:10.1007/s10815-018-1290-6
- Landres, I.V., Milki, A.A., Lathi, R.B. **Karyotype of miscarriages in relation to maternal weight.** Hum. Reprod. 2010; 25: 1123–1126. doi:10.1093/humrep/deq025
- Lashen, H., Fear, K., Sturdee, D.W. **Obesity is associated with increased risk of first trimester and recurrent miscarriage: matched case-control study.** Hum. Reprod. 2004; 19: 1644–1646. doi:10.1093/humrep/deh277
- Leary, C., Leese, H.J., Sturmey, R.G. **Human embryos from overweight and obese women display phenotypic and metabolic abnormalities.** Hum. Reprod. 2015; 30: 122–132. doi:10.1093/humrep/deu276
- Leddy, M.A., Power, M.L., Schulkin, J. **The impact of maternal obesity on maternal and fetal health.** Rev. Obstet. Gynecol. 2008; 1: 170–178
- Leonavicius, K., Royer, C., Preece, C., Davies, B., Biggins, J.S., Srinivas, S. **Mechanics of mouse blastocyst hatching revealed by a hydrogel-based microdeformation assay.** Proc. Natl. Acad. Sci. 2018; 115: 10375–10380. doi:10.1073/pnas.1719930115
- Liang, L.F., Qi, S.T., Xian, Y.X., Huang, L., Sun, X.F., Wang, W.H. **Protective effect of antioxidants on the pre-maturation ageing of mouse oocytes.** Sci. Rep. 2017; 7: 1434–1444. doi:10.1038/s41598-017-01609-3
- Licciardi, F., McCaffrey, C., Oh, C., Schmidt-Sarosi, C., McCulloh, D.H. **Birth weight is associated with inner cell mass grade of blastocysts.** Fertil. Steril. 2015; 103: 382–387. doi:10.1016/j.fertnstert.2014.10.039
- Luzzo, K.M., Wang, Q., Purcell, S.H., Chi, M., Jimenez, P.T., Grindler, N., Schedl, T., Moley, K.H. **High Fat Diet Induced Developmental Defects in the Mouse: Oocyte Meiotic Aneuploidy and Fetal Growth Retardation/Brain Defects.** PLoS One 2012; 7: e49217. doi:10.1371/journal.pone.0049217
- MacKenna, A., Schwarze, J.E., Crosby, J.A., Zegers-Hochschild, F. **Outcome of assisted reproductive technology in overweight and obese women.** JBRA Assist. Reprod. 2017; 21: 79–83. doi:10.5935/1518-0557.20170020
- Metwally, M., Ong, K.J., Ledger, W.L., Li, T.C. **Does high body mass index increase the risk of miscarriage after spontaneous and assisted conception? A meta-analysis of the evidence.** Fertil. Steril. 2008; 90: 714–726. doi:10.1016/j.fertnstert.2007.07.1290
- Moragianni, V.A., Jones, S.-M.L., Ryley, D.A. **The effect of body mass index on the outcomes of first assisted reproductive technology cycles.** Fertil. Steril. 2012; 98: 102–108. doi:10.1016/j.fertnstert.2012.04.004
- Ott, C., Jacobs, K., Haucke, E., Navarrete Santos, A., Grune, T., Simm, A. **Role of advanced glycation end products in cellular signaling.** Redox Biol 2014; 2: 411–429. doi:10.1016/j.redox.2013.12.016
- Perona, R.M., Wassarman, P.M. **Mouse blastocysts hatch *in vitro* by using a trypsin-like proteinase associated with cells of mural trophoderm.** Dev. Biol. 1986; 114: 42–52. doi:10.1016/0012-1606(86)90382-9
- Poorolajal, J., Jenabi, E. **The association between body mass index and preeclampsia: a meta-analysis.** J. Matern. Fetal Neonatal. Med. 2016; 29: 3670–3676. doi:10.3109/14767058.2016.1140738
- Poulsen, M.W., Hedegaard, R.V., Andersen, J.M., de Courten, B., Bügel, S., Nielsen, J., Skibsted, L.H., Dragsted, L.O. **Advanced glycation endproducts in food and their effects on health.** Food Chem. Toxicol. 2013; 60: 10–37. doi:10.1016/j.fct.2013.06.052
- Rittenberg, V., Seshadri, S., Sunkara, S.K., Sobaleva, S., Oteng-Ntim, E., El-toukhy, T. **Effect of body mass index on IVF treatment outcome: an updated systematic review and meta-analysis.** Reprod. Biomed. Online 2011; 23: 421–439. doi:10.1016/j.rbmo.2011.06.018
- Roberts, J.M., Bodnar, L.M., Patrick, T.E., Powers, R.W. **The role of obesity in preeclampsia.** Pregnancy Hypertens. An Int. J. Women's Cardiovasc. Heal. 2011; 1: 6–16. doi:10.1016/j.preghy.2010.10.013
- Saito, S., Nakashima, A. **A review of the mechanism for poor placentation in early-onset preeclampsia: The role of autophagy in trophoblast invasion and vascular remodeling.** J. Reprod. Immunol. 2014; 101–102: 80–88. doi:10.1016/j.jri.2013.06.002
- Salamonsen, L.A., Evans, J., Nguyen, H.P.T., Edgell, T.A. **The Microenvironment of Human Implantation: Determinant of Reproductive Success.** Am. J. Reprod. Immunol. 2016; 75: 218–225. doi:10.1111/aji.12450
- Schliep, K.C., Mumford, S.L., Ahrens, K.A., Hotaling, J.M., Carrell, D.T., Link, M., Hinkle, S.N., Kissell, K., Porucznik, C.A., Hammoud, A.O. **Effect of male and female body mass index on pregnancy and live birth success after *in vitro* fertilization.** Fertil. Steril. 2015; 103: 388–395. doi:10.1016/j.fertnstert.2014.10.048
- Sermondade, N., Huberlant, S., Bourhis-Lefebvre, V., Arbo, E., Gallot, V., Colombani, M., Fréour, T. **Female obesity is negatively associated with live birth rate following IVF: a systematic review and meta-analysis.** Hum. Reprod. Update 2019; 25: 439–451. doi:10.1093/humupd/dmz011
- Shah, D.K., Missmer, S.A., Berry, K.F., Racowsky, C., Ginsburg, E.S. **Effect of obesity on oocyte and embryo quality in women undergoing *in vitro* fertilization.** Obstet. Gynecol. 2011; 118: 63–70. doi:10.1097/AOG.0b013e31821fd360
- Shirasuna, K., Seno, K., Ohtsu, A., Shiratsuki, S., Ohkuchi, A., Suzuki, H., Matsubara, S., Nagayama, S., Iwata, H., Kuwayama, T. **AGEs and HMGB1 Increase Inflammatory Cytokine Production from Human Placental Cells, Resulting in an Enhancement of Monocyte Migration.** Am. J. Reprod. Immunol. 2016; 75: 557–568. doi:10.1111/aji.12506
- Sugiura-Ogasawara, M. **Recurrent pregnancy loss and obesity.** Best Pract. Res. Clin. Obstet. Gynaecol. 2015; 29: 489–497. doi:10.1016/j.bpobgyn.2014.12.001
- Takahashi, N., Harada, M., Azhary, J.M., Kunitomi, C., Nose, E., Terao, H., Koike, H., Wada-Hiraike, O., Hirata, T., Hirota, Y., Koga, K., Fujii, T., Osuga, Y. **Accumulation of Advanced Glycation End Products in follicles is associated with poor oocyte developmental competence.** Mol. Hum. Reprod. 2019; gaz050. doi:10.1093/molehr/gaz050
- Tremellen, K., Pearce, K., Zander-Fox, D. **Increased miscarriage of euploid pregnancies in obese women undergoing cryopreserved embryo transfer.** Reprod. Biomed. Online 2017; 34: 90–97. doi:10.1016/j.rbmo.2016.09.011
- Truong, T., Gardner, D.K. **Antioxidants improve IVF outcome and subsequent embryo development in the mouse.** Hum. Reprod. 2017; 32: 2404–2413. doi:10.1093/humrep/dex330
- Truong, T., Soh, Y.M., Gardner, D.K. **Antioxidants improve mouse preimplantation embryo development and viability.** Hum. Reprod. 2016; 31: 1445–1454. doi:10.1093/humrep/dew098
- Van Der Steeg, J.W., Steures, P., Eijkemans, M.J.C., Habbema, J.D.F., Hompes, P.G.A., Burggraaf, J.M., Oosterhuis, G.J.E., Bossuyt, P.M.M., Van Der Veen, F., Mol, B.W.J. **Obesity affects spontaneous pregnancy chances in subfertile, ovulatory women.** Hum. Reprod. 2008; 23: 324–328. doi:10.1093/humrep/dem371
- Vu, T.-K.H., Liu, R.W., Haakma, C.J., Tomasek, J.J., Howard, E.W. **Identification and cloning of the membrane-associated serine protease, hepsin, from mouse preimplantation embryos.** J. Biol. Chem. 1997; 272: 31315–31320. doi:10.1074/jbc.272.50.31315
- Wilcox, A.J., Baird, D.D., Weinberg, C.R. **Time of Implantation of the Conceptus and Loss of Pregnancy.** N. Engl. J. Med. 1999; 340: 1796–1799. doi:10.1056/NEJM199906103402304
- Wittemer, C., Ohl, J., Bailly, M., Bettahar-Lebugle, K., Nisand, I. **Does body mass index of infertile women have an impact on IVF procedure and outcome?** J. Assist. Reprod. Genet. 2000; 17: 547–552. doi:10.1023/A:1026477628723
- World Health Organization. 2018 **European Health Report 2018: More than numbers – evidence for all.** WHO Regional Office for Europe Copenhagen <https://www.euro.who.int/en/publications/abstracts/european-health-report-2018-more-than-numbers-evidence-for-all-2018>
- Wu, L.L., Russell, D.L., Norman, R.J., Robker, R.L. **Endoplasmic reticulum (ER) stress in cumulus-oocyte complexes impairs pentraxin-3 secretion, mitochondrial membrane potential ($\Delta\Psi_m$), and embryo development.** Mol. Endocrinol. 2012; 26: 562–573. doi:10.1210/me.2011-1362
- Wu, L.L., Russell, D.L., Wong, S.L., Chen, M., Tsai, T.S., St John, J.C., Norman, R.J., Febbraio, M.A., Carroll, J., Robker, R.L. **Mitochondrial dysfunction in oocytes of obese mothers: Transmission to offspring and reversal by pharmacological endoplasmic reticulum stress inhibitors.** Development 2015; 142: 681–691. doi:10.1242/dev.114850
- Xie, J., Méndez, J.D., Méndez-Valenzuela, V., Aguilar-Hernández, M.M. **Cellular signalling of the receptor for advanced glycation end products (RAGE).** Cell. Signal. 2013; 25: 2185–2197. doi:10.1016/j.cellsig.2013.06.013
- Yao, Q., Liang, Y., Shao, Y., Bian, W., Fu, H., Xu, J., Sui, L., Yao, B., Li, M. **Advanced glycation end product concentrations in follicular fluid of women undergoing IVF/ICSI with a GnRH agonist protocol.** Reprod. Biomed. Online 2018; 36: 20–25. doi:10.1016/j.rbmo.2017.09.003
- Zhou, Z., Tang, Y., Jin, X., Chen, C., Lu, Y., Liu, L., Shen, C. **Metformin inhibits Advanced Glycation End Products-induced inflammatory response in murine macrophages partly through AMPK activation and RAGE/NF κ B pathway suppression.** J. Diabetes Res. 2016; 2016: 1–10. doi:10.1155/2016/4847812

Chapter 4:

Normalising the functions of
endometrial cells exposed to obesity
associated AGEs



Chapter 4: Normalising the functions of endometrial cells exposed to obesity associated AGEs

Therapeutic interventions to improve implantation potential

Chapter 3 of this thesis described significant effects of Advanced Glycation Endproducts (AGEs) equimolar to those in the obese uterine fluid on the preimplantation embryo, but these were not fully normalised by therapeutic intervention. This highlighted the need to optimise the maternal environment to support healthy embryo development and implantation. As Antoniotti et al. (2018), demonstrated significantly altered endometrial cell functions in the presence of obese concentrations of AGEs, this chapter focussed on the use of pharmacological interventions to normalise the obese endometrial environment to support a healthy pregnancy.

4.1 Introduction

While the mechanisms linking obesity and reduced endometrial competency are still unclear (Bellver et al., 2013b; DeUgarte et al., 2010; Tremellen et al., 2017), AGEs are emerging as a potential mediator of obesity's detrimental effects on both male and female reproductive systems (Mallidis et al., 2008; Merhi, 2014). Of relevance to the work in this chapter, AGEs are significantly elevated in the uterine cavity of obese women, impairing epithelial cell proliferation and adhesive capacity, stromal cell decidualisation, and trophoblast invasion (Antoniotti et al., 2018). Furthermore, concentrations of AGEs equimolar to those in the obese uterine environment compromise the development and function of trophectoderm cells in the mouse blastocyst, exhibited as a low trophectoderm cell number and reduced blastocyst outgrowth (Chapter 3), further substantiating the link between obesity and poor placental formation and function.

AGEs interact with a variety of cellular receptors, predominantly the Receptor for AGEs (RAGE), AGE Receptor Complex-1 (also known as OST-48), and Toll-Like Receptor 4 (TLR4) (Konishi et al., 2004; Noguchi et al., 2010; Ott et al., 2014). Both RAGE and TLR4 are present within the human endometrium (Antoniotti et al., 2018; Fazeli et al., 2005) but little is known of OST-48. RAGE and TLR4 are involved in chronic inflammation (Gąsiorowski et al., 2018), and the obese uterine environment is highly pro-inflammatory (Antoniotti et al., 2018). Interaction of AGEs with RAGE and TLR4 result in increased cell stress, activation of the unfolded protein response, and increased inflammatory responses through NFκB (Ott et al., 2014; Xie et al., 2013). Further, in first trimester trophoblast cells (Sw.71 cells), inhibition of RAGE and TLR4 was able to prevent the secretion of IL-6 secretion stimulated by AGEs (Shirasuna et al., 2016). This indicates receptor antagonism may be beneficial in normalising endometrial cell functions.

Specific therapies to optimise the success of IVF and ART for obese women would be highly beneficial. Whilst maintenance of a healthy weight should be encouraged, a variety of physical, psychological, and socioeconomic factors may make weight loss difficult for individuals, and weight loss may have only minimal impact on reproductive potential (Norman and Mol, 2018). As a variety of therapeutics were unable to completely reverse detrimental the effects of AGEs on preimplantation development (Chapter 3), optimising the implantation environment may improve conception rates by actions on endometrial receptivity. Thus, the research presented here aimed to ameliorate AGEs-mediated effects on endometrial cell function described by Antoniotti et al. (2018), by application of a RAGE antagonist, metformin, and a previously published trio of antioxidants (Truong et al., 2016). The effects of AGEs on endoplasmic reticulum stress were further investigated in this research to identify additional therapeutic targets to normalise the functions of endometrial cells in the obese uterine environment.

4.2 Methodology

Work in this chapter used standard protocols detailed in Chapter 2. Brief descriptions of methodology are provided where required with results.

4.2.1 Donor demographics for human endometrial stromal cell experimentation

Human endometrial stromal cells were collected as per section 2.4.1.2 between days 10 and 24 of the menstrual cycle and cultured blind to the fertility of the donor. Out of 5 samples, 2 had a history of fertility, and 3 had a history of primary infertility. Donors had an average age of 32 years (range 24-40), and a BMI of 24 kg/m² (range 21-29). One patient had evidence of endometrial fibroids, and one donor was undergoing IVF. Individual donor characteristics are available in Table 4.1.

Table 4.1: Donor characteristics. Stromal cell cultures were generated from 5 endometrial donors. Fertility status, age (years), BMI (kg/m²), cycle phase (histologically determined) and patient reported cycle day at time of collection, are noted. (-) No data available. For donors 1-3, histopathological dating was unavailable.

| Donor # | Fertility status | Age | BMI | Day of cycle | Cycle stage | Notes |
|---------|-------------------|-----|-----|--------------|-----------------|------------------------------------|
| 1 | Fertile | - | 26 | 10 | - | Fibroids |
| 2 | Primary infertile | 40 | 29 | 18 | - | Normal endometrium, undergoing IVF |
| 3 | Fertile | 35 | 21 | 10 | - | Normal endometrium, |
| 4 | Primary infertile | 29 | 22 | 24 | Late secretory | Normal endometrium |
| 5 | Infertile | 24 | 22 | 18 | Early secretory | Normal endometrium |

4.2.2 Therapeutic intervention

ECC-1, human endometrial stromal cells, and the trophoblast cell line HTR8/SVneo, were cultured in the presence of AGEs equimolar to the lean (2 μ M) and obese (8 μ M) uterine fluid, and obese AGEs further supplemented with therapeutics, optimised as in Section 2.4.2.2, and detailed in Table 4.2. Where FPS-ZM1 was added to an experiment, its vehicle DMSO at 0.0005% vol/vol was added to all wells including controls in that experiment. This was not necessary for experiments with metformin and antioxidants

Table 4.2: Therapeutic interventions. Optimised concentrations utilised to remediate the effects of obesity-associated AGEs on endometrial cell functions.

| Therapeutic | | Optimised concentration |
|--------------|-----------------------|-------------------------|
| FPS-ZM1 | | 25 nM |
| Metformin | | 100 μ M |
| Antioxidants | N-Acetyl-L-Cysteine | 10 μ M |
| | N-acetyl-L-Carnitine | 10 μ M |
| | α -Lipoic acid | 5 μ M |

4.2.3 Western immunoblotting

Using standard protocols, ECC-1 cells were seeded at a density of 2.5×10^5 cells per well in a 12 well plate, and left to settle overnight. Cells were starved of serum for 6 h, treated with 10^{-8} M E for 24 h in the presence of lean or obese AGEs alone or obese AGEs further supplemented with therapeutics (Table 4.2), and 10^{-8} M E + 10^{-7} M MPA for an additional 24 h with experimental treatments continued. Cells were lysed in ice-cold RIPA buffer, and Western immunoblotting performed as per Section 2.4.1.5. The concentrations of antibodies used in this chapter are detailed in Table 4.3. The detection of TLR4 could not be optimised due to time constraints.

Table 4.3: Antibodies utilised to examine ER stress. Concentrations of primary and secondary antibodies used to examine ER stress in ECC-1 cell lysates through Western Immunoblotting.

| Target | Primary antibody | Dilution | Secondary antibody |
|--------|--|----------|---|
| RAGE | Mouse monoclonal, Santa Cruz (sc-365154) <i>0.2 mg/mL</i> | 1:2000 | 1:5000 Goat anti Mouse – HRP conjugated |
| CHOP | Rabbit polyclonal, Thermofisher (PA588116) | 1:2000 | 1:5000 Goat anti Rabbit – HRP conjugated |

| | | | |
|---------|---|----------|---|
| | 2.85 mg/mL | | 1:5000 Goat anti Rabbit – HRP conjugated |
| ATF4 | Rabbit polyclonal ThermoFisher (PA519521) 0.8 mg/mL | 1:2000 | |
| B-actin | Rabbit monoclonal HRP conjugated (Cell Signalling Technology #5125) | 1:10,000 | N/A |

4.3 Results

4.3.1 AGE receptors are affected by obesity associated AGEs

Western immunoblotting confirmed the expression of RAGE in ECC-1 cells (Figure 4.1) indicating that antagonism of this receptor is an appropriate therapeutic strategy. A strong band was observed at approximately 45 kDa, the expected molecular weight of RAGE (shown), and two weak bands seen at approximately 60 and 100 kDa, most likely a result of dimerization and glycosylation. No other bands were visible on the blot. Quantification using iLab software (Version 6.1, Bio-Rad) demonstrated a significant modulation of RAGE expression in the presence of AGEs ($P < 0.01$; Figure 4.1 A). Physiologically obese AGEs (8 μ M) significantly increased RAGE expression approximately 1.5-fold compared to lean AGEs (2 μ M; $P = 0.041$) and no AGEs control ($P = 0.047$). RAGE remained elevated in the presence of the antagonist FPS-ZM1 in comparison to lean AGEs (2 μ M; $P = 0.012$) and no AGEs control ($P = 0.013$). With metformin and antioxidants, no significant difference in RAGE expression was detected ($P = 0.39$; Figure 4.1 B), though a similar 1.5-fold increase in RAGE expression was observed with obese AGEs.

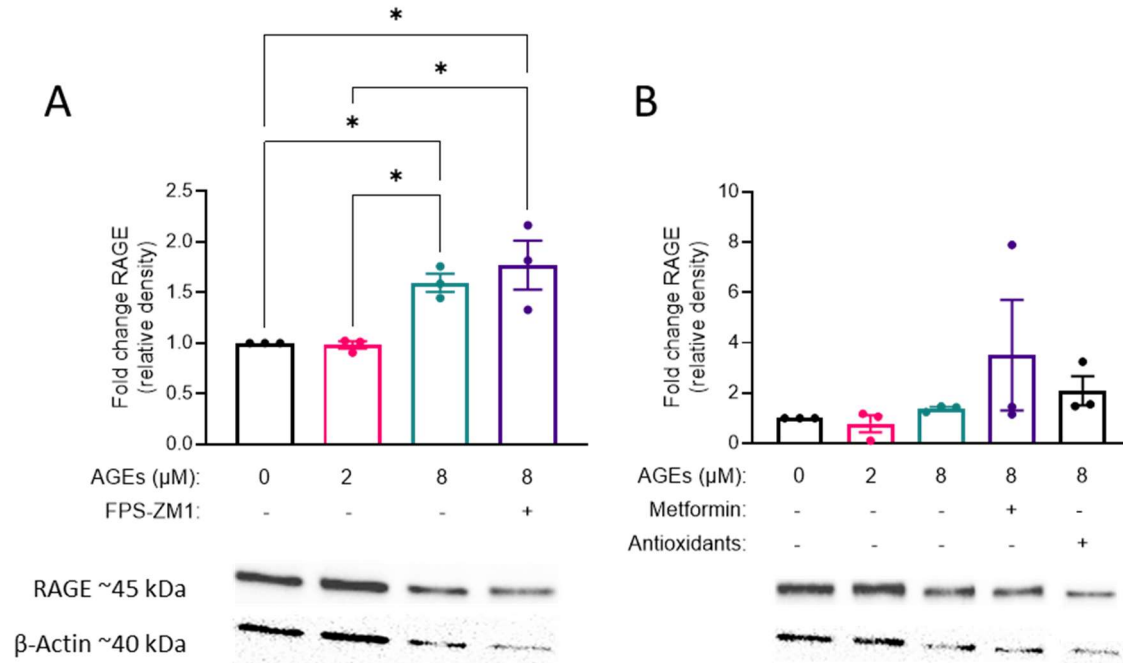


Figure 4.1: RAGE expression in ECC-1 is influenced by obesity-associated AGEs. Representative Western immunoblots of RAGE and β -actin loading control, mean \pm SEM (derived from $n=3$) relative band intensity, normalised to standard culture conditions ($0 \mu\text{M}$ AGEs control). **A)** Obese AGEs ($8 \mu\text{M}$) mediated a significant increase in RAGE expression in comparison to lean ($2 \mu\text{M}$) and no AGEs ($P = 0.012$, 0.048 respectively) while FPS-ZM1 was without further effect. Lean AGEs did not alter RAGE expression relative to control ($P > 0.99$). **B)** Application of metformin or antioxidants did not further alter RAGE expression in the presence of obese AGEs ($P = 0.39$). Individual data points represent independent replicates. One-way ANOVA: $*P < 0.05$.

4.3.2 The effects of AGEs on endometrial epithelial cell proliferation are partially normalised by antioxidants

Previously, AGEs equimolar to the obese uterine environment significantly reduced the adhesion and proliferation of ECC-1 cells (Antoniotti et al., 2018), an effect recapitulated here (Figures 4.2 and 4.3). ECC-1 cells were hormonally primed, and treated with lean and obese concentrations of AGEs (as per Section 4.2.3), or obese AGEs further supplemented with therapeutics (Table 4.1). Adhesion and proliferation of ECC-1 cells on fibronectin was analysed using the xCelligence system (cell culture and xCelligence protocol: Section 2.4.1.4). The rate of adhesion was determined between 0 and 5 h, and the rate of proliferation determined between 12 and 72 h. Obese concentrations of AGEs significantly decreased the rate of proliferation of ECC-1 cells, reflected in a reduced cell index across all time points (Figures 4.2 and 4.3). Of the three therapeutics tested, only antioxidants normalised the rate of proliferation of ECC-1 cells in the presence of obese concentrations of AGEs (Figure 4.3 E), but these antioxidants did not rescue cell index, likely a result of the continued decrease in rate of cell adhesion.

AGEs altered the growth kinetics of ECC-1 alone and in the presence of a RAGE antagonist (Figure 4.2 A). During the period of adhesion (1-5 h; Figure 4.2 B), cell index was not affected at 1 h ($P = 0.13$), but an overall effect of treatment was detected at 2 h ($P = 0.017$), 3 h ($P = 0.018$), 4 h ($P = 0.021$), and 5 h ($P = 0.037$). Obese AGEs reduced cell index in comparison to no AGEs control at 2 h ($P = 0.027$), 3 h ($P = 0.035$) and 4 h ($P = 0.046$). No significant effect of other treatments was detected at these time points. Whilst overall significant, no specific treatment effects were observed at 5 h. Whilst an overall significant effect was seen on the rate of adhesion ($P = 0.036$; Figure 4.2 C), no effect of individual treatments was detected ($P \geq 0.08$ for all comparisons).

During the period of proliferation (12-72 h), a significant effect of AGEs on ECC-1 cell index (Figure 4.2 D) and rate of proliferation (Figure 4.2 E) was observed. An overall effect of treatment was seen on cell index at 12 h ($P = 0.020$), and 24 h ($P = 0.011$), with no specific effect of any treatment. At 36 h, compared to no AGEs control, cell index was significantly reduced in the presence of obese AGEs alone ($P = 0.032$), and obese AGEs supplemented with FPS-ZM1 ($P = 0.036$). Compared to lean (2 μ M) AGEs, obese AGEs significantly reduced cell index ($P = 0.049$). Obese AGEs in the presence of FPS-ZM1 did not significantly reduce cell index in comparison to lean ($P = 0.054$). At 48 h, only obese AGEs in the presence of FPS-ZM1 significantly reduced cell index compared to no AGEs control ($P = 0.038$). No condition was significantly reduced compared to lean AGEs ($P \geq 0.059$ for all). After 60 h, cell index was significantly affected ($P < 0.01$), but no specific treatment effect was detected ($P \geq 0.068$ for all). After 72 h, obese AGEs alone and with FPS-ZM1 reduced cell index in comparison to lean AGEs ($P = 0.048$, 0.037 respectively). There was no effect of any treatment in comparison to no AGEs control ($P \geq 0.061$ for all).

The rate of proliferation of ECC-1 (12-72 h, Figure 4.2 E) was significantly reduced by the presence of obese AGEs and FPS-ZM1 in comparison to no AGEs control ($P = 0.011$) and lean AGEs ($P < 0.01$). The reduced rate of proliferation in the presence of obese AGEs was not significant in comparison to no AGEs control ($P = 0.13$), or in comparison to lean AGEs ($P = 0.09$). The addition of FPS-ZM1 did not further reduce the rate of proliferation in comparison to obese AGEs alone ($P = 0.62$).

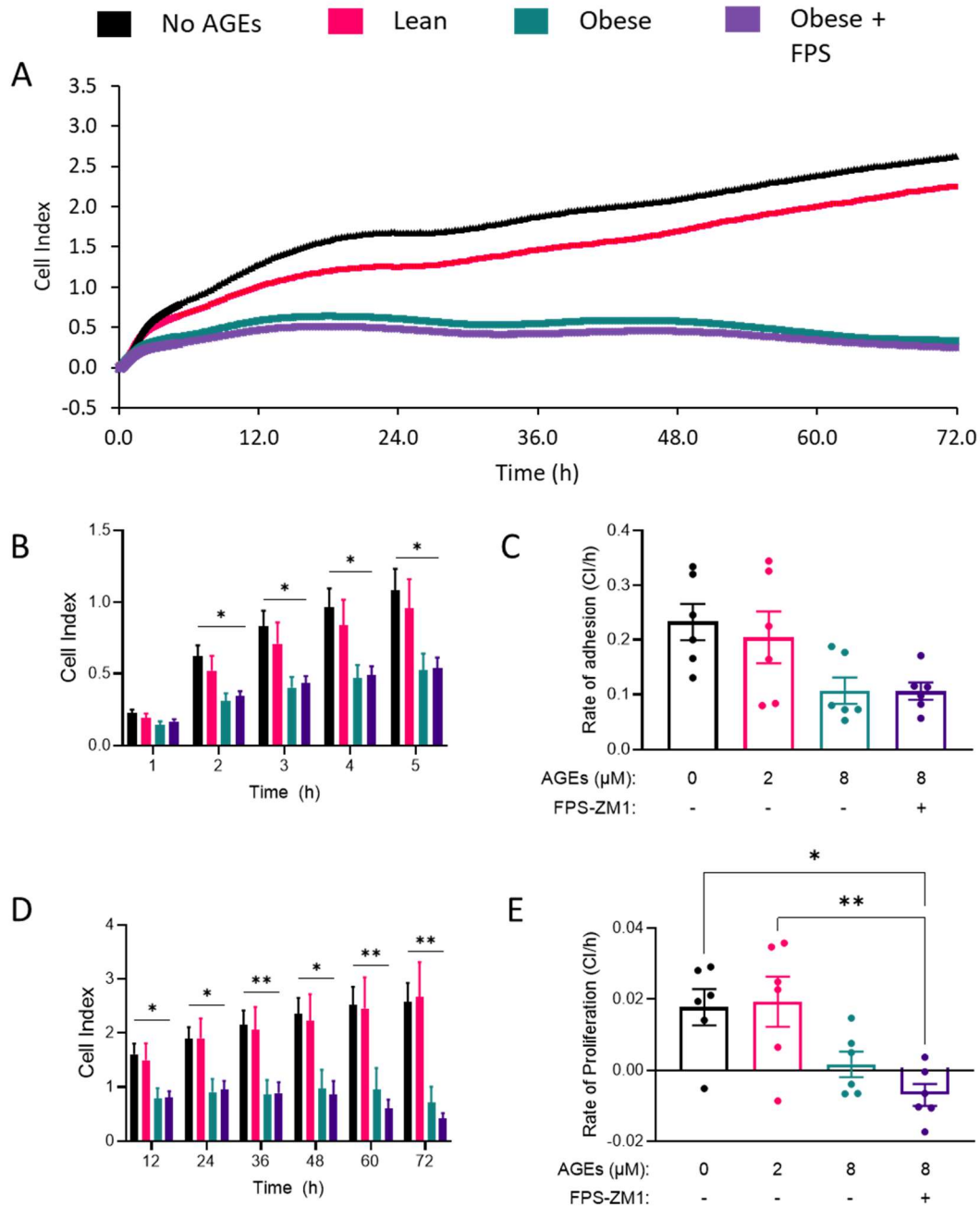


Figure 4.2: RAGE antagonism does not improve endometrial epithelial cell proliferation kinetics in the presence of obese AGEs. Adhesion and proliferation kinetics of ECC-1 cells hormonally primed in the presence of lean ($2\ \mu\text{M}$) or obese ($8\ \mu\text{M}$) concentrations of AGEs either alone or obese AGEs further supplemented with $25\ \text{nM}$ RAGE antagonist FPS-ZM1. PBS was used as a no AGEs control. **A**) Representative real time cell analysis plot showing cell index over time ($n=1$ of 6 replicates). **B**) Cell index (over 1-5 h; the period of adhesion) is significantly affected by treatments; FPS-ZM1 does not improve the cell index in the presence of obese AGEs. **C**) Whilst there was an overall significant effect ($P = 0.035$), the rate of change of cell index (rate of adhesion, 0-5 h) was not significantly affected by obese AGEs in comparison to lean AGEs or no AGEs control ($P \geq 0.08$). **D**) The cell index during the period of cell proliferation (12-72 h) was reduced by obese concentrations of AGEs at specific time points. **E**) Co-culture of ECC-1 in obese concentrations of AGEs supplemented with FPS-ZM1 did not rescue the rate of proliferation. Reduced rate of proliferation in the presence of obese AGEs alone

was not significant in comparison to lean AGEs ($P = 0.09$), or in comparison to no AGEs control ($P = 0.12$). For B-E mean is the derivative of $n = 6$ biological replicates, data expressed as mean \pm SEM. Individual points represent independent replicates. One-way ANOVA/Kruskal-Wallis *, ** $P < 0.05$, 0.01 .

In the presence of metformin and antioxidants, AGEs altered the growth kinetics of ECC-1 (Figure 4.3). During the period of adhesion (1-5 h), cell index was not affected at 1 h ($P = 0.13$), or 2 h ($P = 0.06$), but an overall effect of treatment was detected at 3 h ($P = 0.05$), 4 h ($P = 0.049$), and 5 h ($P = 0.046$). No significant difference was detected between groups at each time point. Whilst an overall significant effect was seen on the rate of adhesion ($P = 0.499$), no effect of individual treatments was detected ($P \geq 0.13$ for all comparisons).

During the period of proliferation (12-72 h), a significant effect of AGEs on cell index (Figure 4.3 D) and rate of proliferation (Figure 4.3 E) was observed. An overall effect of treatment was seen on cell index at 12 h ($P = 0.045$), and 24 h ($P = 0.019$), with no specific effect of any treatment. At 36 h, compared to no AGEs control, cell index was significantly reduced in the presence of obese AGEs alone ($P = 0.026$), and obese AGEs and metformin ($P = 0.013$), and antioxidants ($P = 0.032$). Compared to lean AGEs, obese AGEs alone non-significantly reduced cell index ($P = 0.093$), and obese AGEs in the presence of metformin significantly reduced cell index ($P = 0.047$). Obese AGEs in the presence of antioxidants did not significantly reduce cell index in comparison to lean ($P = 0.11$). At 48 h, only obese AGEs in the presence of metformin significantly reduced cell index compared to no AGEs control ($P = 0.023$). No condition was significantly reduced compared to lean AGEs ($P \geq 0.028$ for all). After 60 h, compared to no AGEs, obese AGEs alone and with metformin significantly reduced cell index ($P = 0.035$, 0.012 respectively). Obese AGEs in the presence of antioxidants did not significantly reduce cell index versus no AGEs ($P = 0.24$). No condition reduced cell index versus lean AGEs ($P \geq 0.13$ for all). After 72 h, compared to no AGEs, obese AGEs alone and with metformin significantly reduced cell index ($P = 0.032$, < 0.01 respectively). Obese AGEs with antioxidants did not reduce cell index versus no AGEs ($P = 0.33$). No condition reduced cell index versus lean AGEs ($P \geq 0.06$ for all).

The rate of proliferation (12-72 h, Figure 4.3 E) was significantly reduced by obese concentrations of AGEs versus no AGEs control ($P < 0.001$), and lean AGEs ($P = 0.036$). In the presence of metformin, the rate of proliferation remained significantly reduced in comparison to no AGEs ($P < 0.001$), and lean AGEs ($P = 0.028$), and was not significantly different versus obese AGEs alone ($P > 0.99$). The addition of antioxidants improved the rate of proliferation such that it was not different to lean AGEs ($P = 0.69$), however was still reduced versus no AGEs control ($P = 0.035$). The rate of proliferation in the presence of obese AGEs and antioxidants was not different to obese AGE alone or with metformin ($P = 0.40$, 0.35 respectively).

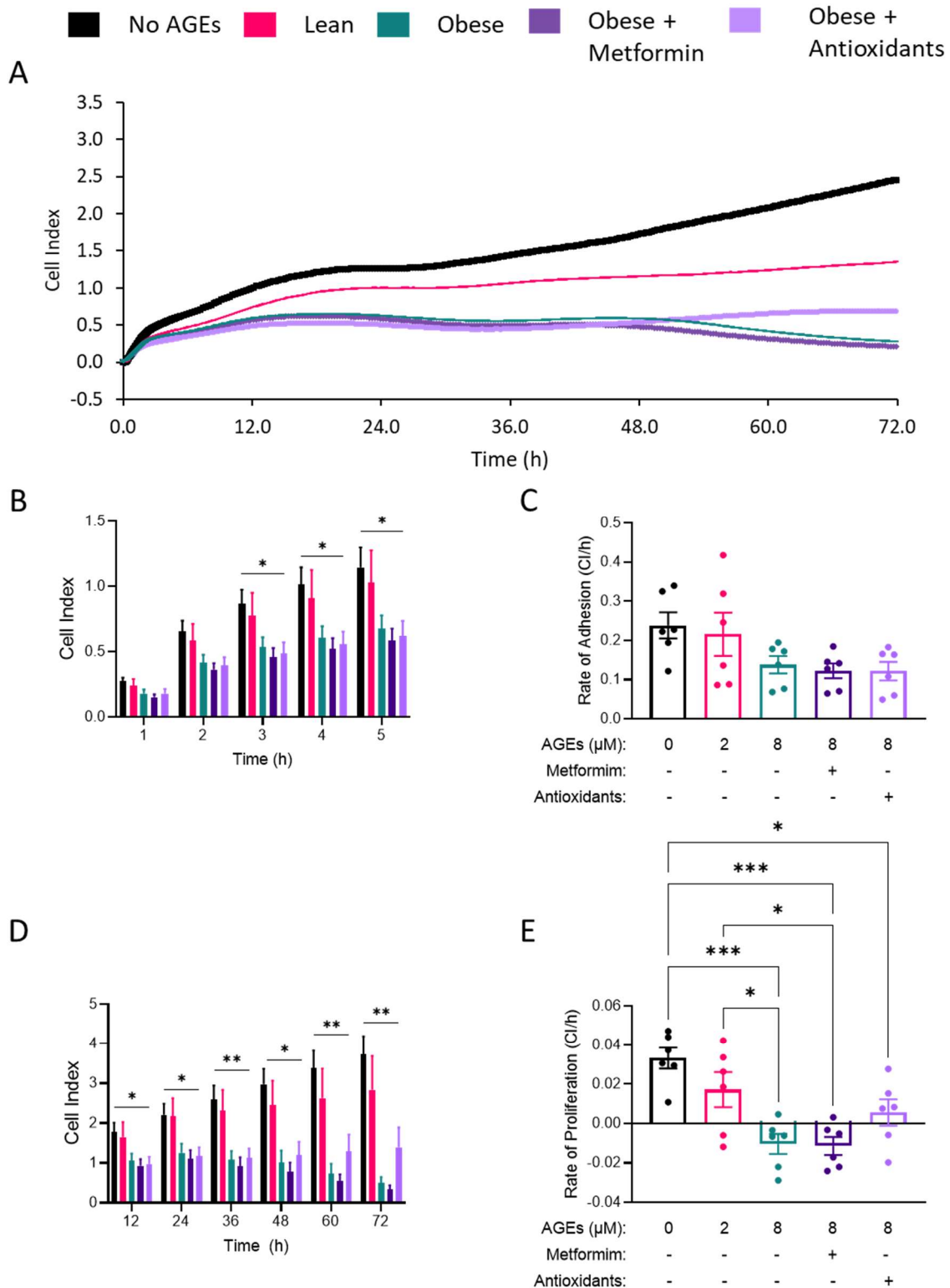


Figure 4.3: Antioxidants but not metformin improve proliferation kinetics of endometrial epithelial cells exposed to obese AGEs. Adhesion and proliferation kinetics of ECC-1 cells hormonally primed in the presence of lean (2 μM) or obese (8μM) concentrations of AGEs either alone or obese AGEs further supplemented with either 100 μM metformin, or a combination of antioxidants. **A)** Representative real time cell analysis plot showing cell index over time (n=1 of 6 replicates). **B)** Cell index (over 1-5 h;

the period of adhesion) is significantly affected by treatments between 3 and 5 h, neither metformin nor antioxidants improve the cell index in the presence of obese AGEs. **C**) While overall significant ($P = 0.05$), no effect of any treatment was seen on rate of adhesion ($P \geq 0.13$). **D**) The cell index during the period of cell proliferation (12-72 h) is reduced by obese concentrations of AGEs at specific time points. **E**) Antioxidants improved rate of proliferation of ECC-1 in the presence of obese AGEs such that rate of proliferation was not significantly different to lean AGEs ($P = 0.69$). For B-E mean is the derivative of $n=6$ biological replicates, data expressed as mean \pm SEM. Individual data points represent independent replicates. One-way ANOVA/Kruskal-Wallis: * $P < 0.05$ vs lean AGEs.

4.3.3 Assessment of endoplasmic reticulum stress

To determine potential mechanisms underpinning AGEs-induced effects, Western immunoblotting was performed as per standard protocols (section 2.4.1.5) for both CHOP and ATF4, to examine endoplasmic reticulum stress. Primary antibody concentrations are provided in Table 4.3.

Two biologically independent replicates are available for the Western immunoblot of CHOP (Figures 4.4 A, 4.4 B, with or without DMSO vehicle respectively), and thus no statistical analysis was performed. A strong band was observed at approximately 30 kDa, the expected molecular weight of CHOP. Following quantification of the 30 kDa band, a trend towards reduction of CHOP in the presence of RAGE antagonism was noted, indication that RAGE signalling may be involved in the ER stress response in ECC-1 cells (Figure 4.4 A), though further replicates are required to determine the significance of this effect (not possible due to time restrictions). Western immunoblotting (Figure 4.4 C, D respectively) demonstrated no significant effect of RAGE antagonism on ATF4 ($P = 0.40, 0.61$ respectively). Metformin and antioxidants may alter the expression of both ATF4 and CHOP. For both ATF4 and CHOP, multiple bands were observed at higher molecular weights, with the band at the anticipated molecular weight of the protein of interest used for densitometry analysis. Because of the outliers in this data, further replication and Western immunoblot optimisation would assist in interpretation—this was not possible because of my limited time in the laboratory in 2020 due to COVID-19-related restrictions.

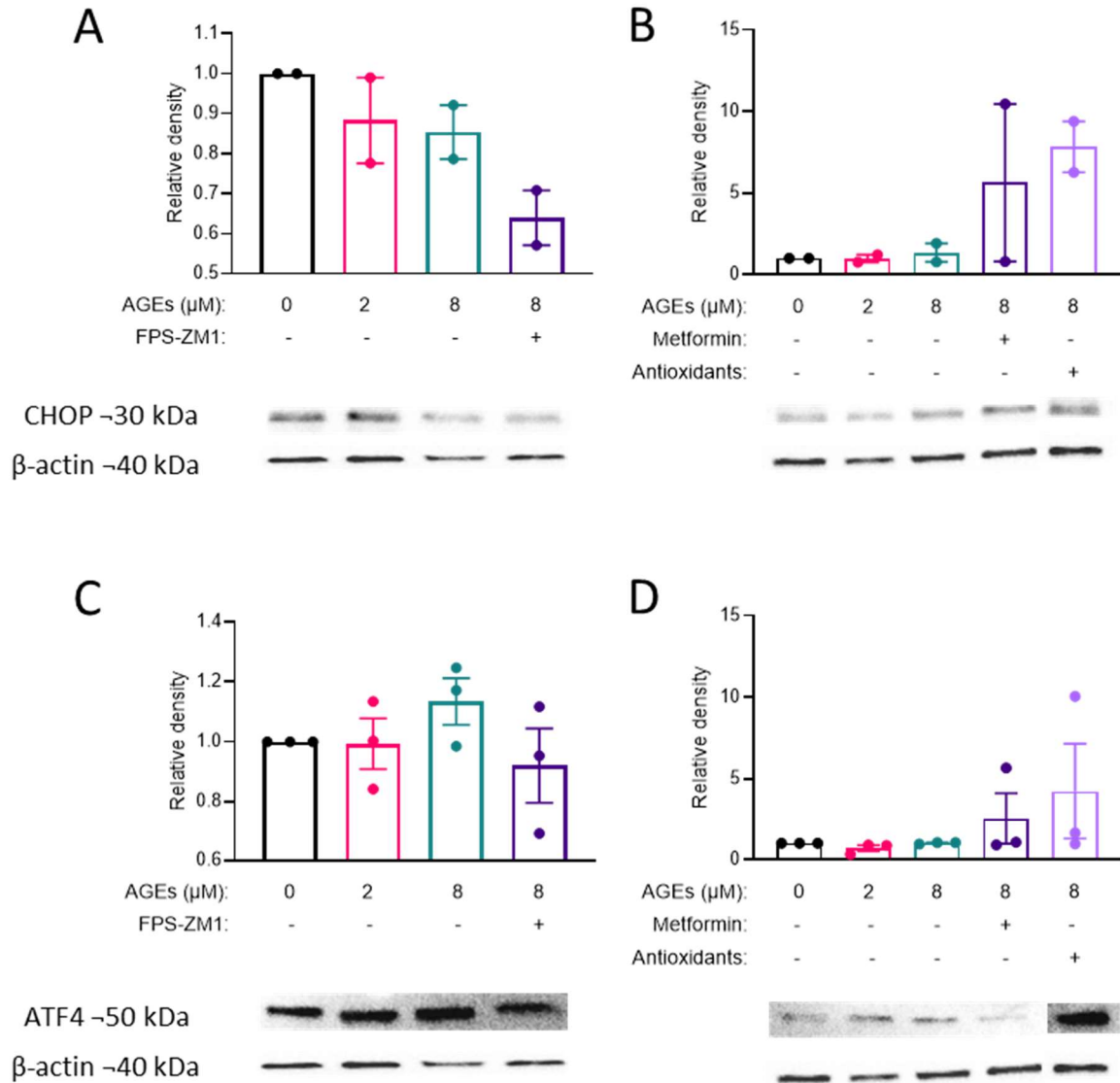


Figure 4.4: Obesity-associated AGEs and therapeutics may impact ER stress in endometrial epithelial cells. **A, B)** Representative Western immunoblot and quantification of CHOP protein abundance in ECC-1 cells treated with lean and obese concentrations of AGEs and potential therapeutics. **C, D)** RAGE antagonism appears to reduce, and metformin and antioxidants increase, expression of CHOP in ECC-1 cells cultured with obese concentrations of AGEs (A-B). No significant effect was seen on ATF4 expression (C, $P = 0.48$; D, $P = 0.58$, one-way ANOVA). β -actin utilised as a loading control and band intensity normalised to lean AGEs. Data expressed as mean \pm SEM derived from 2 (A, B) or 3 (C, D) biologically independent replicates (denoted by individual data points). Density normalised to β actin, and expressed relative to no AGEs control.

4.3.4 Endometrial stromal cell decidualisation

Only one freshly isolated stromal cell preparation was able to be used for this research, and additional replicates used frozen isolated stromal cells from previous isolations (bio-banked). It was not possible to prepare fresh isolations due to the COVID-19 health pandemic. Stromal cells were isolated (Section 2.4.1.2), or thawed, and decidualised for 12 days with 10^{-8} M E + 10^{-7} M MPA (Section 2.4.1.3), in the

presence of AGEs equimolar to those in lean and obese uterine fluid (2 μM and 8 μM respectively), either alone or in the presence of therapeutics (Table 4.2). Only one sample (of 5 separate preparations) showed evidence of decidualisation (evidenced by increased prolactin secretion, Figure 4.5). In this one culture, obese AGEs (8 μM) increased prolactin release, which was further increased with FPS-ZM1, and by antioxidants. Given the limited number of stromal cells available, a no-AGEs control could not be performed. Prolactin levels in conditioned media from the other four stromal cell cultures was reflective of day 2 secretions (basal) (Azlan et al., 2020, this laboratory). As further indication of lack of decidualisation in these cultures, morphology did not change from fibroblastic to the more rounded, cobblestone like appearance expected, with or without AGEs (Antoniotti et al., 2018).

Due the COVID-19 pandemic, no fresh tissue was available for use (from March 2020, ongoing), and previously frozen human endometrial stromal cells were utilised for the majority of replicates (4 out of 5 samples). Their long-term storage in liquid nitrogen is likely to have contributed to reduced functionality (decidualisation *in vitro*). In such absence of primary stromal cells, future experiments could utilise recently developed cell lines such as hESC-PRLY – an immortalised human endometrial stromal cell line with a yellow fluorescence reporter under the control of prolactin expression (Haller et al., 2019).

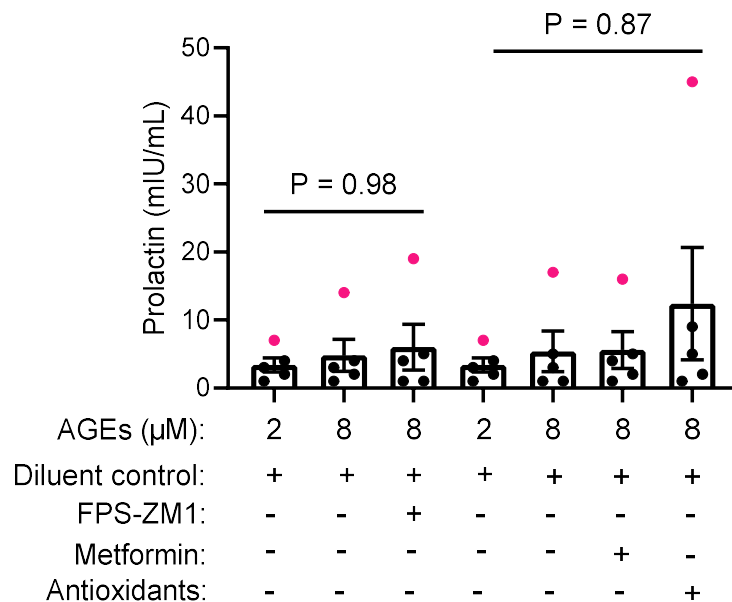


Figure 4.5: Prolactin released from stromal cells co-cultured with AGEs and therapeutics. Mean \pm SEM prolactin (mIU/mL) in conditioned media following 12 days of decidualisation treatment of human endometrial epithelial cells. Pink symbols represent data from the one preparation that showed evidence of prolactin secretion. Mean and SEM are derived from 5 biologically independent replicates, denoted by individual data points. One-way ANOVA.

4.3.5 Implantation competence: invasion of trophoblast cells

Antoniotti et al. (2018), demonstrated a significant reduction in invasive properties of the first trimester invasive extravillous trophoblast cell line HTR8/SVneo, in the presence of obese AGEs (8 μ M) in comparison to lean (2 μ M) but no effect on migration. Here, remediation of the adverse effects of AGEs on trophoblast invasion was examined.

HTR8/SVneo cells were cultured for 24 h in the presence of lean and obese concentrations of AGEs, either alone or supplemented with therapeutics (Table 4.2). Invasion was measured using the xCelligence system (Section 2.4.1.4.2). Cell invasion through Matrigel (measured as an increase in cell index, Figure 4.6) was first observed at approximately 36 h, compared to previously reported 24 h (Antoniotti et al., 2018). Increasing the cell number seeded did not affect the time of invasion (data not shown). No effect of obese concentrations of AGEs compared to lean were observed in the two biological replicates performed. Due to limited wells available in the experimental set up, a no-AGEs control was not performed—the physiological comparison being between lean and obese AGEs. Further optimisation of this technique is beyond the scope of this thesis.

HTR8/SVneo are reportedly a mixture of stromal and trophoblastic cells which may exhibit batch to batch variation (Abou-Kheir et al., 2017). It is possible that during their culture, the stromal phenotype has been promoted, resulting in reduced sensitivity to AGEs. Earlier passages of these cells could be utilised; however due to time constraints in addition to limited access to human endometrial stromal cells, it was decided at the outbreak of the COVID-19 pandemic, that my research would be restructured to focus on the epithelial effects of AGEs only, utilising human endometrial epithelial organoid culture methodologies recently established in our laboratory.

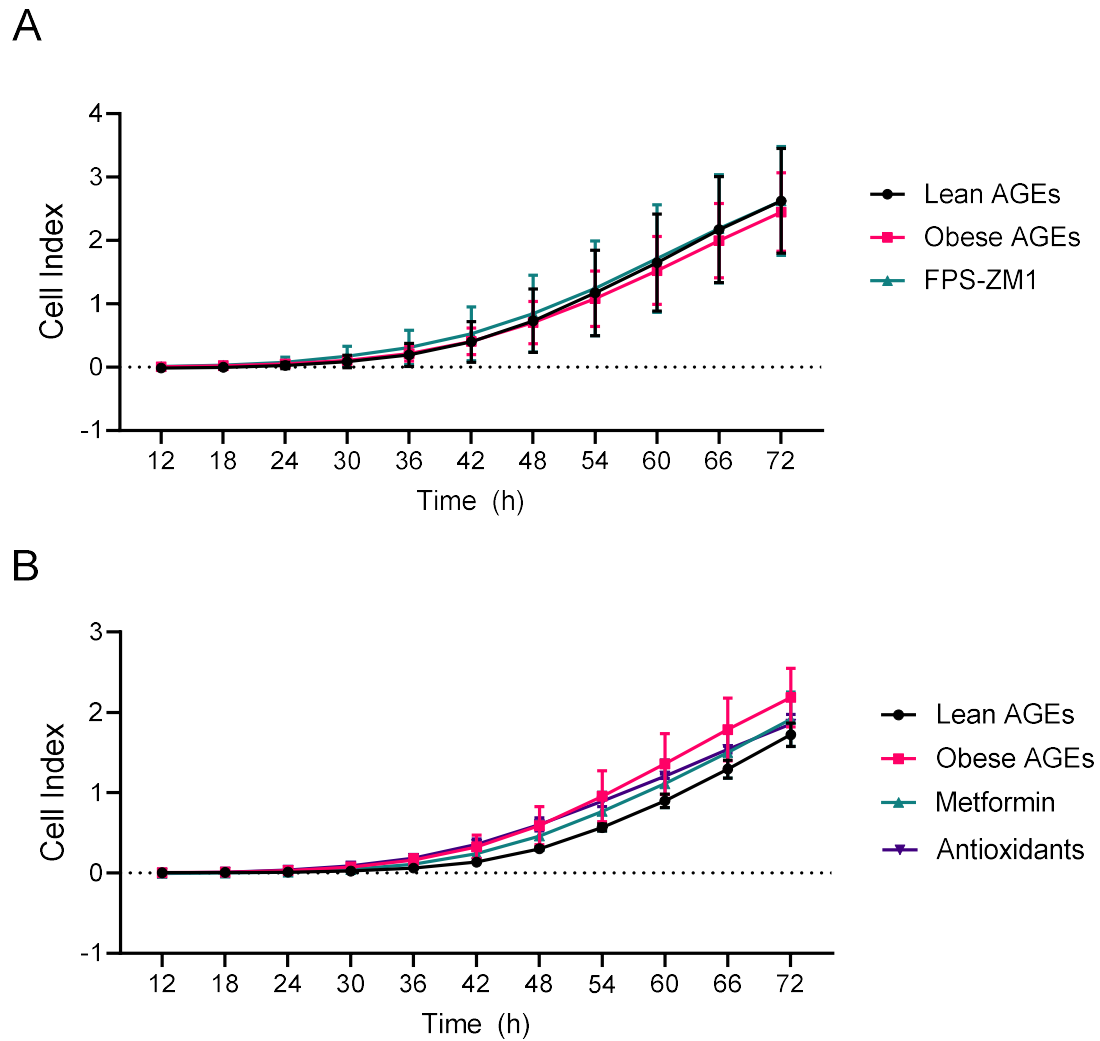


Figure 4.6: The published impact of AGEs on trophoblast invasion was not replicated. AGEs equimolar to the lean ($2 \mu\text{M}$) or obese ($8 \mu\text{M}$) uterine fluid did not affect HTR8/SVneo cell invasion through Matrigel. Co-culture with AGEs and therapeutic interventions likewise did not impact cell invasion. Mean \pm SEM cell index over time, $n = 2$.

4.4 Discussion and conclusions

The human endometrial microenvironment is significantly compromised by concentrations of AGEs equimolar to the obese uterine environment. This chapter aimed to neutralise the effects of AGEs on endometrial cell function by application of therapeutics (Table 4.2) and to further interrogate their mechanism of action.

Significant issues were encountered with stromal cell decidualisation and trophoblast invasion experiments as described above. Given the modest benefits of pharmaceutical intervention on trophectoderm formation and function (Chapter 3), and the difficulties in obtaining fresh endometrial tissue for stromal cell isolation, the effects of AGEs on stromal cells and the adhesion and invasion of trophoblast cells were not fully examined, and will not be discussed further in this thesis.

Here, only general functional effects of epithelial cells (adhesion and proliferation) in the presence of physiologically obese AGEs were examined, and potential therapeutics screened initially using these general functions. The data suggest that antioxidants mitigate inhibitory effects of high concentration AGEs on epithelial cell proliferation. Future work could investigate more specific effects of AGEs on endometrial receptivity and embryo implantation, such as the regulation of tight junctions, and biomarkers of endometrial receptivity (Chapter 6), and the remedial effects of the therapeutics identified here.

4.4.1 RAGE antagonism was insufficient to improve endometrial cell outcomes

ECC-1 cells express RAGE (Figure 4.1), providing an appropriate mechanism for AGEs signalling, thus RAGE antagonism is an appropriate therapeutic strategy. While obese concentrations of AGEs increased relative protein abundance of RAGE, no therapeutic reversed this effect, and indeed RAGE antagonism may exacerbate this (Figure 4.1). The rate of proliferation of ECC-1 was reduced when treated with obese (8 μ M) concentrations of AGEs compared to lean (2 μ M): the negative rate of change in cell index indicative of cell senescence and death, or cellular deadhesion from the fibronectin coated plate (Figures 4.2 and 4.3). Neither metformin nor antagonism of RAGE significantly improved the rate of proliferation; indeed, the effects of AGEs may be enhanced. Following antagonism of RAGE, AGEs may be acting preferentially through an alternative mechanism such as TLR4 (known to be expressed by ECC-1 (Schaefer et al., 2004)), or additional AGE receptors. A multi-therapeutic approach may be required to normalise endometrial epithelial cell function through receptor antagonism. Antagonism of TLR4 through an inhibitory peptide (VIPER), proved cytotoxic to ECC-1 cells (Section 2.4.2.2.1), and inhibition of multiple receptors was unable to be performed. Either alternative TLR4 inhibitors such as the small molecule antagonist TAK242 or inhibition of different receptors (i.e. AGE receptor complex 1/OST-48) could be explored.

4.4.2 Antioxidants improved ECC-1 cell function in the presence of obese AGEs

Application of a cocktail of antioxidants improved the rate of proliferation of ECC-1 cells in the presence of obese (8 μM) AGEs to lean (2 μM AGEs) conditions (Figure 4.3 E). Individually, each component of the antioxidant cocktail has significant anti-AGEs effects, as demonstrated in prior literature. N-Acetyl-L-Carnitine combats the formation of AGEs both *in vitro* and *in vivo* (Rajasekar and Anuradha, 2007), and reduces diabetic complications including cataract formation *in vitro* (Swamy-Mruthinti and Carter, 1999). α -Lipoic acid also helps prevent *in vitro* formation of AGEs (Ghelani et al., 2018), and improves intracellular antioxidant (glutathione) production and NF κ B activation in the presence of AGEs (Bierhaus et al., 1997). N-Acetyl-L-Cysteine (NAC) has numerous anti-AGEs effects: applied at higher concentrations NAC reduces AGEs-induced effects including endoplasmic reticulum stress and generation of reactive oxygen species (Loske et al., 1998). Clinically, oral NAC significantly improves urinary and renal function in rats exposed to high dietary AGEs (Thieme et al., 2016). Trials of individual antioxidants, administered orally or by other means (discussed in Chapter 7) would elucidate if all three antioxidants are required or if N-acetyl-L-cysteine alone is sufficient to combat uterine AGEs.

During optimisation (Section 2.4.2.2), concentrations of antioxidants in combination were trialled at 10-fold higher levels: 100 μM N-acetyl-L-cysteine and N-acetyl-L-carnitine, and 50 μM α -lipoic-acid. While beneficial at micromolar concentrations to embryo trophectoderm cell proliferation (Truong et al., 2016), higher concentrations reduce proliferation, migration, and invasion of various cancer cell lines (Feuerecker et al., 2012; Tripathy et al., 2018). While both these studies use millimolar concentrations, compared to the micromolar concentrations used in this thesis, increasing the concentration of α -lipoic-acid may be detrimental to the proliferation of endometrial cancer cells, possibly resulting in the lack of benefit seen during optimisation.

4.4.3 Mechanisms underpinning the epithelial response to AGEs

As demonstrated in Chapter 3, embryo trophectoderm cells responded to RAGE antagonism, which was of benefit to trophectoderm formation in the presence of obese concentrations of AGEs; neither metformin nor antioxidants were beneficial. In contrast, the only therapeutic to improve endometrial epithelial cell function was the cocktail of antioxidants. Mechanisms of AGEs-induced effects likely differ between the cell types, and a multi-therapeutic may be required for obese women attempting to conceive. The beneficial effects of antioxidants imply oxidative stress as a mechanism underpinning the epithelial response to AGEs, which warrants further investigation. Oxidative stress is a known effect of AGEs, and may be involved in the development of insulin resistance (Unoki et al., 2007).

Antonioti *et al* (2018) identified endoplasmic reticulum stress in the detrimental effect of AGEs, as phospho-PERK was significantly elevated in decidualised stromal cells exposed to obese

concentrations of AGEs. Downstream of PERK, endoplasmic reticulum stress response proteins ATF4 and CHOP are upregulated, leading to both mitochondrial and death receptor pathways of apoptosis (Hu et al., 2019). Following exposure to obese AGEs, an elevation of these proteins would be consistent with the cellular senescence and deadhesion observed using real time cell analysis (xCelligence, Figures 4.2, 4.3). However, when compared to lean, obese concentrations of AGEs did not significantly increase the expression of the ER stress proteins CHOP or ATF4 in endometrial epithelial cells (Figure 4.4). It is possible that AGEs promote endoplasmic reticulum stress in endometrial stromal, but not epithelial cells. Further replicates will clarify this data, not possible for this thesis due to time constraints. In addition, a trend towards increased ER stress proteins by application of antioxidants and metformin was observed. Metformin can activate the ATF4-CHOP endoplasmic reticulum stress pathway (Quentin et al., 2012), additionally, blocking of other AGEs response pathways such as oxidative stress, may lead to alternative effects including endoplasmic reticulum stress.

4.4.4 The organoid phenomenon: restructure of my experimental paradigm

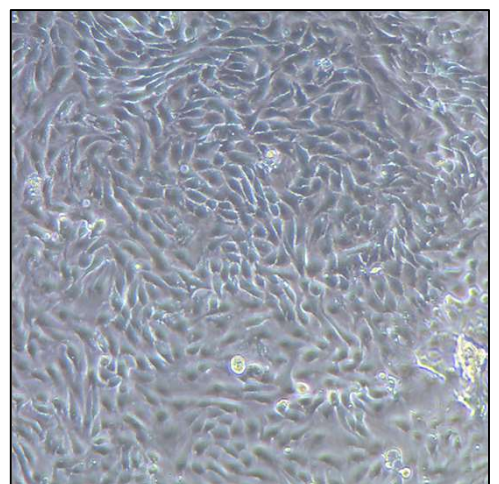
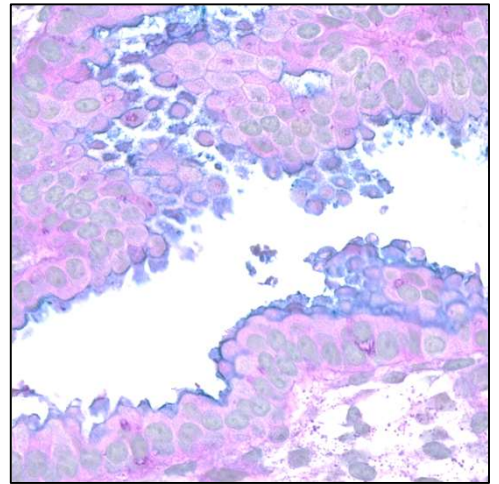
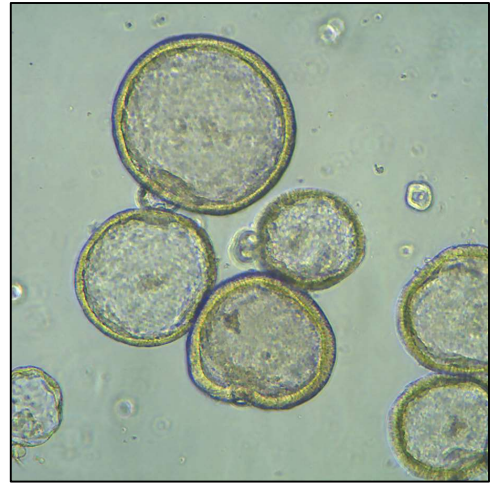
My supervisor, Dr Jemma Evans, introduced the culture of human endometrial epithelial cell organoids (hEEO) to the Salamonsen Laboratory at the end of 2019. Considering the substantial effect of obesity-associated AGEs on ECC-1 cells, I began to use organoids to examine their effect on primary endometrial epithelial cells. When the difficulties in stromal cell culture and trophoblast invasion became evident, my research was restructured to make epithelial cell function a major focus of this research, giving rise to Chapter 5 of this thesis.

4.5 “Take home” message

Obesity-associated AGEs significantly impair endometrial epithelial cell function (adhesion and proliferation). Antioxidants improved endometrial epithelial cell function, whereas RAGE antagonism and metformin had no effect. A closer examination of epithelial cell function in primary cells is required to fully understand the mechanism behind AGEs-induced effects, and subsequently to develop appropriate therapeutic interventions.

Chapter 5:

Use of human endometrial epithelial organoid culture to investigate the effects of AGEs on the human endometrial epithelium



Chapter 5: Use of human endometrial epithelial organoid culture to investigate the effects of AGEs on the human endometrial epithelium

Adopting a physiologically representative model for functional assessment

Chapter 4 of this thesis demonstrated mitigation of the effects of obesity-associated AGEs on ECC-1 (adenocarcinoma derived endometrial epithelial cells) proliferation. Here I turn to a new and more physiologically relevant model, endometrial epithelial organoids, to gain a better understanding of the effect of AGEs on the primary human endometrial epithelium. Before fully examining functional effects of AGEs, it was necessary to scale up primary epithelial cell culture and confirm the viability of these cells to be utilised in real time cell analysis (xCelligence).

5.1 Introduction

A significant limitation of current *in vitro* modelling systems is the use of cell lines which, while versatile and readily available, are not necessarily physiologically representative of the healthy *in utero* environment. The choice of cell line for experimentation is crucial and must take into consideration the physiological features of the experimental design, cell line origin, and expression of appropriate markers (Bazer and Salamonsen, 2008; Hannan et al., 2010; Skok et al., 2020). Primary endometrial epithelial and stromal cells are currently the most valid system to study the functions of the endometrium; however, primary human endometrial epithelial cells have limited capacity for proliferation and passaging *in vitro* (Varma et al., 1982), and stromal cell phenotypes change with progressive passage.

Since the early reports of primary human glandular and surface epithelium formation in an extracellular matrix (Negami and Tominaga, 1989; Rinehart et al., 1988), significant progress has been made in modelling the human endometrium from progenitor cells, yet the luminal epithelium remains elusive (Gargett et al., 2012). Recent advances in female reproductive tract organoids provide exciting new means to culture and examine primary human endometrial epithelial cells (Alzamil et al., 2020). First derived from both mouse and human endometrium by Boretto et al. (2017) and Turco et al. (2017), organoids are stable in culture for prolonged periods of time, and are highly responsive to hormonal stimulation (Fitzgerald et al., 2019; Turco et al., 2017), with recapitulation of phenotypic changes characteristic of the menstrual cycle (Haider et al., 2019). Human endometrial epithelial organoids (hEEO) maintain their constituent cells in a stem-like niche, and can differentiate into epithelial and secretory cells of a glandular nature upon hormonal priming (Fitzgerald et al., 2019). Furthermore, organoid culture provides a unique opportunity to examine epithelial cells under pathological conditions such as polycystic ovarian syndrome, carcinomas, and endometriosis (Boretto et al., 2019; Wiwatpanit et al., 2020), and also to assess individual patient drug responsiveness in a move towards personalised medicine (Boretto et al., 2019; Girda et al., 2017).

Extensive research has used endometrial cancer cell lines to model the physiological endometrial epithelium. Commonly used are ECC-1 and Ishikawa cells. ECC-1 cells are described and utilised as a model of the luminal epithelium. Whilst hormonally responsive and expressing the surface epithelial marker Cytokeratin-13 (Mo et al., 2006), they are of adenocarcinoma origin, have an unstable karyotype (Clarke et al., 1987; Mo et al., 2006), and thus are not truly representative of the healthy endometrial luminal epithelium. Ishikawa cells are also adenocarcinoma derived (Nishida, 2002), and show significant karyotypic abnormalities, including monosomy of the X chromosome (Kasai et al., 2016). As cancer cell lines are in general genetically unstable and metabolically abnormal, primary cell validation of results from cell lines would be valuable. As cells within hEEO are highly proliferative, can be maintained in a stem like state, and have a stable karyotype (Fitzgerald et al., 2019; Turco et al., 2017), these cells could be used as a more physiologically relevant model to further investigate the functional effects seen in cell lines.

Organoid cell culture, as recently established for primary human endometrial epithelial cells by other laboratories (Boretto et al., 2019; Fitzgerald et al., 2019; Turco et al., 2017), enables maintenance and expansion of primary epithelial cells in culture, with the added benefits of biobanking. I thus grew epithelial organoids from primary endometrial tissue and confirmed that they closely resemble those previously published. I further investigated their functional capabilities in comparison to well-established cell lines ECC-1 and Ishikawa. The advantages of this proved invaluable especially during the COVID-19 health pandemic (March 2020—ongoing) when endometrial tissue donations stopped and fresh primary cell isolations ceased, yet the bio-banked cohort of organoids enabled me to continue my research.

Furthermore, in this chapter I used hEEO to interrogate the effects of obesity-associated AGEs on primary human endometrial epithelial cells. I hypothesised that AGEs would exert a similar effect on hEEO to cancer cell lines, altering the functional capacity of these cells. I addressed this by confirming appropriate receptor expression, cell proliferation, and secretion of inflammatory markers in the presence of lean and obese AGEs.

5.2 Methods

This work followed the previously published protocols for the derivation and culture of human endometrial epithelial organoids (Turco et al., 2018); for detailed methodology see Section 2.5.2. A brief description of methodologies is provided within the results of this chapter where required

5.2.1 Donor demographics

All donors were of fertile background (≥ 1 parous pregnancy), with a mean age of 38 years (range 30-48), and an average BMI of 24.8 kg/m² (range 22-27). Following experimentation, two samples (donors 1 and 3, Table 5.1) were retrospectively identified to have either PCOS or an ovarian cyst.

Table 5.1: Donor characteristics. hEEO were generated from 5 fertile endometrial donors. Age (years), BMI (kg/m²), cycle phase (histologically determined) and patient reported cycle day at time of collection are noted. PCOS: polycystic ovary syndrome. (-) No data available. For donors 3-4, histological dating was unavailable.

| Donor # | Age | BMI | Cycle phase (patient reported cycle day) | Notes |
|---------|-----|-----|--|----------------------------------|
| 1 | 34 | 26 | Early secretory (20) | PCOS; Normal endometrium |
| 2 | 42 | 26 | Early-mid secretory (15) | Normal endometrium |
| 3 | 48 | 27 | Not dated (unknown) | Ovarian cyst; normal endometrium |
| 4 | 38 | 22 | Not dated (23) | - |
| 5 | 30 | 23 | Not dated (18) | Normal endometrium |

5.2.2 Immunohistochemistry

The endometrial epithelial identity of organoids was confirmed using immunohistochemistry. The standard protocol and optimised antibody concentrations are set out in Section 2.5.1.1 and Table 2.5.

5.2.3 Western immunoblotting

In triplicate wells, hEEO were hormonally primed in organoid expansion medium (ExM, Table 2.4) either alone or in the presence of AGEs equimolar to the lean (2 μ M) or obese (8 μ M) uterine fluid, containing 0.5% csFCS + 10⁻⁷ M E for 24 h and an additional 24 h in EXM containing 0.5% csFCS + 10⁻⁷ M E + 10⁻⁸ M MPA. PBS was used as a vehicle control for AGEs. hEEO were manually disaggregated from Matrigel, centrifuged at 1000 RCF for 5 minutes, rinsed twice in PBS, and lysed in ice-cold RIPA buffer. Western Immunoblotting was performed as per Section 2.4.1.5. RAGE antibody conditions are provided in Table 4.3.

5.2.4 Real time cell analysis (xCelligence)

Ishikawa and ECC-1 were hormonally primed in their respective culture medium (Table 2.2), as per standard protocols (6 h serum starvation, 24 h basal medium + 0.5% csFCS + 10⁻⁸ M E, and 24 h basal

medium + 0.5% csFCS + 10^{-8} M E + 10^{-7} M MPA). hEEO were hormonally primed as for Western immunoblotting, and dissociated into predominantly single cells for xCelligence analysis of proliferation (Section 2.4.1.4.1). For xCelligence analysis, 2.0×10^4 cells were seeded per well in their respective basal medium (MEM, Ishikawa; DMEM/F-12, ECC-1) or advanced (a)DMEM + 10% ExM (hEEO), all supplemented with 1% FCS, and experimental treatments continued. Unless stated otherwise, ECC-1 and Ishikawa were seeded in technical triplicate, and hEEO seeded in technical quadruplicate.

5.2.5 Multiplex analysis of organoid secretions (Luminex)

In triplicate wells, conditioned medium was collected from hEEO prior to hormonal priming (approximately 48 h incubation), following 24 h in ExM supplemented with 10^{-8} M E + 0.5 % csFCS and either lean or obese AGEs, and following 24 h in 10^{-8} M E + 10^{-7} M MPA + 0.5% csFCS in the continued presence of AGEs. PBS served as a vehicle control, to represent standard culture conditions. Conditioned medium from triplicate wells was pooled and assayed for a panel of chemokines and cytokines in technical duplicate using Luminex technology as described in Section 2.5.1.2, per manufacturer's instructions. To account for differences in cell number across samples and treatments in analysis, each treatment was normalised to the concentration of analyte detected in conditioned medium from the appropriate basal well, in which no AGEs or hormones were present.

5.3 Results

5.3.1 hEEO maintain morphology and secretory characteristics of donor endometrium

Human endometrial epithelial organoids (hEEO) were paraffin embedded and their endometrial epithelial identity validated with histological methods (Figures 5.1-5.3). Human endometrial glands are characterised by predominantly columnar and polarised epithelial cells. H&E staining of hEEO revealed columnar cells with basally located nuclei as well as some squamous cells (Figure 5.1 A-D). In addition, hEEO retain secretory characteristics of their donor endometrium (Figure 5.1 E-H), which shows significant acidic (blue) and neutral (magenta) glandular secretions. Acidic secretions are evident on the apical surface of the epithelial cells, and neutral secretions appear to be released into the extracellular matrix of the epithelial and stromal compartments, in addition to the lumen of the gland. Some acidic secretions are evident in the stromal compartment. The hEEO demonstrate significant acidic secretions into the lumen of the organoid. Some neutral secretions are evident, however, neutral mucins detected external to the organoid may be residual Matrigel. Agar from the fixation process has stained pale blue external to the organoid.

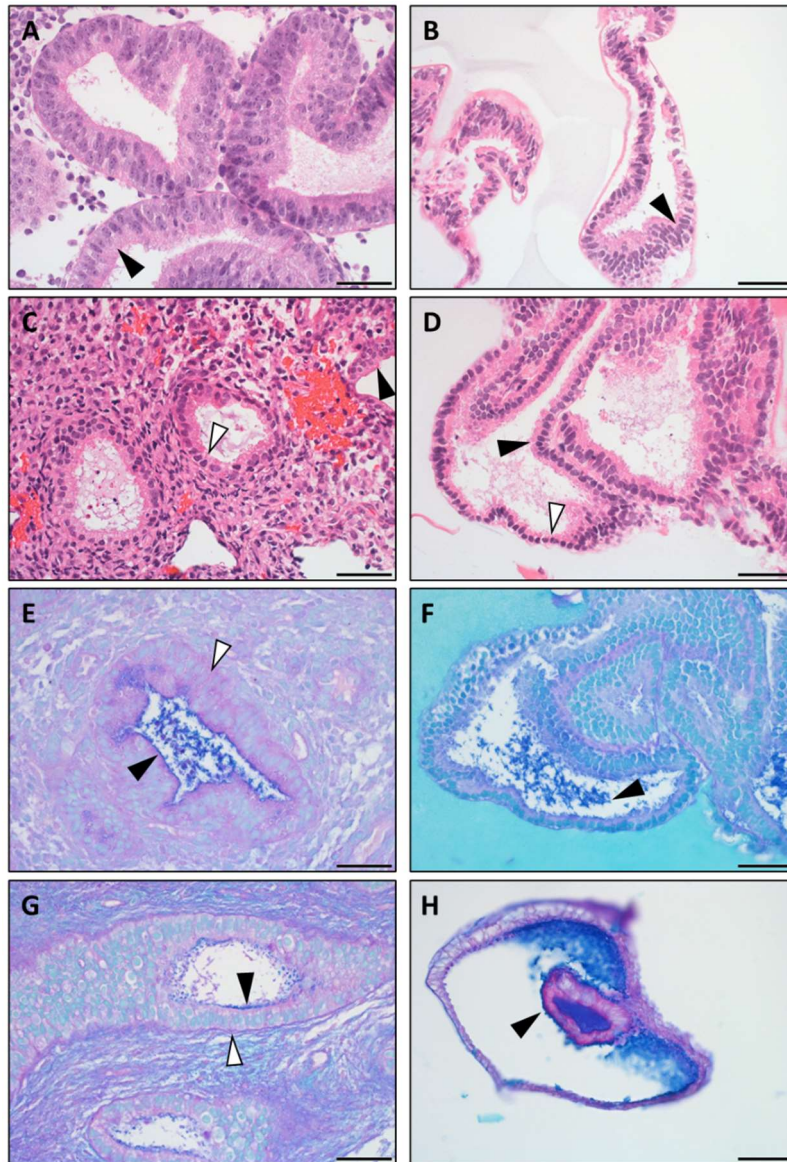


Figure 5.1: Human endometrial epithelial organoids retain morphological and secretory characteristics of donor endometria. Organoid cells (**B, D**) exhibit a combination of squamous (white arrow) and columnar (black arrow) morphology similar to their respective donor endometrium (**A, C**) as visualised with H&E. Both donor endometrium (**E, G**) and organoids (**F, H**) show discrete regions of neutral (white arrow), and acidic (black arrow) secretions. Staining on the basal edge of organoid sections may be a result of remaining Matrigel. Acidic secretion staining is strongly localised in the apical membrane and lumen of both organoids and donor endometrium. Scale bars represent 50 μm . Two independent representative samples are shown.

5.3.2 hEEO maintain endometrial epithelial cell characteristics

Immunohistochemistry compared hEEO and matched donor endometria expression of epithelial markers and cell proliferation. Epithelial glands express cytokeratin 7, which is conserved in the hEEO, however this was not at a consistent level with the donor endometrium: some hEEO showed more intense immunostaining, whereas others displayed reduced immunostaining in comparison to donor tissue (Figure 5.2 A-D).

PCNA was immunolocalised to the nucleus of the endometrial stromal and epithelial cells, and the nucleus of hEEO cells, confirming the proliferative nature of these cells (Figure 5.2 E-G).

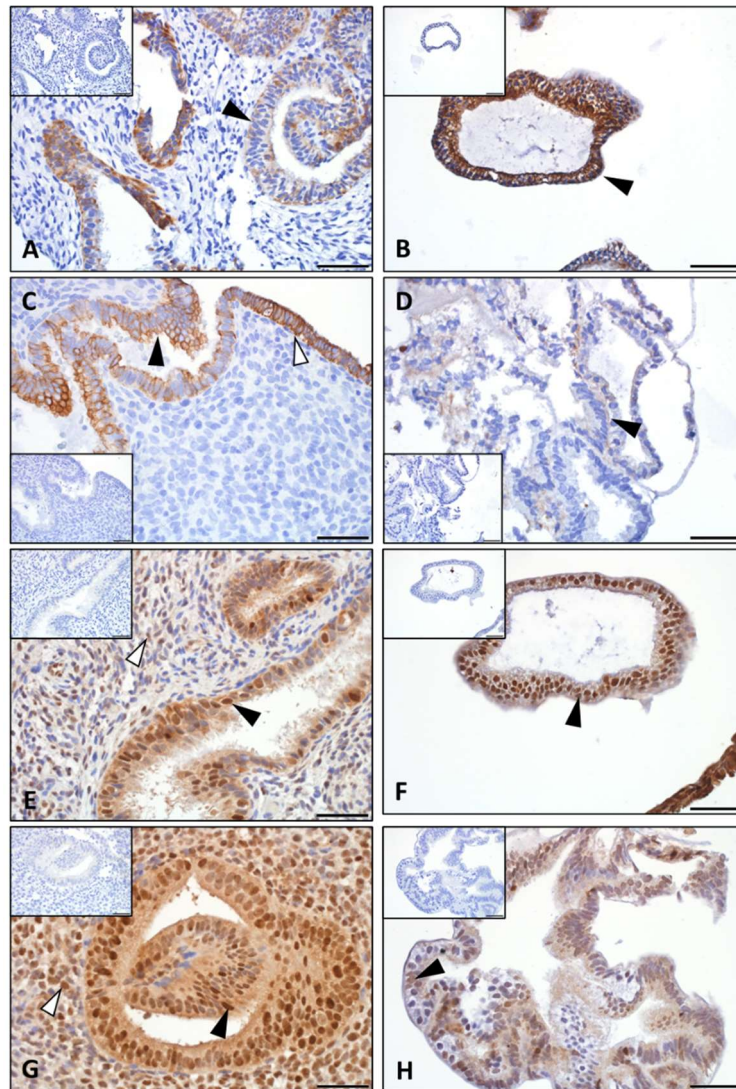


Figure 5.2: hEEO contain proliferating cells of epithelial identity. Cytokeratin 7 was immunolocalised the endometrial glandular (black arrow) and luminal epithelium (white arrow) of the donor endometrium (**A, C**). Staining was identified in the cytoplasm of hEEO (**B, D**). In the donor endometrium (**E, G**), PCNA was identified in the nucleus of epithelial (black arrow) and some stromal (white arrow) cells. Some, but not all nuclei of the hEEO, were positive for PCNA immunostaining (**F, H**). Scale bars represent 50 μm , inserts are isotype controls. Two independent representative samples shown.

5.3.2.1 hEEO express hormone receptors characteristic of the human endometrium

Donor endometria strongly express the receptors for estrogen ($\text{ER}\alpha$) and progesterone (PR) in the cytoplasm and nuclei of epithelial cells and stromal fibroblasts. Cytoplasmic expression is maintained in hEEO cells (Figure 5.3). When activated, $\text{ER}\alpha$ translocates to the nucleus, evident in the epithelial

and stromal cells of the endometrium. Activation is not observed in the hEEO. Immunoreactive PR is evident in the nuclei epithelial and stromal cells of the human endometrium, but is absent in the hEEO (Figure 5.3 E-H).

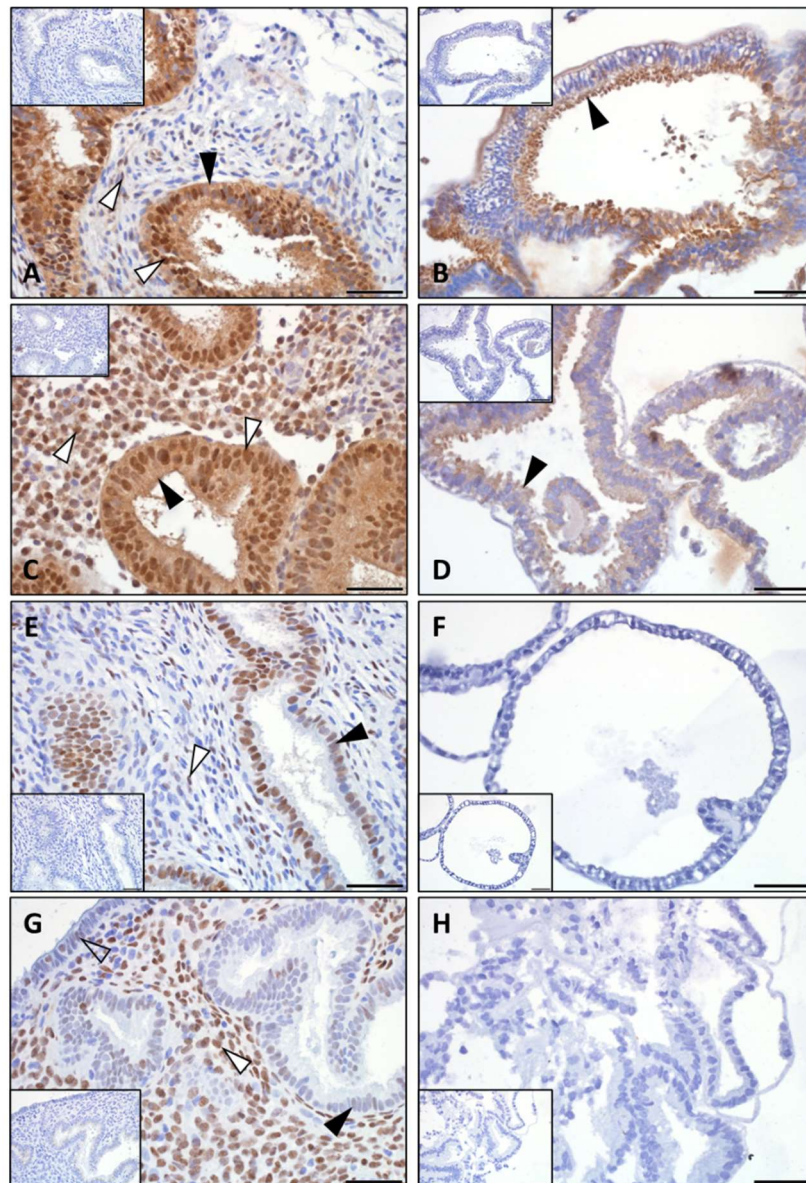


Figure 5.3: Organoids derived from human endometrial epithelial cells maintain appropriate mechanisms to respond to hormones of the menstrual cycle. The human endometrial epithelial and stromal cells express the estrogen receptor ($ER\alpha$; black arrow; **A, C**). Upon activation the receptor translocates to the nucleus (white arrow). hEEO (**B, D**) express $ER\alpha$ within the cytoplasm of the epithelial cells. There is no evidence of receptor activation. Progesterone receptor is upregulated by estrogen and the activated receptor is immunolocalised in the nucleus of the luminal (open arrow) and glandular (black arrow) epithelial cells, and in the stromal cells (white arrow) of the human endometrium (**E, G**). Activated progesterone receptor did not immunolocalise in hEEO (**F, H**). Two independent representative samples shown, isotype controls are in inset. Scale bars represent 50 μm .

5.3.3 hEEO maintain appropriate mechanisms by which to respond to AGEs and have limited prior exposure to endometrial AGEs

Before treatment of hEEO with AGEs, the presence of appropriate receptors was confirmed with immunohistochemistry (Figure 5.4). RAGE was immunolocalised to the luminal and glandular epithelium, and the stromal cells of the human endometrium, as reported previously (Antoniotti et al., 2018). Some staining was also noted on the maternal blood vessels. RAGE was identified predominantly on the apical membrane of hEEO, but limited basal staining was observed. Some non-specific staining was evident in residual Matrigel. TLR4 was immunostained strongly throughout the endometrium, and similarly in the hEEO.

N- ϵ -Carboxymethyl lysine (CML) was immunolocalised throughout the lean and obese endometrium (Antoniotti et al., 2018). Strong immunostaining was observed in obese endometrium that was retrieved from the archive (Figure 5.5 B; positive control). However limited or no immunostaining for CML was identified in the donor endometrium of this cohort, and no staining identified in the hEEO either (Figure 5.5 C-F). All donor women had a BMI less than 30 kg/m², so significant staining is unlikely, however a greater extent was expected as the lean endometrium used as a control also demonstrated immunostaining for CML. As AGEs can impact epigenetic markers, potentially altering gene expression, low prior exposure of these epithelial cells to AGEs will prevent any confounding impacts during functional assessment.

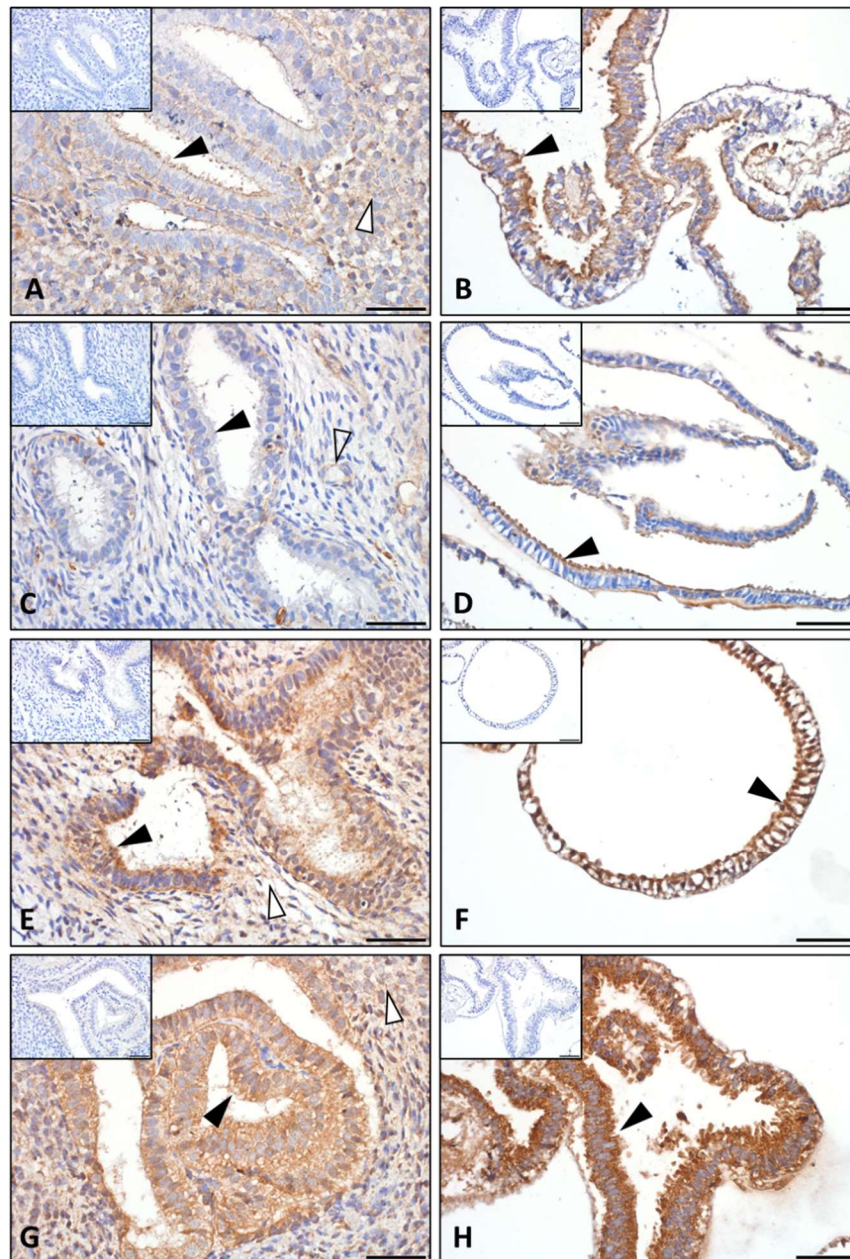


Figure 5.4: Expression of AGEs receptors by hEEO. RAGE (A, C) and TLR4 (E, G) are both immunolocalised in the human endometrium. RAGE is immunolocalised in the glandular epithelium (black arrow), stroma (white arrow), and maternal blood vessels (open arrow). TLR4 is stained strongly in the glandular epithelium and moderately in the stromal compartment of donor endometria. RAGE is immunolocalised on the apical membrane of hEEO (B, D), and TLR4 immunolocalisation is continued in organoid culture (F, H). Two independent representative samples shown. Isotype control inset. Scale bars represent 50 μm .

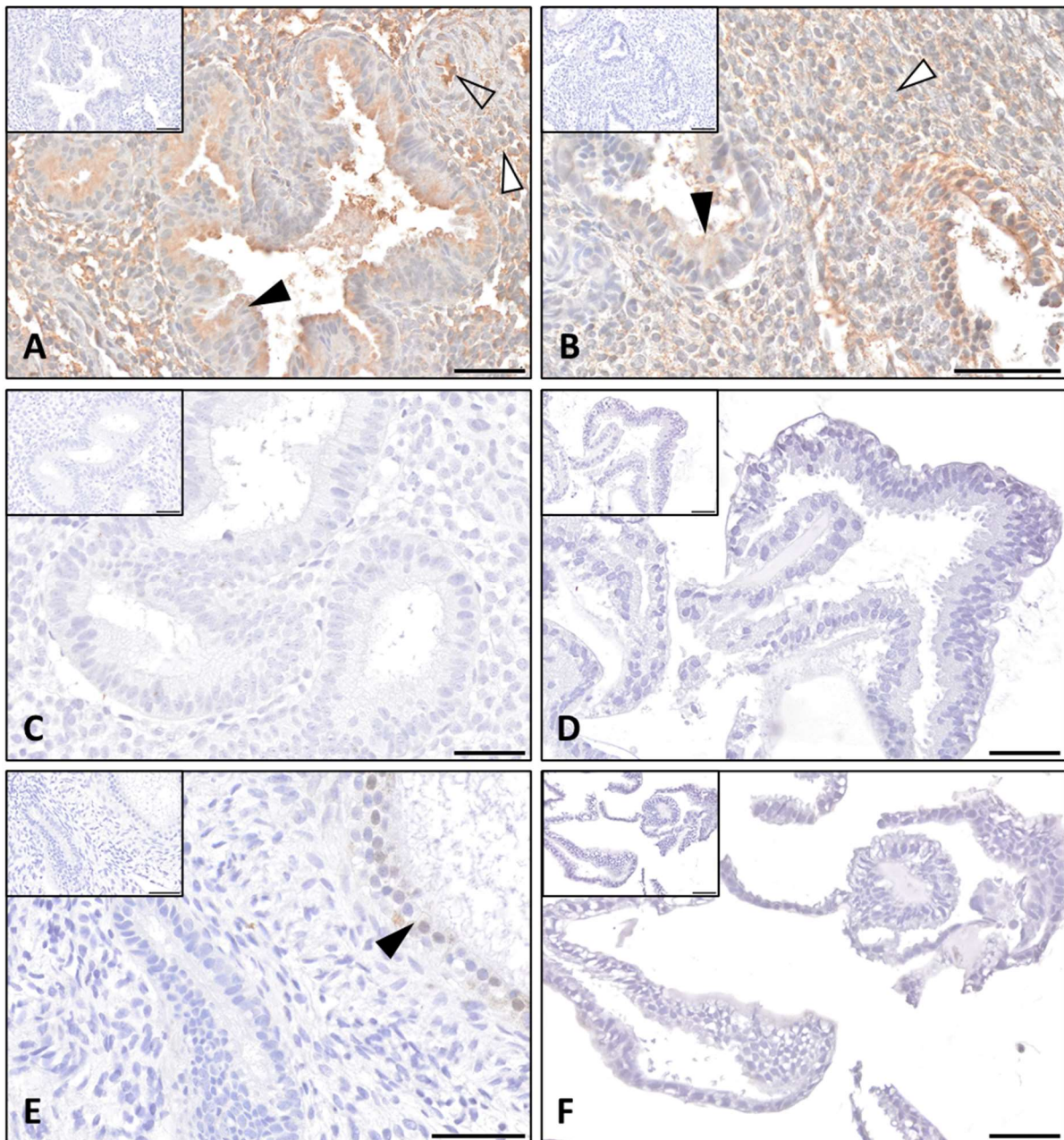


Figure 5.5: Carboxymethyl lysine immunolocalisation in donor endometrium and hEEO. In the lean (A) and obese (B) endometrium retrieved from the archive, CML is immunolocalised to the endometrial stromal cells (white arrow), the glandular epithelium (black arrow), and maternal blood vessels (open arrow). Very limited staining was evident in the donor endometrium (C, E) for organoid cultures, and no staining evident in the hEEO (D, F). Two independent representative images shown. Isotype control inset; scale bars represent 50 µm.

5.3.4 Epithelial cells derived from hEEO have a distinct kinetic profile compared to commonly used cancer cell lines

Using the xCelligence real time cell analysis system (ACEA biosciences), I confirmed that hEEO-derived epithelial cells can be used to examine adhesion and proliferation of primary epithelial cells on fibronectin; however, they display distinct kinetic characteristics in comparison to commonly used

endometrial epithelial cancer cell lines (Figure 5.6). Initially, I tried monolayers of hEEO-derived epithelial cells that continued pan-cytokeratin expression (data not shown) and showed morphology similar to freshly isolated primary endometrial epithelial cells. However, following freeze-thaw of hEEO, it was difficult to maintain them in healthy monolayers. I thus elected to treat the endometrial epithelial cells as intact organoids within the Matrigel dome; hEEO were then manually dissociated from Matrigel and washed twice in aDMEM before dissociation into an approximately single cell solution via manual repetitive pipetting. Cells were seeded and analysed by xCelligence as per section 2.4.1.4 in aDMEM containing 10% ExM (Table 2.4) and 1% FCS. To allow comparison with independent models of endometrial epithelial cells, Ishikawa and ECC-1 cells were hormonally primed following standard protocols, and seeded for xCelligence in their respective culture medium supplemented with 1% FCS (Table 2.2). Five biologically independent hEEO were analysed, and 3 biological replicates of ECC-1 and Ishikawa were assessed. Experiments were performed in technical quadruplicate.

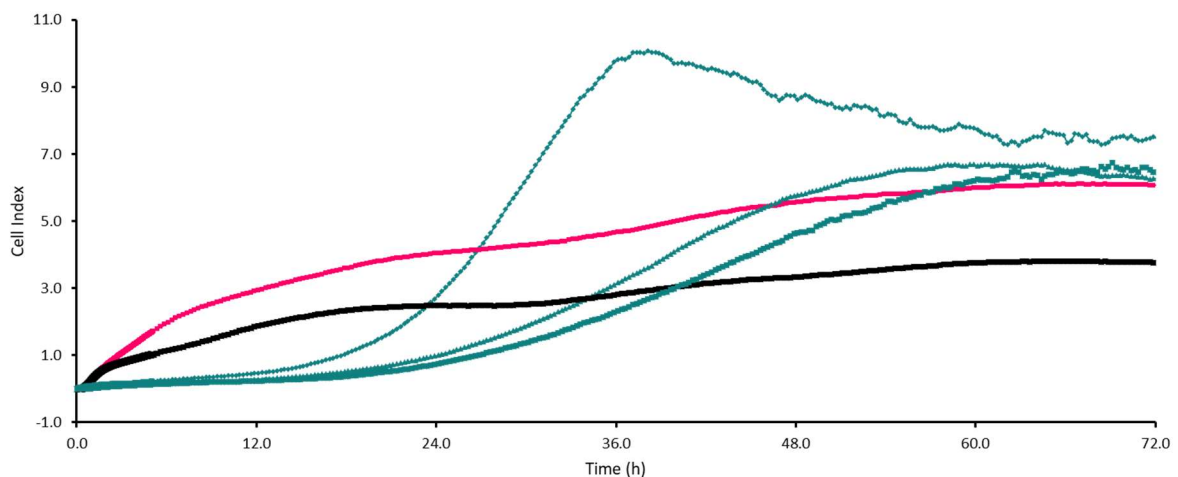


Figure 5.6: Proliferation kinetics of hEEO and cancer cell lines. Representative graph of cell index over time for $n = 1$ representative for ECC-1 (black) and Ishikawa (pink), and $n = 3$ hEEO derived cells (green) under their individual growth conditions. hEEO derived cells exhibit proliferation kinetics distinct from cancer cell lines. Kinetic profiles were similar for biologically independent $n=5$ hEEO derived cell cultures and $n=3$ for each cancer cell line.

Under their own standard growth conditions, each type of epithelial cell exhibits a different kinetic profile as determined by real time cell analysis, highlighting the differences between carcinoma cell lines and primary cells (Figure 5.6). Ishikawa tend to exhibit a higher cell index across time, but show a similar growth pattern to ECC-1 cells. In contrast, hEEO derived epithelial cells show an extended lag phase of growth, up to approximately 16 h, before entering the exponential log phase of cell growth. After approximately 48 h, the cells enter a stationary phase of growth before undergoing senescence and cell death as exhibited by the reduction in cell index. However, this may be due to

cellular deadhesion from fibronectin, and could be confirmed by apoptosis assays. Evidently, once dissociated from organoid culture, the reduced concentration of growth factors maintained in the medium (10%) is able to support finite proliferation but unable to prevent eventual cell senescence.

5.3.5 Obesity associated AGEs do not affect receptor expression

Co-culture of intact hEEO with AGEs representative of the lean or obese uterine fluid throughout hormonal priming did not impact the expression of RAGE relative to no AGEs (standard culture conditions; Figure 5.7; $P = 0.38$). Upon development of the Western immunoblot, a clear, strong band was identified at approximately 45 kDa, the expected size of RAGE, and was used for densitometry analysis. Two bands were identified at approximately 200 kDa, not observed in cell line protein preparations. This may be a protein complex formed within primary epithelial cells and not in ECC-1, and represents an avenue for future investigation. No other clear bands were observed.

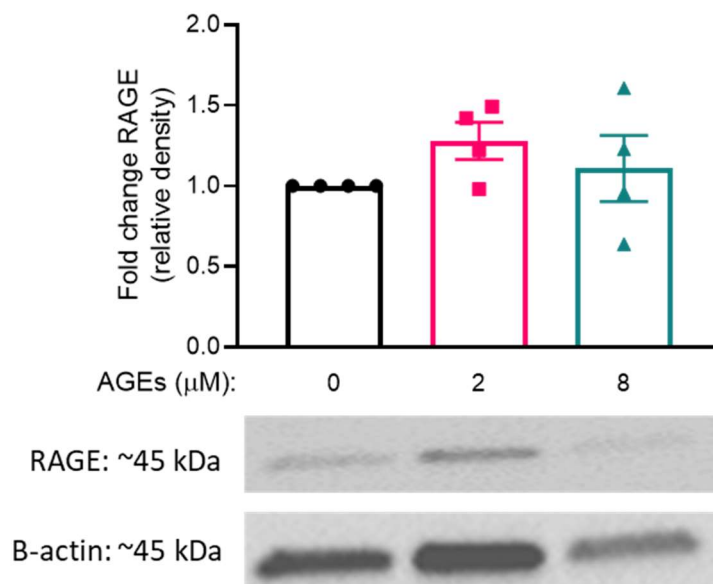


Figure 5.7: AGEs do not impact hEEO expression of RAGE in culture. hEEO were hormonally primed in the presence of lean or obese AGEs. PBS served as a vehicle control for AGEs to represent standard culture. Co-culture with AGEs equimolar to the lean (2 μM) or obese (8 μM) uterine fluid did not significantly impact the expression of RAGE (One-way ANOVA: $P = 0.38$). Mean \pm SEM derived from 4 biologically independent samples, denoted by individual data points.

5.3.6 Obesity associated AGEs impact organoid functions

5.3.6.1 Gross organoid morphology is not impacted by AGEs

hEEO derived epithelial cells were further examined for adhesion and proliferation in the context of obesity-associated AGEs. Throughout hormonal priming in the presence of lean and obese concentrations of AGEs, hEEO did not appear adversely affected by AGEs following visual examination of morphology in the Matrigel droplet (Figure 5.8). There was no obvious disruption in organoid

structure, or accumulation of debris within the lumen, following the application of lean and obese concentrations of AGEs.

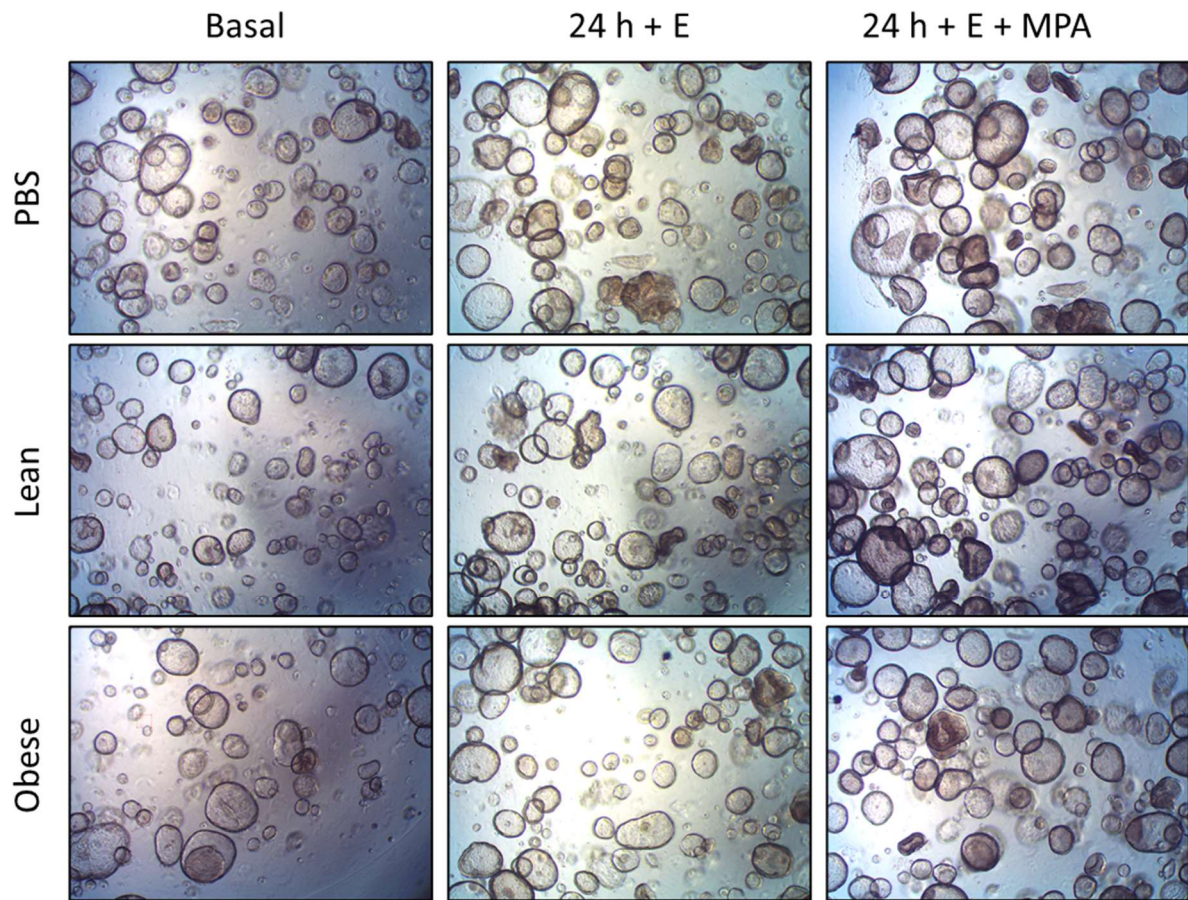


Figure 5.8: Morphology of hEEO exposed to obesity-associated AGEs. hEEO were grown in Matrigel domes and hormonally primed in the presence of lean (2 μ M) or obese (8 μ M) AGEs. PBS was used as a vehicle control to represent standard culture conditions. Hormonal priming of hEEO increased observable number of hEEO. Exposure to elevated AGEs did not impact morphology of hEEO within the Matrigel culture droplet following treatment with E, or E + MPA. Increased AGEs appeared to somewhat increase the observable number of hEEO. Morphology was consistent across 5 biologically independent replicates. Representative images from one biological replicate taken at 4x magnification.

5.3.6.2 AGEs equimolar with the obese uterine fluid impact the proliferation of organoid derived epithelial cells

Intact hEEO were hormonally primed and treated with physiologically lean and obese AGEs, and PBS used as a vehicle control for AGEs. Organoid derived epithelial cells exhibited altered proliferation kinetics in the presence of obese concentrations of AGEs (Figure 5.9). Most organoid derived cells proliferated between 12 and 48 h. Cell index was normalised to no AGEs control at each time point of interest (Figure 5.9 A); at 12 and 24 h, a trend towards increased cell index in comparison to no AGEs control and lean AGEs was observed, though this did not reach significance ($P = 0.65, 0.75$ respectively). The rate of proliferation was altered for each sample (Figure 5.9 B) though overall this

did not reach significance ($P = 0.75$). Three of 5 samples exhibited an increased rate of proliferation in the presence of obese AGEs (8 μM) versus lean AGEs (2 μM) and no AGEs control. In two samples (Donors 1 and 3), the rate of proliferation was reduced versus lean and no AGEs; these samples were retrospectively identified to have been derived from women with either PCOS or an ovarian cyst (Table 5.1).

When examined individually (Figure 5.9 C), organoid derived epithelial cells show a distinct response to obese concentrations of AGEs compared to lean, which is not evident in the combined data. As these represent only one biological replicate, performed in technical quadruplicate, no statistical analysis was performed. Donors 2, 4, and 5 exhibited a higher cell index in the presence of obese AGEs versus lean AGEs. Only donors 1 and 3 exhibited a lower cell index in the presence of obese AGEs versus lean.

Each individual donor culture demonstrated a unique kinetic profile (Figure 5.9 C). The rate of proliferation (steepness of the curve) and maximum cell index varied significantly between donors, highlighting the inherent variation in human samples. The rate of proliferation was reflected in the duplication of organoids in culture (visual observation during routine hEEO maintenance, no data shown). Future work could quantify this rate of duplication, and the effects of hormonal priming and AGEs by use of time-lapse microscopy (not available during my candidature).

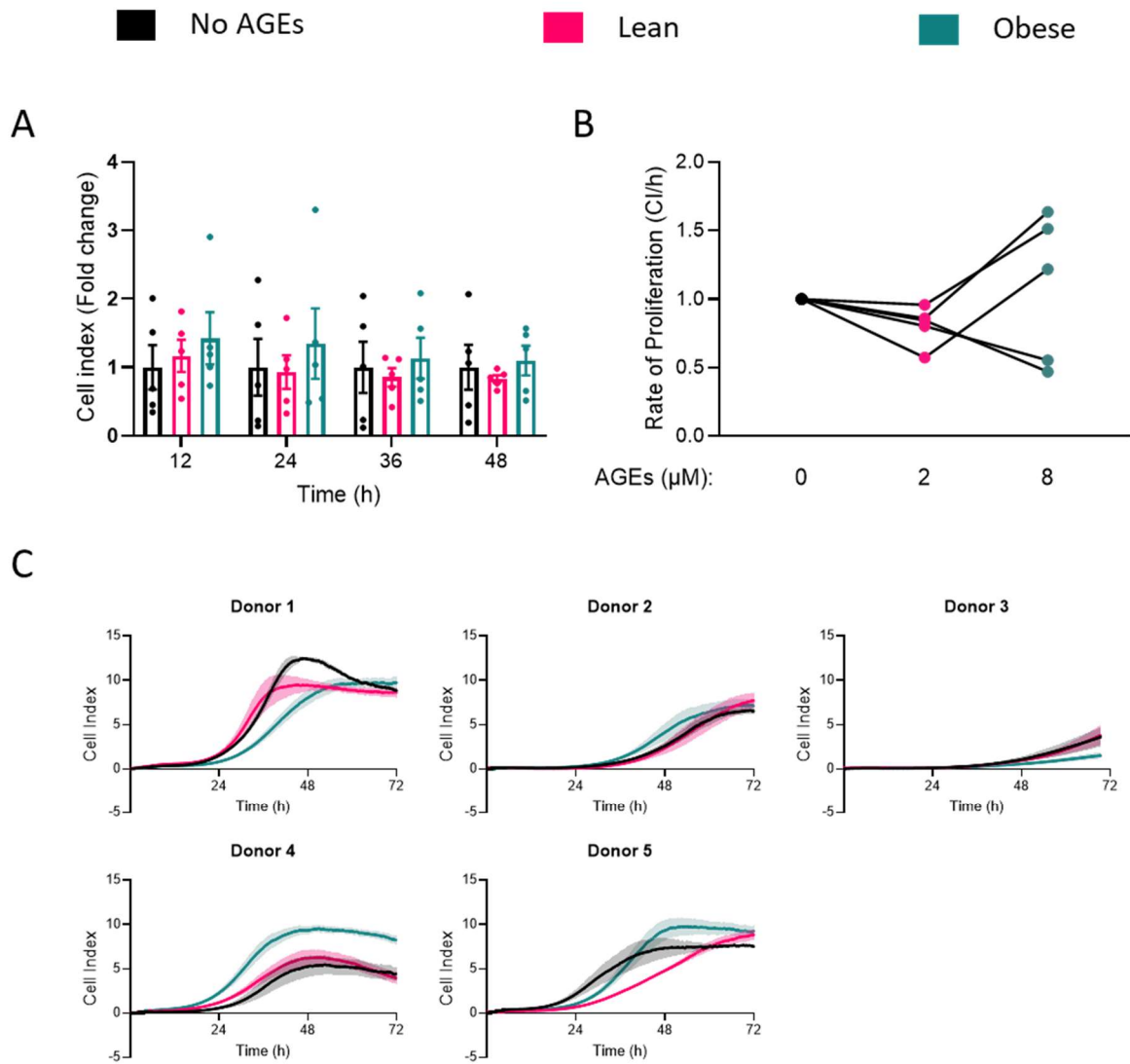


Figure 5.9: Obesity-associated AGEs may influence the proliferation of organoid derived human endometrial epithelial cells. **A)** Mean \pm SEM relative cell index across the period of proliferation (12–48 h), normalised to no-AGEs control, derived from $n = 5$ biologically independent replicates performed in experimental quadruplicate. Individual dot points derived from independent replicates, analysed by One-way ANOVA. Cell index relative to no AGEs control (standard culture conditions; black) was not significantly impacted by lean (2 μM ; pink) or obese AGEs (8 μM ; green) at 12 h ($P = 0.65$), 24 h ($P = 0.75$), 36 h ($P = 0.80$), and 48 h 24 h ($P = 0.71$). **B)** Rate of proliferation normalised to no AGEs control. Each point represents the mean of a biologically independent replicate, performed in experimental quadruplicate. Lines connect data points from the same donor. For 3 of 5 samples, obese AGEs increased the rate of proliferation relative to no AGEs control and lean AGEs. For 2 samples, obese AGEs reduced the rate of proliferation. **C)** Individual donor epithelial cell proliferation curves from which A and B were determined, show significant inter-donor variation. Mean \pm SEM (shaded area) cell index over time, derived from one biological replicate, performed in technical quadruplicate.

5.3.6.3 Obesity associated AGEs affect hEEO secretion of chemokines and cytokines

Under basal conditions (ExM only), hEEO secrete numerous factors, interleukin 8 (IL-8) being the most abundant (approximately 3 ng/mL present in conditioned media). Of all the analytes, placental growth factor (PLGF) was the only one not detected in any sample. Very limited secretion of IL-17A was detected (maximum detected 0.5 pg/mL). Detected analyte concentrations in conditioned medium are provided in Table 5.2.

Secretions following hormonal priming in E and E + MPA were normalised to basal, to account for differing cell numbers within cultures, and are expressed as percent of basal (Figure 5.10). Application of obese AGEs (8 μ M) significantly increased the secretion of CXCL-16 (Figure 5.10 B) in comparison to vehicle control following treatment with E ($P = 0.04$) and with E + MPA ($P = 0.03$), but not in comparison to lean ($P = 0.08$ for both). For most analytes, a clear and distinct trend towards increased secretion was evident in the presence of obese AGEs for example: IL-10 ($P = 0.07$; Figure 5.10 F), and TNF- α ($P = 0.06$; Figure 5.10 I) with the exception of IL-1 β , IL-17A, VEGF-A, and GCSF (Figure 5.10 C, G, H, and J). The P -value for the effect of AGEs on secretion for each analyte is provided with Figure 5.10.

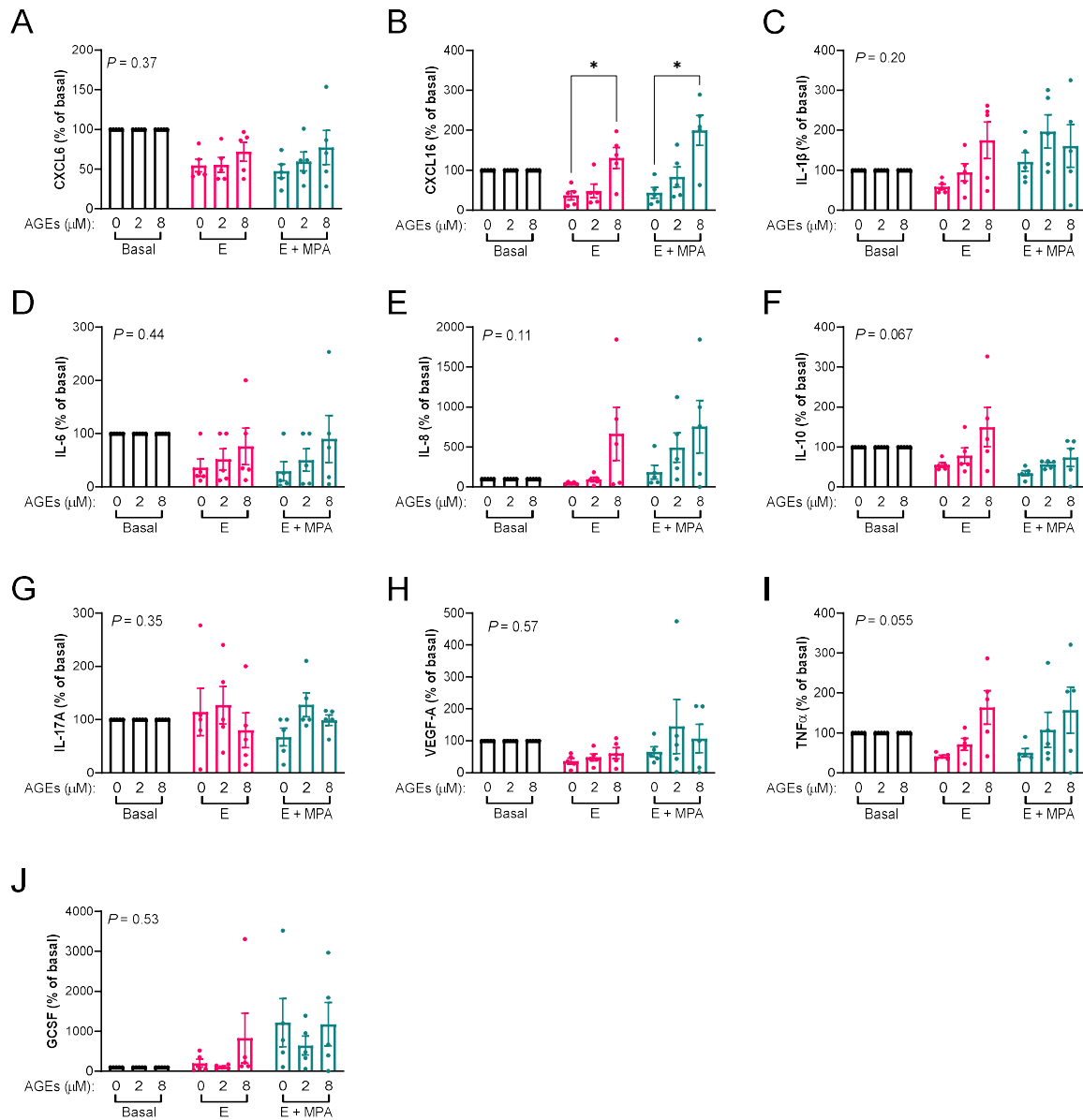


Figure 5.10: The secretion of chemokines and cytokines from hEEO is impacted by obesity-associated AGEs. Mean (%) \pm SEM cytokine secretion from $n = 5$ hormonally primed hEEO, normalised to basal conditions. Individual data points derived from independent replicates. P -value indicates effect of AGEs detected by two-way ANOVA. Application of AGEs equimolar to the obese (8 μM) uterine microenvironment significantly increased the secretion of CXCL-16 (**B**) in comparison to vehicle control (PBS, 0 μM) following 24 h hormonal priming in E + AGEs ($P = 0.04$), and 24 h in E + MPA + AGEs ($P = 0.03$). The increase in comparison to lean (2 μM) approached significance following E ($P = 0.08$) and E + MPA ($P = 0.08$). No significant effect of AGEs on the secretion of CXCL-6 (**A**; $P = 0.37$), IL-1 β (**C**; $P = 0.20$), IL-6 (**D**; $P = 0.44$), IL-8 (**E**; $P = 0.11$), IL-10 (**F**; $P = 0.07$), IL-17A (**G**; $P = 0.35$), VEGF-A (**H**; $P = 0.57$), TNF- α (**I**; $P = 0.06$), and GCSF (**J**; $P = 0.53$) was detected. $*P < 0.05$.

| | AGES (μ M) | CXCL-16 | CXCL6 | IL-1 β | IL-6 | IL-8 | IL-10 | IL17-A | TNF- α | PLGF | GCSF | VEGF-A |
|--------------|---------------------------|---------|--------------|---------------|---------------|------------------|---------------|-----------------|---------------|------|--------------|-----------------|
| Basal | % detectable | 0 | 100 | 100 | 60 | 100 | 100 | 80 | 100 | 0 | 100 | 100 |
| | | 2 | 100 | 100 | 60 | 100 | 100 | 80 | 100 | 0 | 100 | 100 |
| | | 8 | 100 | 100 | 60 | 100 | 100 | 80 | 100 | 0 | 100 | 100 |
| | Range (pg/mL) | 0 | 180 - 520 | 1.7 - 4.1 | <LoD - 41 | 1225 - 5021 | 206 - 2214 | <LoD - 0.4 | 31 - 200 | <LoD | 5 - 52 | 925 - 2708 |
| | | 2 | 185 - 509 | 1.9 - 5.1 | <LoD - 115 | 1362 - 7468 | 212 - 1792 | <LoD - 0.3 | 34 - 236 | <LoD | 7 - 120 | 1037 - 4817 |
| | | 8 | 182 - 673 | 2.0 - 4.8 | <LoD - 54 | 1475 - 5847 | 210 - 1739 | <LoD - 0.3 | 45 - 203 | <LoD | 6 - 40 | 1037 - 4536 |
| | Mean \pm SEM (pg/mL) | 0 | 290 \pm 61 | 2.7 \pm 0.4 | 18 \pm 8 | 2469 \pm 680 | 836 \pm 358 | 0.15 \pm 0.06 | 99 \pm 28 | - | 24 \pm 10 | 1610 \pm 351 |
| | | 2 | 271 \pm 60 | 3.1 \pm 0.6 | 32 \pm 22 | 3122 \pm 1157 | 707 \pm 287 | 0.15 \pm 0.05 | 126 \pm 44 | - | 38 \pm 21 | 2101 \pm 698 |
| | | 8 | 310 \pm 92 | 3.2 \pm 0.5 | 19 \pm 11 | 3015 \pm 843 | 645 \pm 286 | 0.17 \pm 0.05 | 114 \pm 32 | - | 20 \pm 6 | 2171 \pm 641 |
| | Median (pg/mL) | 0 | 236 | 2.7 | 7.7 | 1863 | 540 | 0.1 | 96 | - | 13 | 1331 |
| | 2 | 221 | 2.5 | 4.0 | 1781 | 613 | 0.2 | 89 | - | 17 | 1356 | |
| | 8 | 217 | 2.8 | 4.7 | 2173 | 345 | 0.2 | 91 | - | 22 | 1754 | |
| 24 h + E | % detectable | 0 | 100 | 100 | 60 | 100 | 100 | 60 | 100 | 0 | 100 | 100 |
| | | 2 | 100 | 100 | 60 | 100 | 100 | 80 | 100 | 0 | 100 | 100 |
| | | 8 | 100 | 100 | 80 | 100 | 100 | 80 | 100 | 0 | 100 | 100 |
| | Range (pg/mL) | 0 | 35 - 205 | 0.9 - 2.8 | <LoD - 10 | 722 - 1980 | 113 - 1175 | <LoD - 0.4 | 14 - 106 | <LoD | 4 - 47 | 67 - 982 |
| | | 2 | 44 - 238 | 1.6 - 4.2 | <LoD - 14 | 1181 - 2512 | 142 - 1021 | <LoD - 0.5 | 39 - 148 | <LoD | 5 - 70 | 432 - 1146 |
| | | 8 | 252 - 429 | 2.3 - 7.0 | <LoD - 12 | 1858 - >LoD | 96 - 2258 | <LoD - 0.2 | 74 - 209 | <LoD | 20 - 186 | 397 - 1898 |
| | Mean \pm SEM (pg/mL) | 0 | 95 \pm 29 | 1.6 \pm 0.4 | 4.3 \pm 2.0 | 1088 \pm 229 | 467 \pm 197 | 0.17 \pm 0.09 | 43 \pm 16 | - | 23 \pm 7 | 575 \pm 147 |
| | | 2 | 113 \pm 33 | 2.5 \pm 0.5 | 5.9 \pm 3.1 | 1859 \pm 261 | 519 \pm 202 | 0.18 \pm 0.08 | 69 \pm 20 | - | 34 \pm 13 | 795 \pm 140 |
| | | 8 | 326 \pm 42 | 4.6 \pm 0.8 | 4.6 \pm 2.1 | 13004 \pm 7057 | 937 \pm 415 | 0.10 \pm 0.04 | 140 \pm 27 | - | 81 \pm 34 | 1048 \pm 272 |
| | Median (pg/mL) | 0 | 83 | 1.3 | 1.2 | 930 | 245 | 0.1 | 33 | - | 26 | 600 |
| | 2 | 95 | 2.1 | 0.9 | 1910 | 239 | 0.1 | 52 | - | 20 | 751 | |
| | 8 | 270 | 4.8 | 1.8 | 8422 | 414 | 0.1 | 148 | - | 33 | 1010 | |
| 24 h + E+MPA | % detectable | 0 | 100 | 100 | 40 | 100 | 100 | 80 | 100 | 0 | 100 | 100 |
| | | 2 | 100 | 100 | 40 | 100 | 100 | 80 | 100 | 0 | 100 | 100 |
| | | 8 | 100 | 100 | 80 | 60 | 80 | 80 | 80 | 0 | 100 | 80 |
| | Range (pg/mL) | 0 | 36 - 266 | 1.2 - 5.3 | <LoD - 9 | 704 - 8125 | 28 - 880 | <LoD - 0.2 | 10 - 92 | <LoD | 48 - 267 | 499 - 2465 |
| | | 2 | 78 - 341 | 4.8 - 5.7 | <LoD - 17 | 3274 - 20034 | 119 - 1146 | <LoD - 0.2 | 36 - 172 | <LoD | 47 - 231 | <LoD - 6431 |
| | | 8 | 366 - 627 | <LoD - 6.8 | <LoD - 25 | 0.2 - >LoD | <LoD - 2004 | <LoD - 0.3 | <LoD - 413 | <LoD | 0.8 - 343 | <LoD - 2335 |
| | Mean \pm SEM (pg/mL) | 0 | 119 \pm 40 | 3.2 \pm 0.6 | 2.4 \pm 1.7 | 3644 \pm 1219 | 401 \pm 179 | 0.08 \pm 0.03 | 52 \pm 16 | - | 127 \pm 41 | 1024 \pm 365 |
| | | 2 | 198 \pm 48 | 5.1 \pm 0.2 | 5.2 \pm 3.1 | 11026 \pm 3349 | 418 \pm 190 | 0.18 \pm 0.04 | 92 \pm 26 | - | 121 \pm 37 | 2375 \pm 1083 |
| | | 8 | 498 \pm 54 | 4.8 \pm 1.2 | 6.5 \pm 4.7 | 20187 \pm 8339 | 574 \pm 365 | 0.16 \pm 0.04 | 173 \pm 68 | - | 157 \pm 56 | 1479 \pm 459 |
| | Median (pg/mL) | 0 | 110 | 58 | 3.2 | 3319 | 170 | 0.1 | 48 | - | 85 | 690 |
| | 2 | 193 | 81 | 4.9 | 9528 | 270 | 0.2 | 80 | - | 70 | 2104 | |
| | 8 | 451 | 104 | 6.1 | 11221 | 327 | 0.2 | 165 | - | 167 | 2124 | |

Table 5.2: Secretions from AGEs treated hEEO. Concentrations (pg/mL) of analytes detected in multiplex analysis of n = 5 hEEO conditioned medium prior to treatment (basal), 24 h in the presence of E + AGEs, and 24 h in E + MPA + AGEs. LoD: Limit of detection.

5.4 Discussion and conclusions

The functions of primary human endometrial epithelial cells are notoriously difficult to study *in vitro*, as these cells do not proliferate well and cannot be passaged many times; thus, endometrial cancer cell lines are widely used as a proxy to examine physiological functions of this cell type. I have presented evidence that endometrial epithelial cells derived from organoids can be readily expanded and used to examine cellular functions in a more physiologically relevant manner, and have explored the effects of obesity-associated AGEs on human endometrial epithelial organoids.

5.4.1 Organoid culture: the future of cell line research?

Organoid culture has previously been described for this cell type and examined in some detail (Boretto et al., 2017; Fitzgerald et al., 2019; Turco et al., 2017). My independent reproduction of these methodologies validates and demonstrates the robust nature of such organoids, which is essential in this era of international collaboration that requires scientific rigour and reproducibility of methodologies. The organoids generated in this study appear similar to those of previous studies in terms of their morphology, secretion, and hormone receptor expression. In this study, no hormonal priming was performed before validation, and as such ER α is not activated in the hEEO, and progesterone receptor is not upregulated (Figure 5.3). Other work in our laboratory showed that progesterone receptor is present following an extended period of hormonal priming (Figure 2.13). Retention of similar characteristics to donor endometrium by hEEO, highlights their physiological representation of the human endometrial epithelium. As the organoids presented here are highly secretory, supported by histological examination and Luminex analysis, they are likely to provide a physiologically meaningful model to study endometrial glandular secretions *in vitro*, allowing greater insight into secretory contributions to the complex uterine fluid microenvironment.

Previous studies have focussed on the use of hEEO for modelling the human endometrium and investigating maternal-fetal interactions in a 3D manner in combination with human endometrial stromal cells and trophoblast organoid culture (Abbas et al., 2020; Haider et al., 2018; Turco et al., 2018). This thesis suggests an additional important application of hEEO: to provide sufficient primary epithelial cells to confirm and build upon knowledge gained thus far using cancer cell lines.

Although hEEO are more physiologically representative of the healthy endometrium than adenocarcinoma-derived Ishikawa and ECC-1, they are still an *ex vivo* model and have their own limitations. The inclusion of numerous growth factors and signalling inhibitors maintains the cells in a stem-like state, they are therefore not fully differentiated epithelial cells. By necessity, these hEEO are also generated from predominantly glandular epithelium, and therefore may not be representative of the luminal epithelium, a caution that must be applied when interpreting results and investigating embryo attachment.

Whilst organoid culture will likely result in alterations to human endometrial epithelial cells on a phenotypic or epigenetic level, their physiological relevance is arguably greater than cell lines when not investigating a disease phenotype. Cancer cell lines remain a valuable tool in examining disease related cellular functions, but as demonstrated here, hEEO derived cells provide a more sophisticated way to examine normal physiological functions of the human endometrial epithelium with particular relevance to fertility and endometrial receptivity. Furthermore, intact organoids contain polarised epithelium which is lost on dissociation into single cells until these are grown to confluence. The caveat remains that organoid culture is an artificial, *in vitro* system, primarily representative of glandular rather than luminal epithelium, and the application of growth factors and signalling inhibitors may alter the functions of these epithelial cells from those *in vivo*. After confirming that hEEO maintain appropriate mechanisms to respond hormonal stimulation and to AGEs (Figures 5.3 and 5.4), I used hEEO to examine the impacts of obesity-associated AGEs on these cells.

5.4.2 AGEs influence function but not morphology

The morphology of hEEO within the Matrigel culture droplet is not noticeably affected by exposure to obese concentrations of AGEs (Figure 5.8). Given that AGEs can affect stem cell differentiation (Kume et al., 2005), it was anticipated that AGEs may affect differentiation or the ability of the cells to maintain their stem-like nature in organoid culture. No such effect was observed. Ultrastructural investigation would provide microscopic detail on cellular morphology which may provide more information. While in organoid culture for hormonal priming, hEEO are exposed to numerous growth factors; notably, N-acetyl-L-Cysteine (NAC), which can mitigate the effects of AGEs on other cell processes (Thieme et al., 2016; Wang et al., 2016), including endometrial epithelial cell proliferation (as demonstrated in Chapter 4), which may explain why detrimental effects of AGEs were not observed on intact hEEO. Once dissociated from hEEO, the epithelial cells are exposed to reduced levels of growth factors (maintained in 10% of original concentration).

As demonstrated in Chapter 4, ECC-1 exhibit a reduced cell index over time when exposed to obese AGEs in comparison to lean, and a negative rate of proliferation indicative of cell senescence and apoptosis, which was mitigated by application of antioxidants. In contrast, obese concentrations of AGEs impact the proliferation of the hEEO derived epithelial cells, increasing cell index between 12 and 48 h for 3 of 5 biologically independent samples (Figure 5.9). This is reflected in an elevated higher rate of proliferation during the log phase of growth (approximated as 12-48 h). For the other 2 samples, obese AGEs reduced the rate of proliferation compared to lean, highlighting the biological variation of such human samples. Because of the distinct growth kinetic profiles, a direct comparison to the effects of AGEs on ECC-1 cannot be made. Further, while proliferation of hEEO derived epithelial cells can be used to draw preliminary conclusions and provide “proof of principle” evidence regarding

the functional impact of AGEs on primary endometrial epithelial cells, this process is not yet fully understood and requires further investigation. Given these discrepancies in data between primary endometrial epithelial cells and cell lines, selection of the most physiologically appropriate model for use is clearly important; if possible, validation of cell line data in a primary model should always be performed.

5.4.3 Potential mediators of the differential response to AGEs in primary endometrial epithelial cells

Limited effects were noted on hEEO morphology, cytokine secretion, and proliferation following exposure to AGEs that are physiologically representative of the obese uterine fluid. Given the magnitude of the effect of AGEs on cell index and proliferation (Figure 4.3), anti-AGEs components of the organoid expansion medium (ExM) were considered. As mentioned above, NAC is maintained at 1.25 mM in ExM (Turco et al., 2018; Table 2.4), which may neutralise effects of AGEs during hormonal priming. ExM is diluted to 10% during functional analysis, containing a final concentration of 125 μ M NAC, which is still more than 10-fold greater than the cocktail used in Chapters 3 and 4 of this thesis (10 μ M). This high concentration of NAC may have mitigated the effects of AGEs on hEEO. Future studies in which organoids are co-cultured in obese concentrations of AGEs plus decreasing doses of NAC should provide clarity on AGEs-induced effects and the protective role of this antioxidant.

RAGE was immunolocalised to the apical membrane of cells within hEEO (Figure 5.4). *In vivo*, AGEs from the uterine fluid would be present at the apical surfaces of the luminal and glandular epithelium. However, hEEO are spherical structures with the apical surface facing internally towards the lumen. *In vitro*, AGEs are added to the culture medium and not into the lumen of the hEEO, and will most likely interact with the basal surface of the epithelial cells, where minimal RAGE is present. Whether solubilised AGEs, such as those present in uterine fluid, can pass through cells or through tight junctions is not known. TLR4 is localised throughout the hEEO, and would provide a mechanism for these AGEs to interact with the epithelial cells; indeed, TLR4 appears elevated in the hEEO compared to donor tissue (Figure 5.4), and if validated through quantitative methodologies, this would provide increased receptor availability for AGEs' binding. The ECC-1 cells used in this experimentation were non-polarised and AGEs in the culture medium would be able to interact with RAGE more readily than in the hEEO. Activation of TLR4 increases the proliferation and migration of other epithelial cell types (Eslani et al., 2014); as such, preferential activation of TLR4 may explain the elevated rate of proliferation in the presence of obese concentrations of AGEs rather than the significant reduction observed in ECC-1 cells.

Significant biological variation was noted during real time cell analysis, with two samples exhibiting reduced proliferation of hEEO derived cells following exposure to obese concentrations of

AGEs versus lean, whereas all other samples showed an increased rate of proliferation. To assess factors which may result in this variation, the patient history was re-evaluated. All samples were obtained from women with a history of fertility, within a similar age range, and had a BMI below 30 kg/m² (Table 5.1). Retrospective assessment of patient history revealed that one patient had PCOS, and one showed evidence of an ovarian cyst. PCOS is known to affect serum levels of AGEs (Diamanti-Kandarakis et al., 2005); the influence of PCOS on uterine AGEs is unknown but may contribute to this altered functional response of hEEO derived cells. Further, the altered expression of hormonal receptors in the endometrium of PCOS patients (Quezada et al., 2006) may influence the functional response of hEEO to hormonal priming and elevated AGEs. Similarly, the ovarian cyst may impact the hormonal milieu in the endometrium and have functional consequences for the epithelial cells isolated from this sample. In the future, an increased sample size will help clarify trends within the data presented here; this was not possible due to COVID-19 restricting human endometrial tissue collections in 2020 and 2021.

In addition to patient history, the AGEs content of donor endometrium was assessed using immunohistochemistry to determine whether any sample contained excess AGEs which may influence the functions of isolated cells. No donor endometrium exhibited strong immunostaining for CML (Figure 5.5). Furthermore, no hEEO cultures demonstrated immunostaining for CML. This was as expected; since hEEO continuously remodel and are passaged frequently there is limited extracellular matrix present for a prolonged period of time, on which AGEs could be formed. These results demonstrate it is unlikely that prior exposure to elevated AGEs *in vivo* will have influenced the results of these experiments.

Given that no donor had a BMI over 30 kg/m², intensive immunoreactive CML was not expected; however even the lean endometrium has previously demonstrated significant accumulation of CML (Antoniotti et al., 2018). It was therefore surprising that such limited staining was observed in these samples (Figure 5.5). Indeed, it was not anticipated that five donors, including one with PCOS, to have no CML accumulation in endometrial tissue. Of note, positive controls utilised were archival tissue samples and long-term storage may affect the glycation of proteins. Given the difficulties involved in investigating post-translational surface modifications of proteins, identifying the optimal storage conditions, such as in a desiccated environment or removed from oxygen, must be considered in planning experimentation (Haragan et al., 2020). It is also possible that the heat intensive antigen retrieval may further modify glycation products, such as the earlier Amadori products (representative of the mid-way point of the glycation process), leading to immunohistochemical artifacts (Hayashi et al., 2002). The benefit of archival or bio-banked tissue for human research cannot be understated; however future prospective studies on endometrial AGEs should utilise snap-frozen and OCT

embedded samples which do not require heat-induced antigen retrieval, to prevent such artifact formation. In addition, with archival tissues, processing of samples will be impacted by inter-staff variation, and minor amendments to protocols over the years of sample collection. Variations in the timing of fixation from specimen fixation can affect the glycosylation of proteins in mouse samples, this is likely also the case for human tissue (Donczo et al., 2019), although our laboratory takes great care over this. The endometrial tissue for derivation of organoids was freshly collected and fixed, while the positive controls were archival; it is possible the immunohistochemistry protocol for freshly collected specimens may need to be re-optimised, not possible in the time of my candidature.

5.4.4 Obesity associated AGEs may lead to a pro-inflammatory environment adverse to establishment of a healthy pregnancy

Antoniotti *et al.* (2018) identified that the obese uterine microenvironment was highly pro-inflammatory. Elevated AGEs within the obese uterine microenvironment may stimulate endometrial epithelial cell contributions to the inflammatory milieu of the uterine fluid (Hannan et al., 2011), and peripheral AGEs may further affect the cytokine profile of the uterine fluid. Separating the local and systemic contributions will require significant further work.

To the best of my knowledge, prior to the work described here, limited information was available on the secretions from hEEO. Human endometrial epithelial cells are highly secretory (Fahey et al., 2005), and using multiplex analysis of the hEEO conditioned media I have provided evidence that hEEO maintain this secretory capacity, and that obesity-associated AGEs modulate their secretions (Figure 5.10). Given the significant contribution of inflammation to the progression of the menstrual cycle (Azlan et al., 2020; Evans and Salamonsen, 2012), and human fertility (Edgell et al., 2018; Fitzgerald et al., 2016), the secretory nature of hEEO provides an new opportunity to more closely examine the epithelial contribution to the uterine immune environment in an experimental setting, particularly given that hEEO can be derived from both fertile and infertile women (the latter not used in this study). The cytokines detected within the hEEO conditioned media clearly demonstrate an immunomodulatory effect of AGEs; further impacts may be detected within the luminal fluid of the hEEO which will contain cytokines secreted apically into the lumen.

Cytokines and chemokines play varied and complex roles in embryo implantation and pregnancy (Chavan et al., 2017; Dimitriadis et al., 2005); the regulation of preimplantation embryo development, fetal development, and placentation, are highly sensitive to growth factors and cytokines *in vitro* (Gurner et al., 2020; Jackson et al., 2012) and *in vivo*, with a delicate balance between cytokines beneficial to the embryo and 'embryotoxic' cytokines required for the appropriate development and selection of a viable embryo (Robertson et al., 2018). Chapter 3 of this thesis has linked obesity-

associated AGEs with reduced placentation potential, and the increase in cytokine release induced by AGEs may provide further mechanisms by which their detrimental effects on fertility are exerted.

All cytokines and chemokines assayed, with the exception of PLGF (present in the uterine fluid and important for embryo development (Binder et al., 2016)), were detected in hEEO conditioned media without application of hormones or AGEs (Table 5.2). Elevated serum IL-17A may be related to failed implantation in infertile women following ART (Crosby et al., 2020); however minimal IL-17A was detected in hEEO conditioned media. Across hormonal priming, obese AGEs elevated the secretion of the other chemokines and cytokines, with CXCL-16 being significantly increased compared to standard culture conditions (Figure 5.10 B). IL-8, IL-10, IL-1 β , and TNF α were also somewhat but non-significantly elevated in the presence of obese AGEs. Whilst inflammation is an essential component of the menstrual cycle, excess AGEs may overstimulate this process, leading to a non-receptive cycle: for example IL-8 is elevated in the uterine fluid of infertile women (Edgell et al., 2018). Regrettably, it was not possible to increase the n-values for these analyses due to COVID-19, but if more samples were included, many of the trends in cytokine levels may become significant.

IL-1 β in uterine fluid at the time of embryo transfer is negatively correlated with pregnancy (Boomsma et al., 2009), strengthening the assertion that AGEs-induced inflammation may lead to non-receptivity. Intriguingly, IL-1 β was not detected in the proliferative phase uterine fluid of fertile women, was detected only at low concentrations (2.3 ± 1.3 pg/mL) in idiopathic infertile women (Fitzgerald et al., 2016), and was not detected in uterine fluid when examined by Hannan et al (2011). In this study, IL-1 β was non-significantly elevated by obese AGEs following treatment with estrogen (the primary hormonal driver of the proliferative phase), and was detected at a similar concentration in hEEO conditioned medium to uterine fluid concentrations reported in Fitzgerald et al. (2016). In contrast, the concentration of IL-10 in hEEO conditioned medium is far greater than previous reports of uterine fluid (Boomsma et al., 2009; Fitzgerald et al., 2016; Hannan et al., 2011), potentially due to a different secretory response from that *in vivo*.

TNF α , non-significantly elevated by the application of obese AGEs (Figure 5.10 I), is produced to a greater extent by immune cells from women experiencing conditions including recurrent spontaneous miscarriage and preeclampsia, versus normal pregnancy (Azizieh and Raghupathy, 2015). However, Boomsma et al. (2009) report a positive correlation with clinical pregnancy following embryo transfer, a difference perhaps in peripheral immune cell function and endometrial secretions. AGEs are known to increase the secretion of IL-6 from trophoblast cells, in a TLR4 dependent manner (Shirasuna et al., 2016), and it is known to be present in the uterine fluid (Hannan et al., 2011), and is somewhat elevated in uterine fluid from idiopathic women versus fertile during the proliferative

phase of the menstrual cycle (Fitzgerald et al., 2016). However, no effect of AGEs was demonstrated on the IL-6 secretion from endometrial epithelial cells in this study.

CXCL16, elevated in the plasma of obese individuals (Lopes et al., 2018; Ribeiro et al., 2017), was detected in the hEEO conditioned media and significantly elevated by obese AGEs. CXCL16 has several roles within the maternal-fetal interface and pregnancy (review: Shi et al., 2020), including stromal cell decidualisation, spiral artery remodelling, and trophoblast invasion and migration. First trimester trophoblast secreted CXCL16 in culture, and exogenous CXCL16 increased the proliferation and invasion of primary first trimester trophoblast cells in a dose dependent manner (Huang et al., 2006). CXCL16 is further implicated in pathologies of pregnancy: CXCL16 expression is reduced in the decidua and trophoblast villi from spontaneous abortion versus normal pregnancy; in addition less CXCL-16 is released from the decidua and trophoblast from spontaneous abortion (Mei et al., 2019). Conversely, some studies have demonstrated elevated serum CXCL16 in women experiencing preeclampsia (J. W. Shi et al., 2020; Tok et al., 2019), a pathology disproportionately affecting obese women (Roberts et al., 2011). Given the roles of this chemokine in pregnancy, the effects of AGEs may lead to abnormal placentation.

Clinically, cytokines examined here are associated with poor pregnancy outcomes. In addition, IL-6, IL-1 β , and IL-8 are associated with preterm birth (Lyon et al., 2010). These studies, supported by the AGEs-induced alteration in cytokine secretion, lend further credence to elevated AGEs impacting clinical outcomes. Other cytokines, chemokines, and growth factors not examined here are known to impact embryo development and uterine receptivity; for example, the TGF- β superfamily (Jones et al., 2006) and leukaemia inhibitory factor (LIF) (Paiva et al., 2009). Given this preliminary foray into the complex immune environment of the uterine fluid demonstrated significant effects of AGEs, a broader examination of their effect on immune moieties is of significant interest. Human pregnancy begins with the highly inflammatory process of embryo implantation, an evolution of inflammatory attachment, while gestation occurs in an anti-inflammatory environment (Griffith et al., 2017). Altered maternal inflammation, associated with conditions such as preeclampsia or infection during pregnancy, impacts offspring development (Goldstein et al., 2020; Han et al., 2021). Given the immune requirements for embryo implantation and pregnancy are temporally regulated (Griffith et al., 2017), it would be of interest to examine whether there are correlations between pre-pregnancy uterine AGEs and serum inflammatory markers across gestation.

5.4.4.1 Potential fertility limiting effects of AGEs induced inflammation

This research clearly demonstrates that AGEs within the obese uterine microenvironment stimulate endometrial epithelial cell contributions to the inflammatory milieu. Epithelial gland secretions are fundamental to blastocyst development and in the first trimester of pregnancy before the switch from

histotrophic to haemotrophic nutrition, with glandular function informed by signals from the decidualised stromal cells (review: Burton et al., 2020). The effect of AGEs on the secretions of human endometrial stromal cells was not examined here, but would be of interest to future work. Antoniotti et al. (2018) demonstrated increased prolactin release from decidualised stromal cells in the presence of obese AGEs versus lean. Inflammation and decidualisation are tightly linked, with decidualised endometrial stromal cells secreting inflammatory mediators *in vitro* (Evans and Salamonsen, 2014). Antoniotti et al. (2018) identified endoplasmic reticulum stress in decidual cells co-cultured with obese AGEs, and proposed the elevated prolactin to be due to the unfolded protein response. Regrettably, inflammatory molecules were not measured in this conditioned medium. During the differentiation of stromal fibroblasts into decidual cells, a sub-population enter senescence, and secrete endometrial receptivity associated factors. During endometrial remodelling in the presence of an invading blastocyst, these senescent cells are cleared by uterine natural killer cells (Brighton et al., 2017). The balance of senescent and decidual stromal cells is finely tuned, and alterations can be identified in conditions such as recurrent pregnancy loss (Lucas et al., 2020). It is possible that AGEs promote the decidual phenotype in an excessive proportion of cells, as exogenous CXCL16 stimulates decidualisation of endometrial stromal cells (Mei et al., 2019), resulting in inappropriate remodelling at the maternal-fetal interface and elevated prolactin secretion: biomarker analysis could determine the proportion of decidual and senescent cells in the obese decidual endometrium (Lucas et al., 2020).

5.4.5 Therapeutic potential and future directions

Data from this chapter lends further support to the alteration of the uterine fluid microenvironment in obese women (Antoniotti et al., 2018). The prevailing effect identified in this chapter is the elevation of chemokines and cytokines from hEEO in the presence of obese AGEs. Application of anti-inflammatory therapeutics, or adoption of a diet to lessen systemic inflammation, may be of benefit to women with elevated uterine AGEs attempting to conceive. Further investigation is required into the effects of therapeutics examined previously in this thesis (RAGE antagonism, antioxidants, and metformin) and the normalisation of hEEO cell functions. Translational outcomes of the effect of AGEs on the endometrial environment are discussed further in Chapter 7 of this thesis.

This work has demonstrated that hEEO derived cells are responsive to AGEs in a functional manner. Future work could examine specific functions related to endometrial physiology and receptivity, including trophoblast spheroid adhesion to AGEs-exposed epithelial monolayers. Furthermore, the use of hEEO derived cells may help resolve the considerable discussion as to whether re-epithelialisation of the endometrial surface following menstruation is from stem cells within glands or by 'wound healing' from the more mature cells at the edges of denuded glands and from remaining patches of luminal epithelium (Salamonsen et al., invited review, *in submission*). Glandular secretions

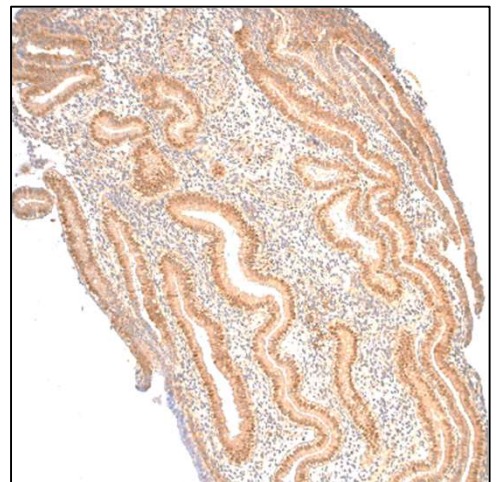
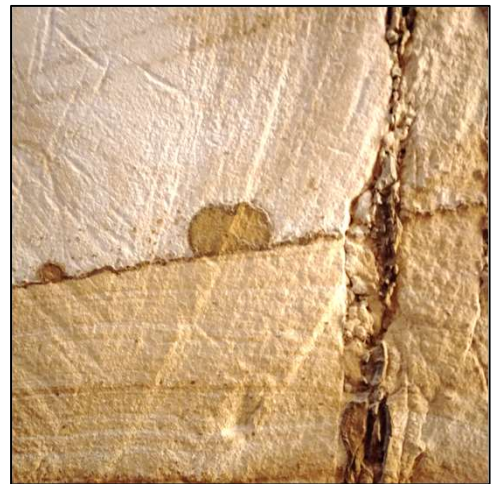
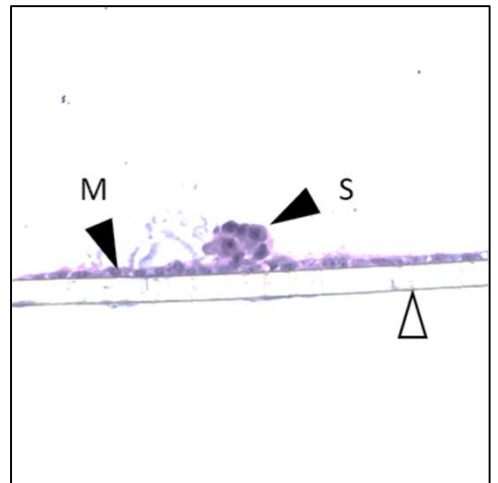
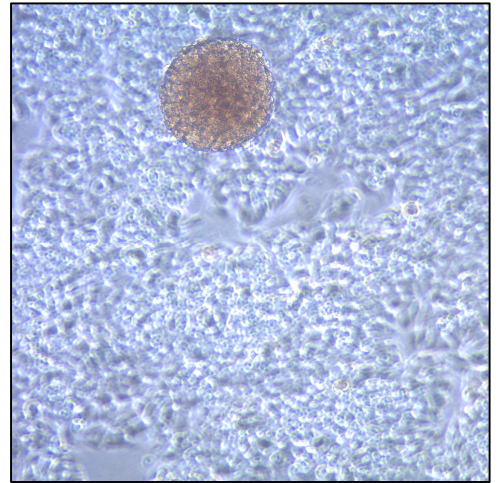
and the impact of obesity could also be investigated through 3D modelling or proteomic analysis of hEEO-derived conditioned medium and fluid within the organoids.

5.5 “Take home” message

Endometrial epithelial organoids are an emerging technique to culture primary human endometrial epithelial cells. They are functionally responsive to obesity-associated AGEs, with preliminary data demonstrating a donor-dependent effect on organoid derived epithelial cell proliferation, and altered secretion of inflammatory molecules detected in conditioned media. Further research is required to understand functional differences between endometrial cancer cell lines and primary cells, to confirm and expand upon these findings, and to investigate the applicability of therapeutics explored in Chapter 4 for use on these primary cells. Importantly, a fine balance of inflammatory factors is required both for endometrial remodelling and for the establishment of pregnancy; modulation by obesity and associated AGEs may tip the balance towards an unfavourable inflammatory milieu that is likely to result in poor pregnancy outcomes and pathologies.

Chapter 6:

Validation and interrogation of novel protein biomarkers of endometrial receptivity



Chapter 6: Validation and interrogation of novel protein biomarkers of endometrial receptivity

Ongoing work concerning the human receptome and adhesome

At the start of my candidature, the primary focus of this thesis was to be the validation and functional interrogation of the human receptome and adhesome (Evans et al., 2020a). As the parallel investigation of obesity-associated AGEs showed significant promise, and with the incorporation of organoid culture into this thesis, this work became a minor aim. This chapter represents a body of ongoing work, for which preliminary data has been published ((Evans et al., 2020a); Appendix 4). While specific components of the receptome and adhesome have been examined, insufficient time remained to investigate the effects of obesity-associated AGEs on these proteins, and their expression in the obese endometrium versus lean, as was the original aim of this work.

6.1 Introduction

Work detailed in this thesis (Chapters 3-5) has clearly shown that elevated AGEs exert functional effects on the preimplantation mouse embryo and the human endometrium, and has identified some beneficial effects of pharmaceutical interventions. To gain a more comprehensive understanding of obesity-associated AGEs, their effects on molecular characteristics of the human endometrium which underpin crucial reproductive processes, including endometrial receptivity, need to be examined.

A receptive endometrium is required for the establishment of pregnancy, and is considered one of the major reasons for implantation failure following transfer of a high-quality blastocyst. However, little is known about the mechanisms by which the endometrium, specifically the luminal endometrial epithelium, becomes receptive to an appropriately developed blastocyst. As such, endometrial receptivity is often referred to as the 'black box of reproduction' (Macklon et al., 2002). A gene expression profile of the 'receptive' endometrium has been described (Díaz-Gimeno et al., 2011); however this analysed endometrial biopsies, which provide little information on the protein changes providing function within the luminal epithelium, the site of initial embryo attachment leading to implantation.

Limited models exist for interrogating endometrial receptivity *in vitro*. Most assays involve spheroid-epithelial interactions to mimic implantation sites. Since the development of early assays (John et al., 1993), systems have been further developed and refined using different cell types to generate more physiologically relevant models (Schmitz *et al.*, 2014; Ho *et al.*, 2012; Thie and Denker, 2002). Most models utilise readily available endometrial cancer derived cell lines, which as described in Chapter 5 of this thesis, are fundamentally altered from the physiologically normal endometrium. Recent work in this laboratory developed a model using primary human endometrial cell monolayers,

which was able to accurately define each donor endometrium as ‘receptive’ or ‘non-receptive’ (reflecting the donor’s fertility status) by the adhesion of trophectoderm cell spheroids which mimic the human blastocyst (Evans et al., 2020b). This model enables significant *in vitro* applications (Kinnear et al., 2019), and has allowed proteomic interrogation of the maternal-fetal interface *in vitro*. A significant advantage of studying protein biomarkers of receptivity compared to genetic microarrays is that these can provide functional information on the proteins present, whereas not all mRNA is translated. The ‘adhesome’ (endometrium/trophectoderm interface) and ‘receptome’ (endometrial epithelium only), were defined by proteomic changes in the receptive endometrium generating potential biomarkers of endometrial receptivity and embryo adhesion (Evans et al., 2020a). The identification of several proteins in this model that are common to genes included in the endometrial receptivity array (Díaz-Gimeno et al., 2011), lends credence to the validity of this model. Preliminary immunolocalisation and functional assessment of receptome and adhesome proteins was performed (Appendix 4); however, more detailed investigation was required to understand the involvement of these novel receptivity biomarkers in the human endometrium.

Box 1: Definition of the human endometrial epithelial receptome and embryo-epithelial adhesome.

*Human endometrial epithelial **receptome**: The proteome of receptive endometrial epithelial monolayers compared to non-receptive monolayers, defined by spheroid adhesion assay.*

*Human endometrial-epithelial **adhesome**: the proteome of adhesive co-cultures (trophectoderm spheroids adherent to receptive endometrial epithelial monolayers) compared to all non-adhesive epithelial conditions (receptive and non-receptive monolayers not exposed to spheroids, and non-adherent co-cultures).*

In this chapter, I describe investigations of 8 specific receptome and adhesome proteins (defined in Box 1) as determined by proteomic investigation (full lists of proteins within the receptome and adhesome are provided in Appendix 3) and assessment of their potential functions. Through this work, both Stem-Loop-Interacting RNA-binding Protein (SLIRP) and Positive Co-factor 4 (PC4) have emerged as potential discriminants of fertility and key players in the regulation of endometrial receptivity. While initial immunohistochemical studies on human endometrium indicated that endometrial epithelial expression of a number of receptome proteins was modulated across the menstrual cycle and between fertile and infertile women (Evans et al., 2020a; Appendix 4), digital quantification as detailed here was unable to report any statistically significant difference for several

proteins. However, siRNA reduction of some specific proteins significantly altered the adhesive capacity of hormonally primed epithelial cells, validating their functions in this model.

This work provides a foundation for subsequent studies, having identified targets for investigation either in the context of the molecular changes related to obesity-associated AGEs or for further examination of endometrial receptivity.

6.2 Materials and methods

6.2.1 Donor demographics

Endometrial biopsies were obtained across the menstrual cycle from women with a history of fertility (at least 1 previous parous pregnancy), or primary infertility (no previous pregnancy). These tissues were formalin fixed and paraffin embedded for histological use.

Table 6.1: Demographics of endometrial donors. Mean \pm SEM AGE (years) and BMI (kg/m^2 ; not available for all donors in this cohort, available n-number listed in table) for endometrial donors used to localise individual receptome and adhesome proteins. n.a.: not available. *, **: $P < 0.05$, < 0.01 versus fertile.

| Proliferative | | |
|----------------------------|---------------|-------------------|
| Fertility | Age | BMI |
| Fertile (n = 15) | 35 \pm 1 | n.a. |
| Early-secretory | | |
| Fertility | Age | BMI |
| Fertile (n = 18) | 38 \pm 1 | 30 \pm 4 (n=3) |
| Primary infertile (n = 25) | 35 \pm 1 * | 25 \pm 1 (n=10) |
| Mid-secretory | | |
| Fertility | Age | BMI |
| Fertile (n = 11) | 39 \pm 2 | 28 \pm 2 (n=6) |
| Primary infertile (n = 17) | 33 \pm 1 ** | 25 \pm 1 (n=9) |

Due to limited available tissue, not all samples could be used for all immunohistochemical investigations, and n-numbers vary accordingly between individual receptome and adhesome proteins; data are displayed as individual points representing biologically independent samples clearly showing the n-number used for each protein. The characteristics of the total available cohort are described in Table 6.1. The donors of both infertile early-secretory and mid-secretory endometrium

were significantly younger than their fertile counterparts. Given these women are recruited following presentation to a clinic for gynaecological procedures, it is unlikely that younger, fertile women will present. Thus, this age difference was anticipated but must be taken into account when interpreting data. No significant difference in age was seen between fertile proliferative and fertile mid-secretory endometrium donors ($P = 0.06$). For those samples for which data are available, BMI did not differ between donor cohorts ($P \geq 0.16$ for all).

6.2.2 Digital quantification of immunohistochemistry

Immunohistochemistry was performed as per Section 2.5.1.1, using the optimised conditions presented in Table 2.8. Three representative images of each section were taken at 5x total magnification on an Olympus B52 microscope, and intensity of epithelial staining digitally quantified using ImageJ software (NIH). To quantify immunostaining, the colour channels of TIFF images were split, and the blue channel used for quantification. Using the full colour image for comparison, an intensity threshold detecting immunostained pixels was set for a representative selection of images (minimum of 3 biologically independent samples), with the average intensity threshold used for quantification. Epithelial areas were manually identified and the number of stained pixels quantified; this was then subtracted from the total number of stained pixels in the tissue section to give epithelial and non-epithelial contributions to staining. Non-epithelial staining contains contributions from stromal fibroblasts, immune cells, maternal blood vessels, and glandular secretions. The same quantification was performed on the isotype control to correct for any non-specific staining. No outlier processing was performed on this data.

6.2.3 qPCR assessment of siRNA knockdown and hormonal regulation of receptome and adhesome genes in ECC-1

The relative expression of individual receptome and adhesome mRNA (PC4, LGMN, KYNU, STMN1, SLIRP, PTGS2, and SERPINE1) following siRNA knockdown (Section 2.6.1.2) was determined using qPCR (Section 2.6.1.4). RPL19 was used as a housekeeper. The overall protocol for the cell culture and hormonal treatments is as described in Section 2.6.1.2. RNA was extracted from sequential time-points across hormonal priming: at the time of addition of serum free medium alone (+ SFM; 72 h after siRNA application), addition also of E (+ E; 78 h after siRNA application), addition of E + MPA (+ E + MPA; 98 h after siRNA application), and at the time of spheroid addition (+ SPR; 118 h after siRNA application).

RNA available from scramble control samples of ECC-1 which underwent standard hormonal priming was considered sufficient for this preliminary data. The mRNA levels following serum starvation, following E treatment, and following E + MPA treatment were determined relative to basal (immediately prior to starvation) for each gene of interest.

6.2.4 Transepithelial resistance

ECC-1 cells underwent siRNA knockdown, were hormonally primed and TER measured across hormonal priming (Section 2.6.1.3). TER from each condition was normalised to the corresponding TER following the prior application: E + MPA compared to E alone, E + MPA compared to serum starvation (SFM), and E alone compared to serum starvation.

6.2.5 Data mining

Single cell RNA sequencing (scRNA-seq) data was obtained with permission from Dr Harriet Fitzgerald (Fitzgerald et al., 2019). This data was derived from experimental data obtained as follows: in technical triplicate, human endometrial epithelial organoids (hEEO) from one donor were primed with 10 nM E for 2 days, followed by a further 6 days of culture in either 10 nM E + 1 µM MPA (EP) or 10 nM E + 1 µM MPA + 1 µM cyclic adenosine monophosphate (cAMP; EPC). hEEO-derived cells were processed for scRNA-seq using an Illumina NextSeq. The fragments per kilobase of transcript per million mapped reads (FPKM) and log fold change values were obtained from the supplementary data provided with the manuscript for the appropriate gene for each receptome and adhesome protein of interest. FPKM values analysed using a T-test or Mann Whitney U-test. Log-fold-change and false discovery rate (FDR) *P*-value as determined by a bioinformatician are provided in Table 6.2.

6.3 Results

The proteins selected for further study fell into three groups: those unique to the receptome (involved in endometrial receptivity only); those common to the receptome and adhesome (receptivity and embryo adhesion); and those unique to adhesome (adhesion specific).

6.3.1 Independent interrogation of receptome-specific proteins

6.3.1.1 Positive Co-factor 4

PC4 is the most highly upregulated protein unique to the receptome, with a fold change in label free quantification (LFQ, relative protein abundance as determined by mass spectrometry) of 1.3×10^5 between receptive and non-receptive epithelial cell cultures (Appendix 3). PC4 is involved in transcriptional regulation and DNA repair (Batta et al., 2009; Conesa and Acker, 2010) and is expressed throughout the body. After oxidative damage, PC4 plays an important role in initiating DNA strand repair (Conesa and Acker, 2010). As PC4 enhances BRCA1 expression and stimulates p53-mediated cellular apoptosis, it has been proposed to play a role in tumour suppression (Banerjee et al., 2004); conversely PC4 has been implicated in breast cancer cell metabolism and metastasis (Luo et al., 2019). Additionally, PC4 is important for reproductive processes as it is involved in modulation of luteinising hormone receptor gene expression by interacting with transcription factor Sp1 at the promoter region (Liao et al., 2011). Holistically, PC4 is a versatile nuclear protein involved in modulation of cellular stress.

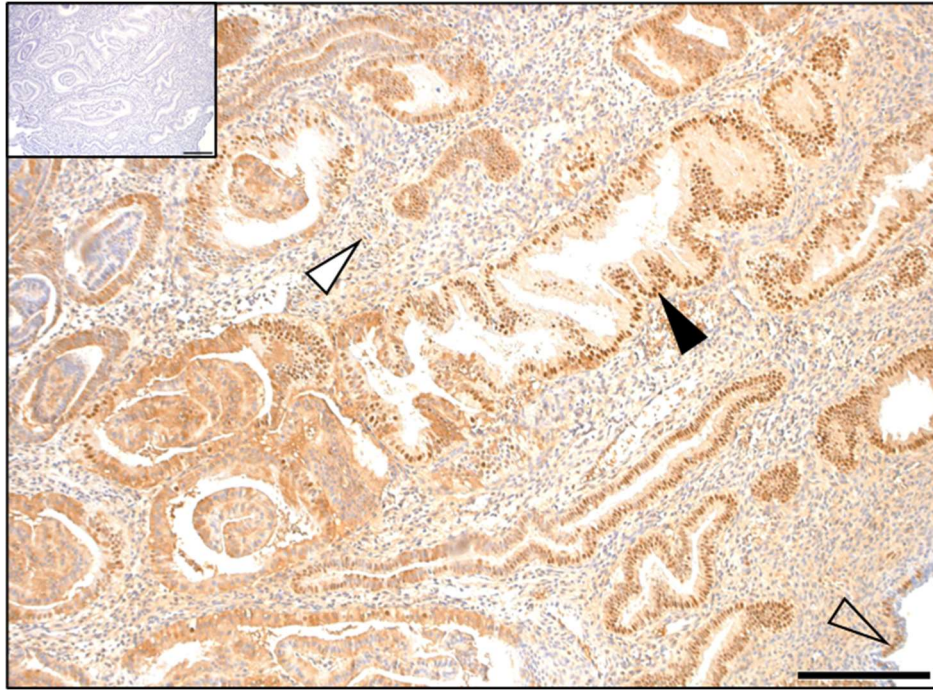


Figure 6.1: PC4 in the human endometrium. Representative PC4 immunostaining in the early-secretory phase human endometrium. PC4 was located in nuclei and localised to the glandular (black arrow) and luminal (open arrow) epithelium, and the stroma (white arrow) of the endometrium. Representative image shown, scale bar represents 200 μm . Isotype control inset.

PC4 is strongly detected in the human endometrium across the proliferative, early-secretory, and mid-secretory phases of the menstrual cycle (representative image, Figure 6.1). Staining is predominantly nuclear, as expected for this protein. A faint wash of staining is evident in the stromal compartment, with some nuclear staining identified. This protein is identified in both the glandular and luminal epithelium, to similar extents. PC4 was not identified within the glandular secretions or contents of the maternal blood vessels.

While epithelial PC4 appeared to be elevated in the mid-secretory endometrium compared to proliferative phase endometrium from fertile women, digital quantification was unable to detect a significant difference in either the epithelial ($P = 0.34$), or non-epithelial ($P = 0.55$) compartments. However, when comparing mid-secretory phase epithelial staining between fertile and infertile women, PC4 immunostaining appeared reduced in the infertile samples ($P = 0.054$). There was no difference in the non-epithelial immunostaining ($P = 0.68$) Within the early secretory endometrium, epithelial PC4 was not reduced ($P = 0.15$), but non-epithelial PC4 was significantly reduced in the infertile endometrium compared to fertile ($P = 0.04$). It is clear that endometrial PC4 can be modulated by infertility and is an important protein of the human epithelial receptome.

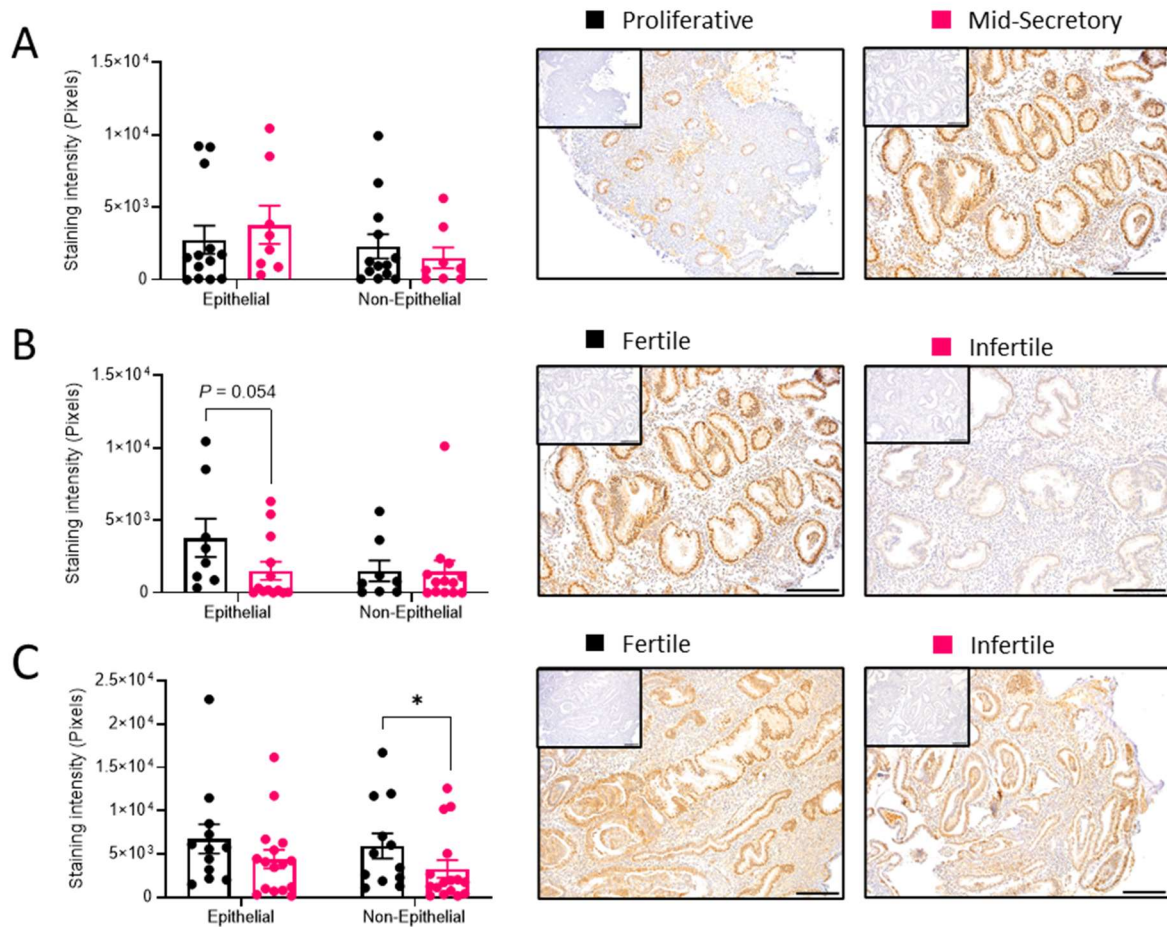


Figure 6.2: Quantification of PC4 expression in the human endometrium. Mean \pm SEM immunostained pixels following digital quantification of staining in the (A) fertile proliferative and mid secretory endometrium, (B) the fertile and infertile mid-secretory and (C) early-secretory endometrium. Epithelial immunoreactive PC4 was not significantly altered across the menstrual cycle (A; $P = 0.34$). PC4 appears reduced in the epithelium of the infertile mid-secretory endometrium compared to fertile (B; $P = 0.054$). PC4 was significantly reduced in the non-epithelial components of the infertile early secretory endometrium (C; $P = 0.04$). Mann-Whitney test: $*P < 0.05$. Representative images shown, isotype control inset. Scale bars represent 200 μm . Individual data points represent biologically independent samples ($n \geq 8$ for each).

An 80% reduction of PC4 mRNA in ECC-1 cells was achieved across all time points examined ($P < 0.01$ for all; Figure 6.3 A). No morphological differences were observed in the cell cultures (data not shown). There was no significant effect of knockdown on the adhesive capacity of ECC-1 cells ($P = 0.85$; Figure 6.3 B). This implies PC4 is not significant in maintaining adhesive capacity function in a cell culture model of the human receptome. Knockdown was not performed on primary cells for this thesis.

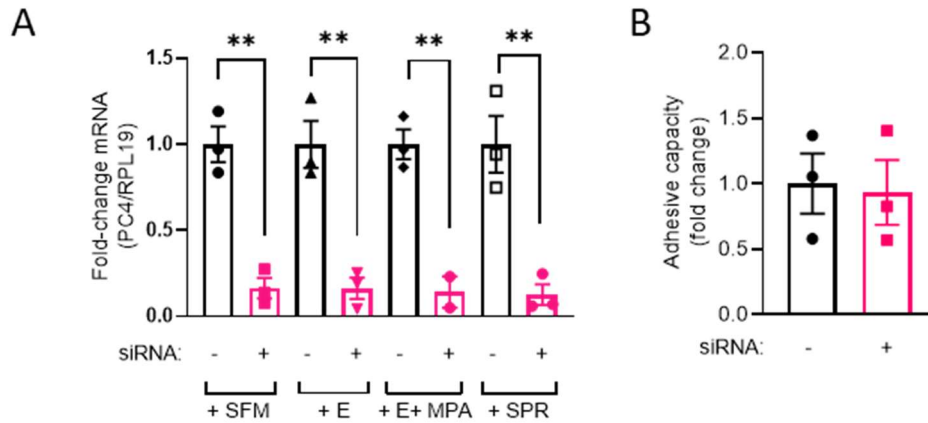


Figure 6.3: siRNA reduction of PC4 does not affect the adhesion of trophectoderm spheroids to ECC-1. **A)** PC4 mRNA was significantly reduced in ECC-1 cells throughout hormonal priming compared to scramble siRNA control: at the addition of serum free medium (+ SFM; $P < 0.01$), addition of E (+ E; $P < 0.01$), addition of E + MPA (+ E + MPA; $P < 0.01$), and at the time of spheroid addition (+ SPR, $P < 0.01$). **B)** Reduction of PC4 in ECC-1 cells did not affect the percent of spheroids that adhered in comparison to scramble control ($P = 0.85$). Data expressed as mean \pm SEM derived from 3 biologically independent replicates, denoted by individual data points. Unpaired t-test: ** $P < 0.01$

6.3.1.2 Stathmin1

Stathmin 1 (STMN1) is uniquely upregulated in the receptome, with a fold change in LFQ of 7.6×10^4 between receptive and non-receptive endometrial epithelial cultures. STMN1 was selected for validation as it is one of the most highly upregulated proteins of the receptome, and has previously been implicated in the human reproductive system (Domínguez et al., 2009). STMN1 regulates microtubule dynamics by promoting depolymerization and preventing tubulin heterodimer formation. Its functions and regulation are critical in proper progression of the cell cycle (Rubin and Atweh, 2004). Furthermore STMN1 is involved in cell motility; it has been shown that STMN1 is an important cofactor in STAT3 mediated T-cell migration (Verma et al., 2009) and is involved in the migration and invasion of malignant glioma cells (Liang et al., 2008).

In the reproductive system, STMN1 has been proposed to promote stromal cell proliferation and maintain a pre-receptive state of the endometrium, as it has been found reduced in stromal cells and glandular epithelium of “receptive” mid-secretory endometrium compared to the “pre-receptive” early secretory (Domínguez et al., 2009). It was also noted that maintaining a refractory endometrium by insertion of an intrauterine device contraceptive increased the prevalence of STMN1 (Domínguez et al., 2009). Proteomic data of the receptome differs from this, showing an upregulation of STMN1 during receptivity. Proteins involved in endometrial receptivity may be differentially regulated throughout all phases of the menstrual cycle and as such early- and mid-secretory phases (both influenced by progesterone) may show different STMN1 regulation to the proliferative phase

(influenced by estrogen); STMN1 may be increased from the proliferative phase to the secretory phase, and subsequently decrease as the secretory phase progresses. In addition, proteomic data (Evans et al., 2020a) examined the prevalence of endometrial STMN1 between fertile and infertile women.

Extensive immunohistochemical optimisation was performed to immunolocalise STMN1 in the human endometrium. However, the available antibody could not be optimised for use in this thesis and alternative antibodies would need to be sourced. This is beyond the scope of this thesis; full validation of STMN1 in the human endometrial epithelial receptome and adhesome is unable to be performed at this time. siRNA experiments were performed in parallel with antibody testing, and the results presented below.

The siRNA reduction of STMN1 mRNA could not be validated ($P \geq 0.19$ for all; Figure 6.4 A). It is possible that existing PCR protocols could be re-optimised for these primers, or new primer pairs designed, both beyond the scope of this thesis. While the knockdown was not validated, treatment of ECC-1 cells with siRNA targeted against STMN1 did not affect TER (Figure 6.4 B), but significantly lowered the adhesion of trophoctoderm spheroids ($P = 0.03$; Figure 6.4 C). This implies that STMN1 may be functionally significant in maintaining the adhesive capacity of endometrial epithelial cells.

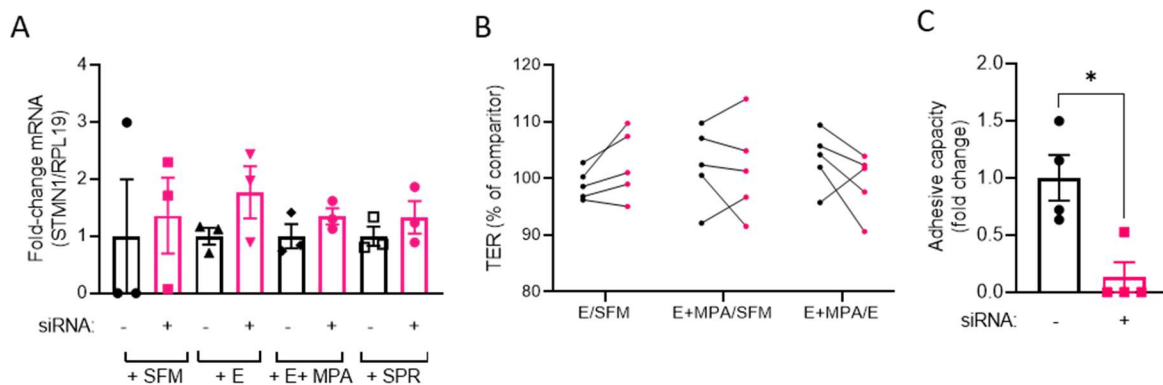


Figure 6.4: siRNA reduction of STMN1 may affect the functions of ECC-1 cells. A) The reduction of STMN1 mRNA could not be confirmed compared to scramble siRNA control (black): at the addition of serum free medium (+ SFM; Mann-Whitney: $P = 0.70$), addition of E (+ E; unpaired t-test: $P = 0.19$), addition of E + MPA (+ E + MPA; unpaired t-test: $P = 0.24$), and at the time of spheroid addition (+ SPR, unpaired t-test: $P = 0.37$). **B)** In comparison to scramble control (black), siRNA reduction of STMN1 (pink) did not affect transepithelial resistance (TER) after hormonal priming with E compared to TER following serum starvation (E/SFM; $P = 0.27$), following priming with E + MPA compared to serum starvation (E+MPA/SFM; $P = 0.89$), or E + MPA compared to TER following E (E+MPA/E; $P = 0.24$). Data connected by lines are from the same experimental replicate, all analysed by unpaired t-test. **C)** STMN1 reduction significantly reduced the adhesive capacity of ECC-1 cells (Mann-Whitney: $P = 0.03$). Individual points represent independent replicates. Data presented as mean \pm SEM, derived from $n = 3$ -5 biologically independent replicates.

6.3.1.3 Cytidine deaminase

Cytidine deaminase (CDA) catalyses the conversion of cytidine to uridine and is important in mRNA editing, particularly in generation of variation in immunoglobulin chains (Cascalho, 2004). CDA is highly upregulated in the receptome (LFQ fold change of 3.1×10^4), and is not further modulated in the adhesome. CDA has previously been implicated in endometrial receptivity as it has been found in genetic signatures corresponding to the receptive endometrium, and is a part of the Endometrial Receptivity Array (Bhagwat et al., 2013; Díaz-Gimeno et al., 2011). This makes CDA a highly interesting candidate for validation and functional evaluation.

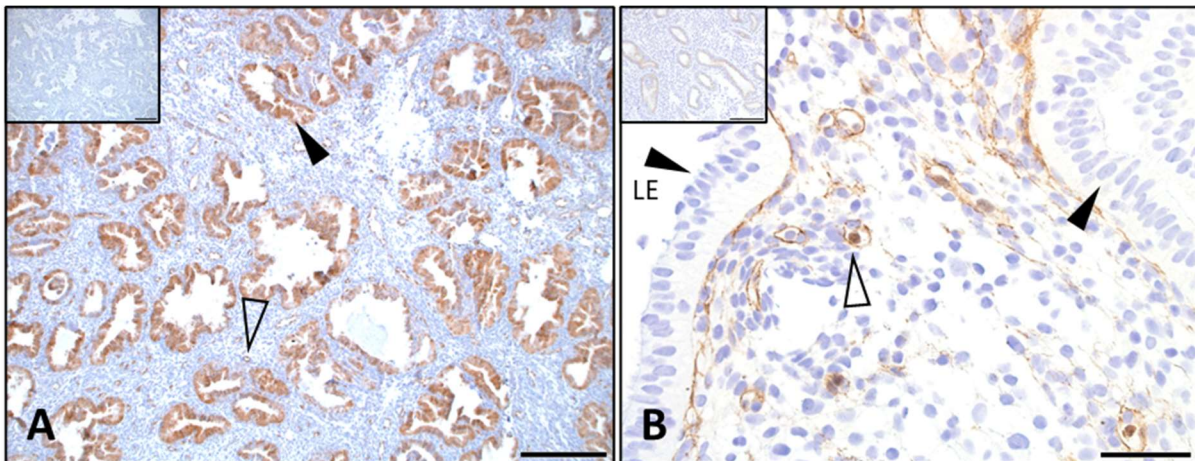


Figure 6.5: CDA immunolocalisation in the human endometrium. A) CDA was immunolocalised to the glandular epithelium of the mid-secretory human endometrium in limited tissues (black arrow), with evidence of staining associated with maternal blood vessels (open arrow) and presumptive immune cells. **B)** In the early secretory endometrium, limited glandular or luminal epithelial (LE) staining was identified (black arrows). Some membrane-associated staining was observed in the stromal compartment, and CDA was immunolocalised to maternal blood vessels (open arrow). Isotype controls inset. Scale bars represent 100 μm (A), 50 μm (B, CDA), and 200 μm (B, isotype control).

During optimisation, epithelial staining was observed in some tissues, but this was not consistently maintained in further investigation, with only 2 of 7 stained fertile mid-secretory tissues demonstrating significant epithelial staining (Figure 6.5 A shows the strongest epithelial stain identified). Few proliferative phase or primary infertile tissues demonstrated epithelial CDA immunostaining. In the majority of endometrial tissues, staining was identified in maternal blood vessels, presumptive immune cells, and within stromal cells. Given the role of CDA in immunoglobulin variation, expression in immune cells is expected. To confirm this colocalization, a dual stain could be performed for CDA and an immune marker such as CD45, and immunolocalisation to maternal blood vessels using an endothelial marker such as CD54. Within the early secretory endometrium, almost no tissues contained epithelial staining for CDA, with some tissues exhibiting a complete absence of CDA from all epithelial cells (Figure 6.5 B).

The presence of CDA in the human receptome may be a result of primary human endometrial epithelial cell differentiation *in vitro*, as expression was not reflected in the *ex vivo* endometrium. Due to its limited epithelial staining and no modulation of expression between 'receptive' and 'non-receptive' endometrial tissue sections, CDA could not be validated as a member of the human receptome, and intensive digital quantification was not performed. Due to limited epithelial staining, no knockdown studies were performed on this protein.

6.3.2 Independent interrogation of proteins common to the receptome and adhesome

6.3.2.1 Kynureninase

Kynureninase (KYNU) is the most highly upregulated protein of the receptome also present in the adhesome, exhibiting a 1.8×10^5 -fold change in LFQ in the receptome, further increased by a factor of 3 in the adhesome. This alone makes KYNU a strong target for validation and functional investigation. Within the proteins upregulated in the receptome, KYNU has no known or predicted interactions; however, in the adhesome KYNU is connected to PPM1G and SQLE. SQLE, squalene epoxidase, is involved in sterol biosynthesis, and PPM1G is a magnesium dependent protein phosphatase (String analysis, Appendix 3). This difference in interactions implies a different role for KYNU in receptivity and adhesion.

KYNU is a member of the amino transferase superfamily, and is involved in the metabolism of tryptophan and the *de novo* synthesis of NAD(P)⁺. In eukaryotes, KYNU catalyses the hydrolysis of 3-hydroxy-L-Kynurenine to 3-hydroxyanthranilic acid (Phillips, 2014). The human protein atlas has shown moderate expression of KYNU in the human endometrium (Uhlén et al., 2015), but KYNU has not previously been linked specifically to endometrial receptivity and embryo adhesion.

KYNU is involved in inflammatory diseases, specifically psoriasis. KYNU positive cells are able to infiltrate lesional skin, and the downstream metabolites of tryptophan promote cell adhesion and induce inflammatory gene expression (Harden et al., 2016). This can be linked back to the enrichment of inflammatory gene ontology terms in the upregulated proteins of the receptome.

In reproduction, homozygous loss of function mutations in KYNU has been identified as contributing to NAD-deficiency related congenital malformations, and confirmed in knock out mouse models, implicating KYNU and its downstream metabolites as important in healthy embryo development (Shi et al., 2017). Using genome wide transcriptomics, KYNU is identified as upregulated in the decidua of preeclamptic placentas, and is associated with the inflammatory response. Enrichment analysis highlights the upregulation of the tryptophan metabolism pathway in preeclamptic placentas, suggesting that KYNU may play an important role in formation and

maintenance of a functional placenta (Loset et al., 2011). KYNU is further implicated in the pathology of endometriosis, as it is dysregulated in human endometrial tissues from women with endometriosis (Pabona et al., 2012). Thus, KYNU is of significant interest when examining the receptome and adhesome.

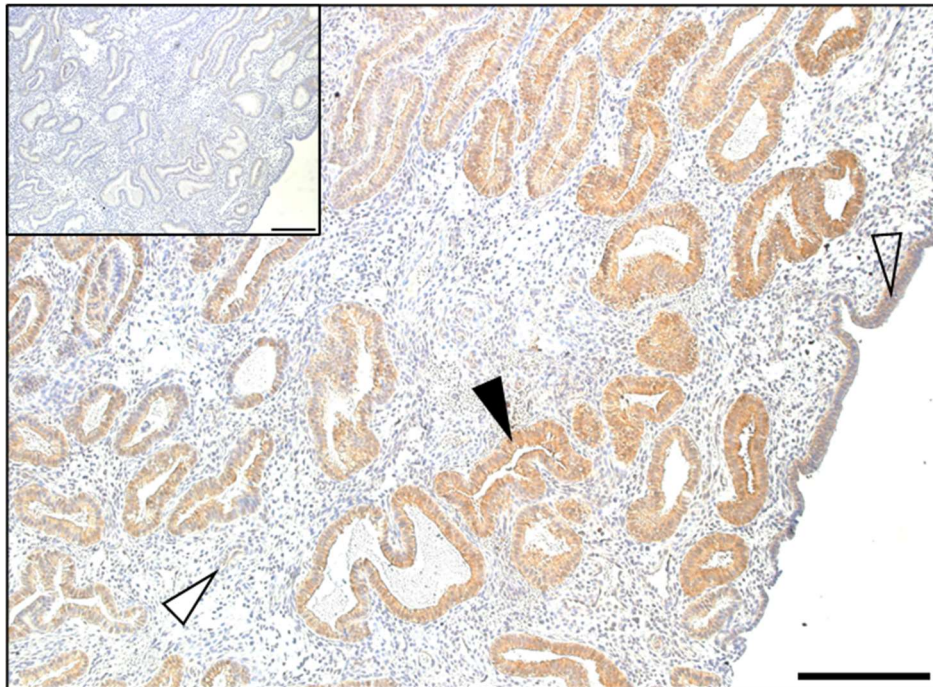


Figure 6.6: KYNU in the human endometrium. Representative KYNU immunostaining in the mid-secretory phase human endometrium. KYNU was localised to the glandular (black arrow) and luminal (open arrow) epithelium, and to a lesser extent within the stroma (white arrow) of the endometrium. Representative image shown, scale bar represents 200 μm . Isotype control inset.

KYNU is immunolocalised in the proliferative and mid-secretory phase human endometrium (representative image, Figure 6.6). Staining is predominantly cytoplasmic, with some nuclear staining observed. KYNU is localised in both the glandular and luminal epithelium, to similar extents. In the proliferative phase, staining is evident in both the stromal and epithelial compartments but in the mid-secretory phase, while staining remains in the stroma, it is predominantly epithelial. In the stromal compartment, KYNU appears in the vicinity of maternal blood vessels. A faint wash of staining is evident throughout the stromal compartment, with some nuclear staining identified.

Quantification revealed predominantly epithelial KYNU immunostaining, which was not significantly different between the proliferative or mid-secretory phase of the menstrual cycle ($P = 0.68$; Figure 6.7 A). Epithelial KYNU was not significantly altered in the infertile mid-secretory endometrium ($P = 0.09$; Figure 6.7 B). Neither cycle stage nor fertility altered non-epithelial staining of KYNU ($P > 0.16$ for both). Immunostaining for KYNU was not performed on early-secretory endometrium.

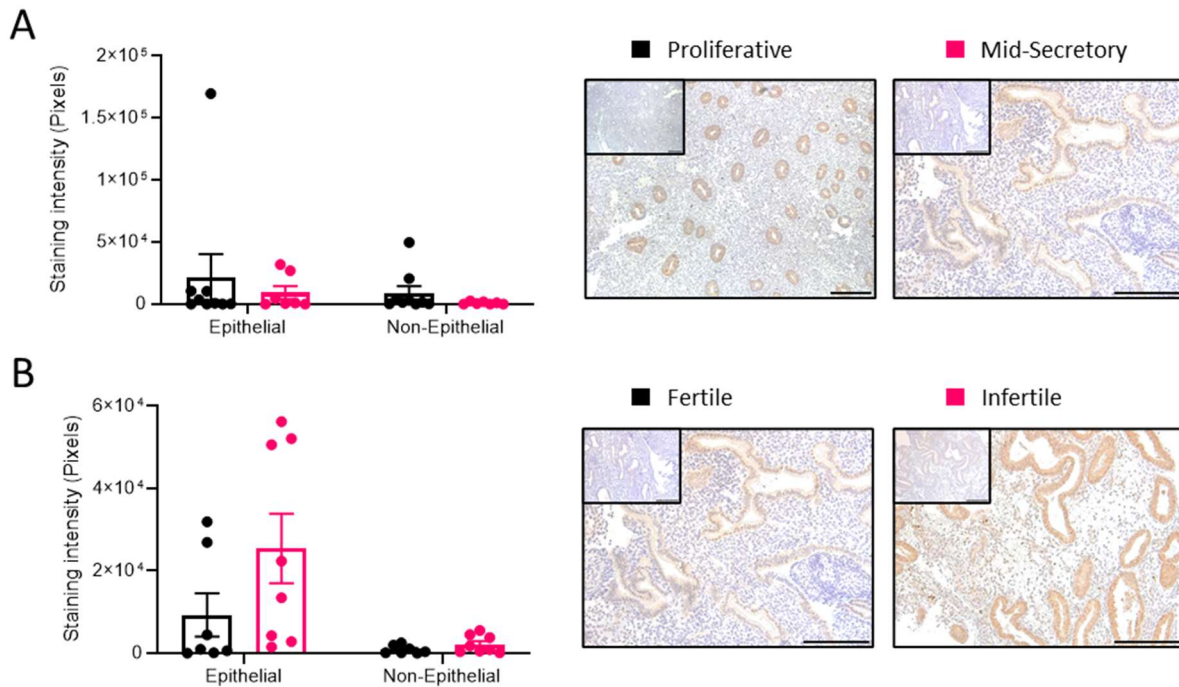


Figure 6.7: Quantification of KYNU immunostaining in the human endometrium. Mean \pm SEM immunostained pixels following digital quantification of KYNU immunostaining contributed by the epithelial and non-epithelial compartments of the fertile human endometrium compared between **(A)** mid-secretory and proliferative phase, and **(B)** comparison of staining between the fertile and primary infertile mid-secretory endometrium. Neither epithelial nor non-epithelial staining were significantly affected by cycle phase or fertility ($P \geq 0.09$ for all). Individual data points represent biologically independent samples ($n \geq 7$ for each). Data expressed as mean \pm SEM, analysed by Mann-Whitney/unpaired t-test.

Following transfection, no morphological effects were observed on ECC-1 monolayers (data not shown). The siRNA reduction of KYNU mRNA could not be validated as the primers used in this work were unable to amplify KYNU in any sample. To confirm the absence of this gene expression, positive control RNA would be required such as from human endometrial epithelial organoids, known to express this gene (Fitzgerald et al., 2019), or alternative primers designed. Further optimisation and investigation are beyond the scope of this thesis. The slight increase in TER between EP and E treatments (E+MPA/E) was reduced in all but one sample following siRNA treatment ($P = 0.28$; Figure 6.8 A). Spheroid adhesion following siRNA treatment was not significantly affected ($P = 0.17$; Figure 6.8 B). Without a confirmed reduction in KYNU expression, no firm conclusions can be drawn from this data.

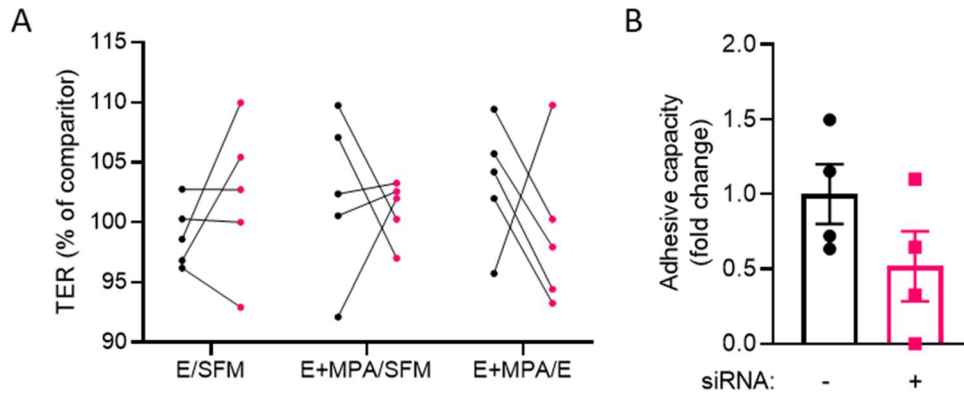


Figure 6.8: siRNA reduction of KYNU does not affect the functions of ECC-1 cells. A) In comparison to scramble control (black), siRNA reduction of KYNU (pink) did not affect transepithelial resistance (TER) after hormonal priming with E compared to TER following serum starvation (E/SFM; $P = 0.32$), following priming with E + MPA compared to serum starvation (E+MPA/SFM; $P = 0.69$), or E + MPA compared to TER following E (E+MPA/E; $P = 0.28$). Data connected by lines are from the same experimental replicate, all analysed by unpaired t-test. **B)** KYNU reduction did not significantly reduce the adhesive capacity of ECC-1 cells (unpaired t-test: $P = 0.17$). Mean and SEM are derived from $n = 4-5$ biologically independent replicates, denoted by individual data points.

6.3.2.2 Legumain

Legumain (LGMN) is upregulated by a factor of 2.2×10^4 in the receptome, and further increased by a factor of 4.6 in the adhesome. No known or predicted interactions of LGMN are seen within these protein cohorts (Appendix 3). LGMN is a cysteine endopeptidase which is involved in antigen processing in the lysosome, but exists in many cellular locations and is involved in several different processes. For a review of the structure and functions of LGMN, see Dall and Brandstetter (2016).

LGMN has been previously identified in the transcriptome of the human embryo trophoctoderm, and in human embryonic stem cells differentiated to a trophoblast lineage, further affirming the validity of the trophoctoderm spheroid adhesion model (Aghajanova et al., 2012), and in the human endometrium (Horcajadas et al., 2008). Previously, LGMN has been suggested to be involved in the remodelling of the extracellular matrix as LGMN gene expression is increased in the bovine endometrium during the pre-attachment period (Bauersachs et al., 2008). For these reasons, LGMN was selected for validation of the receptome and adhesome.

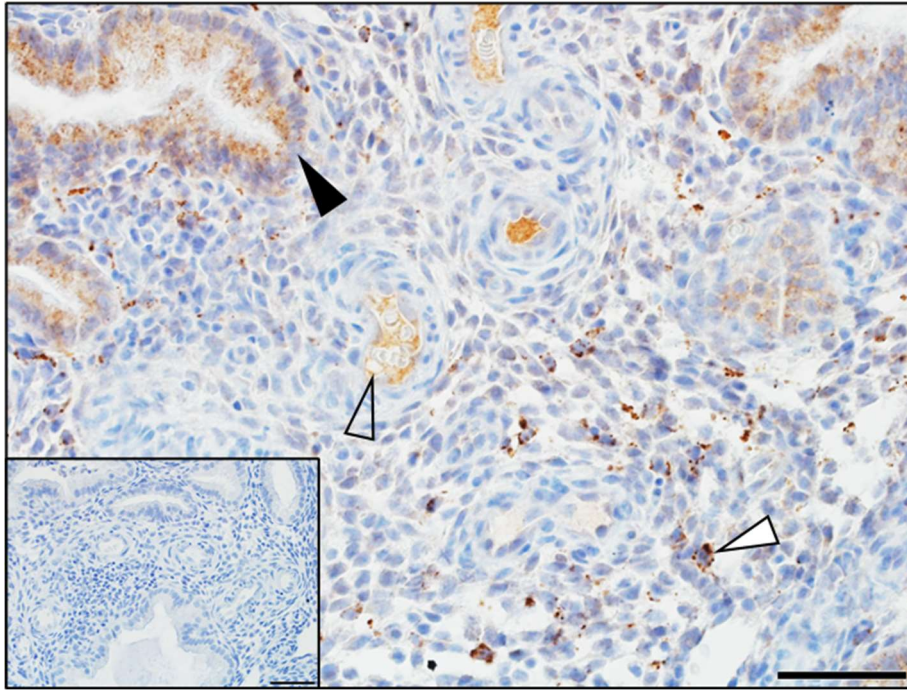


Figure 6.9: LGMN is present in the human mid-secretory endometrium. LGMN was immunolocalised to the glandular epithelium (black arrow), discrete regions of the stromal compartment (white arrow), and within maternal blood vessels (open arrow). Representative image shown, scale bar represents 50 μm . Isotype control inset.

LGMN immunolocalised within the human endometrium in the proliferative, early-secretory, and mid-secretory phases of the menstrual cycle. Shown in Figure 6.9 is a representative image of LGMN immunostaining in the mid-secretory endometrium. Significant staining is identified in the cytoplasm of the glandular epithelium and in sections where luminal epithelium is present, similar staining patterns are observed. Some tissues demonstrate a wash of staining in the stromal compartment, with clear and discrete regions of staining observed in some cells (Figure 6.9); these are likely immune cells and some similar staining was seen in proliferative phase tissue (Figure 6.10 A). No clear nuclear staining was detected in the endometrium. LGMN was also identified within the maternal blood vessels, but not in the red blood cells, indicating LGMN may be secreted and transported in the blood; plasma LGMN secreted from macrophages has been identified as an indicator of atherosclerotic disease (Lunde et al., 2017). No significant difference in staining pattern was noticed between proliferative, early-secretory, and mid-secretory endometrial tissue from fertile and infertile women.

Following digital quantification, LGMN staining was not significantly different between proliferative and mid-secretory tissues in either the epithelial or non-epithelial compartment. (Figure 6.10 A; $P = 0.4$); neither was it significantly increased in the infertile mid-secretory endometrium compared to fertile (Figure 6.10 B; $P = 0.1$). No difference was observed between fertile and infertile

early secretory endometrial epithelium (Figure 6.10 C; $P = 0.4$). No significant difference was seen in the non-epithelial staining for any comparison ($P > 0.2$ for all). In some tissues, a far greater intensity of staining was detected in the mid-secretory period, these may be outliers.

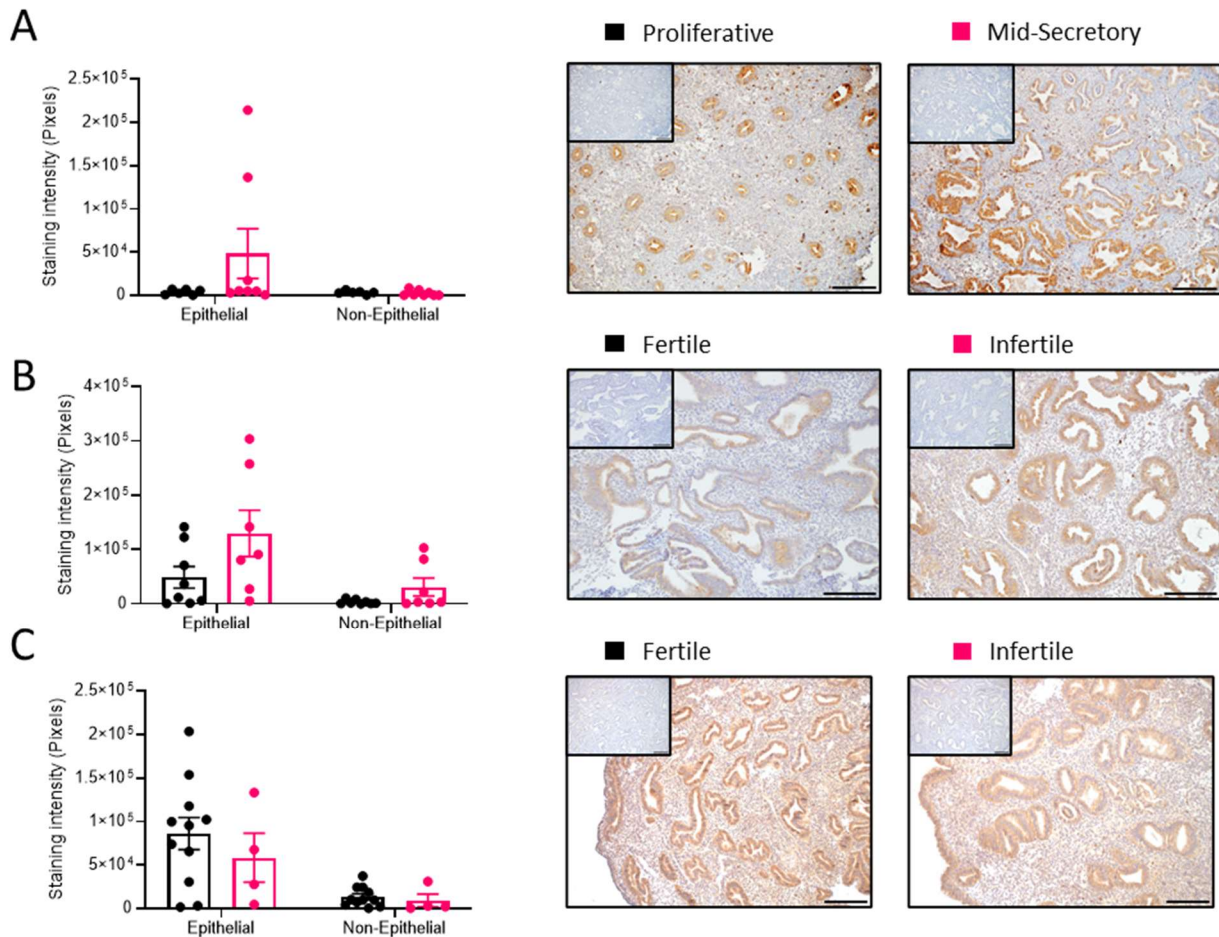


Figure 6.10: Quantification of LGMN immunostaining in the human endometrium. Mean \pm SEM immunostained pixels following digital quantification of LGMN immunostaining in (A) the fertile proliferative and mid secretory endometrium, (B) the fertile and infertile mid-secretory and (C) early-secretory endometrium. No significant difference was seen between epithelial staining in the proliferative versus mid-secretory endometrium (Mann-Whitney: $P = 0.4$), or in the early secretory endometrial epithelium from fertile and infertile women (unpaired t-test: $P = 0.4$). LGMN appeared to be non-significantly increased in the epithelium of the infertile mid-secretory endometrium compared to fertile (unpaired t-test: $P = 0.1$). Scale bars represent 200 μ m, isotype control inset. Individual data points represent biologically independent samples ($n \geq 4$ for each).

In knockdown experiments, a 60% or greater reduction of LGMN mRNA in ECC-1 cells was achieved across all time points examined ($P < 0.01$ for all; Figure 6.11 A). No morphological differences were observed in the cell cultures following transfection (data not shown). No effect of knockdown was seen on the regulation of tight junctions across hormonal priming ($P \geq 0.42$ for all; Figure 6.11 B).

There was no significant effect of knockdown on the adhesive capacity of ECC-1 cells ($P = 0.81$; Figure 6.11 C). This implies LGMN is not significant in maintaining these functions in a cell culture model.

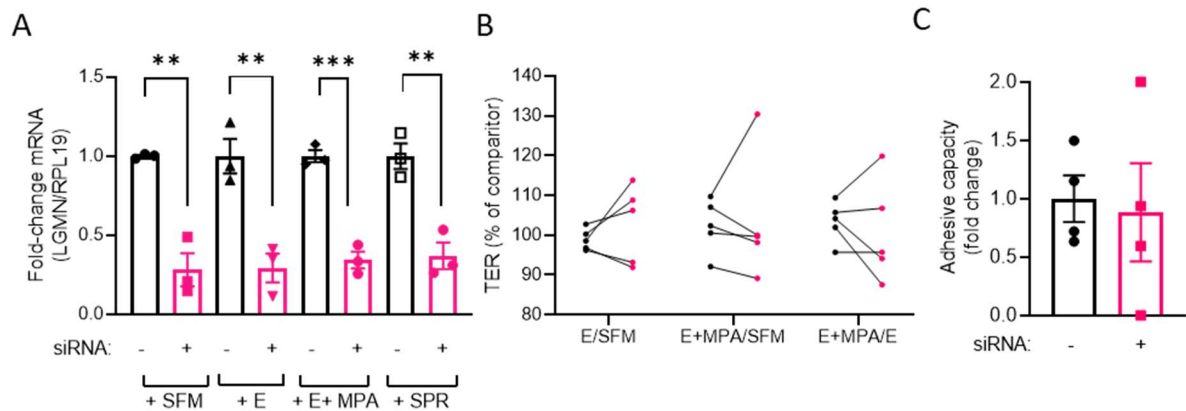


Figure 6.11: siRNA reduction of LGMN does not affect the functions of ECC-1 cells. **A)** LGMN mRNA was significantly reduced in ECC-1 cells throughout hormonal priming compared to scramble siRNA control (black): at the addition of serum free medium (+ SFM; $P < 0.01$), addition of E (+ E; $P < 0.01$), addition of E + MPA (+ E + MPA; $P < 0.001$), and at the time of spheroid addition (+ SPR, $P < 0.01$). All analysed by unpaired t-test. **(B)** In comparison to scramble control (black), siRNA reduction of LGMN (pink) did not affect transepithelial resistance (TER) after hormonal priming with E compared to TER following serum starvation (E/SFM; $P = 0.42$), following priming with E + MPA compared to serum starvation (E+MPA/SFM; $P = 0.89$), or E + MPA compared to TER following E (E+MPA/E; $P = 0.68$). Data connected by lines are from the same experimental replicate, analysed by unpaired-t test. **(C)** LGMN reduction did not significantly reduce the adhesive capacity of ECC-1 cells ($P = 0.81$). Individual points represent independent replicates. Data presented as mean \pm SEM, derived from $n = 3-5$ biologically independent replicates.

6.3.2.3 Stem-Loop-Interacting RNA-binding protein

SLIRP was elevated by a factor of 4.7×10^4 (LFQ value) in receptive epithelial cultures compared to non-receptive, but downregulated by a factor of 3.2×10^{-5} (LFQ value) in the human adhesome (adhesive co-cultures vs all non-adhesive conditions). It was chosen specifically for validation and functional interrogation as it sits at the hub of several previously experimentally determined interactions with other members of the adhesome and receptome as identified by STRING analysis (Appendix 3).

SLIRP is a predominantly mitochondrial protein which regulates protein synthesis and is implicated in male infertility. In both mouse and human, SLIRP impacts the motility of sperm (Colley et al., 2013; Shan et al., 2020). SLIRP binds to RNA, and prevents the activation of specific nuclear receptors, including the Estrogen Receptor α (Hatchell et al., 2006). Within the endometrium it is plausible that SLIRP may contribute to the regulation of hormonal response in the acquisition of endometrial receptivity.

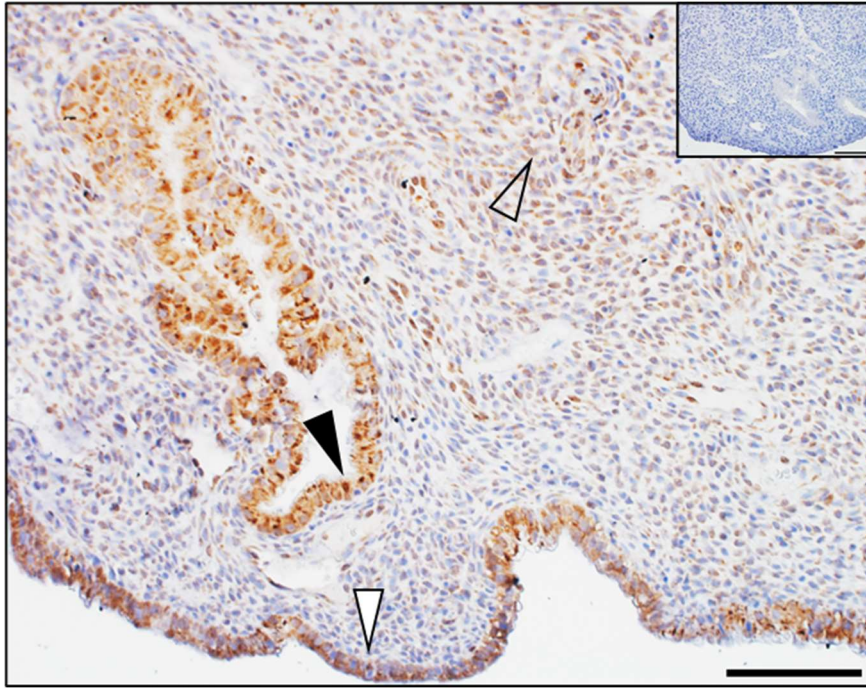


Figure 6.12: SLIRP immunolocalisation in the early-secretory human endometrium. SLIRP was immunolocalised to the glandular (black arrow), and luminal epithelium (white arrow). SLIRP was identified through the stromal compartment (open arrow). Representative image shown, scale bar represents 100 μm . Isotype control inset.

SLIRP has been immunolocalised in the human endometrium and is evident in both the stroma and the epithelium of proliferative, early-secretory, and mid-secretory endometrium of fertile and infertile women. SLIRP appeared predominantly cytoplasmic in the epithelium, with a wash of staining along with specific intracellular staining in some cells evident in the stroma. Some nuclear staining was observed in stromal fibroblasts and in the epithelium. There was no obvious difference in staining localisation between menstrual cycle phases or fertility. A representative image is shown in Figure 6.12, taken from an infertile, early-secretory sample.

Immunostaining of SLIRP was performed by a DEV3990 student, Emily Liang, under my instruction. The quantification and analysis have been reperformed here. SLIRP expression was not significantly altered in the mid-secretory endometrium compared to proliferative ($P = 0.43$ epithelial, $P = 0.64$ non-epithelial; Figure 6.11 A), between the infertile mid-secretory endometrium compared to fertile ($P = 0.20$ epithelial; $P = 0.12$ non-epithelial; Figure 6.13 B) and between the infertile early-secretory endometrium in comparison to fertile ($P = 0.61$ epithelial, $P = 0.22$ non-epithelial; Figure 6.13 C).

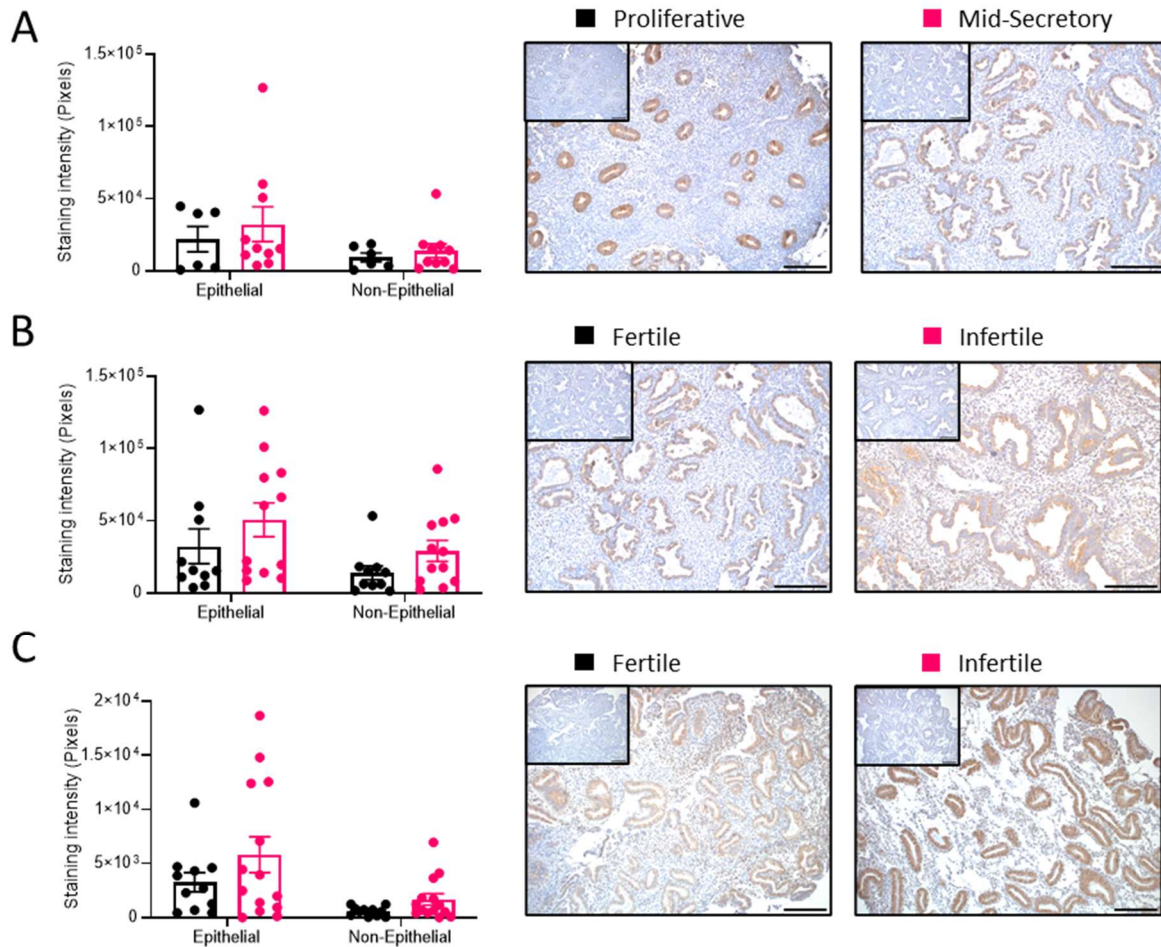


Figure 6.13: Quantification of SLIRP expression in the human endometrium. SLIRP was predominantly detected in the epithelial cells of the human endometrium, with no significant difference in expression of either epithelial or non-epithelial SLIRP between the **(A)** proliferative phase and secretory phase endometrium (Mann-Whitney: $P = 0.4, 0.6$ respectively), or **(B)** between SLIRP in the fertile versus primary infertile mid-secretory endometrium in the epithelial or non-epithelial compartments (Mann-Whitney: $P = 0.2, 0.1$ respectively). **(C)** Within early secretory endometrium, SLIRP expression was not significantly altered between the epithelial or non-epithelial cells of primary infertile endometrium compared to fertile (Mann-Whitney: $P = 0.6, 0.2$ respectively). Representative images shown, isotype control inset, scale bars represent $200 \mu\text{m}$. Individual data points represent biologically independent samples ($n \geq 6$ for each). Data expressed as mean \pm SEM.

In knockdown experiments, an approximate 80% reduction of SLIRP mRNA in ECC-1 cells was achieved across all time points examined ($P < 0.01$ for all; Figure 6.14 A). No significant morphological differences were observed in the cell cultures following transfection (data not shown). When normalised to TER following serum starvation, SLIRP knockdown significantly reduced TER following E (E/SFM; $P = 0.01$; Figure 6.14 B) and E + MPA (E+MPA/SFM; $P = 0.04$; Figure 6.14 B) in comparison to scramble control. No effect was seen on TER following E + MPA when normalised to TER following E treatment (E+MPA/E; $P = 0.28$; Figure 6.14 B). In addition, there was a significant reduction in the

adhesive capacity of ECC-1 cells following SLIRP reduction ($P = 0.03$; Figure 6.12 C). This implies SLIRP is significant in maintaining these functions in a cell culture model.

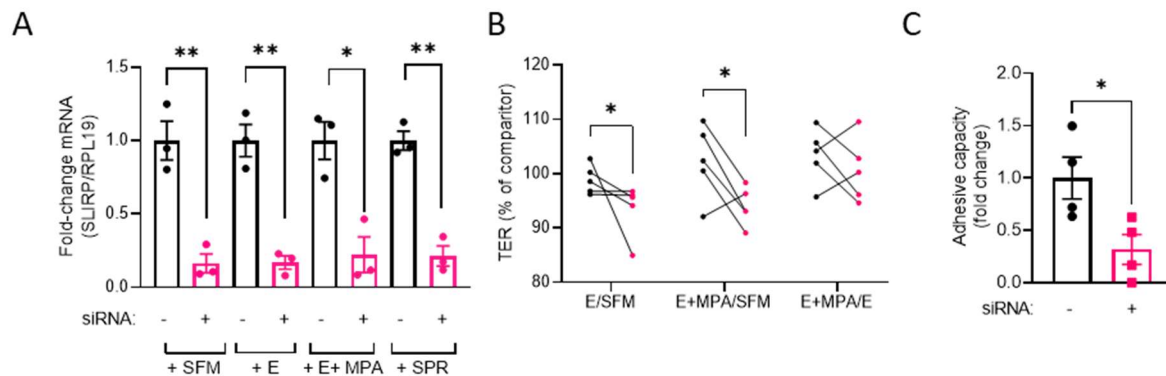


Figure 6.14: siRNA reduction of SLIRP impacts the functions of ECC-1 cells. **A)** SLIRP mRNA was significantly reduced in ECC-1 cells throughout hormonal priming compared to scramble siRNA control: at the addition of serum free medium (+ SFM; $P < 0.01$), addition of E (+ E; $P < 0.01$), addition of E + MPA (+ E + MPA; $P < 0.01$), and at the time of spheroid addition (+ SPR, $P < 0.01$), all analysed by unpaired t-test. **B)** In comparison to scramble control (black), siRNA reduction of SLIRP (pink) significantly reduced transepithelial resistance (TER) after hormonal priming with E compared to TER following serum starvation (E/SFM; Mann-Whitney: $P = 0.01$), and following priming with E + MPA compared to serum starvation (E+MPA/SFM; unpaired t-test: $P = 0.04$), but did not significantly impact TER following E + MPA compared to TER following E (E+MPA/E; unpaired t-test: $P = 0.28$). Data connected by lines are from the same experimental replicate. **C)** SLIRP reduction significantly reduced the adhesive capacity of ECC-1 cells (unpaired t-test: $P = 0.03$). Data presented as mean \pm SEM derived from $n = 3$ -5 biologically independent replicates represented by individual data points.

6.3.3. Independent interrogation of adhesome-specific proteins

The expression of two proteins highly elevated in the human adhesome, PTGS2, and SERPINE1, was investigated in the mid-secretory phase endometrium in a preliminary study to confirm their presence (Figures 6.15, 6.17 respectively).

Prostaglandin G/H Synthase 2 (PTGS2; also known as COX-2) is the most upregulated protein of the adhesome, exhibiting a fold change in LFQ of 3.8×10^5 between adhesion and control conditions. It is not upregulated in the receptome. String analysis reveals no known or predicted interactions of PTGS2 with other proteins upregulated in the adhesome (Appendix 3). PTGS2 is expressed in the mouse endometrium in the luminal epithelium and stroma and is upregulated in the mouse endometrial epithelium in response to an approaching embryo, resulting in the production of prostaglandins required for implantation (Ruan et al., 2012). Functionally it is important for embryo implantation and stromal decidualization in the mouse and human (Han et al., 1996; Lim et al., 1997). Due to its substantial upregulation in the adhesome and its implication as part of the human

implantation factor cascade (Evans et al., 2008), PTGS2 is a promising candidate for validation and functional investigation.

PTGS2 was minimally detected in the epithelial cells of the tissues used in this preliminary study (Figure 6.15), and this was not altered by primary infertility ($P = 0.88$). The non-epithelial staining of PTGS2 was significantly elevated in the infertile endometrium ($P = 0.02$).

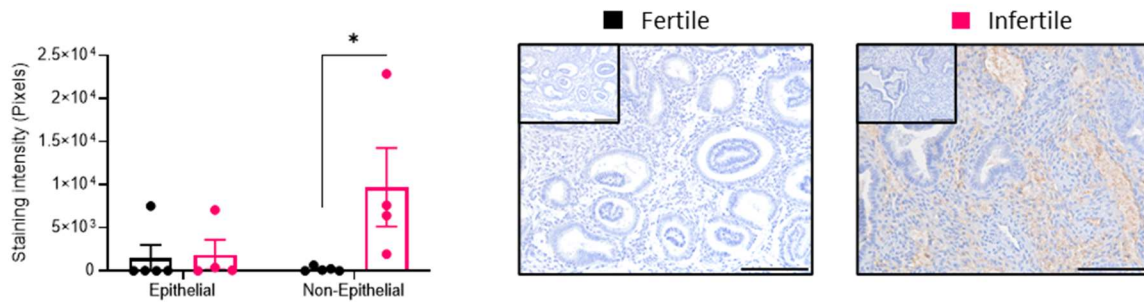


Figure 6.15: PTGS2 is elevated in the infertile mid-secretory endometrium. PTGS2 is elevated in the human endometrium and immunolocalised to the epithelium and stromal cells of the fertile and infertile endometrium. Non-epithelial staining of PTGS2 is significantly higher in the infertile endometrium (Mann-Whitney: $P = 0.02$) but epithelial expression is not altered (unpaired t-test: $P = 0.88$). Scale bars represent 200 μm , isotype controls inset. Individual data points represent biologically independent samples ($n \geq 4$). Data expressed as mean \pm SEM immunostained pixels.

The siRNA reduction of PTGS2 mRNA could not be validated ($P \geq 0.07$ for all; Figure 6.16 A). As above, further optimisation and investigation are beyond the scope of this thesis. While the knockdown was not validated, treatment of ECC-1 cells with siRNA targeted against PTGS2 did not affect TER ($P \geq 0.1$; Figure 6.16 B), or adhesion of trophoctoderm spheroids ($P = 0.15$; Figure 6.16 C). As this is an adhesome protein, knockdown would be required at the time of spheroid adhesion to fully elucidate the effect on adhesive capacity, unlike a receptome protein where changes to the epithelium during hormonal priming may impact the adhesive capacity of the ECC-1 cells. Without a validated knockdown at this time, no clear conclusions can be drawn from this data.

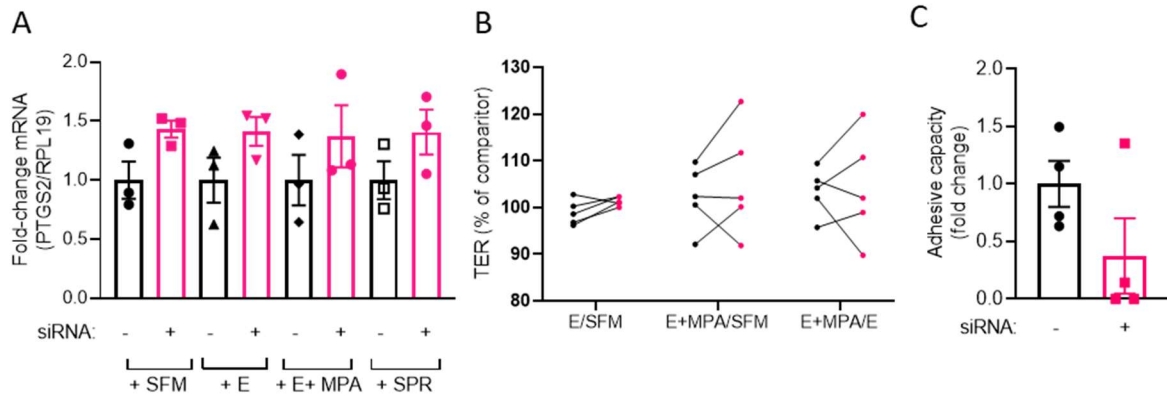


Figure 6.16: siRNA reduction of PTGS2 does not affect the functions of ECC-1 cells. A) The reduction of PTGS2 mRNA was not confirmed compared to scramble siRNA control (black): at the addition of serum free medium (+ SFM; $P = 0.07$), addition of E (+ E; $P = 0.14$), addition of E + MPA (+ E + MPA; $P = 0.34$), and at the time of spheroid addition (+ SPR, $P = 0.18$) all analysed by unpaired t-test. **B)** In comparison to scramble control (black), siRNA reduction of PTGS2 (pink) did not affect transepithelial resistance (TER) after hormonal priming with E compared to TER following serum starvation (E/SFM; $P = 0.09$), following priming with E + MPA compared to serum starvation (E+MPA/SFM; $P = 0.89$), or E + MPA compared to TER following E (E+MPA/E; $P = 0.68$). Data connected by lines are from the same experimental replicate, analysed by unpaired t-test. **C)** PTGS2 reduction did not significantly reduce the adhesive capacity of ECC-1 cells (Mann-Whitney: $P = 0.15$). Individual points represent independent replicates. Data presented as mean \pm SEM, derived from $n = 3$ -5 biologically independent replicates.

Serine protease inhibitor Clade E member 1 (SERPINE1), also known as plasminogen activator inhibitor 1 (PAI-1), is highly upregulated in the adhesome, but not the receptome, showing a fold change in LFQ of 5.9×10^4 between adhesive and non-adhesive conditions. SERPINE1 shows no previously known or predicted interactions with other proteins upregulated in the adhesome (Appendix 3).

Mutations in SERPINE1 have been linked to miscarriage and pregnancy loss (Dossenbach-Glaninger et al., 2008; Magdoud et al., 2013). Transcriptomics of the bovine endometrium suggest that SERPINE1, under the control of Kruppel Like Factor 5, is involved in angiogenesis of the luteal phase bovine endometrium (Bauersachs et al., 2008). As reviewed by Simone et al. (2014), SERPINE1 regulates the proliferation and migration of several cell types, and is especially involved in wound repair. SERPINE1 is activated in response to injury and in any migratory cell or cells undergoing epithelial-mesenchymal transition. Increased expression promotes the migration rather than proliferation of epithelial cells, and overexpression results in reduced cell growth. A further role of SERPINE1 is in the regulation of integrin internalization which is involved in cell detachment from an extracellular matrix. As adhesion and invasion require high levels of proliferation and migration of trophoblast cells, SERPINE1 may regulate this process. Furthermore, invasive implantation can be

considered to “wound” the epithelium, and thus may require SERPINE1-mediated epithelial proliferation and wound repair. These actions of SERPINE1 and its degree of upregulation in the adhesome made this protein a strong candidate for validation and functional assessment.

SERPINE1 was strongly detected in the mid-secretory endometrium (Figure 6.17). Epithelial staining trended towards increased intensity in the infertile endometrium ($P = 0.19$), and non-epithelial staining was significantly higher in the infertile compared to fertile samples ($P = 0.03$).

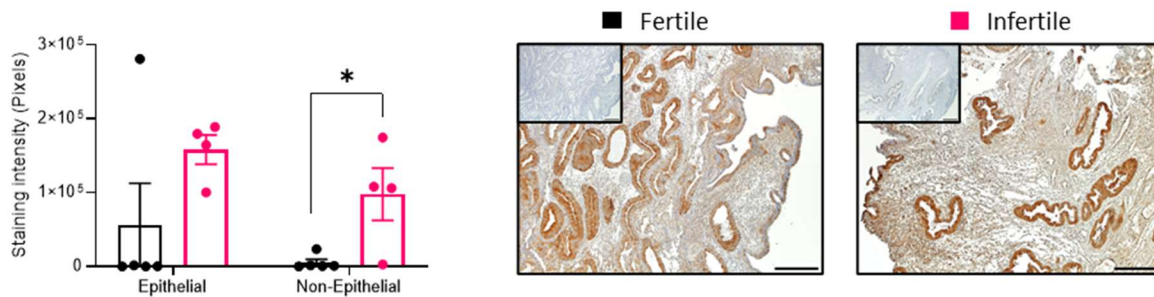


Figure 6.17: SERPINE1 is elevated in the infertile mid-secretory endometrium. PTGS2 is elevated in the human endometrium and immunolocalised to the epithelium and stromal cells of the fertile and infertile endometrium. Non-epithelial staining of both PTGS2 is significantly higher in the infertile endometrium (Mann-Whitney: $P = 0.03$) but epithelial expression is not altered (Mann-Whitney: $P = 0.19$). Scale bars represent 200 μm , isotype controls inset. Individual data points represent biologically independent samples ($n \geq 4$ for each). Data expressed as mean \pm SEM immunostained pixels.

SERPINE1 mRNA was significantly reduced by more than 70% across most timepoints examined; additional replicates would provide further clarity ($P \leq 0.10$ for all; Figure 6.18 A). siRNA knockdown of SERPINE1 in ECC-1 cells did not affect TER (Figure 6.18 B), but significantly lowered the adhesion of trophoctoderm spheroids ($P = 0.04$; Figure 6.18 C). This implies SERPINE1 to be significant in maintaining the adhesive capacity of endometrial epithelial cells, functionally validating its presence in the adhesome.

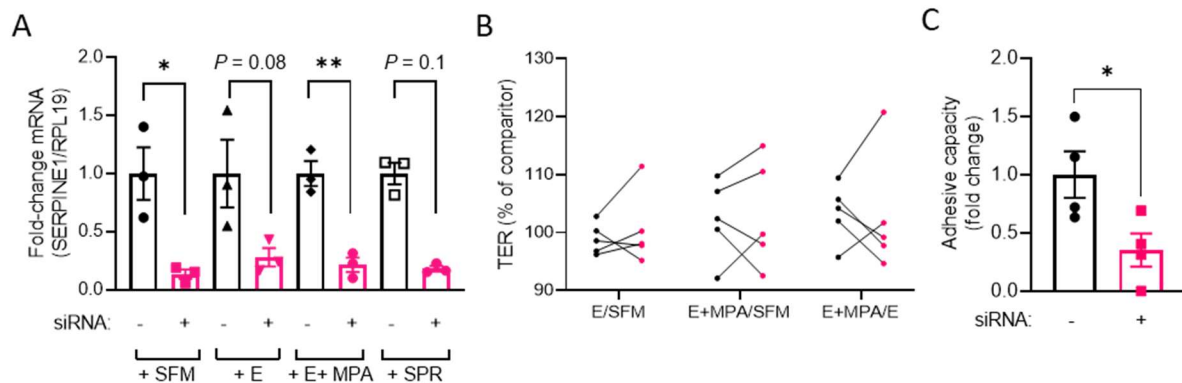


Figure 6.18: siRNA reduction of SERPINE1 affects ECC-1 function. A) SERPINE1 mRNA was reduced in ECC-1 cells at various timepoints throughout hormonal priming compared to scramble siRNA control:

at the addition of serum free medium (+ SFM; unpaired t-test: $P = 0.02$), addition of E (+ E; unpaired t-test: $P = 0.08$), addition of E + MPA (+ E + MPA; unpaired t-test: $P < 0.01$), and at the time of spheroid addition (+ SPR; Mann-Whitney: $P = 0.1$). **B)** In comparison to scramble control (black), siRNA reduction of SERPINE1 (pink) did not affect transepithelial resistance (TER) after hormonal priming with E compared to TER following serum starvation (E/SFM; $P = 0.61$), following priming with E + MPA compared to serum starvation (E+MPA/SFM; $P = 0.88$), or E + MPA compared to TER following E (E+MPA/E; $P = 0.91$). Data connected by lines are from the same experimental replicate, analysed by unpaired t test. **C)** SERPINE1 reduction significantly reduced the adhesive capacity of ECC-1 cells compared to scramble siRNA control (unpaired t-test: $P = 0.04$). Individual points represent independent replicates. Data presented as mean \pm SEM, derived from $n = 3-5$ biologically independent replicates.

6.3.4 Hormonal regulation of receptome and adhesome proteins in ECC-1 cells

RNA was harvested from control ECC-1 cells undergoing siRNA knockdown (exposed to scramble siRNA) across hormonal priming. The expression of receptome and adhesome genes was assessed using qPCR to provide pilot data on hormonal regulation of these genes in ECC-1 cells (Figure 6.19). In comparison to basal conditions, PC4 expression was significantly increased approximately 1.5-fold by application of E ($P = 0.02$; Figure 6.19 A), this was not maintained with addition of MPA ($P = 0.54$). PTGS2 was significantly elevated by application of hormones compared to basal and starved conditions ($P < 0.001$; Figure 6.19 E). No effect of hormonal priming was observed on any other gene investigated. One outlier was removed from the analysis of STMN1, and as such no statistical analysis was performed on the resultant data.

It must be taken into account that the primers utilised for PTGS2 and STMN1 gene expression analysis were unable to validate the siRNA knockdown, and may not give an accurate reflection of the hormonal regulation of these genes. Further investigation with primers of a greater specificity or efficiency is required.

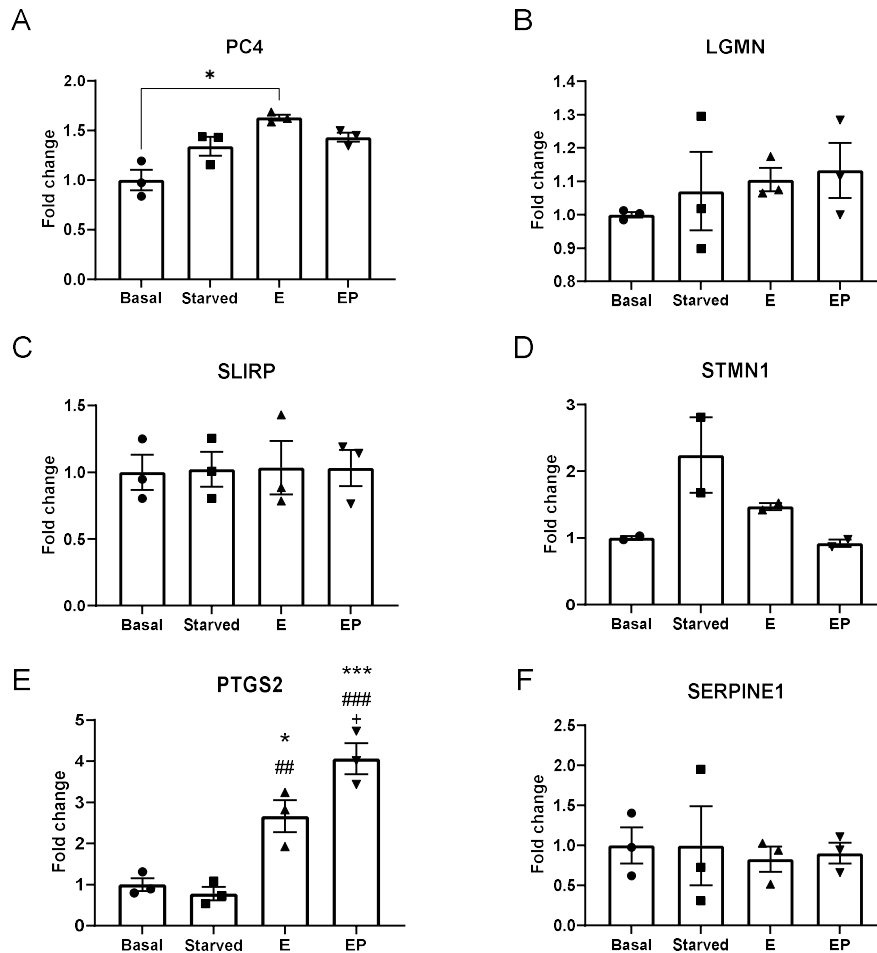


Figure 6.19: Hormonal regulation of receptome and adhesome genes in ECC-1. RNA was collected from ECC-1 cells before and after serum starvation (basal, starved), after treatment with E (E), and after treatment with E + MPA (EP). Fold change of mRNA, normalised to RPL19, was determined for each group compared to basal. Treatment with E significantly increased the expression of PC4 in ECC-1 cells compared to basal levels (A; $P = 0.02$). This was not maintained by treatment with E + MPA (EP, $P = 0.5$). PTGS2 (E) was significantly elevated following treatment with E compared to basal and starved conditions ($P = 0.02$, < 0.01 respectively), and elevated by E + MPA compared to all other conditions ($P < 0.001$ vs basal and starved, $P = 0.04$ compared to E). No effect of hormonal treatment was observed on LGMN (B; $P = 0.60$), SLIRP (C; $P > 0.99$), or SERPINE1 (F; $P = 0.97$). As $n=2$ were available for STMN1 (D), no statistics were performed. Kruskal-Wallis (A)/One-way ANOVA (B, C, E, F): *, ** $P < 0.05 < 0.001$ versus basal; ### $P < 0.001$ versus starved; + $P < 0.05$ versus E. $N=2-3$ biologically independent replicates, denoted by individual data points.

6.3.5 Receptome and adhesome proteins in human endometrial epithelial organoids

As ECC-1 cells did not show the anticipated hormonal regulation of receptome and adhesome proteins, nor did cell culture experiments provide clear results of receptome and adhesome protein functions, I turned to hEEO as a more physiological model. To investigate these proteins in hEEO, I further analysed available scRNA-seq data (Fitzgerald et al., 2019). For each protein investigated in this chapter, corresponding gene expression was detected in at least one condition. The Log fold-

change of FPKM (fragment reads per kilobase transcript per million mapped reads: indicates relative gene expression), and false discovery rate P -value, as determined by a bioinformatician, is provided in Table 6.2. As the log fold-change was inversely representative of regulation, I assessed the FPKM where data was available for a visual representation of regulation (Figure 6.20). No data available indicates that a gene was not differentially regulated between conditions, and not necessarily an absence of expression.

Table 6.2: Log fold change of genes of interest in hormonally treated hEEO as determined by scRNAseq analysis. The log fold change (LogFC) in expression and false discovery rate P value (FDR) were determined by bioinformatics and published in Fitzgerald *et al.* (2019). Note: a negative LogFC is representative of an increase in gene expression. (-) No data available. Performed in technical triplicate, $n = 1$. C, control untreated, E, estrogen treatment; EP estrogen/progesterone, EPC EP+cAMP

| Gene | E vs C | | EP vs C | | EPC vs C | | EPC vs EP | |
|----------|--------|------------------------|---------|------------------------|----------|------------------------|-----------|-----------------------|
| | LogFC | FDR | LogFC | FDR | LogFC | FDR | LogFC | FDR |
| PC4 | -0.22 | 0.17 | - | - | 0.33 | 6×10^{-3} | - | - |
| KYNU | -0.94 | 1.7×10^{-13} | -1.71 | 1.1×10^{-37} | -3.86 | 7.3×10^{-231} | -2.16 | 1.4×10^{-55} |
| LGMN | 0.62 | 5.9×10^{-8} | - | - | - | - | - | - |
| STMN1 | 0.48 | 9.6×10^{-4} | - | - | 2.56 | 6.9×10^{-103} | 0.67 | 1.6×10^{-07} |
| CDA | -1.71 | 1.7×10^{-13} | -3.2 | 2.3×10^{-41} | -4.03 | 7.2×10^{-96} | -0.81 | 1.0×10^{-04} |
| SLIRP | 0.07 | 0.74 | - | - | 0.48 | 1.7×10^{-04} | - | - |
| PTGS2 | -5.52 | 5.7×10^{-270} | -6.33 | 3.1×10^{-144} | -9.00 | 0.00 | -2.68 | 8.3×10^{-25} |
| SERPINE1 | -3.41 | 1.4×10^{-31} | - | - | - | - | - | - |

PC4 (listed as SUB1 in the dataset) was differentially expressed in hEEO treated with hormones (E, EP, EPC; Section 6.2.5) compared to vehicle control (C), reflected in the log fold change values (Table 6.2) and FPKM values (Figure 6.20). PC4 FPKM was non-significantly elevated by application of E ($P = 0.053$) in comparison to vehicle control. Treatment of hEEO with EPC significantly reduced the expression of PC4 ($P < 0.01$). FPKM data was not available for the comparison of EP compared to control and EPC compared to EP.

KYNU was differentially expressed in hormonally primed hEEO compared to vehicle control (Table 6.2, Figure 6.20). The FPKM of KYNU was increased by the application of E ($P < 0.01$), EP ($P < 0.01$), and EPC ($P < 0.0001$) in comparison to vehicle control. EPC further elevated the expression of KYNU in comparison to treatment with EP alone ($P < 0.0001$).

LGMN expression (LogFC and FPKM; Table 6.2, Figure 6.20) was significantly reduced by the application of E ($P < 0.0001$). No data was available for the other conditions.

CDA expression (LogFC and FPKM; Table 6.2, Figure 6.20) was increased by application of E ($P < 0.001$), EP ($P < 0.01$), and EPC ($P < 0.001$). EPC further increased the expression of CDA compared to treatment with EP. While not consistently detected in the endometrial epithelium (Figure 6.15), CDA may be expressed within the epithelium during *in vitro* culture, thus being detected in these hEEO.

The FPKM of STMN1 (protein unable to be detected by immunohistochemistry) trended to reduction by all hormones applied: E and EPC vs control, and EPC vs EP (all $P = 0.10$). LogFC available in Table 6.2. No data was available for the application of EP vs control.

PTGS2 expression (LogFC and FPKM; Table 6.2, Figure 6.20) was significantly increased by E ($P < 0.0001$), EP ($P < 0.0001$), and EPC ($P < 0.0001$) compared to vehicle control. EPC increased the expression of PTGS2 in comparison to EP alone ($P < 0.0001$).

SERPINE1 expression (LogFC and FPKM; Table 6.2, Figure 6.19) was increased by E in comparison to control conditions ($P < 0.01$). No data was available for other conditions.

In summary, this data demonstrates that a number of receptome and adhesome genes are expressed in hEEO, providing a primary culture model more appropriate than ECC-1 cells to validate and interrogate these proteins and determine their functions. Their hormonal regulation gives further credence to these genes being differentially expressed across the menstrual cycle, and their likely involvement in the regulation of endometrial receptivity.

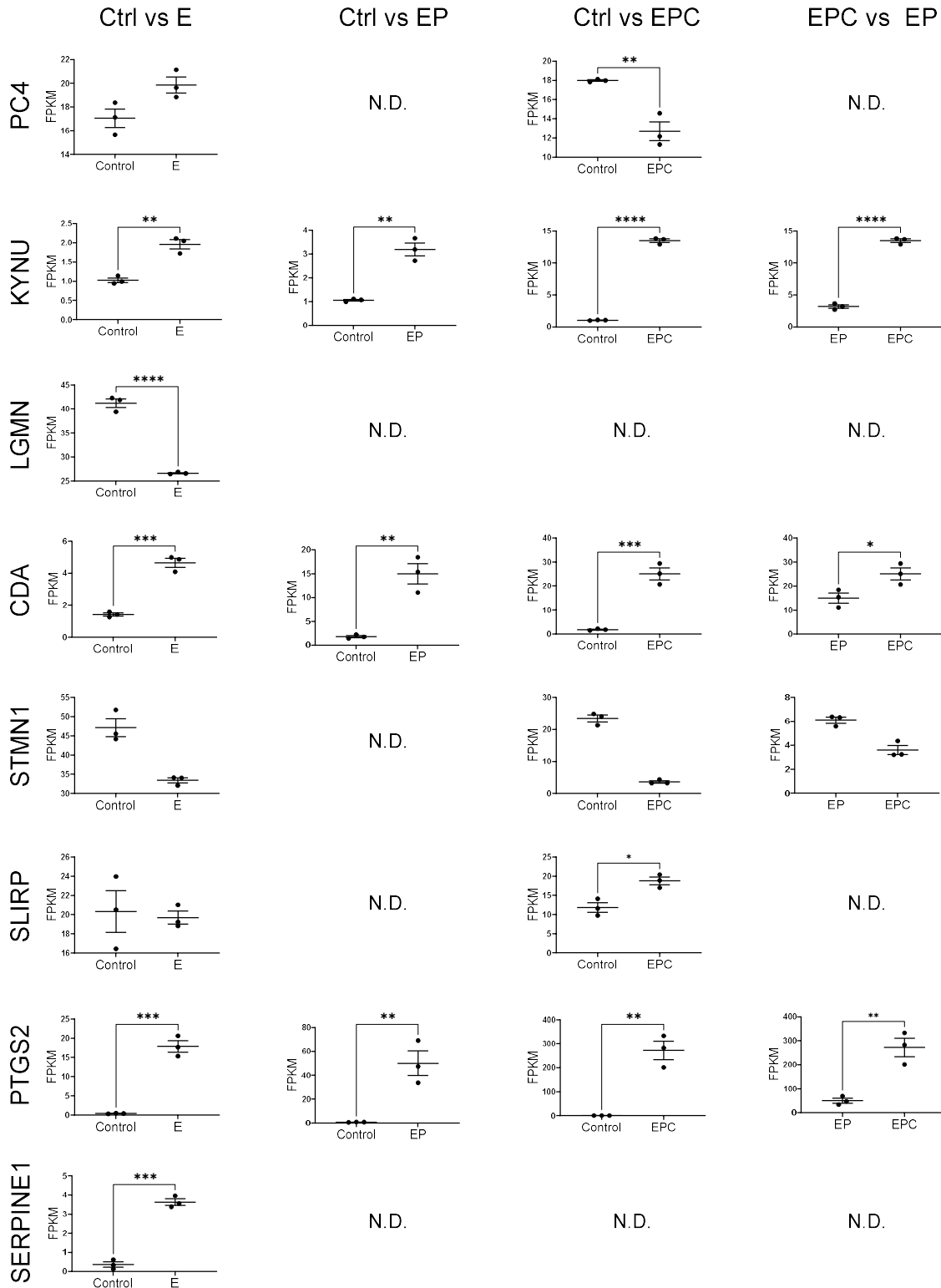


Figure 6.20: Expression of receptome and adhesome genes are hormonally regulated in hEEO. Hormonal priming alters the expression of receptome and adhesome genes in hEEO as determined by scRNAseq (Fitzgerald et al., 2019). C: control; E: primed with E; EP: primed with E + MPA; EPC: Primed with E + MPA + cAMP. Data expressed as mean \pm SEM FPKM derived from n=1 hEEO technical triplicate. N.D.: no data available. Unpaired t-test: * $P < 0.05$; ** $P < 0.01$; *** $P < 0.001$; **** $P < 0.0001$.

6.4 Discussion and conclusions

Previous proteomic analyses of the human endometrial epithelial receptome and embryo-endometrium adhesome defined novel protein biomarkers of human endometrial receptivity and embryo adhesion (Evans et al., 2020a): validation of some individual proteins (my preliminary studies), used qualitative immunohistochemistry on mid-secretory endometrial sections (encompassing the “window of implantation”). In an extension of this work, I have here quantified the expression of 8 individual receptome and adhesome proteins and interrogated their functions: results are summarised in Table 6.3. Of these proteins, PC4 was validated to some extent by immunohistochemistry, while siRNA knockdown indicated SLIRP, STMN1 and SERPINE1 as functional players in endometrial receptivity and embryo adhesion.

Initial proteomic analysis was performed using a human embryo-endometrial adhesion model: a 2D cell culture of primary endometrial epithelial cells in conjunction with embryo “mimics” (trophectodermal cell line formed into spheroids). Interrogation generated a potential receptome (epithelium alone) and adhesome (adhesive co-culture). With the very high resolution of proteomic and large scale bioinformatic data-sets, comes an increased challenge in validation to tease out functions of individual or linked moieties. These issues include: selection of tissues or cells to interrogate; identifying the most significant components for individual investigation while avoiding the red-herrings; and utilising appropriate methods to demonstrate functional effects.

Validation was performed on endometrial tissue sections, and in some cases, immunostaining was evident in both epithelium and stroma. Quantification was predominantly of staining intensity in glandular epithelium, as the luminal epithelium is a delicate structure often lost during tissue processing for histology and thus not present in all tissue sections. However, in the majority of samples in which luminal and glandular epithelium were present, staining was noted at a similar intensity. Given that the original co-culture model typically discriminates between fertile and infertile women under conditions representative of the ‘receptive’ mid-secretory phase (Evans et al., 2020b) it is not surprising that significant differences in immunostaining were typically observed between fertile and infertile tissue of the same phase, rather than as changes across the menstrual cycle. Furthermore, for ‘adhesome’ proteins, appropriate validation would require the presence of an embryo in the model and regrettably sections through the spheroid-epithelial cell interface were not available for interrogation (Section 2.6.1.1).

Table 6.3: Summary of results. The immunolocalisation of 8 receptome and adhesome proteins, their regulation within the endometrium, functional effects of siRNA knockdown, and hormonal regulation

in *in vitro* epithelial cells are summarised. (-) Neither up- or down-regulated; N/A: data not available; ns: no significance in any group; *, **, *** $P < 0.05, 0.01, 0.001$ respectively.

| Protein | Receptome | Adhesome | MS vs P | MS Fertile vs infertile | ES Fertile vs infertile | Knockdown validated? | SPR Adhesion | TER | Hormonal regulation ECC-1 | Hormonal regulation hEEO |
|----------|-----------|----------|----------------------------------|---|---|----------------------|--------------|-------|---------------------------|--------------------------|
| PC4 | ↑ | - | P = 0.34 (Epithelial) $n \geq 8$ | ↓ Primary infertile epithelium (P = 0.054) $n \geq 8$ | ↓ Primary infertile non-epithelial components (*) $n \geq 12$ | ✓ | P = 0.85 | N/A | ↑E (*) | Y |
| KYNU | ↑ | ↑ | P = 0.7 (Epithelial) $n \geq 7$ | (P = 0.09) $n \geq 7$ | N/A | ✗ | P = 0.17 | ns | N/A | Y |
| LGMN | ↑ | ↑ | P = 0.4 (Epithelial) $n \geq 6$ | P = 0.1 (Epithelial) $n \geq 7$ | P = 0.4 (Epithelial and non-epithelial) $n \geq 4$ | ✓ | P = 0.81 | ns | P = 0.60 | Y |
| SLIRP | ↑ | ↓ | P = 0.4 (Epithelial) $n \geq 6$ | P = 0.2 (Epithelial) $n \geq 10$ | P = 0.6 (Epithelial) $n \geq 11$ | ✓ | ↓ (*) | ↓ (*) | P > 0.99 | Y |
| STMN1 | ↑ | - | Unable to optimise IHC | Unable to optimise IHC | Unable to optimise IHC | ✗ | ↓ (*) | ns | n = 2 | Y |
| SERPINE1 | - | ↑ | N/A | ↑ Primary non-infertile epithelial (*) $n \geq 4$ | N/A | ✓ | ↓ (*) | ns | P = 0.97 | Y |
| PTGS2 | - | ↑ | N/A | ↑ Primary non-infertile epithelial (*) $n \geq 4$ | N/A | ✗ | P = 0.15 | ns | ↑E (*/*/**) ↑EP (*) | Y |
| CDA | ↑ | - | Very limited epithelial staining | Almost exclusively non-epithelial | Almost exclusively non-epithelial | N/A | N/A | N/A | N/A | Y |

Unpredictable outliers, as seen within the data, may arise from variability in menstrual cycle length, and from the difficulties in accurate endometrial biopsy dating (Alfer et al., 2020; Díaz-Gimeno et al., 2013; Murray et al., 2004). The samples used herein were dated by classical Noyes criteria (Noyes et al., 1950). Accuracy of dating is improved when sampling follows detection of the LH surge – this is not available in our laboratory. In relation to the obesity focus of this thesis, while BMI did not differ between the groups of donors examined, specific collections from lean or obese women would identify any impact of obesity and potential exposure to elevated AGEs, on significant proteins.

Within the mid-secretory phase of the menstrual cycle, 3 of 8 specific receptome and adhesome proteins were differentially expressed in the fertile and infertile endometrium, namely PC4 (Figure 6.2), PTGS2, and SERPINE1 (Figures 6.15, 6.17). PC4 was reduced in infertile mid-secretory epithelium and significantly lowered in the non-epithelial components of the infertile early-secretory endometrium, indicating a contribution to the infertile phenotype. Given the complex role of this protein in the regulation of gene transcription, DNA repair, and cellular growth (Conesa and Acker, 2010), dysregulation within the infertile endometrium is likely to have widespread effects.

Immunoreactive PTGS2 was low in both fertile and infertile mid-secretory endometrial epithelium but given its identification as an adhesome protein, with modulation by the trophoctoderm spheroid or its secretions, comprehensive validation would require the use of spheroid-epithelium interface sections for immunohistochemistry (Section 2.6.1.1). Additionally, for both the upregulated adhesome proteins PTGS2 and SERPINE1, primary infertility was associated with increased expression within the stromal compartment (Figure 6.15, 6.17). It has been proposed that the stromal compartment can act as a sensor for the quality of an approaching embryo (Brosens et al., 2014; Macklon and Brosens, 2014; Teklenburg et al., 2010), and dysregulation of adhesome proteins may hinder the ability of the endometrium to identify a quality embryo. Alternatively, the involvement of PTGS2 in stromal cell decidualisation (Han et al., 1996; Lim et al., 1997) may result in aberrant decidualisation of the ‘infertile’ stromal fibroblasts, providing an inappropriate environment for embryo implantation. As these adhesome proteins are modulated by the interaction of trophoctodermal cells with the epithelium, it is possible that they may be subsequently regulated in the stromal compartment by the trophoblast once it has traversed the epithelium.

Regulation of gene expression of the selected proteins by estrogen and progesterone was also investigated in both hormonally primed ECC-1 cells and hEEO. Only PTGS2 and PC4 were hormonally modulated in ECC-1 cells (Figure 6.19) but within hEEO, all investigated genes were significantly modulated by estrogen, progesterone, and cAMP (Table 6.2, Figure 6.20; Fitzgerald et al., 2019) strengthening the case for use of primary cells. Furthermore, there is commonly a difference between

the genomic and the proteomic landscape due to a disconnect between transcription and translation. STMN1 gene expression trended towards reduction by all hormones in this study (Table 6.2, Figure 6.20), reflecting the protein data of Dominguez et al. (2009) who identified STMN1 in intact endometrium, rather than in purified epithelial cells *in vitro* (i.e. the receptome); the growth factors present in organoid expansion medium may regulate STMN1 expression in a manner more reflective of the *in vivo* endometrial environment.

The expression patterns of PC4, SLIRP, and PTGS2, with respect to the menstrual cycle and fertility status are presented in Figure 6.21.

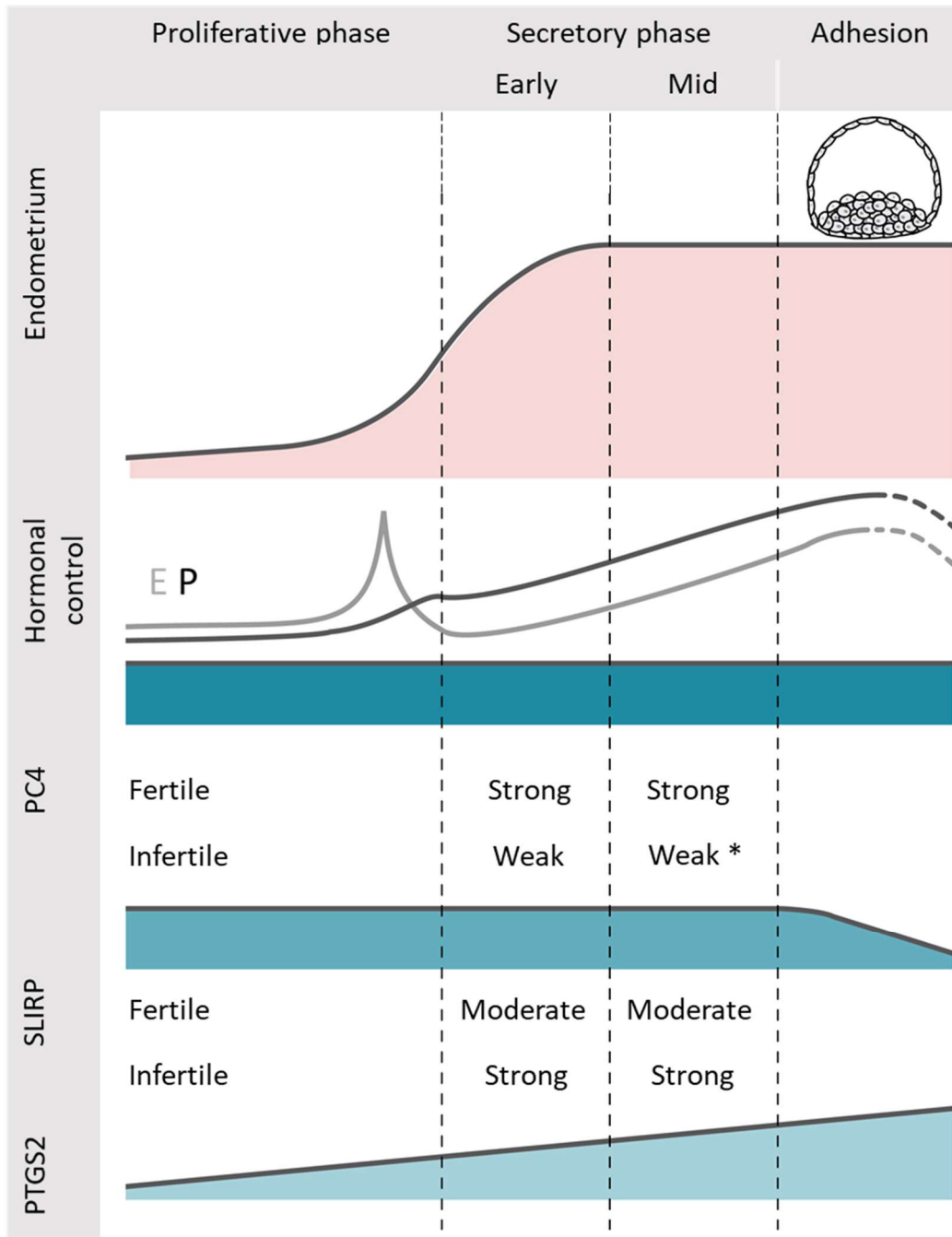


Figure 6.21: Conceptual contribution of receptome proteins to the regulation of endometrial receptivity. SLIRP and PC4 protein levels are not modulated across the menstrual cycle (solid blue bars indicate expression), but is impacted by fertility status. PC4 is a transcriptional regulator more weakly immunolocalised in the infertile endometrium. SLIRP influences the activation of the estrogen receptor α and is somewhat increased by infertility: too much SLIRP may result in deficient response to estrogen including progesterone receptor expression. SLIRP is downregulated in the adhesome (upon embryo adhesion). Together these proteins may regulate other proteins in the receptome and adhesome, such as PTGS2, which is upregulated by Estrogen (E) and progesterone (P), and spheroid adhesion. *: statistically significant difference. Figure generated by David Young, used with permission.

Use of siRNA knockdown to target specific receptome and adhesome proteins revealed that SLIRP, STMN1, and SERPINE1 were significant in modulating functional markers of endometrial receptivity: transepithelial resistance (TER) and adhesion of trophoblast spheroids. The reduction in spheroid adhesion to siRNA-treated ECC-1 for SLIRP, STMN1, and SERPINE1 validates the functions of these proteins in this model. Since siRNA knockdown does not fully delete the protein, future work could focus on complete protein knock-out through genetic manipulation such as CRISPR technologies, to generate knock-out cell lines or to modulate the expression of these proteins in hEEO.

SLIRP was identified within the receptome and adhesome, and was not significantly altered in the endometrium by cycle phase or fertility status (Figure 6.13), but siRNA reduction demonstrated a likely functional role of this protein in maintaining epithelial tight junction integrity (Figure 6.14 B). Physiologically, reduction of this protein at the moment of spheroid or embryo adhesion may enable relaxation of tight junctions facilitating invasive implantation. SLIRP in the receptive endometrial epithelium may help maintain the barrier function of the luminal epithelium prior to adhesion, with its specific reduction at the site of adhesion allowing relaxation of epithelial cell-cell contacts and polarity necessary for implantation. As one function of SLIRP is in repressing estrogen receptor α transactivation (Hatchell et al., 2006), whether ER α action assists in maintaining tight junctions could be examined. Estrogen directly impacts the polarity marker Scribble (Jin et al., 2020), and hormonal priming of ECC-1 reduces their polarity and tight junction integrity (Whitby et al., 2018). Whether SLIRP can indirectly regulate markers of polarity such as Crumbs and Stardust is an avenue for further examination (Whitby et al., 2018). SLIRP is upregulated in receptive endometrial epithelial cells (receptome), and its reduction throughout hormonal priming may have impacted other aspects of receptivity in ECC-1 cells (Figure 6.14 C), hence the reduction in adhesion of trophoblast cells. Further, embryonic secretions may impact the expression of SLIRP at the maternal-fetal interface, orchestrating localised hormonal response. The hypothetical actions of SLIRP in this context are summarised in Figure 6.22. Conversely, while its protein was significantly reduced in the infertile endometrium (Figure 6.2), PC4 knockdown did not impact ECC-1 function (Figure 6.3), indicating potential redundancy or compensatory mechanisms for this protein: an endometrial backup plan for acquiring receptivity. Indeed it is well accepted that redundancy is particularly common in reproductive tissues (Luu et al., 2004).

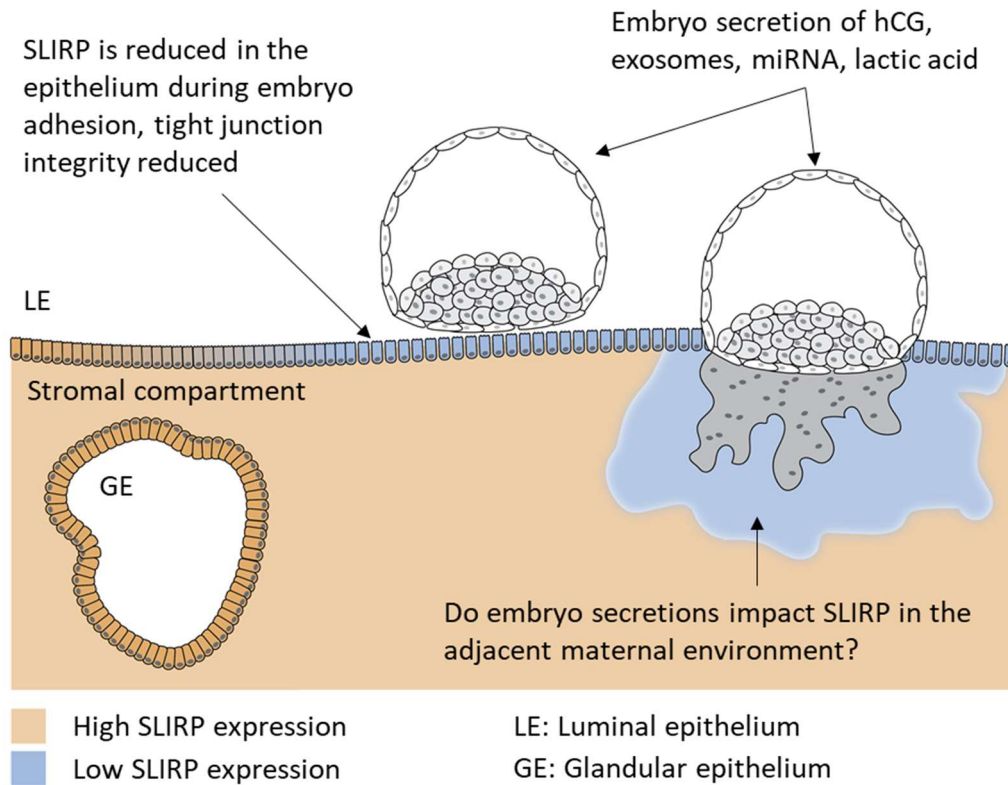


Figure 6.22: Hypothetical actions of SLIRP in embryo adhesion and implantation. SLIRP is a nuclear receptor co-repressor, and is reduced in epithelial cells upon adhesion of trophoblast (embryo mimic, adhesome). The reduction of SLIRP at the maternal-fetal interface relaxes tight junctions, potentially through estrogen-mediated mechanisms which support embryo implantation. SLIRP expression adjacent to the implantation site may provide localised hormone responsiveness and direct an active zone of endometrial receptivity. The role of embryo derived factors on SLIRP expression will provide additional information on the regulation of the maternal-fetal interface. Figure generated by David Young, used with permission.

6.4.1 How physiological is the spheroid adhesion model?

The model used to define the adhesome and receptome provides a clear picture of trophoblast-epithelial interactions using purified cell populations, and discriminates between fertile and infertile women (Evans et al., 2020b). However, this relies on the base assumption that the epithelium and embryo trophoblast form a physical attachment *in vivo*. Mechanisms of embryo implantation differ significantly between species: in contrast to the mouse embryo which induces entosis of luminal epithelial cells enabling invasion into the stroma (Li et al., 2016), it is plausible that the embryo may attach to the glycocalyx and invade around epithelial cells (Bentin-Ley et al., 2000). Presumably there must be at least transient attachment with the embryo tethered to the epithelium, with the ICM apposed to the epithelium in the human, or away from the epithelium in the mouse (Zhang et al., 2014). Whether direct cell-cell contact is made between the embryo and the apical surface of the luminal epithelium is unclear (Aplin and Kimber, 2004; Aplin and Ruane, 2017; Lopata, 1996), and very

few models exist that do not include cancer cell lines or differentiated trophoblast. Remodelling of the glycocalyx, including local reduction of MUC1 cleavage of the glycoprotein dystroglycan—necessary for BeWo trophoblast spheroid adhesion—may not result in cell junction formation between the embryo and the epithelium (Heng et al., 2015; Meseguer et al., 2001). Lopata (1996) argues that such remodelling allows proximity of trophoderm and epithelial membranes such that trophoderm protrusions can invade through the epithelium and provide stability to the maternal-fetal interface. Indeed, in ruminants, the trophoblast develops finger-like villi, inserted into the gland openings to anchor the conceptus (Guillomot et al., 1981). In support of this, gene ontology terms including focal adhesion and cell-cell adherens junctions, are enriched in receptive epithelial cells (the receptome), but while focal adhesion is enriched in the adhesome, cell-cell adhesion and adherens junctions are downregulated.

Conversely, does a non-receptive interaction between the endometrium and embryo mean that no adhesion occurs? It is unknown how the fluid dynamics of the uterine histotroph govern the location of the embryo, and whether the blastocyst will be in proximity to the endometrial epithelium in every conception cycle. The adhesome used here, was generated based on adhesion of spheroids—possibly determined by underlying fertility. Within the milieu of maternal-fetal cross talk, there are several potential mechanisms for non-receptive interactions: 1) The blastocyst secretions are insufficient to inform the endometrium that adhesive interaction is to take place (poor quality embryo), and anti-adhesive molecules such as Mucin 1 are not downregulated (Meseguer et al., 2001); 2) the endometrium is unable to respond to autocrine and paracrine cues to provide an adhesive surface (endometrial non-receptivity); and 3) early adhesion and preliminary invasion occurs with very early pregnancy loss. There is evidence that up to 22% of pregnancies spontaneously end before clinical detection (Wilcox et al., 1988), and that embryos which implant after the presumed window of implantation are highly likely to miscarry: 82% of embryos that implant after 11 days following ovulation resulted in miscarriage in less than 6 weeks (Wilcox et al., 1999). Thus, it is possible in a non-receptive cycle, for an implanting conceptus to be lost at the onset of next menses without maternal recognition of pregnancy, rather than a complete absence of interaction occurring.

Specific aspects of the model used must also be considered in its physiological relevance and translational potential. Namely, how closely does the trophoderm spheroid resemble a blastocyst? In gross morphology, the two entities are significantly different: although of similar size (0.1-0.2 mm (Evans et al., 2020b)), the spheroid is a dense ball of 2500 trophoderm cells, whereas the human embryo contains approximately 170 cells of two distinct lineages, the size being generated by a fluid filled blastocoel (Hardy et al., 1989). On a molecular level, the human blastocyst is a highly metabolic and secretory entity, generating a highly acidic microenvironment which is proposed to influence the

maternal environment and interactions (Gardner, 2015): blastocyst-derived lactic acid induces the release of ATP from luminal epithelial cells and can initiate stromal cell decidualisation, mediating interactions between the blastocyst and endometrium (Gu et al., 2020). Further, metabolism is highly correlated to embryo quality and implantation success (Ferrick et al., 2020), and the secretion of hCG from the blastocyst directs maternal recognition of pregnancy. In addition, the production of exosomes from the embryo contribute to maternal-fetal cross talk (Giacomini et al., 2017). The metabolism, lactic acid production, and hCG secretion of trophoblast spheroids is unknown. Work in this laboratory has recovered functional extracellular vesicles from spheroid-conditioned media (unpublished data), though it has not been possible to compare their cargo to that of vesicles from human embryos. In complementary studies, the human endometrium releases embryo-modulating extracellular vesicles (Blázquez et al., 2018; Gurung et al., 2020) that can be taken up by and modify trophoblast cells (Gurung et al., 2020). In the human blastocyst, communication between the ICM and the trophoblast may regulate trophoblast-endometrium interactions, potentially through extracellular vesicles (B. Simon et al., 2020). The spheroids used here do not contain a blastocoel, unlike some models (Lee et al., 2015). Future work will determine the similarities in secretions and maternal-fetal cross talk between trophoblast spheroids and embryos.

Even considering these substantial differences between a spheroid and a blastocyst, the benefits of these trophoblast spheroids as a proxy are significant. The trophoblast cells in this study are less differentiated than other cell lines (i.e. BeWo, HTR8/SVneo), they actively secrete extracellular vesicles into their surrounding environment, and were used adherent to primary, rather than carcinoma epithelial cells, to define the adhesome and receptome. The discrimination of this adhesion between fertile and infertile parent tissue implies that these spheroids respond to unique maternal cues.

6.4.2 Translational impact and future directions

This validation of specific receptome proteins as modulated by infertility and of functional importance in adhesion of trophoblast spheroids provides a foundation for future research. In the context of other work presented in this thesis, it provides molecular targets for examination of the effects of obesity-related AGEs on endometrial receptivity. If affected, therapeutics could be applied to normalise relative expressions of these proteins. Importantly, while this study has focussed on the endometrium, the relative contribution of the trophoblast to the proteomic adhesome remains to be examined, along with the functional effects of the proteins on trophoblast.

A variety of avenues exist for the translation of this data. The relative expression of specific receptome proteins within the endometrium of women undergoing ART could be assayed to determine if particular treatment courses are impacting the molecular receptivity of the endometrium

and as such advance personalised reproductive medicine. Conversely, these proteins could be targeted in novel contraceptive strategies to retain the endometrium in a non-receptive state, such as using antisense oligonucleotides or specific protein inhibitors, including non-steroidal anti-inflammatory drugs which target PTGS2.

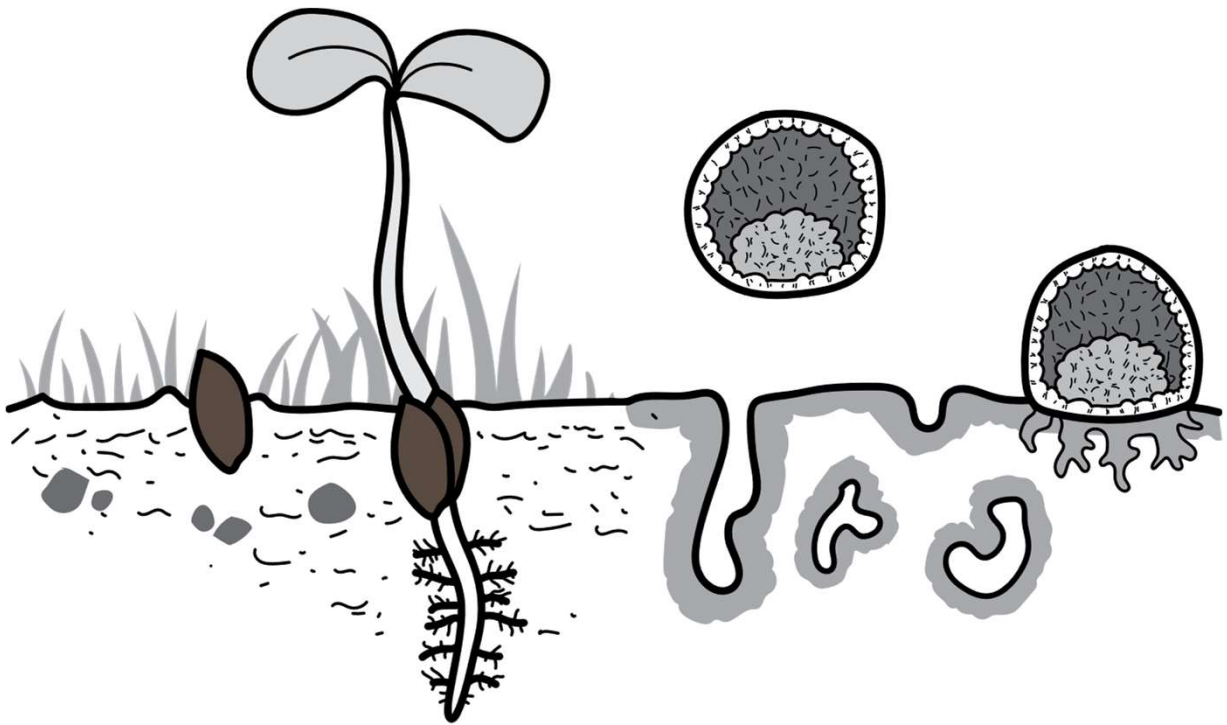
Increasing relative quantities of adhesome and receptome proteins may not necessarily be beneficial to endometrial receptivity and improving the rate of successful implantation, and could instead be too much of a good thing; several receptome proteins are elevated in the infertile mid-secretory endometrium and this may be detrimental to fertility (Edgell et al., 2018). The network of proteins involved in receptivity and adhesion is likely finely tuned, with aberrations in expression leading to disrupted fertility, as seen for CSF-3 in uterine fluid (Edgell et al, 2018). Excess receptive and adhesive proteins could lead to excessive implantation, such as in the condition, placenta previa, or the implantation of a poor-quality embryo. Conversely, too little of each may result in the loss of quality embryos from the endometrium through implantation failure or miscarriage. Given the necessary balance of proteins, disrupting this balance may provide novel avenues for non-hormonal contraceptives. In terms of improving the success of conception, optimising the ratios between receptome proteins across the menstrual cycle may be beneficial.

6.5 “Take home” message

Individual proteins identified in the human endometrial receptome and adhesome were validated as being present in the human endometrium and functionally significant in human endometrial epithelial cells (ECC-1). Specific proteins are likely important in preparing and maintaining the site of implantation within the endometrium, as has been shown by investigation of single proteins. This work provides further understanding of the requisites for implantation at the proteomic level, and provides potential novel protein targets for future research.

Chapter 7:

General discussion
&
Concluding remarks



Chapter 7: General discussion

Contextualising this thesis and its future applications

Obesity affects up to 30% of reproductively aged women, and the prevalence of obesity continues to rise globally (Australian Institute of Health and Welfare, 2017; World Health Organisation). Translation of this research therefore has the potential for significant impact. Advanced Glycation Endproducts (AGEs), highly elevated in the obese uterine environment, are emerging as a potential mediator of obesity-related infertility (Antoniotti et al., 2018). The studies presented in this thesis demonstrate functional effects of obesity-associated AGEs on maternal-fetal interactions with significant clinical implications for fertility and infertility (summarised in Figure 7.1). Specifically, AGEs equimolar with the obese uterine fluid microenvironment were found to detrimentally impact endometrial function, preimplantation embryo development and embryo-endometrium interactions. Antagonism of appropriate receptors and targeting of downstream events mitigate AGEs induced effects.

7.1 Major findings of this thesis

Previous research determined reduced adhesiveness of trophoblast and invasion of trophoblast cells by physiologically obese concentrations of AGEs, indicating there may be impacts of AGEs on the development of the preimplantation embryo. Given the long term effects of altered environments on early embryonic development (the DOHaD hypothesis (Barker, 1995)), it was imperative to understand the implications of obese AGEs on the embryo. In Chapter 3 of this thesis, I showed that AGEs equimolar to the obese uterine fluid microenvironment significantly impacted the blastocyst, with effects noticeable by day four, and continued to day five of development. The hatching rate of blastocysts was reduced, and the embryos were significantly smaller than those cultured in physiologically lean, or no AGEs: the trophoblast comprised fewer cells, this was improved by small molecule antagonism of RAGE, but not metformin nor antioxidants. Trophoblast function was further compromised, with blastocysts cultured in obese AGEs demonstrating reduced outgrowth, an *in vitro* marker of implantation *in vivo* (Binder et al., 2015). These findings substantiate clinical reports of placental insufficiency in obese women, including the disproportionate rates of spontaneous miscarriage of euploid embryos (Bellver et al., 2003; Tremellen et al., 2017) and preeclampsia (Roberts et al., 2011).

Previously, Antoniotti et al. (2018) demonstrated reduced proliferation of endometrial epithelial cells in the presence of obese AGEs. The research described in Chapter 4 recapitulated this effect of obesity-associated AGEs, and the application of antioxidants successfully restored the rate of proliferation of endometrial epithelial cells. Neither receptor antagonism nor metformin were able to improve the rate of proliferation. This provides a promising foundation for normalising the functions of the obese uterine environment therapeutically.

In Chapter 5, I sought to recapitulate work from cell line studies to a more physiologically relevant model of human endometrial epithelium. When exposed to obese levels of AGEs, human endometrial epithelial organoids were affected functionally: increased cytokine secretion from intact organoids and altered proliferation of organoid-derived epithelial cells was observed versus lean AGEs levels. Significant biological variation was noted between samples: those derived from women with ovarian abnormalities (ovarian cyst, PCOS) showed AGEs-induced effects on proliferation in an inverse manner. Thus, AGEs-induced inflammation within the uterine microenvironment may promote a non-receptive phenotype and compromise maternal-fetal interactions.

Earlier published work from this laboratory, had performed proteomic interrogation of trophoblast-spheroid interactions using primary human endometrial epithelial cells from fertile and infertile women and defined the human endometrial epithelial 'receptome' and embryo-endometrial 'adhesome' (Evans et al., 2020a). In Chapter 6, I sought to further validate a number of the highly regulated receptome and adhesome proteins. I identified PC4 as modulated in the infertile endometrium versus fertile, and SLIRP to be functionally important in endometrial epithelial cell function. These proteins may act to regulate the development of endometrial receptivity and hormone-responsiveness of the endometrium. In addition, they represent targets for investigation in the obese uterine environment to understand the mechanisms underpinning obesity-related infertility.

Together, these findings enhance our understanding of maternal-fetal interactions within the obese uterine environment and demonstrate the capacity of AGEs equimolar with those in obese uterine fluid to modulate several functional parameters of the endometrium and the preimplantation embryo. This provides novel potential avenues to assist obese couples, and others with excess levels of uterine AGEs, who may be struggling to conceive. Provision of a targeted fertility strategy to complement the advice of maintaining a healthy weight is of significant benefit for couples approaching reproductive senescence.

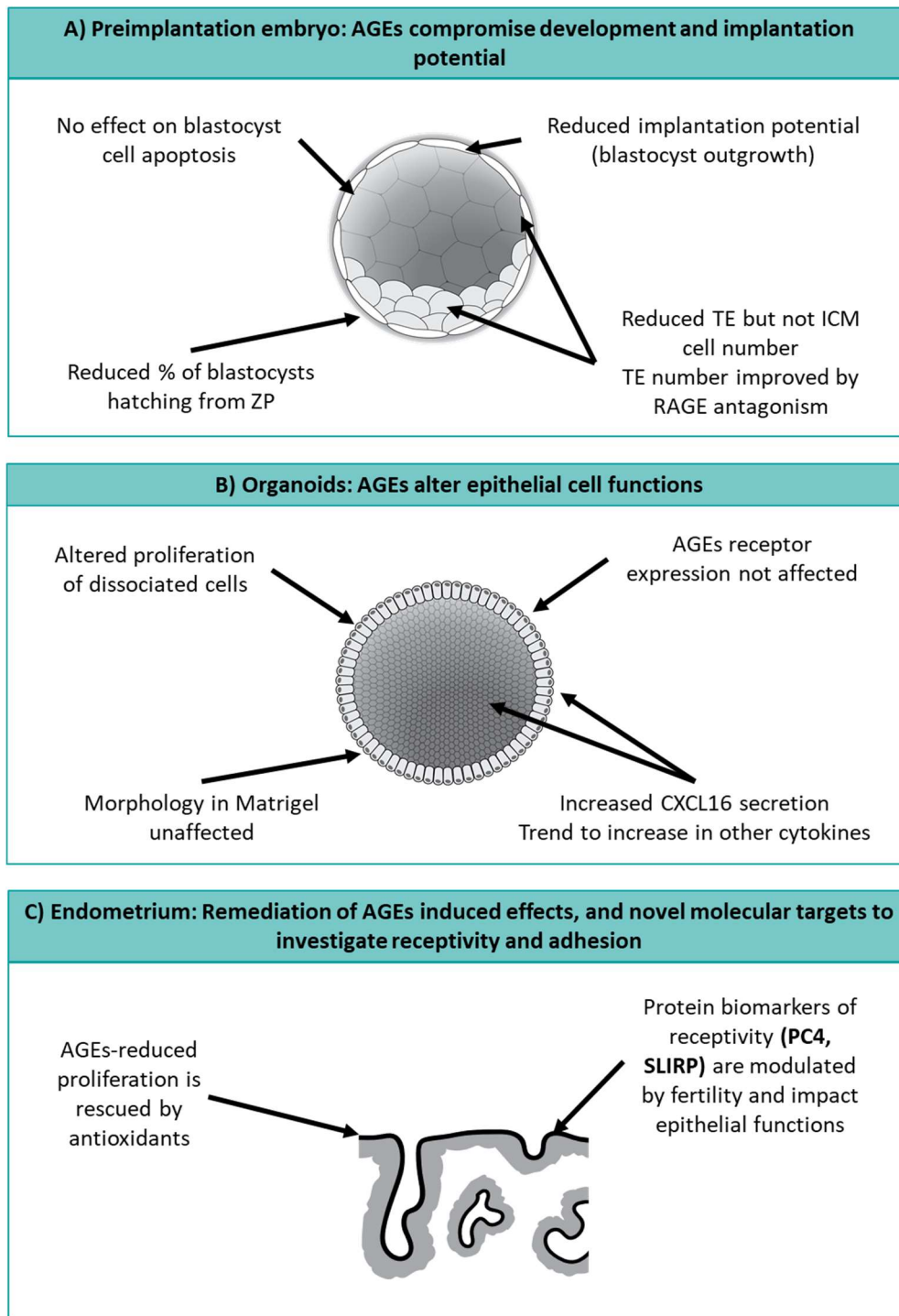


Figure 7.1: Summary of significant findings. **A)** AGEs equimolar with those in the obese uterine fluid significantly impair preimplantation embryo trophoctoderm formation (reduced trophoctoderm cell number) and function (reduced blastocyst outgrowth). Trophoctoderm cell number was improved by RAGE antagonism. TE: trophoctoderm; ICM: inner cell mass. **B)** Obese AGEs altered the proliferation kinetics of organoid derived epithelial cells and the secretion of cytokines/chemokines. **C)** The reduction in ECC-1 proliferation induced by obese AGEs was improved by the application of antioxidants. Novel protein biomarkers of endometrial epithelial cell receptivity and embryo adhesion including PC4 are modulated by infertility and SLIRP is important in epithelial cell function (tight junction integrity and spheroid adhesion).

7.2 Clinical implications of this research

The findings of this thesis have substantial potential for translation to current clinical practices, particularly given the rising numbers of people who experience obesity-related infertility.

7.2.2 To whom does this research apply?

This research is particularly pertinent to obese women experiencing infertility, as an obese BMI is often a barrier to accessing assisted reproduction: an alternative to substantial weight loss would be to their advantage. Further, dependent on their uterine concentrations of AGEs, these results may also be applicable to a broader range of individuals. Numerous conditions, such as diabetes, metabolic syndrome, and PCOS, are known to elevate systemic AGEs, but little is known about the influence of these conditions on uterine AGEs. In addition, people with a diet rich in AGEs or glucose may be at risk of elevated uterine AGEs even with a normal BMI; indeed pre-pregnancy intake of sugary or fast-foods is related to an increased time to pregnancy and altered fetal outcomes (Moran et al., 2018; Okubo et al., 2012). This research can also be applied to women not seeking nor currently undergoing IVF, as reducing intrauterine AGEs could enhance fertility within natural cycles.

7.2.1 What are the clinical implications of this work?

Future work will determine whether serum AGEs correlate to AGEs in uterine fluid, and may identify a “danger zone” in which embryo transfer should be avoided. Identification of women who are at risk of AGEs-induced effects on pregnancy establishment could help diagnose reasons for delayed conception or failed implantation. For obese women who have been attempting to reduce their weight, intrauterine AGEs may have been reduced to a level not adverse to implantation and placentation. This could make women with a borderline BMI eligible to access IVF provided no other substantial and prohibitive risks exist.

Inclusion of quantitative assays, such as ELISA of serum and uterine fluid during patient workup would identify women with high intrauterine AGEs; quality blastocysts generated through *ex vivo* culture could be frozen whilst interventions are undertaken to lower uterine AGEs, maximising the likelihood of establishing a healthy pregnancy following subsequent frozen embryo transfer. Rapid assays would inform clinicians for decision making. However, while mass spectrometry is emerging as the gold standard to investigate AGEs composition and concentration (Perrone et al., 2020), this may not be practical in a clinical setting as uterine AGEs levels would need to be confirmed in the cycle of embryo transfer.

Uterine AGEs pose additional complications for emerging technologies such as womb on a chip and *in vivo* culture of human embryos. For example, in womb on a chip (Chang et al., 2016), inclusion of endometrial cells whose function may have been impacted by excess AGEs could have

downstream effects on the developing embryo. Further, should *in vivo* culture systems be adopted into clinical use (Blockeel et al., 2009), elevated AGEs would be a contraindication for their use, as perfusion of the capsule with uterine fluid would expose the embryo to detrimental levels of AGEs, compromising its implantation potential following transfer.

7.2.3 Application of targeted AGEs reduction strategies

While maintenance of a healthy weight should be encouraged, weight-loss interventions can take significant time: although 75% of women willing to engage in pre-pregnancy weight-loss would consider delaying childbearing during this period (D. Simon et al., 2020), this may not be appropriate for everyone. Though beneficial to serum carboxymethyl lysine levels (Deo et al., 2017), weight-loss alone may not be sufficient to reduce uterine AGEs, and targeted reduction of AGEs or pharmaceutical treatment may provide a more immediate solution for obese women of advanced maternal age wishing to conceive. It is also possible that weight-loss coupled with reduced uterine AGEs may have an additive or synergistic effect on fertility. Of importance, weight-loss may not be required for women with a lean BMI but excess uterine AGEs, with further investigation required around uterine AGEs in conditions such as diabetes and PCOS.

Dependent on individual circumstances, remediation of AGEs-induced effects on maternal-fetal interactions could be performed in three ways: 1) generation of a quality blastocyst through assisted reproduction, complemented with an intrauterine delivery of therapeutics to target the maternal endometrium; 2) a combination therapy of RAGE antagonism and antioxidants to improve both preimplantation embryo and endometrial development during natural conception cycles; 3) a general pre-conception reduction of intrauterine AGEs through dietary or pharmacological intervention. Reduction of intrauterine AGEs would be best performed in the preceding non-conception cycles to improve endometrial remodelling and function for subsequent embryo transfer, as indicated above. Within any conception cycle, intervention must be performed prior to ovulation to prevent additional AGEs-induced effects on the oocyte within the maternal environment, and be maintained during embryo development and implantation. Dietary reduction of AGEs should continue through pregnancy and parturition to prevent exposure of the offspring to AGEs through lactation (Borg et al., 2018; Csongová et al., 2019).

As RAGE is expressed throughout the body (Ott et al., 2014) there is the potential for off target effects of receptor antagonism. In addition, dependent on pharmacokinetics, limited active concentrations of anti-AGEs agents may reach the uterine cavity. To improve this, pharmaceuticals could be preferentially delivered to the uterine microenvironment by targeted delivery systems (Paul et al., 2017), or alternatively be delivered intravaginally which allows for more efficient therapeutic delivery to the uterus while reducing systemic effects (Cicinelli and De Ziegler, 1999; Menkhorst et al.,

2011). Slow release hydrogels have been successful in improving endometrial regeneration in rodent models (Zhang et al., 2017), and application of a hydrogel containing anti-AGEs agents during a conception cycle and at the time of embryo transfer may be a promising potential therapeutic strategy.

Reduction of uterine AGEs rather than mitigation of downstream effects should be the primary focus for long term fertility-improving strategies. This may be achieved either by local or systemic application of the AGEs crosslink breaker Alagebrium (Coughlan et al., 2011), or dietary intervention to reduce exogenous sources of reactive AGEs (Uribarri et al., 2010). Whilst diet influences the composition of uterine fluid (Kermack et al., 2015), future studies are necessary to assess the impact of dietary intervention on local AGEs accumulation within the uterine fluid, as this may not be reflected in serum concentrations. Appropriate clinical trials will be required to assess the efficacy and impact of targeted AGEs reduction on fertility in obese women.

7.3 Identifying the priority for targeted AGEs reduction: the embryo or the endometrium?

As for the method of intervention, individual circumstances will dictate the priority target. Ng et al. (2020), amongst others (Simón et al., 2020), argue that appropriate preparation and receptivity of the endometrium is the primary driver of healthy pregnancy rather than the embryo, and thus should be considered the main focus of therapeutics. For women approaching reproductive senescence in which time is of the essence to conceive (Rosenwaks et al., 1995), the endometrium will likely be the priority for targeted AGEs reduction, as embryos can be cultured *ex vivo*, or may be donated from other couples. However, endometrial health should not be the primary focus at the expense of embryo quality.

Simply focussing on the endometrium might not be sufficient to improve fertility in obese women as a healthy endometrium may not support the implantation of a lower quality blastocyst (Brosens et al., 2014; Macklon and Brosens, 2014): it is necessary to optimise both embryo quality and the maternal environment and neither can be put above the other, particularly for improving natural conception rates. Thus, for younger women, a holistic AGEs reduction approach can be performed to improve multiple aspects of fertility, which may not be possible in the remaining reproductive life span of an older woman.

To tackle the obesity epidemic, interventions are required that will reduce the prevalence of obesity in the next generations, potentially through epigenetic inheritance (Paliy et al., 2014). Given that oocytes are not replenished throughout reproductive life, and have limited capacity for self-repair (Winship et al., 2018), there is currently little that can be done to reverse AGEs induced effects on the

oocyte. As obesity can influence epigenetic modifications in the oocyte (Hou et al., 2016), impacts of AGEs on the gamete may be continued; by reducing systemic and uterine AGEs during follicular maturation and embryo development, we may prevent further changes to the embryonic epigenome.

7.4 Strengths and limitations of this research

In this thesis, I have used a variety of methodologies to assess: 1) endometrial receptivity; 2) the functional impacts of AGEs on embryo development and reproduction; and 3) the detrimental effect of AGEs on cellular functions within the reproductive tract. Replication of AGEs-induced effects across several endpoints highlights the robust nature of these results. The sample sizes used in primary human models was restricted by the limited availability of human endometrial tissue. While the results presented in this thesis are valid, additional samples may provide clarity on trends within datasets. Fertile, secretory phase human tissue is difficult to obtain at the best of times; however, this was further compounded by COVID-19-related restrictions which limited laboratory time in 2020.

A strength of this work is the use of physiologically relevant concentrations of AGEs, quantified in the uterine fluid of lean and obese women (Antoniotti et al., 2018), which is in contrast to a significant proportion of previous reports that apply AGEs by total protein concentration, and do not identify the concentration of particular AGEs moieties. This does not take into account differing degrees of *in vitro* glycation, and may not be physiologically representative. The limitations of the AGEs used in this research is potential differences in AGEs composition in *in vitro* vs *in vivo* (i.e. concentration of CML versus other species such as pentosidine), which could be explored using mass spectrometry techniques.

Organoid research, implemented initially in the Salamonsen lab in 2019 by my supervisor Dr Jemma Evans, represents a significant strength of this thesis. This methodology allowed for the scaling up of primary epithelial cell culture, and would enable repeated measures on the same donor tissue to ensure reproducibility. So, should we switch our experimental paradigms to organoid systems in preference of established cell lines? It could be argued that this is situation specific. Organoid culture is costly and time-consuming versus standard cell culture techniques, but once established, organoids can be successfully biobanked and thawed when required. Although still an *in vitro* system, these cells are more representative of the physiologically normal human endometrium, as the epithelial cells within the organoid retain their polarity; thus not all cell line data will be replicated in organoid research. For example, the organoid studies in this thesis imply that the mode of action of AGEs on primary human endometrial epithelial cells is not primarily proliferative: AGEs may act through TLR4 to stimulate a pro-inflammatory response, rather than suppressing proliferation and promoting de-adhesion as seen in ECC-1 cells. This may represent a fundamental difference between cancer cell lines

and organoid cultured primary cells, and further research into the signalling pathways activated in each cell type is thus warranted. For pilot studies, investigation in established cell lines would provide initial data in a more cost-effective manner, before detailed investigation in organoid culture. Many laboratories do not have access to the primary human endometrium required for organoid production. While organoids have significant benefits, further development is required for these to overtake cell lines as the primary culture system of choice. Organoids as currently used here and elsewhere are comprised of a single endometrial cell type, and inclusion of multiple cell types to enhance the physiology of the model will be required to give a more comprehensive understanding of the *in vivo* environment.

7.4.1 Physiological relevance of the models used

Mouse embryos were used as a necessary proxy to study the earliest stages of embryonic development and provided an indication of how AGEs may affect human preimplantation development. Although implantation and placentation are species-specific processes, the impact of AGEs on human trophoblast and trophoblast cell lines *in vitro* support translation of mouse work. In addition, AGEs-HSA, not glycated mouse serum albumin was applied to mouse embryos, and it is not known what the AGEs contents of the obese mouse uterine environment are. This could be studied in both genetic and diet-induced models of obesity.

Limitations of both cell lines and organoid research must also be considered. As discussed in Chapter 5, adenocarcinoma derived cell lines do not represent the physiology of the healthy endometrium, and the choice of cell line utilised is critical in experimental work (Bazer and Salamonsen, 2008; Hannan et al., 2010). Throughout this thesis, ECC-1 cell investigations have either been used as a *in vitro* complement to primary cell data (receptome and adhesome), or experimental results from these re-examined in organoid cell culture (AGEs). Organoids are advantageous for studying the functions and development of healthy endometrium, but are associated with their own limitations (Huch et al., 2017). Fitzgerald et al. (2019) demonstrate through scRNA-seq that organoids contain clonogenic cells with a mixture of epithelial identities, some cells expressing FOXA2 (a marker of glandular epithelium), and some not, implying both luminal and glandular epithelial cells to be present. This could be further investigated by assessment of putative markers of luminal epithelium such as WNT7A (Wang et al., 2020), and to determine if a luminal identity is present in intact organoids, or is promoted upon dissociation into single cells for monolayer culture. This would be important for the further study of receptivity and adhesion biomarkers as described in Chapter 6, as the luminal epithelium is the first point of contact for the approaching blastocyst.

7.5 Future directions

7.5.1 Personalised medicine: modification of endometrial receptivity

Given the limited ability of the Endometrial Receptivity Array to accurately detect receptivity and improve IVF outcomes (Simón et al., 2020) and the likelihood that protein or other molecular biomarkers will prove more useful, further effort should be applied to determine whether receptome or adhesome proteins may prove useful additional biomarkers. Future studies on AGEs-induced effects on these biomarkers could be examined *in vitro* through use of 3D models of the maternal-fetal interface (Abbas et al., 2020). Understanding the regulation of these proteins in the obese uterine environment would also be important.

7.5.2 Continued development of models

The combined use of individual models presented in this thesis, could improve our understanding of endometrial receptivity and the effects of AGEs on embryo implantation potential. For example, co-culture of organoids and stromal cells to generate a 3D model of the endometrial environment, potentially using prolactin-reporter stromal cell lines (Haller et al., 2019), could be used in conjunction with either trophoblast spheroids or mouse blastocysts to assess the AGEs effects, and development of receptivity at the maternal-fetal interface, and to further examine proteins of the human receptome and adhesome, throughout the implantation process.

7.5.3 Examination of downstream consequences of elevated AGEs in the microenvironment of implantation and placentation

With new clarity of the impact of AGEs on embryos provided here, the downstream consequences and effects of AGEs on offspring should be examined. Embryo transfers following culture in obese levels of AGEs, to recipient normal weight females or to recipients exposed to a high AGEs diet would provide information regarding effects of AGEs on implantation, placentation and on offspring. Complementary *in vitro* studies on trophoblast function and syncytialisation will provide further insight to the molecular and cellular effects of AGEs on placentation.

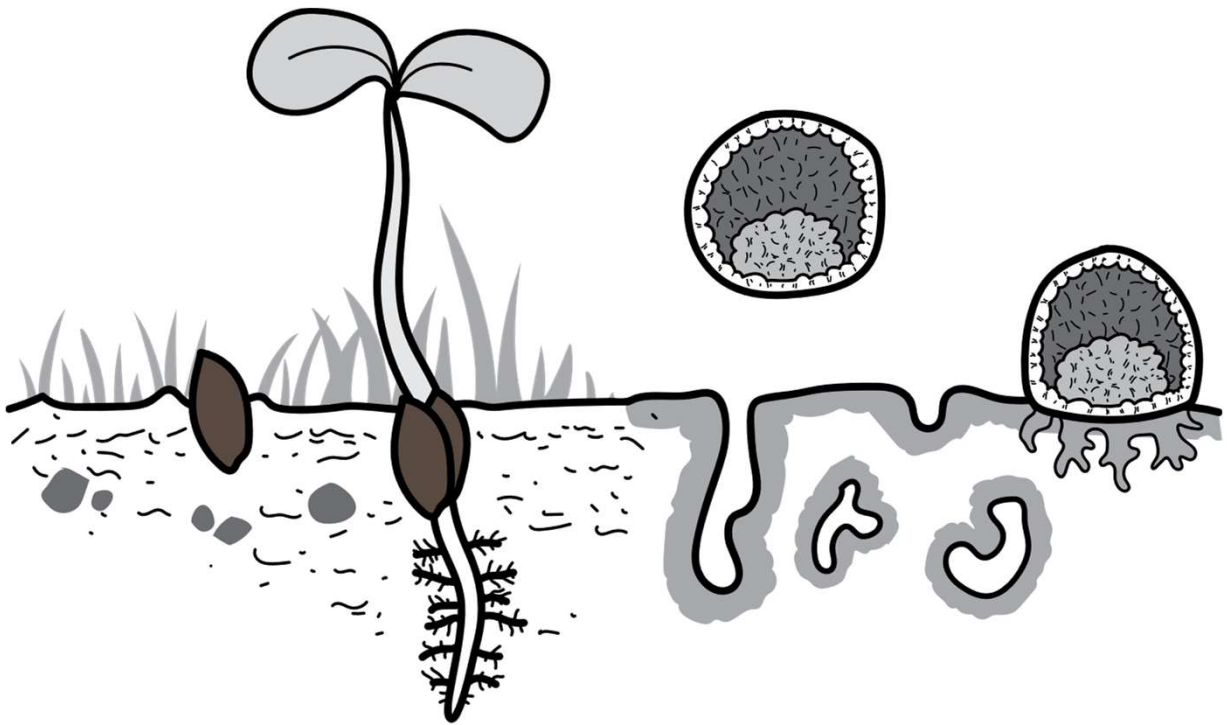
7.5.4 AGEs and male fertility

It is known that elevated male BMI is detrimental to reproduction (Anifandis et al., 2013; MacDonald et al., 2013; Stewart et al., 2009). Assessment of healthy sperm function in a high AGEs environment through sperm motility and chemotaxis assays, and *in vitro* fertilisation in an AGEs rich medium would provide insight on the obese maternal effect on sperm function. Fertility effects of male mice exposed to a high AGEs diet in conjunction with control and high AGEs diet females would ensure the obese male contribution to the couple's fertility is not ignored.

7.6 Concluding remarks

Obese women suffer a disproportionate rate of infertility, but understanding of how excess weight results in reduced fertility is limited. In the doctor's office, and in social situations, weight-loss is often proclaimed as the answer to many problems, which does little to help women approaching reproductive senescence, or individuals who have struggled with their weight for their entire lives. This thesis provides insight into how detrimental effects of obesity on reproduction are mediated, and provides foundations for further investigation into molecular effects of AGEs on implantation potential. *In vitro*, AGEs equimolar to the obese uterine environment promote cellular dysfunction of the preimplantation embryonic trophectoderm, and endometrial epithelial cells. Clinically, reduced uterine AGEs could improve fertility outcomes for women with obesity and other metabolic disorders, and possibly be extrapolated to women with a diet rich in glucose or AGEs. A simple, targeted approach to improving obesity-related infertility may provide profound benefits for those struggling with the invisible burden of infertility, and help break the dogma of weight-loss as a "cure-all" for obese women.

References



References

- Abbas, Y., Brunel, L.G., Hollinshead, M.S., Fernando, R.C., Gardner, L., Duncan, I., Moffett, A., Best, S., Turco, M.Y., Burton, G.J., Cameron, R.E., 2020. Generation of a three-dimensional collagen scaffold-based model of the human endometrium. *Interface Focus* 10. <https://doi.org/10.1098/rsfs.2019.0079>
- Abou-Kheir, W., Barrak, J., Hadadeh, O., Daoud, G., 2017. HTR-8/SVneo cell line contains a mixed population of cells. *Placenta* 50, 1–7. <https://doi.org/10.1016/j.placenta.2016.12.007>
- Adamopoulos, C., Piperi, C., Gargalionis, A.N., Dalagiorgou, G., Spilioti, E., Korkolopoulou, P., Diamanti-Kandarakis, E., Papavassiliou, A.G., 2016. Advanced glycation end products upregulate lysyl oxidase and endothelin-1 in human aortic endothelial cells via parallel activation of ERK1 / 2 – NF- κ B and JNK – AP-1 signaling pathways. *Cell. Mol. Life Sci.* 73, 1685–1698. <https://doi.org/10.1007/s00018-015-2091-z>
- Aghajanova, L., Shen, S., Rojas, A.M., Fisher, S.J., Irwin, J.C., Giudice, L.C., 2012. Comparative Transcriptome Analysis of Human Trophoblast and Embryonic Stem Cell-Derived Trophoblasts Reveal Key Participants in Early Implantation 1. *Biol. Reprod.* 86, 1–21. <https://doi.org/10.1095/biolreprod.111.092775>
- Al-Biate, M.A.S., 2015. Effect of metformin on early pregnancy loss in women with polycystic ovary syndrome. *Taiwan. J. Obstet. Gynecol.* 54, 266–269. <https://doi.org/10.1016/j.tjog.2013.06.020>
- Alexander, K.L., Mejia, C.A., Jordan, C., Nelson, M.B., Howell, B.M., Jones, C.M., Reynolds, P.R., Arroyo, J.A., 2016. Differential Receptor for Advanced Glycation End Products Expression in Preeclamptic , Intrauterine Growth Restricted , and Gestational Diabetic Placentas. *Am. J. Reprod. Immunol.* 75, 172–180. <https://doi.org/10.1111/aji.12462>
- Alfer, J., Fattahi, A., Bleisinger, N., Krieg, J., Behrens, R., Dittrich, R., Beckmann, M.W., Hartmann, A., Classen-Linke, I., Popovici, R.M., 2020. Endometrial dating method detects individual maturation sequences during the secretory phase. *In Vivo (Brooklyn)*. 34, 1951–1963. <https://doi.org/10.21873/invivo.11992>
- Alzamil, L., Nikolakopoulou, K., Turco, M.Y., 2020. Organoid systems to study the human female reproductive tract and pregnancy. *Cell Death Differ.* <https://doi.org/10.1038/s41418-020-0565-5>
- Anifandis, G., Dafopoulos, K., Messini, C.I., Polyzos, N., Messinis, I.E., 2013. The BMI of men and not sperm parameters impact on embryo quality and the IVF outcome. *Andrology* 1, 85–89. <https://doi.org/10.1111/j.2047-2927.2012.00012.x>
- Antoniotti, G.S., Coughlan, M., Salamonsen, L.A., Evans, J., 2018. Obesity associated advanced glycation end products in the uterine cavity adversely impact endometrial function and embryo implantation competence. *Hum. Reprod.* 33, 654–665.
- Aplin, J.D., Kimber, S.J., 2004. Trophoblast-uterine interactions at implantation. *Reprod. Biol. Endocrinol.* 2, 1–12. <https://doi.org/10.1186/1477-7827-2-48>
- Aplin, J.D., Ruane, P.T., 2017. Embryo–epithelium interactions during implantation at a glance. *J. Cell Sci.* 130, 15–22. <https://doi.org/10.1242/jcs.175943>

- Arumugam, T., Simeone, D.M., Schmidt, A.M., Logsdon, C.D., 2004. S100P stimulates cell proliferation and survival via receptor for activated glycation end products (RAGE). *J. Biol. Chem.* 279, 5059–65. <https://doi.org/10.1074/jbc.M310124200>
- Atzmon, Y., Shoshan-Karchovsky, E., Michaeli, M., Aslih, N., Shrem, G., Ellenbogen, A., Shalom-Paz, E., 2017. Obesity results with smaller oocyte in in vitro fertilization/intracytoplasmic sperm injection cycles—a prospective study. *J. Assist. Reprod. Genet.* 34, 1145–1151. <https://doi.org/10.1007/s10815-017-0975-6>
- Audard, J., Godet, T., Blondonnet, R., Joffredo, J.B., Paquette, B., Belville, C., Lavergne, M., Gross, C., Pasteur, J., Bouvier, D., Blanchon, L., Sapin, V., Pereira, B., Constantin, J.M., Jabaudon, M., 2019. Inhibition of the Receptor for Advanced Glycation End-Products in Acute Respiratory Distress Syndrome: A Randomised Laboratory Trial in Piglets. *Sci. Rep.* 9, 9227. <https://doi.org/10.1038/s41598-019-45798-5>
- Australian Institute of Health and Welfare 2017. A picture of overweight and obesity in Australia 2017. Cat. no.PHE 216. Canberra: AIHW.
- Azizieh, F.Y., Raghupathy, R.G., 2015. Tumor necrosis factor- α and pregnancy complications: A prospective study. *Med. Princ. Pract.* 24, 165–170. <https://doi.org/10.1159/000369363>
- Azlan, A., Salamonsen, L.A., Hutchison, J., Evans, J., 2020. Endometrial inflammasome activation accompanies menstruation and may have implications for systemic inflammatory events of the menstrual cycle. *Hum. Reprod.* 35, 1363–1376. <https://doi.org/10.1093/humrep/deaa065>
- Banerjee, S., Kumar, B.R.P., Tapas, K., Kundu, T.K., 2004. General Transcriptional Coactivator PC4 Activates p53 Function. *Society* 24, 2052–2062. <https://doi.org/10.1128/MCB.24.5.2052>
- Barandalla, M., Haucke, E., Fischer, B., Navarrete Santos, Alexander, Colleoni, S., Galli, C., Navarrete Santos, Anne, Lazzari, G., 2017. Comparative Analysis of AGE and RAGE Levels in Human Somatic and Embryonic Stem Cells under H₂O₂-Induced Noncytotoxic Oxidative Stress Conditions. *Oxid. Med. Cell. Longev.* 2017, Article ID: 4240136. <https://doi.org/10.1155/2017/4240136>
- Barcroft, L.C., Offenbergh, H., Thomsen, P., Watson, A.J., 2003. Aquaporin proteins in murine trophoctoderm mediate transepithelial water movements during cavitation. *Dev. Biol.* 256, 342–354. [https://doi.org/10.1016/S0012-1606\(02\)00127-6](https://doi.org/10.1016/S0012-1606(02)00127-6)
- Barker, D.K.P., 1995. Fetal origins of coronary heart disease. *Br. Med. J.* 311, 171–181. <https://doi.org/10.1136/bmj.311.6998.171>
- Batta, K., Yokokawa, M., Takeyasu, K., Kundu, T.K., 2009. Human Transcriptional Coactivator PC4 Stimulates DNA End Joining and Activates DSB Repair Activity. *J. Mol. Biol.* 385, 788–799. <https://doi.org/10.1016/j.jmb.2008.11.008>
- Bauersachs, S., Mitko, K., Ulbrich, S.E., Blum, H., Wolf, E., 2008. Transcriptome studies of bovine endometrium reveal molecular profiles characteristic for specific stages of estrous cycle and early pregnancy. *Exp. Clin. Endocrinol. Diabetes* 116, 371–384. <https://doi.org/10.1055/s-2008-1076714>
- Bazer, F.W., Salamonsen, L.A., 2008. Let's Validate Those Cell Lines. *Biol. Reprod.* 79, 585–585.

- <https://doi.org/10.1095/biolreprod.108.071878>
- Bellofiore, N., Ellery, S.J., Mamrot, J., Walker, D.W., Temple-Smith, P., Dickinson, H., 2017. First evidence of a menstruating rodent: the spiny mouse (*Acomys cahirinus*). *Am. J. Obstet. Gynecol.* 216, 40.e1-40.e11. <https://doi.org/10.1016/j.ajog.2016.07.041>
- Bellver, J., Martínez-Conejero, J.A., Labarta, E., Alamá, P., Melo, M.A.B., Remohí, J., Pellicer, A., Horcajadas, J.A., 2011. Endometrial gene expression in the window of implantation is altered in obese women especially in association with polycystic ovary syndrome. *Fertil. Steril.* 95. <https://doi.org/10.1016/j.fertnstert.2011.03.021>
- Bellver, J., Melo, M.A.B., Bosch, E., Serra, V., Remohí, J., Pellicer, A., 2007. Obesity and poor reproductive outcome: the potential role of the endometrium. *Fertil. Steril.* 88, 446–451. <https://doi.org/10.1016/j.fertnstert.2006.11.162>
- Bellver, J., Mifsud, A., Grau, N., Privitera, L., Meseguer, M., 2013a. Similar morphokinetic patterns in embryos derived from obese and normoweight infertile women: A time-lapse study. *Hum. Reprod.* 28, 794–800. <https://doi.org/10.1093/humrep/des438>
- Bellver, J., Pellicer, A., García-Velasco, J.A., Ballesteros, A., Remohí, J., Meseguer, M., 2013b. Obesity reduces uterine receptivity: Clinical experience from 9,587 first cycles of ovum donation with normal weight donors. *Fertil. Steril.* 100, 1050–1058. <https://doi.org/10.1016/j.fertnstert.2013.06.001>
- Bellver, J., Rossal, L.P., Bosch, E., Zúñiga, A., Corona, J.T., Meléndez, F., Gómez, E., Simón, C., Remohí, J., Pellicer, A., 2003. Obesity and the risk of spontaneous abortion after oocyte donation. *Fertil. Steril.* 79, 1136–1140. [https://doi.org/10.1016/S0015-0282\(03\)00176-6](https://doi.org/10.1016/S0015-0282(03)00176-6)
- Bentin-Ley, U., Horn, T., Sjogren, A., Sorensen, S., Falck Larsen, J., Hamberger, L., 2000. Ultrastructure of human blastocyst-endometrial interactions in vitro. *J. Reprod. Fertil.* 120, 337–350. <https://doi.org/10.1530/jrf.0.1200337>
- Best, D., Avenell, A., Bhattacharya, S., 2017. How effective are weight-loss interventions for improving fertility in women and men who are overweight or obese? A systematic review and meta-analysis of the evidence. *Hum. Reprod. Update* 23, 681–705. <https://doi.org/10.1093/humupd/dmx027>
- Bhagwat, S.R., Chandrashekar, D.S., Kakar, R., Davuluri, S., Bajpai, A.K., Nayak, S., Bhutada, S., Acharya, K., Sachdeva, G., 2013. Endometrial Receptivity: A Revisit to Functional Genomics Studies on Human Endometrium and Creation of HGEx-ERdb. *PLoS One* 8. <https://doi.org/10.1371/journal.pone.0058419>
- Bhandari, H.M., Tan, B.K., Quenby, S., 2015. Superfertility is more prevalent in obese women with recurrent early pregnancy miscarriage 217–222. <https://doi.org/10.1111/1471-0528.13806>
- Bhutada, S., Basak, T., Savardekar, L., Katkam, R.R., Jadhav, G., Metkari, S.M., Chaudhari, U.K., Kumari, D., Kholkute, S.D., Sengupta, S., Sachdeva, G., 2014. High mobility group box 1 (HMGB1) protein in human uterine fluid and its relevance in implantation. *Hum. Reprod.* 29, 763–780. <https://doi.org/10.1093/humrep/det461>
- Bierhaus, A., Chevion, S., Chevion, M., Hofmann, M., Quehenberger, P., Illmer, T., Luther, T.,

- Berentshtein, E., Tritschler, H., Muller, M., Wahl, P., Ziegler, R., Nawroth, P.P., 1997. Advanced glycation end product-induced activation of NF κ B is suppressed by α -lipoic acid in cultured endothelial cells. *Diabetes* 46, 1481–1490.
- Binder, N.K., Evans, J., Salamonsen, L.A., Gardner, D.K., Kaitu'u-Lino, T.J., Hannan, N.J., 2016. Placental growth factor is secreted by the human endometrium and has potential important functions during embryo development and implantation. *PLoS One* 11, 1–15. <https://doi.org/10.1371/journal.pone.0163096>
- Binder, N.K., Hannan, N.J., Gardner, D.K., 2015. In vitro embryo outgrowth is a bioassay of in vivo embryo implantation and development. *Asian Pacific J. Reprod.* 4, 240–241. <https://doi.org/10.1016/j.apjr.2015.06.009>
- Bishop, R.C., Boretto, M., Rutkowski, M.R., Vankelecom, H., Derré, I., 2020. Murine Endometrial Organoids to Model Chlamydia Infection. *Front. Cell. Infect. Microbiol.* 10, 1–9. <https://doi.org/10.3389/fcimb.2020.00416>
- Blázquez, R., Sánchez-Margallo, F.M., Álvarez, V., Matilla, E., Hernández, N., Marinaro, F., Gómez-Serrano, M., Jorge, I., Casado, J.G., Macías-García, B., 2018. Murine embryos exposed to human endometrial MSCs-derived extracellular vesicles exhibit higher VEGF/PDGF AA release, increased blastomere count and hatching rates. *PLoS One* 13, e0196080. <https://doi.org/10.1371/journal.pone.0196080>
- Blockeel, C., Mock, P., Verheyen, G., Bouche, N., Le Goff, P., Heyman, Y., Wrenzycki, C., Höffmann, K., Niemann, H., Haentjens, P., De Los Santos, M.J., Fernandez-Sanchez, M., Velasco, M., Aebischer, P., Devroey, P., Simón, C., 2009. An in vivo culture system for human embryos using an encapsulation technology: A pilot study. *Hum. Reprod.* 24, 790–796. <https://doi.org/10.1093/humrep/dep005>
- Boivin, J., Takefman, J.E., 1996. Impact of the in-vitro fertilization process on emotional, physical and relational variables. *Hum. Reprod.* 11, 903–907. <https://doi.org/10.1093/oxfordjournals.humrep.a019276>
- Bonetti, T.C.S., Borges, E., Braga, D.P.A.F., Iaconelli, A., Kleine, J.P., Silva, I.D.C.G., 2013. Intrafollicular soluble receptor for advanced glycation end products (sRAGE) and embryo quality in assisted reproduction. *Reprod. Biomed. Online* 26, 62–67. <https://doi.org/10.1016/j.rbmo.2012.10.001>
- Boomsma, C.M., Kavelaars, A., Eijkemans, M.J.C., Lentjes, E.G., Fauser, B.C.J.M., Heijnen, C.J., MacKlon, N.S., 2009. Endometrial secretion analysis identifies a cytokine profile predictive of pregnancy in IVF. *Hum. Reprod.* 24, 1427–1435. <https://doi.org/10.1093/humrep/dep011>
- Boots, C.E., Bernardi, L.A., Stephenson, M.D., 2014. Frequency of euploid miscarriage is increased in obese women with recurrent early pregnancy loss. *Fertil. Steril.* 102, 455–459. <https://doi.org/10.1016/j.fertnstert.2014.05.005>
- Boretto, M., Cox, B., Noben, M., Hendriks, N., Fassbender, A., Roose, H., Amant, F., Timmerman, D., Tomassetti, C., Vanhie, A., Meuleman, C., Ferrante, M., Vankelecom, H., 2017. Development of organoids from mouse and human endometrium showing endometrial epithelium physiology and long-term expandability. *Dev.* 144, 1775–1786. <https://doi.org/10.1242/dev.148478>

- Boretto, M., Maenhoudt, N., Luo, X., Hennes, A., Boeckx, B., Bui, B., Heremans, R., Perneel, L., Kobayashi, H., Van Zundert, I., Brems, H., Cox, B., Ferrante, M., Uji-i, H., Koh, K.P., D'Hooghe, T., Vanhie, A., Vergote, I., Meuleman, C., Tomassetti, C., Lambrechts, D., Vriens, J., Timmerman, D., Vankelecom, H., 2019. Patient-derived organoids from endometrial disease capture clinical heterogeneity and are amenable to drug screening. *Nat. Cell Biol.* 21, 1041–1051. <https://doi.org/10.1038/s41556-019-0360-z>
- Borg, D.J., Yap, F.Y.T., Keshvari, S., Simmons, D.G., Gallo, L.A., Fotheringham, A.K., Zhuang, A., Slattery, R.M., Hasnain, S.Z., Coughlan, M.T., Kantharidis, P., Forbes, J.M., 2018. Perinatal exposure to high dietary advanced glycation end products in transgenic NOD8.3 mice leads to pancreatic beta cell dysfunction. *Islets* 10, 10–24. <https://doi.org/10.1080/19382014.2017.1405189>
- Brighton, P.J., Maruyama, Y., Fishwick, K., Vrljicak, P., Tewary, S., Fujihara, R., Muter, J., Lucas, E.S., Yamada, T., Woods, L., Lucciola, R., Lee, Y.H., Takeda, S., Ott, S., Hemberger, M., Quenby, S., Brosens, J.J., 2017. Clearance of senescent decidual cells by uterine natural killer cells in cycling human endometrium. *Elife* 6, e31274. <https://doi.org/10.7554/eLife.31274.001>
- Brosens, J.J., Salker, M.S., Teklenburg, G., Nautiyal, J., Salter, S., Lucas, E.S., Steel, J.H., Christian, M., Chan, Y.W., Boomsma, C.M., Moore, J.D., Hartshorne, G.M., Šučurović, S., Mulac-Jericevic, B., Heijnen, C.J., Quenby, S., Groot Koerkamp, M.J., Holstege, F.C.P., Shmygol, A., Macklon, N.S., 2014. Uterine selection of human embryos at implantation. *Sci. Rep.* 4, 4–11. <https://doi.org/10.1038/srep03894>
- Broughton, D.E., Moley, K.H., 2017. Obesity and female infertility: potential mediators of obesity's impact. *Fertil. Steril.* 107, 840–847. <https://doi.org/10.1016/j.fertnstert.2017.01.017>
- Bu, Z., Hu, L., Su, Y., Guo, Y., Zhai, J., Sun, Y.P., 2020. Factors related to early spontaneous miscarriage during IVF/ICSI treatment: an analysis of 21,485 clinical pregnancies. *Reprod. Biomed. Online* 40, 201–206. <https://doi.org/10.1016/j.rbmo.2019.11.001>
- Burton, G.J., Cindrova-Davies, T., Turco, M.Y., 2020. Review: Histotrophic nutrition and the placental-endometrial dialogue during human early pregnancy. *Placenta* 102, 21–26. <https://doi.org/10.1016/j.placenta.2020.02.008>
- Carver, J., Martin, K., Spyropoulou, I., Barlow, D., Sargent, I., Mardon, H., 2003. An in-vitro model for stromal invasion during implantation of the human blastocyst. *Hum. Reprod.* 18, 283–290. <https://doi.org/10.1093/humrep/deg072>
- Cascalho, M., 2004. Advantages and Disadvantages of Cytidine Deamination. *J. Immunol.* 172, 6513–6518. <https://doi.org/10.4049/jimmunol.172.11.6513>
- Castillo-Martínez, L., López-Alvarenga, J.C., Villa, A.R., González-Barranco, J., 2003. Menstrual cycle length disorders in 18- to 40-y-old obese women. *Nutrition* 19, 317–320. [https://doi.org/10.1016/S0899-9007\(02\)00998-X](https://doi.org/10.1016/S0899-9007(02)00998-X)
- Centres for Disease Control and Prevention, American Society for Reproductive Medicine, Society for assisted reproductive technology, 2017. 2015 Assisted Reproductive Technology Fertility Clinic Success Rates Report. US Dept of Health and Human Services, Atlanta, (GA).

- Chabbert-Buffet, N., Bouchard, P., 2002. The Normal Human Menstrual Cycle. *Rev. Endocr. Metab. Disord.* 3, 173–183.
- Chambers, G.M., Sullivan, E.A., Ishihara, O., Chapman, M.G., Adamson, G.D., 2009. The economic impact of assisted reproductive technology: a review of selected developed countries. *Fertil. Steril.* 91, 2281–2294. <https://doi.org/10.1016/j.fertnstert.2009.04.029>
- Chang, K.W., Chang, P.Y., Huang, H.Y., Li, C.J., Tien, C.H., Yao, D.J., Fan, S.K., Hsu, W., Liu, C.H., 2016. Womb-on-a-chip biomimetic system for improved embryo culture and development. *Sensors Actuators, B Chem.* 226, 218–226. <https://doi.org/10.1016/j.snb.2015.11.004>
- Chavan, A.R., Griffith, O.W., Wagner, G.P., 2017. The inflammation paradox in the evolution of mammalian pregnancy: turning a foe into a friend. *Curr. Opin. Genet. Dev.* 47, 24–32. <https://doi.org/10.1016/j.gde.2017.08.004>
- Chekir, C., Nakatsuka, M., Noguchi, S., Konishi, H., Kamada, Y., Sasaki, A., Hao, L., Hiramatsu, Y., 2006. Accumulation of advanced glycation end products in women with preeclampsia: Possible involvement of placental oxidative and nitrative stress. *Placenta* 27, 225–233. <https://doi.org/10.1016/j.placenta.2005.02.016>
- Choi, I., Dasari, A., Kim, N.H., Campbell, K.H.S., 2015. Effects of prolonged exposure of mouse embryos to elevated temperatures on embryonic developmental competence. *Reprod. Biomed. Online* 31, 171–179. <https://doi.org/10.1016/j.rbmo.2015.04.017>
- Chu, S.Y., Callaghan, W.M., Kim, S.Y., Schmid, C.H., Lau, J., England, Lucinda, J., Dietz, P.M., 2007. Maternal Obesity and Risk of Gestational. *Diabetes Care* 30, 2070–2076. <https://doi.org/10.2337/dc06-2559a.The>
- Cicinelli, E., De Ziegler, D., 1999. Transvaginal progesterone: Evidence for a new functional “portal system” flowing from the vagina to the uterus. *Hum. Reprod. Update* 5, 365–372. <https://doi.org/10.1093/humupd/5.4.365>
- Clarke, C.L., Feil, P.D., Satyaswaroop, P.G., 1987. Progesterone receptor regulation by 17 β -estradiol in human endometrial carcinoma grown in nude mice. *Endocrinology* 121, 1642–1648. <https://doi.org/10.1210/endo-121-5-1642>
- Cnattingius, S., Villamor, E., Johansson, S., Bonamy, A.-K.E., Persson, M., Wikstrom, A.-K., Granath, F., 2013. Maternal obesity and risk of preterm delivery. *JAMA* 309, 2362–2370. <https://doi.org/doi:10.1001/jama.2013.6295>
- Colley, S.M., Wintle, L., Searles, R., Russell, V., Firman, R.C., Smith, S., DeBoer, K., Merriner, D.J., Genevieve, B., Bentel, J.M., Stuckey, B.G.A., Phillips, M.R., Simmons, L.W., de Kretser, D.M., O’Bryan, M.K., Leedman, P.J., 2013. Loss of the Nuclear Receptor Corepressor SLIRP Compromises Male Fertility. *PLoS One* 8, e70700. <https://doi.org/10.1371/journal.pone.0070700>
- Comstock, I.A., Kim, S., Behr, B., Lathi, R.B., 2015. Increased body mass index negatively impacts blastocyst formation rate in normal responders undergoing in vitro fertilization. *J Assist Reprod Genet* 32, 1299–1304. <https://doi.org/10.1007/s10815-015-0515-1>
- Conesa, C., Acker, J., 2010. Sub1/PC4 a chromatin associated protein with multiple functions in

- transcription. *RNA Biol.* 7, 287–290. <https://doi.org/10.4161/rna.7.3.11491>
- Cooke, C.L.M., Brockelsby, J.C., Baker, P.N., Davidge, S.T., 2003. The Receptor for Advanced Glycation End Products (RAGE) Is Elevated in Women with Preeclampsia. *Hypertens. Pregnancy* 22, 173–184. <https://doi.org/10.1081/PRG-120021068>
- Coughlan, M.T., Thallas-bonke, V., Pete, J., Long, D.M., Gasser, A., Tong, D.C.K., Arnstein, M., Thorpe, S.R., Cooper, M.E., Forbes, J.M., 2007. Combination Therapy with the Advanced Glycation End Product Cross-Link Breaker, Alagebrium, and Angiotensin Converting Enzyme Inhibitors in Diabetes: Synergy or Redundancy? *Endocrinology* 148, 886–895. <https://doi.org/10.1210/en.2006-1300>
- Coughlan, M.T., Yap, F.Y.T., Tong, D.C.K., Andrikopoulos, S., Gasser, A., Thallas-Bonke, V., Webster, D.E., Miyazaki, J., Kay, T.W., Slattery, R.M., Kaye, D.M., Drew, B.G., Kingwell, B.A., Fourlanos, S., Groop, P.-H., Harrison, L.C., Knip, M., Forbes, J.M., 2011. Advanced Glycation End Products are direct modulators of β -cell function. *Diabetes* 60, 2523–2532. <https://doi.org/10.2337/db10-1033>
- Cozzolino, M., Diaz-Gimeno, P., Pellicer, A., Garrido, N., 2020. Evaluation of the endometrial receptivity assay and the preimplantation genetic test for aneuploidy in overcoming recurrent implantation failure. *J. Assist. Reprod. Genet.* 37, 2989–2997. <https://doi.org/10.1007/s10815-020-01948-7> ASSISTED
- Crosby, D.A., Glover, L.E., Brennan, E.P., Kelly, P., Cormican, P., Moran, B., Giangrazi, F., Downey, P., Mooney, E.E., Loftus, B.J., McAuliffe, F.M., Wingfield, M., O’Farrelly, C., Brennan, D.J., 2020. Dysregulation of the interleukin-17A pathway in endometrial tissue from women with unexplained infertility affects pregnancy outcome following assisted reproductive treatment. *Hum. Reprod.* 35, 1875–1888. <https://doi.org/10.1093/humrep/deaa111>
- Csongová, M., Gurecká, R., Koborová, I., Celec, P., Domonkos, E., Uličná, O., Somoza, V., Šebeková, K., 2018. The effects of a maternal advanced glycation end product-rich diet on somatic features, reflex ontogeny and metabolic parameters of offspring mice. *Food Funct.* 9, 3432–3446. <https://doi.org/10.1039/c8fo00183a>
- Csongová, M., Renczés, E., Šarayová, V., Mihalovičová, L., Janko, J., Gurecká, R., Troise, A.D., Vitaglione, P., Šebeková, K., 2019. Maternal consumption of a diet rich in maillard reaction products accelerates neurodevelopment in F1 and sex-dependently affects behavioral phenotype in F2 rat offspring. *Foods* 8, 1–22. <https://doi.org/10.3390/foods8050168>
- Cuman, C., Van Sinderen, M., Gantier, M.P., Rainczuk, K., Sorby, K., Rombauts, L., Osianlis, T., Dimitriadis, E., 2015. Human Blastocyst Secreted microRNA Regulate Endometrial Epithelial Cell Adhesion. *EBioMedicine* 2, 1528–1535. <https://doi.org/10.1016/j.ebiom.2015.09.003>
- Dall, E., Brandstetter, H., 2016. Structure and function of legumain in health and disease. *Biochimie* 122, 126–150. <https://doi.org/10.1016/j.biochi.2015.09.022>
- Dardik, A., Schultz, R.M., 1991. Blastocoel expansion in the preimplantation mouse embryo: Stimulatory effect of TGF- α and EGF. *Development* 113, 919–930.
- Deane, R., Singh, I., Sagare, A.P., Bell, R.D., Ross, N.T., LaRue, B., Love, R., Perry, S., Paquette, N.,

- Deane, R.J., Thiyagarajan, M., Zarcone, T., Fritz, G., Friedman, A.E., Miller, B.L., Zlokovic, B. V., 2012. A multimodal RAGE-specific inhibitor reduces amyloid β -mediated brain disorder in a mouse model of Alzheimer disease. *J. Clin. Invest.* 122, 1377–1392.
<https://doi.org/10.1172/JCI58642>
- Del Canto, M., Coticchio, G., Renzini, M., De Ponti, E., Novara, P. V., Bramillasca, F., Comi, R., Fadini, R., 2012. Cleavage kinetics analysis of human embryos predicts development to blastocyst and implantation. *Reprod. Biomed. Online* 25, 474–480.
<https://doi.org/10.1016/j.rbmo.2012.07.016>
- Deo, P., Keogh, J.B., Price, N.J., Clifton, P.M., 2017. Effects of weight loss on advanced glycation end products in subjects with and without diabetes: A preliminary report. *Int. J. Environ. Res. Public Health* 14, 1553. <https://doi.org/10.3390/ijerph14121553>
- DeUgarte, D.A., DeUgarte, C.M., Sahakian, V., 2010. Surrogate obesity negatively impacts pregnancy rates in third-party reproduction. *Fertil. Steril.* 93, 1008–1010.
<https://doi.org/10.1016/j.fertnstert.2009.07.1005>
- Diamanti-Kandarakis, E., Piperi, C., Kalofoutis, A., Creatsas, G., 2005. Increased levels of serum advanced glycation end-products in women with polycystic ovary syndrome. *Clin. Endocrinol. (Oxf)*. 62, 37–43. <https://doi.org/10.1111/j.1365-2265.2004.02170.x>
- Díaz-Gimeno, P., Horcajadas, J.A., Martínez-Conejero, J.A., Esteban, F.J., Alama, P., Pellicer, A., Simon, C., 2011. A genomic diagnostic tool for human endometrial receptivity based on the transcriptomic signature. *Fertil. Steril.* 95, 50–60.
<https://doi.org/10.1016/j.fertnstert.2010.04.063>
- Díaz-Gimeno, P., Ruiz-Alonso, M., Blesa, D., Bosch, N., Martínez-Conejero, J.A., Alamá, P., Garrido, N., Pellicer, A., Simón, C., 2013. The accuracy and reproducibility of the endometrial receptivity array is superior to histology as a diagnostic method for endometrial receptivity. *Fertil. Steril.* 99, 508–517. <https://doi.org/10.1016/j.fertnstert.2012.09.046>
- Dimitriadis, E., Nie, G., Hannan, N.J., Paiva, P., Salamonsen, L.A., 2010. Local regulation of implantation at the human fetal-maternal interface. *Int. J. Dev. Biol.* 54, 313–322.
<https://doi.org/10.1387/ijdb.082772ed>
- Dimitriadis, E., White, C.A., Jones, R.L., Salamonsen, L.A., 2005. Cytokines, chemokines and growth factors in endometrium related to implantation. *Hum. Reprod. Update* 11, 613–630.
<https://doi.org/10.1093/humupd/dmi023>
- Domar, A., Zuttermeister, P., Friedman, R., 1993. The psychological impact of infertility: A comparison with patients with other medical conditions. *J. Psychosom. Obstet. Gynecol.*
- Domínguez, F., Garrido-Gómez, T., López, J.A., Camafeita, E., Quiñonero, A., Pellicer, A., Simón, C., 2009. Proteomic analysis of the human receptive versus non-receptive endometrium using differential in-gel electrophoresis and MALDI-MS unveils stathmin 1 and annexin A2 as differentially regulated. *Hum. Reprod.* 24, 2607–2617.
<https://doi.org/10.1093/humrep/dep230>
- Donczo, B., Kiraly, G., Guttman, A., 2019. Effect of the elapsed time between sampling and formalin

- fixation on the N-glycosylation profile of mouse tissue specimens. *Electrophoresis* 40, 3057–3061. <https://doi.org/10.1002/elps.201900109>
- Dong, L., Zhou, Q., Zhang, Z., Zhu, Y., Duan, T., Feng, Y., 2012. Metformin sensitizes endometrial cancer cells to chemotherapy by repressing glyoxalase I expression. *J. Obstet. Gynaecol. Res.* 38, 1077–1085. <https://doi.org/10.1111/j.1447-0756.2011.01839.x>
- Dossenbach-Glaninger, A., van Trotsenburg, M., Schneider, B., Oberkanins, C., Hopmeier, P., 2008. ACE I/D polymorphism and recurrent first trimester pregnancy loss: interaction with SERPINE1 4G/5G and F13 VAL34Leu polymorphisms. *Br. J. Haematol.* 141, 269–271. <https://doi.org/10.1111/j.1365-2141.2008.07031.x>
- Edgell, T.A., Evans, J., Lazzaro, L., Boyes, K., Sridhar, M., Catt, S., Rombauts, L.J.F., Vollenhoven, B.J., Salamonsen, L.A., 2018. Assessment of potential biomarkers of pre-receptive and receptive endometrium in uterine fluid and a functional evaluation of the potential role of CSF3 in fertility. *Cytokine* 111, 222–229. <https://doi.org/10.1016/j.cyto.2018.08.026>
- Emera, D., Romero, R., Wagner, G., 2012. The evolution of menstruation: A new model for genetic assimilation: Explaining molecular origins of maternal responses to fetal invasiveness. *BioEssays* 34, 26–35. <https://doi.org/10.1002/bies.201100099>
- Emori, C., Sugiura, K., 2014. Role of oocyte-derived paracrine factors in follicular development. *Anim. Sci. J.* 85, 627–33. <https://doi.org/10.1111/asj.12200>
- Eslani, M., Movahedan, A., Afsharkhamseh, N., Sroussi, H., Djalilian, A.R., 2014. The role of toll-like receptor 4 in corneal epithelial wound healing. *Investig. Ophthalmol. Vis. Sci.* 55, 6108–6115. <https://doi.org/10.1167/iovs.14-14736>
- Evans, J., Catalano, R.D., Morgan, K., Critchley, H.O.D., Millar, R.P., Jabbour, H.N., 2008. Prokineticin 1 Signaling and Gene Regulation in Early Human Pregnancy. *Endocrinology* 149, 2877–2887. <https://doi.org/10.1210/en.2007-1633>
- Evans, J., Hannan, N.J., Hincks, C., Rombauts, L.J.F., Salamonsen, L.A., 2012. Defective Soil for a Fertile Seed ? Altered Endometrial Development Is Detrimental to Pregnancy Success 7, 1–12. <https://doi.org/10.1371/journal.pone.0053098>
- Evans, J., Hutchison, J., Salamonsen, L.A., Greening, D.W., 2020a. Proteomic Insights into Endometrial Receptivity and Embryo-Endometrial Epithelium Interaction for Implantation Reveal Critical Determinants of Fertility. *Proteomics* 20, e1900250. <https://doi.org/10.1002/pmic.201900250>
- Evans, J., Salamonsen, L.A., 2014. Decidualized Human Endometrial Stromal Cells Are Sensors of Hormone Withdrawal in the Menstrual Inflammatory Cascade. *Biol. Reprod.* 90, 1–12. <https://doi.org/10.1095/biolreprod.113.108175>
- Evans, J., Salamonsen, L.A., 2012. Inflammation, leukocytes and menstruation. *Rev. Endocr. Metab. Disord.* 13, 277–288. <https://doi.org/10.1007/s11154-012-9223-7>
- Evans, J., Salamonsen, L.A., Winship, A., Menkhorst, E., Nie, G., Gargett, C.E., Dimitriadis, E., 2016. Fertile ground : human endometrial programming and lessons in health and disease. *Nat. Rev. Endocrinol.* 12, 654–667. <https://doi.org/10.1038/nrendo.2016.116>

- Evans, J., Walker, K.J., Bilandzic, M., Kinnear, S., Salamonsen, L.A., 2020b. A novel “ embryo-endometrial ” adhesion model can potentially predict “ receptive ” or “ non-receptive ” endometrium. *J. Assist. Reprod. Genet.* 37, 5–16. <https://doi.org/10.1007/s10815-019-01629-0>
- Fahey, J. V., Schaefer, T.M., Channon, J.Y., Wira, C.R., 2005. Secretion of cytokines and chemokines by polarized human epithelial cells from the female reproductive tract. *Hum. Reprod.* 20, 1439–1446. <https://doi.org/10.1093/humrep/deh806>
- Fan, M., Li, X., Gao, X., Dong, L., Xin, G., Chen, L., Qiu, J., Xu, Y., 2019. LPS Induces Preeclampsia-Like Phenotype in Rats and HTR8/SVneo Cells Dysfunction Through TLR4/p38 MAPK Pathway. *Front. Physiol.* 10. <https://doi.org/10.3389/fphys.2019.01030>
- Fazeli, A., Bruce, C., Anumba, D.O., 2005. Characterization of Toll-like receptors in the female reproductive tract in humans. *Hum. Reprod.* 20, 1372–1378. <https://doi.org/10.1093/humrep/deh775>
- Fedorcsak, P., Dale, P., Storeng, R., Ertzeid, G., Bjercke, S., Oldereid, N., Omland, A.K., Abyholm, T., Tanbo, T., 2004. Impact of overweight and underweight on assisted reproduction treatment. *Hum. Reprod.* 19, 2523–2528. <https://doi.org/10.1093/humrep/deh485>
- Ferrick, L., Lee, Y.S.L., Gardner, D.K., 2020. Metabolic activity of human blastocysts correlates with their morphokinetics, morphological grade, KIDScore and artificial intelligence ranking. *Hum. Reprod.* 35, 2004–2016. <https://doi.org/10.1093/humrep/deaa181>
- Feuerecker, B., Pirsig, S., Seidl, C., Aichler, M., Feuchtinger, A., Bruchelt, G., Senekowitsch-Schmidtko, R., 2012. Lipoic acid inhibits cell proliferation of tumor cells in vitro and in vivo. *Cancer Biol. Ther.* 13, 1425–1435. <https://doi.org/10.4161/cbt.22003>
- Filant, J., Spencer, T.E., 2013. Endometrial Glands Are Essential for Blastocyst Implantation and Decidualization in the Mouse Uterus. *Biol. Reprod.* 88. <https://doi.org/10.1095/biolreprod.113.107631>
- Finger, B.J., Harvey, A.J., Green, M.P., Gardner, D.K., 2015. Combined parental obesity negatively impacts preimplantation mouse embryo development, kinetics, morphology and metabolism. *Hum. Reprod.* 30, 2084–2096. <https://doi.org/10.1093/humrep/dev142>
- Fitzgerald, H.C., Dhakal, P., Behura, S.K., Schust, D.J., Spencer, T.E., 2019. Self-renewing endometrial epithelial organoids of the human uterus. *Proc. Natl. Acad. Sci. U. S. A.* 116, 23132–23142. <https://doi.org/10.1073/pnas.1915389116>
- Fitzgerald, H.C., Salamonsen, L.A., Rombauts, L.J.R., Vollenhoven, B.J., Edgell, T.A., 2016. The proliferative phase underpins endometrial development: Altered cytokine profiles in uterine lavage fluid of women with idiopathic infertility. *Cytokine* 88, 12–19. <https://doi.org/10.1016/j.cyto.2016.08.001>
- Fitzgerald, H.C., Schust, D.J., Spencer, T.E., 2021. In vitro models of the human endometrium: evolution and application for women’s health+. *Biol. Reprod.* 104, 282–293. <https://doi.org/10.1093/biolre/iaaa183>
- Fortune, J.E., 1994. Ovarian follicular growth and development in mammals. *Biol. Reprod.* 50, 225–232. <https://doi.org/10.1095/biolreprod50.2.225>

- Francisco, F.A., Barella, L.F., Silveira, S. da S., Saavedra, L.P.J., Prates, K.V., Alves, V.S., Franco, C.C. da S., Miranda, R.A., Ribeiro, T.A., Tófolo, L.P., Malta, A., Vieira, E., Palma-Rigo, K., Pavanello, A., Martins, I.P., Moreira, V.M., de Oliveira, J.C., Mathias, P.C. de F., Gomes, R.M., 2018. Methylglyoxal treatment in lactating mothers leads to type 2 diabetes phenotype in male rat offspring at adulthood. *Eur. J. Nutr.* 57, 477–486. <https://doi.org/10.1007/s00394-016-1330-x>
- Fujii, E.Y., Nakayama, M., 2010. The measurements of RAGE, VEGF, and AGEs in the plasma and follicular fluid of reproductive women: the influence of aging. *Fertil. Steril.* 94, 694–700. <https://doi.org/10.1016/j.fertnstert.2009.03.029>
- Fujii, E.Y., Nakayama, M., Nakagawa, A., 2008. Concentrations of receptor for advanced glycation end products, VEGF and CML in plasma, follicular fluid, and peritoneal fluid in women with and without endometriosis. *Reprod. Sci.* 15, 1066–1074. <https://doi.org/10.1177/1933719108323445>
- Gardner, D.K., 2016. The impact of physiological oxygen during culture, and vitrification for cryopreservation, on the outcome of extended culture in human IVF. *Reprod. Biomed. Online* 32, 137–141. <https://doi.org/10.1016/j.rbmo.2015.11.008>
- Gardner, D.K., 2015. Lactate production by the mammalian blastocyst: Manipulating the microenvironment for uterine implantation and invasion? *BioEssays* 37, 364–371. <https://doi.org/10.1002/bies.201400155>
- Gardner, D.K., Harvey, A.J., 2015. Blastocyst metabolism. *Reprod. Fertil. Dev.* 27, 638–654. <https://doi.org/10.1071/RD14421>
- Gardner, D.K., Lane, M., Schoolcraft, W.B., 2002. Physiology and culture of the human blastocyst. *J. Reprod. Immunol.* 55, 85–100. [https://doi.org/10.1016/S0165-0378\(01\)00136-X](https://doi.org/10.1016/S0165-0378(01)00136-X)
- Gardner, D.K., Lane, M., Stevens, J., Schlenker, T., Schoolcraft, W.B., 2000a. Blastocyst score affects implantation and pregnancy outcome: Towards a single blastocyst transfer. *Fertil. Steril.* 73, 1155–1158. [https://doi.org/10.1016/S0015-0282\(00\)00518-5](https://doi.org/10.1016/S0015-0282(00)00518-5)
- Gardner, D.K., Schoolcraft, W.B., McMillan, W.H., 2000b. What is the rate limiting factor at implantation: embryo quality or endometrial receptivity? *Va. Med.* 76, S154.
- Gargett, C.E., Ph, D., Ye, L., Ph, D., 2012. Endometrial reconstruction from stem cells. *Fertil. Steril.* 98, 11–20. <https://doi.org/10.1016/j.fertnstert.2012.05.004>
- Gąsiorowski, K., Brokos, B., Echeverria, V., Barreto, G.E., Leszek, J., 2018. RAGE-TLR Crosstalk Sustains Chronic Inflammation in Neurodegeneration. *Mol. Neurobiol.* 55, 1463–1476. <https://doi.org/10.1007/s12035-017-0419-4>
- Ghelani, H., Razmovski-Naumovski, V., Pragada, R.R., Nammi, S., 2018. (R)- α -Lipoic acid inhibits fructose-induced myoglobin fructation and the formation of advanced glycation end products (AGEs) in vitro. *BMC Complement. Altern. Med.* 18, 1–11. <https://doi.org/10.1186/s12906-017-2076-6>
- Giacomini, E., Vago, R., Sanchez, A.M., Podini, P., Zarovni, N., Murdica, V., Rizzo, R., Bortolotti, D., Candiani, M., Viganò, P., 2017. Secretome of in vitro cultured human embryos contains extracellular vesicles that are uptaken by the maternal side. *Sci. Rep.* 7, 1–13.

- <https://doi.org/10.1038/s41598-017-05549-w>
- Girda, E., Huang, E.C., Leiserowitz, G.S., Smith, L.H., 2017. The use of endometrial cancer Patient Derived organoid culture for drug sensitivity testing is feasible. *Int. J. Gynecol. Cancer* 27, 1701–1707. <https://doi.org/10.1097/IGC.0000000000001061>
- Giudice, L.C., 2020. Multidimensional transcriptomic mapping of human endometrium at single-cell resolution. *Nat. Med.* 26, 1513–1514. <https://doi.org/10.1038/s41591-020-1075-1>
- Goldman, K.N., Hodes-Wertz, B., McCulloh, D.H., Flom, J.D., Grifo, J.A., 2015. Association of body mass index with embryonic aneuploidy. *Fertil. Steril.* 103, 744–748. <https://doi.org/10.1016/j.fertnstert.2014.11.029>
- Goldstein, J.A., Gallagher, K., Beck, C., Kumar, R., Gernand, A.D., 2020. Maternal-Fetal Inflammation in the Placenta and the Developmental Origins of Health and Disease. *Front. Immunol.* 11, 1–14. <https://doi.org/10.3389/fimmu.2020.531543>
- Gong, P., Liu, M., Hong, G., Li, Y., Xue, P., Zheng, M., Wu, M., Shen, L., Yang, M., Diao, Z., Hu, Y., 2016. Curcumin improves LPS-induced preeclampsia-like phenotype in rat by inhibiting the TLR4 signaling pathway. *Placenta* 41, 45–52. <https://doi.org/10.1016/j.placenta.2016.03.002>
- Gray, C.A., Bartol, F.F., Tarleton, B.J., Wiley, A.A., Johnson, G.A., Bazer, F.W., Spencer, T.E., 2001. Developmental Biology of Uterine Glands. *Biol. Reprod.* 65, 1311–1323.
- Gray, C.A., Bartol, F.F., Taylor, K.M., Wiley, a a, Ramsey, W.S., Ott, T.L., Bazer, F.W., Spencer, T.E., 2000. Ovine uterine gland knock-out model: effects of gland ablation on the estrous cycle. *Biol. Reprod.* 62, 448–56. <https://doi.org/10.1095/biolreprod62.2.448>
- Gray, C.A., Burghardt, R.C., Johnson, G.A., Bazer, F.W., Spencer, T.E., 2002. Evidence that absence of endometrial gland secretions in uterine gland knockout ewes compromises conceptus survival and elongation 289–300.
- Greening, D.W., Nguyen, H.P.T., Elgass, K., Simpson, R.J., Salamonsen, L.A., 2016a. Human Endometrial Exosomes Contain Hormone-Specific Cargo Modulating Trophoblast Adhesive Capacity: Insights into Endometrial-Embryo Interactions1. *Biol. Reprod.* 94, 1–15. <https://doi.org/10.1095/biolreprod.115.134890>
- Greening, D.W., Nguyen, H.P.T., Evans, J., Simpson, R.J., Salamonsen, L.A., 2016b. Modulating the endometrial epithelial proteome and secretome in preparation for pregnancy: The role of ovarian steroid and pregnancy hormones. *J. Proteomics* 144, 99–112. <https://doi.org/10.1016/j.jprot.2016.05.026>
- Griffith, O.W., Chavan, A.R., Protopapas, S., Maziarz, J., Romero, R., Wagner, G.P., 2017. Embryo implantation evolved from an ancestral inflammatory attachment reaction. *Proc. Natl. Acad. Sci. U. S. A.* 114, E6566–E6575. <https://doi.org/10.1073/pnas.1701129114>
- Gu, X.W., Yang, Y., Li, T., Chen, Z.C., Fu, T., Pan, J.M., Ou, J.P., Yang, Z.M., 2020. ATP mediates the interaction between human blastocyst and endometrium. *Cell Prolif.* 53. <https://doi.org/10.1111/cpr.12737>
- Guedes-Martins, L., Matos, L., Soares, A., Silva, E., Almeida, H., 2013. AGEs , contributors to placental

- bed vascular changes leading to preeclampsia. *Free Radic. Res.* 47, 70–80.
<https://doi.org/10.3109/10715762.2013.815347>
- Guilbaud, A., Niquet-Leridon, C., Boulanger, E., Tessier, F., 2016. How Can Diet Affect the Accumulation of Advanced Glycation End-Products in the Human Body? *Foods* 5, 84.
<https://doi.org/10.3390/foods5040084>
- Guillomot, M., Fléchon, J.E., Wintenberger-Torres, S., 1981. Conceptus attachment in the Ewe: an ultrastructural study. *Placenta* 2, 169–182. [https://doi.org/10.1016/S0143-4004\(81\)80021-5](https://doi.org/10.1016/S0143-4004(81)80021-5)
- Gurner, K.H., Truong, T.T., Harvey, A.J., Gardner, D.K., 2020. A combination of growth factors and cytokines alter preimplantation mouse embryo development, fetal development and gene expression profiles. *Mol. Hum. Reprod.* 26, 953–970. <https://doi.org/10.1093/molehr/gaaa072>
- Gurung, S., Greening, D.W., Catt, S., Salamonsen, L., Evans, J., 2020. Exosomes and soluble secretome from hormone-treated endometrial epithelial cells direct embryo implantation. *Mol. Hum. Reprod.* 27–31. <https://doi.org/10.1093/molehr/gaaa034>
- Haider, S., Gamperl, M., Burkard, T.R., Kunihs, V., Kaindl, U., Junttila, S., Fiala, C., Schmidt, K., Mendjan, S., Knöfler, M., Latos, P.A., 2019. Estrogen Signaling Drives Ciliogenesis in Human Endometrial Organoids. *Endocrinology* 160, 2282–2297. <https://doi.org/10.1210/en.2019-00314>
- Haider, S., Meinhardt, G., Saleh, L., Kunihs, V., Gamperl, M., Kaindl, U., Ellinger, A., Burkard, T.R., Fiala, C., Pollheimer, J., Mendjan, S., Latos, P.A., Knöfler, M., 2018. Self-Renewing Trophoblast Organoids Recapitulate the Developmental Program of the Early Human Placenta. *Stem Cell Reports* 11, 537–551. <https://doi.org/10.1016/j.stemcr.2018.07.004>
- Haller, M., Yin, Y., Ma, L., 2019. Development and utilization of human decidualization reporter cell line uncovers new modulators of female fertility. *Proc. Natl. Acad. Sci. U. S. A.* 116, 19541–19551. <https://doi.org/10.1073/pnas.1907652116>
- Han, S.W., Lei, Z.M., Rao, C. V, 1996. Up-regulation of cyclooxygenase-2 gene expression by chorionic gonadotropin during the differentiation of human endometrial stromal cells into decidua. *Endocrinology* 137, 1791–1797. <https://doi.org/10.1210/endo.137.5.8612516>
- Han, V.X., Patel, S., Jones, H.F., Nielsen, T.C., Mohammad, S.S., Hofer, M.J., Gold, W., Brilot, F., Lain, S.J., Nassar, N., Dale, R.C., 2021. Maternal acute and chronic inflammation in pregnancy is associated with common neurodevelopmental disorders: a systematic review. *Transl. Psychiatry* 11. <https://doi.org/10.1038/s41398-021-01198-w>
- Hannan, N.J., Paiva, P., Dimitriadis, E., Salamonsen, L.A., 2010. Models for Study of Human Embryo Implantation : Choice of Cell Lines? *Biol. Reprod.* 82, 235–245.
<https://doi.org/10.1095/biolreprod.109.077800>
- Hannan, N.J., Pavia, P., Meehan, K.L., Rombauts, L.J.F., Gardner, D.K., Salamonsen, L.A., 2011. Analysis of Fertility-Related Soluble Mediators in Human Uterine Fluid Identifies VEGF as a Key Regulator of Embryo Implantation. *Endocrinology* 152, 4948–4956.
<https://doi.org/10.1210/en.2011-1248>
- Hao, L., Noguchi, S., Kamada, Y., Sasaki, A., Matsuda, M., Shimizu, K., Hiramatsu, Y., Nakatsuka, M.,

2008. Adverse effects of Advanced Glycation End Products on embryonal development. *Acta Med. Okayama* 62, 93–99.
- Haragan, A., Liebler, D.C., Das, D.M., Soper, M.D., Morrison, R.D., Slebos, R.J.C., Ackermann, B.L., Fill, J.A., Schade, A.E., Gosney, J.R., Gruver, A.M., 2020. Accelerated instability testing reveals quantitative mass spectrometry overcomes specimen storage limitations associated with PD-L1 immunohistochemistry. *Lab. Investig.* 100, 874–886. <https://doi.org/10.1038/s41374-019-0366-y>
- Harden, J.L., Lewis, S.M., Lish, S.R., Suárez-Fariñas, M., Gareau, D., Lentini, T., Johnson-Huang, L.M., Krueger, J.G., Lowes, M.A., 2016. The tryptophan metabolism enzyme L-kynureninase is a novel inflammatory factor in psoriasis and other inflammatory diseases. *J. Allergy Clin. Immunol.* 137, 1830–1840. <https://doi.org/10.1016/j.jaci.2015.09.055>
- Hardy, K., Handyside, A.H., Winston, R.M., 1989. The human blastocyst: cell number, death and allocation during late preimplantation development in vitro. *Development* 107, 597–604.
- Hatchell, E.C., Colley, S.M., Beveridge, D.J., Epis, M.R., Stuart, L.M., Giles, K.M., Redfern, A.D., Miles, L.E.C., Barker, A., MacDonald, L.M., Arthur, P.G., Lui, J.C.K., Golding, J.L., McCulloch, R.K., Metcalf, C.B., Wilce, J.A., Wilce, M.C.J., Lanz, R.B., O'Malley, B.W., Leedman, P.J., 2006. SLIRP, a Small SRA Binding Protein, Is a Nuclear Receptor Corepressor. *Mol. Cell* 22, 657–668. <https://doi.org/10.1016/j.molcel.2006.05.024>
- Haucke, E., Navarrete Santos, Alexander, Simm, A., Henning, C., Glomb, M.A., Gürke, J., Schindler, M., Fischer, B., Navarrete Santos, Anne, 2014. Accumulation of advanced glycation end products in the rabbit blastocyst under maternal diabetes. *Reproduction* 148, 169–178. <https://doi.org/10.1530/REP-14-0149>
- Hayashi, C.M., Nagai, R., Miyazaki, K., Hayase, F., Araki, T., Ono, T., Horiuchi, S., 2002. Conversion of Amadori products of the Maillard reaction to N ϵ -(carboxymethyl)lysine by short-term heating: Possible detection of artifacts by immunohistochemistry. *Lab. Investig.* 82, 795–807. <https://doi.org/10.1097/01.lab.0000018826.59648.07>
- Heerwagen, M.J.R., Miller, M.R., Barbour, L.A., Friedman, J.E., 2010. Maternal obesity and fetal metabolic programming: a fertile epigenetic soil. *AJP Regul. Integr. Comp. Physiol.* 299, R711–R722. <https://doi.org/10.1152/ajpregu.00310.2010>
- Heng, S., Hannan, N.J., Rombauts, L.J.F., Salamonsen, L.A., Nie, G., 2011. PC6 levels in uterine lavage are closely associated with uterine receptivity and significantly lower in a subgroup of women with unexplained infertility 26, 840–846. <https://doi.org/10.1093/humrep/der002>
- Heng, S., Paule, S.G., Ying, L., Rombauts, L.J., Vollenhoven, B., Salamonsen, L.A., Nie, G., 2015. Posttranslational removal of α -dystroglycan N terminus by PC5/6 cleavage is important for uterine preparation for embryo implantation in women. *FASEB J.* 29, 4011–4022. <https://doi.org/10.1096/fj.14-269456>
- Hlinka, D., Kal'atova, B., Uhrinova, I., Dolinska, S., Rutarova, J., Rezacova, J., Lazarovska, S., Dudas, M., 2012. Time-lapse cleavage rating predicts human embryo viability. *Physiol. Res.* 61, 513–525. <https://doi.org/10.1016/j.rbmo.2012.07.016>

- Hoad, C.L., Raine-Fenning, N.J., Fulford, J., Campbell, B.K., Johnson, I.R., Gowland, P.A., 2005. Uterine tissue development in healthy women during the normal menstrual cycle and investigations with magnetic resonance imaging. *Am. J. Obstet. Gynecol.* 192, 648–654. <https://doi.org/10.1016/j.ajog.2004.07.032>
- Hogg, K., Western, P.S., 2015. Refurbishing the germline epigenome: Out with the old, in with the new. *Semin. Cell Dev. Biol.* 45, 104–113. <https://doi.org/10.1016/j.semcd.2015.09.012>
- Holdsworth-Carson, S.J., Chung, J., Sloggett, C., Mortlock, S., Fung, J.N., Montgomery, G.W., Dior, U.P., Healey, M., Rogers, P.A., Girling, J.E., 2020. Obesity does not alter endometrial gene expression in women with endometriosis. *Reprod. Biomed. Online* 41, 113–118. <https://doi.org/10.1016/j.rbmo.2020.03.015>
- Homer, H., Rice, G.E., Salomon, C., 2016. Embryo- and endometrium-derived exosomes and their potential role in assisted reproductive treatments-liquid biopsies for endometrial receptivity. *Placenta* 54, 89–94. <https://doi.org/10.1016/j.placenta.2016.12.011>
- Hong, S.G., Jang, G., Oh, H.J., Koo, O.J., Park, J.E., Park, H.J., Kang, S.K., Lee, B.C., 2009. The effects of brain-derived neurotrophic factor and metformin on in vitro developmental competence of bovine oocytes. *Zygote* 17, 187–193. <https://doi.org/10.1017/S0967199409005255>
- Horcajadas, J.A., Mínguez, P., Dopazo, J., Esteban, F.J., Domínguez, F., Giudice, L.C., Pellicer, A., Simón, C., 2008. Controlled Ovarian Stimulation Induces a Functional Genomic Delay of the Endometrium with Potential Clinical Implications. *J. Clin. Endocrinol. Metab.* 93, 4500–4510. <https://doi.org/10.1210/jc.2008-0588>
- Hou, Y.J., Zhu, C.C., Duan, X., Liu, H.L., Wang, Q., Sun, S.C., 2016. Both diet and gene mutation induced obesity affect oocyte quality in mice. *Sci. Rep.* 6, 18858. <https://doi.org/10.1038/srep18858>
- Houghton, F.D., Humpherson, P.G., Hawkhead, J.A., Hall, C.J., Leese, H.J., 2003. Na⁺, K⁺, ATPase activity in the human and bovine preimplantation embryo. *Dev. Biol.* 263, 360–366. <https://doi.org/10.1016/j.ydbio.2003.07.014>
- Hu, H., Tian, M., Ding, C., Yu, S., 2019. The C/EBP homologous protein (CHOP) transcription factor functions in endoplasmic reticulum stress-induced apoptosis and microbial infection. *Front. Immunol.* 9, 3083. <https://doi.org/10.3389/fimmu.2018.03083>
- Huang, Q.T., Zhang, M., Zhong, M., Yu, Y.H., Liang, W.Z., Hang, L.L., Gao, Y.F., Huang, L.P., Wang, Z.J., 2013. Advanced glycation end products as an upstream molecule triggers ROS-induced sFlt-1 production in extravillous trophoblasts: A novel bridge between oxidative stress and preeclampsia. *Placenta* 34, 1177–1182. <https://doi.org/10.1016/j.placenta.2013.09.017>
- Huang, T.T.F., Chinn, K., Kosasa, T., Ahn, H.J., Kessel, B., 2016. Morphokinetics of human blastocyst expansion in vitro. *Reprod. Biomed. Online* 33, 659–667. <https://doi.org/10.1016/j.rbmo.2016.08.020>
- Huang, Y., Zhu, X.Y., Du, M.R., Wu, X., Wang, M.Y., Li, D.J., 2006. Chemokine CXCL16, a scavenger receptor, induces proliferation and invasion of first-trimester human trophoblast cells in an autocrine manner. *Hum. Reprod.* 21, 1083–1091. <https://doi.org/10.1093/humrep/dei436>

- Huch, M., Knoblich, J.A., Lutolf, M.P., Martinez-Arias, A., 2017. The hope and the hype of organoid research. *Development* 144, 938–941. <https://doi.org/10.1242/dev.150201>
- Insogna, I.G., Lee, M.S., Reimers, R.M., Toth, T.L., 2017. Neutral effect of body mass index on implantation rate after frozen-thawed blastocyst transfer. *Fertil. Steril.* 108, 770–776. <https://doi.org/10.1016/j.fertnstert.2017.08.024>
- Institute, A., 2017. A Picture of Overweight and Obesity in Australia 2017.
- Ishibashi, Y., Yamagishi, S.I., Matsui, T., Ohta, K., Tanoue, R., Takeuchi, M., Ueda, S., Nakamura, K.I., Okuda, S., 2012. Pravastatin inhibits advanced glycation end products (AGEs)-induced proximal tubular cell apoptosis and injury by reducing receptor for AGEs (RAGE) level. *Metabolism.* 61, 1067–1072. <https://doi.org/10.1016/j.metabol.2012.01.006>
- Jackson, L.R., Farin, C.E., Whisnant, S., 2012. Tumor necrosis factor alpha inhibits in vitro bovine embryo development through a prostaglandin mediated mechanism. *J. Anim. Sci. Biotechnol.* 3. <https://doi.org/10.1186/2049-1891-3-7>
- Jakubowicz, D.J., Luorno, M.J., Jakubowicz, S., Roberts, K.A., Nestler, J.E., 2014. Effects of Metformin on Early Pregnancy Loss in the Polycystic Ovary Syndrome. *J. Clin. Endocrinol. Metab.* 87, 524–529. <https://doi.org/10.1210/jcem.87.2.8207>
- Jarrell, J., 2018. The Significance and Evolution of Menstruation. *Best Pract. Res. Clin. Obstet. Gynaecol.* 1–9. <https://doi.org/10.1016/j.bpobgyn.2018.01.007>
- Jin, Q., Chen, H., Luo, A., Ding, F., Liu, Z., 2011. S100A14 stimulates cell proliferation and induces cell apoptosis at different concentrations via receptor for advanced glycation end products (RAGE). *PLoS One* 6. <https://doi.org/10.1371/journal.pone.0019375>
- Jin, Z., Liu, H., Xu, C., 2020. Estrogen degrades Scribble in endometrial epithelial cells through E3 ubiquitin ligase HECW1 in the development of diffuse adenomyosis. *Biol. Reprod.* 102, 376–387. <https://doi.org/10.1093/biolre/ioz194>
- Jinno, M., Kondou, K., Teruya, K., 2010. Low-dose metformin improves pregnancy rate in in vitro fertilization repeaters without polycystic ovary syndrome: Prediction of effectiveness by multiple parameters related to insulin resistance. *Hormones* 9, 161–170. <https://doi.org/10.14310/horm.2002.1266>
- Jinno, M., Takeuchi, M., Watanabe, A., Teruya, K., Hirohama, J., Eguchi, N., Miyazaki, A., 2011. Advanced glycation end-products accumulation compromises embryonic development and achievement of pregnancy by assisted reproductive technology. *Hum. Reprod.* 26, 604–610. <https://doi.org/10.1093/humrep/deq388>
- Johannisson, E., Landgren, B.-M., Rohr, H.P., Diczfalusy, E., 1987. Endometrial morphology and peripheral hormone levels in women with regular menstrual cycles. *Fertil. Steril.* 48, 401–408. [https://doi.org/10.1016/S0015-0282\(16\)59406-0](https://doi.org/10.1016/S0015-0282(16)59406-0)
- John, N.T., Linke, M., Denker, H.W., 1993. Quantitation of Human Choriocarcinoma Spheroid Attachment to Uterine Epithelial Cell Monolayers. *In Vitro Cell. Dev. Biol. Anim.* 29A, 461–468.
- Jones, R.L., Stoikos, C., Findlay, J.K., Salamonsen, L.A., 2006. TGF- β superfamily expression and

- actions in the endometrium and placenta. *Reproduction* 132, 217–232.
<https://doi.org/10.1530/rep.1.01076>
- Jungheim, E.S., Schoeller, E.L., Marguard, K.L., Louden, E.D., Schaffer, J.E., Moley, K.H., 2010. Diet-induced obesity model: abnormal oocytes and persistent growth abnormalities in the offspring. *Endocrinology* 151, 4039–4046. <https://doi.org/10.1210/en.2010-0098>
- Jungheim, E.S., Schon, S.B., Schulte, M.B., Deugarte, D.A., Fowler, S.A., Tuuli, M.G., 2013. IVF outcomes in obese donor oocyte recipients: A systematic review and meta-analysis. *Hum. Reprod.* 28, 2720–2727. <https://doi.org/10.1093/humrep/det292>
- Kaitu'u-Lino, T.J., Ye, L., Gargett, C.E., 2010. Reepithelialization of the uterine surface arises from endometrial glands: Evidence from a functional mouse model of breakdown and repair. *Endocrinology* 151, 3386–3395. <https://doi.org/10.1210/en.2009-1334>
- Kasai, F., Hirayama, N., Ozawa, M., Iemura, M., Kohara, A., 2016. Changes of heterogeneous cell populations in the Ishikawa cell line during long-term culture: Proposal for an in vitro clonal evolution model of tumor cells. *Genomics* 107, 259–266.
<https://doi.org/10.1016/j.ygeno.2016.04.003>
- Kelleher, A.M., Burns, G.W., Behura, S., Wu, G., Spencer, T.E., 2016. Uterine glands impact uterine receptivity, luminal fluid homeostasis and blastocyst implantation. *Sci. Rep.* 6, 1–18.
<https://doi.org/10.1038/srep38078>
- Kelley, R.L., Gardner, D.K., 2016. Combined effects of individual culture and atmospheric oxygen on preimplantation mouse embryos in vitro. *Reprod. Biomed. Online* 33, 537–549.
<https://doi.org/10.1016/j.rbmo.2016.08.003>
- Kellow, N.J., Savige, G.S., 2013. Dietary advanced glycation end-product restriction for the attenuation of insulin resistance, oxidative stress and endothelial dysfunction: A systematic review. *Eur. J. Clin. Nutr.* 67, 239–248. <https://doi.org/10.1038/ejcn.2012.220>
- Kerby, A., Shingleton, D., Batra, G., Sharps, M.C., Baker, B.C., Heazell, A.E.P., 2021. Placental Morphology and Cellular Characteristics in Stillbirths in Women With Diabetes and Unexplained Stillbirths. *Arch. Pathol. Lab. Med.* 145, 82–89. <https://doi.org/10.5858/arpa.2019-0524-oa>
- Kermack, A.J., Finn-Sell, S., Cheong, Y.C., Brook, N., Eckert, J.J., Macklon, N.S., Houghton, F.D., 2015. Amino acid composition of human uterine fluid: Association with age, lifestyle and gynaecological pathology. *Hum. Reprod.* 30, 917–924. <https://doi.org/10.1093/humrep/dev008>
- Kinnear, S., Salamonsen, L.A., Francois, M., Harley, V., Evans, J., 2019. Uterine SOX17: a key player in human endometrial receptivity and embryo implantation. *Sci. Rep.* 9, 15495.
<https://doi.org/10.1038/s41598-019-51751-3>
- Konishi, H., Nakatsuka, M., Chekir, C., Noguchi, S., Kamada, Y., Sasaki, A., Hiramatsu, Y., 2004. Advanced glycation end products induce secretion of chemokines and apoptosis in human first trimester trophoblasts. *Hum. Reprod.* 19, 2156–2162. <https://doi.org/10.1093/humrep/deh389>
- Koschinsky, T., He, C.J., Mitsuhashi, T., Bucala, R., Liu, C., Buenting, C., Heitmann, K., Vlassara, H., 1997. Orally absorbed reactive glycation products (glycotoxins): An environmental risk factor in diabetic nephropathy. *Proc. Natl. Acad. Sci. U. S. A.* 94, 6474–6479.

- <https://doi.org/10.1073/pnas.94.12.6474>
- Kukushkina, V., Modhukur, V., Suhorutšenko, M., Peters, M., Mägi, R., Rahmioglu, N., Velthut-Meikas, A., Altmäe, S., Esteban, F.J., Vilo, J., Zondervan, K., Salumets, A., Laisk-Podar, T., 2017. DNA methylation changes in endometrium and correlation with gene expression during the transition from pre-receptive to receptive phase. *Sci. Rep.* 7, 1–11. <https://doi.org/10.1038/s41598-017-03682-0>
- Kume, S., Kato, S., Yamagishi, S.I., Inagaki, Y., Ueda, S., Arima, N., Okawa, T., Kojiro, M., Nagata, K., 2005. Advanced glycation end-products attenuate human mesenchymal stem cells and prevent cognate differentiation into adipose tissue, cartilage, and bone. *J. Bone Miner. Res.* 20, 1647–1658. <https://doi.org/10.1359/JBMR.050514>
- Kupka, M.S., Gnoth, C., Buehler, K., Dahncke, W., Kruessel, J.S., 2011. Impact of female and male obesity on IVF/ICSI: Results of 700,000 ART-cycles in Germany. *Gynecol. Endocrinol.* 27, 144–149. <https://doi.org/10.3109/09513590.2010.487617>
- Lane, M., Gardner, D.K., 1992. Effect of incubation volume and embryo density on the development and viability of mouse embryos in vitro. *Hum. Reprod.* 7, 558–562. <https://doi.org/10.1093/oxfordjournals.humrep.a137690>
- Lane, M., Zander-Fox, D.L., Robker, R.L., McPherson, N.O., 2015. Peri-conception parental obesity, reproductive health, and transgenerational impacts. *Trends Endocrinol. Metab.* 26, 84–90. <https://doi.org/10.1016/j.tem.2014.11.005>
- Lappas, M., Permezel, M., Rice, G.E., 2007. Advanced glycation endproducts mediate pro-inflammatory actions in human gestational tissues via nuclear factor- κ B and extracellular signal-regulated kinase 1/2. *J. Endocrinol.* 193, 269–277. <https://doi.org/10.1677/JOE-06-0081>
- Lashen, H., Fear, K., Sturdee, D.W., 2004. Obesity is associated with increased risk of first trimester and recurrent miscarriage : matched case-control study. *Hum. Reprod.* 19, 1644–1646. <https://doi.org/10.1093/humrep/deh277>
- Lathi, R.B., Ruiz, M., Gómez, E., Rincon-Bertolin, A., Blesa, D., Simón, C., 2014. Obesity and Endometrial Receptivity as Assessed by the Endometrial Receptivity Array (ERA). *Fertil. Steril.* 101, e30–e31. <https://doi.org/10.1016/j.fertnstert.2013.11.113>
- Leary, C., Leese, H.J., Sturmey, R.G., 2015. Human embryos from overweight and obese women display phenotypic and metabolic abnormalities. *Hum. Reprod.* 30, 122–132. <https://doi.org/10.1093/humrep/deu276>
- Lee, K.Y., DeMayo, F.J., 2004. Animal models of implantation. *Reproduction* 128, 679–695. <https://doi.org/10.1530/rep.1.00340>
- Lee, Y., Fong, S., Chen, A.C.H., Li, T., Yue, C., Lee, C., Ng, E.H.Y., Yeung, W.S.B., Lee, K., 2015. Establishment of a novel human embryonic stem cell-derived trophoblastic spheroid implantation model. *Hum. Reprod.* 30, 2614–2626. <https://doi.org/10.1093/humrep/dev223>
- Legro, R.S., Dodson, W.C., Kris-Etherton, P.M., Kunselman, A.R., Stetter, C.M., Williams, N.I., Gnatuk, C.L., Estes, S.J., Fleming, J., Allison, K.C., Sarwer, D.B., Coutifaris, C., Dokras, A., 2015. Randomized controlled trial of preconception interventions in infertile women with polycystic

- ovary syndrome. *J. Clin. Endocrinol. Metab.* 100, 4048–4058. <https://doi.org/10.1210/jc.2015-2778>
- Leonavicius, K., Royer, C., Preece, C., Davies, B., Biggins, J.S., Srinivas, S., 2018. Mechanics of mouse blastocyst hatching revealed by a hydrogel-based microdeformation assay. *Proc. Natl. Acad. Sci.* 115, 10375–10380. <https://doi.org/10.1073/pnas.1719930115>
- Lessey, B.A., 2011. Assessment of endometrial receptivity. *Fertil. Steril.* 96, 522–529. <https://doi.org/10.1016/j.fertnstert.2011.07.1095>
- Leung, C.Y., Zernicka-Goetz, M., 2015. Mapping the journey from totipotency to lineage specification in the mouse embryo. *Curr. Opin. Genet. Dev.* 34, 71–76. <https://doi.org/10.1016/j.gde.2015.08.002>
- Li, Y., Sun, X., Dey, S.K., 2016. Entosis allows timely elimination of the luminal epithelial barrier for embryo implantation. *Cell Rep.* 1848, 358–265. <https://doi.org/10.1016/j.celrep.2015.03.035>
- Liang, X.J., Choi, Y., Sackett, D.L., Park, J.K., 2008. Nitrosoureas inhibit the stathmin-mediated migration and invasion of malignant glioma cells. *Cancer Res.* 68, 5267–5272. <https://doi.org/10.1158/0008-5472.CAN-07-6482>
- Liao, M., Zhang, Y., Kang, J.H., Dufau, M.L., 2011. Coactivator function of Positive Cofactor 4 (PC4) in Sp1-directed Luteinizing Hormone Receptor (LHR) gene transcription. *J. Biol. Chem.* 286, 7681–7691. <https://doi.org/10.1074/jbc.M110.188532>
- Lim, H., Paria, B.C., Das, S.K., Dinchuk, J.E., Langenbach, R., Trzaskos, J.M., Dey, S.K., 1997. Multiple female reproductive failures in cyclooxygenase 2-deficient mice. *Cell* 91, 197–208. [https://doi.org/10.1016/S0092-8674\(00\)80402-X](https://doi.org/10.1016/S0092-8674(00)80402-X)
- Lopata, A., 1996. Blastocyst-endometrial interaction: An appraisal of some old and new ideas. *Mol. Hum. Reprod.* 2, 519–525. <https://doi.org/10.1093/molehr/2.7.519>
- Lopes, L.R., Ribeiro, S.M.L.T., Figueiredo, V.P., Leite, A.L.J., Nicolato, R.L. de C., Gomes, J.A.E., de Oliveira, F.L.P., Talvani, A., 2018. The overweight increases circulating inflammatory mediators commonly associated with obesity in young individuals. *Cytokine* 110, 169–173. <https://doi.org/10.1016/j.cyto.2018.04.024>
- Loset, M., Mundal, S.B., Johnson, M.P., Fenstad, M.H., Freed, K.A., Lian, I.A., Eide, I.P., BjorGe, L., Blangero, J., Moses, E., Rigmor, A., 2011. A transcriptional profile of the decidua in preeclampsia. *Am. J. Obstet. Gynecol.* 204, 84.e1-84.e27. <https://doi.org/doi:10.1016/j.ajog.2010.08.043>
- Loske, C., Neumann, A., Cunningham, A.M., Nichol, K., Schinzel, R., Riederer, P., Münch, G., 1998. Cytotoxicity of advanced glycation endproducts is mediated by oxidative stress. *J. Neural Transm.* 105, 1005–1015. <https://doi.org/10.1007/s007020050108>
- Louden, E.D., Luzzo, K.M., Jimenez, P.T., Chi, T., Chi, M., Moley, K.H., 2014. TallyHO obese female mice experience poor reproductive outcomes and abnormal blastocyst metabolism which is reversed by metformin. *Reprod. Fertil. Dev.* 27, 31–39. <https://doi.org/10.1071/RD14339.TallyHO>

- Lu, Y.C., Yeh, W.C., Ohashi, P.S., 2008. LPS/TLR4 signal transduction pathway. *Cytokine* 42, 145–151. <https://doi.org/10.1016/j.cyto.2008.01.006>
- Lucas, E.S., Vrljicak, P., Muter, J., Diniz-da-costa, M.M., Brighton, P.J., Kong, C., Lipecki, J., Fishwick, K.J., Odendaal, J., Ewington, L.J., Quenby, S., Ott, S., Brosens, J.J., 2020. Recurrent pregnancy loss is associated with a pro-senescent decidual response during the peri-implantation window. *Commun. Biol.* 3, 1–14. <https://doi.org/10.1038/s42003-020-0763-1>
- Ludwig, H., Metzger, H., 1976. The re-epithelization of endometrium after menstrual desquamation. *Arch. Gynakol.* 221, 51–60. <https://doi.org/10.1007/BF00667681>
- Ludwig, H., Spornitz, U.M., 1991. Microarchitecture of the human endometrium by scanning electron microscopy: menstrual desquamation and remodeling. *Ann. New York Acad. Sci.* 622, 28–46.
- Lunde, N.N., Holm, S., Dahl, T.B., Elyouncha, I., Sporsheim, B., Gregersen, I., Abbas, A., Skjelland, M., Espevik, T., Solberg, R., Johansen, H.T., Halvorsen, B., 2017. Increased levels of legumain in plasma and plaques from patients with carotid atherosclerosis. *Atherosclerosis* 257, 216–223. <https://doi.org/10.1016/j.atherosclerosis.2016.11.026>
- Luo, P., Zhang, C., Liao, F., Chen, L., Liu, Zhenyu, Long, L., Jiang, Z., Wang, Y., Wang, Z., Liu, Zujuan, Miao, H., Shi, C., 2019. Transcriptional positive cofactor 4 promotes breast cancer proliferation and metastasis through c-Myc mediated Warburg effect. *Cell Commun. Signal.* 17, 1–13. <https://doi.org/10.1186/s12964-019-0348-0>
- Lutz, W., 2006. Fertility rates and future population trends: Will Europe's birth rate recover or continue to decline? *Int. J. Androl.* 29, 25–33. <https://doi.org/10.1111/j.1365-2605.2005.00639.x>
- Luu, K.C., Nie, G.Y., Hampton, A., Fu, G.Q., Liu, Y.X., Salamonsen, L.A., 2004. Endometrial expression of calbindin (CaBP)-d28k but not CaBP-d9k in primates implies evolutionary changes and functional redundancy of calbindins at implantation. *Reproduction* 128, 433–441. <https://doi.org/10.1530/rep.1.00226>
- Lyon, D., Cheng, C.Y., Howland, L., Rattican, D., Jallo, N., Pickler, R., Brown, L., McGrath, J., 2010. Integrated review of cytokines in maternal, cord, and newborn blood: Part I—associations with preterm birth. *Biol. Res. Nurs.* 11, 371–376. <https://doi.org/10.1177/1099800409344620>
- Maas, J.W., Groothuis, P.G., Dunselman, G.A., de Goeij, A.F., Struyker Boudier, H.A., Evers, J.L., 2001. Endometrial angiogenesis throughout the human menstrual cycle. *Hum. Reprod.* 16, 1557–1561. [https://doi.org/10.1016/S0015-0282\(00\)01103-1](https://doi.org/10.1016/S0015-0282(00)01103-1)
- MacDonald, A.A., Stewart, A.W., Farquhar, C.M., 2013. Body mass index in relation to semen quality and reproductive hormones in New Zealand men: A cross-sectional study in fertility clinics. *Hum. Reprod.* 28, 3178–3198. <https://doi.org/10.1016/j.juro.2014.06.019>
- Macklon, N.S., Brosens, J.J., 2014. The Human Endometrium as a Sensor of Embryo Quality¹. *Biol. Reprod.* 91. <https://doi.org/10.1095/biolreprod.114.122846>
- Macklon, N.S., Geraedts, J.P.M., Fauser, B.C.J.M., 2002. Conception to ongoing pregnancy: The “black box” of early pregnancy loss. *Hum. Reprod. Update* 8, 333–343.

<https://doi.org/10.1093/humupd/8.4.333>

- Magdoud, K., Herbepin, V.G., Touraine, R., Almawi, W.Y., Mahjoub, T., 2013. Plasminogen Activator Inhibitor 1 4G/5G and -844G/A Variants in Idiopathic Recurrent Pregnancy Loss. *Am. J. Reprod. Immunol.* 70, 246–252. <https://doi.org/10.1111/aji.12116>
- Mallidis, C., Agbaje, I.M., Rogers, D.A., Glenn, J. V., Pringle, R., Atkinson, A.B., Steger, K., Stitt, A.W., McClure, N., 2008. Advanced glycation end products accumulate in the reproductive tract of men with diabetes. *Int. J. Androl.* 32, 295–305. <https://doi.org/10.1111/j.1365-2605.2007.00849.x>
- Manejwala, F.M., Cragoe, E.J., Schultz, R.M., 1989. Blastocoel expansion in the preimplantation mouse embryo: Role of extracellular sodium and chloride and possible apical routes of their entry. *Dev. Biol.* 133, 210–220. [https://doi.org/10.1016/0012-1606\(89\)90312-6](https://doi.org/10.1016/0012-1606(89)90312-6)
- Marinić, M., Rana, S., Lynch, V.J., 2020. Derivation of endometrial gland organoids from term placenta. *Placenta* 101, 75–79. <https://doi.org/10.1016/j.placenta.2020.08.017>
- Martinuzzi, K., Ryan, S., Luna, M., 2008. Elevated BMI does not adversely affect IVF outcome in young women. *J. Assist. Reprod. Genet.* 25, 169–175.
- Matorras, R., Ph, D., Exposito, A., Ph, D., Ferrando, M., 2020. Oocytes of women who are obese or overweight have lower levels of n-3 polyunsaturated fatty acids compared with oocytes of women with normal weight 113, 53–61. <https://doi.org/10.1016/j.fertnstert.2019.08.059>
- McCoski, S.R., Vailes, M.T., Owens, C.E., Cockrum, R.R., Ealy, A.D., 2018. Exposure to maternal obesity alters gene expression in the preimplantation ovine conceptus. *BMC Genomics* 19, 737. <https://doi.org/10.1186/s12864-018-5120-0> RESEARCH
- McGee, E.A., Hsueh, A.J.W., 2000. Initial and Cyclic Recruitment of Ovarian Follicles. *Endocr. Rev.* 21, 200–214.
- McNulty, M., Mahmud, A., Feely, J., 2007. Advanced Glycation End-Products and Arterial Stiffness in Hypertension. *Am. J. Hypertens.* 20, 242–247. <https://doi.org/10.1016/j.amjhyper.2006.08.009>
- McPherson, N.O., Bell, V.G., Zander-Fox, D.L., Fullston, T., Wu, L.L., Robker, R.L., Lane, M., 2015. When two obese parents are worse than one! Impacts on embryo and fetal development. *Am. J. Physiol. - Endocrinol. Metab.* 309, E568–E581. <https://doi.org/10.1152/ajpendo.00230.2015>
- Mei, J., Yan, Y., Li, S.Y., Zhou, W.J., Zhang, Q., Li, M.Q., Sun, H.X., 2019. CXCL16/CXCR6 interaction promotes endometrial decidualization via the PI3K/AKT pathway. *Reproduction* 157, 273–282. <https://doi.org/10.1530/REP-18-0417>
- Menkhorst, E., Zhang, J.G., Sims, N.A., Morgan, P.O., Soo, P., Poulton, I.J., Metcalf, D., Alexandrou, E., Gresle, M., Salamonsen, L.A., Butzkueven, H., Nicola, N.A., Dimitriadis, E., 2011. Vaginally administered PEGylated LIF Antagonist blocked embryo implantation and eliminated non-target effects on bone in mice. *PLoS One* 6, e19665. <https://doi.org/10.1371/journal.pone.0019665>
- Merhi, Z., 2019. Vitamin D attenuates the effect of advanced glycation end products on anti-Mullerian hormone signaling. *Mol. Cell. Endocrinol.* 479, 87–92.

- <https://doi.org/10.1016/j.mce.2018.09.004>
- Merhi, Z., 2014. Advanced glycation end products and their relevance in female reproduction. *Hum. Reprod.* 29, 135–145. <https://doi.org/10.1093/humrep/det383>
- Merhi, Z., Buyuk, E., Cipolla, M.J., 2018. Advanced glycation end products alter steroidogenic gene expression by granulosa cells: An effect partially reversible by vitamin D. *Mol. Hum. Reprod.* 24, 318–326. <https://doi.org/10.1093/molehr/gay014>
- Merhi, Z., Du, X.Q., Charron, M.J., 2020. Perinatal Exposure to High Dietary Advanced Glycation End-Products Affects the Reproductive System in Female Offspring in Mice. *Hum. Reprod.*
- Merhi, Z., Irani, M., Doswell, A.D., Ambroggio, J., 2014. Follicular fluid soluble receptor for advanced glycation end-products (sRAGE): A potential indicator of ovarian reserve. *J. Clin. Endocrinol. Metab.* 99, 226–233. <https://doi.org/10.1210/jc.2013-3839>
- Meriq, V., Piccardom, C., Cai, W., Chen, X., Zhu, L., Striker, G.E., Vlassara, H., Uribarri, J., 2010. Maternally Transmitted and Food-Derived Glycotoxins. *Diabetes Care* 33, 2232–2237. <https://doi.org/10.2337/dc10-1058>.
- Meseguer, M., Aplin, J.D., Caballero-Campo, P., O'Connor, J.E., Martín, J.C., Remohí, J., Pellicer, A., Simón, C., 2001. Human endometrial mucin MUC1 is up-regulated by progesterone and down-regulated in vitro by the human blastocyst. *Biol. Reprod.* 64, 590–601. <https://doi.org/10.1095/biolreprod64.2.590>
- Mills, M., Rindfuss, R.R., McDonald, P., te Velde, E., 2011. Why do people postpone parenthood? Reasons and social policy incentives. *Hum. Reprod. Update* 17, 848–860. <https://doi.org/10.1093/humupd/dmr026>
- Mo, B., Vendrov, A.E., Palomino, W.A., DuPont, B.R., Apparao, K.B.C., Lessey, B.A., 2006. ECC-1 Cells: A Well-Differentiated Steroid-Responsive Endometrial Cell Line with Characteristics of Luminal Epithelium. *Biol. Reprod.* 75, 387–394. <https://doi.org/10.1095/biolreprod.106.051870>
- Moran, L.J., Myers, J., Kenny, L.C., Poston, L., Wilson, R.L., Bianco-Miotto, T., Jankovic-Karasoulos, T., McCowan, L., Grieger, J.A., Norman, R.J., Leemaqz, S.Y., Grzeskowiak, L.E., Dekker, G.A., Walker, J.J., Roberts, C.T., 2018. Pre-pregnancy fast food and fruit intake is associated with time to pregnancy. *Hum. Reprod.* 33, 1063–1070. <https://doi.org/10.1093/humrep/dey079>
- Murakami, K., Bhandari, H., Lucas, E.S., Takeda, S., Gargett, C.E., Quenby, S., Murakami, K., Bhandari, H., Lucas, E.S., Takeda, S., Gargett, C.E., Quenby, S., Brosens, J.J., Tan, B.K., 2013. Deficiency in Clonogenic Endometrial Mesenchymal Stem Cells in Obese Women with Reproductive Failure - a Pilot Study. *PLoS* 8, e82582. <https://doi.org/10.1371/journal.pone.0082582>
- Murphy, C.R., 2004. Uterine receptivity and the plasma membrane transformation. *Cell Res.* 14, 259–267. <https://doi.org/10.1038/sj.cr.7290227>
- Murray, M.J., Meyer, W.R., Zaino, R.J., Lessey, B.A., Novotny, D.B., Ireland, K., Zeng, D., Fritz, M.A., 2004. A critical analysis of the accuracy, reproducibility, and clinical utility of histologic endometrial dating in fertile women. *Fertil. Steril.* 81, 1333–1343. <https://doi.org/10.1016/j.fertnstert.2003.11.030>

- Naruse, K., Sado, T., Noguchi, T., Tsunemi, T., Yoshida, S., Akasaka, J., Koike, N., Oi, H., Kobayashi, H., 2012. Peripheral RAGE (Receptor for Advanced Glycation Endproducts)-ligands in normal pregnancy and preeclampsia: Novel markers of inflammatory response. *J. Reprod. Immunol.* 93, 69–74. <https://doi.org/10.1016/j.jri.2011.12.003>
- Negami, A.I., Tominaga, T., 1989. Gland and epithelium formation in vitro from epithelial cells of the human endometrium. *Hum. Reprod.* 4, 620–624. <https://doi.org/10.1093/oxfordjournals.humrep.a136954>
- Nenna, A., Nappi, F., Avtaar Singh, S., Sutherland, F., Di Domenico, F., Chello, M., Spadaccio, C., 2015. Pharmacologic approaches against Advanced Glycation End Products (AGEs) in diabetic cardiovascular disease. *Res. Cardiovasc. Med.* 4, e36949. [https://doi.org/10.5812/cardiovascmed.4\(2\)2015.26949](https://doi.org/10.5812/cardiovascmed.4(2)2015.26949)
- Nevin, C., McNeil, L., Ahmed, N., Murgatroyd, C., Brison, D., Carroll, M., 2018. Investigating the Glycating Effects of Glucose, Glyoxal and Methylglyoxal on Human Sperm. *Sci. Rep.* 8, 1–12. <https://doi.org/10.1038/s41598-018-27108-7>
- Ng, S.W., Norwitz, G.A., Pavlicev, M., Tilburgs, T., Simón, C., Norwitz, E.R., 2020. Endometrial decidualization: The primary driver of pregnancy health. *Int. J. Mol. Sci.* 21, 1–20. <https://doi.org/10.3390/ijms21114092>
- Nguyen, H.P.T., Xiao, L., Deane, J.A., Tan, K.S., Cousins, F.L., Masuda, H., Sprung, C.N., Rosamilia, A., Gargett, C.E., 2017. N-cadherin identifies human endometrial epithelial progenitor cells by in vitro stem cell assays. *Hum. Reprod.* 32, 2254–2268. <https://doi.org/10.1093/humrep/dex289>
- Nishida, M., 2002. The Ishikawa cells from birth to the present. *Hum. Cell* 15, 104–117. <https://doi.org/10.1111/j.1749-0774.2002.tb00105.x>
- Noguchi, T., Sado, T., Naruse, K., Shigetomi, H., Onogi, A., Haruta, S., Kawaguchi, R., Nagai, A., Tanase, Y., Yoshida, S., Kitanaka, T., Oi, H., Kobayashi, H., 2010. Evidence for activation of toll-like receptor and receptor for advanced glycation end products in preterm birth. *Mediators Inflamm.* 2010. <https://doi.org/10.1155/2010/490406>
- Norman, R.J., Mol, B.W.J., 2018. Successful weight loss interventions before in vitro fertilization: fat chance? *Fertil. Steril.* 110, 581–586. <https://doi.org/10.1016/j.fertnstert.2018.05.029>
- Noyes, R.W., Hertig, A.T., Rock, J., 1950. Dating the endometrial biopsy. *Obstet. Gynecol. Surv.* 5, 561–564. <https://doi.org/10.1097/00006254-195008000-00044>
- Okubo, H., Miyake, Y., Sasaki, S., Tanaka, K., Murakami, K., Hirota, Y., Osaka Maternal, Kanzaki, H., Kitada, M., Horikoshi, Y., Ishiko, O., Nakai, Y., Nishio, J., Yamamasu, S., Yasuda, J., Kawai, S., Yanagihara, K., Wakuda, K., Kawashima, T., Narimoto, K., Iwasa, Y., Orino, K., Tsunetoh, I., Yoshida, J., Ito, J., Kaneko, T., Kamiya, T., Kuribayashi, H., Taniguchi, T., Takemura, H., Morimoto, Y., Matsunaga, I., Oda, H., Ohya, Y., 2012. Maternal dietary patterns in pregnancy and fetal growth in Japan: the Osaka Maternal and Child Health Study. *Br. J. Nutr.* 107, 1526–1533. <https://doi.org/10.1017/S0007114511004636>
- Oliver, E.A., Buhimschi, C.S., Dulay, A.T., Baumbusch, M.A., Abdel-Razek, S.S., Lee, S.Y., Zhao, G., Jing, S., Pettker, C.M., Buhimschi, I.A., 2011. Activation of the receptor for advanced glycation end

- products system in women with severe preeclampsia. *J. Clin. Endocrinol. Metab.* 96, 689–698. <https://doi.org/10.1210/jc.2010-1418>
- Orvieto, R., Meltzer, S., Nahum, R., Rabinson, J., Anteby, E.Y., Ashkenazi, J., 2009. The influence of body mass index on in vitro fertilization outcome. *Int. J. Gynecol. Obstet.* 104, 53–55. <https://doi.org/10.1016/j.ijgo.2008.08.012>
- Orvieto, R., Mohr-Sasson, A., Aizer, A., Nahum, R., Blumenfeld, S., Kirshenbaum, M., Haas, J., 2020. Do Follicles of Obese Patients Yield Competent Oocytes/Embryos? *Gynecol. Obstet. Invest.* 290–293. <https://doi.org/10.1159/000508226>
- Ota, K., Yamagishi, S.I., Kim, M., Dambaeva, S., Gilman-Sachs, A., Beaman, K., Kwak-Kim, J., 2014. Elevation of soluble form of receptor for advanced glycation end products (sRAGE) in recurrent pregnancy losses (RPL): Possible participation of RAGE in RPL. *Fertil. Steril.* 102, 782–789. <https://doi.org/10.1016/j.fertnstert.2014.06.010>
- Ott, C., Jacobs, K., Haucke, E., Navarrete Santos, A., Grune, T., Simm, A., 2014. Role of advanced glycation end products in cellular signaling. *Redox Biol.* 2, 411–429. <https://doi.org/10.1016/j.redox.2013.12.016>
- Ouslimani, N., Mahrouf, M., Peynet, J., Bonnefont-Rousselot, D., Cosson, C., Legrand, A., Beaudoux, J.L., 2007. Metformin reduces endothelial cell expression of both the receptor for advanced glycation end products and lectin-like oxidized receptor 1. *Metabolism.* 56, 308–313. <https://doi.org/10.1016/j.metabol.2006.10.010>
- Owusu-Akyaw, A., Krishnamoorthy, K., Goldsmith, L.T., Morelli, S.S., 2019. The role of mesenchymal-epithelial transition in endometrial function. *Hum. Reprod. Update* 25, 114–133. <https://doi.org/10.1093/humupd/dmy035>
- Pabona, J.M.P., Simmen, F.A., Nikiforov, M.A., Zhuang, D., Shankar, K., Velarde, M.C., Zelenko, Z., Giudice, L.C., Simmen, R.C.M., 2012. Krüppel-Like Factor 9 and Progesterone Receptor Coregulation of Decidualizing Endometrial Stromal Cells: Implications for the Pathogenesis of Endometriosis. *J. Clin. Endocrinol. Metab.* 97, E376–E392. <https://doi.org/10.1210/jc.2011-2562>
- Padykula, H. a, Coles, L.G., Okulicz, W.C., Rapaport, S.I., McCracken, J.A., King, N.W., Longcope, C., Kaiserman-Abramof, I.R., 1989. The basalis of the primate endometrium: a bifunctional germinal compartment. *Biol. Reprod.* 40, 681–90. <https://doi.org/10.1095/biolreprod40.3.681>
- Paiva, P., Menkhorst, E., Salamonsen, L., Dimitriadis, E., 2009. Leukemia inhibitory factor and interleukin-11: Critical regulators in the establishment of pregnancy. *Cytokine Growth Factor Rev.* 20, 319–328. <https://doi.org/10.1016/j.cytogfr.2009.07.001>
- Paliy, O., Piyathilake, C.J., Kozyrskyj, A., Celep, G., Marotta, F., Rastmanesh, R., 2014. Excess body weight during pregnancy and offspring obesity: Potential mechanisms. *Nutrition* 30, 245–251. <https://doi.org/10.1016/j.nut.2013.05.011>
- Parker, V.J., Solano, M.E., Arck, P.C., Douglas, A.J., 2013. Diet-induced obesity may affect the uterine immune environment in early – mid pregnancy , reducing NK-cell activity and potentially compromising uterine vascularization. *Int. J. Obes.* 38, 766–774.

- <https://doi.org/10.1038/ijo.2013.164>
- Paul, J.W., Hua, S., Ilicic, M., Tolosa, J.M., Butler, T., Robertson, S., Smith, R., 2017. Drug delivery to the human and mouse uterus using immunoliposomes targeted to the oxytocin receptor. *Am. J. Obstet. Gynecol.* 216, e1-14. <https://doi.org/10.1016/j.ajog.2016.08.027>
- Perdu, S., Castellana, B., Kim, Y., Chan, K., DeLuca, L., Beristain, A.G., 2016. Maternal obesity drives functional alterations in uterine NK cells. *JCI Insight* 1, 1–21. <https://doi.org/10.1172/jci.insight.85560>
- Perrone, A., Giovino, A., Benny, J., Martinelli, F., 2020. Advanced Glycation End Products (AGEs): Biochemistry, Signaling, Analytical Methods, and Epigenetic Effects. *Oxid. Med. Cell. Longev.* 2020. <https://doi.org/10.1155/2020/3818196>
- Peters, H., Byskov, a G., Himelstein-Braw, R., Faber, M., 1975. Follicular growth: the basic event in the mouse and human ovary. *J. Reprod. Fertil.* 45, 559–566. <https://doi.org/10.1530/jrf.0.0450559>
- Phillips, R.S., 2014. Structure and mechanism of kynureninase. *Arch. Biochem. Biophys.* 544, 69–74. <https://doi.org/10.1016/j.abb.2013.10.020>
- Pierre, N., Deldicque, L., Barbé, C., Naslain, D., Cani, P.D., Francaux, M., 2013. Toll-Like Receptor 4 Knockout Mice Are Protected against Endoplasmic Reticulum Stress Induced by a High-Fat Diet. *PLoS One* 8, e65061. <https://doi.org/10.1371/journal.pone.0065061>
- Pikiou, O., Vasilaki, A., Leondaritis, G., Vamvakopoulos, N., Messinis, I.E., 2013. Effects of metformin on fertilisation of bovine oocytes and early embryo development: possible involvement of AMPK3-mediated TSC2 activation. *Zygote* 23, 58–67. <https://doi.org/10.1017/s0967199413000300>
- Pineda, A., Verdin-Terán, S.L., Camacho, A., Moreno-Fierros, L., 2011. Expression of Toll-like Receptor TLR-2, TLR-3, TLR-4 and TLR-9 Is Increased in Placentas from Patients with Preeclampsia. *Arch. Med. Res.* 42, 382–391. <https://doi.org/10.1016/j.arcmed.2011.08.003>
- Provost, M.P., Acharya, K.S., Acharya, C.R., Yeh, J.S., Steward, R.G., Eaton, J.L., Goldfarb, J.M., Muasher, S.J., 2016. Pregnancy outcomes decline with increasing body mass index: Analysis of 239,127 fresh autologous in vitro fertilization cycles from the 2008-2010 Society for Assisted Reproductive Technology registry. *Fertil. Steril.* 105, 663–669. <https://doi.org/10.1016/j.fertnstert.2015.11.008>
- Quentin, T., Steinmetz, M., Poppe, A., Thoms, S., 2012. Metformin differentially activates ER stress signaling pathways without inducing apoptosis. *DMM Dis. Model. Mech.* 5, 259–269. <https://doi.org/10.1242/dmm.008110>
- Quezada, S., Avellaira, C., Johnson, M.C., Gabler, F., Fuentes, A., Vega, M., 2006. Evaluation of steroid receptors, coregulators, and molecules associated with uterine receptivity in secretory endometria from untreated women with polycystic ovary syndrome. *Fertil. Steril.* 85, 1017–1026. <https://doi.org/10.1016/j.fertnstert.2005.09.053>
- Rai, R., Regan, L., 2006. Recurrent Miscarriage. *Lancet* 368, 601–611. <https://doi.org/10.1002/9781119979449.ch7>

- Rajasekar, P., Anuradha, C. V., 2007. L-Carnitine inhibits protein glycation in vitro and in vivo: Evidence for a role in diabetic management. *Acta Diabetol.* 44, 83–90. <https://doi.org/10.1007/s00592-007-0247-5>
- Rajkhowa, M., Mcconnell, A., Thomas, G.E., 2006. Reasons for discontinuation of IVF treatment: A questionnaire study. *Hum. Reprod.* 21, 358–363. <https://doi.org/10.1093/humrep/dei355>
- Ramlau-Hansen, C.H., Thulstrup, A.M., Nohr, E.A., Bonde, J.P., Sørensen, T.I.A., Olsen, J., 2007. Subfecundity in overweight and obese couples. *Hum. Reprod.* 22, 1634–1637. <https://doi.org/10.1093/humrep/dem035>
- Rani, S.G., Sepuru, K.M., Yu, C., 2014. Interaction of S100A13 with C2 domain of receptor for advanced glycation end products (RAGE). *Biochim. Biophys. Acta - Proteins Proteomics* 1844, 1718–1728. <https://doi.org/10.1016/j.bbapap.2014.06.017>
- Reed, B.G., Carr, B.R., 2015. The normal menstrual cycle and the control of ovulation.pdf. Dallas.
- Reynolds, K.A., Boudoures, A.L., Chi, M.M.Y., Wang, Q., Moley, K.H., 2015. Adverse effects of obesity and/or high-fat diet on oocyte quality and metabolism are not reversible with resumption of regular diet in mice. *Reprod. Fertil. Dev.* 27, 716–724. <https://doi.org/10.1071/RD14251>
- Rhee, J.S., Saben, J.L., Mayer, A.L., Schulte, M.B., Asghar, Z., Stephens, C., Chi, M.M.Y., Moley, K.H., 2016. Diet-induced obesity impairs endometrial stromal cell decidualization: A potential role for impaired autophagy. *Hum. Reprod.* 31, 1315–1326. <https://doi.org/10.1093/humrep/dew048>
- Ribeiro, S.M.T.L., Lopes, L.R., Paula Costa, G. de, Figueiredo, V.P., Shrestha, D., Batista, A.P., Nicolato, R.L. de C., de Oliveira, F.L.P., Gomes, J.A.S., Talvani, A., 2017. CXCL-16, IL-17, and bone morphogenetic protein 2 (BMP-2) are associated with overweight and obesity conditions in middle-aged and elderly women. *Immun. Ageing* 14, 1–7. <https://doi.org/10.1186/s12979-017-0089-0>
- Rich-Edwards JW, Spiegelman D, Garland M, Hertzmark E, Hunter DJ, Colditz GA, Willett WC, Wand H, M.J., 2002. Physical Activity, Body Mass Index, and Ovulatory Disorder Infertility. *Epidemiology* 13, 184–190.
- Rinehart, C.A., Lynn-Cook, B.D., Kaufman, D.G., 1988. Gland Formation from Human Endometrial Epithelial Cells in vitro. *Vitr. Cell. Dev. Biol.* 24, 1037–1041.
- Rittenberg, V., Seshadri, S., Sunkara, S.K., Sobaleva, S., Oteng-Ntim, E., El-toukhy, T., 2011. Effect of body mass index on IVF treatment outcome: an updated systematic review and meta-analysis. *Reprod. Biomed. Online* 23, 421–439. <https://doi.org/10.1016/j.rbmo.2011.06.018>
- Roberts, J.M., Bodnar, L.M., Patrick, T.E., Powers, R.W., 2011. The role of obesity in preeclampsia. *Pregnancy Hypertens. An Int. J. Women's Cardiovasc. Heal.* 1, 6–16. <https://doi.org/10.1016/j.preghy.2010.10.013>
- Robertson, S.A., Chin, P.Y., Femia, J.G., Brown, H.M., 2018. Embryotoxic cytokines—Potential roles in embryo loss and fetal programming. *J. Reprod. Immunol.* 125, 80–88. <https://doi.org/10.1016/j.jri.2017.12.003>

- Robker, R.L., 2008. Evidence that obesity alters the quality of oocytes and embryos. *Pathophysiology* 15, 115–121. <https://doi.org/10.1016/j.pathophys.2008.04.004>
- Robker, R.L., Akison, L.K., Bennett, B.D., Thrupp, P.N., Chura, L.R., Russell, D.L., Lane, M., Norman, R.J., 2009. Obese women exhibit differences in ovarian metabolites, hormones, and gene expression compared with moderate-weight women. *J. Clin. Endocrinol. Metab.* 94, 1533–1540. <https://doi.org/10.1210/jc.2008-2648>
- Rogers, J., Mitchess, G.W.J., 1952. The relation of obesity to menstrual disturbances. *N. Engl. J. Med.* 247, 839–840.
- Rosenwaks, Z., Davis, O.K., Damario, M.A., 1995. The role of maternal age in the assisted reproductive technologies. *Hum. Reprod.* 10, 165–173. <https://doi.org/10.1017/S0962279999000149>
- Ruan, Y.C., Guo, J.H., Liu, X., Zhang, R., Tsang, L.L., Dong, J. Da, Chen, H., Yu, M.K., Jiang, X., Zhang, X.H., Fok, K.L., Chung, Y.W., Huang, H., Zhou, W.L., Chan, H.C., 2012. Activation of the epithelial Na⁺ channel triggers prostaglandin E2 release and production required for embryo implantation. *Nat. Med.* 18, 1112–1117. <https://doi.org/10.1038/nm.2771>
- Ruane, P.T., Berneau, S.C., Koeck, R., Watts, J., Kimber, S.J., Brison, D.R., Westwood, M., Aplin, J.D., 2017. Apposition to endometrial epithelial cells activates mouse blastocysts for implantation. *Mol. Hum. Reprod.* 23, 617–627. <https://doi.org/10.1093/molehr/gax043>
- Rubin, C.I., Atweh, G.F., 2004. The role of stathmin in the regulation of the cell cycle. *J. Cell. Biochem.* 93, 242–250. <https://doi.org/10.1002/jcb.20187>
- Ruiz-Alonso, M., Blesa, D., Diaz-Gimeno, P., Gomez, E., Fernandez-Sanchez, M., Carranza, F., Carrera, J., Vilella, F., Pellicer, A., Simon, C., 2013. The endometrial receptivity array for diagnosis and personalized embryo transfer as a treatment for patients with repeated implantation failure. *Fertil. Steril.* 100, 818–824. <https://doi.org/10.1016/j.fertnstert.2013.05.004>
- Salamonsen, L.A., Evans, J., Nguyen, H.P.T., Edgell, T.A., 2016. The Microenvironment of Human Implantation: Determinant of Reproductive Success. *Am. J. Reprod. Immunol.* 75, 218–225. <https://doi.org/10.1111/aji.12450>
- Salamonsen, L.A., Hutchison, J.C., Gargett, C.E., 2021. Cyclical endometrial repair and regeneration in women: mechanisms, insights and opportunities. *Development* (Submitted).
- Salamonsen, L.A., Nie, G., Hannan, N.J., Dimitriadis, E., 2009. Society for Reproductive Biology Founders' Lecture 2009 Preparing fertile soil: the importance of endometrial receptivity. *Reprod. Fertil. Dev.* 21, 923–934. <https://doi.org/10.1071/RD09145>
- Schaefer, T.M., Desouza, K., Fahey, J. V., Beagley, K.W., Wira, C.R., 2004. Toll-like receptor (TLR) expression and TLR-mediated cytokine/chemokine production by human uterine epithelial cells. *Immunology* 112, 428–436. <https://doi.org/10.1111/j.1365-2567.2004.01898.x>
- Schliep, K.C., Mumford, S.L., Ahrens, K.A., Hotaling, J.M., Carrell, D.T., Link, M., Hinkle, S.N., Kissell, K., Porucznik, C.A., Hammoud, A.O., 2015. Effect of male and female body mass index on pregnancy and live birth success after in vitro fertilization. *Fertil. Steril.* 103, 388–395. <https://doi.org/10.1016/j.fertnstert.2014.10.048>

- Schmitz, C., Yu, L., Bocca, S., Anderson, S., Cunha-Filho, J.S., Rhavi, B.S., Oehninger, S., 2014. Role for the endometrial epithelial protein MFG-E8 and its receptor integrin $\alpha\beta 3$ in human implantation: Results of an in vitro trophoblast attachment study using established human cell lines. *Fertil. Steril.* 101, 874–882. <https://doi.org/10.1016/j.fertnstert.2013.12.015>
- Schurman, L., McCarthy, A.D., Sedlinsky, C., Gangoiti, M. V., Arnol, V., Bruzzone, L., Cortizo, A.M., 2008. Metformin reverts deleterious effects of advanced glycation end-products (AGEs) on osteoblastic cells. *Exp. Clin. Endocrinol. Diabetes* 116, 333–340. <https://doi.org/10.1055/s-2007-992786>
- Sebastian-León, P., Garrido, N., Remohí, J., Pellicer, A., Diaz-Gimeno, P., 2018. Asynchronous and pathological windows of implantation: Two causes of recurrent implantation failure. *Hum. Reprod.* 33, 626–635. <https://doi.org/10.1093/humrep/dey023>
- Semba, R.D., Najjar, S.S., Sun, K., Lakatta, E.G., Ferrucci, L., 2009. Serum carboxymethyl-lysine, an advanced glycation end product, is associated with increased aortic pulse wave velocity in adults. *Am. J. Hypertens.* 22, 74–79. <https://doi.org/10.1038/ajh.2008.320>
- Sermondade, N., Huberlant, S., Bourhis-Lefebvre, V., Arbo, E., Gallot, V., Colombani, M., Fréour, T., 2019. Female obesity is negatively associated with live birth rate following IVF: a systematic review and meta-analysis. *Hum. Reprod. Update* 25, 439–451. <https://doi.org/10.1093/humupd/dmz011>
- Seshagiri, P.B., Sen Roy, S., Sireesha, G., Rao, R.P., 2009. Cellular and molecular regulation of mammalian blastocyst hatching. *J. Reprod. Immunol.* 83, 79–84. <https://doi.org/10.1016/j.jri.2009.06.264>
- Seth, B., Arora, S., Singh, R., 2013. Association of obesity with hormonal imbalance in infertility: A cross-sectional study in North Indian Women. *Indian J. Clin. Biochem.* 28, 342–347. <https://doi.org/10.1007/s12291-013-0301-8>
- Shan, D., Arhin, S.K., Zhao, J., Xi, H., Zhang, F., Zhu, C., Hu, Y., 2020. Effects of SLIRP on Sperm Motility and Oxidative Stress. *Biomed Res. Int.* 2020, 9060356–9060356. <https://doi.org/10.1155/2020/9060356>
- Sharma, C., Kaur, A., Thind, S.S., Singh, B., Raina, S., 2015. Advanced glycation End-products (AGEs): an emerging concern for processed food industries. *J. Food Sci. Technol.* 52, 7561–7576. <https://doi.org/10.1007/s13197-015-1851-y>
- Sharma, I., Dhawan, V., Saha, S.C., Rashmi, B., Dhaliwal, L.K., 2010. Implication of the RAGE-EN-RAGE axis in endometriosis. *Int. J. Gynecol. Obstet.* 110, 199–202. <https://doi.org/10.1016/j.ijgo.2010.03.037>
- Shen, C., Ma, Y., Zeng, Z., Yin, Q., Hong, Y., Hou, X., Liu, X., 2017. RAGE-Specific Inhibitor FPS-ZM1 Attenuates AGEs-Induced Neuroinflammation and Oxidative Stress in Rat Primary Microglia. *Neurochem. Res.* 42, 2902–2911. <https://doi.org/10.1007/s11064-017-2321-x>
- Shi, H., Enriquez, A., Rapadas, M., Martin, E.M.M.A., Wang, R., Moreau, J., Lim, C.K., Szot, J.O., Ip, E., Hughes, J.N., Sugimoto, K., Humphreys, D.T., McInerney-Leo, A.M., Leo, P.J., Maghzal, G.J., Halliday, J., Smith, J., Colley, A., Mark, P.R., Collins, F., Sillence, D.O., Winlaw, D.S., Ho, J.W.K.,

- Guillemin, G.J., Brown, M.A., Kikuchi, K., Thomas, P.Q., Stocker, R., Giannoulatou, E., Chapman, G., Duncan, E.L., Sparrow, D.B., Dunwoodie, S.L., 2017. NAD Deficiency, Congenital Malformations, and Niacin Supplementation. *N. Engl. J. Med.* 377, 544–552. <https://doi.org/10.1056/NEJMoa1616361>
- Shi, J.W., Yang, H.L., Fan, D.X., Yang, S.L., Qiu, X.M., Wang, Y., Lai, Z.Z., Ha, S.Y., Ruan, L.Y., Shen, H.H., Zhou, W.J., Li, M.Q., 2020. The role of CXC chemokine ligand 16 in physiological and pathological pregnancies. *Am. J. Reprod. Immunol.* 83. <https://doi.org/10.1111/aji.13223>
- Shi, Y., Qian, J., Zhang, Q., Hu, Y., Sun, D., Jiang, L., 2020. Advanced glycation end products increased placental vascular permeability of human BeWo cells via RAGE / NF- κ B signaling pathway. *Eur. J. Obstet. Gynecol.* 250, 93–100. <https://doi.org/10.1016/j.ejogrb.2020.04.058>
- Shimizu, K., Kamada, Y., Sakamoto, A., Matsuda, M., Nakatsuka, M., Hiramatsu, Y., 2017. High Expression of High-Mobility Group Box 1 in Menstrual Blood: Implications for Endometriosis. *Reprod. Sci.* 24, 1532–1537. <https://doi.org/10.1177/1933719117692042>
- Shirasuna, K., Seno, K., Ohtsu, A., Shiratsuki, S., Ohkuchi, A., Suzuki, H., Matsubara, S., Nagayama, S., Iwata, H., Kuwayama, T., 2016. AGEs and HMGB1 Increase Inflammatory Cytokine Production from Human Placental Cells, Resulting in an Enhancement of Monocyte Migration. *Am. J. Reprod. Immunol.* 75, 557–568. <https://doi.org/10.1111/aji.12506>
- Simon, B., Bolumar, D., Amadoz, A., Jimenez-Almazán, J., Valbuena, D., Vilella, F., Moreno, I., 2020. Identification and characterization of extracellular vesicles and its DNA cargo secreted during murine embryo development. *Genes (Basel)*. 11, 203. <https://doi.org/10.3390/genes11020203>
- Simón, C., Gómez, C., Cabanillas, S., Vladimirov, I., Castellón, G., Giles, J., Boynukalin, K., Findikli, N., Bahçeci, M., Ortega, I., Vidal, C., Funabiki, M., Izquierdo, A., López, L., Portela, S., Frantz, N., Kulmann, M., Taguchi, S., Labarta, E., Colucci, F., Mackens, S., Santamaría, X., Muñoz, E., Barrera, S., García-Velasco, J.A., Fernández, M., Ferrando, M., Ruiz, M., Mol, B.W., Valbuena, D., 2020. A 5-year multicentre randomized controlled trial comparing personalized, frozen and fresh blastocyst transfer in IVF. *Reprod. Biomed. Online* 41, 402–415. <https://doi.org/10.1016/j.rbmo.2020.06.002>
- Simon, D., Kaimal, A.J., Oken, E., Hivert, M.-F., 2020. Reaching women with obesity to support weight loss before pregnancy: feasibility and qualitative assessment. *Ther. Adv. Reprod. Heal.* 14, 1–10. <https://doi.org/10.1177/2633494120909106>
- Simone, T.M., Higgins, C.E., Czekay, R., Law, B.K., Higgins, S.P., Archambeault, J., Kutz, S.M., Higgins, P.J., 2014. SERPINE1 : A Molecular Switch in the Proliferation-Migration Dichotomy in Wound-“ Activated ” Keratinocytes. *Adv. wound care* 3, 281–290. <https://doi.org/10.1089/wound.2013.0512>
- Singh, R., Barden, A., Mori, T., Beilin, L., 2001. Advanced glycation end-products: A review. *Diabetologia* 44, 129–146. <https://doi.org/10.1007/s001250051591>
- Skok, K., Maver, U., Gradišnik, L., Kozar, N., Takač, I., Arko, D., 2020. Endometrial cancer and its cell lines. *Mol. Biol. Rep.* 47, 1399–1411. <https://doi.org/10.1007/s11033-019-05226-3>
- Smoak, I.W., 1999. Glucose metabolism in mouse embryos exposed to metformin in vitro. *Toxicol.*

- Vitr. 13, 27–33. [https://doi.org/10.1016/S0887-2333\(98\)00061-7](https://doi.org/10.1016/S0887-2333(98)00061-7)
- Sohouli, M.H., Sharifi-Zahabi, E., Lari, A., Fatahi, S., Shidfar, F., 2020. The impact of low advanced glycation end products diet on obesity and related hormones: a systematic review and meta-analysis. *Sci. Rep.* 10, 22194. <https://doi.org/10.1038/s41598-020-79216-y>
- Son, M., Kang, W.C., Oh, S., Bayarsaikhan, D., Ahn, H., Lee, J., Park, H., Lee, S., Choi, J., Lee, H.S., Yang, P.C., Byun, K., Lee, B., 2017. Advanced glycation end-product (AGE)-albumin from activated macrophage is critical in human mesenchymal stem cells survival and post-ischemic reperfusion injury. *Sci. Rep.* 7, 11593. <https://doi.org/10.1038/s41598-017-11773-1>
- Stensen, M.H., Tanbo, T., Storeng, R., Fedorcsak, P., 2014. Advanced glycation end products and their receptor contribute to ovarian ageing. *Hum. Reprod.* 29, 125–134. <https://doi.org/10.1093/humrep/det419>
- Stewart, T.M., Liu, D.Y., Garrett, C., Jørgensen, N., Brown, E.H., Baker, H.W.G., 2009. Associations between andrological measures, hormones and semen quality in fertile Australian men: Inverse relationship between obesity and sperm output. *Hum. Reprod.* 24, 1561–1568. <https://doi.org/10.1093/humrep/dep075>
- Sugiura-ogasawara, M., 2015. Recurrent pregnancy loss and obesity. *Best Pract. Res. Clin. Obstet. Gynaecol.* 29, 489–497. <https://doi.org/10.1016/j.bpobgyn.2014.12.001>
- Swamy-Mruthinti, S., Carter, A.L., 1999. Acetyl- L -Carnitine Decreases Glycation of Lens Proteins : in vitro Studies. *Exp. Eye Res.* 69, 109–115.
- Szklanna, P.B., Wynne, K., Nolan, M., Egan, K., Áinle, F.N., Maguire, P.B., 2017. Comparative proteomic analysis of trophoblast cell models reveals their differential phenotypes, potential uses, and limitations. *Proteomics* 17, 6–11. <https://doi.org/10.1002/pmic.201700037>
- Tadros, W., Lipshitz, H.D., 2009. The maternal-to-zygotic transition: A play in two acts. *Development* 136, 3033–3042. <https://doi.org/10.1242/dev.033183>
- Takahashi, N., Harada, M., Azhary, J.M., Kunitomi, C., Nose, E., Terao, H., Koike, H., Wada-Hiraike, O., Hirata, T., Hirota, Y., Koga, K., Fujii, T., Osuga, Y., 2019. Accumulation of Advanced Glycation End Products in follicles is associated with poor oocyte developmental competence. *Mol. Hum. Reprod.* gaz050. <https://doi.org/10.1093/molehr/gaz050>
- Tanaka, Y., Uchino, H., Shimizu, T., Yoshii, H., Niwa, M., Ohmura, C., Mitsuhashi, N., Onuma, T., Kawamori, R., 1999. Effect of metformin on advanced glycation endproduct formation and peripheral nerve function in streptozotocin-induced diabetic rats. *Eur. J. Pharmacol.* 376, 17–22. [https://doi.org/10.1016/S0014-2999\(99\)00342-8](https://doi.org/10.1016/S0014-2999(99)00342-8)
- Taylor, A., 2003. ABC of subfertility: extent of the problem. *Br. Med. J.* 327, 434–6. <https://doi.org/10.1136/bmj.327.7412.434>
- Teklenburg, G., Salker, M., Molokhia, M., Lavery, S., Trew, G., Aojanepong, T., Mardon, H.J., Lokugamage, A.U., Rai, R., Landles, C., Roelen, B.A.J., Quenby, S., Kuijk, E.W., Kavelaars, A., Heijnen, C.J., Regan, L., Brosens, J.J., Macklon, N.S., 2010. Natural selection of human embryos: Decidualizing endometrial stromal cells serve as sensors of embryo quality upon implantation. *PLoS One* 5, 2–7. <https://doi.org/10.1371/journal.pone.0010258>

- Thie, M., Denker, H.W., 2002. In vitro studies on endometrial adhesiveness for trophoblast: Cellular dynamics in uterine epithelial cells. *Cells Tissues Organs* 172, 237–252.
<https://doi.org/10.1159/000066963>
- Thieme, K., Da Silva, K.S., Fabre, N.T., Catanozi, S., Monteiro, M.B., Santos-Bezerra, D.P., Costa-Pessoa, J.M., Oliveira-Souza, M., Machado, U.F., Passarelli, M., Correa-Giannella, M.L., 2016. N-Acetyl Cysteine Attenuated the Deleterious Effects of Advanced Glycation End-Products on the Kidney of Non-Diabetic Rats. *Cell. Physiol. Biochem.* 40, 608–620.
<https://doi.org/10.1159/000452574>
- Thomsen, L., Humaidan, P., Bungum, L., Bungum, M., 2014. The impact of male overweight on semen quality and outcome of assisted reproduction. *Asian J. Androl.* 16, 749–754.
<https://doi.org/10.4103/1008-682X.125398>
- Tok, A., Seyithanoğlu, M., Ozer, A., ErKayıran, U., Karaküçük, S., Çelebi, A., 2019. The serum level of soluble CXCL16 is increased in preeclampsia and associated with hepatic/renal damage. *J. Matern. Neonatal Med.* 7058. <https://doi.org/10.1080/14767058.2019.1638361>
- Tomic, V., Kasum, M., Vucic, K., 2020. Impact of embryo quality and endometrial thickness on implantation in natural cycle IVF. *Arch. Gynecol. Obstet.* 301, 1325–1330.
<https://doi.org/10.1007/s00404-020-05507-4>
- Tremellen, K., Pearce, K., Zander-Fox, D., 2017. Increased miscarriage of euploid pregnancies in obese women undergoing cryopreserved embryo transfer. *Reprod. Biomed. Online* 34, 90–97.
<https://doi.org/10.1016/j.rbmo.2016.09.011>
- Tripathy, J., Tripathy, A., Thangaraju, M., Suar, M., Elangovan, S., 2018. α -Lipoic acid inhibits the migration and invasion of breast cancer cells through inhibition of TGF β signaling. *Life Sci.* 207, 15–22. <https://doi.org/10.1016/j.lfs.2018.05.039>
- Trott, J.F., Simpson, K.J., Moyle, R.L.C., Hearn, C.M., Shaw, G., Nicholas, K.R., Renfree, M.B., 2003. Maternal regulation of milk composition, milk production, and pouch young development during lactation in the tammar wallaby (*Macropus eugenii*). *Biol. Reprod.* 68, 929–936.
<https://doi.org/10.1095/biolreprod.102.005934>
- Truong, T., Gardner, D.K., 2017. Antioxidants improve IVF outcome and subsequent embryo development in the mouse. *Hum. Reprod.* 32, 2404–2413.
<https://doi.org/10.1093/humrep/dex330>
- Truong, T., Soh, Y.M., Gardner, D.K., 2016. Antioxidants improve mouse preimplantation embryo development and viability. *Hum. Reprod.* 31, 1445–1454.
<https://doi.org/10.1093/humrep/dew098>
- Tsukahara, H., Ohta, N., Sato, S., Hiraoko, M., Shukunami, K.I., Uchiyama, M., Kawakami, H., Sekine, K., Mayumi, M., 2004. Concentrations of pentosidine, an advanced glycation end-product, in umbilical cord blood. *Free Radic. Res.* 38, 691–695.
<https://doi.org/10.1080/1071576042000220256>
- Turco, M.Y., Gardner, L., Hughes, J., Cindrova-Davies, T., Gomez, M.J., Farrell, L., Hollinshead, M., Marsh, S.G.E., Brosens, J.J., Critchley, H.O., Simons, B.D., Hemberger, M., Koo, B.K., Moffett, A.,

- Burton, G.J., 2017. Long-term, hormone-responsive organoid cultures of human endometrium in a chemically defined medium. *Nat. Cell Biol.* 19, 568–577. <https://doi.org/10.1038/ncb3516>
- Turco, M.Y., Gardner, L., Kay, R.G., Hamilton, R.S., Prater, M., Hollinshead, M.S., McWhinnie, A., Esposito, L., Fernando, R., Skelton, H., Reimann, F., Gribble, F.M., Sharkey, A., Marsh, S.G.E., O’rahilly, S., Hemberger, M., Burton, G.J., Moffett, A., 2018. Trophoblast organoids as a model for maternal–fetal interactions during human placentation. *Nature* 564, 263–281. <https://doi.org/10.1038/s41586-018-0753-3>
- Uhlén, M., Fagerberg, L., Hallström, B.M., Lindskog, C., Oksvold, P., Mardinoglu, A., Sivertsson, Å., Kampf, C., Sjöstedt, E., Asplund, A., Olsson, I., Edlund, K., Lundberg, E., Navani, S., Szigartyo, C.A., Odeberg, J., Djureinovic, D., Takanen, J.O., Hober, S., Alm, T., Edqvist, P, H., Berling, H., Tegel, H., Mulder, J., Rockberg, J., Nilsson, P., Schwenk, J.M., Hamsten, M., von Feilitzen, K Forsberg, M., Persson, L., Johansson, F., Zwahlen, M., von Heijne, G., Nielsen, J., Pontén, F., 2015. Tissue-based map of the human proteome. *Science* (80-). 347, 1260419. <https://doi.org/10.1126/science.1260419>
- Unoki, H., Bujo, H., Yamagishi, S. ichi, Takeuchi, M., Imaizumi, T., Saito, Y., 2007. Advanced glycation end products attenuate cellular insulin sensitivity by increasing the generation of intracellular reactive oxygen species in adipocytes. *Diabetes Res. Clin. Pract.* 76, 236–244. <https://doi.org/10.1016/j.diabres.2006.09.016>
- Uribarri, J., Cai, W., Woodward, M., Tripp, E., Goldberg, L., Pyzik, R., Yee, K., Tansman, L., Chen, X., Mani, V., Fayad, Z.A., Vlassara, H., 2015. Elevated serum advanced glycation endproducts in obese indicate risk for the metabolic syndrome: A link between healthy and unhealthy obesity? *J. Clin. Endocrinol. Metab.* 100, 1957–1966. <https://doi.org/10.1210/jc.2014-3925>
- Uribarri, J., Woodruff, S., Goodman, S., Cai, W., Chen, X., Pyzik, R., Yong, A., Striker, G.E., Vlassara, H., 2010. Advanced Glycation End Products in Foods and a Practical Guide to Their Reduction in the Diet. *J. Am. Diet. Assoc.* 110, 911–916. <https://doi.org/10.1016/j.jada.2010.03.018>
- Valckx, S.D.M., De Pauw, I., De Neubourg, D., Inion, I., Berth, M., Fransen, E., Bols, P.E.J., Leroy, J.L.M.R., 2012. BMI-related metabolic composition of the follicular fluid of women undergoing assisted reproductive treatment and the consequences for oocyte and embryo quality. *Hum. Reprod.* 27, 3531–3539. <https://doi.org/10.1093/humrep/des350>
- Van Der Steeg, J.W., Steures, P., Eijkemans, M.J.C., Habbema, J.D.F., Hompes, P.G.A., Burggraaff, J.M., Oosterhuis, G.J.E., Bossuyt, P.M.M., Van Der Veen, F., Mol, B.W.J., 2008. Obesity affects spontaneous pregnancy chances in subfertile, ovulatory women. *Hum. Reprod.* 23, 324–328. <https://doi.org/10.1093/humrep/dem371>
- Varma, V.A., Melin, S.A., Adamec, T.A., Dorman, B.H., Siegfried, J.M., Walton, L.A., Carney, C.N., Norton, C.R., Kaufman, D.G., Varma, V.A., Melin, S.A., Adamec, T.A., N, B.H.D., Siegfried, J.M., Walton, L.A., Carney, C.N., Norton, C.R., Kaufman, D.G., 1982. Monolayer Culture of Human Endometrium : Methods of Culture and Identification of Cell Types Published by : Society for In Vitro Biology Stable URL. *In Vitro* 18, 911–918.
- Veleva, Z., Tiitinen, A., Vilksa, S., Tomas, C., Hyden-Granskog, C., Martikainen, H., Tapanainen, J.S., 2008. High and low BMI increase the risk of miscarriage after IVF / ICSI and FET. *Hum. Reprod.*

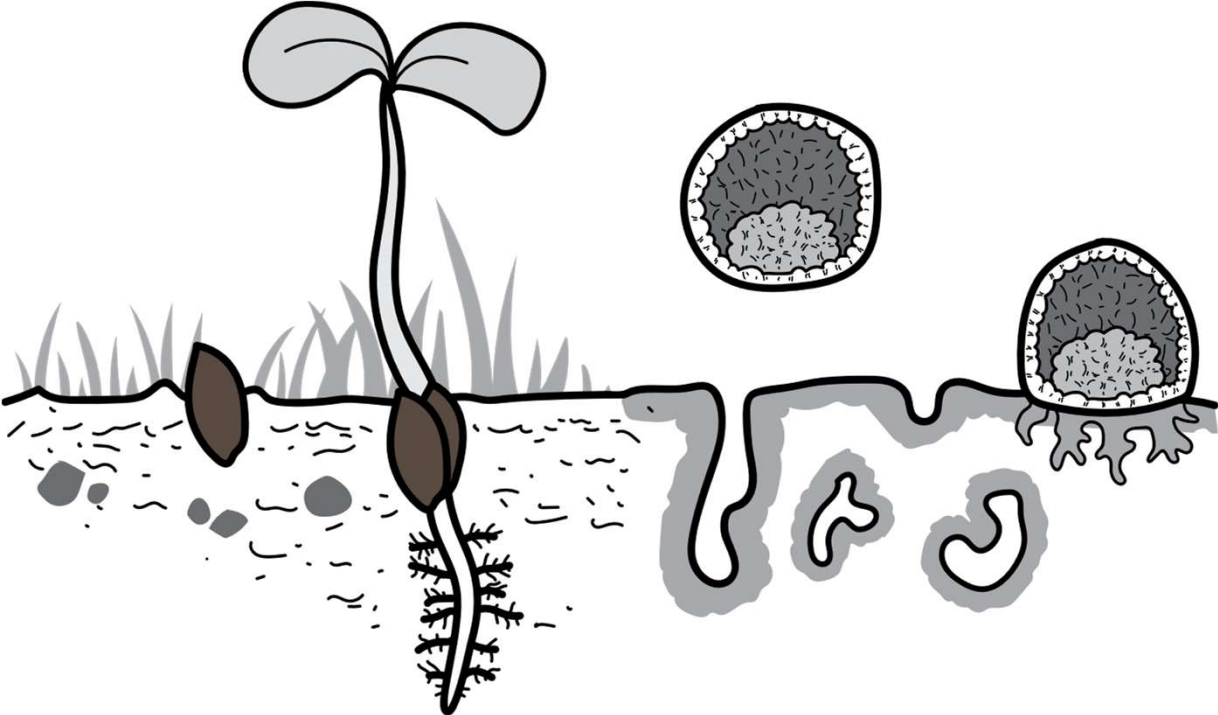
23, 878–884.

- Verma, N.K., Dourlat, J., Davies, A.M., Long, A., Liu, W.Q., Garbay, C., Kelleher, D., Volkov, Y., 2009. STAT3-stathmin interactions control microtubule dynamics in migrating T-cells. *J. Biol. Chem.* 284, 12349–12362. <https://doi.org/10.1074/jbc.M807761200>
- Vutyavanich, T., Saeng-Anan, U., Sirisukkasem, S., Piromlertamorn, W., 2011. Effect of embryo density and microdrop volume on the blastocyst development of mouse two-cell embryos. *Fertil. Steril.* 95, 1435–1439. <https://doi.org/10.1016/j.fertnstert.2010.05.005>
- Wale, P.L., Gardner, D.K., 2016. The effects of chemical and physical factors on mammalian embryo culture and their importance for the practice of assisted human reproduction. *Hum. Reprod. Update* 22, 2–22. <https://doi.org/10.1093/humupd/dmv034>
- Wale, P.L., Gardner, D.K., 2010. Time-lapse analysis of mouse embryo development in oxygen gradients. *Reprod. Biomed. Online* 21, 402–410. <https://doi.org/10.1016/j.rbmo.2010.04.028>
- Walker, D., Lue, L.F., Paul, G., Patel, A., Sabbag, M.N., 2015. Receptor for Advanced Glycation Endproduct Modulators: A new therapeutic target in Alzheimer’s Disease. *Expert Opin. Investig. Drugs* 24, 292–200. <https://doi.org/10.1517/13543784.2015.1001490>
- Walters, E.A., Brown, J.L., Krisher, R., Voelkel, S., Swain, J.E., 2020. Impact of a controlled culture temperature gradient on mouse embryo development and morphokinetics. *Reprod. Biomed. Online* 40, 494–499. <https://doi.org/10.1016/j.rbmo.2019.12.015>
- Wang, H., Pilla, F., Anderson, S., Martínez-Escribano, S., Herrer, I., Moreno-Moya, J.M., Musti, S., Bocca, S., Oehninger, S., Horcajadas, J.A., 2012. A novel model of human implantation: 3D endometrium-like culture system to study attachment of human trophoblast (Jar) cell spheroids. *Mol. Hum. Reprod.* 18, 33–43. <https://doi.org/10.1093/molehr/gar064>
- Wang, W., Vilella, F., Alama, P., Moreno, I., Mignardi, M., Isakova, A., Pan, W., Simon, C., Quake, S.R., 2020. Single-cell transcriptomic atlas of the human endometrium during the menstrual cycle. *Nat. Med.* 26, 1644–1653. <https://doi.org/10.1038/s41591-020-1040-z>
- Wang, X., Zhang, Z., Tao, H., Liu, J., Hopyan, S., Sun, Y., 2018. Characterizing Inner Pressure and Stiffness of Trophoblast and Inner Cell Mass of Blastocysts. *Biophys. J.* 115, 2443–2450. <https://doi.org/10.1016/j.bpj.2018.11.008>
- Wang, Z., Li, H., Guo, R., Wang, Q., Zhang, D., 2016. Antioxidants inhibit advanced glycosylation end-product-induced apoptosis by downregulation of miR-223 in human adipose tissue-derived stem cells. *Sci. Rep.* 6, 1–11. <https://doi.org/10.1038/srep23021>
- Wattanakumtornkul, S., Damario, M.A., Stevens Hall, S.A., Thornhill, A.R., Tummon, I.S., 2003. Body mass index and uterine receptivity in the oocyte donation model. *Fertil. Steril.* 80, 336–340. [https://doi.org/10.1016/S0015-0282\(03\)00595-8](https://doi.org/10.1016/S0015-0282(03)00595-8)
- Weimar, C.H.E., Post Uiterweer, E.D., Teklenburg, G., Heijnen, C.J., Macklon, N.S., 2013. In-vitro model systems for the study of human embryo-endometrium interactions. *Reprod. Biomed. Online* 27, 673–688. <https://doi.org/10.1016/j.rbmo.2013.10.004>
- Whitby, S., Salamonsen, L.A., Evans, J., 2018. The endometrial polarity paradox: Differential

- regulation of polarity within secretory-Phase human endometrium. *Endocrinology* 159, 506–518. <https://doi.org/10.1210/en.2016-1877>
- Wilcox, A.J., Baird, D.D., Weinberg, C.R., 1999. Time of Implantation of the Conceptus and Loss of Pregnancy. *N. Engl. J. Med.* 340, 1796–1799. <https://doi.org/10.1056/NEJM199906103402304>
- Wilcox, A.J., Weinberg, C.R., O'connor, J.F., Baird, D.D., Schlatterer, J.P., Canfield, R., Armstrong, E.G., Nisula, B.C., 1988. Incidence of early loss of pregnancy 319, 189–194. <https://doi.org/10.1056/NEJM198807283190401>
- Winship, A.L., Stringer, J.M., Liew, S.H., Hutt, K.J., 2018. The importance of DNA repair for maintaining oocyte quality in response to anti-cancer treatments , environmental toxins and maternal ageing 24, 119–134. <https://doi.org/10.1093/humupd/dmy002>
- Wittemer, C., Ohl, J., Bailly, M., Bettahar-Lebugle, K., Nisand, I., 2000. Does body mass index of infertile women have an impact on IVF procedure and outcome? *J. Assist. Reprod. Genet.* 17, 547–552.
- Wiwatpanit, T., Murphy, A.R., Lu, Z., Urbanek, M., Burdette, J.E., Woodruff, T.K., Kim, J.J., 2020. Scaffold-Free Endometrial Organoids Respond to Excess Androgens Associated With Polycystic Ovarian Syndrome. *J. Clin. Endocrinol. Metab.* 105, 769–780. <https://doi.org/10.1210/clinem/dgz100>
- Wolf, W.M., Wattick, R.A., Kinkade, O.N., Olfert, M.D., 2018. Geographical prevalence of polycystic ovary syndrome as determined by region and race/ethnicity. *Int. J. Environ. Res. Public Health* 15, 2859. <https://doi.org/10.3390/ijerph15112589>
- Wolffenbuttel, B.H.R., Boulanger, C.M., Crijns, F.R.L., Huijberts, M.S.P., Poitevin, P., Swennen, G.N.M., Vasan, S., Egan, J.J., Ulrich, P., Cerami, A., Levy, B.I., 1998. Breakers of advanced glycation end products restore large artery properties in experimental diabetes. *Proc. Natl. Acad. Sci. U. S. A.* 95, 4630–4634. <https://doi.org/10.1073/pnas.95.8.4630>
- Wu, G., Bazer, F.W., Cudd, T. a, Meininger, C.J., Spencer, T.E., 2004. Recent Advances in Nutritional Sciences Maternal Nutrition and Fetal. *J. Nutr.* 134, 2169–2172.
- Wu, L.L., Russell, D.L., Wong, S.L., Chen, M., Tsai, T.S., St John, J.C., Norman, R.J., Febbraio, M.A., Carroll, J., Robker, R.L., 2015. Mitochondrial dysfunction in oocytes of obese mothers: Transmission to offspring and reversal by pharmacological endoplasmic reticulum stress inhibitors. *Development* 142, 681–691. <https://doi.org/10.1242/dev.114850>
- Wu, Y., He, J., Guo, C., Zhang, Y., Yang, W., Xin, M., Liang, X., Yin, X., Wang, J., Liu, Y., 2017. Serum biomarker analysis in patients with recurrent spontaneous abortion. *Mol. Med. Rep.* 16, 2367–2378. <https://doi.org/10.3892/mmr.2017.6890>
- Xie, J., Méndez, J.D., Méndez-Valenzuela, V., Aguilar-Hernández, M.M., 2013. Cellular signalling of the receptor for advanced glycation end products (RAGE). *Cell. Signal.* 25, 2185–2197. <https://doi.org/10.1016/j.cellsig.2013.06.013>
- Yamabe, S., Hirose, J., Uehara, Y., Okada, T., Okamoto, N., 2013. Intracellular accumulation of advanced glycation end products induces apoptosis via endoplasmic reticulum stress in chondrocytes. *FEBS J.* 280, 1617–1629. <https://doi.org/10.1111/febs.12170>

- Yao, Q., Liang, Y., Shao, Y., Bian, W., Fu, H., Xu, J., Sui, L., Yao, B., Li, M., 2018. Advanced glycation end product concentrations in follicular fluid of women undergoing IVF/ICSI with a GnRH agonist protocol. *Reprod. Biomed. Online* 36, 20–25. <https://doi.org/10.1016/j.rbmo.2017.09.003>
- Yu, Y., Hanssen, K.F., Kalyanaraman, V., Chirindel, A., Jenkins, A.J., Nankervis, A.J., Torjesen, P.A., Scholz, H., Henriksen, T., Lorentzen, B., Garg, S.K., Menard, M.K., Hammad, S.M., Scardo, J.A., Stanley, J.R., Wu, M., Basu, A., Aston, C.E., Lyons, T.J., 2012. Reduced soluble receptor for advanced glycation end-products (sRAGE) scavenger capacity precedes pre-eclampsia in Type 1 diabetes. *BJOG An Int. J. Obstet. Gynaecol.* 119, 1512–1520. <https://doi.org/10.1111/j.1471-0528.2012.03463.x>
- Zaadstra, B.M., Seidell, J.C., Van Noord, P.A., te Velde, E.R., Habbema, J.D., Vrieswijk, B., Karbaat, J., 1993. Fat and female fecundity: prospective study of effect of body fat distribution on conception rates. *Bmj* 306, 484–487. <https://doi.org/10.1136/bmj.306.6876.484>
- Zdravkovic, T., Nazor, K.L., Larocque, N., Gormley, M., Donne, M., Hunkapillar, N., Giritharan, G., Bernstein, H.S., Wei, G., Hebrok, M., Zeng, X., Genbacev, O., Mattis, A., McMaster, M.T., 2015. Human stem cells from single blastomeres reveal pathways of embryonic or trophoblast fate specification 1, 4010–4025. <https://doi.org/10.1242/dev.122846>
- Zhang, E., Li, X., Zhang, B., Cai, L., Tao, X., Xing, W., Tao, X., 2012. Relationship Between Obesity and Menstrual Disturbances Among Women of Reproductive Age. *Heart* 98, E156.1-E156. <https://doi.org/10.1136/heartjnl-2012-302920h.3>
- Zhang, Q., Wang, Y., Fu, L., 2020. Dietary advanced glycation end-products: Perspectives linking food processing with health implications. *Compr. Rev. Food Sci. Food Saf.* 19, 2559–2587. <https://doi.org/10.1111/1541-4337.12593>
- Zhang, S., Kong, S., Wang, B., Cheng, X., Chen, Y., Wu, W., Wang, Q., Shi, J., Zhang, Y., Wang, S., Lu, J., Lydon, J.P., DeMayo, F., Pear, W.S., Han, H., Lin, H., Li, L., Wang, Hongmei, Wang, Y.L., Li, B., Chen, Q., Duan, E., Wang, Haibin, 2014. Uterine Rbpj is required for embryonic-uterine orientation and decidual remodeling via Notch pathway-independent and -dependent mechanisms. *Cell Res.* 24, 925–942. <https://doi.org/10.1038/cr.2014.82>
- Zhang, S.S., Xia, W.T., Xu, J., Xu, H.L., Lu, C.T., Zhao, Y.Z., Wu, X.Q., 2017. Three-dimensional structure micelles of heparin-poloxamer improve the therapeutic effect of 17 β -estradiol on endometrial regeneration for intrauterine adhesions in a rat model. *Int. J. Nanomedicine* 12, 5643–5657. <https://doi.org/10.2147/IJN.S137237>

Appendices



Appendix 1: Widely used Solutions

A1.1: Tris Buffered Saline (10X)

Tris buffered saline (TBS) was used to wash sections in immunohistochemistry and membranes in Western Immunoblotting. Stock solution diluted to 1X in distilled water immediately prior to use.

- 80 g NaCl
- 24.2 g Trizma Base (Sigma)
- Volume adjusted to 1 L using distilled water
- pH adjusted to 7.4 with concentrated HCl

TBS-T was made by addition of 2 mL Tween-20 to 1 L of 1X TBS (0.2% vol/vol).

A1.2: Phosphate Buffered Saline (10X)

Phosphate buffered saline (PBS) was used to dialyse AGEs-HSA solutions (made in-house) and wash sections for immunohistochemistry (Thermofisher).

- 80 g NaCl
- 2 g KCl
- 14.4 g Na₂HPO₄ anhydrous
- 2.4 g KH₂PO₄
- Volume adjusted to 1 L using distilled water
- pH adjusted to 7.4 using concentrated HCl

Stock solution was diluted to 1X in distilled water immediately prior to use.

A1.3: Sodium Citrate antigen retrieval solution (10X)

In all optimised immunohistochemistry protocols, antigen retrieval was performed by immersion of sections in boiling 10 mM sodium citrate buffer.

- 2.94 g trisodium citrate dehydrate (Sigma)
- Volume adjusted to 1 L with distilled water
- pH adjusted to 6.0 with concentrated HCl
- 0.05 % Tween-20 (% vol/vol)

Stock solution was diluted to 1X in distilled water immediately prior to use.

A1.4 SDS buffer for gel electrophoresis (4X)

SDS buffer was used to denature protein samples for Western Immunoblotting.

- 4 mL glycerol (100%)
- 2.4 mL 1 M Tris/HCl (pH 6.8)
- 0.8 g SDS
- Volume adjusted to 10 mL with distilled water

Dithiothreitol was added to a final concentration of 0.1 M immediately prior to use. Buffer diluted to 1X in sample for use in gel electrophoresis.

Appendix 2: Endometrial 3D Co-Gel

To generate spheroid-monolayer interfaces, a 3D co-gel was utilised to attempt to make a cross section more amenable to sectioning. The 3D co-gel was developed by a previous PhD student in this laboratory, Harriet Fitzgerald. Presented here is her optimised protocol, as detailed in her thesis. The volumes of reagents were doubled to allow generation of the co-gel in a 12-well cell culture insert, rather than in the original 24-well insert.

Components:

- Fibrinogen (Sigma, 5 mg/mL)
- Thrombin (Sigma, 100 units/mL)
- CaCl₂ (2M)
- Collagen I (Sigma, 3 mg/mL)
- NaOH (0.1 M)
- Aprotinin (Sigma, 10 mg/mL)
- Protease inhibitor cocktail (Millipore, reconstituted as per manufacturer's recommendation)

On ice, 87.5 μ L thrombin and 0.75 μ L CaCl₂ were combined. In a 12-well cell culture insert, 250 μ L collagen and 45 μ L NaOH were mixed gently (final pH 7.3). Two μ L of the trypsin inhibitor aprotinin and protease inhibitor cocktail were added to the collagen mix in the transwell insert. The thrombin/CaCl₂ mixture was removed from ice and added to the gel mix. Finally, 175 μ L fibrinogen was added to the gel mix, and the gel set by incubation at 37°C for approximately 1 h. In DMEM/F-12 medium containing 4 μ L/mL PI cocktail and 40 μ g/mL aprotinin, 10% FCS, and 1% Ab/Am, 1.5×10^5 ECC-1 cells were seeded on top of the co-gel, and allowed to settle overnight. Hormonal priming was performed as per standard protocols with the addition of protease inhibitors and aprotinin in the media.

Appendix 3: The human adhesome and receptome

Prior to the start of my candidature, proteins involved in endometrial epithelial receptivity and adhesion of trophoblast spheroids were identified by proteomics in collaboration with Dr David Greening, and interrogated to define the human endometrial epithelial “receptome”, and the embryo-epithelial “adhesome”. The proteomic identification of these, and my preliminary validation have been published (Appendix 4).

For ease of reference, presented here are the proteins identified in the receptome (receptive vs non-receptive monolayers) and adhesome (adhesive co-cultures vs all non-adhesive conditions) from our published report. Proteins that are unique, or exclusive to either the receptome or adhesome were not identified to be differentially regulated in the alternative. For example, PC4 is uniquely upregulated in the receptome, as it is not identified to be differentially expressed between adhesive cultures and non-adhesive conditions, the adhesome. In contrast, PTGS2 is highly upregulated in the adhesome (in adhesive conditions vs non-adhesive conditions), and is not found either upregulated or downregulated in the receptome (between receptive vs non-receptive monolayers).

A3.1 String analysis of protein interactions

The protein names from each category of receptome and adhesome proteins were uploaded and their interactions analysed using STRING version 10.5 (<http://string-db.org>).

A3.1.1 String analysis: total upregulated proteins of the receptome

136 proteins in total were upregulated in the epithelial receptome. These proteins are the combination of the proteins uniquely upregulated, upregulated in the receptome and adhesome, and proteins upregulated in the receptome and downregulated in the adhesome.

String analysis shows clusters of proteins known to interact within this cohort, but the majority of the upregulated proteins of the receptome have no previously identified or predicted interactions (Figure A3.1), not surprising as the endometrium is currently understudied. These proteins may not interact directly but may work together to orchestrate endometrial receptivity. Proteins known to interact that may pose interesting targets for functional investigation include SLIRP which is connected to SRRM2, U2SURP, AQE, SARNP, and PC4 (here denoted as SUB1). Connections between proteins represent known or predicted interactions. Knockdown of interconnected proteins will likely result in the loss of interactions which may significantly hinder the acquisition of receptivity and thus determination of proteins which sit at the hub of a number of interactions will enable us to more appropriately target proteins for functional knockdown studies.

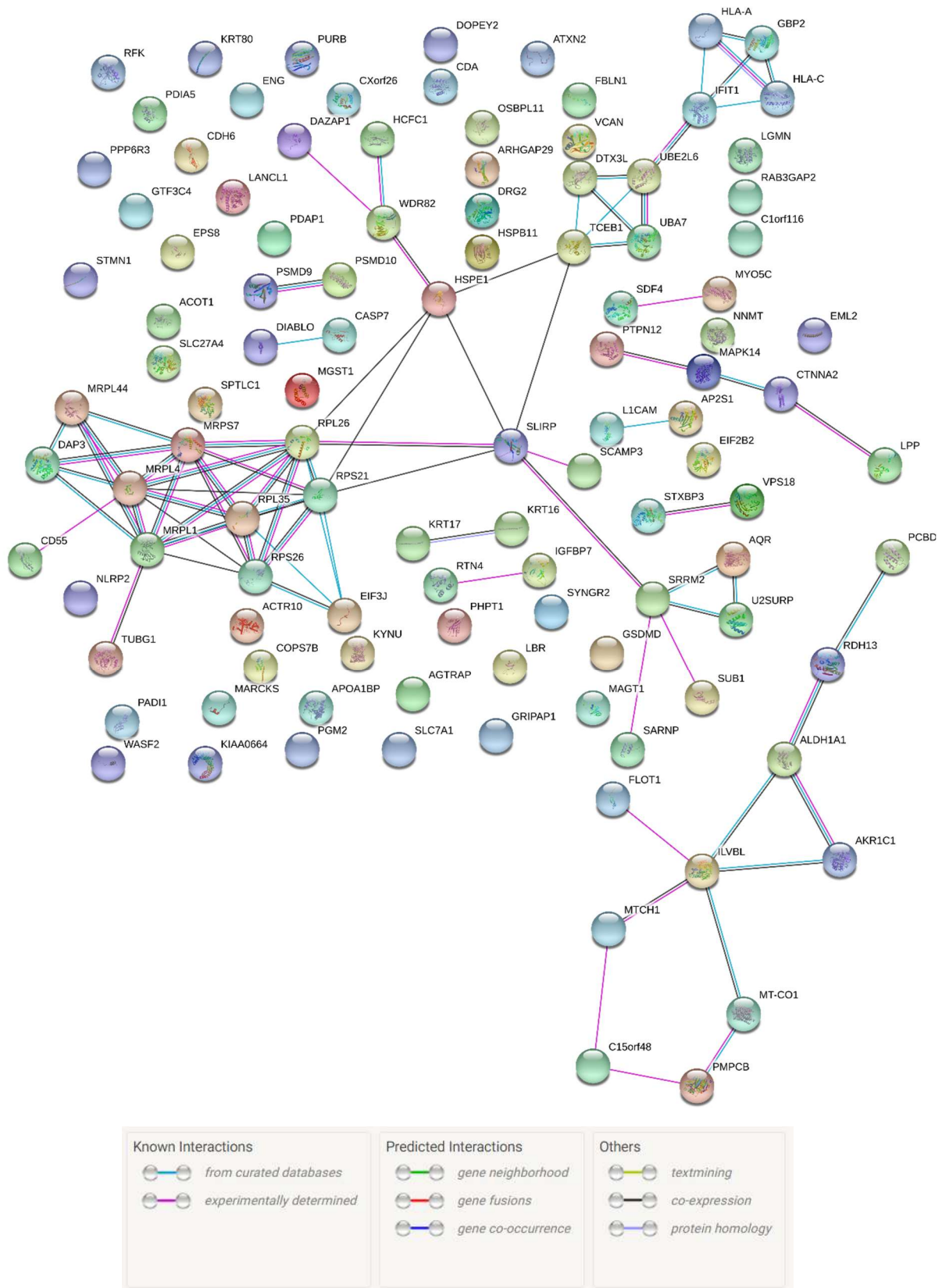


Figure A3.1: Interactions of the proteins upregulated in the receptome. String analysis of the total proteins upregulated in the receptome.

A3.1.2 String analysis: total downregulated proteins of the receptome

131 proteins in total were downregulated in the epithelial receptome. These proteins are the combination of the proteins uniquely downregulated, commonly downregulated in the receptome and adhesome, and downregulated in the receptome whilst upregulated in the adhesome.

Subsets of proteins downregulated in the receptome have known or are predicted to have interactions (Figure A3.2). A large number of proteins have no known interactions; however, it is possible they work together to regulate endometrial receptivity and have not been investigated together before. Interconnecting proteins of interest for further studies include SNRPD2, which is connected to NUP43, R8M25, EFTUD1, and RPS 29; and MTOR which is connected to SMARCA4, LAMTOR3, PRKAA1 and MON2. Overexpression of these proteins may significantly affect the receptivity of endometrial epithelial cells.

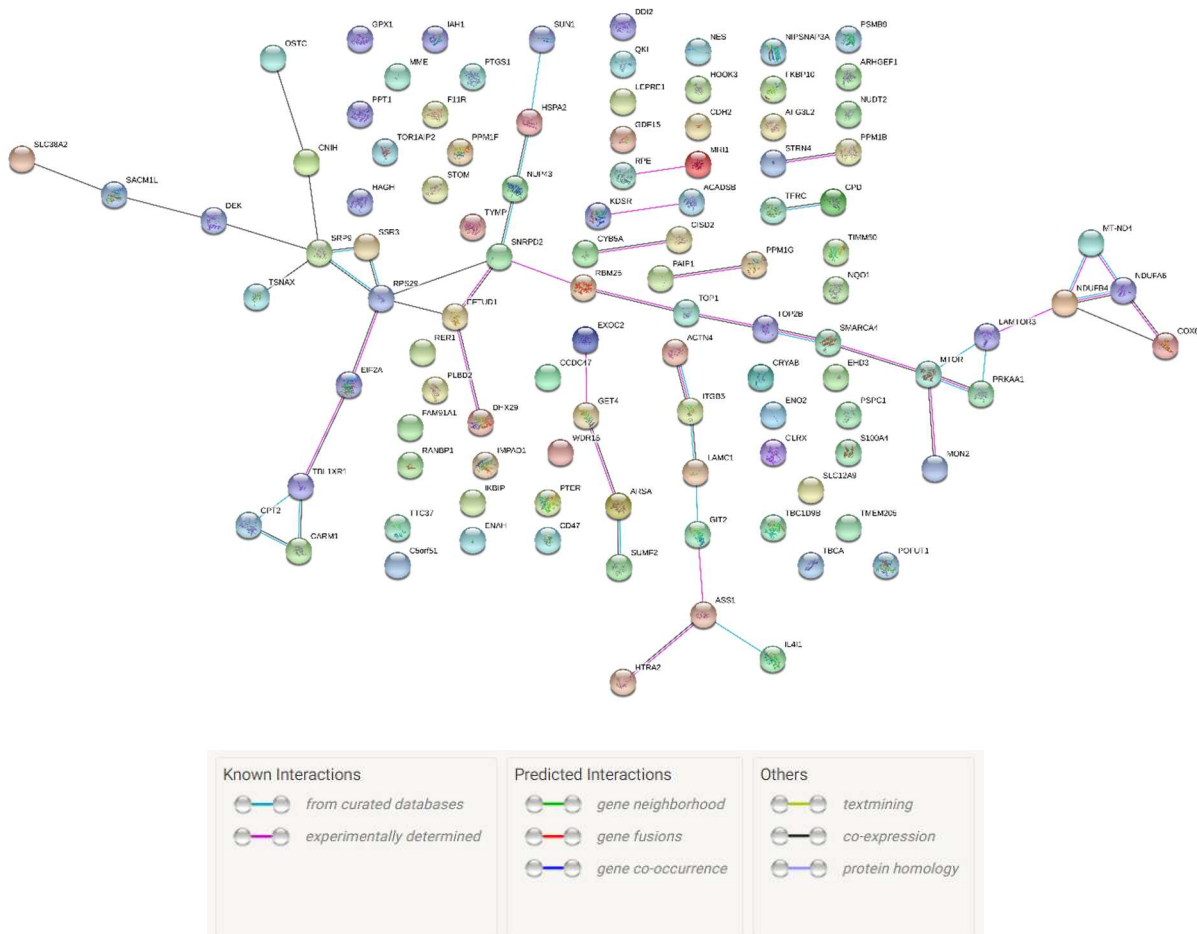
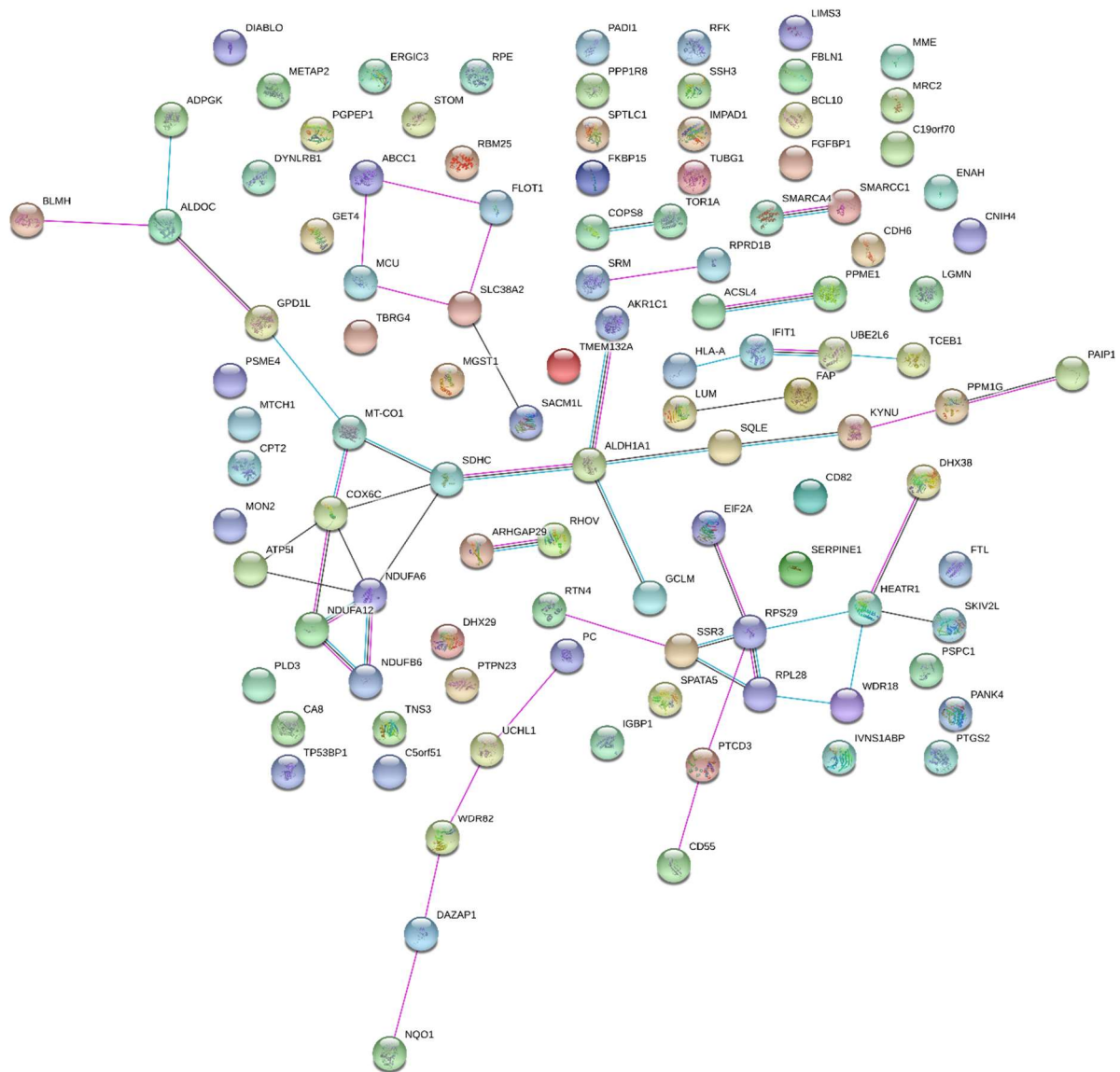


Figure A3.2: String analysis of the proteins downregulated in the receptome. Known and predicted interactions of the total proteins downregulated in the receptome.

A3.1.3 String analysis: total proteins upregulated in the adhesome

In total, 142 proteins were found to be upregulated in the adhesome. These comprise the proteins uniquely upregulated, commonly upregulated with the receptome, and upregulated in the adhesome whilst downregulated in the receptome.

There are several networks of known or predicted interactions in the proteins upregulated in the adhesome (Figure A3.3). For example, KYNU, which is upregulated in the receptome, and further upregulated in the adhesome, is connected to SQLE and PPM1G, and SDHC is connected to MT-CO1, COX6C, NDUFA6, and ALH1A1. These proteins are of interest for knockdown studies as their removal would interrupt a network of protein interactions. Highly upregulated proteins including PTGS2 and SERPINE1 do not show previously identified or predicted interactions, however it is likely that this cohort of proteins do interact in some manner to regulate human embryo adhesion but this has not previously been demonstrated in other systems which are typically curated to perform these interaction analyses.



Nodes:

Network nodes represent proteins

splice isoforms or post-translational modifications are collapsed, i.e. each node represents all the proteins produced by a single, protein-coding gene locus.

Node Color

-  *colored nodes: query proteins and first shell of interactors*
-  *white nodes: second shell of interactors*

Node Content

-  *empty nodes: proteins of unknown 3D structure*
-  *filled nodes: some 3D structure is known or predicted*

Edges:

Edges represent protein-protein associations

associations are meant to be specific and meaningful, i.e. proteins jointly contribute to a shared function; this does not necessarily mean they are physically binding each other.

Known Interactions

-  *from curated databases*
-  *experimentally determined*

Predicted Interactions

-  *gene neighborhood*
-  *gene fusions*
-  *gene co-occurrence*

Others

-  *textmining*
-  *co-expression*
-  *protein homology*

Figure A3.3: Interactions of the proteins upregulated in the adhesome. String analysis of the total proteins upregulated in the adhesome.

A3.1.4 String analysis: total proteins downregulated in the adhesome

Clusters of proteins with known and predicted interactions exist within the cohort of 143 proteins downregulated in the human adhesome, as shown in Figure A3.4. Proteins of interest include NUP62, CRKL, DENR, and SRSF11 as they have multiple interactions. As these proteins are downregulated in the adhesome, their overexpression may significantly affect embryo adhesion and are therefore of interest in functional studies.

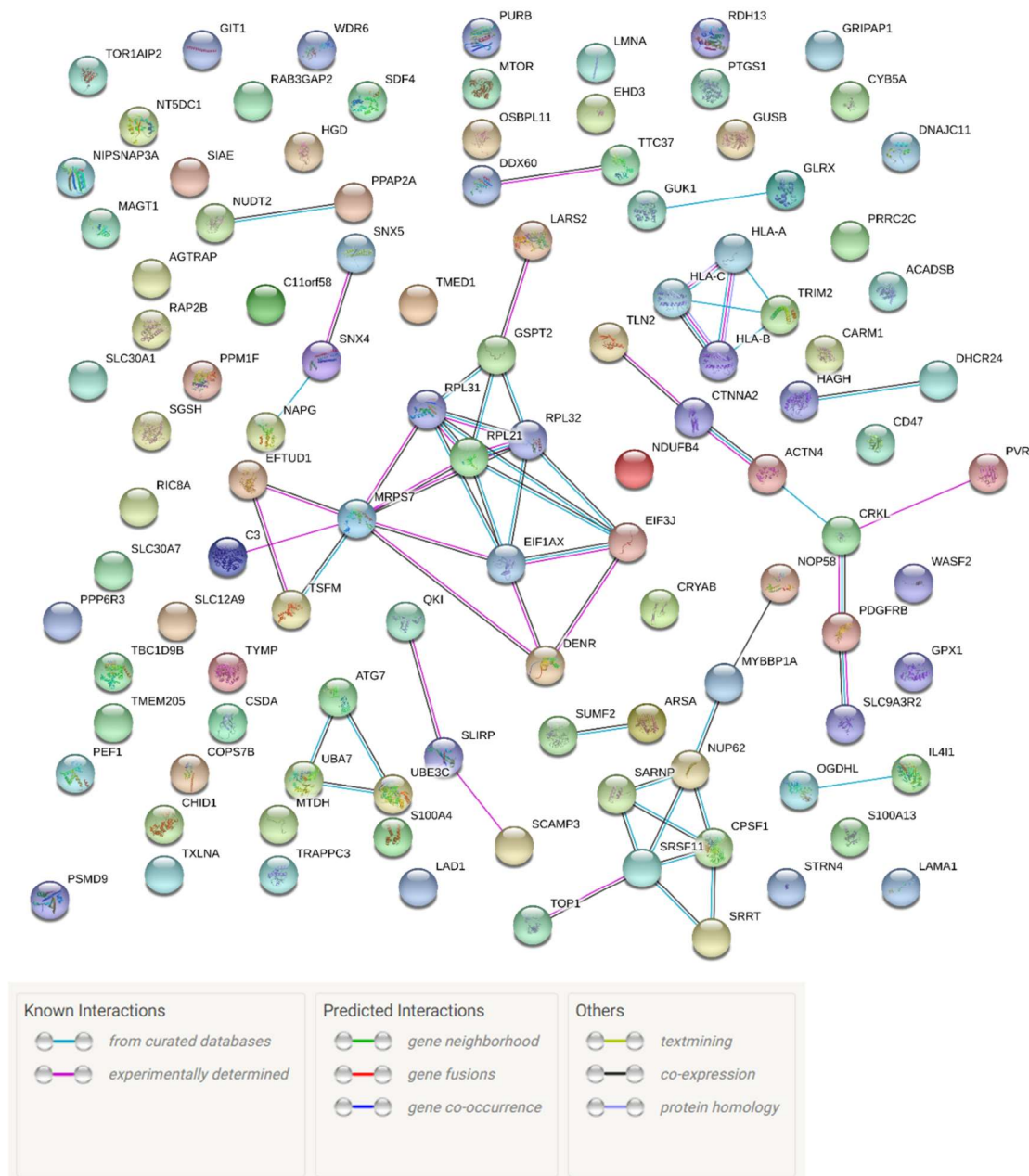


Figure A3.4: String analysis of the proteins downregulated in the adhesome. Known and predicted interactions of the total proteins identified to be down regulated in the adhesome.

A3.2 Unique proteins of the receptome

A3.2.1 Proteins uniquely upregulated in the epithelial receptome

136 proteins were found to be upregulated, and 132 proteins were downregulated in the receptome in total. In comparison with the adhesome, 78 proteins were uniquely upregulated in the receptome (Table A3.1), and 61 proteins uniquely downregulated (Table A3.2). These may be considered to more accurately define biomarkers for the receptive endometrium.

Table A3.1: Proteins uniquely upregulated in the receptome. Proteomic data of proteins found only to be upregulated in receptive epithelial monolayers.

| <i>Proteins uniquely up-regulated in the Receptome</i> | | | |
|--|-------------|------------------|----------------|
| <i>Protein</i> | | <i>LFQ Ratio</i> | <i>P-Value</i> |
| <i>Accession Number</i> | <i>Name</i> | | |
| A0A024RB14 | RPS26 | 148828.99 | 4.1E-03 |
| Q6IBA2 | PC4 | 132259.85 | 2.4E-03 |
| Q9UNM1 | EPFP1 | 125494.85 | 2.3E-02 |
| Q53GD1 | Q53GD1 | 115212.97 | 4.0E-173 |
| Q8WVC2 | RPS21 | 115176.96 | 2.2E-04 |
| J3QRI7 | RPL26 | 112715.89 | 4.6E-178 |
| P42766 | RPL35 | 86455.29 | 1.8E-02 |
| A0A024R5U4 | C15orf48 | 80461.85 | 2.4E-05 |
| A2A2D0 | STMN1 | 75958.04 | 8.3E-04 |
| V5NQE0 | HLA-C | 71489.02 | 1.7E-187 |
| A0A024R8T9 | SYNGR2 | 61886.91 | 3.1E-03 |
| B2R6X6 | B2R6X6 | 60357.49 | 2.0E-02 |
| Q6FGB3 | PCBD | 51061.54 | 3.5E-04 |
| V9HWC4 | HEL-S-132P | 43154.94 | 8.6E-03 |
| P29966 | MARCKS | 40722.89 | 1.5E-179 |
| Q13442 | PDAP1 | 34331.49 | 7.2E-05 |
| P53680 | AP2S1 | 31265.26 | 1.6E-05 |
| P32320 | CDA | 30701.14 | 4.5E-05 |
| H3BMT0 | JPT2 | 29823.77 | 1.1E-161 |
| Q8NCW5 | NAXE | 27517.36 | 2.3E-04 |
| A1Z1D7 | HLA-A | 23096.80 | 1.8E-173 |
| E5RFX7 | PLPBP | 22960.59 | 6.1E-03 |
| Q9BW04 | SARG | 21905.71 | 4.0E-02 |
| Q9Y547 | HSPB11 | 21117.36 | 4.6E-03 |
| Q6KB66 | KRT80 | 20845.58 | 2.0E-03 |
| J3QR71 | DRG2 | 18796.20 | 8.0E-160 |
| Q9BVG4 | PBDC1 | 17788.84 | 2.1E-05 |
| A1L0T0 | ILVBL | 16316.56 | 2.0E-04 |
| B4E0K5 | MAPK14 | 15491.64 | 1.7E-05 |
| Q96CP5 | PMPCB | 12049.93 | 6.3E-05 |
| K7ES61 | MRPL4 | 11752.44 | 1.3E-05 |
| Q14554 | PDIA5 | 11260.18 | 1.3E-168 |

| | | | |
|------------|-------------|---------|----------|
| A0A024R3R5 | LBR | 9809.16 | 6.6E-08 |
| O95834 | EML2 | 9365.59 | 3.5E-04 |
| G3V4F2 | ACOT1 | 9359.16 | 1.3E-162 |
| Q9BPX4 | EIF2B2 | 9077.49 | 3.5E-05 |
| A0PJ79 | MRPL1 | 8743.71 | 2.9E-03 |
| Q6FHH6 | LANCL1 | 8510.19 | 3.0E-04 |
| B4DW31 | B4DW31 | 8355.47 | 6.5E-03 |
| B1AJY5 | PSMD10 | 8243.06 | 5.4E-04 |
| J3KN39 | NLRP2 | 7982.91 | 3.2E-04 |
| A0A024R8D2 | SLC27A4 | 7890.20 | 7.2E-167 |
| Q05209 | PTPN12 | 7696.50 | 4.9E-06 |
| A0A024R473 | MRPL44 | 7235.14 | 8.2E-04 |
| P55210 | CASP7 | 7212.21 | 8.9E-04 |
| P51398 | DAP3 | 6755.70 | 3.0E-02 |
| P32456 | GBP2 | 6611.56 | 2.2E-163 |
| Q96G03 | PGM2 | 6541.01 | 1.2E-163 |
| A0A0A8K9B7 | SLC7A1 | 6259.10 | 3.5E-07 |
| B4DX55 | B4DX55 | 6078.08 | 2.0E-03 |
| Q8TDB6 | DTX3L | 5690.09 | 1.2E-07 |
| P57764 | GSDMD | 4984.02 | 4.8E-157 |
| Q12929 | EPS8 | 4294.24 | 2.9E-03 |
| A8K6Q9 | A8K6Q9 | 4143.29 | 2.9E-02 |
| A0A024R9R3 | VPS18 | 3884.76 | 1.9E-02 |
| O15042 | U2SURP | 3331.45 | 1.1E-02 |
| O00186 | STXBP3 | 3301.91 | 1.3E-02 |
| B4DHG4 | B4DHG4 | 3014.09 | 1.9E-04 |
| I3L2B0 | CLUH | 2939.40 | 2.8E-04 |
| Q05CN7 | GTF3C4 | 2772.90 | 2.7E-05 |
| H0YH87 | ATXN2 | 1748.80 | 3.5E-02 |
| Q9UQ35 | SRRM2 | 1725.25 | 7.5E-166 |
| Q9Y3R5 | DOPEY2 | 1524.46 | 1.1E-04 |
| A0A024R9L1 | AQR | 1422.96 | 7.2E-03 |
| P51610 | HCFC1 | 1331.61 | 1.5E-158 |
| Q9NQX4 | MYO5C | 1116.19 | 3.1E-154 |
| E9PF17 | VCAN | 5.78 | 1.2E-10 |
| A0A087WZF1 | LPP | 3.16 | 1.4E-05 |
| Q53GU8 | Q53GU8 | 2.92 | 4.9E-05 |
| A0A024RDA6 | IGFBP7 | 2.38 | 7.2E-04 |
| Q6FH49 | NNMT | 2.26 | 1.6E-03 |
| Q53G64 | Q53G64 | 2.25 | 1.8E-03 |
| Q7Z3Z9 | L1CAM | 2.20 | 2.1E-03 |
| Q5T9B9 | ENG | 2.16 | 2.5E-03 |
| P08779 | KRT16 | 2.15 | 3.4E-03 |
| Q04695 | KRT17 | 2.14 | 3.1E-03 |
| A0A024QZ62 | hCG_1998851 | 2.11 | 3.4E-03 |
| Q05DQ7 | ACTR10 | 2.00 | 6.2E-03 |

A3.2.2 Proteins uniquely downregulated in the receptome

61 proteins were found exclusively in the downregulated receptome, as listed in Table A3.2.

Table A3.2: Proteins uniquely downregulated in the receptome. Proteomic data of proteins found only to be downregulated in receptive epithelial monolayers.

| <i>Proteins uniquely down-regulated in Receptome</i> | | | |
|--|-------------|----------------------|----------------|
| <i>Protein</i> | | <i>LFQ Ratio</i> | <i>P-Value</i> |
| <i>Accession Number</i> | <i>Name</i> | | |
| A0A087WUD3 | OSTC | 8.4x10 ⁻⁶ | 1.3E-02 |
| A4D110 | LOC401309 | 6.7x10 ⁻⁶ | 6.2E-06 |
| P62316 | SNRPD2 | 7.0x10 ⁻⁶ | 3.5E-07 |
| C9JJ34 | RANBP1 | 1.0x10 ⁻⁵ | 1.1E-04 |
| Q59GA0 | Q59GA0 | 1.1x10 ⁻⁵ | 6.9E-04 |
| P49458 | SRP9 | 1.7x10 ⁻⁵ | 3.1E-04 |
| E5RIW3 | TBCA | 2.1x10 ⁻⁵ | 4.9E-02 |
| Q9UHA4 | LAMTOR3 | 2.3x10 ⁻⁵ | 7.1E-06 |
| G3V5P8 | CNIH1 | 2.5x10 ⁻⁵ | 1.6E-03 |
| P14854 | COX6B1 | 2.8x10 ⁻⁵ | 4.2E-03 |
| O95168 | NDUFB4 | 2.8x10 ⁻⁵ | 2.6E-165 |
| Q70UQ0 | IKBIP | 3.5x10 ⁻⁵ | 6.1E-05 |
| A0A024R6B5 | HSPA2 | 4.1x10 ⁻⁵ | 1.7E-04 |
| Q8N5K1 | CISD2 | 4.4x10 ⁻⁵ | 1.3E-05 |
| Q3ZCQ8 | TIMM50 | 5.1x10 ⁻⁵ | 6.2E-07 |
| B4DFG0 | DEK | 5.2x10 ⁻⁵ | 6.7E-03 |
| A0A024R3V8 | TSNAX | 5.4x10 ⁻⁵ | 6.3E-06 |
| A2ACR1 | PSMB9 | 5.7x10 ⁻⁵ | 6.2E-05 |
| Q9H488 | POFUT1 | 5.8x10 ⁻⁵ | 1.0E-04 |
| Q96A33 | CCDC47 | 6.7x10 ⁻⁵ | 6.6E-05 |
| A8K6V7 | A8K6V7 | 6.9x10 ⁻⁵ | 5.5E-03 |
| Q53FX5 | Q53FX5 | 7.2x10 ⁻⁵ | 1.6E-02 |
| B4DMV0 | B4DMV0 | 7.2x10 ⁻⁵ | 1.0E-170 |
| D3DVF0 | F11R | 7.3x10 ⁻⁵ | 4.6E-04 |
| H7C5G1 | IAH1 | 8.2x10 ⁻⁵ | 8.0E-159 |
| Q99988 | GDF15 | 8.3x10 ⁻⁵ | 1.3E-162 |
| A0A0C4DG44 | HOOK3 | 1.0x10 ⁻⁴ | 9.8E-08 |
| A0A0C4DG44 | HTRA2 | 1.0x10 ⁻⁴ | 1.0E-163 |
| A0A024R292 | FVT1 | 1.0x10 ⁻⁴ | 1.9E-160 |
| B3KML1 | B3KML1 | 1.1x10 ⁻⁴ | 4.0E-02 |
| A0PJK4 | NUP43 | 1.1x10 ⁻⁴ | 1.7E-03 |
| Q96BW5 | PTER | 1.1x10 ⁻⁴ | 5.9E-160 |
| A0A024RC42 | CDH2 | 1.3x10 ⁻⁴ | 1.4E-04 |
| Q8NHP8 | PLBD2 | 1.3x10 ⁻⁴ | 8.1E-165 |
| Q9BV20 | MRI1 | 1.4x10 ⁻⁴ | 7.1E-04 |
| Q4GG69 | NADH4 | 1.4x10 ⁻⁴ | 1.9E-161 |
| C9JIR6 | PPM1B | 1.4x10 ⁻⁴ | 1.9E-158 |
| D3DUJ0 | AFG3L2 | 1.4x10 ⁻⁴ | 5.4E-05 |

| | | | |
|------------|----------|----------------------|----------|
| H0Y6N5 | SUN1 | 1.5x10 ⁻⁴ | 9.8E-03 |
| B4DSH1 | B4DSH1 | 1.6x10 ⁻⁴ | 2.2E-03 |
| Q6ZNJ9 | FLJ00319 | 1.8x10 ⁻⁴ | 9.1E-158 |
| A0A024R0R1 | ARHGEF1 | 1.9x10 ⁻⁴ | 1.2E-04 |
| Q5TDH0 | DDI2 | 2.1x10 ⁻⁴ | 2.4E-02 |
| Q9BZK7 | TBL1XR1 | 2.1x10 ⁻⁴ | 6.6E-157 |
| Q13131 | PRKAA1 | 2.3x10 ⁻⁴ | 6.6E-03 |
| A0A024QZT2 | EXOC2 | 2.9x10 ⁻⁴ | 3.0E-03 |
| F8WAK2 | GIT2 | 3.2x10 ⁻⁴ | 3.4E-04 |
| O75976 | CPD | 3.3x10 ⁻⁴ | 1.9E-02 |
| E7ER68 | FAM91A1 | 3.4x10 ⁻⁴ | 3.4E-03 |
| Q71UH4 | TOP2B | 3.6x10 ⁻⁴ | 7.2E-03 |
| D3DVC4 | NES | 0.38 | 2.7E-04 |
| Q5T6L4 | ASS | 0.43 | 1.5E-03 |
| A0A024R972 | LAMC1 | 0.44 | 2.5E-03 |
| Q6FHV6 | ENO2 | 0.45 | 2.6E-03 |
| P50897 | PPT1 | 0.46 | 3.4E-03 |
| P02786 | TFRC | 0.47 | 4.2E-03 |
| Q32P28 | P3H1 | 0.47 | 5.4E-03 |
| A8KA19 | A8KA19 | 0.49 | 6.4E-03 |
| Q5T094 | RER1 | 0.49 | 6.9E-03 |
| L7RT22 | ITGB5 | 0.49 | 8.6E-03 |
| A0A024R1W3 | FKBP10 | 0.50 | 9.3E-03 |

A3.3 Unique proteins of the adhesome

A3.3.1 Upregulated proteins of the adhesome

In total, 143 proteins were found to be upregulated in the adhesome, and 137 proteins were downregulated in the adhesome. In comparison with the receptome, 78 proteins were uniquely upregulated in the adhesome (Table A3.3), and 78 proteins uniquely downregulated (Table 2.4). These may more accurately represent the proteins involved in the *in vivo* adhesion process. Of the 78 upregulated proteins unique to the adhesome, 27 have previously been implicated in endometrial receptivity.

Table A3.3: Proteins uniquely upregulated in the adhesome. Proteomic data of proteins found only to be upregulated in receptive epithelial monolayers co-cultured with trophectoderm spheroids versus non-adhesive conditions.

| <i>Up-regulated in Adhesome</i> | | | |
|---------------------------------|-------------|------------------|----------------|
| <i>Protein</i> | | <i>LFQ Ratio</i> | <i>P-Value</i> |
| <i>Accession Number</i> | <i>Name</i> | | |
| P35354 | PTGS2 | 381848.79 | 1.2E-171 |
| H0YMF4 | RPL28 | 141956.25 | 4.7E-13 |
| A6NLH6 | CNIH4 | 58664.24 | 7.6E-10 |
| A0A024QYT5 | SERPINE1 | 58522.14 | 6.1E-34 |

| | | | |
|------------|---------------|----------|---------|
| P56385 | ATP5I | 43444.45 | 9.6E-17 |
| D3DVH1 | SDHC | 32531.11 | 3.6E-14 |
| P19623 | SRM | 32200.88 | 8.1E-15 |
| A0A0D9SEN1 | FAP | 31278.30 | 5.0E-24 |
| Q9NP97 | DYNLRB1 | 28654.86 | 1.5E-02 |
| POCW19 | LIMS3 | 26485.72 | 2.1E-02 |
| P51884 | LUM | 25932.84 | 5.9E-10 |
| B7Z2X4 | B7Z2X4 | 22524.82 | 3.8E-16 |
| A0A024R9M9 | CHP | 21904.79 | 9.9E-17 |
| E9PGT6 | COPS8 | 19223.51 | 5.2E-10 |
| Q14512 | FGFBP1 | 19114.82 | 6.0E-14 |
| A8K0F7 | A8K0F7 | 18944.51 | 9.5E-05 |
| P48507 | GCLM | 17213.50 | 2.1E-10 |
| O95139 | NDUFB6 | 15950.00 | 5.6E-09 |
| Q9NXJ5 | PGPEP1 | 15266.83 | 5.1E-03 |
| Q68D50 | DKFZp779I1858 | 14179.98 | 0.0E+00 |
| Q8NE86 | MCU | 13951.85 | 4.3E-03 |
| A0A024R0Q4 | PLD3 | 13447.69 | 0.0E+00 |
| A2TJK5 | ERGIC3 | 12690.95 | 3.5E-17 |
| B0S7P4 | B0S7P4 | 12058.79 | 3.7E-04 |
| B4DRW6 | B4DRW6 | 11855.37 | 0.0E+00 |
| A8K5M0 | A8K5M0 | 11124.66 | 9.8E-04 |
| Q9HC03 | Q9HC03 | 9971.09 | 2.6E-28 |
| O95999 | BCL10 | 9832.05 | 6.3E-10 |
| Q13867 | BLMH | 8615.17 | 1.3E-12 |
| Q9NQG5 | RPRD1B | 8354.09 | 3.9E-04 |
| B4DLP6 | B4DLP6 | 8306.92 | 1.3E-10 |
| P78318 | IGBP1 | 7299.90 | 4.0E-27 |
| P50579 | METAP2 | 6994.07 | 1.1E-09 |
| B7Z4K8 | B7Z4K8 | 6965.39 | 1.2E-32 |
| Q561W4 | PPP1R8 | 5927.07 | 1.1E-03 |
| B4DKY3 | B4DKY3 | 5582.91 | 4.6E-02 |
| D3DVL7 | TBRG4 | 5455.92 | 2.6E-11 |
| Q8N335 | GPD1L | 4471.51 | 8.3E-40 |
| E7EVQ6 | SQLE | 4343.84 | 0.0E+00 |
| B4DM28 | B4DM28 | 4141.64 | 9.0E-08 |
| Q9Y6Y0 | IVNS1ABP | 4107.22 | 1.1E-05 |
| Q9H3S7 | PTPN23 | 4011.86 | 4.1E-09 |
| B2RBA6 | B2RBA6 | 3202.04 | 4.6E-06 |
| B3KM81 | B3KM81 | 3174.54 | 1.8E-08 |
| Q68CZ2 | TNS3 | 2949.16 | 2.5E-02 |
| Q58EY4 | SMARCC1 | 2930.05 | 3.2E-09 |
| E9PHT6 | PANK4 | 2784.08 | 6.3E-18 |
| A8KAQ3 | A8KAQ3 | 2721.98 | 1.1E-23 |
| Q96EY7 | PTCD3 | 2512.29 | 1.2E-03 |
| Q8NB90 | SPATA5 | 2410.38 | 0.0E+00 |
| B4DS55 | B4DS55 | 2204.24 | 2.4E-04 |
| B7Z670 | B7Z670 | 2151.84 | 3.3E-25 |

| | | | |
|------------|----------|---------|---------|
| Q5T1M5 | FKBP15 | 1995.76 | 6.5E-10 |
| A0A024R5C5 | PC | 1823.20 | 2.1E-03 |
| A6NNK5 | TP53BP1 | 1802.91 | 2.4E-03 |
| P35219 | CA8 | 5.69 | 5.5E-05 |
| V9HW74 | HEL-117 | 5.62 | 2.2E-19 |
| Q9UI09 | NDUFA12 | 4.97 | 5.2E-05 |
| Q14997 | PSME4 | 4.93 | 2.0E-03 |
| A0A024R3R7 | HEATR1 | 4.27 | 5.0E-05 |
| I1VE18 | SEC22B | 4.23 | 7.7E-03 |
| B2RB23 | B2RB23 | 4.05 | 4.8E-06 |
| B4E318 | B4E318 | 4.02 | 1.2E-12 |
| Q9BRR6 | ADPGK | 3.74 | 1.2E-04 |
| A0A024QZ64 | ALDOC | 3.45 | 7.0E-06 |
| Q5XKP0 | MIC13 | 3.35 | 2.1E-02 |
| Q9UBG0 | MRC2 | 3.30 | 9.0E-05 |
| Q9NPK3 | SKIV2L | 3.05 | 3.1E-03 |
| B4DM30 | DHX38 | 2.98 | 4.6E-03 |
| O60488 | ACSL4 | 2.94 | 4.0E-08 |
| I3L4X2 | ABCC1 | 2.67 | 2.9E-04 |
| A0A024R5J4 | SSH3 | 2.62 | 2.6E-03 |
| A0A024R9B7 | COX6C | 2.45 | 2.2E-03 |
| Q9Y570 | PPME1 | 2.43 | 5.3E-04 |
| P02792 | FTL | 2.21 | 6.5E-05 |
| Q24JP5 | TMEM132A | 2.11 | 1.8E-04 |
| O14656 | TOR1A | 2.06 | 2.9E-04 |
| Q6LETO | KAI1 | 2.01 | 9.6E-03 |

A3.3.2 Proteins downregulated in the adhesome

78 proteins were found to be uniquely downregulated in the adhesome (Table A3.4).

Table A3.4: Proteins uniquely downregulated in the adhesome. Proteomic data of proteins identified only as downregulated in receptive epithelial monolayers co-cultured with trophectoderm spheroids.

| <i>Down-regulated in Adhesome</i> | | | |
|-----------------------------------|-------------|-----------------------|----------------|
| <i>Protein</i> | | <i>LFQ Ratio</i> | <i>P-Value</i> |
| <i>Accession Number</i> | <i>Name</i> | | |
| Q6IAX2 | RPL21 | 4.69x10 ⁻⁶ | 4.1E-05 |
| H7C2W9 | RPL31 | 6.42x10 ⁻⁶ | 1.4E-06 |
| Q99584 | S100A13 | 1.1x10 ⁻⁵ | 1.5E-05 |
| D3YTB1 | RPL32 | 1.8x10 ⁻⁵ | 1.9E-178 |
| P47813 | EIF1AX | 2.5x10 ⁻⁵ | 5.1E-05 |
| Q53F37 | Q53F37 | 3.0x10 ⁻⁵ | 1.1E-06 |
| P51688 | SGSH | 3.5x10 ⁻⁵ | 3.7E-06 |
| A8K7A4 | A8K7A4 | 3.5x10 ⁻⁵ | 2.1E-177 |
| B4DQW0 | B4DQW0 | 3.6x10 ⁻⁵ | 8.4E-169 |
| W8QE H3 | LMNA | 3.9x10 ⁻⁵ | 1.6E-183 |

| | | | |
|------------|---------------|----------------------|----------|
| B4DHY8 | TSFM | 4.5x10 ⁻⁵ | 4.4E-04 |
| Q8NCJ3 | Q8NCJ3 | 5.2x10 ⁻⁵ | 2.1E-02 |
| Q5JQ44 | DKFZp547A0616 | 5.3x10 ⁻⁵ | 1.3E-03 |
| Q8IYD1 | GSPT2 | 5.3x10 ⁻⁵ | 1.5E-08 |
| Q9Y6M5 | SLC30A1 | 5.4x10 ⁻⁵ | 1.0E-177 |
| B4DY59 | B4DY59 | 5.5x10 ⁻⁵ | 1.3E-03 |
| E9PM92 | C11orf58 | 6.0x10 ⁻⁵ | 2.3E-02 |
| Q9UBV8 | PEF1 | 6.1x10 ⁻⁵ | 4.5E-04 |
| A0A024RBR3 | DENR | 6.3x10 ⁻⁵ | 3.2E-169 |
| A8KAQ5 | A8KAQ5 | 6.4x10 ⁻⁵ | 4.3E-02 |
| A0A024RAV4 | CSDA | 6.5x10 ⁻⁵ | 1.9E-02 |
| A8K885 | A8K885 | 7.8x10 ⁻⁵ | 5.2E-170 |
| Q8NEW0 | SLC30A7 | 7.9x10 ⁻⁵ | 6.9E-169 |
| Q96IN2 | GUK1 | 8.1x10 ⁻⁵ | 4.7E-02 |
| B2RB07 | B2RB07 | 9.1x10 ⁻⁵ | 4.4E-07 |
| V9HWA9 | HEL-S-62p | 1.1x10 ⁻⁴ | 1.0E-04 |
| Q9NVH1 | DNAJC11 | 1.1x10 ⁻⁴ | 1.4E-03 |
| Q68DQ4 | DKFZp779L0468 | 1.1x10 ⁻⁴ | 4.4E-02 |
| M0QXN5 | NUP62 | 1.2x10 ⁻⁴ | 2.2E-05 |
| A0A024RCB5 | CHID1 | 1.2x10 ⁻⁴ | 3.2E-05 |
| Q13445 | TMED1 | 1.3x10 ⁻⁴ | 3.7E-158 |
| Q5TFE4 | NT5DC1 | 1.4x10 ⁻⁴ | 3.9E-04 |
| P46109 | CRKL | 1.5x10 ⁻⁴ | 3.2E-161 |
| Q9Y5X3 | SNX5 | 1.5x10 ⁻⁴ | 1.4E-02 |
| O43617 | TRAPPC3 | 1.5x10 ⁻⁴ | 3.0E-04 |
| P09619 | PDGFRB | 1.5x10 ⁻⁴ | 7.0E-06 |
| O95219 | SNX4 | 1.6x10 ⁻⁴ | 4.0E-05 |
| Q86U75 | Q86U75 | 1.6x10 ⁻⁴ | 1.0E-02 |
| Q9Y2X3 | NOP58 | 1.6x10 ⁻⁴ | 3.3E-02 |
| A0A024R1K8 | Nbla03646 | 1.7x10 ⁻⁴ | 8.6E-161 |
| Q9NPQ8 | RIC8A | 1.7x10 ⁻⁴ | 2.0E-03 |
| Q15599 | SLC9A3R2 | 1.7x10 ⁻⁴ | 6.2E-04 |
| Q8NBL9 | Q8NBL9 | 1.7x10 ⁻⁴ | 1.4E-03 |
| Q6KEQ1 | HLA-B | 1.8x10 ⁻⁴ | 1.4E-163 |
| Q05BU6 | SFRS11 | 1.9x10 ⁻⁴ | 9.0E-158 |
| Q9H9B7 | Q9H9B7 | 2.1x10 ⁻⁴ | 1.8E-04 |
| P40222 | TXLNA | 2.2x10 ⁻⁴ | 4.7E-163 |
| Q9ULD0 | OGDHL | 2.2x10 ⁻⁴ | 1.7E-03 |
| Q93099 | HGD | 3.0x10 ⁻⁴ | 9.4E-154 |
| K7EKE8 | NECTIN2 | 3.0x10 ⁻⁴ | 3.4E-153 |
| Q53HG5 | Q53HG5 | 3.1x10 ⁻⁴ | 4.5E-154 |
| Q96SW8 | Q96SW8 | 3.2x10 ⁻⁴ | 1.0E-156 |
| Q9C040 | TRIM2 | 3.2x10 ⁻⁴ | 8.9E-165 |
| I3L1L3 | MYBBP1A | 3.3x10 ⁻⁴ | 1.2E-05 |
| Q9BXB4 | OSBPL11 | 3.8x10 ⁻⁴ | 4.7E-03 |
| B4E1Q7 | B4E1Q7 | 4.2x10 ⁻⁴ | 9.1E-150 |
| A7E261 | OPLAH | 4.2x10 ⁻⁴ | 4.7E-163 |
| A0A024QZS3 | PPAP2A | 4.8x10 ⁻⁴ | 2.7E-06 |

| | | | |
|------------|---------------|----------------------|----------|
| Q8NDH0 | DKFZp434F1720 | 4.9x10 ⁻⁴ | 8.0E-156 |
| Q9HAT2 | SIAE | 5.3x10 ⁻⁴ | 1.1E-152 |
| A0A024R2E9 | ATG7 | 5.3x10 ⁻⁴ | 3.6E-152 |
| Q6FHY4 | NAPG | 5.5x10 ⁻⁴ | 1.4E-153 |
| Q15386 | UBE3C | 6.1x10 ⁻⁴ | 2.9E-02 |
| B4E1E2 | B4E1E2 | 6.2x10 ⁻⁴ | 1.4E-154 |
| E9PHM2 | LARS2 | 6.7x10 ⁻⁴ | 2.4E-155 |
| B3KTS4 | B3KTS4 | 7.1x10 ⁻⁴ | 3.7E-155 |
| Q9BXP5 | SRRT | 6.8x10 ⁻⁴ | 4.2E-02 |
| A0A0C4DGN6 | GIT1 | 7.2x10 ⁻⁴ | 9.4E-05 |
| P25391 | LAMA1 | 1.4x10 ⁻³ | 5.6E-20 |
| Q9Y4G6 | TLN2 | 1.6x10 ⁻³ | 5.5E-04 |
| D3DWL9 | CPSF1 | 1.9x10 ⁻³ | 2.9E-03 |
| Q8IY21 | DDX60 | 3.4x10 ⁻³ | 1.1E-02 |
| E7EPN9 | PRRC2C | 3.9x10 ⁻³ | 5.7E-154 |
| E3UPC4 | HLA-C | 0.39 | 5.6E-05 |
| P08236 | GUSB | 0.46 | 5.4E-04 |
| Q6IPJ9 | LAD1 | 0.47 | 7.7E-04 |
| X5D2K4 | HLA-A | 0.49 | 1.4E-03 |
| A0A024R9D2 | MTDH | 0.49 | 1.5E-03 |

A3.4 Proteins common to the receptome and adhesome

33 proteins were found to be commonly upregulated in both the epithelial receptome and the adhesome (Table A3.5). 40 proteins were found to be downregulated in both the epithelial receptome and the adhesome (Table A3.6).

Table A3.5: Proteins upregulated in both the receptome and adhesome. Proteomic data of proteins found upregulated in both cohorts.

| <i>Up-regulated in Receptome and Adhesome</i> | | | | | |
|---|-------------|------------------|----------------|------------------|----------------|
| <i>Protein</i> | | <i>Receptome</i> | | <i>Adhesome</i> | |
| <i>Accession Number</i> | <i>Name</i> | <i>LFQ Ratio</i> | <i>P-Value</i> | <i>LFQ Ratio</i> | <i>P-Value</i> |
| Q16719 | KYNU | 178099.64 | 2.9E-09 | 3.14 | 3.6E-07 |
| B2R577 | B2R577 | 137062.59 | 2.1E-178 | 4.99 | 1.2E-16 |
| E5RHG8 | ELOC | 62608.62 | 2.3E-02 | 2.01 | 2.6E-02 |
| Q502X2 | DIABLO | 57987.46 | 1.7E-02 | 2.49 | 7.8E-04 |
| A0A059RPW0 | COX1 | 31333.99 | 8.5E-05 | 2.95 | 7.9E-03 |
| E5FQ49 | HLA-A | 27503.20 | 2.2E-06 | 2.97 | 2.8E-05 |
| H3BLV0 | CD55 | 24814.93 | 2.1E-05 | 4.16 | 7.6E-05 |
| G3V4E4 | LG MN | 22065.77 | 1.2E-02 | 4.64 | 1.7E-04 |
| K7EQ02 | DAZAP1 | 20140.57 | 3.0E-04 | 2.97 | 5.3E-03 |
| O14933 | UBE2L6 | 19588.02 | 2.6E-03 | 2.34 | 1.7E-03 |
| B3KM58 | B3KM58 | 19364.33 | 5.7E-06 | 3.60 | 2.6E-05 |
| B7Z5F9 | B7Z5F9 | 18587.02 | 4.5E-02 | 3.48 | 8.9E-05 |
| Q04828 | AKR1C1 | 18192.67 | 1.1E-168 | 9.62 | 4.2E-32 |
| P09914 | IFIT1 | 18112.13 | 1.5E-08 | 2.49 | 1.1E-04 |

| | | | | | |
|------------|-----------|----------|----------|------|---------|
| Q9NQC3 | RTN4 | 16674.50 | 1.4E-08 | 2.08 | 2.6E-03 |
| B2R761 | B2R761 | 15465.51 | 2.1E-03 | 2.06 | 9.1E-03 |
| B7ZAC1 | B7ZAC1 | 12308.73 | 2.3E-174 | 3.40 | 6.6E-07 |
| P23142 | FBLN1 | 11564.30 | 1.0E-06 | 2.05 | 5.0E-03 |
| A8YXX5 | PIG60 | 10478.91 | 1.2E-02 | 3.25 | 8.5E-03 |
| A8K4C2 | A8K4C2 | 9786.04 | 8.7E-169 | 2.13 | 1.9E-04 |
| Q59GM9 | Q59GM9 | 9468.05 | 4.4E-173 | 3.12 | 6.7E-09 |
| Q9ULC6 | PADI1 | 9132.33 | 3.6E-169 | 2.29 | 8.5E-03 |
| A0A024R333 | TMEM113 | 8163.58 | 7.5E-04 | 4.34 | 2.1E-05 |
| Q969G6 | RFK | 7268.39 | 4.0E-147 | 3.63 | 3.5E-05 |
| P23258 | TUBG1 | 6948.12 | 1.9E-160 | 3.19 | 5.8E-05 |
| Q6IB58 | FLOT1 | 5866.75 | 2.7E-04 | 5.23 | 5.0E-14 |
| P55285 | CDH6 | 5395.70 | 1.2E-04 | 2.91 | 8.9E-03 |
| B4DH44 | B4DH44 | 5281.56 | 3.0E-03 | 2.17 | 4.0E-03 |
| A0A024R277 | SPTLC1 | 4979.49 | 3.4E-02 | 3.49 | 9.8E-05 |
| A8K6Q9 | A8K6Q9 | 4143.29 | 2.9E-02 | 2.95 | 9.0E-02 |
| Q52LW3 | ARHGAP29 | 3243.62 | 1.4E-05 | 2.04 | 3.3E-02 |
| V9HW83 | HEL-S-53e | 4.98 | 2.7E-09 | 5.74 | 1.3E-19 |
| Q6LET6 | MGST1 | 2.49 | 4.1E-04 | 2.17 | 9.3E-05 |

Table A3.6: Proteins downregulated in both the receptome and adhesome. Proteomic data of proteins identified as downregulated in both cohorts.

| <i>Down-regulated in Receptome and Adhesome</i> | | | | | |
|---|-------------|----------------------|----------------|----------------------|----------------|
| <i>Protein</i> | | <i>Receptome</i> | | <i>Adhesome</i> | |
| <i>Accession Number</i> | <i>Name</i> | <i>LFQ Ratio</i> | <i>P-Value</i> | <i>LFQ Ratio</i> | <i>P-Value</i> |
| AOA024RAM2 | GLRX | 1.4x10 ⁻⁵ | 1.7E-171 | 4.3x10 ⁻⁵ | 3.8E-160 |
| K7EM09 | TMEM205 | 1.7x10 ⁻⁵ | 2.6E-04 | 2.4x10 ⁻⁵ | 2.3E-02 |
| Q08722 | CD47 | 2.1x10 ⁻⁵ | 4.2E-181 | 6.2x10 ⁻⁵ | 9.4E-170 |
| P26447 | S100A4 | 2.2x10 ⁻⁵ | 3.7E-165 | 6.6x10 ⁻⁵ | 8.2E-154 |
| P00167 | CYB5A | 2.2x10 ⁻⁵ | 3.8E-02 | 2.9x10 ⁻⁵ | 1.1E-02 |
| P15289 | ARSA | 2.4x10 ⁻⁵ | 5.4E-06 | 3.6x10 ⁻⁵ | 6.4E-05 |
| Q70UQ0 | NDUFB4 | 2.8x10 ⁻⁵ | 2.6E-165 | 8.4x10 ⁻⁵ | 1.3E-158 |
| Q9UFN0 | NIPSNAP3A | 3.6x10 ⁻⁵ | 1.5E-170 | 1.1x10 ⁻⁴ | 3.2E-02 |
| A0A087X296 | PTGS1 | 5.5x10 ⁻⁵ | 4.1E-05 | 1.8x10 ⁻⁴ | 4.0E-07 |
| Q7LD69 | Q7LD69 | 5.5x10 ⁻⁵ | 6.2E-163 | 1.7x10 ⁻⁴ | 4.0E-02 |
| B2R5I8 | B2R5I8 | 6.4x10 ⁻⁵ | 3.4E-02 | 1.0x10 ⁻⁴ | 2.1E-02 |
| B7Z7Q6 | B7Z7Q6 | 6.5x10 ⁻⁵ | 6.7E-169 | 1.9x10 ⁻⁴ | 1.5E-157 |
| H3BPK3 | HAGH | 6.6x10 ⁻⁵ | 7.8E-03 | 1.0x10 ⁻⁴ | 4.0E-05 |
| B7Z5V6 | B7Z5V6 | 6.7x10 ⁻⁵ | 5.9E-175 | 1.0x10 ⁻⁴ | 2.1E-174 |
| B2RDN1 | B2RDN1 | 7.0x10 ⁻⁵ | 5.9E-03 | 1.0x10 ⁻⁴ | 3.0E-161 |
| B4DM76 | B4DM76 | 7.4x10 ⁻⁵ | 1.2E-02 | 2.2x10 ⁻⁴ | 7.8E-154 |
| C9JL30 | SUMF2 | 7.5x10 ⁻⁵ | 3.6E-163 | 1.2x10 ⁻⁴ | 3.5E-160 |
| K7EJH8 | ACTN4 | 8.4x10 ⁻⁵ | 2.1E-155 | 2.5x10 ⁻⁴ | 4.1E-153 |
| Q9NZN3 | EHD3 | 8.4x10 ⁻⁵ | 2.0E-169 | 2.5x10 ⁻⁴ | 3.3E-163 |
| P50583 | NUDT2 | 9.7x10 ⁻⁵ | 1.0E-150 | 2.9x10 ⁻⁴ | 3.6E-144 |

| | | | | | |
|------------|----------|----------------------|----------|----------------------|----------|
| P11387 | TOP1 | 9.9x10 ⁻⁵ | 3.8E-03 | 1.5x10 ⁻⁴ | 2.8E-03 |
| Q86X55 | CARM1 | 1.0x10 ⁻⁴ | 7.0E-04 | 1.7x10 ⁻⁴ | 1.4E-05 |
| Q9H8D6 | Q9H8D6 | 1.2x10 ⁻⁴ | 6.7E-04 | 2.0x10 ⁻⁴ | 7.6E-05 |
| Q96PU8 | QKI | 1.2x10 ⁻⁴ | 1.2E-02 | 3.7x10 ⁻⁴ | 6.8E-157 |
| Q0VGL7 | PPM1F | 1.5x10 ⁻⁴ | 1.5E-04 | 4.4x10 ⁻⁴ | 1.8E-147 |
| A0A024R957 | TOR1AIP2 | 1.5x10 ⁻⁴ | 1.6E-160 | 2.3x10 ⁻⁴ | 2.9E-02 |
| F5GYK2 | STRN4 | 1.8x10 ⁻⁴ | 6.9E-03 | 5.3x10 ⁻⁴ | 2.2E-159 |
| Q9NX47 | 38412 | 1.9x10 ⁻⁴ | 1.4E-03 | 2.8x10 ⁻⁴ | 1.3E-02 |
| D6W5X5 | SLC12A9 | 2.2x10 ⁻⁴ | 1.1E-154 | 6.5x10 ⁻⁴ | 2.4E-143 |
| B3KPZ7 | B3KPZ7 | 2.2x10 ⁻⁴ | 1.0E-156 | 3.5x10 ⁻⁴ | 3.2E-02 |
| A1L3A9 | TBC1D9B | 2.4x10 ⁻⁴ | 5.0E-167 | 4.1x10 ⁻⁴ | 9.2E-04 |
| P45954 | ACADSB | 2.6x10 ⁻⁴ | 8.0E-152 | 7.9x10 ⁻⁴ | 6.2E-146 |
| Q7Z2Z2 | EFL1 | 3.5x10 ⁻⁴ | 1.8E-160 | 1.1x10 ⁻³ | 4.0E-149 |
| B3KNC3 | B3KNC3 | 4.3x10 ⁻⁴ | 8.1E-04 | 5.9x10 ⁻⁴ | 8.5E-154 |
| Q6PGP7 | TTC37 | 5.0x10 ⁻⁴ | 5.2E-03 | 7.6x10 ⁻⁴ | 1.1E-02 |
| P42345 | MTOR | 7.0x10 ⁻⁴ | 6.5E-04 | 1.0x10 ⁻³ | 6.3E-03 |
| A0A087WUQ6 | GPX1 | 0.32 | 2.2E-05 | 2.0x10 ⁻⁵ | 2.8E-10 |
| Q96RQ9 | IL4I1 | 0.38 | 3.4E-04 | 0.38 | 2.5E-05 |
| C9JGI3 | TYMP | 0.38 | 3.3E-04 | 0.35 | 8.2E-06 |
| E9PR44 | CRYAB | 0.46 | 3.4E-03 | 0.48 | 1.1E-03 |

A3.5 Proteins differentially regulated in the receptome and adhesome

A subset of proteins was found to be conversely regulated between the epithelial receptome and the adhesome. 26 proteins were upregulated in the receptome while downregulated in the adhesome (Table A3.7) and 32 proteins were downregulated in the receptome while upregulated in the adhesome (Table A3.8).

Table A3.7: Proteins upregulated receptivity but downregulated in adhesion. Proteomic data of proteins identified to have opposing regulation in the adhesome and receptome.

| <i>Up-regulated in receptome/down-regulated in adhesome</i> | | | | | |
|---|-------------|------------------|----------------|----------------------|----------------|
| <i>Protein</i> | | <i>Receptome</i> | | <i>Adhesome</i> | |
| <i>Accession Number</i> | <i>Name</i> | <i>LFQ Ratio</i> | <i>P-Value</i> | <i>LFQ Ratio</i> | <i>P-Value</i> |
| Q53F35 | Q53F35 | 70594.67 | 1.4E-12 | 2.1x10 ⁻⁵ | 1.7E-181 |
| A0A087WUN7 | SLIRP | 47042.76 | 2.5E-03 | 3.2x10 ⁻⁵ | 5.8E-165 |
| Q6RW13 | AGTRAP | 29356.81 | 1.9E-05 | 1.0x10 ⁻⁴ | 4.6E-02 |
| Q567R9 | CIP29 | 26358.89 | 6.2E-03 | 1.1x10 ⁻⁴ | 2.0E-157 |
| A0A024R084 | SDF4 | 16701.84 | 8.7E-05 | 1.8x10 ⁻⁴ | 1.9E-02 |
| A0A024R5S5 | EIF3S1 | 16286.05 | 6.9E-03 | 7.6x10 ⁻⁵ | 5.7E-167 |
| P26232 | CTNNA2 | 15800.98 | 6.9E-181 | 1.9x10 ⁻⁴ | 1.9E-04 |
| Q6FHJ5 | SCAMP3 | 15646.11 | 2.9E-04 | 1.1x10 ⁻⁴ | 1.5E-166 |
| R9RVK4 | HLA-A | 15208.55 | 5.9E-07 | 2.0x10 ⁻⁴ | 9.5E-04 |
| B7ZAH9 | B7ZAH9 | 14471.71 | 7.3E-163 | 2.1x10 ⁻⁴ | 1.6E-151 |
| Q9H0U3 | MAGT1 | 13508.56 | 1.9E-05 | 1.4x10 ⁻⁴ | 8.2E-04 |
| J3KN29 | PSMD9 | 12436.34 | 2.7E-03 | 1.3x10 ⁻⁴ | 4.5E-158 |

| | | | | | |
|------------|----------|----------|----------|----------|----------|
| B6VEX5 | B6VEX5 | 12436.00 | 1.6E-02 | 9.5x10-5 | 1.7E-03 |
| Q9Y6W5 | WASF2 | 11659.97 | 4.3E-04 | 1.2x10-4 | 1.5E-03 |
| Q96QR8 | PURB | 11595.19 | 2.2E-162 | 2.6x10-4 | 8.2E-159 |
| B4DEB4 | B4DEB4 | 11538.40 | 3.8E-02 | 2.6x10-4 | 3.8E-03 |
| J3QQS1 | MRPS7 | 11117.83 | 5.2E-154 | 2.7x10-4 | 3.6E-148 |
| J3QT95 | COPS7B | 9005.11 | 1.3E-149 | 3.3x10-4 | 4.4E-03 |
| B4DMZ0 | B4DMZ0 | 6770.80 | 1.2E-03 | 2.2x10-4 | 5.8E-03 |
| A0A024R4M8 | RDH13 | 4793.96 | 1.5E-151 | 6.3x10-4 | 3.3E-140 |
| Q9BXB4 | OSBPL11 | 4432.75 | 4.3E-04 | 3.8x10-4 | 4.7E-03 |
| B4E0K0 | B4E0K0 | 3396.52 | 8.3E-151 | 8.8x10-4 | 9.0E-03 |
| A0A087WT45 | GRIPAP1 | 3188.02 | 1.1E-157 | 9.4x10-4 | 2.4E-146 |
| A0A024R5F3 | SAPS3 | 2540.82 | 1.1E-02 | 5.2x10-4 | 1.1E-02 |
| P41226 | UBA7 | 2233.00 | 2.3E-03 | 5.0x10-4 | 7.0E-04 |
| Q9H2M9 | RAB3GAP2 | 1548.50 | 4.6E-02 | 8.7x10-4 | 4.6E-04 |

Table A3.8: Proteins upregulated adhesion but downregulated in receptivity. Proteomic data of proteins identified to have opposing regulation in the adhesome and receptome.

| Up-regulated in adhesome/down-regulated in receptome | | | | | |
|--|---------|----------------------|----------|-----------|---------|
| Protein | | Receptome | | Adhesome | |
| Accession Number | Name | LFQ Ratio | P-Value | LFQ Ratio | P-Value |
| A0A024R882 | STOM | 1.5x10 ⁻⁴ | 1.8E-02 | 12.24 | 5.6E-36 |
| P08473 | MME | 1.4x10 ⁻⁴ | 2.6E-167 | 9.25 | 8.3E-23 |
| P23786 | CPT2 | 2.4x10 ⁻⁴ | 2.2E-02 | 4.82 | 1.6E-04 |
| B4DPY0 | B4DPY0 | 2.2x10 ⁻⁵ | 4.8E-02 | 4.14 | 3.4E-04 |
| B2R7C2 | B2R7C2 | 2.4x10 ⁻⁴ | 7.7E-161 | 4.10 | 2.0E-09 |
| A0A024R0W3 | SLC38A2 | 6.3x10 ⁻⁵ | 1.2E-172 | 3.91 | 4.4E-06 |
| B3KNG6 | B3KNG6 | 1.1x10 ⁻⁴ | 4.1E-159 | 3.53 | 6.5E-11 |
| A7E2E1 | SMARCA4 | 1.1x10 ⁻³ | 4.0E-151 | 3.49 | 1.2E-03 |
| U3KQC1 | WDR18 | 1.4x10 ⁻⁴ | 1.0E-158 | 3.47 | 2.8E-05 |
| A8K369 | A8K369 | 1.7x10 ⁻⁴ | 1.6E-02 | 3.47 | 4.6E-03 |
| P15559 | NQO1 | 2.0x10 ⁻⁵ | 2.3E-10 | 3.31 | 1.4E-08 |
| A0A024R7W0 | IMPAD1 | 3.9x10 ⁻⁵ | 2.2E-174 | 3.30 | 7.2E-06 |
| A8K923 | A8K923 | 2.4x10 ⁻⁴ | 2.4E-05 | 3.27 | 1.1E-03 |
| Q9BY44 | EIF2A | 1.7x10 ⁻⁴ | 4.4E-02 | 3.26 | 3.9E-02 |
| C9JA28 | SSR3 | 2.4x10 ⁻⁵ | 3.0E-171 | 3.23 | 1.5E-09 |
| A0A024R094 | PAIP1 | 7.6x10 ⁻⁵ | 2.0E-163 | 3.16 | 1.6E-04 |
| B4E295 | B4E295 | 2.6x10 ⁻⁴ | 1.1E-161 | 3.04 | 7.2E-04 |
| Q7L5D6 | GET4 | 1.2x10 ⁻⁴ | 3.3E-02 | 3.03 | 4.5E-02 |
| Q96AT9 | RPE | 1.1x10 ⁻⁴ | 2.0E-154 | 2.99 | 2.6E-08 |
| A0A024RDP4 | PSPC1 | 4.8x10 ⁻⁵ | 5.8E-05 | 2.92 | 1.9E-02 |
| Q9UES0 | Q9UES0 | 3.0x10 ⁻⁵ | 2.4E-02 | 2.74 | 4.2E-03 |
| A0A0C4DGW6 | C5orf51 | 6.4x10 ⁻⁵ | 8.4E-157 | 2.73 | 4.9E-03 |
| P49756 | RBM25 | 3.3x10 ⁻⁴ | 2.7E-03 | 2.70 | 1.8E-03 |
| Q7Z478 | DHX29 | 3.6x10 ⁻⁴ | 7.7E-163 | 2.65 | 2.0E-03 |
| Q6IAU5 | PPM1G | 1.0x10 ⁻⁴ | 1.2E-02 | 2.62 | 2.3E-04 |
| B3KWE2 | B3KWE2 | 2.3x10 ⁻⁴ | 1.9E-03 | 2.45 | 8.0E-03 |
| P62273 | RPS29 | 3.8x10 ⁻⁶ | 2.0E-180 | 2.45 | 7.8E-03 |
| A8K509 | A8K509 | 4.6x10 ⁻⁵ | 1.0E-169 | 2.26 | 2.3E-02 |
| Q8N8S7 | ENAH | 2.3x10 ⁻⁴ | 4.8E-02 | 2.24 | 3.7E-03 |
| Q9NTJ5 | SACM1L | 1.1x10 ⁻⁴ | 1.0E-05 | 2.13 | 4.0E-03 |
| A0A0C4DGS0 | NDUFA6 | 4.4x10 ⁻⁵ | 1.2E-03 | 2.12 | 5.1E-03 |
| B7ZM73 | MON2 | 1.1x10 ⁻³ | 2.0E-04 | 2.11 | 3.7E-03 |

Appendix 4: Publication of the human receptome and adhesome

Provided here is the published manuscript detailing the proteomic determination of the human receptome and adhesome. For this paper I assisted with *in silico* analysis of the receptome and adhesome, contributed immunolocalisation of receptome and adhesome proteins in the human endometrium, and siRNA knockdown data (Figure 6). Full author contributions are provided in the declaration of thesis including published works.

Evans, J., **Hutchison, J.**, Salamonsen, L. A., Greening D. W. (2020). Proteomic insights into endometrial receptivity and embryo-endometrial epithelium interaction for implantation reveal critical determinants of fertility. *Proteomics*, 20(1), e1900250.

Proteomic Insights into Endometrial Receptivity and Embryo-Endometrial Epithelium Interaction for Implantation Reveal Critical Determinants of Fertility

Jemma Evans,* Jennifer Hutchison, Lois A. Salamonsen, and David W. Greening*

In vitro fertilization has overcome infertility issues for many couples. However, achieving implantation of a viable embryo into the maternal endometrium remains a limiting step in optimizing pregnancy success. The molecular mechanisms which characterize the transient state of endometrial receptivity, critical in enabling embryo-endometrial interactions, and proteins which underpin adhesion at the implantation interface, are limited in humans despite these temporally regulated processes fundamental to life. Hence, failure of implantation remains the “final frontier” in infertility. A human coculture model is utilized utilizing spheroids of a trophoblast (trophoblast stem) cell line, derived from pre-implantation human embryos, and primary human endometrial epithelial cells, to functionally identify “fertile” versus “infertile” endometrial epithelium based on adhesion between these cell types. Quantitative proteomics identified proteins associated with human endometrial epithelial receptivity (“epithelial receptome”) and trophoblast adhesion (“adhesome”). As validation, key “epithelial receptome” proteins (MAGT-1/CDA/LGMN/KYNU/PC4) localized to the epithelium of receptive phase (mid-secretory) endometrium obtained from fertile, normally cycling women but is largely absent from non-receptive (proliferative) phase tissues. Factors involved in embryo-epithelium interaction in successive temporal stages of endometrial receptivity and implantation are demonstrated and potential targets for improving fertility are provided, enhancing potential to become pregnant either naturally or in a clinical setting.

epithelial surface of the endometrium that lines the uterine cavity. These are the first steps of implantation, which then proceeds by the invasion of the trophoblast (the outer cellular layer of the blastocyst) through the decidualized endometrial stroma, until it invades and reconstructs the spiral arterioles to fully form the placenta which comprises both maternal and fetal cells. The early processes whereby the endometrium attains receptivity and the trophoblast first attaches, are little understood. They cannot be studied in vivo in humans, while animal models demonstrate significant differences in basic physiology and there is a paucity of appropriate human models.^[1]

We recently developed a novel model for human embryo implantation that enables detailed examination of the adhesion of human embryo mimics to endometrial epithelial cells.^[2] This utilized a human trophoblast stem cell line^[3] developed from donated human embryos, and which had characteristics of trophoblastic cells (TEAD4, CDX2, geminin, HMGA2, LIFR, GDF15, and LGR5 expression). These “trophoblast” cells formed into spheroids,

consistently the size of human blastocysts. Their adhesion to primary human endometrial epithelial cells could be manipulated with the hormonal milieu and importantly, these trophoblast spheroids could discriminate, via adhesion/

1. Introduction

Establishment of a human pregnancy requires that an embryo (at blastocyst stage), becomes attached to and invades the receptive

Dr. J. Evans, J. Hutchison, Prof L. A. Salamonsen
Hudson Institute of Medical Research
Monash University
Clayton, Victoria 3168, Australia
E-mail: jemma.evans@hudson.org.au

Dr. J. Evans, J. Hutchison, Prof L. A. Salamonsen
Department of Molecular and Translational Science
Monash University
Clayton Victoria 3168, Australia

Dr. D. W. Greening
Baker Heart and Diabetes Institute
Molecular Proteomics
Melbourne, Victoria 3004, Australia
E-mail: david.greening@baker.edu.au

Dr. D. W. Greening
Department of Biochemistry and Genetics
La Trobe Institute for Molecular Science
La Trobe University
Bundoora, Victoria 3086, Australia

 The ORCID identification number(s) for the author(s) of this article can be found under <https://doi.org/10.1002/pmic.201900250>

DOI: 10.1002/pmic.201900250

non-adhesion, between endometrial epithelial cells obtained from fertile versus infertile women, respectively.

Using this model, we have here applied a proteomic approach to identify a unique adhesion protein network and define a human embryo implantation “adhesome” in fertile endometrial epithelial cell-trophoblast spheroid cocultures. Using trophoblast spheroid adhesion to define primary endometrial epithelial cells as “receptive” or “non-receptive” to implantation, we also identify a human endometrial epithelial “receptome.” Interrogation of these protein networks and composition has enabled novel insight into endometrial receptivity and the adhesion stage of human implantation, providing potential novel biomarkers for the identification of endometrial epithelial receptivity and insights into embryo adhesion that will assist in improving outcomes of assisted reproduction.

2. Experimental Section

2.1. Ethics and Tissue Collection

Ethical approval for tissue collections was obtained from Institutional Ethics Committees at Monash Health and Monash Surgical Private Hospital. Written informed consent was obtained from all subjects prior to tissue collection.

2.2. Endometrial Tissue Collection and Patient Details

Endometrial biopsies for culture were collected by curettage from normally cycling women (28–32 day cycles), ≤ 40 undergoing hysteroscopy and curettage. Women were undergoing investigation as indicated in **Table 1** and had not used steroid hormone therapy/contraception in the preceding 6 months. These women were of proven fertility (≥ 1 parous pregnancy) and had normal endometrium at hysteroscopy and morphologically normal endometrium as assessed by experienced endometrial histopathologists. Likewise, biopsies were taken from infertile women in an IVF program as indicated in **Table 1**, with non-endometrial indications (i.e., no diagnosis of fibroids, endometriosis, adenomyosis, or other endometrial related disorders) for their infertility, and who were otherwise of similar characteristics. Women were normally cycling and experienced regular menstruation. Women were noted to have normal endometrium at hysteroscopy and patent, unblocked fallopian tubes. As these tissues were collected via altruistic donation from women consented immediately before entry to operating theatre through a private hospital, only limited patient background data is available.

2.3. Epithelial Cell Isolation from Human Endometrial Tissue

Performed per previous protocols.^[4] In brief, within 16 h of collection, endometrial tissues were washed in phosphate buffered saline (PBS), finely chopped, and incubated with 1200 U collagenase type III and 100 mg mL⁻¹ DNase in 2 mL of phosphate buffered saline (PBS) for 45 min at 37 °C with shaking at

Significance Statement

Infertility affects 1:6 couples worldwide and this is increasing. In vitro fertilization (IVF) pregnancy success rates are <25% per cycle and couples using such technologies face both financial and emotional hardship. Implantation of a healthy embryo into a receptive endometrium is a critical step in the establishment of pregnancy but both receptivity and implantation are considered the “black box” of reproduction; little is known of the underlying mechanisms or how these are disturbed in infertile women. Importantly, much remains to be discovered about the basic protein interactions that govern trophoblast–endometrial epithelium adhesion. Significantly, this study provides a unique functional proteomic strategy to identify the composition of factors involved in embryo-epithelial interactions in the critical stages of receptivity and implantation, which may be targeted to improve fertility without or with existing technologies.

130 rpm. Digestion was terminated by the addition of 4 volumes of DMEM/F12 containing 1% v/v penicillin/streptomycin (p/s). Digested tissue was passed through a 45 μ m filter (endometrial stromal cells pass through the filter) and retained epithelial fragments washed off, centrifuged, resuspended in DMEM/F12 containing 10% v/v fetal bovine serum (FBS, Gibco, Invitrogen) and 1% p/s and seeded into 24 well plates (2 cm² surface area). Epithelial fragments were allowed to attach for 48 h before thorough washing with PBS to remove stromal and other cells. Endometrial epithelial cell preparations were visually assessed for contamination with endometrial stromal fibroblasts and only those with $\geq 95\%$ epithelial cells were used for experimental purposes. Primary human endometrial epithelial cells (pHEECs) were not passaged and were used at p0 (i.e., at first seeding after isolation) as, in the authors' experience, this reduces the likelihood of stromal cell contamination of the cultures. pHEECs at p0 were used for experimental purposes within 1 week of isolation. An example of morphologically pure epithelial preparation with characteristic “rounded” morphology and no contaminating stromal fibroblasts is provided in **Figure 1a**. This is the typical appearance of epithelial cultures used in the current study.

2.4. Cell Culture

L2-TSC (trophoblastic) cells are human trophoblast stem cells (kind gift of Prof. Susan Fisher, UCSF)^[3]; these cells were developed from individual blastomeres of donated human embryos. L2-TSCs have characteristics of trophoblastic cells (TEAD4, CDX2, geminin, HMGA2, LIFR, GDF15, and LGR5 expression) and can be manipulated to differentiate toward a syncytiotrophoblast or cytotrophoblast fate. However, routine maintenance in a 1:1 mix of DMEM:F12 Glutamax (Gibco, Invitrogen) supplemented with 1% p/s and 10% v/v FBS with the addition of 10 ng mL⁻¹ basic fibroblast growth factor (bFGF, 233-FB-025, R&D systems) and 10 μ m SB431542 (#1614, Tocris

Table 1. Characteristics of women used in coculture studies.

| | Endometrial findings | Parity | Age | BMI | Reason for hysteroscopy/D&C | Fertility status |
|------------------|----------------------|----------|-----|------|---|-----------------------|
| Fertile | | | | | | |
| P1 | Normal | P3 | 39 | 31.2 | Mirena insertion | Fertile |
| P2 | Normal | P2 | 40 | 22.8 | Benign ovarian cyst assessment | Fertile |
| P3 | Polyps | P1 | 30 | 17.6 | Polypectomy | Fertile |
| Infertile | | | | | | |
| P4 | Normal | P1 (IVF) | 39 | 20.8 | Pain | Secondary infertility |
| P5 | Normal | | 28 | 27.5 | Tubal assessment: patent, unblocked tubes present | Secondary infertility |
| P6 | Normal | | 36 | 30.9 | Tubal assessment: patent, unblocked tubes present | Primary infertility |

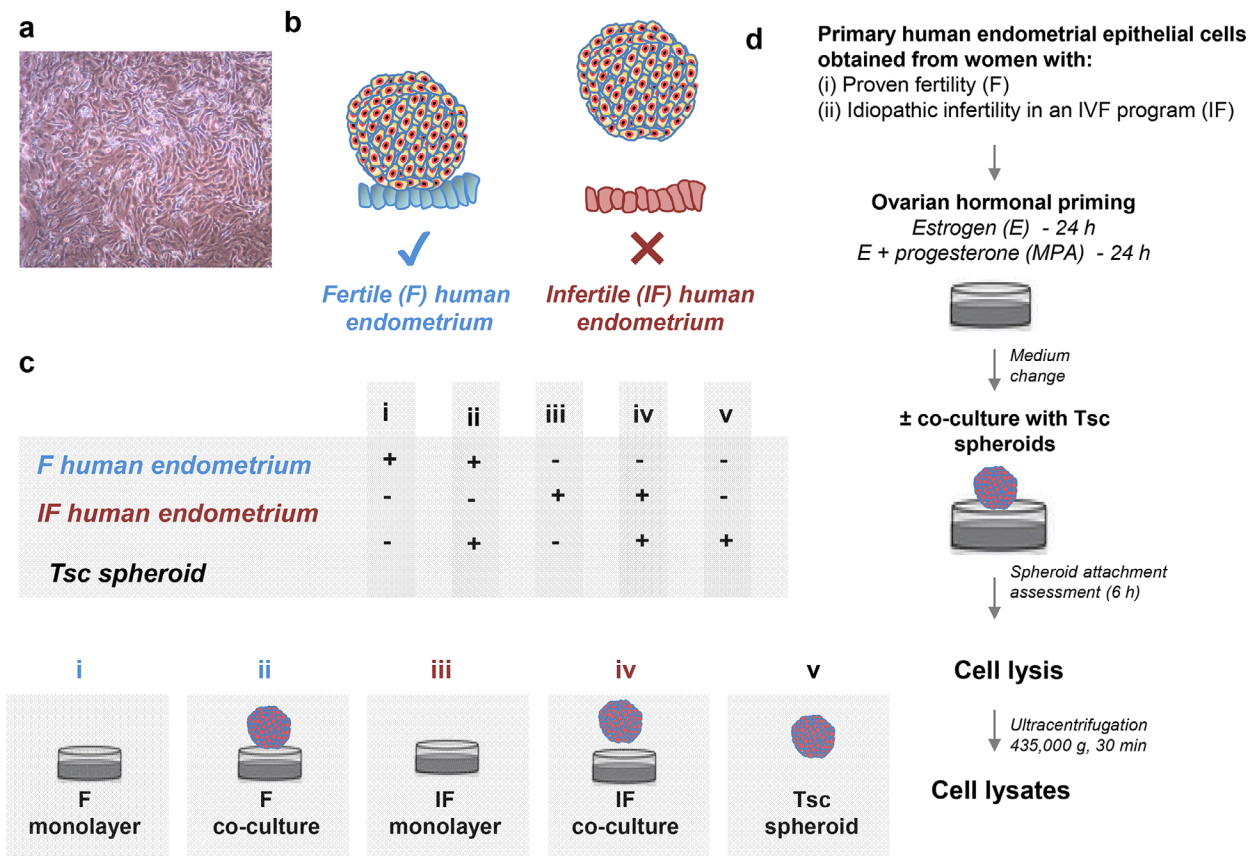


Figure 1. Experimental design to understand human trophoblast–endometrial adhesion during fertility. a) Representative image of morphologically normal primary human endometrial epithelial cells at >95% purity. b) To understand the adhesion network between trophoblast spheroids (outer layer of embryo) and endometrium during fertility, we employed primary human endometrial epithelial cells from women with proven fertility (F, ✓, morphologically normal endometrium), and from infertile women in an IVF program (IF, ✗, with non-endometrial indications for infertility). c) Cells from each woman were independently grown in monolayer culture in the presence of estrogen/progesterone, either alone or in the presence of trophoblast spheroids. They were then defined as “receptive” (i) or “non-receptive” (iii) depending on whether trophoblast spheroids attached (adhesion (ii); non-adhesion (iv)) to matched endometrial monolayers. Spheroids were also maintained in isolation (v). d) Experimental design of endometrial cells hormonally primed with estrogen/progesterone, and where applicable, spheroid coculture and attachment, before imaging and outgrowth quantification, and cell lysis performed.

Bioscience)^[5] as used herein maintains these cells in their “stem cell” trophoblast like state (henceforth termed trophoblast medium). Cells were grown on flasks coated with 0.5% gelatin (G1393, Sigma Aldrich). Human endometrial adenocarcinoma cells, ECC-1^[6,7] were used as a model of human endometrial

luminal epithelial cells. These were cultured and maintained as previously described^[6] in DMEM/F-12 supplemented with 10% FBS, and incubated at 37 °C with 5% CO₂.^[8] ECC-1 cells were validated by Karyotype analysis^[9] according to the ATCC guidelines, with allele match in STR profile of 100%.

2.5. Preparation of Trophectodermal Spheroids

Methylcellulose (4000 centipoises, Sigma Aldrich) at 1.5% w/v, dissolved in DMEM was centrifuged (90 min/3500 rpm) to remove insoluble methylcellulose. 2500 trophoctoderm cells (optimized cell number based on initial studies^[2,5]) in 150 μ L of 20% methylcellulose/80% trophoctoderm medium^[10] were seeded into a round bottomed well in which one spheroid formed gradually in each well over 48 h; each spheroid was approximately the same size as a human blastocyst (0.1–0.2 mm). Any mis-formed spheroids (<5%) were discarded. Spheroids were thoroughly washed to remove methylcellulose and trophoctoderm media prior to coculture with endometrial epithelial cell monolayers. In brief, spheroids were collected into 15 mL sterile polypropylene tubes using wide bore 1 mL tips to prevent disturbing the 3D structure of the spheroids. These spheroids were centrifuged at 800 \times g for 8 min followed by the removal of media. Serum-free DMEM/F12 media was added to the tubes and the spheroids gently resuspended by flicking the tube with resuspension visually confirmed. The spheroids were again centrifuged, and this process repeated a total of three times.

2.6. Endometrial Epithelial Cell-Trophectoderm Spheroid Coculture and Lysate Preparation

It was previously demonstrated that spheroids of trophoctoderm cells discriminate between endometrial epithelial cells isolated from fertile (Figure 1a, fertile) and idiopathic infertile (Figure 1a, infertile) women based on spheroid adhesion after coculture with pHEECs for 6 h.^[2] For the current study, primary human endometrial epithelial cells monolayers in 0.5% charcoal stripped (cs)FBS/DMEM/F12 were sequentially treated with 10^{-8} M 17β -estradiol (estrogen: E) for 24 h followed by estrogen/ 10^{-7} M medroxyprogesterone acetate (progestin: MPA) for a further 24 h to mimic in vivo hormonal regulation during the receptive phase of the menstrual cycle (hormonal priming).^[11] After 48 h of total hormonal priming, spheroids were resuspended in E/MPA media (concentrations as above) containing 1% FBS and cocultured with hormonally primed endometrial epithelial cell monolayers for 6 h (per previously developed protocol, Figure 1b-ii,iv). Control spheroids incubated in the absence of endometrial epithelial cells (adherence to plastic only) were also treated with estrogen/progestin media for 6 h (Figure 1b-v). Spheroid adhesion was determined by a) counting total spheroids present under an inverted light microscope; b) removing medium and gently washing cocultures with PBS; c) re-counting firmly adhered spheroids. Adhered spheroids were expressed as percentage of total spheroids.^[2] Endometrial cell monolayers which supported spheroid adhesion were defined as “adhesive” (Figure 1b-ii) while those that did not were defined as “non-adhesive” (Figure 1b-iv). “Receptive” or “non-receptive” endometrial monolayers were prepared by hormonal priming as above. These cells were maintained under the same treatment conditions as the endometrial epithelial-trophectoderm spheroid cocultures but without the addition of spheroids. If spheroids adhered to the matched endometrial epithelial monolayers (i.e., cells obtained from the same woman, present on the same culture plate, treated in the same manner), the cells were defined

as receptive (Figure 1b-i); if no adhesion was exhibited, the cells were defined as non-receptive (Figure 1b-iii). All cultures were lysed on ice (15 min) with 100 μ L SDS sample buffer (4% w/v SDS, 20% v/v glycerol, 0.01% v/v bromophenol blue, 0.125 M Tris-HCl, pH 6.8). Cell lysates were ultracentrifuged at 435 000 \times g/30 min at 4 $^{\circ}$ C (TLA-100 rotor, Beckman Coulter).^[11,12] This procedure is outlined in Figure 1c.

2.7. siRNA Knockdown: ECC-1 Endometrial Epithelial Cells

ECC-1 cells seeded at 1.5×10^5 cells per well in 12 well plates in DMEM/F12 containing 10% v/v FBS without p/s and allowed to attach and proliferate overnight. 2 μ L of 10 μ M siRNA/scrambled stock (Santa-Cruz Biotechnology) was added then to 100 μ L of OptiMEM transfection media (Invitrogen), and 2 μ L of lipofectamine (Life Technologies) was added to 100 μ L of OptiMEM, each for 5 min. These solutions were mixed gently and incubated for 30 min before the addition of 800 μ L of OptiMEM. Cells were washed twice with OptiMEM, then siRNA/scrambled transfection mix added and incubated (8 h). Media were replaced with DMEM/F12/FBS media as above, for 48 h before cell starvation for 6 h. siRNA/scrambled ECC-1 cells were sequentially treated with 10^{-8} M E for 24 h followed by E plus 10^{-7} M MPA for a further 24 h to mimic the receptive phase of the menstrual cycle,^[6] and trophoctoderm spheroid adhesion assay performed (as above) for 6 h.

2.8. Protein Quantification

Protein content was determined by microBCA colorimetric protein quantification (Life Technologies, 23235) or quantified by Qubit fluorescence using Qubit 4.0 (Life Technologies, Q33212) as per manufacturer's instructions.

2.9. Proteomic Sample Preparation of Endometrial Epithelial Cell-Trophectoderm Spheroid Cocultures

Lysates from cell monolayers (primary endometrium; receptive and non-receptive), cocultures (primary endometrium with spheroid adhesion assay; adhered and non-adhered), or spheroids alone (20 μ g total protein) were solubilized in SDS sample buffer (4% w/v SDS, 20% v/v glycerol, and 0.01% v/v bromophenol blue, 0.125 M Tris-HCl, pH 6.8) with protease inhibitor cocktail (Complete, EDTA-free protease inhibitor cocktail, Roche), lysed at 95 $^{\circ}$ C for 5 min, then fractionated by short-range SDS-PAGE, with fractions ($n = 2$) representing the entire gel excised.^[12] Each fraction was destained (50 mM ammonium bicarbonate/50% v/v acetonitrile [ACN]) for 30 min at 27 $^{\circ}$ C.^[13] Samples were reduced with 2 mM tri (2-carboxyethyl) phosphine hydrochloride (Sigma-Aldrich, C4706) at RT 1 h on gentle rotation, alkylated by treatment with 25 mM iodoacetamide (Sigma-Aldrich) for 30 min (in the dark), and digested with trypsin (Promega, V5111) for 18 h at 37 $^{\circ}$ C. The peptide solutions were acidified to a final concentration of 1% formic acid (FA) and 0.1% trifluoroacetic acid (TFA) and desalted with a C18 Sep-Pak column (Waters). Each Sep-Pak column was

activated with 100 μ L of methanol, washed with 30 μ L of 80% acetonitrile, and equilibrated with $3 \times 30 \mu$ L 0.1% TFA. Samples were loaded and each column was washed with $2 \times 20 \mu$ L 0.1% TFA. Elution was performed with two rounds of 20 μ L of 50% acetonitrile. Samples were lyophilized (SpeedVac; Savant, Thermo Fisher Scientific) and acidified with 0.1% FA, 2% ACN, and peptide concentrations estimated from A_{280} absorbance (Thermo Scientific Nanodrop 2000).

2.10. Mass-Spectrometry-Based Proteomics

Proteomic experiments performed in biological triplicate, with technical replicates ($n = 2$), with MIAPE-compliance.^[5,14] MS analyses performed on an Orbitrap LTQ Elite mass spectrometer (ThermoFisher Scientific) with a nanoelectrospray ion source coupled online to a Waters nanoAcquity UPLC. Peptides were loaded (Acclaim PepMap100, 5 mm \times 300 μ m i.d., μ -precolumn packed with 5 μ m C18 beads, Thermo Fisher Scientific) and separated over a 120 min gradient run using a BioSphere C18 analytical column (1.9 μ m 120 \AA , 360/75 μ m \times 400 mm, NanoSeparations) at 45 $^{\circ}$ C. Trapping was for 3 min at 5 μ L min^{-1} , 98% buffer A (99% water, 0.1% formic acid), and 2% buffer B (0.1% v/v FA in 80% v/v ACN), before eluting at 2–100% 0.1% FA in acetonitrile (2–40% from 0 to 100 min, 40–80% from 100 to 110 min (flow rate, 250 nL min^{-1})).

The mass spectrometer was operated in data-dependent mode where up to 20 dynamically chosen, most abundant precursor ions in the survey scan (350–1500 Th) were selected for MS/MS fragmentation. Survey scans were acquired at a resolution of 120 000, with MS/MS resolution of 15 000. Unassigned precursor ion charge states and singly charged species were rejected, and peptide match disabled. The isolation window was set to 2.0 Th and selected precursors fragmented by collisional dissociation with normalized collision energies of 35 with a maximum ion injection time of 110 ms. Ion target values were set to 3×10^6 and 1×10^5 for survey and MS/MS scans, respectively. Dynamic exclusion was activated for 90 s. Samples were run in regional blocks, with sample groups interspersed throughout to allow correction of batch effects. Data was acquired using Xcalibur software v4.0 (Thermo Fisher Scientific). Raw mass spectrometry data deposited in the PeptideAtlas (#PASS01121) and can be accessed at <http://www.peptideatlas.org/PASS/PASS01121>.

2.11. Data Analysis

Peptide identification and quantification were performed using MaxQuant (v1.6.0.1) with its built-in search engine Andromeda.^[15] Tandem mass spectra were searched against a human reference proteome (71 798 entries, downloaded 10/2018) supplemented with common contaminants. Search parameters included carbamidomethylated cysteine as fixed modification and oxidation of methionine and N-terminal protein acetylation as variable modifications. Data was processed using either trypsin/P as the proteolytic enzyme with up to two missed cleavage sites allowed. Where possible, peptide identification information was matched between runs of the fractionated samples within MaxQuant. Precursor tolerance was set to ± 4.5 ppm,

and fragment ion tolerance to ± 10 ppm. Results were adjusted to 1 % false discovery rate (FDR) on peptide spectrum match (PSM) level employing a target-decoy approach at the peptide and protein levels. In cases of redundancy, shared peptides were assigned to the protein sequence with the most matching peptides, thus adhering to principles of parsimony. The label-free quantification (LFQ) algorithm^[16] in MaxQuant was used to obtain quantification intensity values. Perseus (v1.6.0.7) was further used to process data, where the resulting p -values were adjusted by the Benjamini–Hochberg multi-test adjustment method for a high number of comparisons^[17] and statistics performed as previously described.^[18] For pathway analyses, Kyoto Encyclopedia of Genes and Genomes (KEGG) and NIH Database for Annotation, Visualization and Integrated Discovery Bioinformatics Resources 6.7 (DAVID) resources were utilized using recommended analytical parameters.^[19] For gene ontology enrichment and network analyses, UniProt (www.uniprot.org) database resource (biological process, molecular function), Ingenuity Pathway Analysis, and Reactome knowledgebase were utilized. Clustering of samples was performed by principal component analysis (PCA) and visualized using ggplot2^[20] and ggfortify (<https://cran.r-project.org/web/packages/ggfortify/index.html>). The heat map of proteins used gplots (<https://cran.r-project.org/web/packages/gplots/index.html>).

2.12. Immunohistochemistry

For immunohistochemistry^[21] proliferative (non-receptive) and secretory (receptive) phase endometrial tissues were incubated with antibodies directed against MAGT1, KYNU, CDA, LGMN, or PC4 (all Santa-Cruz Biotechnology) overnight at 4 $^{\circ}$ C or isotype matched IgG negative controls. Biotin-labeled secondary antibodies were applied followed by avidin-HRP before colorimetric development with diaminobenzidine and counterstaining with hematoxylin.

2.13. Statistics

GraphPad Prism v7.0 was used with all data pre-tested for normality. If the data was non-parametric, a Kruskal–Wallis with a Tukey's post-hoc test or Mann–Whitney U analysis was performed and if parametric, one-way ANOVA with a Tukey's post-hoc test or unpaired t -test was applied. All data presented as mean plus/minus standard error of the mean (mean \pm SEM). Statistical testing of proteomic data used Poisson distribution with EdgeR software (v3.2). Student's t -test used GraphPad Prism v7.0). In all analyses, $*p < 0.05$ were considered statistically significant.

The accession number for the mass spectrometry data reported in this paper is PeptideAtlas Consortium via the PeptideAtlas proteomics repository: PASS01121.

3. Results

Implantation of a healthy embryo into a receptive endometrium is a critical step in the establishment of pregnancy but this is considered the “black box” of infertility^[22]; little is known

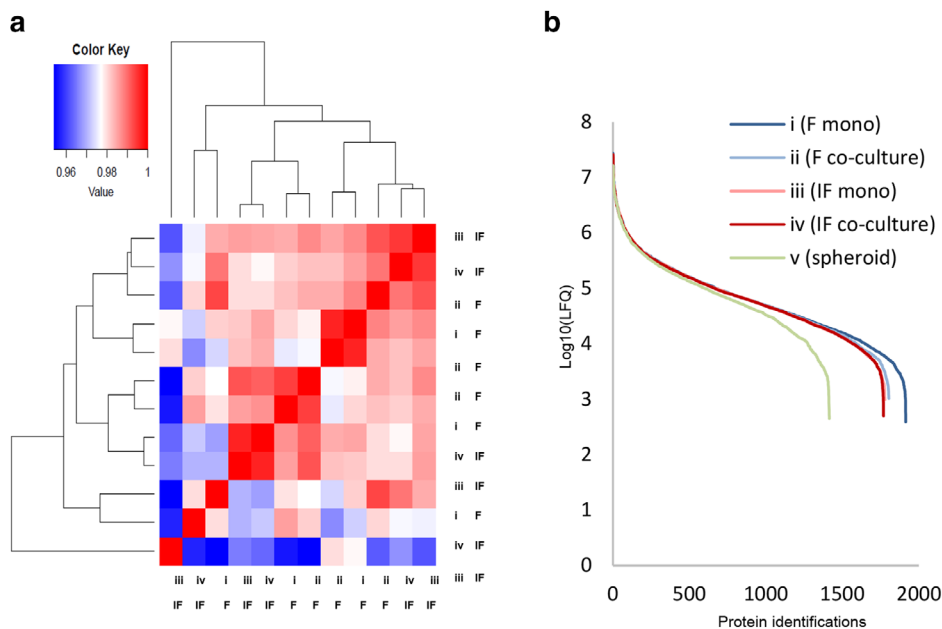


Figure 2. Protein landscape of endometrial receptome and adhesome. a) Protein expression heatmap of proteins identified in receptive (i, F) and non-receptive (iii, IF) epithelium, depending whether matched monolayers demonstrated adhesion (ii, F) or non-adhesion (iv, IF) with trophoctodermal spheroids (monitored alone, v). Scale represents label-free quantitation intensity. b) Estimated abundance by LFQ intensity (\log_{10}) of proteins identified in endometrial receptome and adhesome, indicating the sampling depth of each dataset spanning over five orders of magnitude.

of the underlying mechanisms of endometrial receptivity, the adhesion stage of implantation, or how these are disturbed in infertile women. To gain critical insights into this interaction, we performed functional integration of human endometrial epithelial cell adhesion (from patients with proven fertility, and in patients with infertility) to trophoctoderm spheroids. Here, we demonstrate for the first time, proteins and their associated networks that can be identified as associated with trophoctoderm–epithelium adhesion in an unbiased fashion (Figure 1). Significantly, this study provides a unique insight into the composition of factors involved in embryo–endometrial epithelium interaction in temporal stages of receptivity and implantation, and key changes in these networks associated with endometrial-associated infertility.

3.1. Functional Adhesion of Endometrial Epithelial Cells from Fertile and Non-Fertile Women

We previously demonstrated that our trophoctoderm–epithelium coculture system clearly differentiates between endometrial epithelial cells derived from fertile women or those with idiopathic fertility.^[2] Indeed, trophoctoderm spheroids adhered to 85% of fertile tissues assessed (11/13), but only to 11% of infertile tissues (2/18, $p < 0.001$) despite appropriate *in vitro* hormonal (estrogen/progesterin) priming. The present study design, described above, and in Figure 1, enabled complex analyses between receptive and non-receptive endometrial epithelium (the receptome) and attachment between epithelium and spheroids in coculture (the adhesome). Characteristics of women used in these coculture studies are presented in Table 1. No significant differences were found between the groups.

3.2. Proteome Analysis of Human Trophoctoderm–Epithelium Adhesion

Proteomic profiling was performed on adhesive/non-adhesive cocultures, receptive versus non-receptive primary cell monolayers, and on spheroids alone (with control for spheroid protein expression upon adhesion to plastic and spheroid quality) (Figure 1b–v). Endometrial epithelial monolayers and cocultures (per Figure 1b) were terminated after 6 h of coculture/media change (for monolayers) and cell lysates processed for analysis by nanoLC-MS/MS data-dependent acquisition. Samples were analyzed in biological triplicate, with technical replicates, and a stringent metric for protein and peptide identification. A total 3760 proteins were identified in the global proteomics analysis (Figure S1 and Table S1, Supporting Information) representing the largest human embryo mimetic (trophoctoderm) protein dataset yet reported. The protein expression heatmap of endometrial monolayers and trophoctoderm coculture analyses is shown (Figure 2a). The proteins identified in this study represent significantly low abundant factors as judged from normalized LFQ values (Figure 2b), indicating an increased sampling depth collectively spanning over five orders of magnitude.

3.3. Defining the Human Endometrial “Epithelial Receptome”

Proteomic comparison of adhesive endometrial monolayers from fertile women (Figure 1b–i) with non-adhesive monolayers from infertile women (Figure 1b–iii, both estrogen/progesterone treated) led to the identification of an “epithelial receptome” (Figure 3a). Of the 2048 proteins identified, 137 were unique to

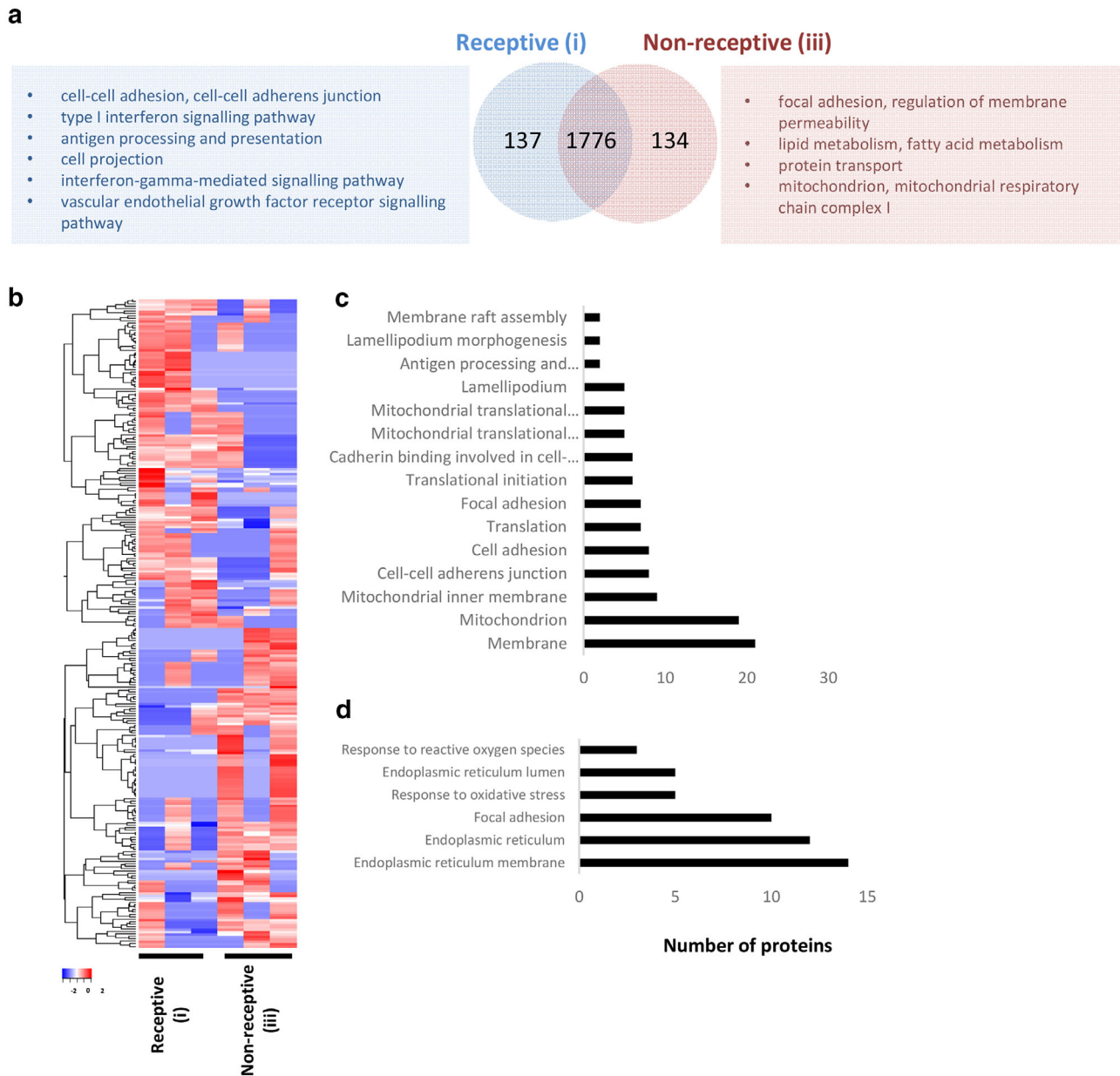


Figure 3. Protein landscape of endometrial receptome. a) Venn diagram of proteins identified in receptive (i, F) and non-receptive (iii, IF) epithelium, with functional annotation of each unique subset. b) Protein expression heatmap of proteins identified in receptive (i) and non-receptive epithelium (iii). Scale represents label-free quantitation intensity. Protein functional annotation and pathway analysis for significantly ($p \leq 0.05$) enriched (c) and downregulated (d) components between i versus iii, “epithelial receptome” using Gene Ontology, STRING, and Reactome.

receptive fertile group, while 134 proteins were identified in the infertile, non-receptive group (Figure 3a; Table S2, Supporting Information). Protein functional annotation and pathway analysis of unique protein subset associated with receptivity in the fertile group revealed protein categories associated with cell–cell adhesion ($1.40E-03$), cell–cell adherens junctions ($1.60E-04$), type I interferon signaling pathway ($7.04E-02$), antigen processing and presentation ($6.81E-03$), cell projection ($4.32E-03$), and vascular endothelial growth factor receptor signaling pathway ($7.22E-02$). For unique proteins from non-receptive endometrium, functional annotation and pathway analysis revealed

proteins associated with focal adhesion ($4.95E-04$), regulation of membrane permeability ($1.81E-02$), lipid metabolism ($8.25E-03$), fatty acid metabolism ($4.29E-03$), protein transport ($1.03E-02$), mitochondrion ($4.80E-02$), and mitochondrial respiratory chain complex I ($3.36E-02$) (Figure 3a). Taking these findings together, this analysis shows that the receptive endometrial proteome is tailored to cell adhesion and cellular attachment, interaction/projection, while in contrast metabolic regulation (including lipid and mitochondrial function), and membrane permeability and attachment are prominently represented in the non-receptive, infertile endometrium.

For proteins differentially expressed, label-free quantitation (LFQ, precursor ion intensity, normalized by maxLFQ^[23]) demonstrated significant differential expression of 296 proteins (i, F mono in comparison to iii, IF mono); 136 proteins upregulated and 132 proteins downregulated (ratio fold change ≥ 2 , $p \leq 0.05$) in the hormonally primed adhesive monolayer versus hormonally primed non-adhesive monolayer (Figure 3b, Table S1, Supporting Information [total proteome]; Table S3, Supporting Information [epithelial receptome only]). Of the 136 upregulated proteins, 50 have previously been associated with endometrial receptivity (Table S4, Supporting Information 1), 4 included within endometrial receptivity array^[24], yielding 86 potential new protein markers for receptivity. Functions/biological pathways significantly ($p \leq 0.05$) enriched in the “epithelial receptome” included components associated with membrane (cell membrane, membrane raft assembly), translation (translation initiation), mitochondria/membrane, and cellular adhesion changes (cell adhesion, focal adhesion, cell–cell adherens junctions, cadherin binding involved in cell–cell adhesion) (Figure 3c, Table S5, Supporting Information). This was confirmed by enrichment analyses using orthogonal approaches including STRING^[25] where the “epithelial receptome” showed significant ($p \leq 0.05$) enrichment for translational initiation, translational elongation, and membrane organization. Downregulated processes during receptivity included endoplasmic reticulum functions, focal adhesion, and response to oxidative stress/oxygen species (Figure 3d).

3.4. Definition of a Human Embryo Implantation “Adhesome”

To understand embryo-endometrium interactions at the time of implantation, we first compared proteins identified in adhesive endometrium (adhesome), in comparison to non-adhesive, and subsequently examined whether this adhesome network was also involved in the trophoctoderm–endometrial epithelium interaction (Figure 4). For the “adhesome”, the proteomes of receptive endometrial monolayer (Figure 1b-i) and non-adhesive endometrial epithelial cells (Figure 1b-iii,iv) were compared to adhesive coculture (Figure 1b-ii), 143 components were significantly upregulated (≥ 2 ratio, $p \leq 0.05$), and 143 components significantly downregulated (≤ -2 ratio, $p \leq 0.05$) in expression (Table S6, Supporting Information). Of the upregulated proteins, 42 have previously been associated with endometrial receptivity/embryo implantation (Table S6, Supporting Information 2) yielding 100 novel proteins for further investigation. Networks associated with membrane, calcium ion binding, cell proliferation, translation, cell–cell adhesion, cytoskeletal/cell projection, and lamellipodia were identified (Figure 4a), along with establishment of protein localization to membrane, and membrane organization determined by STRING network enrichment analysis. Downregulated processes (Figure 4b) included cell–cell adhesion and specific molecules involved in this adhesion which may reflect alterations in the epithelial cell monolayer to promote implantation.

To determine whether adhesome proteins were specific to trophoctoderm–endometrial epithelium interaction or simply regulated upon trophoctoderm spheroid adhesion to a non-specific substrate (plastic, as used in other “implantation” studies^[26]), the adhesome and spheroid-only proteomes were

compared (Figure 4c). 44 of the 143 upregulated adhesome proteins were also expressed upon adhesion of trophoctoderm spheroids alone to the plastic substrate, with 31/143 proteins expressed in $\geq 50\%$ of the plastic adhered trophoctoderm spheroid samples examined. Importantly, 78/143 proteins (54.5%) were exclusive to the adhesome proteome (Table S7, Supporting Information); these proteins are exclusively upregulated upon trophoctoderm–endometrial epithelial adhesion. Uniquely identified adhesome proteins included CNIH4 and SDHC (previously implicated in receptivity/implantation) and DYNLRB1 and LIMS3, neither of which has been previously associated with receptivity/implantation. Cross-referencing of the adhesome list with: i) proteins not previously implicated in endometrial receptivity/embryo implantation; implicated in receptivity/embryo implantation, (Table S6, Supporting Information 1) and ii) those exclusive to trophoctoderm–endometrial epithelial adhesome (Table S7, Supporting Information 2) revealed 55 unique proteins which together provide a valuable resource for future investigation of embryo implantation (Table S7, Supporting Information).

Further, of the 2212 proteins identified across adhesive and non-adhesive endometrium (Figure 4), 116 were unique to the fertile implantation/adhesion group (ii), while 74 proteins were identified in the infertile non-implantation/non-adhesion group (Figure 4d; Table S8, Supporting Information). Protein functional annotation and pathway analysis of unique protein subset associated with implantation (adhesome) in the fertile group revealed protein categories associated with cell–cell adhesion (1.20E-02), cell–cell adherens junctions (1.84E-02), endocytosis (1.51E-02), protein biosynthesis (2.75E-02), cell projection (4.32E-03), and microtubule cytoskeleton organization (4.92E-02). For unique proteins from infertile non-implantation/non-adhesion endometrium (not identified in fertile implantation/adhesion endometrium or spheroid alone) (Figure 4d), functional annotation and pathway analysis revealed proteins associated with protein binding (7.61E-03), ubiquitin activating enzyme activity (1.62E-02), antigen processing and presentation (1.75E-02), cell–cell adherens junction (1.83E-02), glutathione biosynthetic process (5.0E-02), and membrane (3.72E-02). Taking these findings together, this analysis shows that the fertile implantation/adhesion endometrial proteome (as distinct from infertile non-implantation/non-adhesion endometrium, and trophoctoderm alone; i.e., adhesome) is tailored to cell adhesion and cellular attachment, and organization of the membrane and cytoskeletal network, while in contrast immune regulation (antigen presentation), cell–cell adhesion, glutathione, and ubiquitin activities are prominently represented in the infertile endometrium which cannot support implantation.

3.5. “Epithelial Receptome” versus “Adhesome”: Commonalities, Differences, and Unique Protein Signature

A subset of proteins was commonly expressed between “receptome” and “adhesome” (33 upregulated proteins, 40 downregulated proteins [Table S9, Supporting Information]) suggestive of roles in both processes. Proteins exclusive to the “receptome” or “adhesome” may be considered to define more accurately, epithelial receptivity and embryo adhesion, respectively. 139 proteins

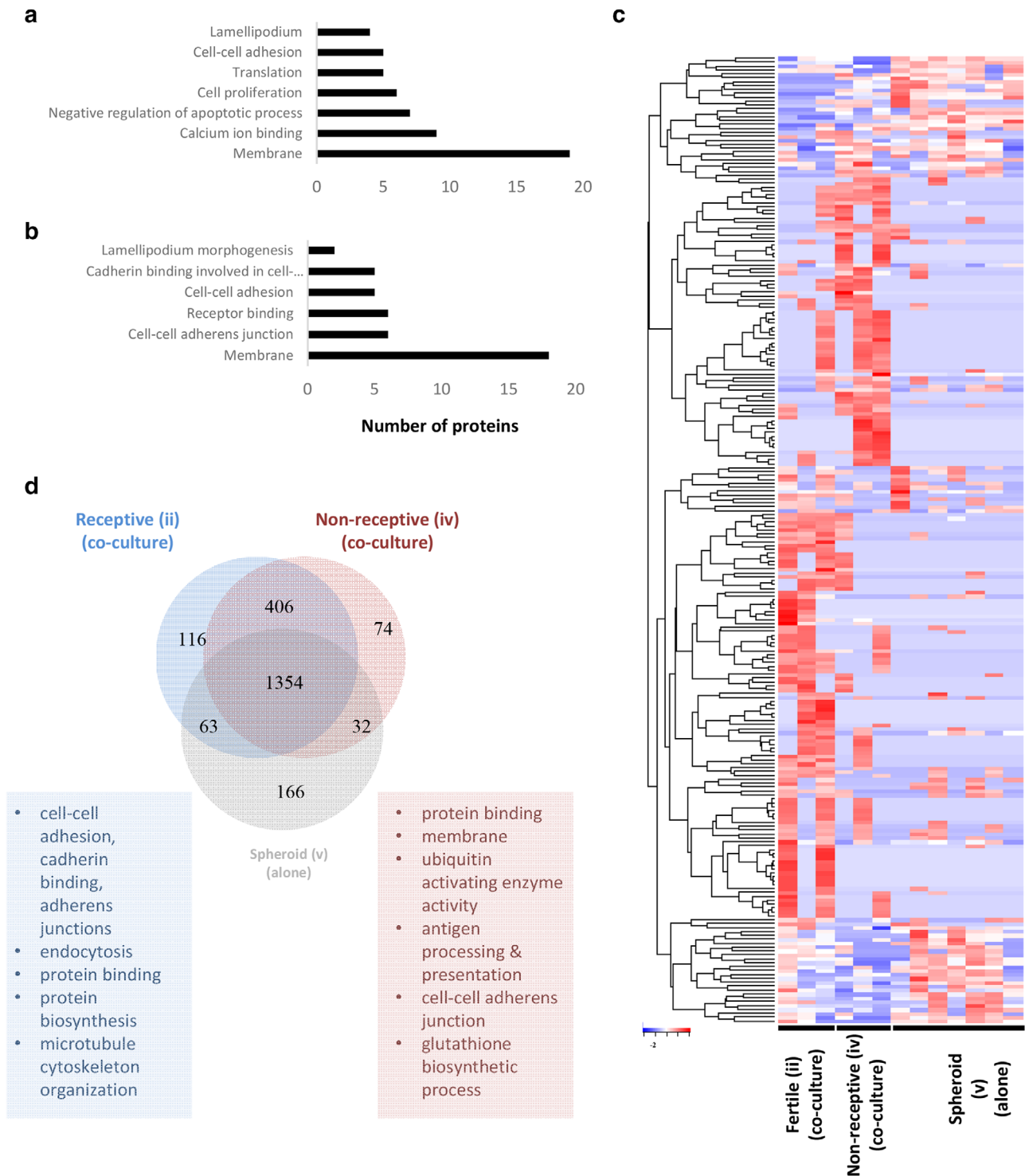


Figure 4. Protein landscape of human embryo implantation “adhesome.” a,b) Functional metrics of differentially ($p \leq 0.05$) enriched ((a) and down-regulated (b)) proteins between adherent (ii) and non-adherent (iv) coculture, based on enrichment analysis (Gene Ontology, STRING, and Reactome) and analyzed by hierarchical clustering. c) Protein expression heatmap of proteins identified in implantation “adhesome” for fertile (ii) and infertile (iv) coculture, relative to trophectodermal spheroids (v). Scale represents label-free quantitation intensity. d) Venn diagram of proteins identified in fertile adhesome (ii) and infertile (non-adherent) endometrium coculture (iv), with trophectodermal spheroids alone (v).

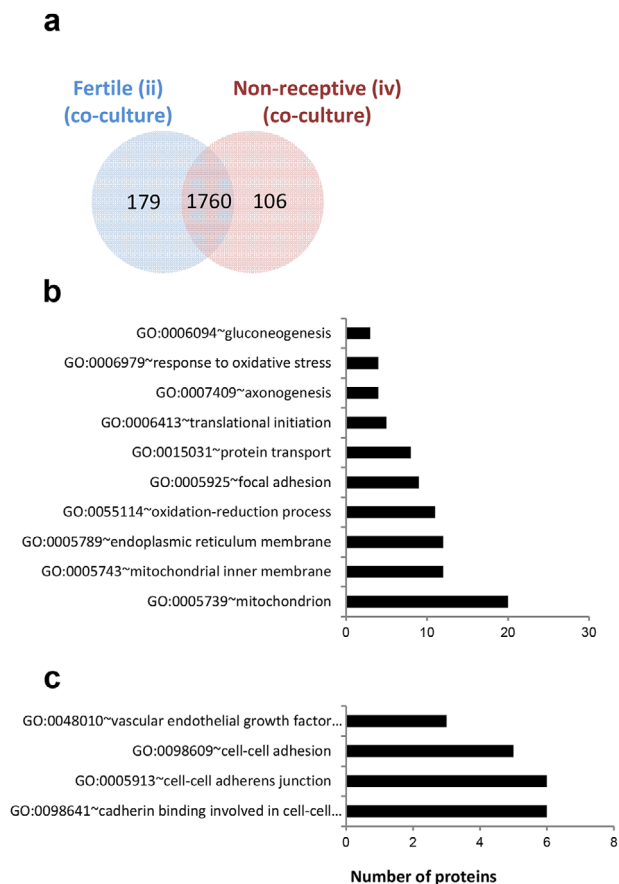


Figure 5. Endometrial adhesion to trophoctoderm influences proteome. a) Venn diagram of proteins identified in fertile adhesome (ii) and infertile (non-adherent) endometrium coculture (iv), indicating differences in cellular proteome based on coculture. b) Functional metrics of differentially ($p \leq 0.05$) enriched proteins between adherent and non-adherent endometrium to trophoctoderm spheroids, performed based on enrichment analysis (Gene Ontology, STRING, and Reactome). Data were analyzed by hierarchical clustering. c) Significantly ($p \leq 0.05$) downregulated proteins (based on enrichment analysis as above) using Gene Ontology, STRING, and Reactome were analyzed by hierarchical clustering.

were exclusive to “receptivity”, 78 upregulated, 61 downregulated (Table S10, Supporting Information). 156 proteins were exclusively associated with adhesion, 78 upregulated, 78 downregulated (Table S7, Supporting Information).

3.6. Protein Landscape of Trophoctoderm Coculture with Adherent and Non-Adherent Endometrium

To directly compare the protein landscape of trophoctoderm between adherent and non-adherent monolayer and spheroid models, we performed cell-morphology-based proteomic profiling (Figure 5a; Table S11, Supporting Information). Proteins differentially (≥ 2 ratio) expressed between adherent and non-adherent monolayer and spheroid models revealed 114 proteins were selectively upregulated (Figure 5b), associated with membrane, mitochondria, cell adhesion (focal adhesion), protein transport, response to oxidative stress, and gluconeogenesis; 358 proteins

were downregulated in this comparison (Figure 5c). Functional enrichment analyses of spheroid growth condition revealed networks associated with cell adhesion (cadherin binding, cell–cell adherens junction, cell–cell adhesion, focal adhesion) and vascular endothelial growth factor receptor signaling pathway. This comparison reveals important cellular protein network changes between monolayer and spheroid trophoctoderm models with regards to their adhesive protein landscape.

3.7. Tissue Expression of Endometrium Validates Receptome Protein Expression

Immunostaining for KYNU, LGMN, PC4, CDA, and MAGT1 (Figure 6a–e, respectively) was evident within receptive phase (mid-secretory) endometrium, mainly localized to epithelial cells, with minimal/no immunostaining within non-receptive (proliferative) endometrium (Figure 6f–j), confirming the validity of our proteomic approach (Figure 6k) in the identification of potential receptivity proteins. PC4 clearly demonstrates some degree of staining within the proliferative phase endometrium (Figure 6h). Importantly, this endometrial tissue expression approach validates receptome protein expression of several protein targets identified by proteomic profiling, but does not distinguish between stromal and epithelial components of the endometrium.

3.8. Validation of Adhesome Function: Perturbing the Interaction between Trophoctoderm and Endometrium

Given that the ultimate aim of this study was to examine and understand “embryo” (trophoctoderm spheroid) adhesion to the endometrial epithelium in a human model, validation in mouse knockout models was inappropriate due to the different modes of implantation between species. We targeted proteins identified in the proteomic profile of fertile implantation/adhesion endometrium (adhesome; ii), in comparison to infertile non-receptive endometrium (iii) and infertile non-implantation/non-adhesion endometrium (iv) (Figure 6l). Knockdown of LGMN, SERPINE1, and PTGS2 in the human ECC-1 cell line followed by E/MPA treatment of the knockdown/scrambled construct cells demonstrated significantly reduced trophoctoderm spheroid adhesion associated with LGMN ($p < 0.01$) and SERPINE1 ($p < 0.05$), and reduced adhesion associated with PTGS2 (ns) knockdown versus scrambled construct (sc siRNA; control, Figure 6m). This further validates our functional proteomic strategy and confirms the functional involvement of these proteins in adhesion between trophoctoderm and endometrium.

4. Discussion

This work interrogates and validates the cellular proteomes of the endometrial epithelium at the human implantation site, in terms of the “receptome” and the adhesome. The “receptome” data defines the state of the epithelium for that very short period of time in each menstrual cycle when the endometrium is appropriately differentiated to enable embryo implantation, while

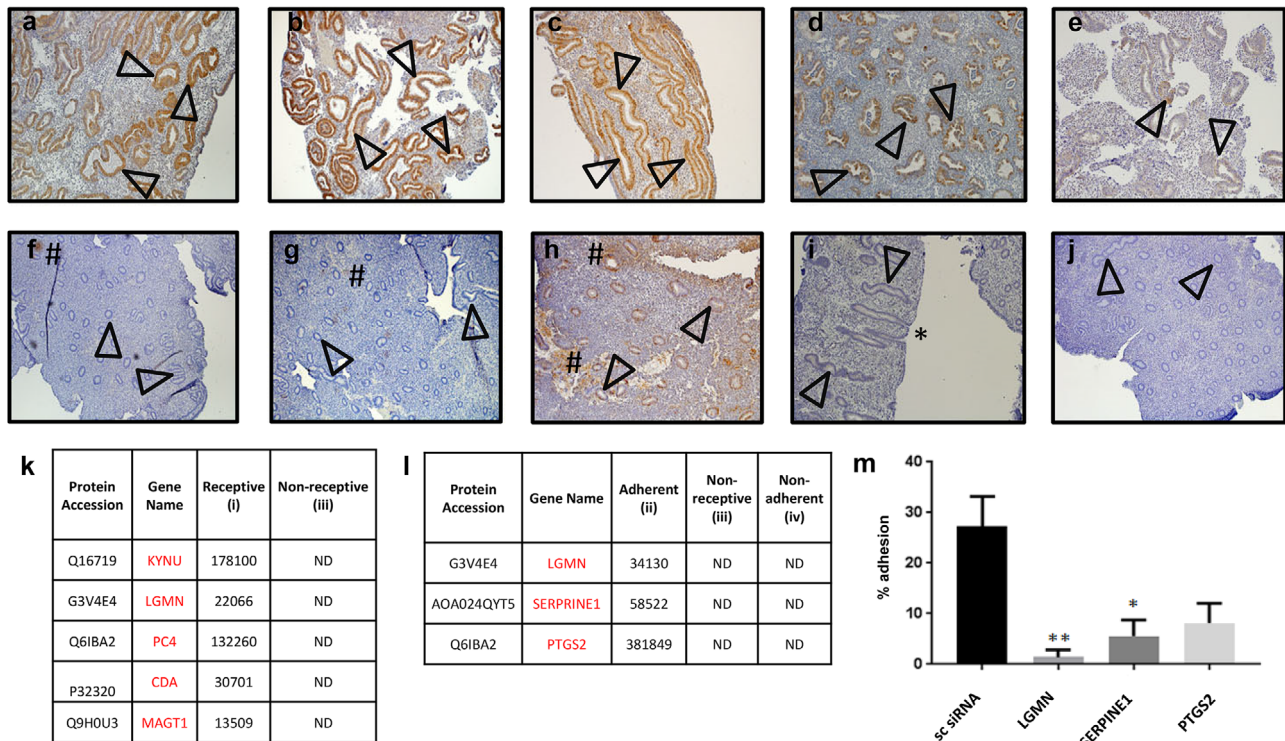


Figure 6. Protein expression validation of receptome markers in human receptive endometrial tissue. Immunohistochemistry of receptome proteins KYNU (a), LGMN (b), PC4 (c), CDA (d), and MAGT1 (e) positively immunostain endometrial epithelial cells within receptive (mid-secretory phase) human endometrium with minimal/no staining within endometrial epithelial cells of proliferative phase endometrium for KYNU (f), LGMN (g), PC4 (h), CDA (i), or MAGT1 (j). Closed arrowheads indicate endometrial glandular epithelium, * indicates endometrial glands invaginating from luminal epithelium, # indicates endometrial stromal localization. k) Protein abundance by LFQ intensity of proteins identified in receptive (i) and non-receptive (iii) endometrium. l) Protein abundance by LFQ intensity of LGMN, SERPINE1, and PTGS2 identified in adherent endometrium coculture (ii, F), non-adherent endometrium monolayer (iii), and non-adherent endometrium coculture (iv, IF). Knockdown of LGMN (■, $p < 0.01$), SERPINE1 (■, $p < 0.05$), and PTGS2 (■) within endometrial epithelial cells reduced trophoblast adhesion versus scrambled control (■, m).

the “adhesome” represents receptive endometrial epithelium that has additionally been influenced by the presence of a blastocyst. The study utilizes a recently developed coculture model of implantation, using true trophoblast cells and primary in-vivo-derived receptive and non-receptive endometrial cells, and offers promise for identifying and improving endometrial receptivity in women.^[3] Importantly, the data provides uniquely regulated proteins of importance for both receptivity and adhesion, critical for establishing pregnancy in women.

It is clear from the proteomic data, that a differential response to a high-quality human embryo may be mounted by the endometrial epithelial cells depending on the fertility status of the woman^[27] as highlighted by our embryo mimic. These essential changes within the luminal epithelium in the initial stages of implantation are not replicated in some infertile women. Indeed, in such women, the barrier function of the epithelium cannot be appropriately modulated to enable trophoblast attachment, thus resulting in implantation failure.^[28]

A global understanding of human endometrial receptivity remains elusive, most likely due to the plethora of cell types included in analyses and the variability between women. Furthermore, endometrial receptivity may be pathological, display altered timing or be a combination of pathological and altered in timing.^[29] Such differentiation and determination of fertility

issues may be aided by the current model. Since the first contact between the embryo and endometrium is the epithelium which lines the uterine cavity, the current study specifically examines the functional status of endometrial epithelium and associated changes in its proteome. Its strength lies in the unique power of the trophoblast spheroid model to discriminate between “fertile” and “infertile” endometrium rather than reliance on menstrual cycle day or apparent/previous fertility status, both of which are unreliable “fertility determinants.” Proteomic analysis of appropriately hormone-primed (estrogen/progesterone) endometrial epithelial cells, defined as “receptive” or “non-receptive” based on trophoblast spheroid adhesion, has revealed a protein signature encompassing a large number of proteins not previously investigated in this role. Our “epithelial receptome” analysis has a concordance of 36.7% with previous studies investigating endometrial receptivity (Supporting Information references: epithelial receptome). This is encouraging, particularly considering the overlap of a number of the proteins identified with genes utilized by the endometrial receptivity array to predict whether the endometrium is capable of supporting a pregnancy,^[24] and that our proteome is specific to epithelium. However, it is not surprising that the concordance rate is relatively low given the lack of agreement between the many existing genomic and proteomic studies of endometrial receptivity^[30]

and that the only previous study globally analyzing epithelium alone, found distinct mRNA signatures for epithelium and stroma.^[31]

As anticipated, many cellular adhesion proteins were upregulated within receptive endometrial epithelial cells preparing for embryo adhesion, together with cell membrane alterations supporting a “plasma membrane transformation.”^[32] Focal adhesion proteins were downregulated, also encompassing aspects of the plasma membrane transformation whereby the cells become less adherent to each other and to their underlying basal lamina. Independent immunohistochemical validation of five receptome proteins localized them primarily to endometrial epithelial cells of receptive (secretory) endometrium. Collectively, these findings provide validity to our analyses, which are a unique resource for studies of essential epithelial-specific changes and for diagnosis of receptivity.

Identifying mechanisms that regulate/characterize the adhesion phase of embryo implantation, is important if we are to improve establishment of pregnancy.^[22] The “adhesome” at the trophoctoderm–epithelial interface, includes many previously unidentified proteins in this setting. Differentially expressed cell-surface ligands, cell–cell, and cell–matrix adhesion and receptors identified herein, need defining both in normal implantation and when adhesion, cellular reprogramming, and specific cell interactions are disturbed with infertility and complications of early pregnancy. Important upregulated adhesome proteins included PTGS2 (previously implicated in implantation^[33]), LGMN, and SERPINE1, for which mutations are associated with recurrent pregnancy loss.^[34] Importantly, knockdown of three of these proteins in epithelial cells functionally reduced their adhesive capacity. Knockdown of PTGS2 did not significantly reduce adhesion, potentially suggesting this protein may be of lesser importance in the adhesive process. The proteins identified display a 30% concordance with previous studies investigating receptivity and implantation (Supporting Information references; adhesome) (annotated, Table S6, Supporting Information). This relatively low concordance likely reflects the human focus of the current model as opposed to previous studies conducted in mouse models.

5. Summary

Identification of the proteome of receptive endometrium represents a key step toward alleviating some infertility and provides potential targets for the inhibition of receptivity as a contraceptive strategy. Furthermore, this first classification of the human adhesome provides strong new targets for further investigation of the basic mechanisms underpinning the critical first step in implantation. Both the epithelial receptome and the adhesome provide a valuable resource for future studies focused on improving embryo implantation by endogenous/exogenous interventions. In addition, our proteomic strategy is broadly applicable to other cell surface, developmental and stem cell systems. Future work to enhance our endometrial/embryo proteomic resource could include alternative methodologies to enrich membrane and cell surface subsets, or related modifications associated with these cell subsets. In addition, human extracellular protein and RNA cellular datasets should be integrated to generate detailed knowledge of the intra- and extracellular signaling pathways (i.e., me-

diated through exosomes^[5] and soluble mediators) that regulate receptivity and implantation.

Supporting Information

Supporting Information is available from the Wiley Online Library or from the author.

Acknowledgements

The authors thank the patients who gave their consent for this study and Sister Judi Hocking for collecting human tissue samples. The authors thank Prof. Susan Fisher for her kind gift of L2-TSC trophoctodermal cells. This work was supported by NHMRC Project Grants #1057741 and #1139489, and by the Victorian Government's Operational Infrastructure funding to the Hudson Institute. J.E. is supported by a Fielding Foundation fellowship, School of Clinical Sciences, Monash University Career Development Fellowship, Society for Reproductive Investigation Bridge grant, and the Hudson Institute of Medical Research. J.H. is supported by an Australian Government Research Training Program Scholarship. L.A.S. is supported by the Hudson Institute of Medical Research. D.W.G. is supported by Baker Institute, La Trobe Institute for Molecular Science Fellowship, and La Trobe University Leadership RFA grant.

Author Contributions

J.E. conceived and designed the experiments. J.E. and D.W.G. carried out the majority of experiments. J.H. performed experimental work. D.W.G. performed proteomic analysis, bioinformatics. L.A.S. helped develop project, wrote and edited manuscript, and provided critical insight. J.E., L.A.S., and D.W.G. wrote, reviewed, and edited the manuscript. All authors approved the final manuscript.

Conflict of Interest

The authors declare no conflict of interest.

Keywords

adhesion, cell–cell interactions, endometrium, implantation, receptivity, trophoctoderm

Received: July 24, 2019
Revised: November 25, 2019

-
- [1] a) N. M. E. Fogarty, A. McCarthy, K. E. Snijders, B. E. Powell, N. Kubikova, P. Blakeley, R. Lea, K. Elder, S. E. Wamaitha, D. Kim, V. Maciulyte, J. Kleinjung, J. S. Kim, D. Wells, L. Vallier, A. Bertero, J. M. A. Turner, K. K. Niakan, *Nature* **2017**, *550*, 67; b) N. S. Macklon, J. P. Geraedts, B. C. Fauser, *Hum. Reprod. Update* **2002**, *8*, 333; c) G. L. Harton, S. Munne, M. Surrey, J. Grifo, B. Kaplan, D. H. McCulloh, D. K. Griffin, D. Wells; PGD Practitioners Group, *Fertil. Steril.* **2013**, *100*, 1695.
- [2] J. Evans, K. J. Walker, M. Bilandzic, S. Kinnear, L. A. Salamonsen, *J. Assist. Reprod. Gen.* **2019**, <https://doi.org/10.1007/s10815-019-01629-0>.

- [3] T. Zdravkovic, K. L. Nazor, N. Larocque, M. Gormley, M. Donne, N. Hunkapillar, G. Giritharan, H. S. Bernstein, G. Wei, M. Hebrok, X. Zeng, O. Genbacev, A. Mattis, M. T. McMaster, A. Krtolica, D. Valbuena, C. Simon, L. C. Laurent, J. F. Loring, S. J. Fisher, *Development* **2015**, 142, 4010.
- [4] P. Paiva, N. J. Hannan, C. Hincks, K. L. Meehan, E. Pruyers, E. Dimitriadis, L. A. Salamonsen, *Hum. Reprod.* **2011**, 26, 1153.
- [5] J. Evans, A. Rai, H. P. T. Nguyen, Q. H. Poh, K. Elglass, R. J. Simpson, L. A. Salamonsen, D. W. Greening, *Proteomics* **2019**, 19, 1800423.
- [6] D. W. Greening, H. P. Nguyen, K. Elgass, R. J. Simpson, L. A. Salamonsen, *Biol. Reprod.* **2016**, 94, 38.
- [7] Y. H. Ng, S. Rome, A. Jalabert, A. Forterre, H. Singh, C. L. Hincks, L. A. Salamonsen, *PLoS One* **2013**, 8, e58502.
- [8] H. Ji, D. W. Greening, T. W. Barnes, J. W. Lim, B. J. Tauro, A. Rai, R. Xu, C. Adda, S. Mathivanan, W. Zhao, Y. Xue, T. Xu, H. J. Zhu, R. J. Simpson, *Proteomics* **2013**, 13, 1672.
- [9] a) B. Mo, A. E. Vendrov, W. A. Palomino, B. R. DuPont, K. B. Apparao, B. A. Lessey, *B Reprod* **2006**, 75, 387; b) C. Korch, M. A. Spillman, T. A. Jackson, B. M. Jacobsen, S. K. Murphy, B. A. Lessey, V. C. Jordan, A. P. Bradford, *Gynecol. Oncol.* **2012**, 127, 241.
- [10] M. Bilandzic, K. L. Stenvers, *J. Vis. Exp.* **2014**, <https://doi.org/10.3791/51655>.
- [11] D. W. Greening, H. P. Nguyen, J. Evans, R. J. Simpson, L. A. Salamonsen, *J. Proteomics* **2016**, 144, 99.
- [12] A. Rai, D. W. Greening, M. Chen, R. Xu, H. Ji, R. J. Simpson, *Proteomics* **2019**, 19, 1800148.
- [13] A. Shevchenko, H. Tomas, J. Havlis, J. V. Olsen, M. Mann, *Nat. Protoc.* **2006**, 1, 2856.
- [14] D. W. Greening, H. Ji, M. Chen, B. W. Robinson, I. M. Dick, J. Creaney, R. J. Simpson, *Sci. Rep.* **2016**, 6, 32643.
- [15] J. Cox, M. Mann, *Nat. Biotechnol.* **2008**, 26, 1367.
- [16] C. A. Lubber, J. Cox, H. Lauterbach, B. Fancke, M. Selbach, J. Tschoop, S. Akira, M. Wiegand, H. Hochrein, M. O'Keeffe, M. Mann, *Immunity* **2010**, 32, 279.
- [17] Y. Benjamini, Y. Hochberg, *J. R. Stat. Soc. Ser. B-Stat. Methodol.* **1995**, 57, 289.
- [18] B. J. Tauro, R. A. Mathias, D. W. Greening, S. K. Gopal, H. Ji, E. A. Kapp, B. M. Coleman, A. F. Hill, U. Kusebauch, J. L. Hallows, D. Shteynberg, R. L. Moritz, H. J. Zhu, R. J. Simpson, *Mol. Cell. Proteomics* **2013**, 12, 2148.
- [19] W. Huang da, B. T. Sherman, R. A. Lempicki, *Nat. Protoc.* **2009**, 4, 44.
- [20] H. Wickham, *ggplot2: Elegant Graphics for Data Analysis*, Springer-Verlag, New York **2009**.
- [21] S. Whitby, L. A. Salamonsen, J. Evans, *Endocrinology* **2018**, 159, 506.
- [22] J. Cha, X. Sun, S. K. Dey, *Nat. Med.* **2012**, 18, 1754.
- [23] J. Cox, M. Y. Hein, C. A. Lubber, I. Paron, N. Nagaraj, M. Mann, *Mol. Cell. Proteomics* **2014**, 13, 2513.
- [24] P. Diaz-Gimeno, J. A. Horcajadas, J. A. Martinez-Conejero, F. J. Esteban, P. Alama, A. Pellicer, C. Simon, *Fertil. Steril.* **2011**, 95, 50.
- [25] D. Szklarczyk, A. Franceschini, S. Wyder, K. Forslund, D. Heller, J. Huerta-Cepas, M. Simonovic, A. Roth, A. Santos, K. P. Tsafou, M. Kuhn, P. Bork, L. J. Jensen, C. von Mering, *Nucleic Acids Res.* **2015**, 43, D447.
- [26] a) A. Deglincerti, G. F. Croft, L. N. Pietila, M. Zernicka-Goetz, E. D. Siggia, A. H. Brivanlou, *Nature* **2016**, 533, 251; b) M. N. Shahbazi, A. Jedrusik, S. Vuoristo, G. Recher, A. Hupalowska, V. Bolton, N. N. M. Fogarty, A. Campbell, L. Devito, D. Ilic, Y. Khalaf, K. K. Niakan, S. Fishel, M. Zernicka-Goetz, *Nat. Cell Biol.* **2016**, 18, 700.
- [27] a) Y. L. Lee, S. W. Fong, A. C. Chen, T. Li, C. Yue, C. L. Lee, E. H. Ng, W. S. Yeung, K. F. Lee, *Hum. Reprod.* **2015**, 30, 2614; b) N. C. Rivron, J. Frias-Aldeguer, E. J. Vrij, J. C. Boisset, J. Korving, J. Vivie, R. K. Truckenmuller, A. van Oudenaarden, C. A. van Blitterswijk, N. Geijsen, *Nature Protoc.* **2018**, 13, 1586.
- [28] a) D. K. Gardner, *BioEssays* **2015**, 37, 364; b) M. N. Shahbazi, A. Scialdone, N. Skorupska, A. Weberling, G. Recher, M. Zhu, A. Jedrusik, L. G. Devito, L. Noli, I. C. Macaulay, C. Buecker, Y. Khalaf, D. Ilic, T. Voet, J. C. Marioni, M. Zernicka-Goetz, *Nature* **2017**, 552, 239; c) X. Chen, L. Jiang, C. C. Wang, J. Huang, T. C. Li, *Fertil. Steril.* **2016**, 105, 1496; d) M. Salker, G. Teklenburg, M. Molokhia, S. Lavery, G. Trew, T. Aojanepong, H. J. Mardon, A. U. Lokugamage, R. Rai, C. Landles, B. A. Roelen, S. Quenby, E. W. Kuijk, A. Kavelaars, C. J. Heijnen, L. Regan, N. S. Macklon, J. J. Brosens, *PLoS One* **2010**, 5, e10287.
- [29] P. Sebastian-Leon, N. Garrido, J. Remohi, A. Pellicer, P. Diaz-Gimeno, *Hum. Reprod.* **2018**, 33, 626.
- [30] S. Altmae, F. J. Esteban, A. Stavreus-Evers, C. Simon, L. Giudice, B. A. Lessey, J. A. Horcajadas, N. S. Macklon, T. D'Hooghe, C. Campoy, B. C. Fauser, L. A. Salamonsen, A. Salumets, *Hum. Reprod. Update* **2014**, 20, 12.
- [31] G. E. Evans, J. A. Martinez-Conejero, G. T. Phillipson, C. Simon, L. A. McNoe, P. H. Sykes, J. A. Horcajadas, E. Y. Lam, C. G. Print, I. L. Sin, J. J. Evans, *Fertil. Steril.* **2012**, 97, 1365.
- [32] a) C. R. Murphy, *J. Reprod. Fertil. Suppl.* **2000**, 55, 23; b) C. R. Murphy, *Hum. Reprod.* **2000**, 15, 182.
- [33] H. Lim, B. C. Paria, S. K. Das, J. E. Dinchuk, R. Langenbach, J. M. Trzaskos, S. K. Dey, *Cell* **1997**, 91, 197.
- [34] a) K. Magdoud, V. G. Herbein, R. Touraine, W. Y. Almawi, T. Mahjoub, *Am. J. Reprod. Immunol.* **2013**, 70, 246; b) A. Dossenbach-Glaninger, M. van Trotsenburg, B. Schneider, C. Oberkanins, P. Hopmeier, *Br. J. Haematol.* **2008**, 141, 269.